High-Tech Fibrous Materials

Composites,
Biomedical Materials,
Protective Clothing,
and
Geotextiles

Edited by
Tyrone L. Vigo
and Albin F. Turbak

ACS Symposium Series 457

ACS SYMPOSIUM SERIES **457**

High-Tech Fibrous Materials

Composites, Biomedical Materials, Protective Clothing, and Geotextiles

Tyrone L. Vigo, EDITOR
U.S. Department of Agriculture

Albin F. Turbak, EDITOR
Southern College of Technology

Developed from a symposium sponsored
by the Cellulose, Paper, and Textile Division
of the American Chemical Society
at the 198th National Meeting,
Miami Beach, Florida, September 10–15, 1989

American Chemical Society, Washington, DC 1991

Downloaded by 89.163.34.136 on August 6, 2012 | http://pubs.acs.org
Publication Date: April 3, 1991 | doi: 10.1021/bk-1991-0457.fw001

Downloaded by 89.163.34.136 on August 6, 2012 | http://pubs.acs.org
Publication Date: April 3, 1991 | doi: 10.1021/bk-1991-0457.fw001

Library of Congress Cataloging-in-Publication Data

High-tech fibrous materials: composites, biomedical materials, protective clothing, and geotextiles
Tyrone L. Vigo, editor, Albin F. Turbak, editor

Developed from a symposium sponsored by the Cellulose, Paper, and Textile Division of the American Chemical Society at the 198th National Meeting, Miami Beach, Florida, September 10–15, 1989.

p. cm.—(ACS symposium series, ISSN 0097–6156; 457)

Includes bibliographical references and indexes.

ISBN 0–8412–1985–0

1. Textile fabrics—Congresses. 2. Textile fibers—Congresses. 3. Geotextiles—Congresses. 4. Protective clothing—Congresses.

I. Vigo, Tyrone L., 1939– . II. Turbak, Albin F., 1929– . III. American Chemical Society. Cellulose, Paper, and Textile Division. IV. Series.

TS1300.H54 1991
677—dc20 90–28996
CIP

The paper used in this publication meets the minimum requirements of American National Standard for Information Sciences—Permanence of Paper for Printed Library Materials, ANSI Z39.48–1984. ∞

Copyright © 1991

American Chemical Society

All Rights Reserved. The appearance of the code at the bottom of the first page of each chapter in this volume indicates the copyright owner's consent that reprographic copies of the chapter may be made for personal or internal use or for the personal or internal use of specific clients. This consent is given on the condition, however, that the copier pay the stated per-copy fee through the Copyright Clearance Center, Inc., 27 Congress Street, Salem, MA 01970, for copying beyond that permitted by Sections 107 or 108 of the U.S. Copyright Law. This consent does not extend to copying or transmission by any means—graphic or electronic—for any other purpose, such as for general distribution, for advertising or promotional purposes, for creating a new collective work, for resale, or for information storage and retrieval systems. The copying fee for each chapter is indicated in the code at the bottom of the first page of the chapter.

The citation of trade names and/or names of manufacturers in this publication is not to be construed as an endorsement or as approval by ACS of the commercial products or services referenced herein; nor should the mere reference herein to any drawing, specification, chemical process, or other data be regarded as a license or as a conveyance of any right or permission to the holder, reader, or any other person or corporation, to manufacture, reproduce, use, or sell any patented invention or copyrighted work that may in any way be related thereto. Registered names, trademarks, etc., used in this publication, even without specific indication thereof, are not to be considered unprotected by law.

PRINTED IN THE UNITED STATES OF AMERICA

American Chemical Society
Library
1155 16th St., N.W.
Washington, D.C. 20036

Downloaded by 89.163.34.136 on August 6, 2012 | http://pubs.acs.org
Publication Date: April 3, 1991 | doi: 10.1021/bk-1991-0457.fw001

ACS Symposium Series

M. Joan Comstock, *Series Editor*

1991 ACS Books Advisory Board

V. Dean Adams
Tennessee Technological University

Paul S. Anderson
Merck Sharp & Dohme Research Laboratories

Alexis T. Bell
University of California—Berkeley

Malcolm H. Chisholm
Indiana University

Natalie Foster
Lehigh University

Dennis W. Hess
University of California—Berkeley

Mary A. Kaiser
E. I. du Pont de Nemours and Company

Gretchen S. Kohl
Dow-Corning Corporation

Michael R. Ladisch
Purdue University

Bonnie Lawlor
Institute for Scientific Information

John L. Massingill
Dow Chemical Company

Robert McGorrin
Kraft General Foods

Julius J. Menn
Plant Sciences Institute, U.S. Department of Agriculture

Marshall Phillips
Office of Agricultural Biotechnology, U.S. Department of Agriculture

Daniel M. Quinn
University of Iowa

A. Truman Schwartz
Macalaster College

Stephen A. Szabo
Conoco Inc.

Robert A. Weiss
University of Connecticut

Foreword

THE ACS SYMPOSIUM SERIES was founded in 1974 to provide a medium for publishing symposia quickly in book form. The format of the Series parallels that of the continuing ADVANCES IN CHEMISTRY SERIES except that, in order to save time, the papers are not typeset, but are reproduced as they are submitted by the authors in camera-ready form. Papers are reviewed under the supervision of the editors with the assistance of the Advisory Board and are selected to maintain the integrity of the symposia. Both reviews and reports of research are acceptable, because symposia may embrace both types of presentation. However, verbatim reproductions of previously published papers are not accepted.

Downloaded by 89.163.34.136 on August 6, 2012 | http://pubs.acs.org
Publication Date: April 3, 1991 | doi: 10.1021/bk-1991-0457.fw001

Preface

FIBROUS MATERIALS TECHNOLOGY is a dynamic field in which exciting, high-performance products are being developed almost daily to benefit such diverse areas as biomedical and aerospace engineering, construction, transportation, pollution control, and body protection. In recent years, scientists have learned to capitalize on advanced materials technology to produce products with high-performance features.

The four-day conference upon which this book is based highlighted four major areas—composites, biomedical materials, protective clothing, and geotextiles—where advanced textile fibers and structures have had and are having a significant impact. Symposium sessions on each of these four areas were developed by Christopher Pastore (North Carolina State University), Donald J. Lyman (University of Utah), Tyrone L. Vigo (U.S. Department of Agriculture, Southern Regional Research Laboratories), and Ian Peggs (GeoSyntec, Inc.). The resulting book highlights the main focuses of the symposium.

The section on composites includes such important topics as 3–D braiding, 3–D multilayer woven fabrics, multiaxial warp knit structures, braided reinforced vehicles, and silicon-coated wood fiber fillers for polyethylene.

Design of laminated semiabsorbable bone plates, theoretical modeling of geometric forms and laminates for deformation behavior in bioapplication requirements for fibrous materials, and recent advances in suture developments are highlighted in the section on biomedical materials.

Chapters on protective-clothing technology present in-depth discussions on uses of high-performance fibers such as Spectra 1000, the world's strongest fiber, and PBI (polybenzimidazole) blended with Kevlar and Nomex in clothing that offers protection from knife and bullet wounds. Also included is information on printing Nomex. Thermal transmission properties of wool blends with Kevlar, Nomex, Ryton, and Inidex for firefighters' clothing, the effects of simultaneous application of intense heat and dynamic mechanical forces on protective clothing, and the melt–stick performance of flame-treated polyester–cotton blends further expand the coverage on protective clothing. The symposium presented the first reports on user test experience with NeutraTherm, the permanently affixed polyethylene glycol phase-change treated textiles for controlling clothing temperature next to the skin, and those results are presented in Chapter 15. This exciting technological advance represents a totally new concept in design and comfort.

Downloaded by 89.163.34.136 on August 6, 2012 | http://pubs.acs.org
Publication Date: April 3, 1991 | doi: 10.1021/bk-1991-0457.pr001

Geotextiles are given extensive treatment in the book's final section, which encompasses the chemical compatibility and long-term stability of geotextiles and their use in waste containment, transportation, and related areas. Polyester durability, polyolefin stabilization, and fiber glass yarns are discussed in detail.

As conference co-chairmen and co-editors of this book, we would like to thank the symposia chairmen, the various individual contributors, and the staff of the American Chemical Society.

TYRONE L. VIGO*
Southern Regional Research Center
Agricultural Research Service
U.S. Department of Agriculture
New Orleans, LA 70179

ALBIN F. TURBAK*
Applied Research Center
Southern College of Technology
Marietta, GA 30060

November 30, 1990

Downloaded by 89.163.34.136 on August 6, 2012 | http://pubs.acs.org
Publication Date: April 3, 1991 | doi: 10.1021/bk-1991-0457.pr001

***Also adjunct professor, Textile Department, University of Georgia, Athens, Georgia.**

Downloaded by 89.163.34.136 on August 6, 2012 | http://pubs.acs.org
Publication Date: April 3, 1991 | doi: 10.1021/bk-1991-0457.ch001

Chapter 1

High-Tech Textiles

Evolution or Revolution

Albin F. Turbak[1] and Tyrone L. Vigo[2]

[1]Southern College of Technology, 1110 South Marietta Parkway,
Marietta, GA 30060
[2]Agricultural Research Service, U.S. Department of Agriculture,
P.O. Box 19687, New Orleans, LA 70179

The new world of textile technology now encompasses realms of products that were not even dreamed of ten years ago. High-tech textiles are prevalent as major components in such diverse products as artificial organs, structural bone replacements, rocket motors and nozzles, space shuttle shields, the Stealth bomber and most of the new design military, commercial and civilian aircraft, boats, bicycles, high-performance sporting goods, road beds, food/water removal systems, pollution control devices, translucent roofs for stadiums, airports and shopping malls, components for converting sea water into potable water, optical fibers for transmission of laser-pulsed communication and extended, temperature-controlled garments. Fibers that are five to ten times as strong as steel on a weight basis now provide the lead technology for making automobiles that are 50% lighter, safer and twice as fuel-efficient as current models. These examples and the history of the development of this technology will be reviewed and discussed in depth in this book.

The textile industry is one of American's major industries and employs 2.3 million people for producing yarn and converting it into finished textile products. The American consumer spends $110 billion annually for apparel and an additional $120 billion for other textiles such as upholstery, furnishings, carpets, etc. (1). Over two-thirds of all carpets made in the United States and one-third of all carpets made in the world are produced in the Dalton, Georgia area. This constitutes about 1.3 billion pounds of this textile product annually (2). Major U. S. automobile manufacturers (such as General Motors, Ford and Chrysler) use approximately 18 million yards of fabric in their vehicles. The textile industry purchases $2 billion worth of new foreign machinery annually on which they pay

0097–6156/91/0457–0001$06.00/0

$110 million in import taxes (3). In spite of this massive machinery purchase and fantastic domestic consumption, the United States still produces only 13 billion pounds of fiber while it consumes 16 billion pounds -- a 3 billion pound shortfall (4).

With such impressive statistics, one would assume that textiles should be in a very strong economic position. Yet, exactly the opposite is true! In 1988, foreign imports of textiles accounted for a $20 billion deficit second only to the monstrous $55 billion auto import deficit (5). New developments by U. S. textile companies are few because of two main factors:

1. Leveraged buy outs of textile companies usually leave the new owners with such massive debt and interest payments that research and development are immediately sacrificed to improve cash flow.

2. While the federal government collects $110 million in import taxes each year on the textile machinery purchases, not one cent of these revenues is returned to universities engaged in textile education and research. A return of such revenues for R & D could help the domestic industry remain healthy and globally competitive. Moreover, there is an urgent need for the establishment of a National Textile Institute patterned along the lines of NSF to coordinate such R & D (6). This could initially be achieved by allocating at least $10 million of the $110 million import taxes now being collected for the foreign machinery purchases.

Downloaded by 89.163.34.136 on August 6, 2012 | http://pubs.acs.org
Publication Date: April 3, 1991 | doi: 10.1021/bk-1991-0457.ch001

While the staid textile industry is working out its dubious future in areas of conventional uses, forward-looking companies and entrepreneurs have begun to capitalize on advanced materials technology by utilizing modified natural and specially constructed synthetic fibers to produce textile products with exciting and high tech features. This high tech evolution or revolution is worldwide. However, the contributions in this book are all from American scientists and companies, indicating that substantial progress has already been achieved and more innovative developments are on the horizon. Although the tenacity of these new textile fibers has not yet reached the theoretically predicted 100 gram-per-denier level and the new textile products are not yet in the realm of the apparel in the classic movie "The Man in the White Suit", there are many exciting innovations in diverse areas of technology. These include, but are not limited to:

1. Biomedical uses for artificial hearts, heart valves, artificial kidneys and arteries (Figures 1 and 2), improved prosthetic devices, knee and hip joints, antimicrobial sutures, and optical fibers to guide lasers for pulverizing kidney stones and for vaporizing arterial-plaque blockage.

2. Transportation uses for making lighter weight and more fuel-efficient airplanes (Figure 3), vehicles, faster boats, rocket nozzles and ablative heat shield tiles for the aerospace program.

Downloaded by 89.163.34.136 on August 6, 2012 | http://pubs.acs.org
Publication Date: April 3, 1991 | doi: 10.1021/bk-1991-0457.ch001

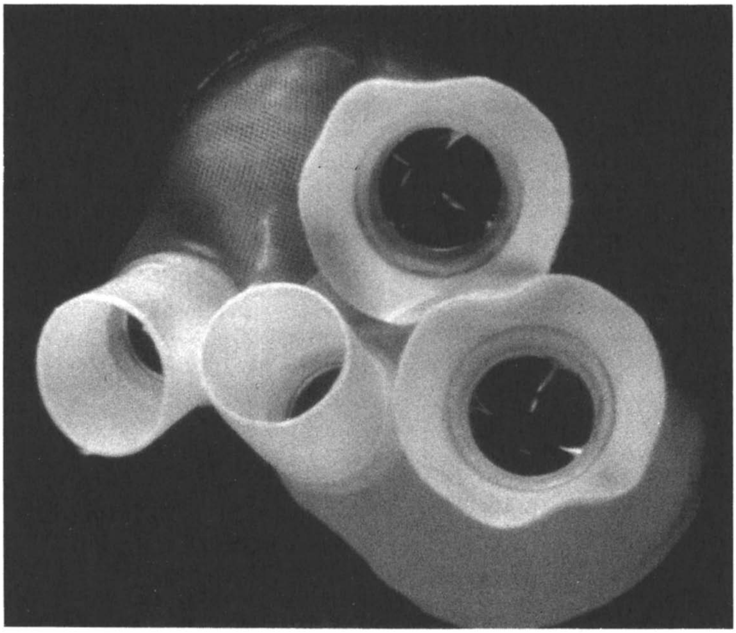

Figure 1. Artificial heart -- 50% textile fiber content

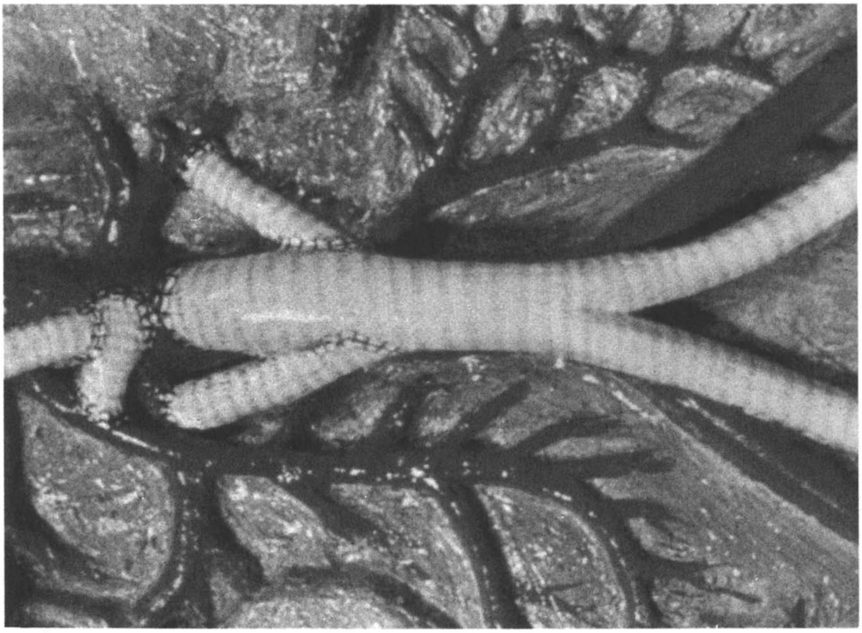

Figure 2. Knit polyester artificial arteries

3. Protective clothing that can stop bullets (Figure 4) and resist flame, gloves that can't be readily cut with a razor blade and can catch white rivets with impunity, lumberjack trousers with built-in pads that can stop a chain saw, total body suits for protection against the newest skin-contact nerve gases while allowing for moisture transport from within, and comfort clothing that simulates natural down or that literally and reversibly absorbs and releases heat based on incorporation of phase change materials.

4. Geotextiles used in civil engineering applications such as road-bed liners to minimize pothole formation, prevent retainer-wall movement and collapse as well as shifting of earth embankments, strengthen the dikes in Holland, minimize soil erosion and gully formation, prevent undesirable water seepage into subterranean aquifers or commercial structures, pond liners to preserve valuable water resources, and reverse osmosis units that supply 300 hundred cities worldwide with up to 3.5 million gallons of drinking water daily for each city.

5. Architectural and construction uses where flexible composites of glass and silicone are used for fabricating roofs for the Hubert Humphrey Dome in Minneapolis (Figure 5), the airport terminal in Saudia Arabia (Figure 6a and 6b), translucent roofs for modern shopping centers, and silos for storage of grain and agricultural products. These also include horticultural uses of pigmented polyolefin fabrics for shade covers and fiber composite roofs for greenhouses.

6. Recreational uses in which carbon-fiber reinforced composites make possible lightweight and strong tennis rackets, golf clubs, snowmobiles, spas, bicycles, speedboats, and other recreational equipment and accessories.

7. Specially constructed nonwoven fabric assemblies for filtration of gases and liquids in a variety of industries and applications such as dairy, pollution control, chemical and water purification, for reduction of dust/ particles and as clean room garments in the computer and biomedical industries. For example, "Intersept"-treated fabrics, filters and carpets (7) which prevent bacterial, mold and growth on fabrics used in hospitals and provide a cleaner and healthier office and living environment. Also, high-temperature resistant fibers which are used to filter hot exhaust gases up to 2000°C.

While "High Tech " Textiles are impacting our daily lives in significantly new ways, commodity fibers have also been employed to extend their horizons of utility. These changes include bicomponent, carbon-loaded conductive nylon and polyester fibers for elimination of static charge, "Flecton" metal-coated fibers and fabrics for electromagnetic shielding (8), melt-blown polypropylene structures for diaper liners to wick away moisture more effectively, acrylic PAN fibers for

Downloaded by 89.163.34.136 on August 6, 2012 | http://pubs.acs.org
Publication Date: April 3, 1991 | doi: 10.1021/bk-1991-0457.ch001

Downloaded by 89.163.34.136 on August 6, 2012 | http://pubs.acs.org
Publication Date: April 3, 1991 | doi: 10.1021/bk-1991-0457.ch001

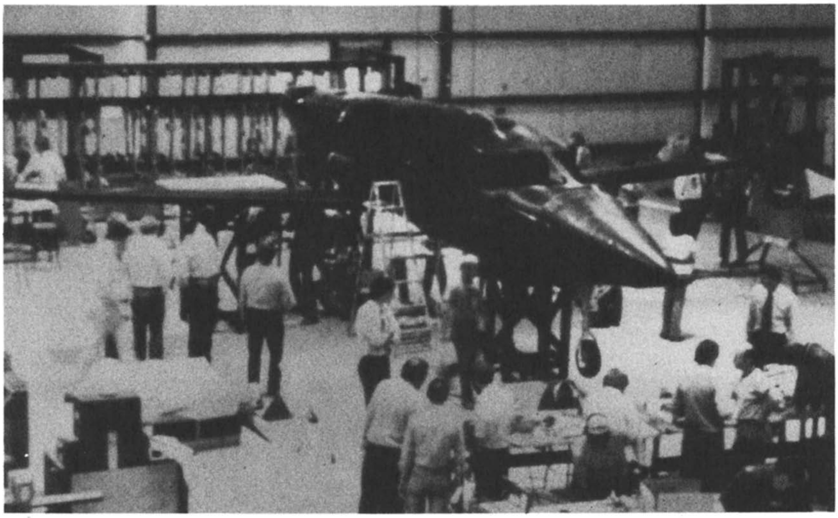

Figure 3. Lear Jet -- 98% carbon fiber composite -- world's most fuel-efficient airplane

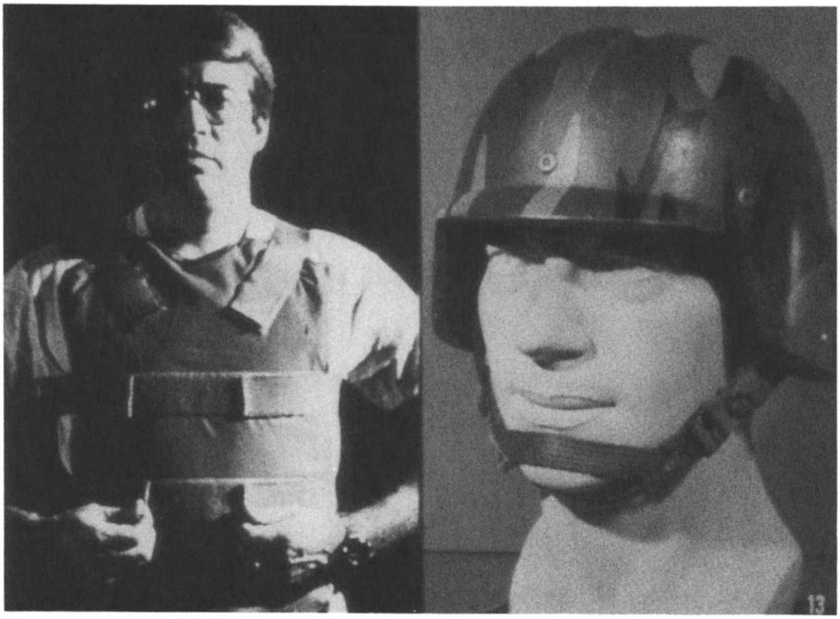

Figure 4. High tech fiber body protection -- bullet-proof vest and new army helmet

Downloaded by 89.163.34.136 on August 6, 2012 | http://pubs.acs.org
Publication Date: April 3, 1991 | doi: 10.1021/bk-1991-0457.ch001

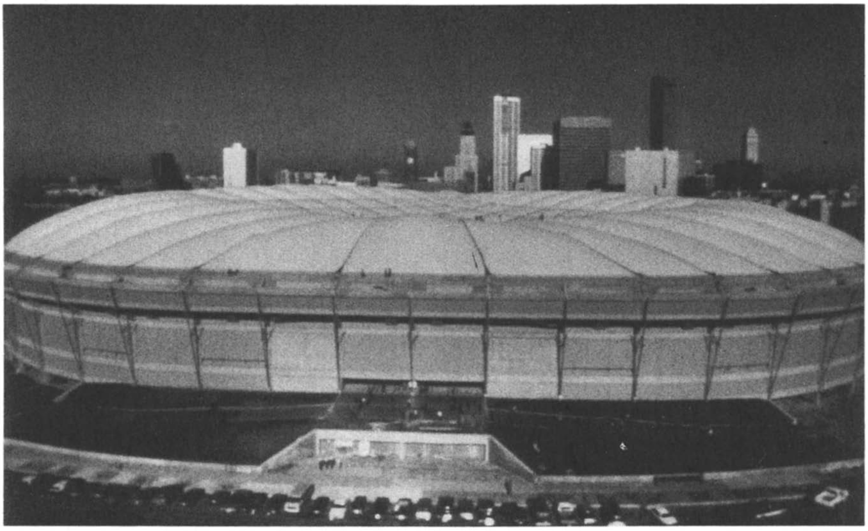

Figure 5. Hubert Humphrey Fabric-Domed Sports Arena, Minneapolis, MN

Downloaded by 89.163.34.136 on August 6, 2012 | http://pubs.acs.org
Publication Date: April 3, 1991 | doi: 10.1021/bk-1991-0457.ch001

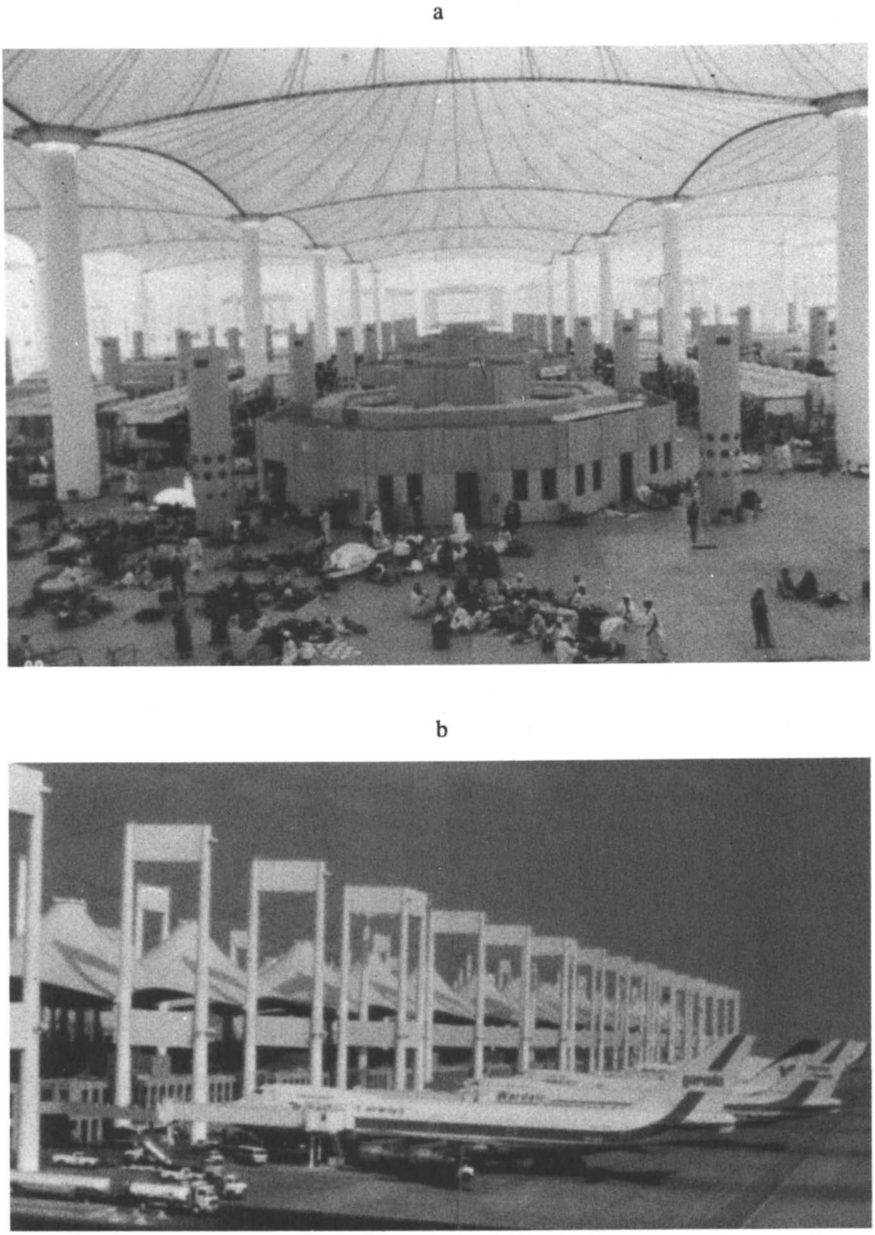

Figure 6. Fabric roof of Saudi Arabian Airport Terminal: (a) inside and (b) outside

concrete reinforcement and modified nylons for stain-resistant carpets. Such modifications are obviously important, but the inherent properties of standard fibers will limit their upper performance levels for consideration in a number of high tech areas.

With these kinds of advances taking place, it is difficult to contain an enthusiasm for the future of what had been dubbed in the early 1980's by A. F. Turbak as **Hi Tech Textiles** (9). In each of the above-mentioned areas, new types of structured fibers with outstanding properties resulted in their advantageous utilization for exciting new areas of use. In considering these advances, it is important to realize that new fibers and textile products have resulted from fundamental and applied discoveries of a dual chemical and physical nature.

High-Tech-Fiber Evolution

Some excellent examples of high-tech-fiber evolution are found in the historical development of nylon, polyethylene and carbon fibers. In the case of nylon, Dr. Wallace Carothers at duPont first discovered in the early 1930's that aliphatic dibasic acids could be linked with aliphatic diamines or aliphatic glycols to form respectively polyamides and polyesters. The physical form of these polymers varied from oils and greases to meltable solids capable of being drawn into fibers by removing water as the reaction proceeded from 90 to 99.999+ % completion. His equation (Equation 1) relating degree of polymerization (DP) to the extent of completion of water removal was basic to giving direction to the new science of polymer formation via condensation technology:

$$DP = 1/(1 - B) \qquad (1)$$

where DP = degree of polymerization and B = decimal % of reaction completion. These then new polymers exhibited tenacities of 6-10 grams per denier (gpd) whereas cotton, wool, rayon and acetate fibers at that time had only 1.5-3.5 gpd.

It took 40 more years before Dr. Stephanie Kwolek (also of duPont) utilized "aromatic polyamides" having a length to width (or aspect) ratio of at least 10/1 to produce "liquid crystal" solutions of nylon. Upon dissolving this type of polymer, she discovered that as the concentration was increased, there came a point where the viscosity began to drop rather than increase. At this point, it was also observed that the solution became iridescent, and she reasoned that these concurrent phenomena were due to the close association of these more linear polymer chains into clusters or liquid crystals.

Such "pre-organized" chain bundles ultimately led to the spinning of a nylon having a strength of 22 gpd -- 10 times the strength of cotton and other natural fibers (10-14). This type of material was finally commercialized as "Kevlar" in a wide variety of products requiring high tenacity and high modulus such as bullet-proof vests, truck tires and cut-proof gloves. Kevlar also has a melting temperature of about 700°F compared to about 480°F for regular aliphatic nylon. This led to use of aromatic polyamides for a wide variety of high

Downloaded by 89.163.34.136 on August 6, 2012 | http://pubs.acs.org
Publication Date: April 3, 1991 | doi: 10.1021/bk-1991-0457.ch001

temperature applications such as nonwoven batting covers for airplane seats to retard combustion of the polyurethane foam in the seats and as an asbestos replacement in vehicular brakes.

A similar story exists for polyethylene which for years was nothing more than a refinery by-product that housewives used to melt seal the tops of their jams and preserves. While some preliminary efforts were made to produce high-molecular-weight polyethylene by use of high pressures, it wasn't until 1953 that Dr. Carl Ziegler discovered his special $Al(Et)_3/TiCl_4$ heterogeneous catalyst system used to produce highly crystalline, high-density, linear, high-molecular-weight polyethylene at room temperature and atmospheric pressure. Shortly thereafter, he showed his invention to his friend Dr. Julio Natta who promptly returned to his native Italy and used the catalyst system to produce stereoregular isotactic polypropylene and other polyolefins that resulted in a totally new array of textile and related products. For his discovery, Ziegler ultimately shared a Nobel Prize in Chemistry with Natta in 1963.

But now as Paul Harvey says, you need to know "the rest of the story!" Up through the mid 1970's, everyone involved in polymers had reasoned that the high strength of nylon over cotton or wool was due to the high degree of hydrogen bonding that occurred between chains. No one really took much time to note that Dr. Kwolek's Kevlar discovery, in fact, might have led to less hydrogen bonding energy because aromatic nitrogens were less basic and the rigid-chain structures had less tortuosity, thus limiting atomic proximities while the product still gave significantly higher strengths. This observation, along with Ziegler's discovery of stereoregularity, were the first concrete suggestions that structure perhaps played as great as, or an even greater role than, chemical composition in determining ultimate fiber and film properties and performance.

In the 1970's the effects of structural considerations were finally brought into focus as researchers such as Dr. A. J. Pennings and his associates in Holland made another startling discovery. They found that by spinning high molecular weight, high-density polyethylene from a hot solution into a nonsolvent, they could affect what they called "Gel Spinning." This process gave them control of extremely high orientation and continuity between crystalline and amorphous regions (minimizing chain folding into a lamellar structure) thereby producing fiber strengths of 44 gpd -- twice the strength previously achieved with Kevlar (15). Thus, the strongest fiber in the world is now being made from a hydrocarbon nonpolar monomer (ethylene) that simply cannot have a high degree of hydrogen bonding. This fiber has been recently commercialized by the Allied-Signal Company as "Spectra 1000" with the commercial version having strengths in the 32-35 gpd range. It is now obvious that we are finally beginning to understand how to approach the truly available fiber strengths of about 100 gpd calculated on a theoretical bond-strength basis.

It is also important to demonstrate that old technology is always worth examining more closely, and no better example of this can be found than in the history of carbon-fiber production. When rayon was first produced in 1880, Count Hilaire de Chardonnet of France took some rayon samples to Switzerland and left them with his friends. They tried to combust them in an atmosphere of limited oxygen and succeeded in making the first carbon fibers. Their driving

Downloaded by 89.163.34.136 on August 6, 2012 | http://pubs.acs.org
Publication Date: April 3, 1991 | doi: 10.1021/bk-1991-0457.ch001

force for this work was that Swan in England and Thomas Edison in America had both just invented the light bulb and were urgently seeking new filament materials that would last longer than two hours; moreover, Edison was willing to pay the unheard price of $2.00 per pound for such a material. The carbon fibers were a great improvement and gave illumination for several weeks compared to the other materials, but they were ultimately replaced by the special metal alloy filaments still in use today.

Carbon-fiber technology lay in abeyance for nearly 80 years until 1963, when the new space program required fibers that had exceptional heat resistance, high modulus, reasonable textile processability and excellent ablative performance to protect space vehicles which were experiencing extreme heat generation on returning to earth. The best fiber combining all these properties is carbon fiber which is finally graphitized at temperatures of up to 3000°C (5432°F). Today, the rocket nozzles made of graphite-fiber composites are used to contain the flames from the lift-off, propulsion-rocket-motor combustion and also are the best ablative tile materials applied to the front and bottom surfaces of the shuttle vehicle itself for re-entry into the earth's atmosphere (Figure 7).

Carbon fibers can be made from a number of different precursor materials, the three most common raw materials being rayon, polyacrylonitrile (PAN) and meso pitch. The two prime contenders at present are rayon and PAN fibers. Of these two, rayon currently has a performance advantage for aerospace in two important areas: density and thermal protection (as illustrated in Table I).

Downloaded by 89.163.34.136 on August 6, 2012 | http://pubs.acs.org
Publication Date: April 3, 1991 | doi: 10.1021/bk-1991-0457.ch001

Table I. Carbon Fiber Properties from Various Precursors (16)

Precursor	Density	Thermal Conductivity (W/mK)
Rayon	1.44-1.52	3.7-4.1
Polyacrylonitrile	1.55-1.78	8.5-43
Pitch	1.88-2.00	22-120

The main disadvantage of rayon as a carbon-fiber precursor has been its unpredictability as a raw material since the sole supplier of the proper type of rayon, Avtex, Inc., was temporarily closed in 1988 and finally closed in 1989 by the state of Virginia for pollution; thus, the government agencies had to scramble to try to develop a second source of supply to keep various space and rocket programs intact. This situation seems presently to be temporarily under control. As future research improves the performance of PAN-based materials, this precursor may well replace rayon in these critical applications. However, gaining acceptance as a "qualified fiber" for NASA uses will take several years of testing, and thus rayon can be expected to maintain its dominant position for space use for the foreseeable feature. For less critical uses not involving the specific needs of the space program, PAN fibers presently offer sufficient advantages over rayon in that they are the materials of choice for ease of handling, ease of carbonization and have superior specific fiber properties. Pitch-based carbon fibers offer cost advantages compared to the other two precursor materials. Some experimental work has also been undertaken using Kevlar as a graphite-fiber precursor material, but the fiber produced did not exhibit any spectacular improvement in its final fiber properties. The main research areas currently requiring the most attention are: (a) how to greatly increase the speed of carbonization and (b) how to improve carbon fiber adhesion to polymeric matrices.

High-Tech-Fiber Utilization

In many instances, fibers are preferred over films or other structural shapes because of the high-surface area available for a given weight of material. A good example of this is found in artificial kidneys where such devices were first made from cellophane tubing having a flat width of about an inch (Kolf dialyzers) or from cellophane sheets arranged as a parallel plate filter (Kiil dialyzers). Each of these designs presented significantly less surface and resulted in significantly more blood retention than the present artificial kidneys which employ bundles of 7,000 hollow fibers. These fiber bundles are about 12 inches long and have fibers of 10 microns outer diameter with a hole about half that size. These newer units allow for much more rapid patient dialysis rates with a drastically reduced serum retention and clotting.

A recent extension of the application of the artificial kidney is the use of extracorporeal dialysis to cleanse the blood of individuals who have taken an overdose of sleeping pills, accidentally consumed toxic chemical or overdosed with drugs. This rapid means of removing excess harmful material is helping to save many more lives.

An opposite situation from dialysis occurs in the case of reverse osmosis where similar types of modules with different fibers are used to filter salt from sea water or to concentrate dilute feed streams. It is possible to employ the proper polymer and copolymers to achieve either **Ultrafiltration** or **Hyperfiltration**. Such units have found extensive commercial use in water desalination and purification, effluent pollution abatement and concentration of materials that cannot endure heat without undergoing significant alteration or decomposition. Over 300 cities depend on hyperfiltration to supply their daily potable water of up to 3.5 million gallons per day (Figure 8). The typical cost for water purification by reverse osmosis is about 80 cents per 1000 gallons which includes investment depreciation and operating expenses. By comparison, regular purification of river water costs about 60 cents per 1000 gallons. "Hybrinet" polysulfone hollow fiber modules are available for use in bioreactors to grow mammalian and plant cell cultures (17).

Since reverse osmosis media have pores small enough to reject salt, they are also capable of rejecting bacteria and viruses. In Japan, small reverse osmosis units are installed under sinks in the operating rooms and deliver sterile water when a physician steps on a pump-starting pedal. In space, the astronauts use reverse osmosis units to recycle their water to minimize the total weight of water that must be carried on each trip. Recently, a retired engineer and his wife

Downloaded by 89.163.34.136 on August 6, 2012 | http://pubs.acs.org
Publication Date: April 3, 1991 | doi: 10.1021/bk-1991-0457.ch001

Downloaded by 89.163.34.136 on August 6, 2012 | http://pubs.acs.org
Publication Date: April 3, 1991 | doi: 10.1021/bk-1991-0457.ch001

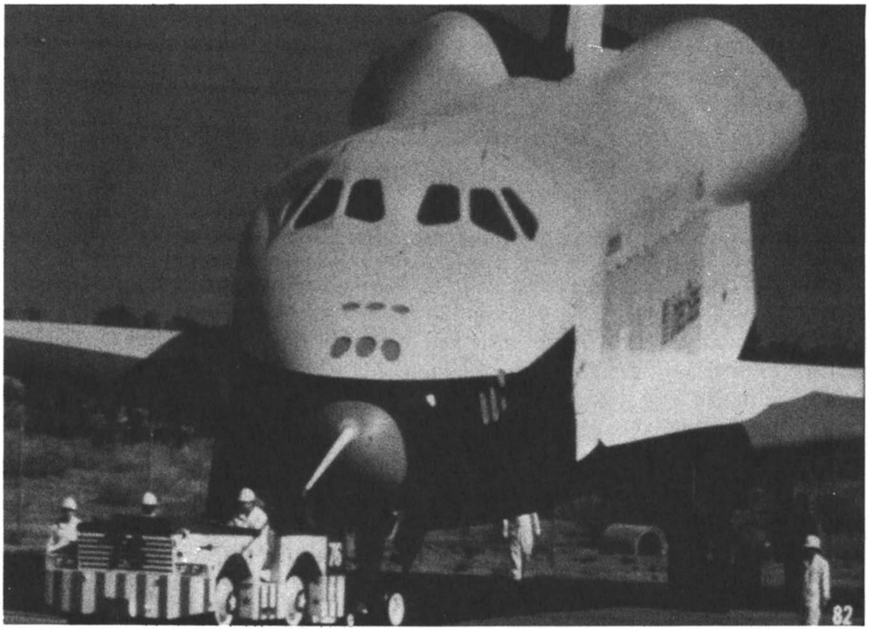

Figure 7. NASA Space Shuttle with carbon fiber heat shield

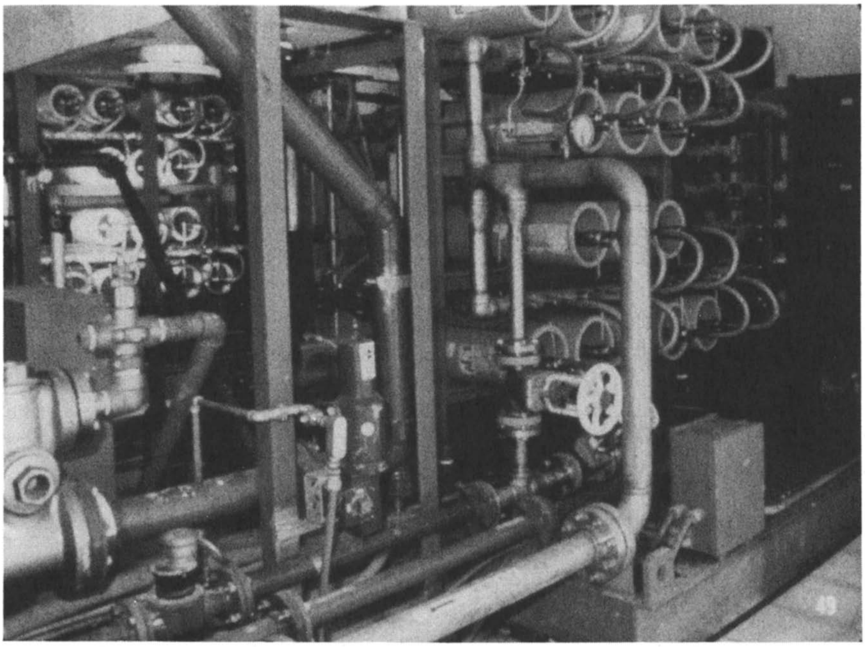

Figure 8. Commercial reverse osmosis fiber, potable-water installation

Downloaded by 89.163.34.136 on August 6, 2012 | http://pubs.acs.org
Publication Date: April 3, 1991 | doi: 10.1021/bk-1991-0457.ch001

sailing in the Pacific had their craft sunk by a school of whales, but they survived for 44 days because they had included a hand-operated reverse osmosis unit on their raft.

In the medical area, optical fibers are finding increased uses in directing laser beams. Optical fibers and lasers are now being used to locate and disintegrate kidney stones by well-established procedures. Recent extensions of this technique utilize high-intensity, ultraviolet-excimer laser beams to destroy arterial plaque. This technique may ultimately replace the now standard angioplasty which uses inflatable balloons to compress such life-threatening cholesterol and low-density, lipoprotein plaque material against the arterial wall and usually requires repeated treatments. While this technique is still experimental, the initial results have been very promising with a very high level of success and low side effects. Excimer lasers differ from regular Yag and similar infrared ray lasers in that they have a significantly smaller focus diameter and they leave essentially no scar tissue since they do not generate heat.

In the aerospace, aircraft and transportation areas, high performance fibers are rapidly becoming indispensable materials for advanced structural use. The new "Stealth Bomber" is an obvious example of such use. The high- specific tensile and modulus values coupled with the high-temperature stability achievable by use of these fibers have led to composites that greatly outperform metals. This High-Tech aspect of textile composites is currently being actively pursued by the three largest American automobile manufacturers who have now formed a "Composites Consortium" to jointly fabricate the composite car of the future.

The exceptional weight savings that can be achieved with composites over metals coupled with the much simpler fabrication of complex shapes easily justifies these efforts. Data in Table II indicate some of the weight advantages of composites over metals in vehicles.

Table II. Automobile Weight-Saving with Carbon Fiber Composites

Component Part	Steel (lb)	Graphite (lb)	Reduction (lb)	Reduction %
Hood	40.00	15.00	25.00	62
Door, right rear	30.25	12.65	17.60	58
Hinge, upper left front	2.25	0.47	1.78	79
Hinge, lower left front	2.67	0.77	1.90	71
Door, guard beam	3.85	2.40	1.45	37
Suspension arm, upper	3.85	1.68	2.17	56
Suspension arm, lower	2.90	1.27	1.63	56
Transmission support	2.35	0.55	1.80	77
Drive shaft	27.40	12.00	15.40	56
Air conditioner (lateral brace)	9.50	3.25	6.25	66
Air conditioner (compressor bracket)	5.63	1.35	4.28	76

The major weight savings, however, will come from use of composites in the engines where such engines will be designed with ceramic sleeves for combustion chambers. The gasoline automobile of the future, therefore, will weigh about half of its present weight, be stronger and easier to manufacture and repair and will have significantly improved gasoline mileage per gallon. Figure 9 compares the strength and stiffness of composites made from different high-tech fiber materials.

In the area of geotextiles, a great deal has already been accomplished through the use of High-Tech Textiles. Nonwoven mats such as the heavy nylon denier "ENKAMAT" have been extensively used to retain soil on the sides of new highways for preventing erosion, and this same type of material is now used in Holland to help reinforce dikes and prevent leakage. A modified version of this concept is now also being used by construction engineers to lay along the sides of new high-rise building foundations to prevent water seepage into subterranean levels. This type of construction also has vastly improved mildew resistance. Other geotextile products are being used as liners to control polluted water run-off from land fills, while polypropylene "TYVEK" nonwovens are being used as sublayers or liners in the construction of road beds, particularly where a soft sub-base is involved (Figure 10).

In the area of protective clothing, High-Tech Textiles are playing a key role. The use of "KEVLAR" for bullet-proof vests and cut-proof gloves is well known. The new "SPECTRA" fibers, however, can now provide the same type of protection at a much lighter weight. Thus, today's bullet-proof vests for police work weigh about half that of earlier vests because of the much lower density of the "SPECTRA" polyethylene vs. the "KEVLAR" aromatic polyamide. However, "SPECTRA" does not have the high-temperature performance characteristics of "KEVLAR."

High-temperature fibers are rapidly becoming very important industrially. The current FAA rulings require that airplane seats have improved flame resistance, and now a nonwoven batting comprised of "NOMEX" and "KEVLAR" (both aromatic polyamides) is being placed over the polyurethane cushions of all new airplane seats to meet these new specifications. It is entirely conceivable that similar standards will ultimately be required for school-bus seats and even for automobile seats.

High-temperature fibers are also very important to the space program where polybenzimidazole (PBI) yarns produced by Hoechst-Celanese Corporation are being used for the astronauts' suits worn during blast-off of the shuttle (Figure 11). The polyphenylene sulfide (PPS) fibers from Phillips Petroleum Co. are also rapidly establishing a niche in related areas. What is still missing is a lighter weight fireman's suit. Even with all our current technology, the fireman's suit still weighs about 75 to 85 pounds, and thus represents a major detriment to fire-fighting efficiency, especially when they have to carry out victims and climb ladders with this heavy clothing. Similarly absent are improved quality cold-water suits for airmen downed into icy water where the present expected time of survival is only five minutes.

Downloaded by 89.163.34.136 on August 6, 2012 | http://pubs.acs.org
Publication Date: April 3, 1991 | doi: 10.1021/bk-1991-0457.ch001

Downloaded by 89.163.34.136 on August 6, 2012 | http://pubs.acs.org
Publication Date: April 3, 1991 | doi: 10.1021/bk-1991-0457.ch001

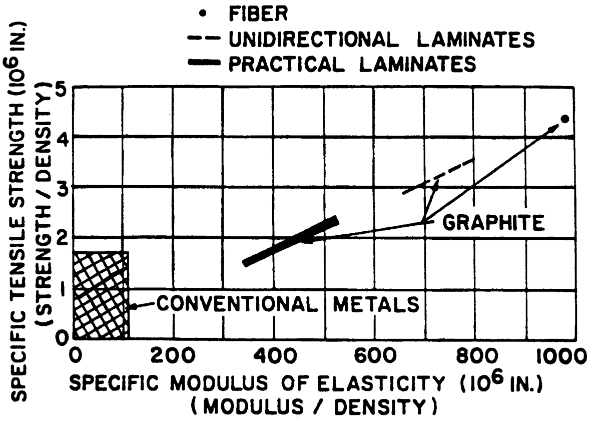

Figure 9. Comparison of strength and stiffness of various high tech fiber composites

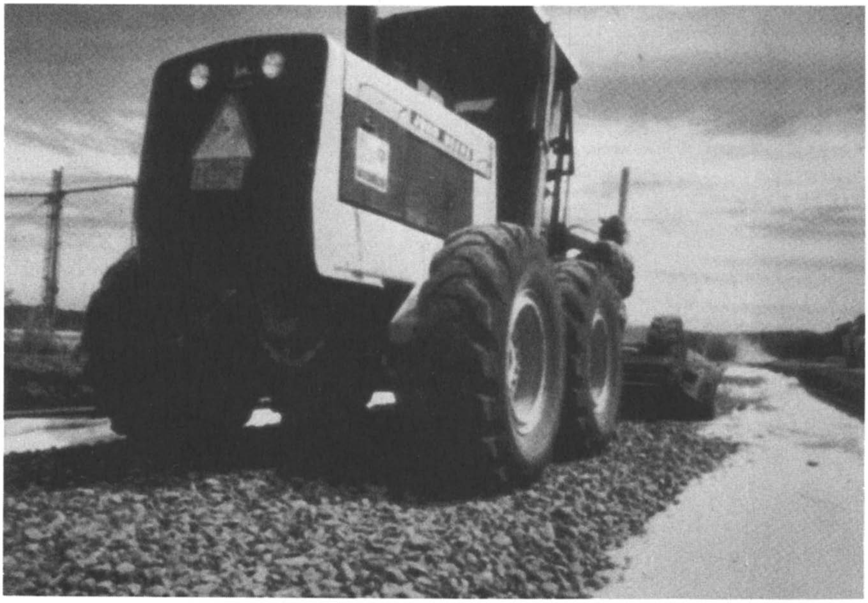

Figure 10. Tyvek nonwoven road bed liners

Downloaded by 89.163.34.136 on August 6, 2012 | http://pubs.acs.org
Publication Date: April 3, 1991 | doi: 10.1021/bk-1991-0457.ch001

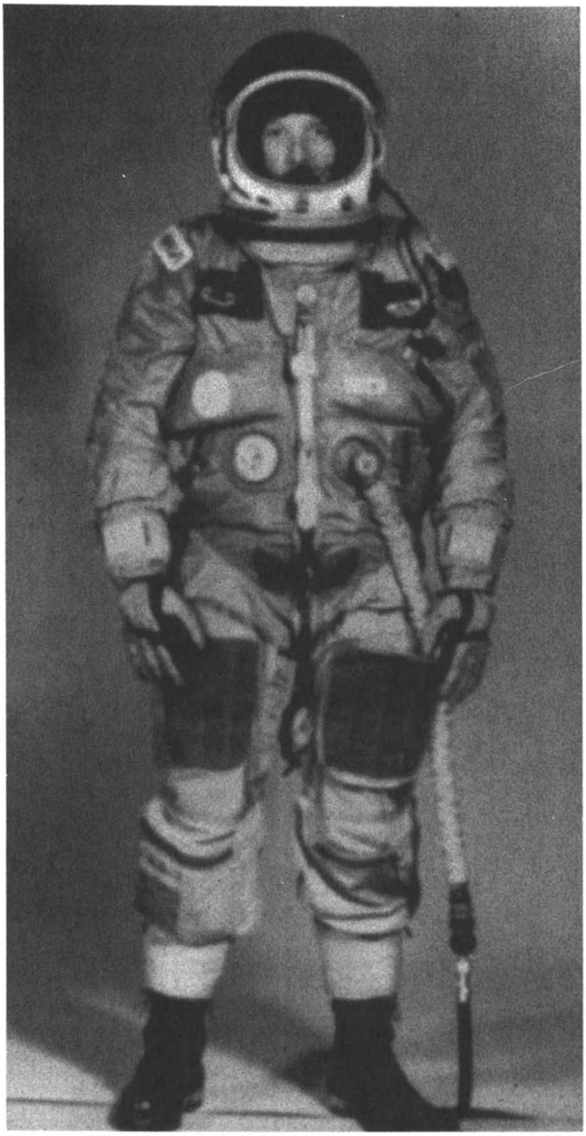

Figure 11. Astronaut's polybenzimidazole (PBI) lift-off suit

Downloaded by 89.163.34.136 on August 6, 2012 | http://pubs.acs.org
Publication Date: April 3, 1991 | doi: 10.1021/bk-1991-0457.ch001

Wool-blend fabrics containing Kevlar, Nomex, Inidex, or similar fibers have been shown to be suitable for use in firefighters' uniforms and other forms of protective clothing, and typify the use of combinations of diverse types of fibers to produce materials with technological advantages. The production of apparel and other textile products with improved thermal comfort and insulation has progressed from traditional concepts utilizing layers of fabrics to trap air as an insulator to more hi-tech concepts and approaches. Over the past twenty years, a variety of hollow synthetic fibers have been developed (18) that effectively increase the amount of trapped air in the fibrous assembly. These are typified by Dupont's Holofil polyester fibers that reduce convective heat loss and by 3M's Thinsulate, a blend of 65% polypropylene microfibers and 35% polyester regular denier fibers. More recently, an ultrafine polyester fiber (Primaloft) has been produced that is a mixture of small and large diameter fibers and has properties comparable to that of natural down.

The next class of innovations in this area is based on membrane-laminated or coated fabrics that vary from nonporous to microporous and are permeable to air and water vapor, but impermeable to liquid water. The introduction of Gortex in the late 1970's, a microporous polytetrafluoroethylene membrane that can be laminated to fabrics, was followed by several commercial fabrics with breathable/waterproof characteristics. The third and newest class of fibrous materials for thermal comfort are based on the ability of the modified fiber to reversibly absorb and release heat under diverse environmental conditions. The principles and applications for these materials have been recently reviewed (Vigo, T. L. and Bruno, J. S. in High Performance Fibers; Preston, J. and Lewin, M., Eds.; Marcel Dekker, New York, in press). Physical incorporation and/or chemical binding of phase change compounds or polymers (such as eicosane, neopentyl glycol and polyethylene glycols of varying molecular weight) to almost any type of fiber or fabric construction produce this thermal adaptability in the textile product.

Two fundamental trends that are receiving much more attention in Europe and the Pacific Rim than in the continental United States are:

(a) the development of textile products with multifunctional properties by a single process and

(b) modification of fiber and fabric surfaces by high energy techniques such as plasma, lasers and glow discharge.

On a practical as well as fundamental level, these advances are already producing textiles with enhanced properties not available by conventional techniques. Continuing emphasis in these areas will lead to new high-tech textiles for a variety of applications.

The International Wool Secretariat was successful in applying shrinkproofing polymers to wool and in modifying wool to produce flame-retardancy and repellency to oil, water, acid and gasoline by a single-bath application. This laid the foundation for later work in which a variety of silicon polymers were applied to different types of fabrics and fibers to impart several functional properties:

improved hand, elasticity, dimensional stability, water repellency and reduced pilling (19). This was followed by a more extensive approach to produce fabrics with multifunctional properties by a single process: insolubilization of polyethylene glycols by their reaction with a resin and subsequent curing under mild conditions. The work in this area has been reviewed (Vigo, T. L. and Bruno, J. S. in High Performance Fibers; Preston, J. and Lewin, M., Eds.; Marcel Dekker, New York, in press), and the applicability of this process to all natural and synthetic fiber types/blends/ fabric constructions was demonstrated to simultaneously improve the following properties: thermal adaptability, oily soil release, tearing or bursting strength, flex and flat abrasion, antistatic, water absorption, lint and particle loss, wind resistance, pilling, odor retention and resiliency. Needless to say, the use of facile in situ or related types of polymerization to impart multifunctional characteristics to textiles is in its infancy, and more sophisticated and targeted approaches and strategies are likely to evolve.

Another area that was initially investigated in the United States, but is now being vigorously pursued in Japan and Western Europe, is the modification of fiber and fabric surfaces by high energy sources such as lasers, plasma and glow discharge sources. Research studies conducted at the USDA Western Regional Research Laboratory in the early 1970's (20) demonstrated that the use of cold plasma was effective in shrinkproofing wool by surface modification. Since that time, there has been a fairly intense effort outside the U.S. to modify fiber and fabric surfaces by these techniques to improve adhesion and bonding characteristics between dissimilar surfaces and/or to improve such properties as dyeability, wettability and dimensional stability. The investigations of Professor Schollmeyer in West Germany are typical of current efforts in this field. For example, when synthetic fibers are irradiated by pulsed ultraviolet (excimer) lasers, "dissipative surfaces" are formed that improve adhesion, wettability, adsorption and other fiber surface properties (21). Such surface modifications allow for the formation of new types of fibrous composites, protective clothing and other multi-material textile products for existing and new applications.

HIGH-TECH textiles thus may be considered both an evolution (of existing and novel structures and fundamental concepts) and a revolution (combination of science and technologies from diverse and allied fields) to produce fibrous substrates that improve the quality and richness of life.

Literature Cited

1. Textile World, 1989 Statistics, 4170 Ashford Dunwoody Road, Suite 420, Atlanta, GA 30319.
2. Carpet and Rug Institute, P. O. Box 2048, Dalton, GA 30722.
3. American Textile Manufacturing Institute, Marketing Dept., 1801 K St., N. W., Suite 900, Washington, D. C. 20036
4. American Textiles International, Marketing Statistics, 2100 Powers Ferry Road, Atlanta, GA 30339
5. Fortune May 22, 1989, p.93.
6. American Textiles International March, 1987, 102-104.

Downloaded by 89.163.34.136 on August 6, 2012 | http://pubs.acs.org
Publication Date: April 3, 1991 | doi: 10.1021/bk-1991-0457.ch001

7. Intersept Antimicrobial, Product Bulletin 101, Interface Research Corp., 100 Chastain Center Blvd., Suite 165, Kennesaw, GA. 30144.
8. Silverman, B.; Henn, A. R., EMC Technology 1990, Sept.-Oct.
9. Turbak, A. F., The World and I January, 1987, 210-227.
10. Kwolek, S. L. U. S. Patents 3 600 350, 1971; 3 617 542, 1972; and 3 819 587, 1974.
11. Papkov, S.; Kulichiklin, V. G.; Kalmykova, V. D.; Malkin, A. Y., J. Poly. Sci., Poly. Phys. Ed. 1974, 12, 1753-1770.
12. Morgan, P. W.; Kwolek, S. L., Macromol. 1975, 8, 104-111.
13. Kwolek, S. L.; Morgan, P. W.; Schafgen, J. R.; Gulrich, L. W., Macromol. 1977, 10 (6), 1390-1396.
14. Blair, T. I.; Morgan, P. W.; Killian, F. L., Macromol. 1977, 10 (6), 1396-1400.
15. Meihuizen, C. E.; Pennings, A. J.; Zwijnenburg, A. U. S. Patent 4 137 394, 1976.
16. Thornel Carbon Fibers, Technical Bulletin, Amoco Performance Products, Inc., Ridgefield, CT, Feb. 1989.
17. Hybrinet Bioreactors for Cell Culture, Technical Bulletin, Kinetek Systems, 11802 Borman Drive, St. Louis, MO. 19894.
18. Anon., Outside Business May, 1989, 37-39.
19. Hardt, P., Textilveredlung 1984, 19 (5), 143-146.
20. Pavlath, A. E.; Slater, R. F., Appl. Poly. Symp. 18, Pt. 2 1971, 1317-1324.
21. Bahmers, T.; Schollmeyer, E., Angew. Makrmol. Chem. 1987, 151, 19-38.

RECEIVED October 23, 1990

Downloaded by 89.163.34.136 on August 6, 2012 | http://pubs.acs.org
Publication Date: April 3, 1991 | doi: 10.1021/bk-1991-0457.ch001

Downloaded by PENNSYLVANIA STATE UNIV on August 6, 2012 | http://pubs.acs.org
Publication Date: April 3, 1991 | doi: 10.1021/bk-1991-0457.ch002

Chapter 2

Analysis and Modeling of Three-Dimensional Textile Structural Composites

Joon-Hyung Byun, Guang-Wu Du, and Tsu-Wei Chou

Center for Composite Materials and Department of Mechanical Engineering, University of Delaware, Newark, DE 19716

The fabric geometric model based on a stiffness averaging method is utilized to analytically characterize two-step braided composites. The fiber architecture of the braided preform is investigated by identifying the geometric and braiding parameters which include the linear density ratio between axial and braider yarns, the pitch length of braider yarns, as well as the aspect ratios of axial and braider yarns. Parametric studies show a wide range of variability in the elastic constants of the composites. Results of the elastic properties are presented in the form of performance maps.

The recent development of textile manufacturing technology has expanded the application of composites in various areas. Among many fabric structures, three-dimensional(3-D) braided fabrics attract much interest due to their improvement in damage tolerance as well as capability of direct formation of complex shapes. Compared to other 3-D braiding processes, 2-step braiding has a relatively simple carrier motion and provides a large number of axial yarns for efficient reinforcement. Figure 1 shows the yarn movements in the 2-step braiding process for manufacturing a rectangular bar. In the first step, the braider yarns on the outside of the preform move diagonally while axial yarns move longitudinally (into the paper). In the second step, the braider yarns move along the other diagonal direction. This sequence is repeated to produce the desired preform shape.

In order to fully utilize the potential of textile composites, it is necessary to control the 3-D orientation of the reinforcing fibers. Correspondingly, the prediction

0097–6156/91/0457–0022$06.00/0

Downloaded by PENNSYLVANIA STATE UNIV on August 6, 2012 | http://pubs.acs.org
Publication Date: April 3, 1991 | doi: 10.1021/bk-1991-0457.ch002

of mechanical properties has an important part in designing the 3-D textile composites. Ma,Yang, and Chou predicted elastic moduli of 3-D braided composites based on an energy method(1) and on the extension of lamination theory to 3-D structures(2). Whitney and Chou(3) demonstrated the succesful application of the lamination theory to the prediction of elastic moduli of angle-interlocked fabric composites. The prediction of tensile strength of 3-D braided composites were made by Ko and Pastore(4) using the netting analysis. The combination of textile engineering methodology and a modified lamination theory was applied to predict the stiffness and stress-strain behavior of 3-D braided composites(5).

A different model to predict thermomechanical properties of 3-D textile composites was proposed by Hatta and Mura(6) based on the Eshelby's equivalent inclusion method. More attention was paid to achieve isotropic properties of 3-D composites by changing fiber orientation distribution. Recently, Du et al.(Du,G-W., Chou,T-W. and Popper,P. J. Mat. Sci., submitted for publication) have developed a model to relate the process variables and braiding parameters with the structural characteristics such as braider yarn orientation, fiber volume fraction and jamming criterion of braider yarns.

Since the 3-D braided composites usually have thick sections, the properties in the thickness direction as well as in-plane direction need to be determined for a tailored design. In this paper, elastic constants of 3-D braided composites are predicted based on the structural geometry and volume averaging of the stiffness of individual fiber bundles with different orientations.

Geometric Relations

The geometric model for 2-step braided composites is based on the cross-section of axial yarns after resin impregnation. Figure 2 shows the distribution of center, side and corner axial yarns with braider yarns interlocking the axial yarns. Ten braider yarns are incorporated into this specific sample.

The dimensions of each yarns (unit = mm) are obtained in terms of yarn properties and processing parameters:

$$S_{ac} = \frac{1}{3}\sqrt{\frac{D_{ac}}{\rho_a \gamma_a \sin\theta}} \qquad (1)$$

$$S_{am} = \frac{D_{as} - D_{ac}/2}{18\ S_{ac}\ \rho_a \gamma_a \cos(\theta/2)} \qquad (2)$$

Downloaded by PENNSYLVANIA STATE UNIV on August 6, 2012 | http://pubs.acs.org
Publication Date: April 3, 1991 | doi: 10.1021/bk-1991-0457.ch002

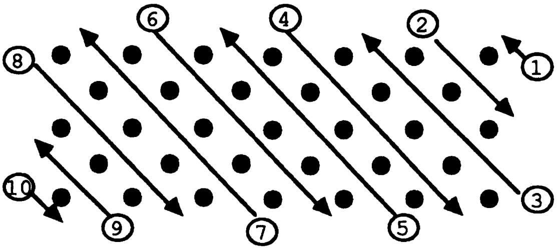
⑥
④
②
⑧
①
③
⑩
⑨
⑦
⑤

(a) Step 1

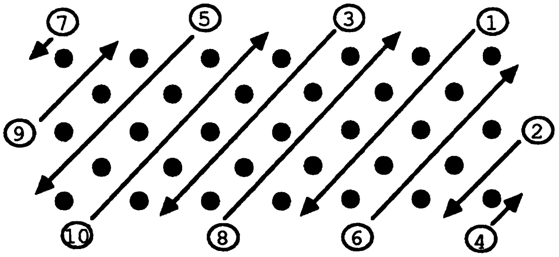
⑦
⑤
③
①
⑨
②
⑩
⑧
⑥
④

(b) Step 2

Figure 1: The 2-step braiding process for 7 column and 5 layers rectangular beam.

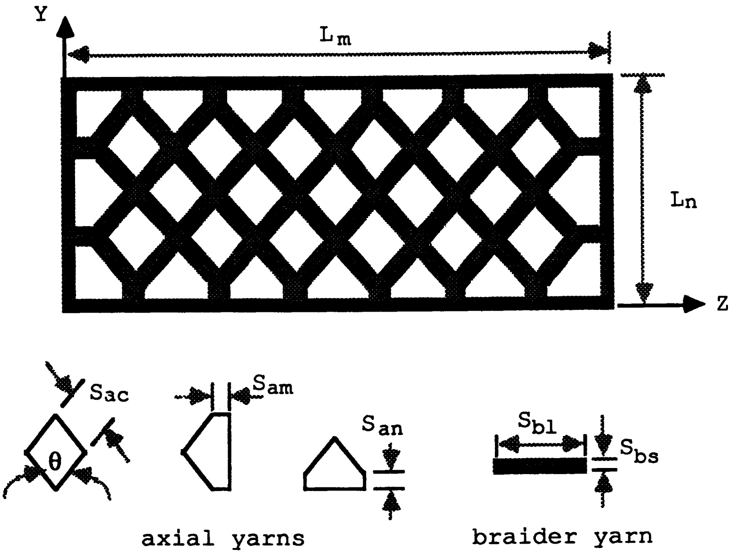
Y
Lm
Ln
Z
Sac
θ
Sam
San
Sbl
Sbs
axial yarns
braider yarn

Figure 2: Cross-section of 2-step braided composite.

$$S_{an} = \frac{D_{as} - D_{ac}/2}{18\ S_{ac}\rho_a\ \gamma_a \sin(\theta/2)} \tag{3}$$

$$S_{bs} = \frac{1}{3}\sqrt{\frac{D_b\ f_b}{\rho_b\,\gamma_b}} \tag{4}$$

where D_{ac}, D_{as}, D_b = linear density of center axial yarns, side axial yarns, and braider yarns, respectively (denier); ρ_a, ρ_b = density of axial and braider yarn, respectively (kg/m^3); γ_a, γ_b = fiber packing fraction of axial and braider yarn, respectively; and f_b = aspect ratio of braider yarn ($f_b = S_{bs}/S_{bl}$).

Since the cross-sections of axial yarns are different depending on their locations in the center and on the corner or side of the preform, the unit cell is defined as the whole cross-sectional area with a pitch length, H. The total volume of the unit cell is:

$$V_t = L_m\, L_n\, H \tag{5}$$

where L_m and L_n are given for the preform of m-column and n-layer axial yarns,

$$L_m = (m-1)\left(2S_{ac}\sin(\theta/2) + \frac{S_{bs}}{\cos(\theta/2)}\right) + 2(S_{bs}+S_{am}) \tag{6}$$

$$L_n = (n-1)\left(S_{ac}\cos(\theta/2) + \frac{S_{bs}}{2\sin(\theta/2)}\right) + 2(S_{bs}+S_{an}) \tag{7}$$

In the specific sample shown in Figure 2, m=7 and n=5.

In order to determine the volume of axial yarns in a unit cell, three different cross-sections of axial yarns are identified: diamond shape and two rectangular shapes. The volume of axial yarns (V_a) is

$$V_a = H[S_{ac}^2 \sin\theta(n-1)(m-1) + 4mS_{ac}S_{an}\sin(\theta/2) + 2(n-1)S_{ac}S_{am}\cos(\theta/2)] \tag{8}$$

Since the reinforcement directions are different between the surface and the inside of a braided composite, the volume calculations for these two cases are carried out separately. First, braider orientation angle (ϕ) is determined in order to calculate the length of inclined braider yarns. Since all braider yarns traverse the same pitch length during each step, the traveling length at the corner is shorter than the length at the center. The braider yarn orientation at the corner is therefore less

Downloaded by PENNSYLVANIA STATE UNIV on August 6, 2012 | http://pubs.acs.org
Publication Date: April 3, 1991 | doi: 10.1021/bk-1991-0457.ch002

Downloaded by PENNSYLVANIA STATE UNIV on August 6, 2012 | http://pubs.acs.org
Publication Date: April 3, 1991 | doi: 10.1021/bk-1991-0457.ch002

than that of the center. In order to deal with difficulties of including all the variations in the modeling, the maximum traveling length of braider yarns is considered. Figure 3 shows the configuration of six braider yarns which consist the cross-section of the preform. Each braider yarn has the same maximum traveling length. Since the configuration of yarn segment(a) is the same as others in terms of length and inclination angle, it represents all the other inclined braider yarns within a unit cell.

Using trigonometric relations in Figure 4, in which the yarn segment(a) is shown schematically:

$$\phi = \tan^{-1}\left(\frac{2L_c}{H}\right) \qquad (9)$$

where L_c is the length of braider yarn projected on the y-z plane;

$$L_c = (n-1)\left(S_{ac} + \frac{S_{bs}}{\sin\theta}\right) + 2S_{an} \qquad (10)$$

Thus,the length of inclined braider yarn(L_b) is

$$L_b = \frac{L_c}{\sin\phi} = \frac{H/2}{\cos\phi} \qquad (11)$$

Since (n+1) braider yarns are incorporated into the unit cell as shown in Figure 3, the total length is $2L_b(n+1)$. The volume of inclined braider yarns V_{bi} located inside of the unit cell is

$$V_{bi} = S_{bs}\, S_{bl}\, L_b\, 2(n+1)$$
$$= \frac{2(n+1)S_{bs}^2}{f_b \sin\phi}\left((n-1)\left(S_{ac}+\frac{S_{bs}}{\sin\theta}\right)+2S_{an}\right) \qquad (12)$$

The volume of top and bottom surfaces(V_{bt}) and that of side surface(V_{bs}) can be easily obtained as follows;

$$V_{bt} = \frac{4S_{bs}^2}{f_b}\,[mS_{ac}\sin(\theta/2)] \qquad (13)$$

$$V_{bs} = \frac{2S_{bs}^2}{f_b}\,[(n-1)S_{ac}\cos(\theta/2) + 2S_{an}] \qquad (14)$$

Relating the Equations 5-8 and 12-14, the yarn volume fractions of individual reinforcing direction can be obtained.

Downloaded by PENNSYLVANIA STATE UNIV on August 6, 2012 | http://pubs.acs.org
Publication Date: April 3, 1991 | doi: 10.1021/bk-1991-0457.ch002

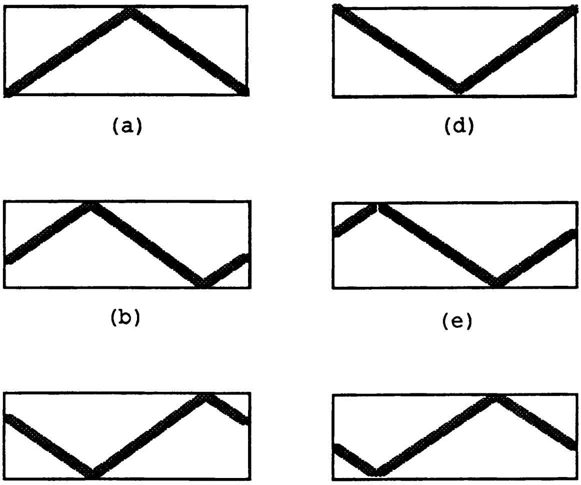
(a) (d)

(b) (e)

(c) (f)

Figure 3: Configurations of six braider yarns traveling the same pitch length (into the paper direction).

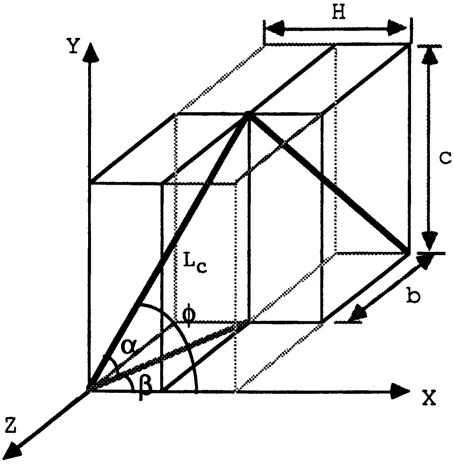

Figure 4: Inclined braider yarn within a unit cell.

Downloaded by PENNSYLVANIA STATE UNIV on August 6, 2012 | http://pubs.acs.org
Publication Date: April 3, 1991 | doi: 10.1021/bk-1991-0457.ch002

Compliance of Spatially Oriented Yarns

In the modeling of three-dimensionally reinforced composites, the yarns can be assumed to be a unidirectional composite rod as shown in Figure 5. The components of stiffness matrix of the rod depend on the specific orientation ϕ (which is the braider yarn angle). The direction cosines between the xyz-coordinate system and the 123-coordinate system can be established by setting the 2-axis perpendicular to the y-axis:

$$\begin{array}{lll} l_{1x}=\cos\alpha\cos\beta, & l_{2x}=-\sin\beta, & l_{3x}=\sin\alpha\cos\beta, \\ l_{1y}=\sin\alpha, & l_{2y}=0, & l_{3y}=-\cos\alpha, \\ l_{1z}=\cos\alpha\sin\beta, & l_{2z}=\cos\beta, & l_{3z}=\sin\alpha\sin\beta \end{array} \tag{15}$$

Referring to Figure 4, it is possible to relate the angles ϕ, α and β:

$$\tan\alpha = \frac{\tan\phi}{\sqrt{R^2(1+\tan^2\phi) + 1}} \tag{16}$$

$$\tan\beta = \frac{R\tan\phi}{\sqrt{R^2 + 1}} \tag{17}$$

where $R=c/b$, $b=[L_m - 2S_{bs} - 2S_{ac}\sin(\theta/2)]/2$ and $c=L_n$.

Thus, the direction cosines of spatially oriented yarns are expressed in terms of braider orientation and specimen geometry. Using these direction cosines, the compliance matrix (S) of the unidirectional composite rod referring to the 123-coordinate system can be transformed to that referring to the xyz-coordinate system:

$$S'_{ijmn} = l_{pi}\, l_{qj}\, l_{rm}\, l_{sn}\, S_{pqrs} \qquad (i,j,m,n,p,q,r,s = 1,2,3) \tag{18}$$

From symmetry conditions and using contracted notation, Equation 18 is reduced to a simple form:

$$S'_{ij}=q_{mi}\, q_{nj}\, S_{mn} \qquad (i,j,m,n = 1\text{-}6) \tag{19}$$

where q_{ij} denotes the element belonging to the i-th row and j-th column of the transformation matrix (7). For a unidirectional composites of transversely isotropic, the compliance matrix has 5 independent constants:

$$\begin{pmatrix} 1/E_{11} & -\nu_{21}/E_{22} & -\nu_{21}/E_{22} & 0 & 0 & 0 \\ -\nu_{12}/E_{11} & 1/E_{22} & -\nu_{32}/E_{22} & 0 & 0 & 0 \\ -\nu_{12}/E_{11} & -\nu_{23}/E_{22} & 1/E_{22} & 0 & 0 & 0 \\ 0 & 0 & 0 & 1/G_{23} & 0 & 0 \\ 0 & 0 & 0 & 0 & 1/G_{12} & 0 \\ 0 & 0 & 0 & 0 & 0 & 1/G_{12} \end{pmatrix} \quad (20)$$

where E_{11} and E_{22} are the elastic moduli for longitudinal and transverse tensions respectively, G's and ν's are respectively, shear moduli and Poisson's ratios.

Numerical Calculations

Given the yarn properties, processing parameters, and fiber and matrix properties, the effective three-dimensional elastic properties can be calculated based on the volume average of stiffness.

In order to calculate the compliance matrix of unidirectional composites, it is necessary to know the elastic moduli of the constituents. In the absence of measurements of some of the required values, the equations in (8) are used. These expressions provide the elastic constants of unidirectional composites in terms of the corresponding properties of their contituents. Then, the compliance matrix in Equation 20 is transformed based on Equation 19 according to the reinforcing directions of yarns. Depending on the angles α and β, there are four different reinforcing directions in this example (Figure 2) ,namely, axial yarns($\alpha=0,\beta=0$), braider yarns on top and bottom surfaces($\alpha=0,\beta=\phi$), braider yarns on side surfaces ($\alpha=\phi,\beta=0$) and inclined braider yarns($\alpha=f(\phi),\beta=g(\phi)$). In order to determine the effective stiffness matrix of composite, the compliance matrices are inverted into stiffness matrices, and then averaged over the volume:

$$[C]^c = \sum_{n=1}^{4} [C]_n \frac{V_n}{V_t} \quad (21)$$

where $[C]_n$ and V_n/V_t are the stiffness matrices and yarn volume fractions for an individual reiforcing direction, respectively. Finally, the stiffness matrix of the composite is inverted into the compliance matrix $[S]^c$. The engineering elastic constants are then obtained from the compliance matrix. For example, $E_{xx} = 1/S_{11}^c$, $E_{yy} = 1/S_{22}^c$ and $\nu_{xy} = -S_{12}^c/S_{22}^c$, etc.

Downloaded by PENNSYLVANIA STATE UNIV on August 6, 2012 | http://pubs.acs.org
Publication Date: April 3, 1991 | doi: 10.1021/bk-1991-0457.ch002

Downloaded by PENNSYLVANIA STATE UNIV on August 6, 2012 | http://pubs.acs.org
Publication Date: April 3, 1991 | doi: 10.1021/bk-1991-0457.ch002

Results and Discussion

Numerical calculations for prediction of engineering constants have been performed in the case of a 2-step braided Kevlar/epoxy composites. Kevlar 29 and 49 were used for the axial and braider yarns,respectively. The epoxy resin was a mixture of Epon resin 9405 and Epon curing agent 9470. Table I gives the fibers and matrix properties utilized in the analysis.

Table I. Fiber and Matrix Properties Utilized in the Prediction

	E_L(GPa)	E_T(GPa)	G_{LT}(GPa)	ν
Kevlar 29	63	4.2	2.9	0.32
Kevlar 49	131	4.2	2.9	0.32
Epon 9405	4.0	4.0	1.46	0.37

The braided preform was consolidated by resin transfer molding process. The cross-section of the braided composite was in a rectangular shape of 15.5 mm in width and 7 mm in thickness. The processing and geometric parameters were determined as shown in Table II.

Table II. Summary of Measured Parameters

Linear density of axial yarn	30000 (denier)
Linear density of braider yarn	2280 (denier)
Density of axial and braider yarns	1.44 (g/cm^3)
Braider pitch length	5.0 (mm)
Aspect ratio of axial yarn	0.76
Aspect ratio of braider yarn	0.05
Packing fraction of axial and braider yarns	0.78

Based on the input data summarized in Table I and II, model prediction of engineering constants for 2-step braided composite are given in Table III, with comparison of experimental results. The discrepancies between the model prediction and experimental results are quite large in shear modulus and Poisson's ratio. Part of the reason would be that certain properties of Kevlar fibers were not available and thus, assumed values were used in this prediction. Another possibility is the great difficulty in accurately measuring the shear response of 3-D composites with current test methods due to the lack of reproduction and scattering data.

Figures 6 and 7 show the variation of selected Young's moduli and shear moduli as functions of process parameters, respectively. The aspect ratio of axial yarn was defined as tan(θ), where θ is the inner angle of axial yarn(Figure 2). The maximum volume fraction of axial yarn was obtained when the angle was around 90 degrees, which also gave the maximum E_{xx} and G_{yz}.

Downloaded by PENNSYLVANIA STATE UNIV on August 6, 2012 | http://pubs.acs.org
Publication Date: April 3, 1991 | doi: 10.1021/bk-1991-0457.ch002

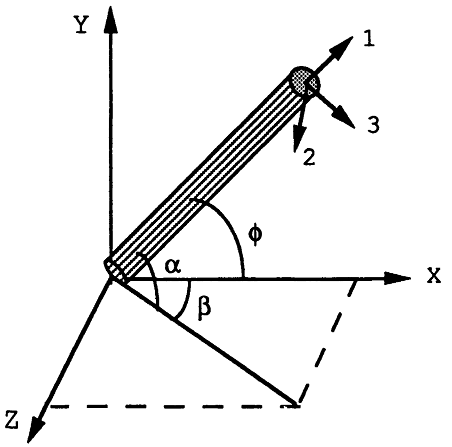

Figure 5: The spatially oriented composite cylinder.

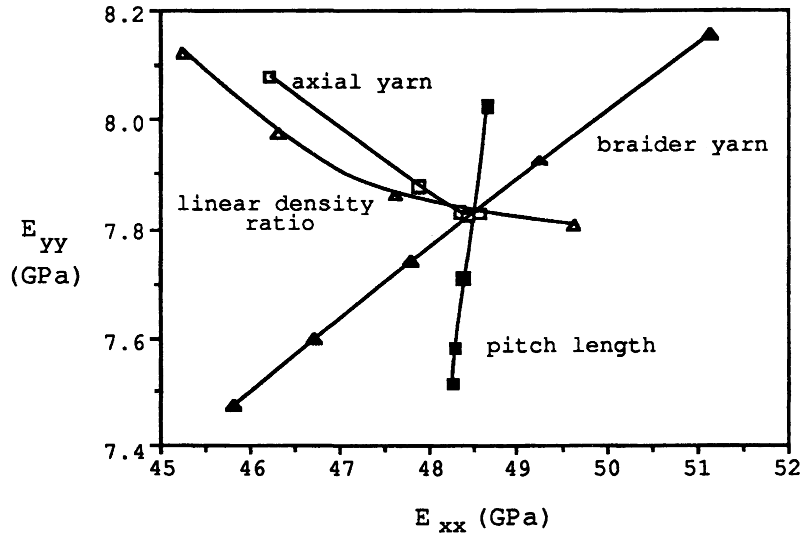

Figure 6: Performance map of Young's modulus as a function of process parameters.(□ aspect ratio of axial yarn,0.2-1, increment:0.2; ▲ aspect ratio of braider yarn,0.1-0.02, decrement:0.02; △ linear density ratio of braider/axial yarn,0.25-0.05, decrement:0.05; ■ pitch length,10-4, increment;2)

Downloaded by PENNSYLVANIA STATE UNIV on August 6, 2012 | http://pubs.acs.org
Publication Date: April 3, 1991 | doi: 10.1021/bk-1991-0457.ch002

Table III. Comparison of Model Prediction and Experimental Results

	Model	Experiment
E_{xx} (GPa)	48.4	52.4
E_{yy} (GPa)	7.83	
E_{zz} (GPa)	8.05	
G_{xy} (GPa)	2.58	1.45
G_{yz} (GPa)	2.68	
G_{xz} (GPa)	2.59	
ν_{xy}	0.36	0.53
ν_{yz}	0.32	
ν_{xz}	0.34	

SOURCE: Data for the Experiment column comes from ref. 9.

Equations 1-4 show that the yarn cross-sections become larger as the linear density of the yarn increases. Increasing the linear density ratio of axial to braider yarn results in an increase in axial yarn volume fraction while the braider yarn volume fraction becomes smaller. Since the stiffness in the longitudinal and transverse directions of the 2-step braided composite are primarily due to the contribution of the axial yarns and braider yarns, respectively, increasing the volume fraction of axial yarn yields increased E_{xx} as shown in Figure 6. However, there are corresponding decreases in E_{yy} and G_{yz} because the volume fraction of braider yarns becomes smaller.

Increasing the aspect ratio of braider yarns results in an increase in their thickness, which in turn causes larger volume of matrix pocket. Since the total fiber volume fraction is reduced due to the increased volume of the composite, all the components of Young's moduli and shear moduli are reduced as the aspect ratio of braider yarns become bigger. Increasing the pitch length gives smaller volume fraction and smaller orientation angle of braider yarn. Thus, E_{yy} and G_{yz} decrease as the pitch length of the braider yarn increases.

Conclusions

The model prediction of engineering constants based on volume averaging of stiffness was performed for 2-step braided Kevlar/epoxy composite material. Geometry of yarns was determined using yarn properties and processing parameters. The key parameters, such as aspect ratios and linear density of axial yarns and braider yarns, and braider pitch length were identified to determine how the structural varialbles affects the predicted elastic constants. Some discrepancies exist between the predicted engineering elastic constants and experimental results. Refined experimental techniques are needed for testing 3-D composites.

Downloaded by PENNSYLVANIA STATE UNIV on August 6, 2012 | http://pubs.acs.org
Publication Date: April 3, 1991 | doi: 10.1021/bk-1991-0457.ch002

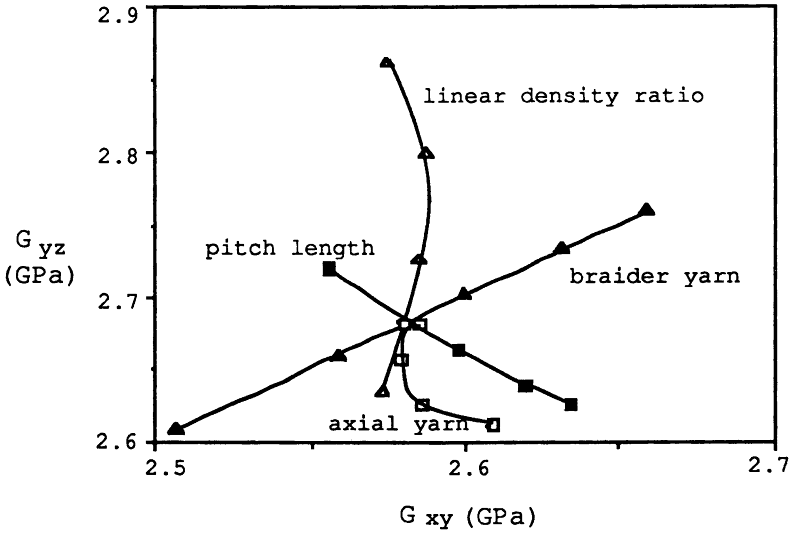

Figure 7: Performance map of shear modulus as a function of process parameters.(□ aspect ratio of axial yarn,1-0.2, decrement:0.2; ▲ aspect ratio of braider yarn,0.02-0.1, increment:0.02; △ linear density ratio of braider/axial yarn,0.25-0.05, decrement:0.05; ■ pitch length,4-10, increment;2)

Literature Cited

1. Ma, C-L.; Yang, J-M.; Chou, T-W. Composite Materials: Testing and Design, ASTM STP 893 ;Philadelphia, Pa, 1986; p 405.
2. Yang, J-M.; Ma, C-L.; Chou, T-W. J. Comp. Mat. 1986, 20, 472-84.
3. Whitney, T.J.; Chou, T-W. J. Comp. Mat. 1989, 23, 890-911.
4. Ko, F.K.; Pastore, C.M Composite Materials: Testing and Design, ASTM STP 864; Philadelphia, Pa, 1985; p 428.
5. Ko, F.K. Textile Structural Composites; Pipes, R.B., Ed.; Elsevier: New York, 1989; Vol 3, Chapter 5.
6. Hatta, H.; Murayama, K. Proc. 4th ICCS, 1987-1988, p 408.
7. Lekhnitskii, S.G. Theory of Elasticity of an Anisotropic Elastic Body; Holden-Day, San Francisco, 1963; p 35.
8. Tsai, S.W.; Hahn, H.T. Introduction to Composite Materials; Technomic: Westport, 1980; Chapter 9.
9. Whitney, T.J. Master's thesis, University of Delaware, Delaware, 1989.

RECEIVED April 2, 1990

Downloaded by UNIV OF ARIZONA on August 6, 2012 | http://pubs.acs.org
Publication Date: April 3, 1991 | doi: 10.1021/bk-1991-0457.ch003

Chapter 3

Mechanics of Three-Dimensional Braiding

Basic Requirements for Process Automation

Wei Li[1], Mohamed Hammad, and Aly El-Shiekh

**College of Textiles and Mars Mission Research Center, North Carolina
State University, Raleigh, NC 27695–8301**

Three dimensional (3-D) braiding processes have been recognized for their outstanding advantages in fabricating integrated and near net-shape preforms for advanced composite materials. A real challenge, however, is the automation of the processes to produce uniform, repeatable and cost-effective products. In our 3-D Braiding Laboratory, two lab-scale machines have been automated and the efforts, principles, and limits are presented in this paper. Some basic engineering aspects for designing and automating these processes such as machine bed size, carrier requirement and design etc. are analyzed and discussed.

The advent in the 1970s of advanced composites which apply new high performance fibers as reinforcements was claimed the biggest technical revolution since the jet engine (1). For predetermined fiber and matrix materials with proper impregnation and curing conditions, the fiber geometry and volume fraction play dominant roles in determining the properties of composites and consequently their end use performance. To achieve desired fiber geometry and cost effective production techniques, textile processes are often used to produce preforms for composites. Among these, three dimensional (3-D) braiding has the capability of fabricating 3-D integrated structures, and also provides an easy method for forming complex structural shapes. This technique allows for the direct fabrication of the preforms into the nearly net shapes of the final products of the composites by manipulating the relative positions of the individual fiber tows in the braiding machine bed. These two distinct advantages of 3-D braiding technology have attracted much attention from various industries, and have made 3-D braided composites a very active and prominent branch of advanced composite materials.

---

[1] **Current address: BASF Fiber Company, Asheville, NC 28728**

0097–6156/91/0457–0034$06.00/0

Downloaded by UNIV OF ARIZONA on August 6, 2012 | http://pubs.acs.org
Publication Date: April 3, 1991 | doi: 10.1021/bk-1991-0457.ch003

Many 3-D braiding concepts have been proposed (2-8), and the exploration of new methods is still under way. Currently, there are mainly two groups of 3-D braiding techniques, namely the 4-step process (often referred to as Magnaweave, Cartisian or Row & column or braiding) and 2-step process (9). In the 4-step process, the braiding is accomplished with at least four distinct motions in each machine cycle, while the 2-step process involves two distinct motions within each machine cycle.

Equipment has been developed to achieve these braiding concepts. In the 4-step braiding process, each row and column consists of discrete eyelets or carrier blocks in the Bluck and Florentine patents (3,5). However, in the Maistre patent and the Atlantic Research machines (4,7), row motion is accomplished by shifting grooved tracks containing fiber carriers, and column motion consists of shifting the discrete fiber carriers. A prototype machine bed was constructed in 1983 by Florentine, which was a 21 row and 21 column square bed, and actuated by pneumatic cylinders through a switching control that alternately powered row and column cylinders (10). In Atlantic Research Corporation, a larger machine consisting of 64 slides with 194 slots per slide has been constructed (11). It is able to mount up to 12,222 fiber tows for the simplest 1x1 rectangular braid pattern. This machine employs 124 double action and 388 single action air cylinders. 962 pneumatic valves allow complete control of the fiber carrier motions.

The 2-step 3-D braiding process is quite new compared to the 4-step process. It was first introduced by Popper and McConnell in 1987 (8,12). Popper and McConnell (12) claim that this process is much easier to automate because it possesses fewer moving parts, simpler motion, and possibly no beating-up motion. Little progress in machine development concerning the 2-step process has been reported. Du et al (13) proposed a concept for automation of the 2-step braiding process. They suggested to use motorized carriers and a reformable track system. The motorized carrier consists of a small DC motor, a bobbin holder, contact brushes for power, and a micro-switch for on/off control. The track system guides the carriers with a T-slot and supplies power to carriers.

Structures of both the 4-step and 2-step braided preforms have been studied extensively (14,15). In this paper, the efforts to automate the 3-D braiding processes in our laboratory are reviewed, and some basic requirements for designing and automating these processes are analyzed and discussed.

Process Analysis and Automation

To demonstrate the feasibility of automating 3-D braiding processes, two lab scale machines, one for each process, have been constructed and automated using computer control.

The 4-step Process. The basic idea of this process is illustrated in Figure 1 which shows the braiding pattern for a rectangular slab, the simplest structural shape. The fiber tows are arranged in rows and columns to form the required shape, then additional tows are added to the outside of the array at alternating locations. Four steps of motion constitute one machine cycle which will braid the tows. First the rows and then the columns are moved both in alternating directions. These movements are then reversed to complete one machine cycle of the 4-step process. As these steps of motion continue, the tows move throughout the cross-section and are interlaced to form the structure. This is the simplest and most widely used braiding pattern. It is referred to as 1x1 pattern (11,16).

Aside from the 1x1, there are many other braiding patterns such as 1x3, 1x1x1/2F, etc, where the first number represents the number of spaces in a carrier track or row shift and the second number represents the number of spaces in a fiber carrier or column shift (11,16). The 1x1x1/2F pattern braids the same way as the 1x1 but including additionally about half the number of the total tows fixed in the structure. These different braiding patterns result in different fiber geometries. The cross-sectional shape of a braided structure is dependent on the machine-loading arrangement.

An analytical model of the 4-step 1x1 structure was established by the present authors (14). Figure 2 shows an idealized repeat unit inside the 1x1 structure which reflects the real yarn path and interlacing. Based on the repeat unit, structural parameters of the preform such as fiber orientation and volume fraction were predicted by relating them to the constituent yarn and machine operation conditions. The selected parameter reflecting the braiding operation is the preform pitch length, h, as shown in Figure 2. One pitch of preform is formed in one machine cycle. Figure 3 gives a basic relation between the fiber orientation and the normalized pitch length which is the pitch length normalized by the yarn diameter (h_d=h/d). Figure 4 shows the effect of the normalized pitch length on the yarn volume fraction of a 4-step 1x1 braid.

Figure 5 is a picture of the 4-step braiding machine in our lab. The machine bed consists of 12 slides with 16 slots in each slide, for a maximum of 164 braiding fiber tows. The braiding motions are actuated by pneumatic cylinders controlled by a microcomputer. Figure 6 demonstrates the controlling system which consists of a microcomputer, a control board interfaced to the computer, and solenoid air valves. According to the structure being braided, a corresponding program pre-written and stored in a floppy disc is loaded to the CPU of the computer. After receiving the defining parameters from the operator through the computer keyboard, the program runs continuously at the desired speed until a stop signal is received through the keyboard, or can automatically stop after a preassigned number of braiding cycles. The programs are written in combination of BASIC and Assembly languages. The Key or the working part of the program which controls the sequence and speed

Downloaded by UNIV OF ARIZONA on August 6, 2012 | http://pubs.acs.org
Publication Date: April 3, 1991 | doi: 10.1021/bk-1991-0457.ch003

Downloaded by UNIV OF ARIZONA on August 6, 2012 | http://pubs.acs.org
Publication Date: April 3, 1991 | doi: 10.1021/bk-1991-0457.ch003

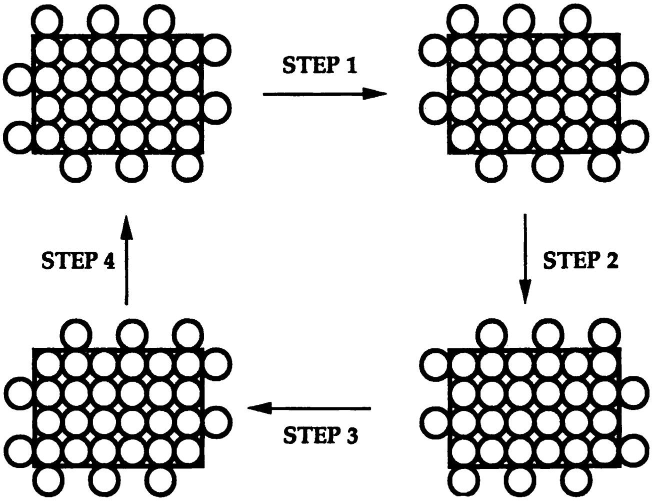

Fig.1 The 4-step 1x1 Braiding Pattern

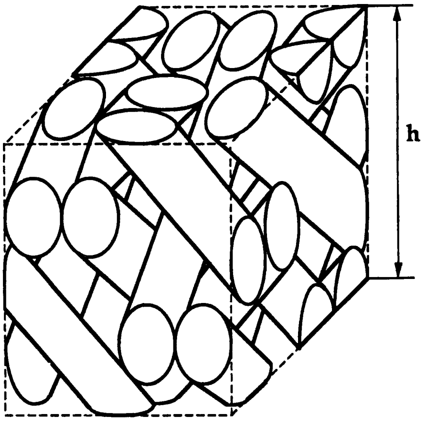

Fig.2 A Repeat Unit of The 4-step Braid [14]

Downloaded by UNIV OF ARIZONA on August 6, 2012 | http://pubs.acs.org
Publication Date: April 3, 1991 | doi: 10.1021/bk-1991-0457.ch003

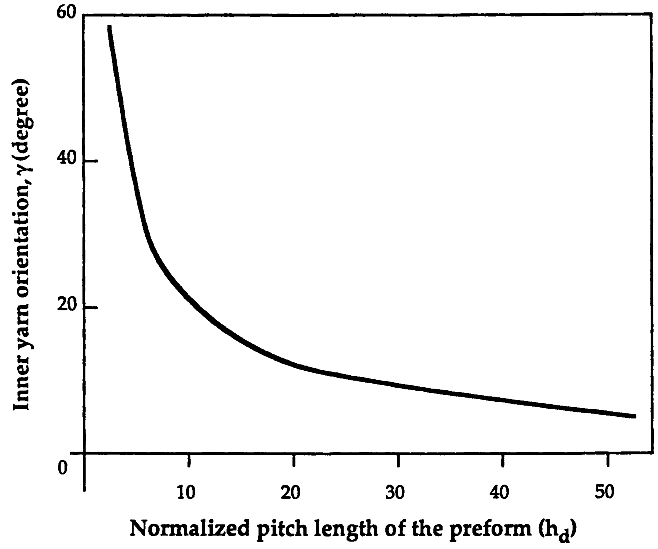

Fig.3 Yarn Orientation Angle of 4-step Braids [14]

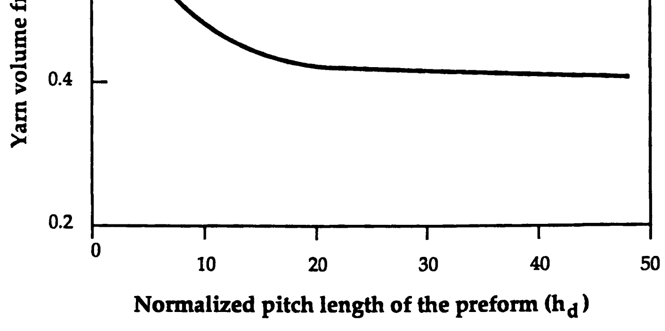

Fig.4 Yarn Volume Fraction of 4-step Braids

Downloaded by UNIV OF ARIZONA on August 6, 2012 | http://pubs.acs.org
Publication Date: April 3, 1991 | doi: 10.1021/bk-1991-0457.ch003

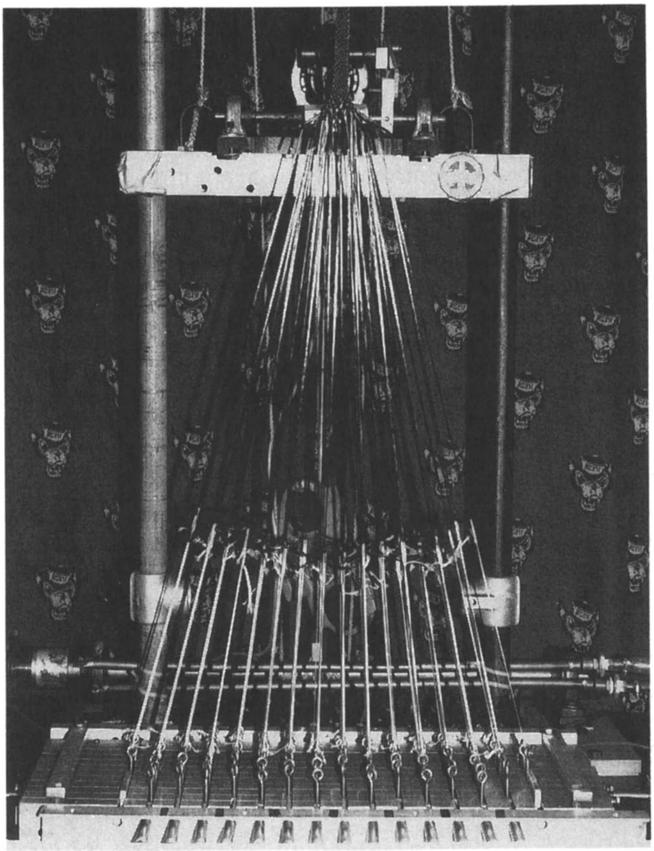

Fig.5 The 4-step Braiding Machine at NCSU

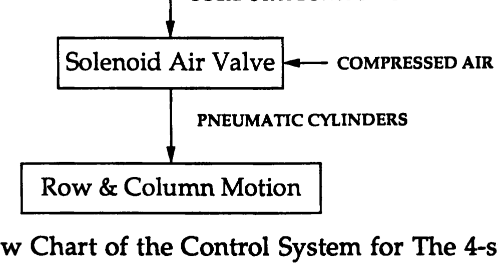
Microcomputer
DIGIT-ANALOG
Control Card
SOLID STATE SWITCHES
Solenoid Air Valve
COMPRESSED AIR
PNEUMATIC CYLINDERS
Row & Column Motion

Fig.6 A Flow Chart of the Control System for The 4-step Machine

of the braiding motions is written in Assembly language so that a precise control can be achieved, while the accessory parts are written in BASIC and then compiled. There are a number of parallel-connected solid state switches mounted on the control board. The running program generates a series of digital signals which are then converted to analog signals and sent to the control board continuously. Each solid state switch is used to control a group of solenoid air valves activating the air cylinders.

The fiber carrier used in this machine is very simple, and only carries a certain length of fiber tow with a short length of elastic material attached at the end to compensate for the rewinding requirement, which is a very critical problem associated with the 3-D braiding processes. This will be discussed in detail in a later part of this paper. A larger machine with a continuous yarn supply is currently under construction, and will be in operation soon.

The machine has a movable beating mechanism driven by two motors with separate controllers. The beating motion is accomplished by a combing device mounted on a crank, which oscillates in a 90 degree angle. Because fixed lengths of preforms are being made, the forming point of the preform moves in a top to bottom direction toward the machine bed during braiding, so that the beating position which determines the forming point has to move down during processing. The speed of this downward movement is equivalent to the take-off speed in other textile processes, and its ratio to the braiding speed determines the pitch length of the preforms. In our machine, one motor controls the oscillating speed of the crank or the beating frequency, and the second one controls the downward speed of the beating mechanism.

Downloaded by UNIV OF ARIZONA on August 6, 2012 | http://pubs.acs.org
Publication Date: April 3, 1991 | doi: 10.1021/bk-1991-0457.ch003

The 2-step Process. The 2-step structure is described by Figure 7 which shows the braiding pattern for a small T-beam. There are two principal sets of yarns arranged in the machine bed: axials and braiders. The axials are placed in the fabric-forming direction and remain approximately straight in the structure without any interlacing. The braiders move between the stationary axials in a special pattern, which cinches the axials and stabilizes the shape of the braid. The basic process consists of two steps of motion. In each one, the braiders are moved in the direction and to the extent indicated by the arrows in Figure 7. As the two machine steps are repeated, the braiders completely intercinch the structure after several cycles. One advantage of this process is that it can form almost any cross-sectional shape with relatively few technical restrictions.

An idealized model of the 2-step structure has also been established (15). Based on a repeat unit inside the structure as shown in Figure 8, structural parameters of the preform such as fiber orientation and volume fraction were related to the constituent yarns and machine operation. Figs.9 and 10, respectively, show the effect of the normalized pitch length on the braiding yarn orientation and yarn volume fraction of a 2-step braid.

Downloaded by UNIV OF ARIZONA on August 6, 2012 | http://pubs.acs.org
Publication Date: April 3, 1991 | doi: 10.1021/bk-1991-0457.ch003

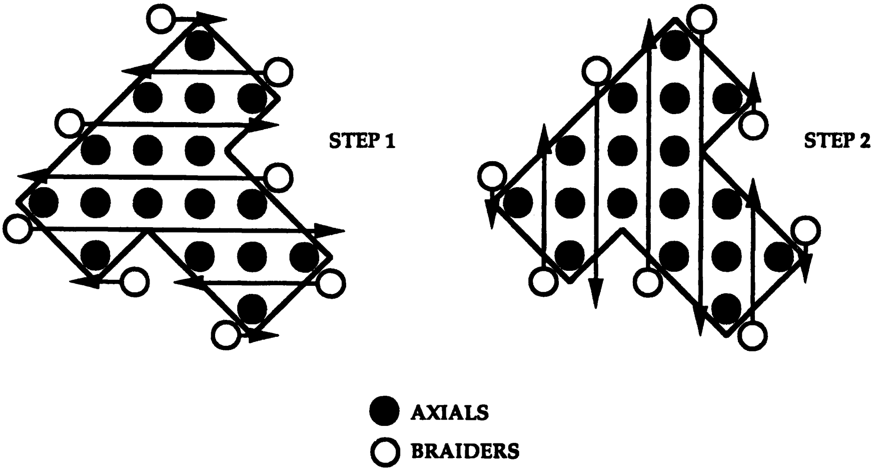

Fig.7 The Basic Braiding Pattern for The 2-step Process

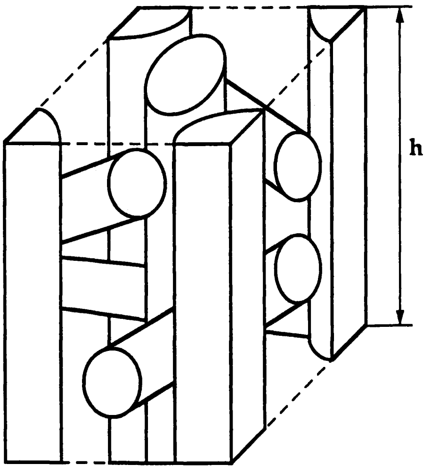

Fig.8 A Repeat Unit of The 2-step Braid [15]

Downloaded by UNIV OF ARIZONA on August 6, 2012 | http://pubs.acs.org
Publication Date: April 3, 1991 | doi: 10.1021/bk-1991-0457.ch003

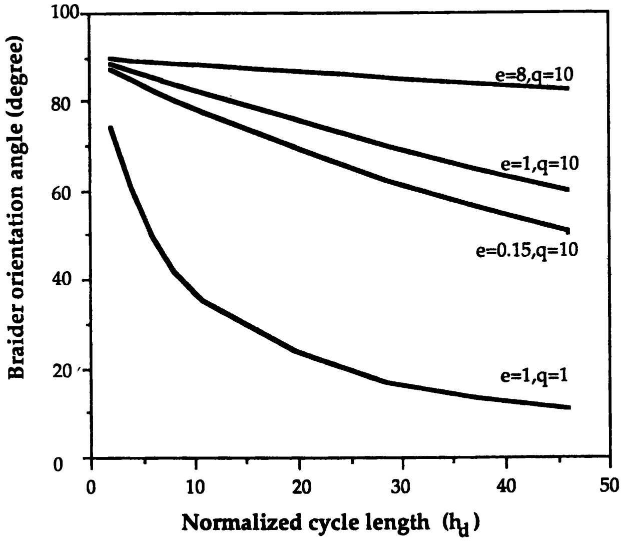

Fig.9 Braider Orientation Angle of 2-step Braids [15]

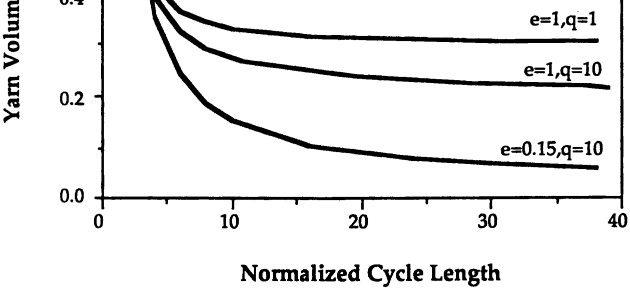

Fig.10 Yarn Volume Fraction of 2-step Braids [15]

Figure 11 shows a picture of the 2-step machine built in our lab. The machine bed is assembled by unit tiles of aluminum plates embedded with orthogonal T-grooves. The size of the unit tiles is 12"x12"x1". The distance between the grooves is 3". The standardization of the unit tiles makes it easy to expand the machine anytime if there is a need. The first version of this machine we built was composed of 4 unit tiles, and then was expanded to 9 unit tiles for the current version.

In a 2-step process, most fiber carriers move across the whole machine bed in one braiding motion. This feature makes the pneumatic actuation eventually impractical due to two reasons: very long air cylinders will be required for large machines; and both the machine length and width will be tripled if each side sticks out as much as the machine bed. Other driving methods have to be worked out to solve this problem.

In our machine, a timing gear-belt combination is applied to push the fiber carriers. The timing belts are reinforced with discrete aluminum sheets, so that they are "rigid" inside the grooves and become "flexible" outside. By this arrangement, the machine size is only a little larger than the machine bed. The timing gears are driven by stepping motors, so the pushing distance can be very precisely controlled.

There are eight stepping motors mounted on this lab scale machine. Four of these are used for pushing the carriers across the bed with one taking care of each side. Every motor together with a combination of a gear and a length of reinforced belt are mounted on an aluminum carriage forming a driving unit. The other four stepping motors transport these carriages to the preassigned positions during braiding. This arrangement enables that only eight motors are required to drive the machine no matter how large the machine. Therefore, the cost of the machine was largely reduced and as a result, the braiding speed was also reduced. It is worth applying this arrangement to a lab stage machine which is mainly concerned with demonstrating ideas rather than speed. For commercial machines, this arrangement could be altered to increase the speed by mounting one motor for each machine slot if this can be economically justified.

Figure 12 shows the flowchart of the controlling system which is composed of a computer terminal, an APPCOR IMC-8 controller, and stepping motors. The stepping motors are controlled by the APPCOR IMC-8 controller. This controller consists of a built-in microprocessor, an input/output card and eight axis cards. The microprocessor communicates with each axis card by means of a high-speed parallel bus. Once an axis card has been configured for a move, and instructed to start, it runs independently of the main processor which is then free to communicate with the input/output card or the other axis cards. The maximum pulse rate of the axis card is 25 khz. An IBM portable personal computer is connected to the controller through a RS232 port, and serves as a terminal. Programs are written as files by word processing software,

Downloaded by UNIV OF ARIZONA on August 6, 2012 | http://pubs.acs.org
Publication Date: April 3, 1991 | doi: 10.1021/bk-1991-0457.ch003

Downloaded by UNIV OF ARIZONA on August 6, 2012 | http://pubs.acs.org
Publication Date: April 3, 1991 | doi: 10.1021/bk-1991-0457.ch003

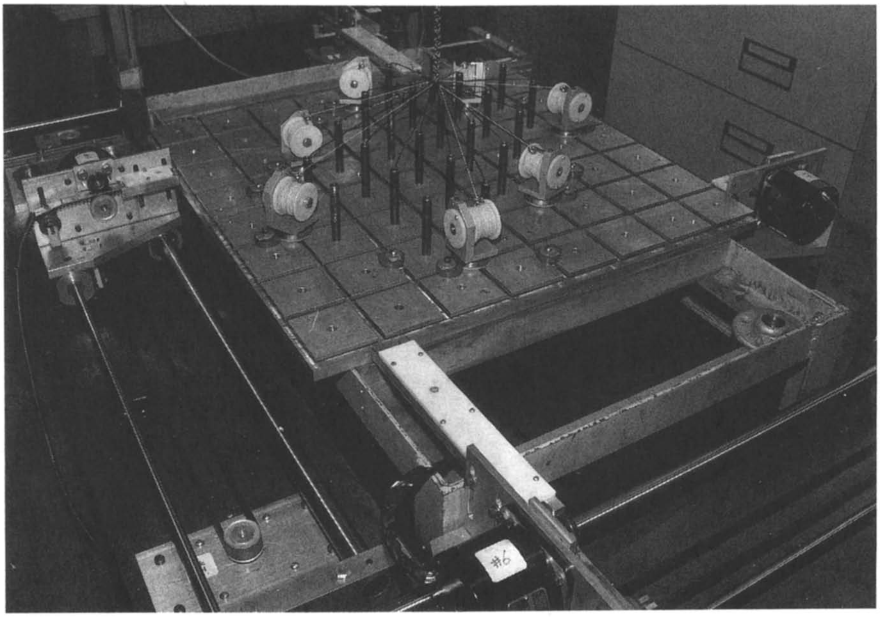

Fig.11 The 2-step Braiding Machine at NCSU

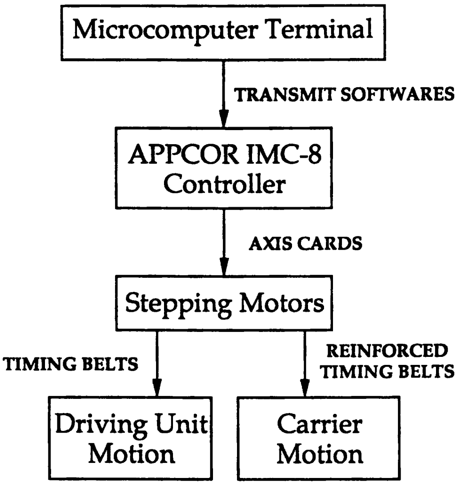
Microcomputer Terminal
TRANSMIT SOFTWARES
APPCOR IMC-8 Controller
AXIS CARDS
Stepping Motors
TIMING BELTS
REINFORCED TIMING BELTS
Driving Unit Motion
Carrier Motion

Fig.12 A Flow Chart of The Control System for The 2-step Machine

Downloaded by UNIV OF ARIZONA on August 6, 2012 | http://pubs.acs.org
Publication Date: April 3, 1991 | doi: 10.1021/bk-1991-0457.ch003

and then transmitted to the CPU of the controller. Each program is responsible for one braiding pattern.

A large rewinding length of yarn for the carriers becomes necessary due to the large moving distances of the carriers across the machine bed. To meet this requirement, the fixed length with elastic compensation is no longer feasible, and carriers with continuous yarn supply have to be applied. Most yarn carriers available in the market do supply yarn continuously but the rewinding lengths are very limited. Therefore, designing proper fiber carriers becomes a prerequisite for automation of the 2-step 3-D braiding machine. Carriers with continuous yarn supply and large rewinding lengths have been designed and manufactured at NCSU, and have been running for several months. A full discussion on carriers will be given later in a separate section.

A Comparison of the Two Processes. Due to different braiding concepts, the two 3-D braiding processes discussed above are quite different, and so are their product structures and properties, as well as the engineering treatments in automation. Table I gives a general comparison of these two processes.

Some Basic Aspects

Special attention has to be paid to several basic aspects in automating 3-D braiding processes, namely the machine bed size, the rewinding requirement, and the design of proper carriers. Automation of the 3-D braiding processes is only feasible when these basic problems are well understood and solved.

Ratio of Machine Bed to Preform Size. Since large quantities of fiber tows are often involved in the 3-D braiding process, the large machine bed tends to complicate their construction. Therefore, to estimate and determine the machine size is the first step needed before designing.

For a 4-step process, 1x1 braiding pattern, it has been shown that a preform width or length of any side with k tows arranged in the main part is given by

$$W_k = (\sqrt{2}\,k + 1)\,d \qquad (1),$$

where W_k is the side length and d is the effective diameter of the fiber tows (14). To braid a side with k tows in the main part requires (k+2) slots in that direction. Therefore, the length of the machine bed in this direction will be given by

$$M_k = S\,(k + 2) \qquad (2),$$

Downloaded by UNIV OF ARIZONA on August 6, 2012 | http://pubs.acs.org
Publication Date: April 3, 1991 | doi: 10.1021/bk-1991-0457.ch003

Table I. A Comparison Between 4-Step and 2-Step Processes

PROCESSES FEATURES	4-STEP (1X1)	2-STEP
CAPABILITY TO BRAID COMPLEX SHAPES	GOOD	GOOD
FABRIC FORMING	BEATING	CONVERGING
RATIO OF BRAIDERS TO TOTAL ENDS	MORE THAN 0.5	LESS THAN 0.5
LOCATION OF THE BRAIDERS	ALL OVER	OUTSIDE OF AXIALS
COMSUMPTION OF YARN PER LENGTH OF BRAID	MODERATE	AXIALS: ABOUT 1 BRAIDERS: HIGH
MAXIMUM BRAIDER ORIENTATION ANGLE	55^0	APPROACHING 90^0
MAXIMUM YARN VOLUME FRACTION	0.685	0.569 - 0.785
NET SHAPE FORMABILITY	GOOD	GOOD
PREFORM STABILITY	MODERATE	GOOD
CURVATURE OF BRAIDERS AT SURFACE	MODERATE	LARGE
TENSILE MODULUS IN THE AXIAL DIRECTION	HIGH	HIGHER
TORSIONAL RIGIDITY	MODERATE	LOW

where M_k is the machine width and S is the distance between center lines of two adjacent slots in that direction. Then the ratio of the machine width to the preform width is

$$\eta = \frac{M_k}{W_k} = \frac{k+2}{\sqrt{2}\,k+1}\,\frac{S}{d} = \lambda\, S_d \qquad (3),$$

where S_d [S/d] is the slot space normalized by the fiber tow diameter and λ [$(k+2)/(\sqrt{2}k+1)$] is a coefficient depending on the value of k. The ratio of the machine width to the preform width, η, indicates how large a machine bed is needed for fabricating a certain size preform, or vice versa indicates the capacity of how large a preform can be made with an existing machine. This ratio is obviously a function of S_d and λ (or k).

For a 2-step process, it has been shown that a preform width or length of any side with k tows arranged in the main part is given by

$$W_k = [(\sqrt{2}\,k - 0.414)\,(1 + e) + 1]\,d \qquad (4),$$

where e is the diameter ratio of the axials to the braiders (15). To braid a side with k tows in the main part requires (k+1) slots in that direction. Because the preform sides are arranged across the slots in a 45 degree angle (15), the length of the machine bed required for this side is

$$M_k = \sqrt{2}\,S\,(\,k + 1\,) \qquad (5),$$

where S is the center distance of two adjacent slots. Then the ratio of the machine width to the preform width is

$$\eta = \frac{M_k}{W_k} = \frac{\sqrt{2}\,(k+1)}{(\sqrt{2}\,k - 0.414)\,(1+e) + 1}\,\frac{S}{d} = \lambda\, S_d \qquad (6),$$

where the coefficient λ [$[\sqrt{2}\,(k + 1)]/[(\sqrt{2}\,k - 0.414)\,(1 + e) + 1)]$] depends on the values of k and e.

Figure 13 shows how λ varies with k for a 4-step and with k and e for a 2-step process. The figure indicates that in most cases, the value of λ is in the range from 0.71 to 0.75 for the 4-step process. With the desired S_d value, it is then very easy to determine the width ratio η. For example, if the tow diameter is 0.03" and the slots spacing is 0.75", η is therefore in the range from 17.75 to 18.75 or the machine side will be approximately 18 times the preform side. For 2-step machines, however, λ is greatly affected by the e value. It can be seen that all the curves for the 2-step

Downloaded by UNIV OF ARIZONA on August 6, 2012 | http://pubs.acs.org
Publication Date: April 3, 1991 | doi: 10.1021/bk-1991-0457.ch003

American Chemical Society
Library
1155 16th St., N.W.
Washington, D.C. 20036

Downloaded by UNIV OF ARIZONA on August 6, 2012 | http://pubs.acs.org
Publication Date: April 3, 1991 | doi: 10.1021/bk-1991-0457.ch003

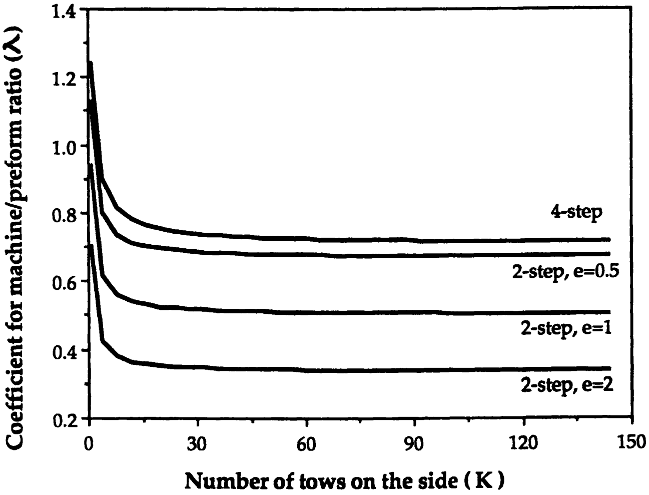

Fig.13 Coefficient of Machine/Preform Ratio for Both Processes

process are under the 4-step curve, which means that a 2-step machine has a smaller λ value. However it should be noticed that 2-step braids are often arranged diagonally on the machine bed, therefore a factor of $\sqrt{2}$ should be taken into account.

The above discussion shows that the distance between the slots, S, plays a critical role in determining the size of the machines. To achieve the minimum η value, the smaller the S the better. However on the other hand, the value of S is limited by the size of the fiber carrier.

Rewinding Requirement for Fiber Carriers. When a fiber carrier moves from outside (position 1) to the center of the machine bed (position 2) during braiding, the length of tow between the carrier top to the converging point of the preform is reduced. This reduction in length has to be rewound by the tow carrier, otherwise it becomes entangled. If the original length at position 1 is L_1, the final length at position 2 is L_2, and the length of tow taken-up because of the forming of preform during this period is L_f, then the excessive length to be rewound is given

$$L_r = L_1 - L_2 - L_f \qquad (7).$$

In a 4-Step braiding machine with n_c columns and n_r rows, and the space between columns and rows are S_c and S_r respectively, then the maximum L_1 is equal to $\sqrt{(S_c(n_c\text{-}1)/2)^2+(S_r(n_r\text{-}3)/2)^2+H^2}$ and the minimum L_2 is H, where H is the height of the converging point. The yarn length taken-up in one machine cycle is approximately $h\sec\gamma$, where h is the pitch length of the preform and γ is the inner yarn orientation angle. Based on the fiber geometries [14], the minimum value of $h\sec\gamma$ is 4.88d, where d is the tow diameter. Thus the maximum rewinding length required is given by

$$L_r = \sqrt{(S_c(n_c\text{-}1)/2)^2+(S_r(n_r\text{-}3)/2)^2+H^2} - H - 4.88dX \qquad (8),$$

where X is the number of machine cycles for a carrier to move from the most outside to the center of the machine. X is dependent on the numbers of columns and rows. If we assume that $n_c > n_r$, the approximated formula to calculate X is

$X = (n_c\text{-}1)/4,$ for a square machine or when n_r approaches n_c

$X = (n_c\text{-}1)(n_r\text{-}1)/4(n_r\text{-}2),$ when $n_r << n_c$; and (9).

Downloaded by UNIV OF ARIZONA on August 6, 2012 | http://pubs.acs.org
Publication Date: April 3, 1991 | doi: 10.1021/bk-1991-0457.ch003

For the 2-step process, since the carrier moves from the outside, passing the center of the machine in a single motion, the length of tow taken-up during this period, L_f, is almost zero. In 2-step machines, there are the same amount of rows and columns, and the row and column spacings are also the same. So the required rewinding length is then given by

$$L_r = \sqrt{(S\frac{2}{n-1})^2 + H^2} - H \qquad (10).$$

As a demonstration, Figure 14 shows how the required rewinding lengths vary with the changes in the converging point heights for different row and column numbers. The yarn diameter used is 0.03" which is close to a 12K 7μm carbon fiber tow. The selected row spacing is 1.5" and column spacings is 1.125" for the 4-step process, and the slot spacing is 3" for the 2-step process. For different row and column spacings, the absolute values will be different but the trend remains the same.

Carrier Design. The foregoing discussion shows that a large rewinding length is required for the fiber carrier of the 3-D braiding processes. Carriers for conventional braiding usually have only a few inches rewinding length which is not enough for 3-D braiding. Therefore, designing a carrier which possesses a large rewinding length becomes a prerequisite for automation of the 3-D braiding processes.

Figure 15 shows a carrier configuration we designed and manufactured. The key part of the carrier is the mechanical clutch. There are three main functions of the mechanical clutch, namely yarn feeding, rewinding, and tensioning. It provides a continuous supply of fiber tow under certain tension. Once the tow becomes slack, say the carrier moves toward the inside of the machine bed, the mechanical clutch will rewind the excess yarn onto the carrier spool. For a rectangular carrier of 1.5" wide, 1" thick, and 4" high made in our lab, the rewinding length is up to 15 feet. Much higher rewinding capability can be achieved if needed.

Conclusions

Based on the forgoing presentation, the following conclusions can be drawn:

(1) Automation of both the 4-step and 2-step 3-D braiding processes is feasible, and innovative ideas are specially important in this issue.

(2) For 3-D braiding processes, a large machine/preform ratio is generally expected.

(3) Because of (2), a large rewinding length is usually required for the fiber carriers to be used.

Downloaded by UNIV OF ARIZONA on August 6, 2012 | http://pubs.acs.org
Publication Date: April 3, 1991 | doi: 10.1021/bk-1991-0457.ch003

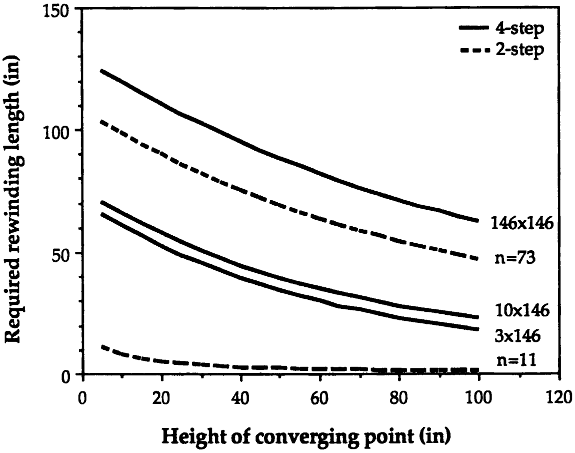

Fig.14 Required Rewinding Length for Both Processes

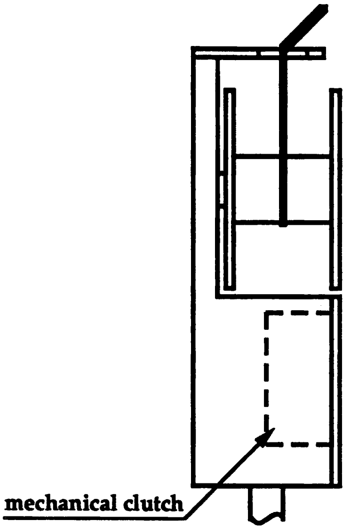

Fig.15 Schematic Drawing of A New Developed Fiber Carrier

Downloaded by UNIV OF ARIZONA on August 6, 2012 | http://pubs.acs.org
Publication Date: April 3, 1991 | doi: 10.1021/bk-1991-0457.ch003

(4) The carriers presented are prominent candidates for commercial 3-D braiding machines or similar applications.

Acknowledgments

This work is partially supported by NASA Head quarters under Grant No. NAGW-1331, and the authors are grateful for this support. The authors would also like to extend their appreciations to Mr. William Roberts of the College's machine shop for his help and interest in designing and machining of our 3-D braiding equipment.

Literature Cited

1. Kuno, J. K. 31st International SAMPE Symposium, April 7-10, 1986, p 725.
2. Stover, E. R., Mark, W. C., Marfowitz, I., and Mueller, W., AFML-TR-70-283, March 1971.
3. Bluck, B. M., U.S. Patent 3,426,804, Feb. 11, 1969.
4. Maistre, M. A., AIAA/SAE 11th Propulsion Conference Proceedings, Sept. 1975.
5. Florentine, R., U.S. Patent 4,312,261, January 26, 1982.
6. Cole, P. M., US Patent 4,737,399, Apr. 12, 1988.
7. Brown, R.T. and Ratliff, E.D., U.S. Patent 4,621,560, Nov.11, 1986.
8. McConnell, R. and Popper, P., U.S. Patent 4,719,837, Jan. 19, 1988.
9. Li, W. and El-Shiekh, A., SAMPE Quarterly, Vol.19, No.4, July 1988, p 22.
10. Florentine, R. A., 15th National SAMPE Technical Conference, 1983, p 700.
11. Brown, R. T., 30th National SAMPE Symposium, March 19-21, 1985, p 1509.
12. Popper, P. and McConnell, R., 32nd International SAMPE Symposium and Exhibition, 1987, P 92.
13. Du, G., Popper, P., and Chou, T., NASA Conference publication 3038, 1988, p 217.
14. Li, W., Kang, T. and El-Shiekh, A., NASA Conference publication 3001, 1987, p 115.
15. Li, W. and El-Shiekh, A., NASA Conference publication 3038, 1988, p 249.
16. Macander, A. B., Crane, R. M., and Camponeschi, E. T. Jr., Composite Materials: Testing and Design (7th Conference) ASTM STP893, 1986, p 422.

RECEIVED March 20, 1990

Downloaded by UNIV OF ARIZONA on August 6, 2012 | http://pubs.acs.org
Publication Date: April 3, 1991 | doi: 10.1021/bk-1991-0457.ch003

Downloaded by UNIV OF GUELPH LIBRARY on August 6, 2012 | http://pubs.acs.org
Publication Date: April 3, 1991 | doi: 10.1021/bk-1991-0457.ch004

Chapter 4

Three-Dimensional Multilayer Woven Preforms for Composites

Peter S. Tung and Sundaresan Jayaraman[1]

School of Textile and Fiber Engineering, Georgia Institute of Technology, Atlanta, GA 30332

The interlaminar mechanical properties of laminated complex shape composite structures tend to be poor due to the presence of delamination effects in the structures. One approach of tackling the delamination problem is to use multilayer woven preforms in the fabrication of composites instead of single-ply woven fabrics. Research efforts on modifying traditional weaving methods to introduce through-the-thickness or "Z" direction yarns for the production of such multilayer woven preforms are discussed. The advantages of this approach over traditional methods of composite fabrication are also discussed. These include the accurate placement of fibers for the optimization of the final composite properties, reduced fiber damage due to reduction in fiber handling and reduced labor cost in composite fabrication.

Composites are gaining increasing acceptance as viable replacements in structural load bearing applications. The advanced composites market totalled 39 million pounds in 1987 and is expected to grow at a yearly rate of 10% for the next decade (*1*). The strongest growth potential for advance composites is projected to be in the aircraft/aerospace/military segment of the market.

The properties demanded for these applications are being met by fiber reinforced composites, with woven fabric constituting the primary form of reinforcement. Woven fabrics offer ease of handling, the ability to conform to complex shapes, as well as inplane properties that are more isotropic than unidirectional composites.

---

[1] Address correspondence to this author.

0097–6156/91/0457–0053$08.00/0

In applications where high performance is required, laminated composites are used. The behavior of these structures is based upon the combined properties of the individual layers. One method of fabricating a laminated composite consists of stacking multiple layers of two-dimensional reinforcement on top of one another, impregnating with uncured resin and then curing the aggregate. Another method consists of stacking multiple layers of prepregs (which are partially cured preimpregnated fibrous materials) and then applying heat and pressure to consolidate the layers into a unified composite material.

Although the choice of matrix and reinforcement materials is important to composite properties, of paramount significance is the way in which the constituents are arranged. For example, continuous parallel fibers provide excellent properties in the longitudinal direction of the material, but contribute very little to the transverse properties. A major attribute of lamination is that the materials can be tailored to give directional properties by specifying the fiber orientation of each ply in order to meet the end use loading requirements encountered by the composite. For example, to obtain quasi-isotropic properties, each unidirectional ply in a four-ply laminate may be laid up with fiber orientations of 0°, +30°, +60°, and +90°. Although this ply arrangement would exhibit quasi-isotropic properties in-plane to the laminate, when the important through-the-thickness or "Z" direction is taken into consideration, there is a general lack of isotropy in the whole structure. This anisotropy is due to the "Z" direction properties of a laminate being solely dependent upon matrix properties which are much lower than those of the reinforcement.

Downloaded by UNIV OF GUELPH LIBRARY on August 6, 2012 | http://pubs.acs.org
Publication Date: April 3, 1991 | doi: 10.1021/bk-1991-0457.ch004

Delamination in Composites. A manifestation of the weak out-of-plane properties of a laminated structure is delamination. According to Schwartz (*2*), shearing stresses are introduced between layers in a laminate. These stresses are caused by the tendency of each layer to deform independently of each other, due to their different properties (at least from the standpoint of orientation of principal machine directions). Shearing stresses are largest at the edges of the laminate, where they may cause delamination. Transverse normal stress may also cause delamination.

Laminated composite structures have many design features that can result in interlaminar forces which in turn can induce the growth of delamination from either pre-existent manufacturing defects or in-service damage. One of the most common forms of in-service damage found in the aircraft industry is caused by dropped tools or from stones flung up from the runway. These occurrences produce impacts that can cause a significant amount of sub-surface delamination with very little evidence on the surface that the material has suffered damage. (*3*).

Browning and Schwartz (*4*) reported that delamination is the failure mechanism that is the most life-limiting growth mode in advanced composite structures. It is the fundamental issue in the evaluation of laminated composite structures for both durability and damage tolerance.

Another impediment to the use of laminated composites is the reproducibility of parts and the high cost/performance factor. Most laminated composites are fabricated by the hand lay-up process, particularly in parts where curvatures are involved. This makes it difficult to reproduce composite parts that are identical in dimensions, constituent volume fractions and therefore physical properties in the final composite. In the hand lay-up procedures there is also a greater risk of fiber damage from the rough handling that is sometimes required to lay successive plies of material over each other or the mold. Because hand lay-up processes used in fabricating laminated are highly labor intensive, the cost of the finished parts prohibits their use in applications other than the aerospace/military/aircraft industries.

Downloaded by UNIV OF GUELPH LIBRARY on August 6, 2012 | http://pubs.acs.org
Publication Date: April 3, 1991 | doi: 10.1021/bk-1991-0457.ch004

Purpose of the Research. The majority of textile reinforcements presently used in composites are still two-dimensional, biaxially woven fabrics. The primary objective of the present research is to design and develop three-dimensional woven fabrics on modified weaving machines. This will be accomplished by the introduction of a system of through-the-thickness or "Z" direction yarns. These "Z" direction yarns will interlace with other yarns to form an integral three-dimensional woven structure. It is anticipated that composites fabricated from these structures will have improved interlaminar mechanical properties (increased resistance to delamination).

The ultimate goals for this approach to produce woven structures are the accurate placement of fibers for the optimization of the final composite properties, to keep fiber damage to a minimum by reducing fiber handling and to optimize the cost/performance ratio of the composite by reducing the amount of labor involved in composite fabrication. This would provide a cost effective method of fabricating composites, with the added benefits of superior properties.

Another objective of this research is to determine the influence of yarn orientation upon the properties of the fabricated composite. This has been accomplished by producing fabrics with different weave geometries and then analyzing the properties of the composite structures fabricated from these fabrics.

Review of Literature

There has been a great amount of literature published on the subject of three-dimensional structures and reinforcements for composites made from fibrous materials. Nearly all known textile formation systems have been used or modified to produce these types of structures, with varying degrees of success.

The reinforcements produced by these methods can be classified into four different categories, determined by their method of production. They are (*5*):

- Nonwoven Orthogonals
- Multilayer Woven Fabrics
- Multilayer Knitted or Stitched Fabrics
- Three-Dimensional Braids

Downloaded by UNIV OF GUELPH LIBRARY on August 6, 2012 | http://pubs.acs.org
Publication Date: April 3, 1991 | doi: 10.1021/bk-1991-0457.ch004

Nonwoven Orthogonals. Nonwoven orthogonals consist of straight, continuous fibers arranged in all three directions with no interlacing. In its simplest form, the three yarn directions are oriented at 90° to each other. The most elementary method of constructing such a preform is by hand, placing each yarn in the desired position, one at a time. Obviously, this method is utilized only where economics is not a factor. In most cases, however, the hand method of fabricating nonwoven orthogonals is aided by the use of machinery (*6-10*).

Multilayer Woven Fabrics. Multilayer fabrics are comprised of multiple layers of woven fabric which are interlaced at selected points within the thickness of the structure. This interlacement is accomplished by utilizing at least one set of yarns which traverses around other yarns to anchor them in position and to thereby form an integral structure (*11-15*).

Multilayer Knitted or Stitched Fabrics. Multilayer knitted fabrics for composite applications are usually fabricated using warp knitting machines. These machines can stitch multiple layers of yarns, even if oriented in different directions, together to hold them in fixed positions (*16-17*).

Three-dimensional Braids. Three-dimensional braiding consists of intertwining multiple yarns so that a particular yarn will follow a path that would take it completely across the structure several times (*18-19*). Other braiding methods for fabricating three-dimensional structures include: X-Y braiding (*20*), through-the-thickness braiding (*21*) and the 2-step braiding process (*22*).

The literature reviewed in the area of three-dimensional preforms for composites did not provide substantial information on multilayer woven fabrics in which the threads of the individual layers are interlaced to form an integral structure for use in composites. This provided additional motivation for the present research.

Downloaded by UNIV OF GUELPH LIBRARY on August 6, 2012 | http://pubs.acs.org
Publication Date: April 3, 1991 | doi: 10.1021/bk-1991-0457.ch004

Three-Dimensional Fabrics: Design and Development

Three-dimensional fabric preforms were produced in three different weave constructions. The number of layers, type and size of thread used and the end density were kept constant for the three fabrics. The variable parameters were the weave geometry and the filling density.

Weave Design. Many different weave constructions are possible in designing three-dimensional woven fabrics. In the angle interlock system, multiple layers of warp and fill yarns are interconnected by yarns which traverse in the "Z" or through-the-thickness direction. The number of layers which the "Z" direction yarns interlace can be varied from a minimum of two layers to a construction in which these yarns pass entirely through the body of the fabric from one fabric surface to the other and back.

Designated as Weave A, B, and C, the three structures were designed as angle interlock structures. Each fabric had a total of five layers, a layer being defined as containing both a warp and fill yarn. Weave A consisted of a layer-to layer interlacement with warp yarns being used to interconnect each layer to the adjacent layer. In weave B, warp yarns penetrated a depth of three layers and in Weave C, warp yarns penetrated a depth of four layers. Weave plans as well as the schematics of the cross sections along the warp direction are shown in Figures 1a and b, Figures 2a and b, and Figures 3a and b, respectively.

Fiber. The fiber chosen for producing the three-dimensional fabrics had to meet the property requirements necessary for high performance composites. These properties included low density, high tensile strength and good impact resistance. One of the fibers which met these requirements was du Pont's Kevlar, an aramid fiber. The three different types of Kevlar produced by du Pont are Kevlar 49, Kevlar 29 and Kevlar. Since Kevlar 49 is extensively used as reinforcements for high performance composites, it was chosen for the production of these fabrics. Kevlar 49 has a tensile strength of 400 ksi, a modulus of 18 msi and an elongation to break of 2.5% (*23*). A 1420 denier, 1000 filament yarn was used. A tensile stress-strain curve of this yarn is shown in Figure 4 (*24-25*).

Equipment Used for Fabric Formation. The experimental set-up designed and fabricated for the production of the fabrics is shown in Figure 5. It consists of three different sections: the loom, the creel and the tension frame.

The characteristics of Kevlar such as its high modulus and propensity for fiber damage from abrasion with smooth metallic surfaces were taken into consideration during the design of the equipment. Some of the other design features of the equipment included:

Downloaded by UNIV OF GUELPH LIBRARY on August 6, 2012 | http://pubs.acs.org
Publication Date: April 3, 1991 | doi: 10.1021/bk-1991-0457.ch004

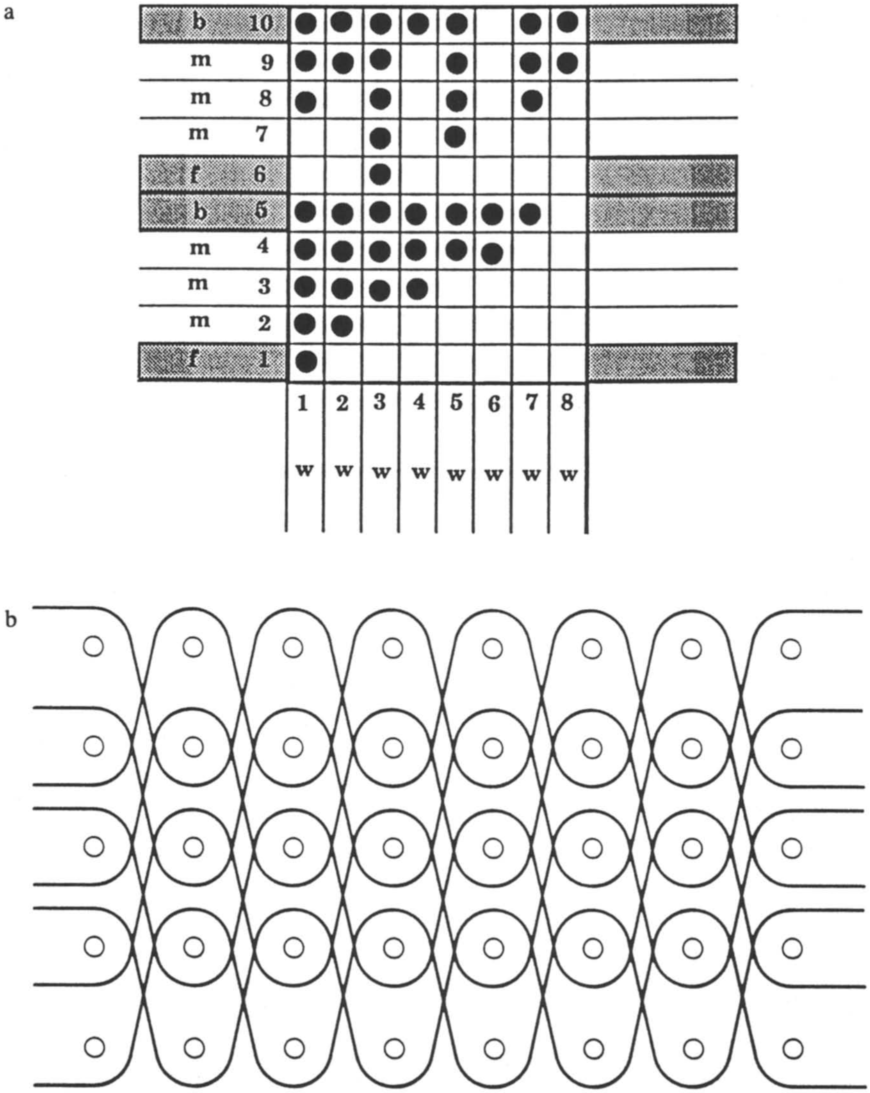

		1	2	3	4	5	6	7	8
b	10	●	●	●	●	●		●	●
m	9	●	●	●		●		●	●
m	8	●		●		●		●	
m	7			●		●			
f	6			●					
b	5	●	●	●	●	●	●	●	
m	4	●	●	●	●	●	●		
m	3	●	●	●	●				
m	2	●	●						
f	1	●							
		w	w	w	w	w	w	w	w

Figure 1. (a) Weave plan for weave A; (b) Schematic for weave A.

Downloaded by UNIV OF GUELPH LIBRARY on August 6, 2012 | http://pubs.acs.org
Publication Date: April 3, 1991 | doi: 10.1021/bk-1991-0457.ch004

Legend For Weave Plan

Vertical Columns- Positions of warp (0°) yarns. " "," " and " " are intersections of warp and filling yarns where the warp is over the filling.

Horizontal Rows- Positions of filling (90°) yarns. " " is and intersection of warp and filling where the filling is over the warp.

Yarn Element	Code	Shade	Location and Movement
Face Warp	f	░	Longitudinal yarn (0°) with one layer of transverse yarns forming the face and back fabric surface. The frequency of the interlacing is two yarns per repeat.
Back Warp	b	░	
Web Warp	w	☐	Longitudinal yarn (0°) moving thru 2,3 or 4 layers of transverse yarns. Through the thickness repeats every 10 filling yarns (90°).
Middle Warp	m	▒	Longitudinal yarn (0°) interlacing with one layer of transverse yarns (M_2) forming a middle plane. Frequency of interlacing is two yarns per repeat.
Face Filling	f	░	Transverse (90°) yarns interlacing with one longitudinal yarn forming the face and back of the fabric.
Back Filling	b	░	
Middle Filling	m_1	☐	Transverse yarns interlacing with web yarns forming the fabric between the face and the back.
Middle Filling	m_2	▓	Special transverse yarns interlacing with middle warp yarns at a frequency of two yarns per repeat.

Downloaded by UNIV OF GUELPH LIBRARY on August 6, 2012 | http://pubs.acs.org
Publication Date: April 3, 1991 | doi: 10.1021/bk-1991-0457.ch004

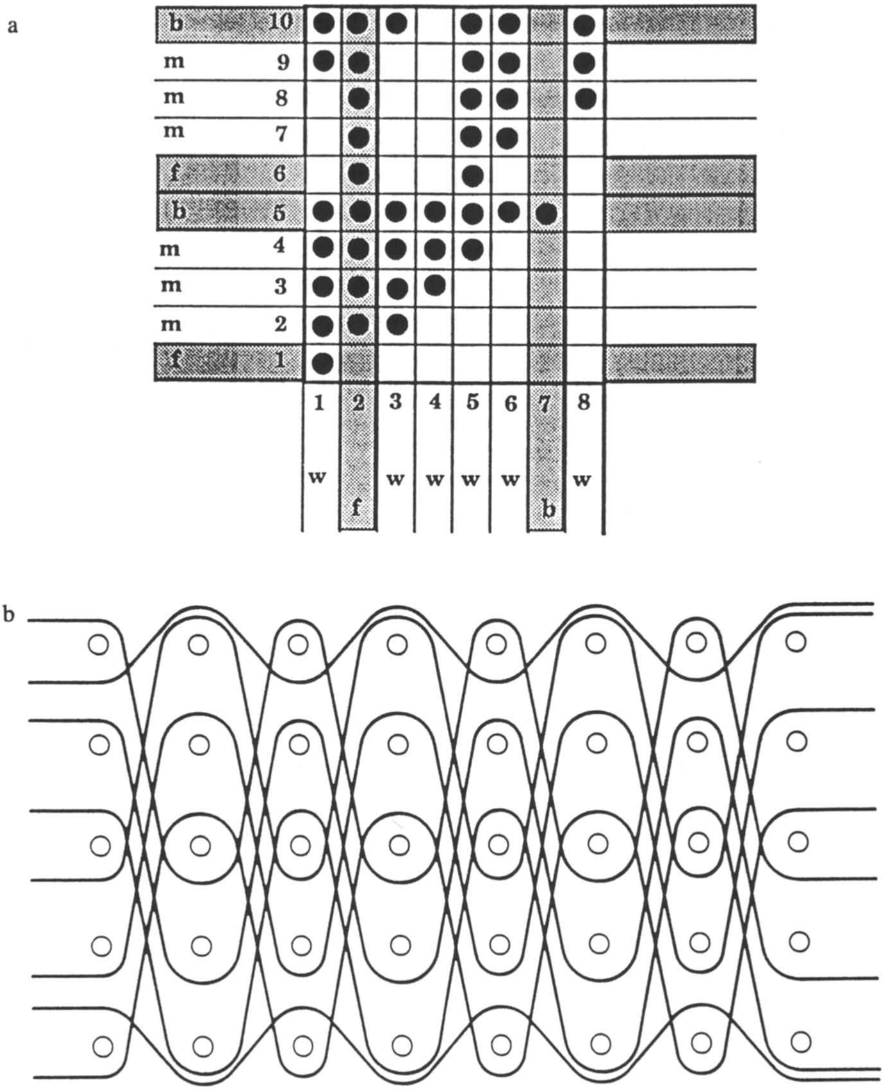

		1	2	3	4	5	6	7	8
b	10	●	●	●		●	●		●
m	9	●	●			●	●		●
m	8		●			●	●		●
m	7		●			●	●		
f	6		●			●			
b	5	●	●	●	●	●	●	●	
m	4	●	●	●	●	●			
m	3	●	●	●	●				
m	2	●	●	●					
f	1	●							
		w	f	w	w	w	w	b	w

Figure 2. (a) Weave plan for weave B; (b) Schematic for weave B.

Downloaded by UNIV OF GUELPH LIBRARY on August 6, 2012 | http://pubs.acs.org
Publication Date: April 3, 1991 | doi: 10.1021/bk-1991-0457.ch004

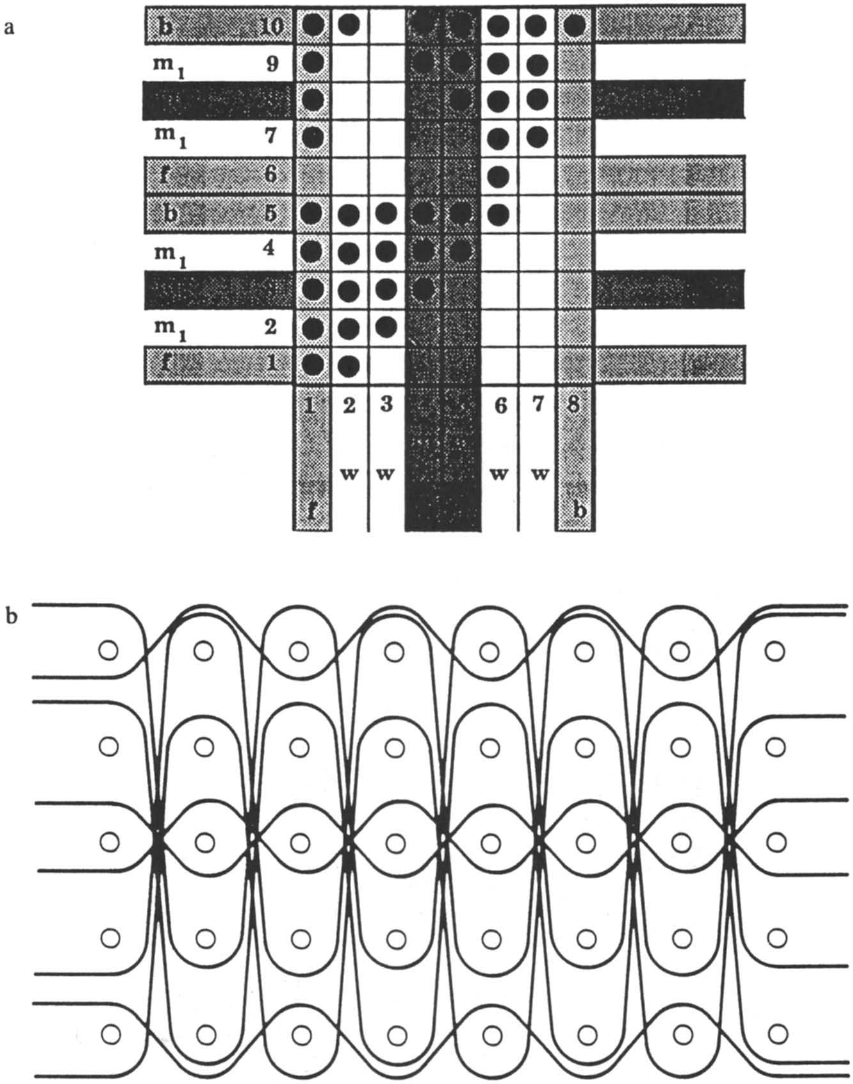
a
b 10
m1 9
m1 7
f 6
b 5
m1 4
m1 2
f 1
1
2
3
6
7
8
w
w
w
w
f
b
b

Figure 3. (a) Weave plan for weave C; (b) Schematic for weave C.

In High-Tech Fibrous Materials; Vigo, T., et al.;
ACS Symposium Series; American Chemical Society: Washington, DC, 1991.

Downloaded by UNIV OF GUELPH LIBRARY on August 6, 2012 | http://pubs.acs.org
Publication Date: April 3, 1991 | doi: 10.1021/bk-1991-0457.ch004

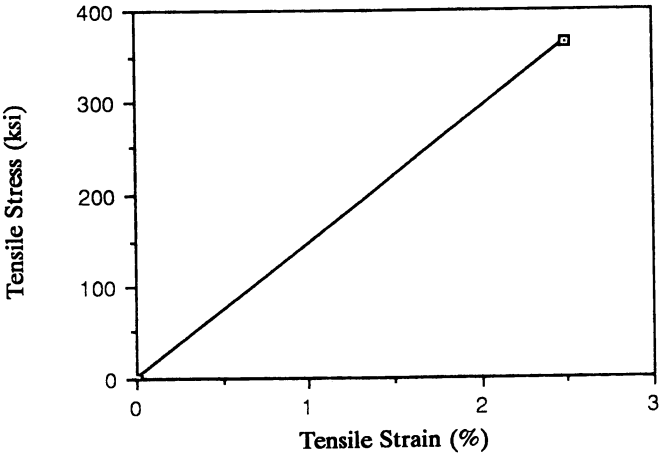

Figure 4. Tensile Stress-Strain Curve of Kevlar 49 Yarn.

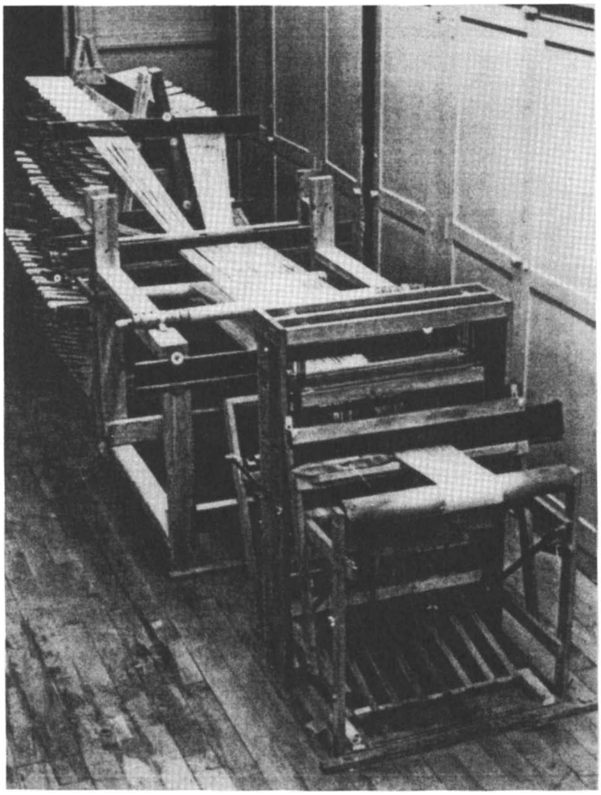

Figure 5. Weaving Set-up

- Yarn paths were designed to minimize contact with other surfaces and to give the least amount of angularity to the threadline.
- All contact surfaces were cleaned and sanded smooth.
- To reduce surface friction, rubber coated drag rolls were utilized.
- The warp sheet entered the loom at the same height as the breast beam of the loom.
- The breast beam of the loom, which would have required the fabric to follow a sharp right-angled path, was replaced with a freely rotating cylinder.

Loom

Due to the thickness of the three-dimensional fabrics, the warp densities are much greater than conventional two-dimensional fabrics. Therefore, the interaction among warp ends in going from one shed to the next would be very severe. To exercise complete control over the weaving process, a hand loom was chosen. A hand loom would provide the fundamental capabilities of a power loom while providing the ability to control the speed and placement of the yarns.

The minimum number of harnesses required to weave the three fabrics was eight. As only four-harness hand looms were available at the facility, two of them were dismantled and reconstructed to form an eight-harness loom. This floor loom, shown in Figure 6, had a working width of 22 inches and the harness motion was controlled by means of four treadles. The reed spacing was 12 dents per inch.

Creel

In conventional looms, the warp yarns are fed from the weaver's beam. Although the beam holds numerous ends, all the ends have to advance at the same rate. The fabric construction required by the three weave geometries necessitated that the warp ends follow paths of varying lengths. Therefore, the warp beam was eliminated and a creel arrangement, as shown in Figure 7, was fabricated. This creel consisted of a wooden frame into which creel pins were attached. Conventional quills or tubes inserted onto the creel pins allowed for ease in let-off by rotation, as well as for yarn storage. The creel had the capability of storing a total of 648 warp ends. It also allowed each end to be individually tensioned and to advance independently of one another thus permitting allowances for the varying yarn crimp demanded by the fabric construction. The warp ends were divided into three different layers and were drawn through combs to further separate the individual ends. This facilitated the drawing-in of ends through the heddles of the loom and also the identification of an individual end in the creel.

Downloaded by UNIV OF GUELPH LIBRARY on August 6, 2012 | http://pubs.acs.org
Publication Date: April 3, 1991 | doi: 10.1021/bk-1991-0457.ch004

Downloaded by UNIV OF GUELPH LIBRARY on August 6, 2012 | http://pubs.acs.org
Publication Date: April 3, 1991 | doi: 10.1021/bk-1991-0457.ch004

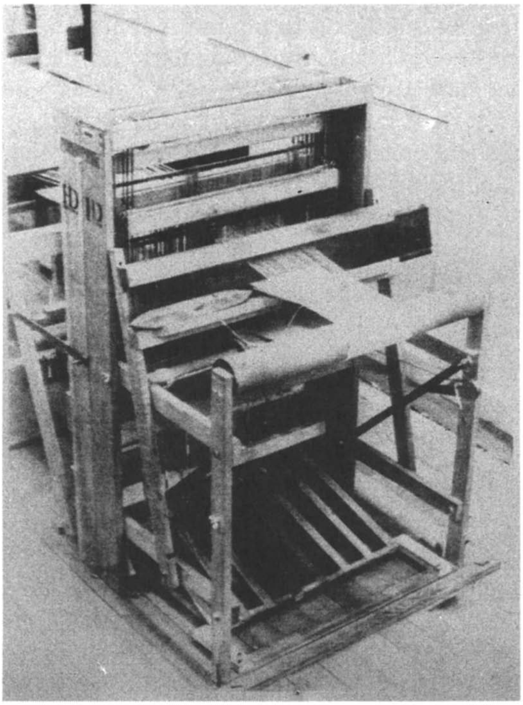

Figure 6. Loom

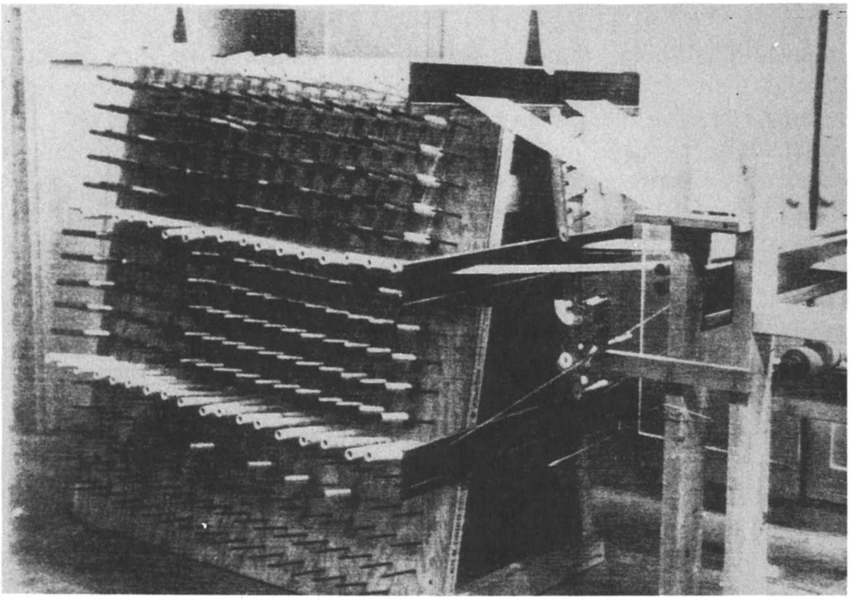

Figure 7. Creel

Downloaded by UNIV OF GUELPH LIBRARY on August 6, 2012 | http://pubs.acs.org
Publication Date: April 3, 1991 | doi: 10.1021/bk-1991-0457.ch004

Tension Device

In any weaving operation, it is important to maintain proper tension of the warp yarns. In order to obtain a stable fabric and to form a proper shed, a high degree of tension had to be applied to the warp ends. The high tension is particularly important when weaving Kevlar due to its low elongation. Slack ends in the warp transform into slack ends in the fabric, which cause entanglements in the warp and prevent the formation of a clear shed.

The tension device, shown in Figure 8, consisted of two rubber coated drag rolls mounted onto a frame. The rubber coated rollers were used instead of polished chrome, smooth stainless steel or glass because these types create high surface friction and damage the Kevlar filaments (*25*). The degree of warp tension necessary for optimum weavability was adjusted by varying the position of the drag rolls relative to each other. In addition, each warp end was drawn through an individual dent in two combs located in the front and back of the tension frame. These combs allowed the consolidation of all the warp ends exiting from the creel into a single layer of one yarn diameter thickness. This separation also minimized the frictional drag between adjacent yarns travelling at different speeds and prevented the yarns from riding on each other.

Preparation For Weaving. In preparation for weaving, the Kevlar warp yarns were wound onto wooden quills and placed on the creel. A total of 328 quills was prepared. The yarns were then individually placed between the teeth of the comb, around the drag rolls of the tension frame, between the teeth of the second comb, drawn-in through the appropriate heddles on the harnesses and through the appropriate dents in the reed. The final arrangement is shown in Figure 5. For all three fabric structures, the warp ends were drawn-in using a straight draw with a reed plan of 4 ends per dent. Finally all the ends were securely tied to the fabric take-up roll on the front of the loom.

Filling preparation consisted of winding the yarn onto quills for subsequent use in the hand shuttle. The shuttle selected had a low profile to ensure abrasion-free travel through the shed.

Sizing the Warp

Du Pont's Elvanol T-66 polyvinyl alcohol size was used to size the yarns. It was supplied in granular solid form and was formulated to obtain a 3% solution. This size formulation was lower than the recommended 4% (*25*) for sizing Kevlar yarns because the method of size application warranted a low viscosity mixture.

Downloaded by UNIV OF GUELPH LIBRARY on August 6, 2012 | http://pubs.acs.org
Publication Date: April 3, 1991 | doi: 10.1021/bk-1991-0457.ch004

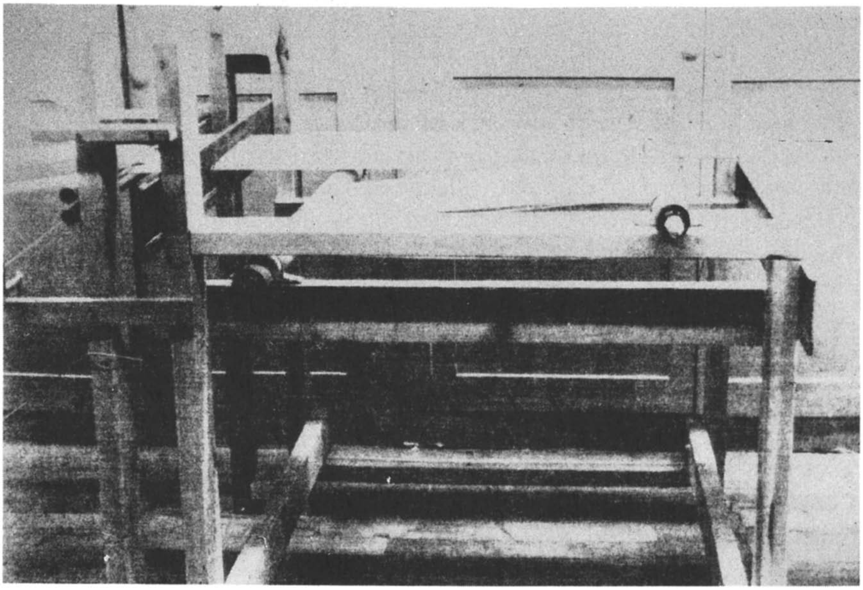

Figure 8. Tension Device

Downloaded by UNIV OF GUELPH LIBRARY on August 6, 2012 | http://pubs.acs.org
Publication Date: April 3, 1991 | doi: 10.1021/bk-1991-0457.ch004

Production of Fabric Samples. Since the fabrics were multi-layered and entirely hand woven, the production process was slow. The 328 warp ends, reeded 4 ends/dent, with a reed density of 12 dents/inch were woven into a fabric approximately 6.5 inches in width.

Figures 9 a, b and c show the lifting plans for weaving the three structures. The plan represents the pattern in which the harnesses were raised or lowered for each pick. The vertical columns represent harnesses numbered 1 through 8 and the horizontal rows represent the picks numbered 1 though 10. Each pattern for the three structures repeated on 10 picks.

Table I shows the sequence of harness movements corresponding to Figure 9a, required to produce one repeat of Weave A. Between each set of harness movements, the filling was placed in the open shed and beaten-up. To provide adequate material for composite fabrication and testing, a total of twelve yards of each structure was produced.

Fabric Finish

In order to obtain the maximum interfacial adhesion between the matrix and the reinforcement, the fabric was desized by scouring in a dye jig.

Composite Fabrication and Testing

The first stage in converting the fabric preforms into composites was preimpregnation of the fabric with matrix material. This operation was performed by American Cyanamid of Havre de Grace, Maryland. The fabrics were impregnated with Cyanamid's Cycom 1806, a 350° F cure epoxy resin. The resin content of the prepregs was fixed at 50%.

Composite Curing. The prepregs were cured into final composites using the facilities of Lockheed-Georgia. The curing system utilized a vacuum bag lay-up cured in an autoclave. A bleeder cloth was utilized to provide partial bleedout of resin, thereby increasing the fiber volume of the final composite (see Figure 10). In addition to curing, this system provided the means for theoretically reducing the number of voids in the composite.

In preparation for curing, the frozen prepregs were warmed to room temperature and then cut to the desired size. The panels were 6.5 inches wide by 36 inches long.

The composite curing cycle is shown in Figure 11.

Materials Characterization. For comparison between the fabric and the final composite, the three fabric preforms were evaluated for thickness, yarn density and fabric weight. In addition, photomicrographs were taken of the three fabric cross-sections. After prepreg curing, the resulting composites were tested to obtain constituent volume fractions and various mechanical properties.

Downloaded by UNIV OF GUELPH LIBRARY on August 6, 2012 | http://pubs.acs.org
Publication Date: April 3, 1991 | doi: 10.1021/bk-1991-0457.ch004

a

●	●	●	●	●		●	●	10
●	●	●		●		●	●	9
●		●		●		●	●	8
		●		●				7
		●						6
●	●	●	●	●	●	●		5
●	●	●	●	●	●			4
●	●	●	●					3
●	●							2
●								1
1	2	3	4	5	6	7	8	

b

●	●	●		●	●		●	10
●	●			●	●		●	9
	●			●	●		●	8
	●			●	●			7
	●			●				6
●	●	●	●	●	●	●		5
●	●	●	●	●				4
●	●	●	●					3
●	●	●						2
●								1
1	2	3	4	5	6	7	8	

c

●	●		●	●	●	●	●	10
●			●	●	●	●		9
●				●	●	●		8
●					●	●		7
					●			6
●	●	●	●	●	●			5
●	●	●	●	●				4
●	●	●	●					3
●	●	●						2
●	●							1
1	2	3	4	5	6	7	8	

Figure 9. (a) Lift plan for weave A; (b) Lift plan for Weave B; (c) Lift plan for Weave C

Downloaded by UNIV OF GUELPH LIBRARY on August 6, 2012 | http://pubs.acs.org
Publication Date: April 3, 1991 | doi: 10.1021/bk-1991-0457.ch004

TABLE I. Sequence Of Harness Movements For Weave A

Pick Number	Position Of Harnesses Raised	 Lowered
1	1	2,3,4,5,6,7,8
2	1,2	3,4,5,6,7,8
3	1,2,3,4	5,6,7,8
4	1,2,3,4,5,6	7,8
5	1,2,3,4,5,6,7	8
6	3	1,2,4,5,6,7,8
7	3,5	1,2,4,6,7,8
8	1,3,5,7	2,4,6,8
9	1,2,3,5,7,8	4,6
10	1,2,3,4,5,7,8	6

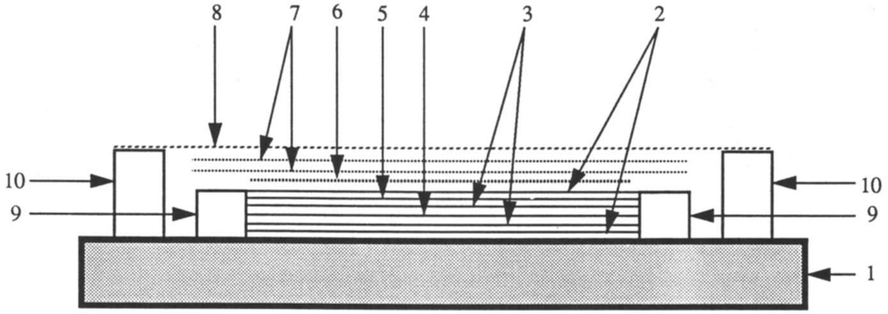

1. Tool Plate
2. Teflon Film
3. Amalon
4. Fabric
5. Bleeder Cloth
6. Caul Plate
7. Woven Fiberglass Fabric
8. Mylar
9. Air Dam
10. Cromate

Figure 10. Schematic of Curing Set-up

Downloaded by UNIV OF GUELPH LIBRARY on August 6, 2012 | http://pubs.acs.org
Publication Date: April 3, 1991 | doi: 10.1021/bk-1991-0457.ch004

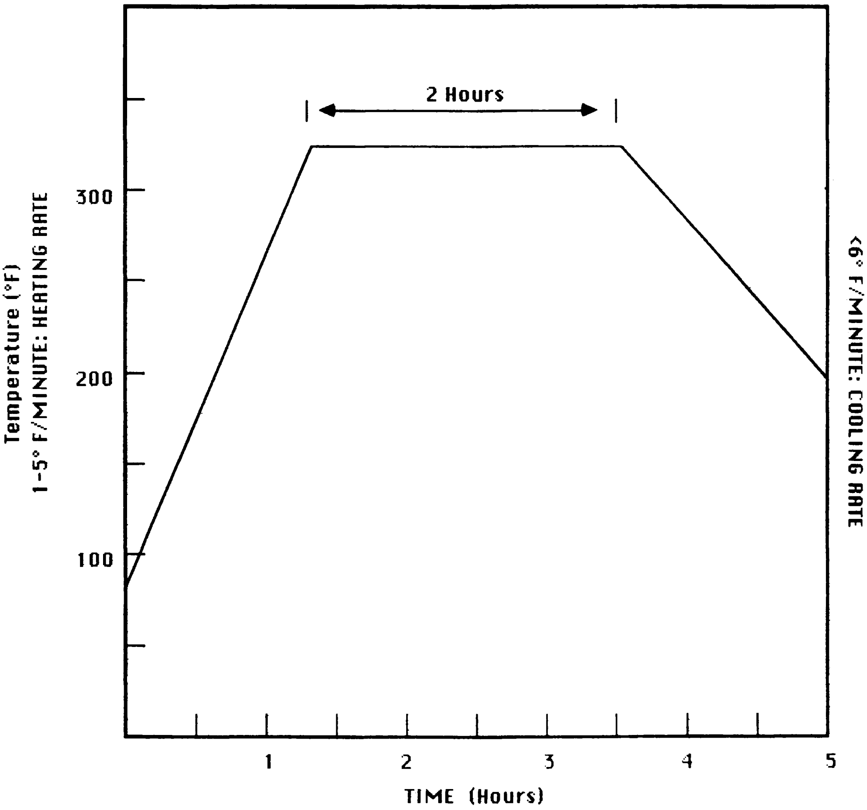

Figure 11. Composite Curing Cycle

Downloaded by UNIV OF GUELPH LIBRARY on August 6, 2012 | http://pubs.acs.org
Publication Date: April 3, 1991 | doi: 10.1021/bk-1991-0457.ch004

Preform Characterization. The evaluation of the preforms was carried out using the testing procedures specified in the following ASTM Standards:

- D1777-75 Thickness of Textile Materials
- D3775-85 Fabric Count of Woven Fabric
- D3776-85 Mass Per Unit Area (Weight) of Woven Fabric

Photomicrographs. Fabric specimens were prepared for photomicrography by embedding the fabric structures in mounting epoxy. After the epoxy was cured, the plane corresponding to the warp cross-sections was polished to obtain a smooth surface parallel to the warp yarn. The micrography apparatus used was a Bausch and Lomb Balphot II Metallograph. Illumination was by polarized light using a xenon lamp as a light source. A magnification of 50X was used.

Photomicrographs shown in Figures 12, 13, and 14 correspond to Weave A, Weave B and Weave C, respectively. The five individual layers of the fabrics as well as the difference in yarn crimp between the three structures can be clearly seen in the photomicrographs. From Weave A to Weave B to Weave C, the progressively increasing levels of warp yarn crimp can be discerned. The photomicrographs also show how the cross-sections of individual weft yarn bundles deform to fill the interstices created by interlacement with warp yarns.

Composite Characterization. The fiber volume fraction is one of the most important parameters which influence the physical properties of composites. The fiber volume fraction of the composites was determined as follows: the weight per unit area of the preform and the final composite were measured. The difference between the two i.e., the fiber weight fraction, was converted to fiber volume fraction using the fiber and matrix densities.

Composite Testing. The composites fabricated from Weaves A, B, C were tested according to the following ASTM Standards (*26*):

- D3039-76 Tensile Properties of Fiber-Resin Composites
- D790M-86 Flexural Properties of Unreinforced and Reinforced Plastics and Electrical Insulation Materials
- D2344-84 Apparent Interlaminar Shear Strength of Parallel Fiber Composite by Short-Beam Method

In preparation for testing, the composite panels were cut to the required dimensions. This was accomplished with the use of a machine customarily employed for cutting metal plates. The cutting device consisted of a pair of fixed and opposing metal blades which cut the samples by a shearing action.

Downloaded by UNIV OF GUELPH LIBRARY on August 6, 2012 | http://pubs.acs.org
Publication Date: April 3, 1991 | doi: 10.1021/bk-1991-0457.ch004

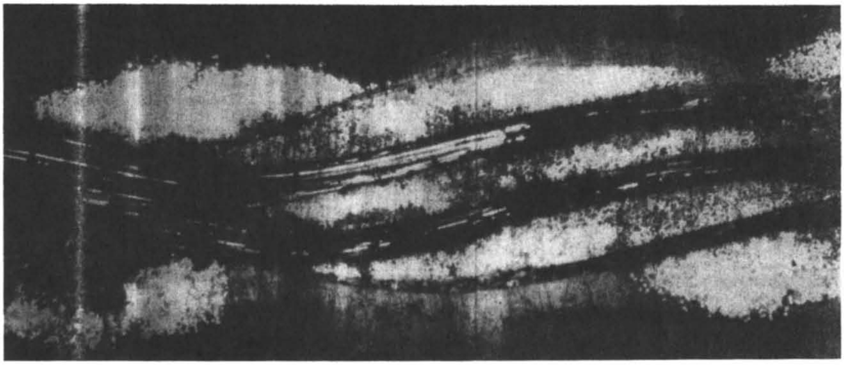

Figure 12. Photomicrograph of Weave A

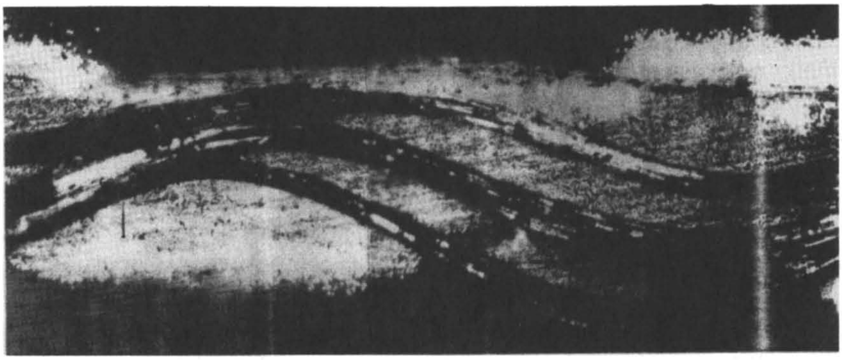

Figure 13. Photomicrograph of Weave B

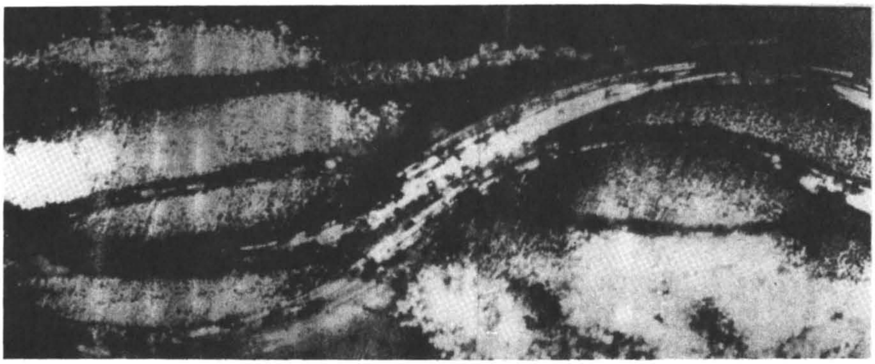

Figure 14. Photomicrograph of Weave C

Downloaded by UNIV OF GUELPH LIBRARY on August 6, 2012 | http://pubs.acs.org
Publication Date: April 3, 1991 | doi: 10.1021/bk-1991-0457.ch004

For the three tests, specimens were cut so that testing could be performed in both the warp (0°) and filling (90°) directions. Composites fabricated from Weave A, B, and C were designated as Composite A, B, and C, respectively.

Tensile Test

Tensile tests were performed using an Instron Tensile testing Machine Model TTP. The test conditions are shown in Table II. The tensile strength and modulus of each sample were calculated from the following formulas:

$$S=P/bd \tag{1}$$

Where:

S = Tensile Strength, psi
P = Maximum Breaking Load
b = Width, in
d = Thickness, in

$$E = (\Delta P/bd)(L/\Delta L) \tag{2}$$

Where:

E = Modulus of Elasticity, psi
ΔP = Load Increment, lbf
bd = Cross-Sectional Area, in^2
L = Gauge Length, in
ΔL = Increase in gauge length at the load increment ΔP, in

Flexure Test

The samples were tested for flexural properties using a three point loading system according to ASTM D790-86, Method I. For this system, the sample was supported at both ends and was center loaded midway between the supports.

The flexural yield strength of each sample tested was calculated from the following formula:

$$S = 3PL/2\,bd^2 \tag{3}$$

where:

S = Flexural yield strength, psi
P = load at the point Y, lbs
L = Support span, in
b = width of the sample, in
d = thickness of the sample, in

During the interlaminar shear strength test, the samples did not fracture in shear indicating that the test method might have been inappropriate for the structures. Consequently, this test was eliminated.

Results and Discussion

The results obtained from testing the fabric for thickness, yarn count and weight are shown in Table III. The specifications for Composites A, B and C are shown in Table IV.

Composite Properties. Table V gives the average values of five samples for tensile strength, tensile modulus and flexural yield strength. Shown in Figure 15 and Figure 16 are typical tensile stress-strain curves of Composites A, B and C at 0° and 90°.

Discussion. Multilayer woven fabric preforms offer advantages over both two dimensional fabrics and other categories of three-dimensional preforms. Compared to a laminate fabricated from multiple layers of two-dimensional fabrics, multilayer fabrics offer better processability in areas such as ease of handling and fabric lay up. This was evident during the lay up process prior to curing. In addition, due to the elimination of the number of processing steps involved in laminate fabrication, there would be a reduction in labor with the added benefit of better reproducibility in composite properties.

Other categories of three-dimensional preforms require extensive modification of present equipment or development of new equipment which can be major time and cost factors, whereas multilayer woven fabrics can be produced using existing textile manufacturing techniques on conventional equipment with few modifications. Preforms produced by this method would provide the greatest immediate benefit in applications that were previously considered prohibitive.

As shown in Table III, the end densities of Weaves A, B and C were identical and pick densities decrease progressively from A to C. Although the pick density of A was greater than B, A had lower fabric weight (23.6 oz/yd^2) compared to B (23.9 oz/yd^2). This may be attributed to the differences in weave geometry resulting in greater yarn crimp in Weave B. This was confirmed by the greater thickness of Weave B (0.051 in) when compared to Weave A (0.049 in). Therefore the total amount of yarn per unit volume in B was greater than in A, which corresponded to the fabric weights obtained.

A comparison of Composites A, B, and C in terms of thickness, weight and fiber volume fraction is shown in Table IV. Due to the pressures exerted during composite curing, the prepregs were compressed to a uniform thickness of 0.038 inches.

Downloaded by UNIV OF GUELPH LIBRARY on August 6, 2012 | http://pubs.acs.org
Publication Date: April 3, 1991 | doi: 10.1021/bk-1991-0457.ch004

TABLE II. Tensile Testing Conditions

	0°(warp)	90°(filling)
Gauge Length	5"	3"
Full Scale Load	1500 lb	5000 lb
Chart Speed	0.5 in/min	0.5 in/min
Cross Head Speed	0.05 in/min	0.05 in/min
Number of Tests	5	5

TABLE III. Fabric Specifications

Weave	Thickness (Inches)	End Density (ends per inch)	Pick Density (picks per inch)	Fabric Weight (oz per yd^2)
Weave A	0.49	49	74	23.6
Weave B	0.52	49	70	23.9
Weave C	0.51	49	61	22.5

TABLE IV. Composite Specifications

Composite	Thickness (inches)	Weight (oz per yd^2)	Fiber Vol. Fraction (%)
Composite A	.038	34.3	68.8
Composite B	.038	32.6	73.3
Composite C	.038	31.3	71.9

TABLE V. Composite Properties
(Average of 5 Tests)

	Tensile Strength (ksi)	Modulus (ksi)	Flexural Yield Strength (ksi)
Composite A (0°)	36.9	522.8	18.1
Composite B (0°)	30.5	441.0	21.5
Composite C (0°)	30.8	527.1	14.4
Composite A (90°)	49.7	464.4	35.1
Composite B (90°)	42.8	357.7	24.6
Composite C (90°)	51.4	460.5	21.6

Downloaded by UNIV OF GUELPH LIBRARY on August 6, 2012 | http://pubs.acs.org
Publication Date: April 3, 1991 | doi: 10.1021/bk-1991-0457.ch004

Downloaded by UNIV OF GUELPH LIBRARY on August 6, 2012 | http://pubs.acs.org
Publication Date: April 3, 1991 | doi: 10.1021/bk-1991-0457.ch004

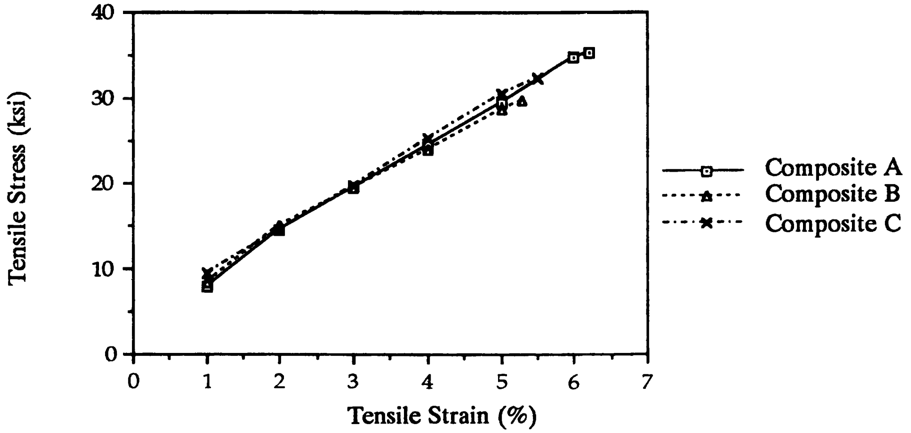

Figure 15. Typical 0° Tensile Stress-Strain Curves of Composites A, B and C.

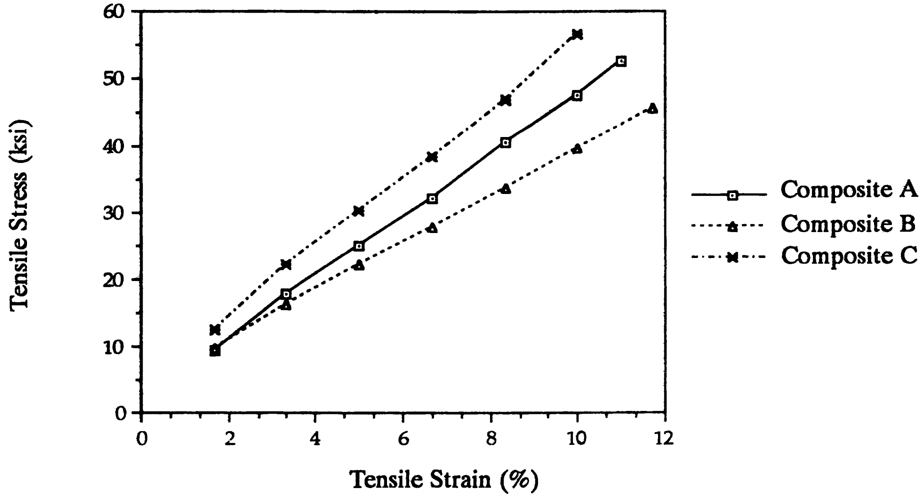

Figure 16. Typical 90° Tensile Stress-Strain Curves of Composites A, B and C.

Downloaded by UNIV OF GUELPH LIBRARY on August 6, 2012 | http://pubs.acs.org
Publication Date: April 3, 1991 | doi: 10.1021/bk-1991-0457.ch004

It was difficult to compare the mechanical properties of the three composites since there were significant variations in specifications among them and there was no satisfactory method of normalizing the data obtained from mechanical testing. The only comparable specification occurred in Composites A, B and C having the same end density. Therefore comparison of data obtained in tests at 0° would be more conclusive than tests at 90°.

Table V gives the average values of tensile strength, modulus and flexural yield strength for the three composites. The tensile strengths in both 0° and 90° were statistically analyzed by the Analysis of Variance technique (*27*). The results indicated that at 0.05 level of significance, the differences among the averages of Composites A, B and C in both 0° and 90° directions were not significant. Moreover, the tensile strength of the composites at 0° could not be compared to the tensile strength of the composites at 90° since the gauge length of the samples were different.

Tensile moduli data were analyzed in the same manner as the tensile strength data. The results indicated that at 0.05 level of significance, the differences among the averages at 0° were not significant but were significant at 90°. In comparing tensile moduli at 90°, there appears to be no dependence upon yarn density or weave geometry.

In analyzing data on flexural yield strength, the differences among averages in both 0° and 90° tests were significant. In comparing 0° flexural yield strength values, Composite B had the highest value (21.45 ksi) then A (18.091 ksi) followed by C (14.37 ksi). As the end densities for the three composites were the same, the values obtained did not show any dependence upon weave geometry. The flexural yield strength values from 90° testing were inconclusive and could not be compared since both pick density and weave geometry were different for the three composites.

C-Scan. C-Scan measurements performed on the composites showed numerous voids dispersed throughout the structures. According to Mallick (*28*), the presence of voids is considered the most critical defect in influencing the mechanical properties of a composite, with a high void content (over 2% by volume) usually leading to increased variation. Regardless of resin type, fiber type and fiber surface treatment, the interlaminar shear strength of a composite material decreases approximately 7% for each 1% of voids up to a total void content of 4% (*29*).

Conclusions and Recommendations

This research has shown that modified conventional weaving equipment can be used to produce three-dimensional multilayer fabrics for use in composites. Preforms produced by this method would provide the greatest immediate benefit in applications that were previously considered prohibitive.

To provide a low cost, automated fabrication method and also eliminate some of the problem in preform fabrication, a power loom in conjunction with a creel should be used. In a power loom, the beat-up of weft yarns is controlled mechanically, which would provide a uniform pick density. In addition, different preforms with identical pick densities can be produced. With end and pick densities equal for all preforms, a more conclusive comparison could be made on the effect of fiber orientation upon composite properties.

For weaving fine filament yarns of low strain to break, the best preform quality would be obtained by a loom with the most gentle yarn treatment. Such a loom would be the rapier, in which the weft yarns are positively controlled throughout the picking cycle. In addition, since the height of the rapier head is smaller than shuttle heights, the shed height and angles of deflection of warp yarns in the heddles could be made lower than on shuttle looms, thereby reducing warp tensions.

The composites fabricated in the research contained a high void content as evidenced in the C-scan results. Voids are due to incomplete wetting out of dry fibers by the resin system, caused by fibers tightly packed fibers and/or highly resin viscosity. Voids can also be caused by processing conditions in composite curing. Therefore, to reduce voids, the matrix system should be changed or process parameters during composite curing modified.

Due to constraints in the number of harnesses available in the loom, the maximum number of layers in each fabric was limited to five. With increased number of harnesses, fabrics with more layers and therefore increased thickness could be fabricated.

With the equipment utilized in this research, there are numerous possibilities in tailoring fiber geometry and component materials to meet performance specifications. For example, the intensity of stitching could be regulated according to the amount of interlaminar strength required, or hybrid fabrics produced where the stitching yarns could be of a different type or size of fiber. Another possibility could be to have regions of warp in which end density or component yarn sizes are different. This would produce variations in thickness across the width of the fabric and continuously along the length. Composites from this preform may be used in applications that require stiffeners in specific regions.

Acknowledgments

The authors would like to thank United Technologies for supporting part of this research through a graduate fellowship (to PST). Thanks are also due American Cyanamid and Lockheed-Georgia for their assistance in prepregging and composite fabrication, respectively.

Downloaded by UNIV OF GUELPH LIBRARY on August 6, 2012 | http://pubs.acs.org
Publication Date: April 3, 1991 | doi: 10.1021/bk-1991-0457.ch004

Downloaded by UNIV OF GUELPH LIBRARY on August 6, 2012 | http://pubs.acs.org
Publication Date: April 3, 1991 | doi: 10.1021/bk-1991-0457.ch004

Literature Cited

1. Huntoon, R. H. *America's Textile International*, May **1988**, *72*.
2. Schwartz, M. *Composite Materials Handbook*, McGraw-Hill Book Company, New York, **1984**, p. 313.
3. Williams, J. F.; Stouffer, D. C.; Illic, S.; and Jones, R. *Composite Structures*, Vol. 5, March **1986**, *204*.
4. Browning, C. E. and Schwartz, H. S. *Composite Materials; Testing and Design (Seventh Conference)*, ASTM STP 893, J. M. Whitney, Ed., American Society for Testing and Materials, Philadelphia, **1986**, p. 256.
5. *Technology Sensor*, Battelle, Columbus, Ohio, No. 45, April **1987**, *1*.
6. King, R. W. U.S. Patent 3,904,464, Sept. 9, **1975**.
7. Stover, E. R. U.S. Patent 4,400,421, Aug. 23, **1983**.
8. Vasilos, T. U.S. Patent 4,209,506, June 24, **1980**.
9. Bruno, P. S.; Keith, D. O.; Vicaro, Jr., A. A. *SAMPE Quarterly*, Vol. 17, No. 4, July **1986**, *10-17*.
10. Rolinick, P. G. Jr., 32nd International SAMPE Symposium, April 6-9, **1987**, *195-207*.
11. Banos, J.; Cantagrel, J.; Cahuzac, G.; Darrieux, Jean-Louis U.S. Patent 4,346,741, Aug. 31, **1982**.
12. Holman, H. A.; Kallmeyer, A. W; Weaver, W. Weaving Machine and Method, U.S. Patent 3,750,714, Aug. 7, **1973**.
13. Male, M. E. *Process Design News*, Vol. 2, No. 9, September **1974**, *14*.
14. Fukuta, K.; Onooka, R.; Aoki, E.; Tsumuraya, S. U.S. Patent 4,336,296, June 22, **1982**.
15. Cahuzac, G. J. J., U.S. Patent 4,492, 096, Jan. 8, **1985**.
16. Wilkens, C. U.S. Patent 4,518,640, May 21, **1985**.
17. Hutson, H. K. U.S. Patent 4,484 459, Nov. 27, **1984**.
18. Florentine, R. A. U.S. Patent 4,312,216, Jan. 26, **1982**.
19. Ko, F., Fourth International Conference on Composite Materials, Tokyo, Japan, **1982**.
20. Macander, A. B.; Crane, R. M.; Camponeschi, E. T. Jr. *Composite Materials: Testing and Design, (Seventh Conference)*, J. M. Whitney, editor ASTM STP 893, American Society for Testing and Materials, **1986**.
21. Brown, R. T., 30th National SAMPE Symposium, March 19-21, **985**.
22. Popper, P., and McConnell, R., "A New 3D Braid for Integrated Parts Manufacture and Improved Delamination Resistance- The 2-Step Process," 32nd International SAMPE Symposium, April 6-9, **1987**.
23. "Characteristics and Uses of Kevlar 49 Aramid High Modulus Organic Fiber," *Bulletin K-5*, E. I. du Pont de Nemours and Co., September **1981**.

24. *Kevlar- The Tough, Lightweight Material for Composite Structures*, E.I. du Pont de Nemours & Co.
25. *Bulletin K-E*, E.I. du Pont de Nemours and Co., Dec. **1978**.
26. Zweben, C.; Smith, W. S.; and Wardle, M. W. *Composite Materials: Testing and Design (Fifth Conference)*, ASTM STP 674, S. W. Tsai, Ed., American Society for Testing and Materials, **1979**, p. 223.
27. Miller, I. and Freund, J. E. *Probability and Statistics for Engineers*, 2nd Edition, Prentice-Hall, Inc., Englewood Cliffs, New Jersey, **1977**, pp. 331-341.
28. Mallick, P. K. *Fiber-Reinforced Composites: Materials, Manufacturing and Design*, Marcel Dekker, Inc., New York, New York, **1988**, p. 66, 329.
29. Hull, D. *An Introduction to Composite Materials*, Cambridge University Press, Cambridge, **1981**, p. 75.

RECEIVED September 10, 1990

Downloaded by UNIV OF GUELPH LIBRARY on August 6, 2012 | http://pubs.acs.org
Publication Date: April 3, 1991 | doi: 10.1021/bk-1991-0457.ch004

Chapter 5

Industrial Applications of Multiaxial Warp Knit Composites

James R. Kaufmann

PBI Products Division, Hoechst Celanese Corporation, P.O. Box 32414, Charlotte, NC 28232

Downloaded by CORNELL UNIV on August 6, 2012 | http://pubs.acs.org
Publication Date: April 3, 1991 | doi: 10.1021/bk-1991-0457.ch005

Over the past few years, Multiaxial Warp Knit (MWK) fabrics have made significant inroads into the industrial composites arena. This paper will examine the use of MWK fabrics in industrial composite applications. Although the focus will be on current applications of MWK fabrics in composites, this paper will also discuss the physical properties, advantages and disadvantages of MWK fabrics. The author will also offer possibilities for the future of MWK fabrics in the industrial composites arena.

According to a Frost and Sullivan study, the demand for high performance composite materials in the USA should more than triple between 1987 and 1992 (3). A yearly growth rate of high performance composite materials for this same period has been forecast to be at least 25%. Others predict that the worldwide market for composite materials, currently at $2 billion will grow to $20 billion by the year 2000 (8). One of the biggest reasons for this projected growth is the ever-expanding use of composite structures in industrial applications.

Advanced composite structures, high strength materials combined with a resin system, are being used in the most diverse sectors of the industrial arena. One fabric that is playing an increasingly important roll in this arena is the Multiaxial Warp Knit (MWK). MWK fabrics are ideally suited for this type of end use because of their flexibility and engineerability. MWK fabrics, produced in a one-step process, have properties similar to those of quasi-isotropic layup structures. Besides good handleability, MWK fabric preforms are extremely conformable.

This paper will examine the use of MWK fabrics in industrial composite applications. The focus will be on the MWK fabric itself, and why it is being used as a preform in industrial composites. Current end use applications for the MWK fabric composites will be discussed and possibilities for the future of MWK fabrics in the industrial composites arena will also be offered.

0097–6156/91/0457–0081$06.00/0

What Is An MWK Fabric Composite

The basic principle of fabric composites is to combine the singular properties of more than one substrate and/or medium to create a single structure that performs much better than any of the individual components. An advanced composite is based on the same principle as using steel reinforced concrete to build a bridge, or straw and mud to make a brick for building a fireplace. In advanced composite structures, reinforcing fibers or fabrics are embedded in resin systems such as epoxy or other binders. Multiaxial warp knitting is a means of manufacturing stable reinforcing fabrics from fibers such as graphite, glass, Kevlar, ceramic, or other textile fibers which have the ability to resist stress and strain from any direction.

MWK fabrics are unique structures which are produced by warp knitting techniques. With these techniques, straight ends of parallel and uncrimped yarns are inlaid into the knitted structure at virtually any desirable angle. Because of the versatility of this process, fabric characteristics can be engineered into the structure to give the ideal combination of mechanical properties at a favorable production cost. This produces MWK fabrics, with the combined advantages of design flexibility, performance, productivity, and availability, the potential to become a major fabric preform for industrial composites.

An industrial composite can be defined as any composite structure that is not being used as a household good such as kitchen utensils, furniture, clothing, jewelry, and/or sporting goods.

Downloaded by CORNELL UNIV on August 6, 2012 | http://pubs.acs.org
Publication Date: April 3, 1991 | doi: 10.1021/bk-1991-0457.ch005

THE MWK FABRIC

MWK fabrics generally possess up to four different load bearing yarn systems arranged so that each can take on stress and strain in virtually all directions. Since these load bearing yarns lie straight in the fabric, with no crimp, the physical parameters of the individual yarn system is fully utilized.

From a structural geometry viewpoint (see Figure 1), MWK fabrics consist of warp (0 degrees), weft (90 degrees), and bias (+/- various degrees) yarns that are stitched together during the warp knitting process by a fifth yarn system through the thickness of the fabric structure (4). The warp and weft yarns stabilize the fabric in the machine and cross machine directions while the diagonally arranged or biased yarns absorb tension from any required angle. The fifth yarn precisely binds together all of the load bearing yarn systems. The bias or diagonal yarns in the fabric can be inlaid at any angle along the plane of the machine direction, the most common of which is +/- 45 degrees. It should be noted that all four load bearing yarn systems do not have to be used in a MWK fabric construction. Also, different yarn types and counts can be used in each of the yarn systems. MWK fabrics allow the designer freedom of choice in the arrangement of load bearing yarns in the structure. This provides the fabric designer with a tremendous amount of design flexibility.

Unlike the crimp inserted into the yarn in woven fabrics during weaving, the load bearing yarn in MWK fabrics lies straight and parallel to other yarns in its yarn system. This characteristic of MWK fabrics allows for the yarn properties to be more fully utilized

Downloaded by CORNELL UNIV on August 6, 2012 | http://pubs.acs.org
Publication Date: April 3, 1991 | doi: 10.1021/bk-1991-0457.ch005

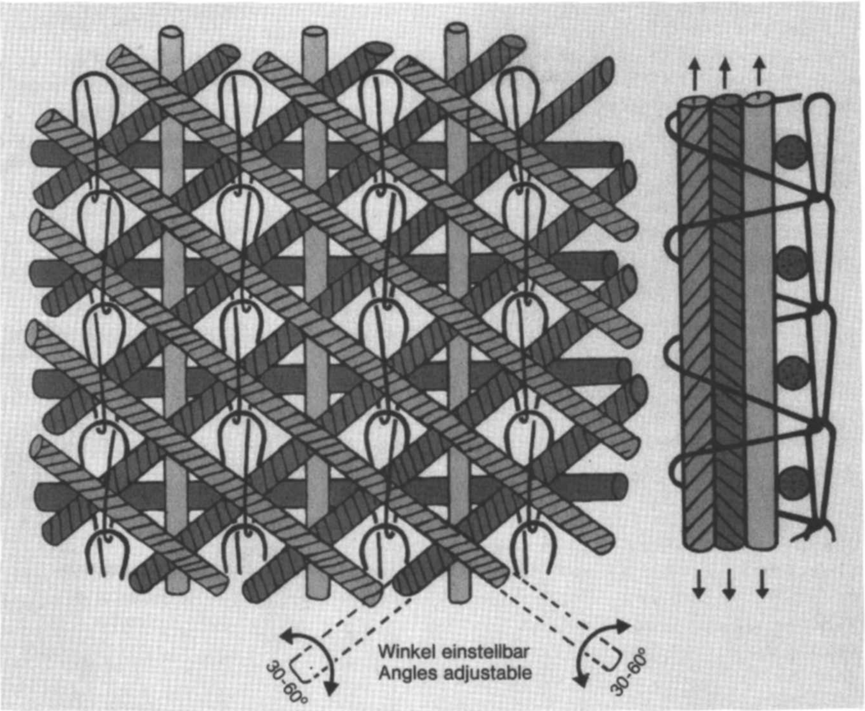

Figure 1. Structural representation of MWK fabric. (Reproduced with permission from ref. 10. Copyright Mayer Textile Machine Corporation.)

in withstanding in-plane forces. Fabric design is made easier because the designer can more accurately calculate the tensile load of a MWK fabric with a much higher degree of confidence than had been previously attainable with woven fabrics. Testing is still required to verify the estimates, but the starting points can be calculated instead of guessed at. In addition to design flexibility, isotropic stress and strain resistance, excellent tear resistance, and improved conformability to complex shapes are also characteristics of the MWK family of fabrics.

MWK fabrics are capable of withstanding stresses and strains in an optimum fashion. This is due largely to the parallel and straight arrangement of the load bearing yarns in the MWK fabric. Because the load bearing yarns lie straight in the fabric, their tensile properties are fully utilized and are able to absorb tension without the elasticity that occurs when the yarns are crimped or in a wavelike form, such as in a woven fabric. Because of the arrangement of the yarn systems at various angles (see Figure 1), the MWK fabric is able to withstand shear forces from various angles (7). This isotropic ability is particularly important in many of the advanced composite structures and a primary reason for the use of MWK fabrics.

Downloaded by CORNELL UNIV on August 6, 2012 | http://pubs.acs.org
Publication Date: April 3, 1991 | doi: 10.1021/bk-1991-0457.ch005

Due to the parallel nature of the load bearing yarns in the MWK fabric, excellent tear propagation resistance is achieved. If a tear were to occur in the MWK, the yarn layers would shift slightly under the force of the tear and bunch together. The inherent movement of the load bearing yarns and the diagonal element would act to reinforce the area and prevent further tearing (7). This resistance to tear propagation becomes increasingly important when a MWK structure is damaged while in use (such as in a sail, inflatable structure, or aircraft skin). The damage is minimized by the resistance to further tearing (2).

Because the yarn systems are not interwoven, but rather lie directly on top of each other and are held together by the fifth yarn system, conformability of the fabric is greatly improved. This allows the MWK fabric preforms to conform to many complex geometrical shapes and still maximize the translation of fiber mechanical properties to the composite structure. The conformability of the uncured MWK fabric also provides good shape retention during the laying up and curing process.

By combining a web or nonwoven fabric (usually nylon, polyester or fiberglass) to the MWK fabric during the knitting process, it is possible to control many other physical aspects of the fabric structure. Both the MWK fabric and the web can demonstrate their specific advantages. Because the web is fed into the knitting machine during production of the MWK fabric, it is linked to the load bearing yarns by the stitch yarn, rather than being rigidly bonded. This allows for a certain amount of give to the MWK and web structure.

Adding a web to the MWK structure allows the designer even greater design flexibility. Addition of a web can further control the strength and elongation of the MWK fabric, and at the same time provide variations of fabric cover and density, water and air permeability, stiffness, thickness, initial tear resistance, increased tear propagation resistance, and yarn slippage resistance; all of which can be tailored by the designer to meet the end use requirements of the MWK fabric. The web also provides greater stability of the yarn layers during the further processing stages of creating an industrial composite. It has been shown that the addition of a web to the MWK preform increases the flow of resin during the resinating process in making the advanced composite structure. This results in better processing times and lower production costs (5).

Few, if any other fabric production techniques, offer such a wide range of properties with such versatility in relation to type and count as MWK fabrics. Although a comprehensive data base is not yet available for MWK fabrics due to their relatively recent introduction into the industrial composites arena, several studies have been done and are being carried out to assess their potential (6). The obvious properties that MWK fabric composites offer the industrial composites arena are their incredible design flexibility, isotropic stress and strain resistance, tear propagation resistance, and conformability (9).

Downloaded by CORNELL UNIV on August 6, 2012 | http://pubs.acs.org
Publication Date: April 3, 1991 | doi: 10.1021/bk-1991-0457.ch005

Table I. Listing of MWK Composite Applications by Category

INDUSTRY	MARINE	AEROSPACE	OTHER
Estimated % of MWK Fabric Composite Market	65%	20%	15%
Applications	-hulls -decks superstructure substructure -support beams -motor bays -sails -racing shells	-aircraft skin -tail units -fuselage paneling -leading edges on wings and rudders -engine paneling -rotor blades -ballistic protection	-flooring -geotextiles -wall panels -automotive applications -protective helmets -industrial belting -inflatables

End Use Applications of Industrial Composites Using MWK Fabrics

Because the MWK fabrics are relatively new to the industrial composites arena, the number of recognizable end use applications is relatively small when compared to those of traditional woven fabrics. But when given the head start that woven fabrics have had, some several hundred years, the progress made by MWK fabrics in the industrial composites arena is nothing less than phenomenal.

The majority of current end uses for industrial composites made from MWK fabrics can be separated into two different industries, marine and aerospace. Probably 65 percent of all MWK fabrics currently made are used in marine composite applications, while another 20 percent is used in the aerospace industry. The remaining 15 percent encompass all of the varied end use applications being evaluated with MWK fabric composites. Table I divides many of the current end uses into the three categories.

MWK fabrics are becoming the fabric preform of choice in the marine industry, especially in yachts, sailboats, and high speed racing boats. The MWK fabric composite is generally used in these vessels for the hulls, deck superstructures and substructures, and motor bays.

Because of the isotropic properties of the MWK fabric structure, boat designers are finding that they can use less MWK fabric in the composite structure and still maintain, or often improve upon, the structural integrity and torsional stiffness of the boat. This also means that boat hulls made of MWK fabric composites can withstand greater stresses and strains with less overall weight. Less overall weight obviously requires less energy to power the boat, which translates into fuel savings and/or faster boats. The improved structural integrity makes the boat safer at higher speeds.

MWK fabric composites are being used in most of the fastest ocean going racing boats and yachts because of their increased stability and weight savings. The hulls and masts of several of the sailboats used in the America's Cup competition were made of MWK fabric composites because of the performance edge experienced by using these composite structures. Partially as a result of using MWK fabric composite structures, speed boats and racing boats are achieving speeds previously thought to be unreachable with any degree of safety.

Another example of improved performance as a result of using MWK composite structures in marine applications was seen in a new generation of racing shells used by some of the top rowing teams in the country. The shells (long narrow row boats, usually powered by 8 rowers) were found to give a greater translation of power into speed because of the improved torsional stiffness. This allowed energy to be translated more directly into speed rather than being absorbed by the shell when flexing.

MWK fabrics are also being looked at for applications in sails. In this case, however, the composite structure is the MWK fabric combined with a plastic film, usually through laminating. Because of the lack of crimp in the yarn in the MWK composite structure, the force of the wind is immediately translated into power and not absorbed at all by the crimp deformation associated with woven fabric structures.

Fabric composites of all types are being used in the marine industry because of their inherent resistance to corrosion. This saves on the manufacturing cost because expensive metal treatments and repeated paintings are not needed to protect the craft from the corrosive nature of salt water.

In the aerospace industry, which includes the military, aerospace and commercial aircraft industries, MWK fabric composites are being used more and more. Relatively speaking, they are being used in this industry for many of the same reasons as in the marine industry, namely reduced weight, and increased strength and integrity. Because of the flexibility and tailorability of mechanical and physical properties, MWK fabric composites can be customized for the application and specific properties can be emphasized to suit the particular need.

Currently, there are very few aircraft that use MWK fabric composites in critical structures such as the fuselage or wings. Most current applications center around the skin of the aircraft. Other areas of use are in the top and side tail units, fuselage paneling, leading edges on side rudders, and engine paneling. MWK fabric composites are also being evaluated for rotor blades, outer skin, and ballistic protection for helicopters. It is thought that the use of MWK composites is also being evaluated in the new military plane/helicopter, the V-22 Osprey, and the all-composite Beech Starship business plane (8).

Downloaded by CORNELL UNIV on August 6, 2012 | http://pubs.acs.org
Publication Date: April 3, 1991 | doi: 10.1021/bk-1991-0457.ch005

The lower weight achieved through the use of MWK composite structures means that less fuel is consumed by the aircraft, which translates into significant energy savings for the user. Also, because of the improved structural integrity offered by the MWK fabric composite, it is believed that safety is enhanced.

Other various applications for MWK fabric composites can be found in the industrial composites arena. In Europe, MWK fabric composites are being used for flooring in sports halls where the combination of multi-directional force distribution and excellent tear resistance are beneficial. The MWK fabric composite also helps to improve the sound damping characteristics of the flooring. MWK fabrics coated with rubber are also being used in the industrial roofing industry.

The Future of MWK Fabric Composites In Industrial Applications

Downloaded by CORNELL UNIV on August 6, 2012 | http://pubs.acs.org
Publication Date: April 3, 1991 | doi: 10.1021/bk-1991-0457.ch005

The main obstacle in gaining acceptance for MWK fabric composites in the industrial composites arena has been the lack of confidence derived from inexperience and a lack of sustained performance data for MWK composites. With the advent of time, these obstacles will undoubtedly be overcome and MWK fabric composite usage will dramatically increase (1).

Numerous end use possibilities exist for MWK fabric composites. They can not only be used to replace traditional materials, but also to improve the performance of many new industrial composites which seem to have reached their performance limit. MWK fabric composites can be used to replace traditional structural materials such as concrete, wood, and steel, thus creating new possibilities in various industries and end uses.

The advantages of using MWK fabrics in composite structures are clearly the flexibility and freedom of choice in the desired properties in all directions which can be matched to individual needs. As a result, MWK fabric composites are uniquely suited to a wide range of industrial applications.

MWK fabric composites incorporating a nonwoven are ideally suited for many high strength geotextile applications, where isotropic strength, resistance to tear and tear propagation, good water permeability, low creep, and good fabric/soil interaction are required.

With the flexibility of fiber placement and potentially high productivity, MWK fabric composites are ideally suited for many structural load bearing applications in the automotive and aerospace industries. MWK fabrics, because of their structural makeup, have good flexibility which allows them to be formed during molding into virtually any desired shape. The through thickness reinforcement provided by the stitching process helps to reduce the possibility of delamination of layers in the composite structure.

Numerous applications for MWK fabric composites also include protective helmets and armored protection of vehicles, buildings, and people. Various drive belts, V-belts, fan belts, and conveyor belts will benefit from the availability of diagonal load bearing yarns in the composite structure. Inflatable rafts, cushions, balloons, and fuel cells are ideal applications due to the MWK fabric composite's isotropic strength and tear resistance.

There are probably hundreds or even thousands of other areas that could benefit via the use of MWK fabric composites. The flexibility of the MWK fabric system provides endless potential end use applications. All that is needed is for the designers and engineers of the world to dare to improve upon what they already have and open their minds to the future.

Conclusions

The MWK process offers limitless possibilities for the formation of new fabric preforms for the composites industry. By varying the angle of the load bearing yarn systems, and the type and count of yarn used, the strength in any fabric direction can be tailored to the requirement, rather than the requirement being tailored to the fabric available. Because of the complete versatility of the MWK fabric, design flexibility is virtually limitless.

MWK fabric composites offer many never before realized advantages to the industrial composites arena, giving the designer flexibility that he or she has never before had. The ability to design a composite structure with the load bearing systems aligned precisely where it is needed provides opportunities to make better, more cost efficient structures.

The use of MWK fabric composites in many of the areas mentioned earlier shows that their development is worthwhile. New end uses are being developed daily and in many cases MWK fabric composite structures are being used to replace expensive, heavier or technically inferior constructions produced from other materials. Many times these replacements are converted directly into cost savings. Also, with each new application, comes more experience and an addition to that ever-expanding data base, which so many engineers and designers require. All that is needed is for them to open their minds and give MWK fabric composites a try.

Acknowledgments

The author wishes to thank the people at Karl Mayer Textile Machine Corporation and Advanced Textiles, Inc. for their help and support in supplying much of the information used for this paper. Their assistance was greatly appreciated. The author would also like to thank his employer Hoechst Celanese for allowing him the time and facilities to produce this paper.

References

1. Allbee, Nancy, "Tapping the Market for Industrial Applications," Advanced Composites Magazine, July/August, 1989, pp. 49-52.
2. "Excellent Tear Propagation Resistance Properties of Bi- and Multi-Axial Structures," Kettenwirk Praxis, February, 1989, p. 65.
3. "Industrial Textiles With High Growth Rates," Kettenwirk Praxis, February, 1989, p. 45.
4. Ko, F., "Multiaxial Warp Knit Composites: Structure, Properties, and Analysis," International Man-Made Fibres Congress, September, 1986.
5. "Multiaxial Structures With Web Inserts and Diagonal Yarns in Alternate Directions," Kettenwirk Praxis, March, 1988, pp. 5-10.

Downloaded by CORNELL UNIV on August 6, 2012 | http://pubs.acs.org
Publication Date: April 3, 1991 | doi: 10.1021/bk-1991-0457.ch005

6. Raz, S., "Bi-Axial and Multi-Axial Warp Knitting Technology," Kettenwirk Praxis, March, 1987, pp. 11-16.
7. Raz, S., "The Karl Mayer Guide to Technical Textiles," Special Supplement to Kettenwirk Praxis, January/February, 1989, pp. 60-94.
8. Slutsker, Gary, "Don't Screw It, Glue It," Forbes Magazine, November 28, 1988, pp. 234-239.
9. Technical Bulletin, Mayer Textile Machine Corporation, 7102 Sherwin Extraordinary Strength Properties Achieved Through Multi-Axial Magazine-Weft Insertion."
10. Technical Bulletin, Mayer Textile Machine Corporation, 7102 Sherwin Road, Greensboro, N.C. 27410, "RS-2-DS."

RECEIVED September 10, 1990

Downloaded by CORNELL UNIV on August 6, 2012 | http://pubs.acs.org
Publication Date: April 3, 1991 | doi: 10.1021/bk-1991-0457.ch005

Downloaded by UNIV MASSACHUSETTS AMHERST on August 6, 2012 | http://pubs.acs.org
Publication Date: April 3, 1991 | doi: 10.1021/bk-1991-0457.ch006

Chapter 6

Design and Fabrication of a Braided Composite Monocoque Bicycle Frame

Nicholas Casale[1,3], Daniel Bristow[1,4], and Christopher M. Pastore[2]

[1]Department of Mechanical Engineering, Drexel University, Philadelphia, PA 19104
[2]Department of Textile Engineering, Chemistry, and Science, North Carolina State University, Raleigh, NC 27695–8301

In the fast growing field of competitive bicycle racing, there exists an increasing demand for high performance, lightweight bicycle frames. Whereas there have been advances in the replacement of traditional steel alloy frames with lighter weight aluminum alloys, the frames available today have reached a minimum weight. By utilizing today's high-strength, lightweight composite materials, bicycle frames can now achieve weights never before possible without sacrificing strength or rigidity.

Textile structural composites have been employed as the engineering material for the fabrication of a light weight road-racing bicycle frame. The use of these materials provides advantages over metallic structures in terms of high specific strength and stiffness as well as the ability to engineer the properties of the material to enhance structural design. The use of textiles as the reinforcing element of the composite provides advantages over traditional filament wound systems by increaseing the damage tolerance of the material and reducing the fabrication labor intensity.

In this paper, an integrated design methodology (1) is presented for the design and fabrication of a composite frame. The objective is to develop design procedures which go beyond the traditional "black aluminum" design approach (i.e., direct subsitution of composites for metal) and develop a technique for exploiting the unique and anisotropic properties of composite materials. The integrated design approach incorporates composite mechanics, processing of composite materials and finite element analysis in an iterative mode to identify locally optimal fiber architectures and frame geometries, as

[3]Current address: Phillips 66 Company, Advanced Composites, Bartlesville, OK 74004
[4]Current address: G.E. Nuclear Energy, King of Prussia, PA 19406

0097–6156/91/0457–0090$06.00/0

Downloaded by UNIV MASSACHUSETTS AMHERST on August 6, 2012 | http://pubs.acs.org
Publication Date: April 3, 1991 | doi: 10.1021/bk-1991-0457.ch006

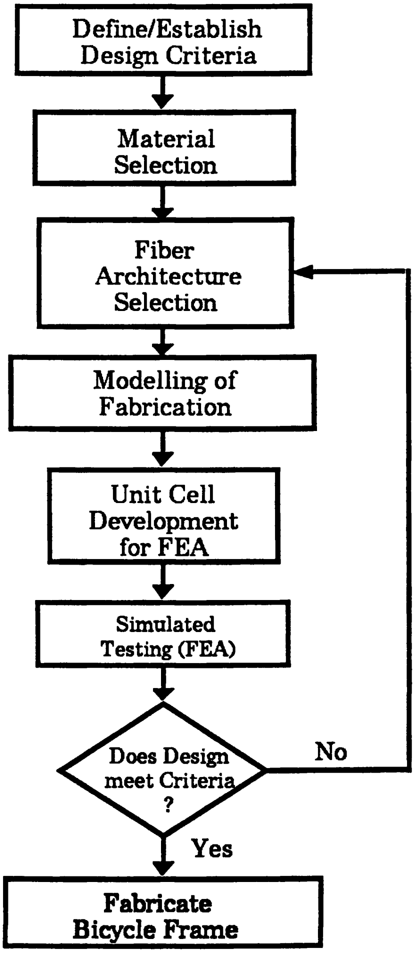
Define/Establish Design Criteria
Material Selection
Fiber Architecture Selection
Modelling of Fabrication
Unit Cell Development for FEA
Simulated Testing (FEA)
Does Design meet Criteria ?
No
Yes
Fabricate Bicycle Frame

Figure 1. Logical Flow of Integrated Design Methodology.

illustrated in Figure 1. To maximize the strength required by the frame, and without adding unnecessary weight, frame designs were evaluated using three dimensional stress analysis for the candidate frame geometries. By concentrating the frame's strength at critical stress areas, all excess material (hence weight) can be eliminated. To properly engineer the frame, each tube of the frame needs individual attention. The cross-sectional geometry, wall thickness, fiber orientation, and fiber volume fraction were designed specifically to meet each tube's individual stress requirements.

The result of this research is a design and subsequent fabrication of a light weight road racing frame built from textile structural composites. In addition to developing a minimal weight frame, this research also addressed the issue of manufacturing. The fabrication technique takes advantage of an automated braiding process which allows for hybrid materials to be incorporated into the frame in a single processing step. The structural geometry was designed to incorporate an attractive aesthetic design which coincides with its intended purpose. To this end, one of the main tubes that appears in a conventional frame was eliminated.

Five prototype frames have been constructed to validate the design. Qualitative tests were performed on this frame to evaluate the composite processing and joining techniques used.

Downloaded by UNIV MASSACHUSETTS AMHERST on August 6, 2012 | http://pubs.acs.org
Publication Date: April 3, 1991 | doi: 10.1021/bk-1991-0457.ch006

Material Selection and Verification

A material selection phase was carried out to identify the most promising fibers and matrices for the composite frame. The choice of material system was based upon four principal criteria: weight, stiffness, strength, and cost. Whereas strength and stiffness are necessary for the successful development of the frame, the issues of weight and cost provide the engineering constraints to the project. In particular, since the composite is a moving vehicle, minimization of weight translates to reduced energy expenditures for riding. Additionally, the materials cost for the frame should not be high or the frame is unrealistic.

Fibers. The selection of fibrous materials for the reinforcement of the composite is critical to the performance and weight of the frame. An initial investigation was carried out examining the effects of combining different materials into a single fabric. Using the braiding process as the method of preform fabrication, it is possible to construct hybrid fabrics (2,3). The braiding machine consists of a set of oriented (braider) yarns, and one set of longitudinal yarns. It is possible to use a different fibrous material in each of these sets. Additionally, it is possible to subdivide the braider yarns into two different materials. Initially, analysis was carried out to investigate the effects of combining one fibrous material in the braiders and another in the longitudinals. The materials which were analytically investigated singly and in hybrid form are:

E-Glass
Kevlar (aramid)
Silicon Carbide
Graphite
Spectra (polyethylene)

Using a basis of 50° braider yarn orientation, and one half the number of longitudinals as braiders, predictions were carried out for these hybrid composites. All of the predictions are based upon 55% fiber volume fraction. Table I shows the predicted densities of the composite corresponding with the various hybrids. It can be clearly seen that the use of Spectra reduces the weight of the composite significantly in any combination.

Table I. Density in g/cc of Candidate Hybrid Systems

	Longitudinals				
Braiders	E-Glass	Kevlar	Graphite	SiC	Spectra
E-Glass	2.04	1.83	1.90	2.00	1.73
Kevlar	1.61	1.39	1.46	1.56	1.29
Graphite	1.75	1.53	1.60	1.70	1.43
SiC	1.95	1.73	1.80	1.90	1.63
Spectra	1.42	1.20	1.27	1.37	1.10

Based on the weight considerations, E-glass and SiC fibers were eliminated from further evaluation. In addition to the weight considerations of the composite material, predictions of the composite properties were made using a modified laminate theory approach, accounting for the interlacing of the yarns in the fabric (4-6). The details of the analysis are not incorporated in this paper, but are as described in the references.

Figure 2 illustrates a comparison of the tensile moduli of the remaining nine hybrid combinations in composite form. This shows both the predicted axial modulus (E_x) and the transverse, or hoop-direction modulus (E_y).

It can be seen that graphite fibers greatly contribute to the tensile modulus of the composite. This stiffness is critical for the development of a rigid frame. However, since graphite is the heaviest of the fibers under consideration, it is still desirable to include one of the polymeric fibers.

In addition to modulus, tensile strengths were also predicted for these material systems. A summary of the results are illustrated in Figure 3. This figure compares the predicted axial (S_x) and hoop (S_y) strengths of the various composite systems. Although generally the frame performance is stiffness critical, strength is a primary concern in areas of stress concentration, such as joins and bends, and particularly in the bottom bracket.

The Spectra fiber, due to its highly oriented microstructure, provides the greatest strength of the hybrids. Combining these predictions with the modulus and density predictions, a hybrid of graphite and Spectra can be identified as the most promising material system; graphite for its light weight and high stiffness properties and the Spectra for its extreme light weight and high tensile strength.

However, concerns exist with the choice of Spectra as the strong, light weight hybrid. Due to its intrinsic chemistry (highly oriented polyethylene), Spectra will not bond well with resin. The design intention is to translate fiber properties to the composite through stress transfer at the interface between fiber and resin. In order to get a good interface between Spectra and a resin system, it is necessary to modify the surface of the fiber (using a process such as plasma or chemical etching) which will introduce surface microcracks to the fiber. It has been demonstrated that the surface

Downloaded by UNIV MASSACHUSETTS AMHERST on August 6, 2012 | http://pubs.acs.org
Publication Date: April 3, 1991 | doi: 10.1021/bk-1991-0457.ch006

Downloaded by UNIV MASSACHUSETTS AMHERST on August 6, 2012 | http://pubs.acs.org
Publication Date: April 3, 1991 | doi: 10.1021/bk-1991-0457.ch006

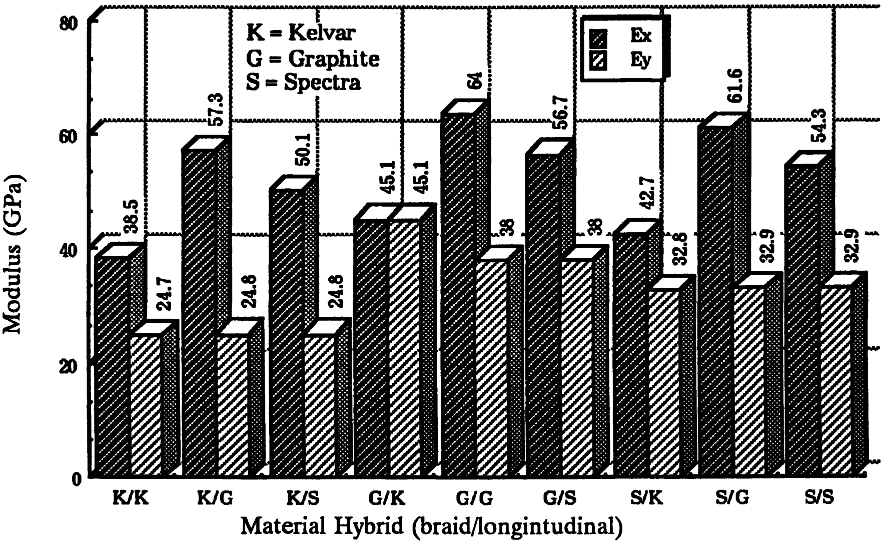

Figure 2. Predicted Tensile Module of the Hybrid Composites.

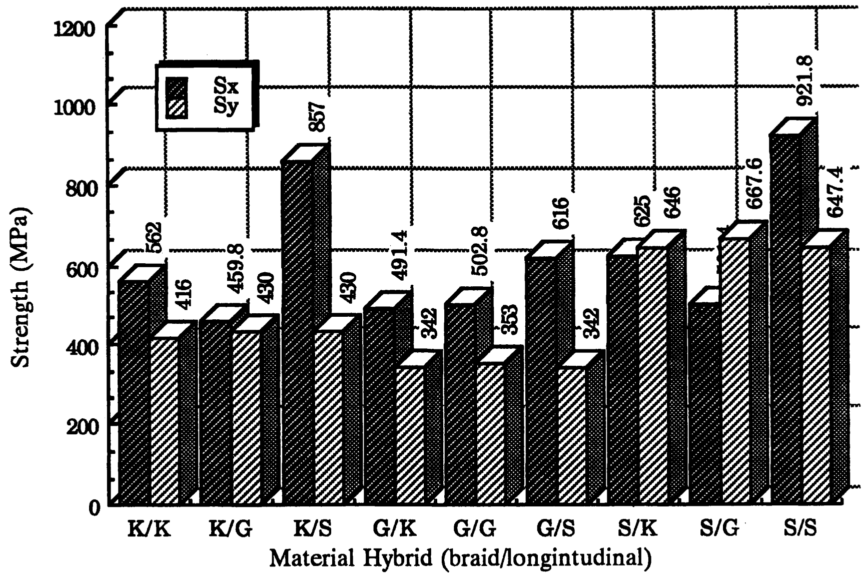

Figure 3. Predicted Tensile Strength of Hybrid Composites.

Downloaded by UNIV MASSACHUSETTS AMHERST on August 6, 2012 | http://pubs.acs.org
Publication Date: April 3, 1991 | doi: 10.1021/bk-1991-0457.ch006

modification of Spectra provides good bonding with resin systems. However, the cost of surface modification is high, and is considered to be out of the scope of this research.

Additionally, other concerns have arisen with regards the creep resistance of Spectra and the low glass transition temperature. Using Spectra will require constraints applied to the material system, principally that the composite cannot go through a cure cycle over 100°C without risking a recrystallization of the polyethylene, so the resin must be chosen accordingly. Substituting another highly drawn polymeric fiber, such as Kevlar, can increase the creep characteristics and T_g while maintaining toughness. Additionally, the good chemical bond between Kevlar and resin will provide additional strength, reduced cost, and reduced processing constraints.

The exchange of Kevlar for Spectra results in a 15% weight increase. However, the additional strength and reduced processing complexities provided by Kevlar is viewed as a good reason to accept this extra weight. Considering the additional factor of safety associated with using Kevlar, it was decided that the weight increase was within the target of performance. Based on this and matrix system selection, an engineering decision was made to switch the material system from Spectra/graphite to Kevlar/graphite for the final frame.

Matrix System. Having selected a fibrous material system, it is necessary to identify a suitable matrix material. The program calls for a low density polymeric resin, with wetting, gelling, and curing properties suitable for the frame geometry. Epon 828 (Shell Chemical Co.) was chosen as the base resin for the epoxy system. Epon 828 is very versatile due to its low reactivity with respect to the polystyrene foam core used as a mandrel. Excellent mechanical and adhesive properties can be achieved, and it is very chemically resistant. With the selection of 828 as the resin, investigations were carried out to determine the optimal curing agent for this particular project. Three curing agents were identified for investigation:

- V-40
- U-80
- D-230 (Jeffamine)

Table II shows a brief summary of typical properties of the epoxies formed with the various curing agents.

Table II. Properties of 828/Curing Agent Epoxies

		V-40	U-80	D-230
Viscosity @ 25°C (Poise)	118	155	8	
Pot life (hours, 400 g @ 25°C)		1.25	0.3	5.5
Cure time (days @ 25° C)	7	10	10	
Cure time (hours @ 80° C)	26	1	2	
Tensile Modulus (GPa)	2.1	3.5	3.1	
Tensile Strength (MPa)	51	51	67	

SOURCE: Data from ref. 7. EPON Resin 828, March 1987.

To evaluate these systems, sample preforms were fabricated and the resin was applied to make a composite. The yarns were wound onto braiding packages and then braided into elliptical cylinders with comparable dimensions to the frame tubes. The braided preforms were then made into composites by consolidating the fabric under atmospheric pressure. The composites were consolidated and sectioned. The sections were examined optically to provide a microscopic analysis of the resin penetration characteristics.

Examination of the composites after consolidation were carried out both in terms of contained porosity determined through density calculations and optical methods. Density measurements showed a high density (8% void) and optical examinations indicated a good wetting between the fibers and matrix. Considering that the composite was densified without vacuum or pressure, the results from this test were considered to be satisfactory.

In order to optimize wetting, the resin must be heated, providing a significantly lower viscosity, hence better flow characteristics through the preform. The need for thermal energy also provides impetus for switching the polymeric hybrid system from Spectra (which softens at 90° C) to Kevlar (service temperature above 220° C). Further experiments were carried out using the U-80 and D-230 curing agents. Through these investigations results indicated that D-230 was the best curing agent for this program. The selection was based upon the relatively short cure time and low viscosity.

Downloaded by UNIV MASSACHUSETTS AMHERST on August 6, 2012 | http://pubs.acs.org
Publication Date: April 3, 1991 | doi: 10.1021/bk-1991-0457.ch006

Structural Analysis

In order to verify the effectiveness of the bicycle frame design, the geometry of the frame was modelled using ANSYS finite element analysis. Figure 4 illustrates the geometry of the bicycle frame. The model was carried out using a space truss analysis with beam elements. The structural analysis was performed by Schwinn Bicycle Company. The structural analysis was run with five standard loading conditions as defined by Schwinn.

The input data for the analysis consisted of bending and torsional stiffness as well as cross-sectional area for each of the beam elements. In this way, it is possible to modify the performance characteristics of individual tubes independently of the others. The input data was based on the predictions of the composite material properties and the geometry of the tubes.

Using the input data, the FEA model was carried out and reviewed. Of principal concern was the deflection of the frame under standard loading. The data was compared to a high performance steel frame with a standard (seven tube) geometry. The results of the first test showed a relatively large deflection at the seat indicating a lack of stiffness in the seat/rear stay area of the frame. Based on these results, a redesign of some of the individual tube geometries was carried out to reduce the seat deflection.

The analysis was carried out again using the new tube geometries, and the results from the second analysis were more acceptable. The deflections decreased by two thirds, which is comparable to the deflection of a steel racing frame under the same loads. Although the seat deflection is still above standard, the value of seat deflection subject to a maximum downward load was on the order of one millimeter, which is within the performance window. Table III details the final design of the tube geometries and moment properties.

Table III. Geometry and Moments of the Frame Tubes

Tube	X-Sect. Geometry	I (in^4)	K (in^4)
Top	Elliptical	0.1747	0.1584
Down	Elliptical	0.1411	0.1639
Chain stay	Rectangular	0.0967	0.0781
Seat stay	Rectangular	0.1818	0.1004
Seat Yoke	Elliptical	0.1980	0.2276

Prototype Fabrication

Having identified a desirable frame and tube geometry, the manufacturing of the frame proceeded. For each tube element, the geometry of the tube and the desired fiber architecture was quantified and the manufacturing parameters determined. The fabrication was carried out by forming net shape mandrels and supplying the yarn in braided fabric form around the mandrel.

A prototype frame was fabricated by braiding carbon and Kevlar fibers over a polystyrene foam core. The polystyrene core was made from blocks of foam shaped to the desired dimensions taken from the full scale engineering drawings, as shown in Figure 5. Although there is a considerable amount of manual labor associated with shaping the foam in this prototyping activity, this can be eliminated through the use of a mold for fabricating the mandrels.

A method for braiding over such a complex structure with sharp angles and transitional tubes like the seat yoke and bottom bracket where one tube breaks off into two is needed. This problem was resolved by breaking the frame into four individual tubes, the top tube/head tube, down tube/bottom bracket, and two rear/chain stays. At this point each section was treated as an individual mandrel.

These mandrels were then inserted into the braiding machine and the braided preform was laid on top of the mandrel, as shown in Figure 6. The first steps in braiding these mandrels were to braid four layers of 12k carbon fiber and Kevlar fibers at ±50° (braiders) with 12k carbon fiber longitudinals. This braid configuration results in the proper tube thickness for the frame.

After braiding the tubes individually, a joining method was required. This is a very complex problem since the fibers at these joints are discontinuous and must be joined (mechanically) to their mating tubes without affecting the structural integrity of the frame. For the prototype frame, the

Downloaded by UNIV MASSACHUSETTS AMHERST on August 6, 2012 | http://pubs.acs.org
Publication Date: April 3, 1991 | doi: 10.1021/bk-1991-0457.ch006

Downloaded by UNIV MASSACHUSETTS AMHERST on August 6, 2012 | http://pubs.acs.org
Publication Date: April 3, 1991 | doi: 10.1021/bk-1991-0457.ch006

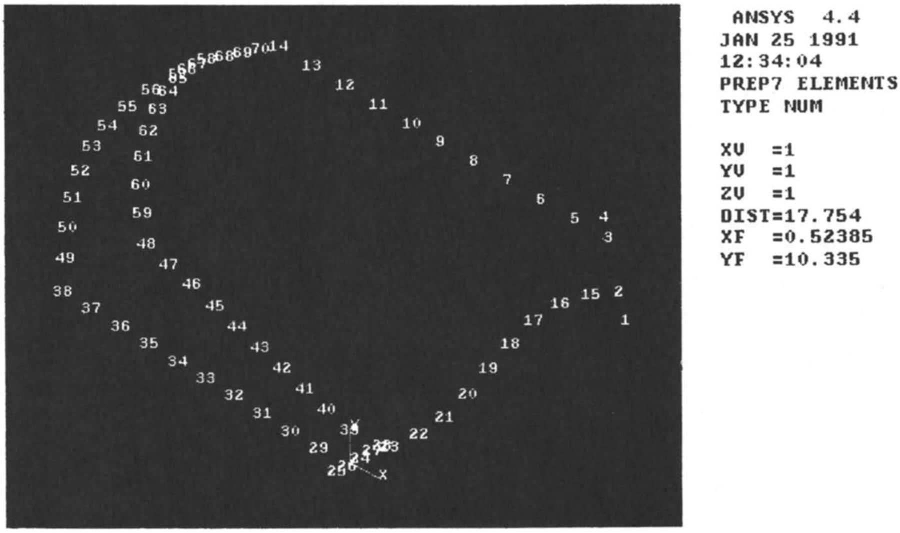

```
ANSYS  4.4
JAN 25 1991
12:34:04
PREP7 ELEMENTS
TYPE NUM

XV   =1
YV   =1
ZV   =1
DIST=17.754
XF   =0.52385
YF   =10.335
```

1
2
3
4
5
6
7
8
9
10
11
12
13
14
15
16
17
18
19
20
21
22
29
30
31
32
33
34
35
36
37
38
40
41
42
43
44
45
46
47
48
49
50
51
52
53
54
55
56
59
60
61
62
63
Y
X

Figure 4. Frame Geometry for Finite Element Analysis.

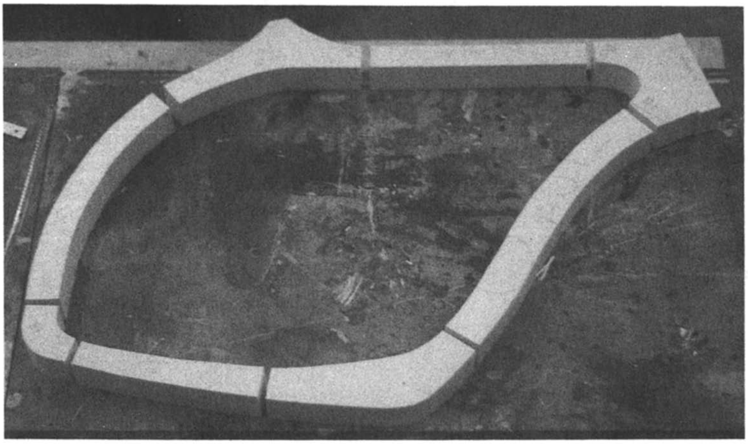

Figure 5. Shaped Foam Mandrels for Preform Processing.

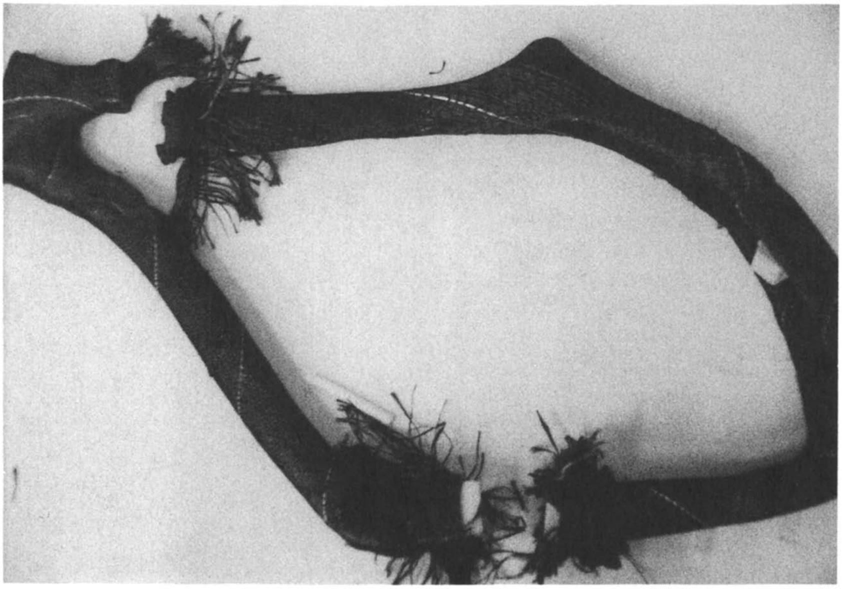

Figure 6. Braiding Over a Mandrel.

fiber ends at the joints were lapped into the braided fiber structure of the adjoining tubes and then braided over once again. The fibers must be at least a critical length (l_c) to assure sufficient stress transfer with the resin and other fibers. It was calculated that these joints will be stronger than if they had been braided alone. This is due to the increase in fibrous material and specific areal coverage at these critical regions.

The braid was formed around the foam mandrel (shaped from styrofoam blocks) and the assembled preform was consolidated, shrink wrapped (to simulate hydrostatic consolidation pressure), and cured at 80°C for 2 hours in a convection oven.

Conclusions

This project demonstrated the ability to design and fabricate a composite structure using an integrated design approach. In particular, the research took advantage of the composite material properties rather than using a "black aluminum" design approach. The results of analytical work were realized as a physical object in the form of a composite bicycle frame.

Downloaded by UNIV MASSACHUSETTS AMHERST on August 6, 2012 | http://pubs.acs.org
Publication Date: April 3, 1991 | doi: 10.1021/bk-1991-0457.ch006

Downloaded by UNIV MASSACHUSETTS AMHERST on August 6, 2012 | http://pubs.acs.org
Publication Date: April 3, 1991 | doi: 10.1021/bk-1991-0457.ch006

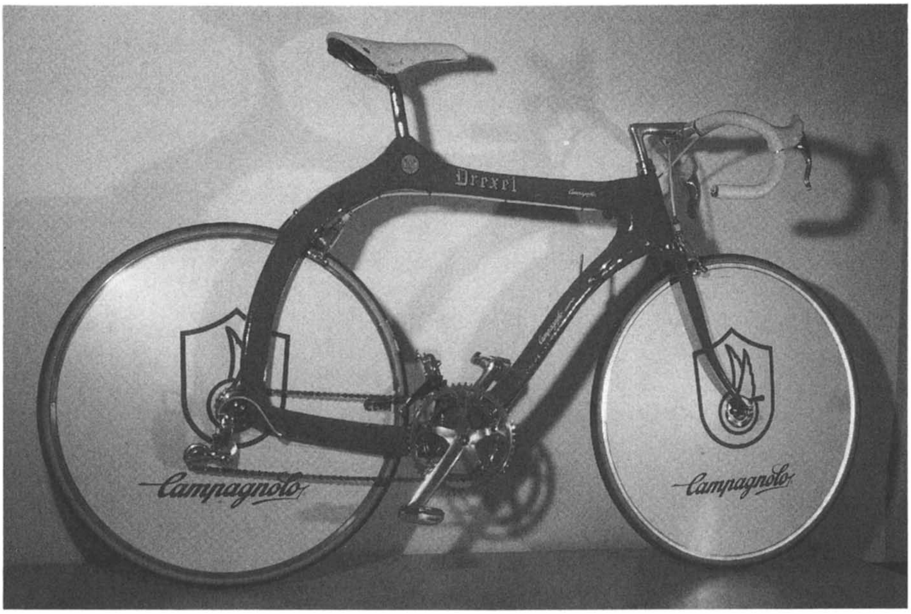

Figure 7. Completed Bicycle Frame.

Through the use of the integrated design, it was possible to produce a light weight frame by taking advantage of the specific material properties available from composite materials. This approach is somewhat generic to composite design, and is currently employed in a number of various structural composite design programs (8,9). The application of this technique to a bicycle frame is a demonstration of the fundamental concept as well as an enjoyable research project.

Five prototype frames were completed during this project. A completed frame is shown in Figure 7. The completed frames are currently being ridden by various bicyclists to evaluate long term effects. Early responses from the riders indicate that the frames feel as stiff as a good steel racing frame, but the benefits of reduced weight are evident.

Acknowledgments

The authors would like to acknowledge the assistance of Campagnolo Corporation, for the support of this project and the donation of components; Mr. Jerry Casale for his support, and assistance in frame specifications and fabrication; Mr. John Kutz for composite processing advice; and Schwinn Bicycle Company for finite element analysis.

Downloaded by UNIV MASSACHUSETTS AMHERST on August 6, 2012 | http://pubs.acs.org
Publication Date: April 3, 1991 | doi: 10.1021/bk-1991-0457.ch006

Literature Cited

1. Tan, T.M., Pastore, C.M., and Ko, F. "Engineering Design of Tough Ceramic Matrix Composites for Turbine Components", Journal of Engineering for Gas Turbines and Power, in press.

2. Douglass, W.A., "Braiding and Braiding Machinery", Centrex Publishing Company, Eindhoven, 1964.

3. Goseberg, Fiedhelm, "The Construction of Braided Goods", Band and Flechtindustrie, No. 2, pp. 65-72, 1969.

4. Ransom, J.B., and Knight, N.F., "Global/Local Stress Analysis of Composite Panels", NASA Technical Memorandum 101622, June 1989.

5. Tarnopol'ckii, Zhigun, and Polyakov, Prostranstvenno-Armirovannyye Komposzitsionnyye Materialy: Spravochnik (Spatially Reinforced Composite Materials: A Handbook), Mashinostroyeniyie Publishing House, Moscow, USSR, 1987.

6. Pastore, C., and Foye, R., "Computer Aided Modeling of Fabric Reinforced Composite Microstructures", Procedings of Fiber-Tex '89, Greenville, SC, Oct. 30-Nov. 1, 1989.

7. Technical Bulletin Shell Chemical Company, SC:235-85.828

8. Ko, F.K., and Pastore, C.M., "Fabric Geometry and Finite Cell Models for Three Dimensional Composites" F. Ko and C. Pastore, 1st US/USSR Conference on Composite Materials, Riga, USSR, May 20-25, 1989.

9. T.M. Tan, C. Pastore, and F. Ko, "Engineering Design of Tough Ceramic Matrix Composites for Turbine Components", presented at Gas Turbine and Aeroengine Congress and Exposition, June 4-8, 1989, Toronto, Ontario, Canada, accepted for publication in Transactions of the ASME.

RECEIVED July 31, 1990

Chapter 7

Linear Low-Density Polyethylene Filled with Silane-Coated Wood Fibers

R. G. Raj and B. V. Kokta

Centre de Recherche en Pâtes et Papiers, Université du Québec, C.P. 500, Trois-Rivières, Québec G9A 5H7, Canada

Downloaded by STANFORD UNIV GREEN LIBR on August 6, 2012 | http://pubs.acs.org
Publication Date: April 3, 1991 | doi: 10.1021/bk-1991-0457.ch007

Silane precoated wood fibers were used as filler in linear low density polyethylene (LLDPE). Chemithermomechanical pulp (CTMP) of aspen was pretreated with silane coupling agents (silane A-172, A-174 and A-1000) having different functional groups. LLDPE filled with silane A-174 pretreated (0.5% by weight of fiber) wood fibers (50% filler weight) produced a 31% increase in tensile strength and 124% increase in tensile modulus compared to unfilled LLDPE. The effect of variation in filler concentration, silane concentration and type of initiator, on mechanical properties of the composites was examined.

The rising cost of resin and the need to enhance mechanical properties are incentives to use low cost fillers as extenders or reinforcements in plastics. Different inorganic fillers such as glass fiber, mica, talc, clay etc. are being incorporated into thermoplastics (1,2). Cellulosic fillers have recently attracted greater attention due to their lower price, low density, biodegradable and renewable in nature (3-5). The use of wood fiber in urea- or phenol-formaldehyde are already common, where the fiber provides a degree of toughness which is not attainable in the relatively brittle thermosetting resins in the absence of some reinforcing fiber. Thus, the use of wood fiber as a filler or reinforcing agent in high volume thermoplastic resins seems to be the main area where the potential of wood fiber is not fully exploited. The surface characteristic of the reinforcing fiber is an important factor due to its role in the transfer of stress from matrix to fiber. Chemically, the hydroxyl-rich surface of lignocellulosic material is

0097-6156/91/0457-0102$06.00/0

Downloaded by STANFORD UNIV GREEN LIBR on August 6, 2012 | http://pubs.acs.org
Publication Date: April 3, 1991 | doi: 10.1021/bk-1991-0457.ch007

advantageous because it provides the potential for reaction with the coupling agent or matrix (phenol or urea formaldehyde).

Another factor which is also important is the physical difference between the fibers commonly used as filler/reinforcing agent in plastics. Synthetic fibers usually have a smooth surface and are relatively straight, whereas the normal wood fiber is twisted and has an irregular surface. Thus, the wood fiber is likely to exhibit a greater resistance to withdrawal from the matrix compared to the synthetic fibers (6). The main disadvantage of the wood fiber is the compatability problem between the hydrophilic fiber and the hydrophobic polymer. A sufficient degree of adhesion between the filler and polymer matrix is a necessary condition to maximize the mechanical performance of the composite. For this reason, a coupling agent which promotes adhesion between the fiber surface and matrix is desirable (7,8). The principal objective for the use of coupling agent in a composite is to effect a significant improvement in the strength of finished product. Assuming that the optimum reactive groups for the filler surface and matrix can be selected, the objective then is to maximize the interaction. In the present work, different silane coupling agents were used to improve the fiber-matrix adhesion. The effect of variation in filler concentration, silane concentration and the type of initiator, on mechanical properties of the composites was examined.

Experimental

LLDPE Navopal LLGR-0118-A was supplied by Novacor Chemicals Ltd. The reported properties of LLDPE are: melt index: 1 g/10 min; density: 0.918 g/cc. CTMP (aspen) was prepared in a sund defibrator (9). The average fiber aspect ratio (L/D) was 11.9. Three silane coupling agents (Union Carbide) were used:
a) Vinyltri(2-methoxy ethoxy)silane (silane A-172)
b) γ- Methacryloxypropyltrimethoxysilane (silane A-174)
c) γ- Aminopropyltriethoxysilane (silane A-1100)

Pretreatment of wood fiber

The wood fibers were pretreated with different silane coupling agents.

a) Oven dried wood fibers (50 g) were placed in a flask to which 300 mL of carbon tetrachloride was added, followed by the addition of dicumyl peroxide (2%) and 2% of silane A-172 or A-174. The above mixture was refluxed for 3 hours. After cooling, the carbon tetrachloride was evaporated and the fibers were dried at 55°C for 24 hours before mixing with the polymer. A series of pretreated wood fibers were prepared using other peroxides (2%), benzoyl or di-t-butyl peroxide.

b) Pretreatment of wood fibers with silane A-1100 was carried out by a two-stage mixing procedure. In the first stage, a mixture of wood fiber, silane A-1100 (2%) and dicumyl peroxide (2%) was refluxed for 3 hours in carbon tetrachloride. In the second stage, a small amount of polymer, to reduce the fiber-fiber interaction, was added to the mixture. The polymer (LLDPE, 5%) was dissolved in p-xylene, to which maleic anhydride (2%) and benzoyl peroxide (0.05%) were added. The mixture was refluxed for 3 hours; then the contents of first stage were added to the precoated polymer and the resulting mixture was again refluxed for 2 hours. The mixture was then cooled to room temperature, filtered, washed with distilled water and then dried at 105°C for 12 hours.

Preparation of composites

Compounding of LLDPE and pretreated wood fibers (0-50% by weight) was done in a C.W. Brabender Roll Mill No.065. The above mixture was compression molded into dog-bone shaped tensile specimens. The molding was done at 150°C with a pressure of 3.2 MPa. After heating the mold for 15 min., the samples were slowly cooled to room temperature with the pressure maintained during the process.

Mechanical tests

Instron model 4201 was used to study the tensile properties of the composites. The full-scale load was 500 N and the cross-head speed was 10 mm/min. The test results were automatically calculated by a HP86B computing system using the Instron 2412005 General Tensile Test Program. The average coefficient of variation of the reported properties was less than 6.0%.

Results and Discussion

The mechanical properties of thermoplastic-wood fiber composites depend upon the properties of the polymer matrix, wood fiber and of the polymer-fiber interface. Wood fibers are relatively short, flexible and coarse in comparison to most of the fillers used for reinforcing the thermoplastic polymers. Thus, bonding of the matrix to the fiber is an important factor in determining whether or not the full strength of wood fiber can be utilized in a composite. Figures 1-3 illustrate the influence of silane pretreatment of fibers on mechanical properties of the composite. The composites containing untreated wood fibers (control) gradually lost their tensile strength with an increase in filler concentration. Both coupling agents (silane A-172 and A-174) provided a considerable increase in tensile strength relative to the untreated fiber composites.

Figure 1 compares the tensile properties of LLDPE

Downloaded by STANFORD UNIV GREEN LIBR on August 6, 2012 | http://pubs.acs.org
Publication Date: April 3, 1991 | doi: 10.1021/bk-1991-0457.ch007

filled with untreated and silane A-172 or A-174 pretreated wood fibers (2% dicumyl peroxide). Tensile strength increased steadily with filler concentration in silane A-172 and A-174 treated fibers, which indicates that the silane treatment influences the bonding at the interface. At 40% fiber level, tensile strength of the silane A-174 treated wood fiber composites is more than four times greater than the untreated fiber composites.

Figure 2 shows that the increase in filler concentration has a negative effect on the elongation of the composites. The elongation decreased sharply with an increase in filler content in the polymer. The silane pretreatment had little influence on the elongation of the composites. The effect of fiber treatment on tensile modulus of the composites is presented in Figure 3. The addition of filler results in an appreciable stiffening effect of the matrix as was observed in an earlier study by Klason et al. (5). At 30% filler level, modulus rose from 132 MPa (unfilled LLDPE) to 350 MPa. An increase in modulus was also observed in the case of silane A-172 and A-174 pretreated wood fiber composites.

A possible coupling mechanisim of polymer-coupling agent-wood fiber is shown in Figure 4. The coupling agent can be represented as

$$Y\text{-}R\text{-}Si\text{-}X_3,$$

where X is a hydrolyzable alkoxy group, Y is a functional organic group (vinyl in silane A-172 and methacryl in silane A-174) and R is an aliphatic linkage. During fiber pretreatment, the reaction of the coupling agent with the hydroxyl groups of wood fiber surface produces the hydrolysis product silanol, $-Si(OH)_3$. A coupling agent silanol can develop either covalent (siloxane bond) or hydrogen bonds with OH groups of cellulose. Subsequent reaction of the functional organic group (vinyl or methacryl) with the polymer completes the establishment of a molecular bridge between the polymer and fiber.

The effect of silane A-174 concentration (2% benzyol peroxide) on tensile properties of the composites are presented in Tables I and II. A significant increase in tensile strength, with the increase in filler content, was achieved even at lower concentrations of silane A-174. The results also indicate that the coupling agent is effective at very low concentrations than at higher concentrations (2 and 4%). Elongation decreased drastically at higher filler concentrations and the silane pretreatment had less effect on elongation.

The incorporation of wood fibers in the polymer matrix increased the tensile modulus as can be observed from Table II. Tensile modulus increased linearlly with filler concentration. The rise in tensile modulus of the composite is due to the higher modulus of the wood fiber. Fracture energy, calculated by the area under the stress-

Downloaded by STANFORD UNIV GREEN LIBR on August 6, 2012 | http://pubs.acs.org
Publication Date: April 3, 1991 | doi: 10.1021/bk-1991-0457.ch007

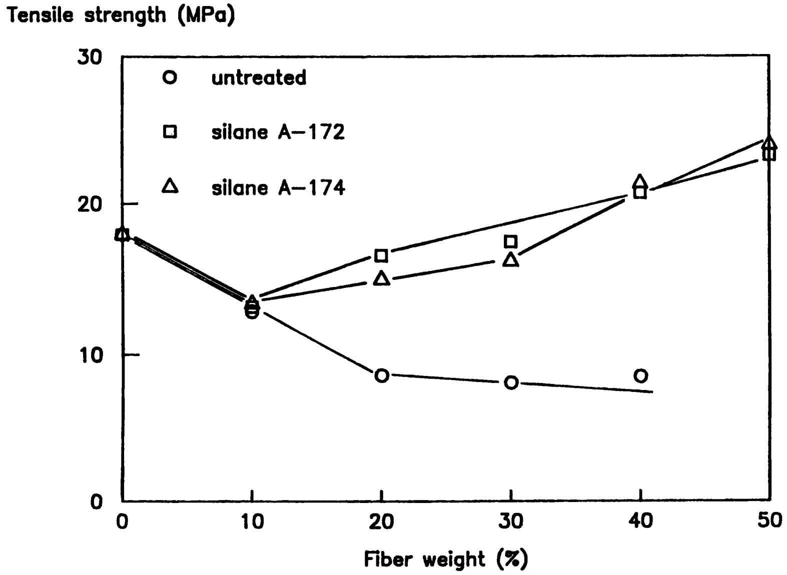

Figure 1. Effect of silane pretreatment on tensile strength of LLDPE-wood fiber composites.

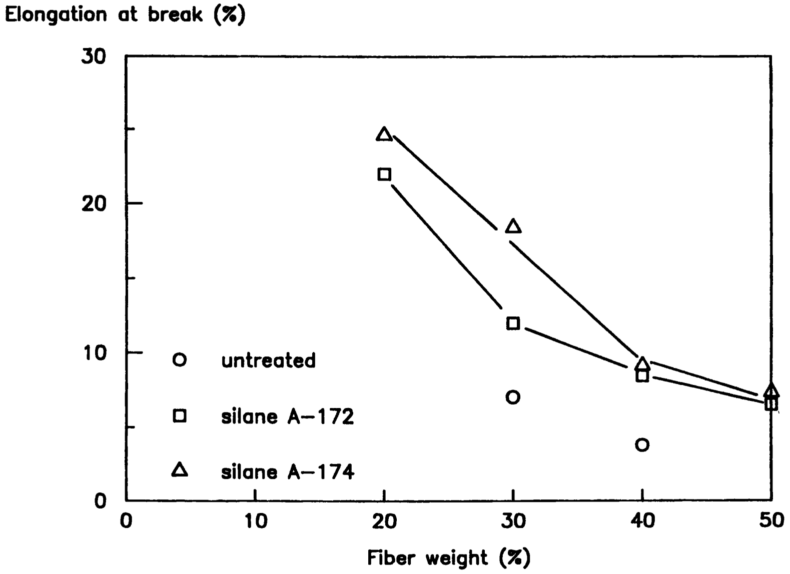

Figure 2. Effect of silane pretreatment on elongation of LLDPE-wood fiber composites.

Downloaded by STANFORD UNIV GREEN LIBR on August 6, 2012 | http://pubs.acs.org
Publication Date: April 3, 1991 | doi: 10.1021/bk-1991-0457.ch007

Downloaded by STANFORD UNIV GREEN LIBR on August 6, 2012 | http://pubs.acs.org
Publication Date: April 3, 1991 | doi: 10.1021/bk-1991-0457.ch007

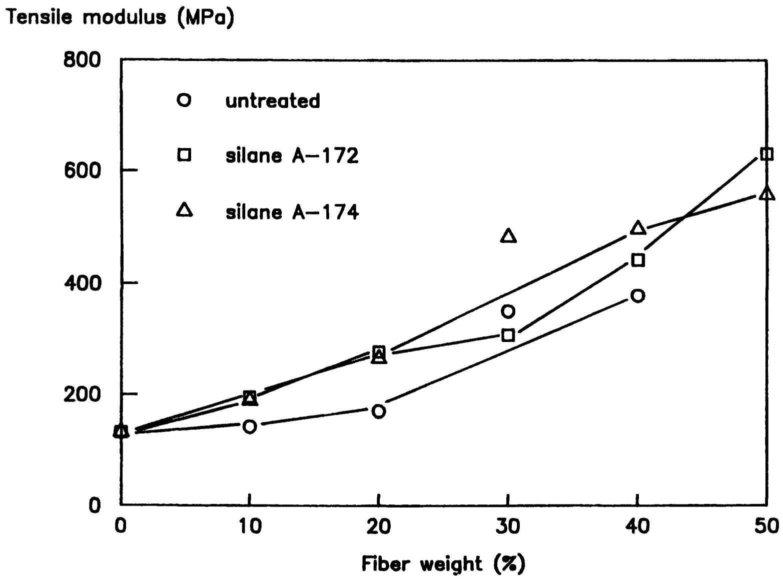

Figure 3. Effect of silane pretreatment on tensile modulus of LLDPE-wood fiber composites.

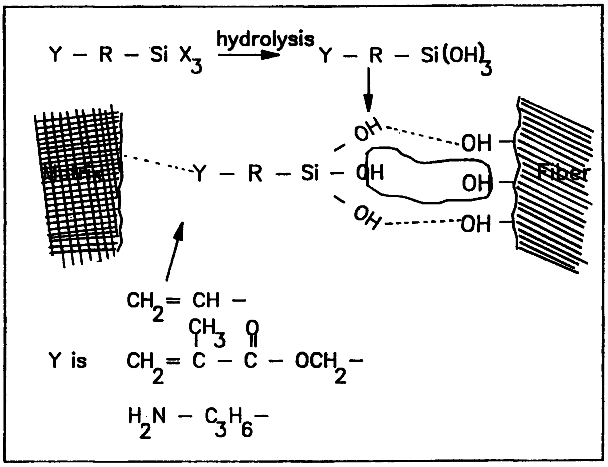
Y – R – Si X3
hydrolysis
Y – R – Si(OH)3
Matrix
Y – R – Si –
OH
OH
OH
OH
OH
OH
Fiber
CH2= CH –
Y is
CH3
O
CH2= C – C – OCH2 –
H2N – C3H6 –

Figure 4. Possible coupling mechanism at the fiber-matrix interface.

strain curve, can provide a measure of the toughness of the composite.

Table I EFFECT OF SILANE A-174 CONCENTRATION ON TENSILE PROPERTIES OF LLDPE-PRETREATED WOOD FIBER COMPOSITES

Fiber	Tensile strength (MPa)				Elongation (%)			
(% wt.)	10	20	30	40	10	20	30	40
Silane A-174								
0%	12.6	8.6	8.1	8.5	782	242	7.3	3.8
1%	12.7	14.4	20.4	23.0	573	23.7	8.9	5.4
2%	12.6	14.8	19.4	21.1	249	37.1	9.3	6.8
4%	12.3	14.5	18.1	19.4	332	42.3	14.8	10.5

Table II EFFECT OF SILANE A-174 CONCENTRATION ON TENSILE PROPERTIES OF LLDPE-PRETREATED WOOD FIBER COMPOSITES

Fiber	Fracture energy (J)				Tensile modulus (MPa)			
(% wt.)	10	20	30	40	10	20	30	40
Silane A-174								
0%	7.3	1.92	0.31	0.19	142	201	337	392
1%	2.7	0.51	0.42	0.34	162	230	298	347
2%	5.8	0.59	0.48	0.40	167	242	291	384
4%	3.6	0.53	0.47	0.31	158	265	326	375

The above results show that the fracture energy decreased steadily with an increase in filler concentration. The loss in fracture energy can be attributed to an increase in fiber pull-out, due to the higher stress generated at the fiber-matrix interface when the fiber is strained in tension, at the interface (6). Improvement in toughness can be achieved only if there is an increase in interfacial bond strength between the fiber and matrix.

Different types of peroxides were used during the

Downloaded by STANFORD UNIV GREEN LIBR on August 6, 2012 | http://pubs.acs.org
Publication Date: April 3, 1991 | doi: 10.1021/bk-1991-0457.ch007

Downloaded by STANFORD UNIV GREEN LIBR on August 6, 2012 | http://pubs.acs.org
Publication Date: April 3, 1991 | doi: 10.1021/bk-1991-0457.ch007

pretreatment of wood fiber. Tables III and IV show the effect of peroxide on tensile properties of LLDPE-silane A-174 pretreated wood fiber composites. The results show that a considerable gain in tensile properties can be achieved with the proper selection of the initiator.

Table III EFFECT OF PEROXIDE ON TENSILE PROPERTIES OF LLDPE-SILANE A-174 PRETREATED WOOD FIBER COMPOSITES

Fiber	Tensile strength (MPa)				Elongation (%)			
(% wt.)	10	20	30	40	10	20	30	40
Dicumyl peroxide	12.6	16.2	21.5	26.8	127	39.2	12.6	9.7
Benzoyl peroxide	12.7	14.4	20.4	23.0	573	23.7	8.9	5.4
Di-t-butyl peroxide	11.7	13.1	16.3	18.7	684	17.3	9.6	5.1

Table IV EFFECT OF PEROXIDE ON TENSILE PROPERTIES OF LLDPE-SILANE A-174 PRETREATED WOOD FIBER COMPOSITES

Fiber	Fracture energy (J)				Tensile modulus (MPa)			
(% wt.)	10	20	30	40	10	20	30	40
Dicumyl peroxide	1.4	0.56	0.52	0.47	172	223	324	413
Benzoyl peroxide	2.7	0.51	0.42	0.34	162	230	298	347
Di-t-butyl peroxide	3.1	0.47	0.28	0.16	141	206	291	322

Higher tensile strength, with increase in fiber content, was observed when dicumyl peroxide was used as an initiator (Table III). Tensile modulus seems to be less influenced by the type of the peroxide used. As observed earlier, fracture energy decreased with the addition of fiber in the matrix (Table IV). The chemical

Downloaded by STANFORD UNIV GREEN LIBR on August 6, 2012 | http://pubs.acs.org
Publication Date: April 3, 1991 | doi: 10.1021/bk-1991-0457.ch007

structure and the physical characteristics of the peroxide seems to influence the reaction with filler surface. It is also possible that the peroxide can generate free radicals on the polymer which can aid in the formation of chemical bonding with the coupling agent (10).

Organic peroxides are thermally unstable and undergo homolytic cleavage at the oxygen-oxygen bonds to form radicals. The relative stability and the reactivity of the radicals can be correlated to the structure of the peroxide (11). The radicals can extract hydrogen from polyethylene and add to the functional group of the coupling agent to form covalent bonds. It is also possible that the radicals can initiate vinyl groups in silane which can be linked to the polymer. In addition, there is also the possibility of crosslinking of the polyethylene chains which can change the physical properties of the matrix.

The effect of silane pretreatment on the morphology of polymer-wood fiber composites was studied by SEM. Micrographs of the fractured surfaces of the samples are shown in Figures 5 and 6. As can be seen, the untreated fiber composites show a poor dispersion of fiber in the polymer matrix (Figure 5). Also there is a lack of adhesion at the interface, which leads to more fiber pull-out from the matrix. In silane A-174 pretreated wood fiber composites, good bonding at the fiber-matrix interface greatly reduces the fiber pull-out (Figure 6).

Figures 7 and 8 summarize the tensile properties of LLDPE filled with different silane treated (2% by weight) fibers. It can be seen that the % increase in tensile strength in all silane treated fiber composites is higher than the untreated fiber composites (Figure 7). It was also observed that with an increase in fiber concentration, a significant gain in tensile strength can be achieved. The % increase in tensile modulus is much lower compared to the tensile strength of silane pretreated fiber composites (Figure 8). This explains why good bonding at the interface is a primary condition for the improvement of tensile strength, whereas a significant gain in modulus can be achieved simply by increasing the filler content in the polymer matrix.

The results also indicate that silane A-174 (methacryl functional group) performed better as a coupling agent than silane A-172 or A-1100. Vinyl group in silane A-172 may react with the matrix through radical reaction, whereas this may not be the case with aminopropyl groups in silane A-1100. In an earlier study on silane coupling agents, Ishida observed that silanes tend to be ordered in the interphase and the degree of organization depends largly on the organofunctionality of the silane. The orientation and organization of the silane affects the reinforcement mechanism (12). Silanes with large and flexible functional groups tend to form more cyclic structures than the silanes with smaller and more rigid

Downloaded by STANFORD UNIV GREEN LIBR on August 6, 2012 | http://pubs.acs.org
Publication Date: April 3, 1991 | doi: 10.1021/bk-1991-0457.ch007

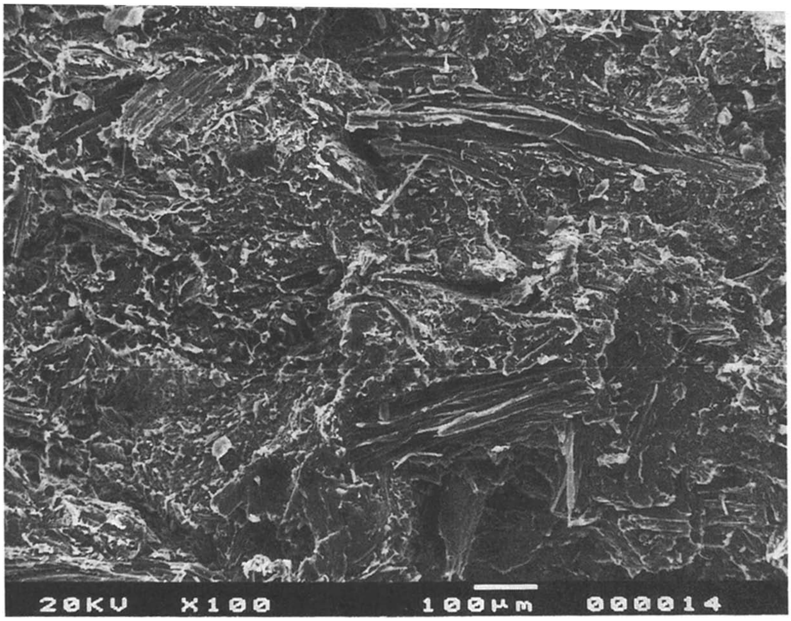

Figure 5. Fracture surface of LLDPE-untreated wood fiber Composite (30% fiber weight).

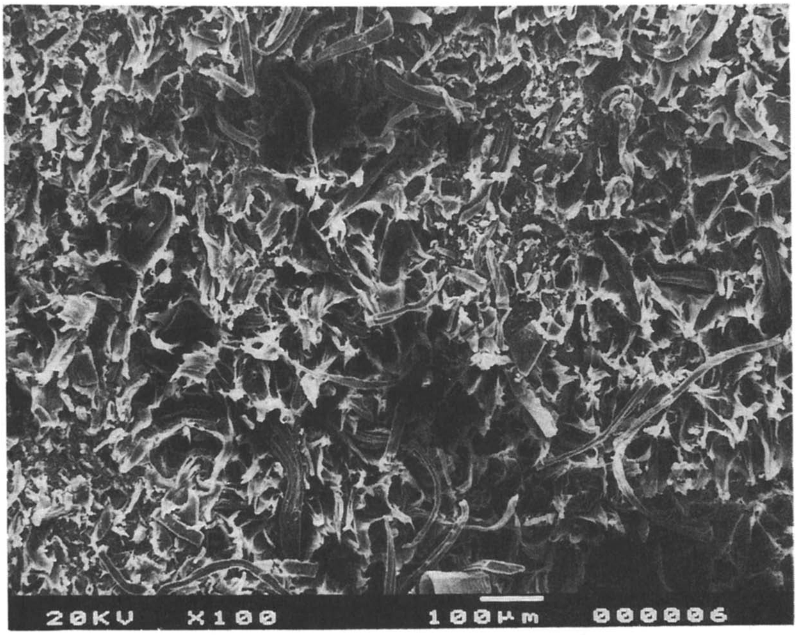

Figure 6. Fracture surface of LLDPE-silane A-174 pretreated wood fiber composite (30% fiber weight).

Downloaded by STANFORD UNIV GREEN LIBR on August 6, 2012 | http://pubs.acs.org
Publication Date: April 3, 1991 | doi: 10.1021/bk-1991-0457.ch007

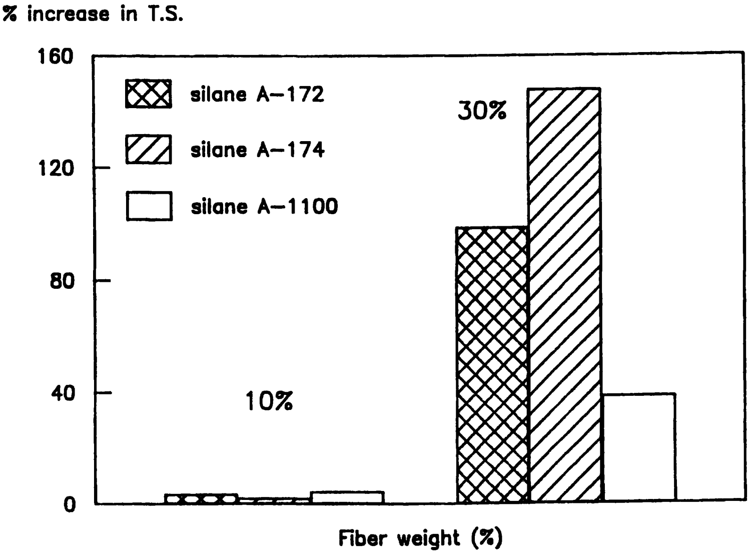

Figure 7. Effect of different silane pretreatments on tensile strength of LLDPE-wood fiber composites.

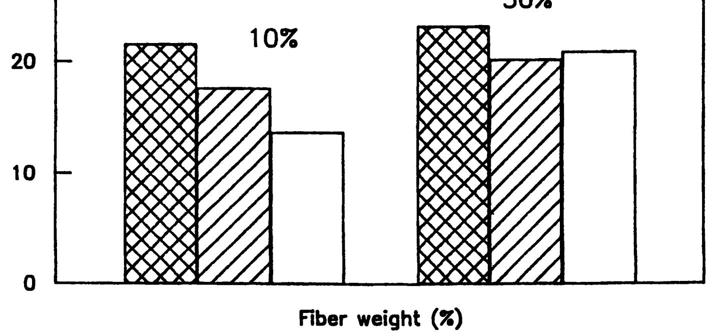

Figure 8. Effect of different silane pretreatments on tensile modulus of LLDPE-wood fiber composites.

substituents. In the present case, the vinyl and methacryloxy groups in silanes exhibit a stronger interaction with the wood fiber surface and polymer matrix than the aminopropyl group. This may explain the reason for higher tensile strength values observed in silane A-172 and A-174 pretreated wood fiber composites than silane A-1100.

Conclusions

The potential of wood fiber as a low cost reinforcing filler in LLDPE was shown to be promising. A significant improvement in tensile properties can be achieved with the pretreatment of wood fiber with silane coupling agent. The concentration of wood fiber in the polymer matrix, the type of the silane coupling agent and their concentration were found to be important factors in achieving optimum strength properties of the composites. Silane A-174 with methacryl functional group was found as a most effective coupling agent for LLDPE-wood fiber composites. Dicumyl peroxide as an initiator gave best improvement in mechanical properties of the composites. SEM studies of silane A-174 pretreated wood fiber composites showed good bonding at the interface with less fiber pull-out from the polymer matrix.

Literature Cited

1. Theberge, J.E.; Hohn, K. Polym. Plast. Technol. Eng. 1981, 16, 41-52.
2. Chun, I; Woodhams, R.T. Polymer Composites 1984, 5, 250-263.
3. Kokta, B.V.; Chen, R.; Daneault, C.; Valade, J.L. Polymer Composites 1983, 4, 229-232.
4. Nakajima, Y. Japan Patent Kokai 127 632, 1981.
5. Klason, C.; Kubat, J.; Strömvall, H.-E. Intern. J. Polymeric Mater. 1984, 11, 9-38.
6. Mckenzie, A.W.; Yuritta, J.P. Appita 1979, 32, 460-465.
7. Morrell, S.H. Plastics and Rubber Processing and Applications 1981, 1, 179-186.
8. Goettler, L.A. U.S. Patent 4 376 144, 1983.
9. Beshay, A.D.; Kokta, B.V.; Daneault, C. Polymer Composites 1985, 6, 261-271.
10. Raj, R.G.; Kokta, B.V.; Daneault, C. J. Appl. Polym. Sci. 1989, 37, 1089-1103.
11. Callais, P.A.; Kazmierczak, R.T. Proc. of SPI 47th Annual Technical Conf., 1989, p 1368.
12. Ishida, H. Polymer Composites 1984, 5, 101-123.

RECEIVED July 18, 1990

Downloaded by STANFORD UNIV GREEN LIBR on August 6, 2012 | http://pubs.acs.org
Publication Date: April 3, 1991 | doi: 10.1021/bk-1991-0457.ch007

Chapter 8

Fibers in Medicine

From Antiquity to the Future

D. J. Lyman

Department of Materials Science and Engineering, University of Utah, Salt Lake City, UT 84112

Downloaded by CORNELL UNIV on August 6, 2012 | http://pubs.acs.org
Publication Date: April 3, 1991 | doi: 10.1021/bk-1991-0457.ch008

Fibrous materials will always play an important role in the advancement of medicine and surgery. Their uses range from non-implantables to extracorporeal devices and implants. Some examples of implants and the extracorporeal devices are discussed to show how the past is guiding us to the future.

Fibrous materials and fibers have always intrigued mankind with their potential uses. This is understandable when one considers that these materials can be tied, woven, knitted or made into paper. Indeed, if we look at the first uses of foreign materials in medicine, they are of fibrous materials and date back to well over 4000 years ago. The first recorded use is mentioned in the Edwin Smith Surgical Papyrus (1), nearly 4000 years old, describing the use of stitches (sutures) in wound repair. Extensive use of a variety of suture materials was also recorded in the Indian literature (1). The Susruta Samhita, written 2500 years ago, describes suturing materials of braided horsehair, leather strips, cotton fibers, animal sinews, and the fibrous bark from the Ashmantaka tree.

Today, fibers are utilized in almost every facet of medicine and surgery (see Table I). While the major volume of uses are for the nonimplantables, we will be discussing some of the extracorporeal and implantable applications of fibers and fibrous materials that are used in affecting repair of the body.

Fibers in Implants and in Extracorporeal Devices.

Sutures. A suture is a strand of material, either monofilament or multifilament, used to tie (ligate) or to sew (suture) tissue. Many materials have been used throughout the centuries of medicine: bark, animal tendons and leather strips, intestinal tissue, gold, silver, iron wire, silk, linen, cotton, and now stainless steel wire and synthetic polymers. While ideally one should only be concerned with the tensile strength of the suture (i.e. its strength must be in excess of that required to hold tissue in opposition to whatever strains are imposed by

0097–6156/91/0457–0116$06.00/0

Table I. Fibers in Medicine

Nonimplantables
Drapes, pillows, wash cloths, surgical dressings, gauze, elastic stockings.
Gowns, caps, surgical masks.
Extracorporeal
Fabric reinforcements for dialysis and oxygenator membranes, silicone rubber, UV curable cast materials and catheters.
Hollow fibers for dialyzers and oxygenators.
Implantables
Sutures
Fabrics for sewing rings (heart valves, percutaneous leads), patches for heart repair, surgical reinforcement meshes.
Vascular grafts, reinforcement tubular meshes for veins and polymer grafts.
Velours for blood contacting surfaces (artificial heart and assist devices).
Fiber reinforcement for hard polymers (bone plates, etc) and soft polymers (ligaments, etc).
Restraining loops for intraocular lenses.

postoperative conditions), in actual use one must be concerned about a number of characteristics. These are: a) *absorption*. A suture must not be absorbed nor lose its tensile strength for a period of 10 to 12 days after implantation so that sufficient healing can occur to restore strength to the wound; b) *pliability*. This refers to the resistance of a strand to bending forces. The suture should handle comfortably and naturally to the surgeon without too much stiffness or kinking; c) *knot tying and holding*. Strands should not be too wiry and resist the firm setting of the knot (for example, the springy polyproplene would actually untie itself) nor have too hard or smooth a surface which would allow the knot to slip or loosen; d) *tissue reaction*. The suture must cause only a minimal tissue reaction. Degradation (absorption) of the suture must not cause any excess chemical irritation.

Infection has also become a concern in terms of suture selection (2,3). For example, monofilament polymeric sutures elicited less infection than multifilament polymeric sutures or metallic sutures. Also, the chrome cross-linked collagen sutures elicited less infection than untreated collagen sutures. A general ranking of the potential of a variety of sutures to develop wound infection is as follows: polypropylene, polyglycolic and lactic acid esters, nylon < collagen, polyethylene terephthalate << silk < stainless steel << chromic collagen, cotton. Coatings on polymers appear to render then more prone to infection.More recent studies (4,5) have been concerned with the role of bacterial adherence to polymers and this appears to correlate well with the earlier suture implant studies.

Sutures can be grouped into several categories in terms of their origin (i.e. the naturally occurring materials such as those based on collagen, silk, cotton or

Downloaded by CORNELL UNIV on August 6, 2012 | http://pubs.acs.org
Publication Date: April 3, 1991 | doi: 10.1021/bk-1991-0457.ch008

linen or metallic materials such as stainless steel, tantalum and aluminum or synthetic polymers such as polyethylene, polypropylene, nylon, polyethylene terephthalate, polytetrafluoroethylene, polycaprolactam, polyglycolic and polylactic acid esters, polydioxanone and the Spandex elastomers), or they may be categorized in terms of their degradation rates. For example, if a suture degrades within 2 to 3 months, it is considered an absorbable suture; if the degradation rate is greater than 6 months it is considered a non-absorbable suture. Silk, cellulose, polyamide, polyterephthalates, and polyhydrocarbon sutures are considered nonsorbable sutures. Collagen and the polyglycolic and polylactic acid sutures are considered sorbable sutures. It is of interest that the new synthetic absorbable sutures, the polyglycolic and polylactic acid ester materials, had their origin in the pioneering polymer studies of Carothers (6) where he first synthesized aliphatic polyesters based on diols and dicarboxcylic acids. These aliphatic polyesters were found to readily degrade in water and thus were not suitable for textile fibers. Today, the aliphatic polyhydroxyesters, an offshoot of these early studies, represent a major class of sutures.

Elastic fibers represent a class of sutures whose potential is yet to be realized. Early studies (7) using elastic silicone rubber sutures in the treatment of rectal prolapse showed less complications than when more conventional stiff sutures were used. However, the silicone rubber sutures could only be made in large diameters and thus were not suitable for fine surgery. Later studies (8,9) using the copolyurethane textile fiber Lycra showed that even fragile tissue could be easily snugged up to provide approximation without tissue damage. Tissue reaction was also very good and the elastic suture showed improved wound healing over the more conventional stiff sutures. However, to date, the sutures available commercially (such as the Matsuda elastic surgical suture, Matsuda Ika Kogyo Co.) are too elastic (elongations of 900-1000%) and are of too heavy a denier for uses other than purse string or U stitch around a catheter in open-heart surgery. The possibility of tailoring the mechanical properties of the block copolyurethanes to obtain their optimal tensile strength and elasticity for suturing while retaining their biocompatiblity represents a yet untapped area of suture materials.

Downloaded by CORNELL UNIV on August 6, 2012 | http://pubs.acs.org
Publication Date: April 3, 1991 | doi: 10.1021/bk-1991-0457.ch008

Vascular Grafts. It was a suture that showed the way to the types of vascular grafts that we know today. In the 1940s, investigators such as Hufnagel were exploring ways to repair damaged blood vessels using polymeric materials instead of metals as was done in WWI. These studies primarily involved solid wall tubes to interconnect damaged arteries. While limited success was obtained in larger vessels of high flow, the overall results were not good, with clotting being the major problem.

In 1952, Voorhees (10) noticed that a silk suture which had been hanging free in the heart had become coated with endothelial cells. From this observation he hypothesized that a fabric graft might do the same and thus avoid the clotting problem. A simple tube made by sewing a piece of sail cloth together proved his hypothesis and led to hundreds of studies by a large number of investigators on the role of the material and the fabric design on graft performance. Local fabric stores became the unknowing suppliers of materials

Downloaded by CORNELL UNIV on August 6, 2012 | http://pubs.acs.org
Publication Date: April 3, 1991 | doi: 10.1021/bk-1991-0457.ch008

for vascular implants. A wide variety of textile fibers, such as nylon, Dacron, Orlon, silk, as well as commercial fabrics of Teflon and various polyvinyl chloride materials were tried. From this research evolved the methods to improve the workability of the graft ends, to reduce kinking, to balance the initial need for low permeability to reduce blood leakage with the later need for higher permeability to achieve optimal cellular ingrowth, to be easy for the surgeon to use and to select the material having the best stability in the biological environment. This led to the current woven and knitted Dacron arterial grafts that are used today. These Dacron arterial grafts have shown good success in the repair of large and medium sized arteries. However, the success rate for arteries below 10 mm ID drops dramatically and in general they have not been successful in the repair of arteries of 6 mm and under. This is due to the nature of the healing process in these woven and knitted prostheses. The cellular ingrowth which renders the graft compatible, results in an inner capsule being formed which is several millimeters thick. This can lead to the occlusion of the small diameter protheses. Thus for small artery repair, the surgeon had to use autogenous veins excised from another part of the patients' body. For some patients, this is not possible because their veins were too diseased. Thus began the search for new prostheses for the repair of small diameter vessels.

Small Diameter Grafts. One of the first small diameter arterial grafts to appear was the graft made from expanded polytetrafluroethylene (ePTFE). While Teflon fiber grafts were found wanting in the 1950s because the heavy denier fibers were too difficult to weave or knit, the novel biaxial mechanical stretching process developed by Gore led to a structure in which solid nodes were interconnected by fine, strong fibrils. Initially these materials had their success as waterproof barriers for camping gear, clothing, etc. Initial studies by Soyer using large diameter tubes and later Campbell in the United States and Matsumoto in Japan using small diameter ePTFE tubes for artery repair showed good patency results in experimental animals (11). This ePTFE graft material had internodule distances (or fibril length or pore size) of 10 to 30 microns; the pore volume was 85-90%. The initial results of these new small diameter arterial grafts were quite good with graft dilation and suture pull-out being the major problems. Eventually the pore volume was slightly reduced (which also seemed to give a preferred orientation of the fibrils thus reducing creep), and the grafts were wrapped with a thin PTFE mesh so as to reduce the graft dilation and the tendency for suture pull-out. These new grafts have enabled the surgeon to achieve good surgical repair in the 10-6 mm ID range. However, while repair in vessels under 6 mm ID is being done, the results are not as good as for 6 mm and larger, and for these small diameter vessels the autogenous vein is still the implant of choice. It would appear that the stiffness (or non-compliance) of these ePTFE grafts (as with the Dacron grafts) which leads to mechanical trauma and hemodynamical disturbances at the graft/natural vessel anastomosis is the possible reason for the hyperplasia which is a major cause of implant failure. Thus, current research has been focusing on the more elastic, or compliant, polymers such as the block copolyurethanes which more nearly match the compliance of the natural vessel and show good blood compatibility.

Annis, using the ICI technology, has explored the electrostatic spinning of fibers as a route to forming small diameter arterial grafts (12). In this approach, a dimethyl acetamide solution of a copolyurethane based on polytetramethylene glycol was electrostatically precipitated in fibrous form onto a revolving mandrel. The residual solvent in the 1-2 μm fibrils caused then to fuse into a fibrous mat about 500 μm thick. The fiber orientation, and thus the mechanical properties of the graft, could by somewhat controlled by the speed of the mandrel rotation and the back and forth movement of the spinnerette. Implantation in experimental animals showed that an intima developed, and that tissue ingrowth into the bulk of the graft was only to a depth of about 5 μm. The grafts maintained their pulsatile characteristics after implantation. Other small diameter arterial grafts using elastic copolyurethane materials have also been developed (13-15). The fabrication of these compliant grafts involved either wet or dry coagulation processes; while the wall structure of these grafts were more foam-like, some of them were made as fabric composites. Unlike the electrostatic spun grafts, these coagulated grafts were usually porous to some degree. These grafts showed good suturability and had pulsatile characteristics similar to those of the natural vessels. The compliant nature of these grafts as well as the improved blood compatibility of the polymers used in their construction contributed to their excellent implant results for 3 and 4 mm ID sizes in experimental animals when compared to even the ePTFE grafts. One would expect that in the future, these new materials will be available for human use and will provide a suitable alternative to the autogenous saphenous vein. Also, these new materials should enable the development of workable grafts for venous repair. At present venous repair is primarily done using autogenous tissue.

Another approach to improve the blood-vessel interface was to seed endothelial cells onto knitted Dacron protheses (16), and later onto ePTFE protheses (17). While improved patency over the non-seeded grafts has been demonstrated, it has also been reported that intimal hyperplasia did develop distally in all grafts. Although the use of a compliant graft as the seeding substrate should reduce this hyperplasia, it has been reported that the copolyurethane material by itself endothelialized in dogs (18) and thus not need seeding.

Miscellaneous uses of fabrics in surgery. Fabrics of Dacron and polypropylene have also been widely used as reinforcing meshes in abdominal repair. However, their use has not been without complications (19).

Fabrics have also been used in tracheal and esophageal repair, usually as a composite structure in which a tubular fabric is coated with silicone rubber or with collagen. Fabrics in flat sheet form have been used in artificial skin materials for treatment of burns. Again these fabrics have been coated with a variety of materials to control moisture and air diffusion and to present a more biological tolerant surface for regenerating tissue.

Hollow fibers: One of the most successful extracorporeal devices has been the blood dialyzer, or artificial kidney. This device has also benefitted from fiber

Downloaded by CORNELL UNIV on August 6, 2012 | http://pubs.acs.org
Publication Date: April 3, 1991 | doi: 10.1021/bk-1991-0457.ch008

Downloaded by CORNELL UNIV on August 6, 2012 | http://pubs.acs.org
Publication Date: April 3, 1991 | doi: 10.1021/bk-1991-0457.ch008

technology. The artificial kidney had its beginning in the blood dialyzer of Abell, Rowntree, and Turner in 1913 (20). This device used semipermeable cellulose nitrate tubes to remove unwanted solutes from blood by dialysis. While the actual tubes used were relatively large, it was interesting to note that in their article was the statement "very small tubes would undoubtedly prove valuable when the necessary time and trouble are not prohibitive", in essence predicting the hollow fiber artificial kidney in use clinically today. However, other problems including the need for better membrane materials prevented this blood dialyzer from becoming more than an interesting laboratory experiment. These problems have occupied the attention of researchers over the next 50 years. It was in 1945, nearly 33 years later that the first patient survived acute kidney failure by being dialyzed with the rotating drum device developed by Kolff. It was an additional 15 years before a functioning blood access system was developed to allow the treatment of chronic kidney failure patients. By this time the twin coil kidney using regenerated cellulose tubes and the Kiil dialyzer using flat sheets of regenerated cellulose were available for use. In 1964, Stewart (21) experimented with some cellulosic desalination hollow fibers in a simple dialyzer which resemble a miniature version of the Abell, Rowntree and Turner device. While this device was not too successful, this was primarily due to the plugging of the hollow fibers with micro clots. Enlargement of the hollow fibers to 200-300 μm ID, with a wall thickness of about 10-20 μm, the use of a larger bundle of fibers, and improved manifolding resulted in a successful hollow fiber artificial kidney similar to that in use today. For pediatric patients, this has been a real benefit since less blood is outside the body (30-50 ml in these hollow fiber devices). For adult patients these is a less clear advantage. The coil, flat sheet, and the hollow fiber kidneys are all rather similar in performance.

Plasmapheresis, or plasma exchange, is a more recent development in which the blood dialyzer has been a real benefit. Initially it was used to harvest plasma from blood donors and now it is used to remove myeloma protein from patients with hyperviscosity syndromes. By use of the dialyzer instead of the centrifuge, more plasma can be removed at a single session with the patient and thus makes possible the treatment of immunologically mediated diseases (22).

Another extracorporeal device using hollow fibers that is currently being investigated is the artificial pancreas(23). The discovery of insulin by Banting and Best over 60 years ago affected the lives of millions of diabetics. However, the injection method of giving the insulin resulted in complications such as retinopathy, neuropathy, premature atherosclerosis, etc. If the insulin could be administered in response to need these problems should be avoided. One approach that is being explored is the artificial pancreas in which Islet cells are on one side of the semi-permeable membrane of the hollow fiber (thus protected from rejection by the body) and the blood to be treated is on the other side of the hollow fiber membrane. Since the smaller molecules such as glucose and insulin can freely diffuse through the membrane, regulation can be obtained. Devices have worked in animals for only short periods of time, a major problem being occlusion of the device at the connection to the natural blood vessel. Thus improvements in small diameter blood vessel research should be applicable in this area and thus these devices show great promise for the future.

The use of a membrane in an artificial lung, or blood oxygenator device has reduced the amount of blood damage resulting from direct blood/gas contact. Newer blood oxygen devices are using hollow fibers as well as flat sheet membranes from ePTFE, expanded polypropylene, silicone rubber coated fabrics and papers, and polyurethane-coated fabrics and papers.

Optical Fibers. Glass and polymethyl methacrylate fibers when appropriately coated become excellent conductors of light. These optical fibers are beginning to provide the means for surgeons to visualize internal problems without the need for surgical invasion of the body. For example, the cystoscope can be easily inserted into the colon and allows visualization of the colon surface (through the optical fibers) for tumors. Since the optical fibers can also be used as transmitters of laser light, a second fiber can be used to treat the condition as well. The optical fibers can transmit an Argon pumped dye laser at 630 nanometers to the tumor site. With the tumor tissue stained with the red hemoporphyrin dyes, the destruction of the tumor by the laser is enhanced. Optical fibers for lasers are also being tried in conjunction with angioplasty. The compression of plaques by angioplasty itself has not been an unqualified success since recurrence is greater than 30%. Also, when the vessel is occluded, the balloon can not be inserted. The use of lasers to destroy the plaque has been even worse since the laser beam is difficult to direct and could damage the vessel wall. By combining the balloon with a laser, the laser can be positioned by the balloon so that it is directed to the center of the plaque; the vessel can then be partially opened making compaction possible. While these technologies are still in their exploratory phase, they hold much promise for the future. The use of UV (excimer) lasers which do not liberate heat may be advantageous in eliminating scar tissue formation.

Fibers in Composites. Fibers have also been used in a variety of composites, ranging from coatings on the stems of hip prostheses, as fiber bundles in ligament and tendon prostheses, to the more traditional types of polymer/fiber composites for hard tissue materials, bone plates, etc. Carbon fibers are nonantigenic (not rejected by the body) and will be used more extensively in future prosthetic efforts. Also, by making composites with controlled porosity it is possible to have replacement parts that can more readily integrate natural fiber growth into the implant.

Conclusion.

Fibrous materials have and will always play an important role in the advancement of medicine and surgery. The following papers in this symposium will cover in more detail the areas of fibrous wound closure materials, fabrics for implant applications, and fiber composites in orthopedics. However, if we are to make progress in the future, one must have these fibrous materials in the right physical form and be made of the right polymer. Many of the problems of the past have occurred when this simple concept was ignored.

Downloaded by CORNELL UNIV on August 6, 2012 | http://pubs.acs.org
Publication Date: April 3, 1991 | doi: 10.1021/bk-1991-0457.ch008

Literature Cited.

1. Snyder, C.C., Seare, W.J., Johnson, Herzog, B. Symposium on Plastic and Reconstruction Surgery, American College of Veterinary Surgeons Annual Meeting. October 31, 1973. Chicago, Illinois.
2. Evertt, W.G., Progr. Surg. 1970, 8,14-37.
3. Edlich, R.F.; Panek, P.H.; Rodeheaven, G.T.; et al., Ann. Surg. 1973, 177, 679-688.
4. Gristina, A.G.; Costerton, J.W.; Leake, E.; et al., Orthop. Trans., 1980, 4, 355.
5. Katz, S.; Izhar, M.; Mirelman, D., Ann. Surg. 1981, 194, 35-41.
6. Mark, H.; Whitby, G.T., Eds.; Collected Papers of Wallace Hume Carothers, Interscience: New York, 1940.
7. Hopkinson, B.R.; Hardman, J., J. Proc. Royal Soc. Med. 1973, 66, 1095.
8. Boretos, J.W.; Detmer, D.E.; Donachy, J.H., J. Biomed. Mater. Res. 1971, 5, 373-387.
9. Wagner, M.; Reul, J.T.; Kayser, K.L., Am. J. Surg. 1966, 111, 838-841.
10. Voorhees, A.B.; Jaretski, A.; Blakemore, A.H., Ann. Surg. 1952, 135, 332.
11. Campbell, C.D.; Brooks, D.H.; Bahnson, H.T., In Vascular Grafts; Sawyer, P.N.; Kaplitt, M.J. Eds.; Appleton-Century-Crofts: New York, 1978; Chapter 31.
12. Annis, D.; Bornat, A.; Edwards, R.; et al, Trans. Am. Soc. Artif. Intern. Organs 1978, 24, 209-214.
13. Lyman, D.J.; Albo, D.; Jackson, R.; et al, Trans. Am. Soc. Artif. Intern. Organs 1977, 23, 253-260.
14. Gilding, D.K.; Reed, A.M.; Askill, I.N.; et al, Trans. Am. Soc. Artif. Intern. Organs 1984, 30, 571-576.
15. Goldberg, L.; Bosco, P.; Shors, E.; et al, Trans. Am. Soc. Artif. Intern. Organs 1981, 28, 195-198.
16. Herring, M.B.; Gardner A.L.; and Glover, J., Surg. 1978, 84, 498-504.
17. Graham, L.M.; Burkel, W.E.; Ford, J.W.; et al, Surg. 1982, 91, 550-559.
18. Lyman, D.J.; Lyman, E.C.; Eichwald, E., Trans. 3rd World Biomaterials Congress 1988, 11, 55.
19. Voyles, C.R., Ann. Surg. 1981, 194, 219-223.
20. Abell, J.J.; Rowntree, L.C.; Turner, B.B., J. Pharmacol. Exp. Ther. 1913-1914, 5, 275.
21. Stewart, R.D.; Cerny, J.C.; Mahon, H.I., Univ. Michigan Med. Centre J. 1964, 30,116.
22. Rees, A.J., In Replacement of Renal Function by Dialysis; Drukker, W.; Parsons, F.M.; Mahe, J.F., Eds.; Martinus Nijhoff: Boston, 2nd ed., 1983, Chapter 48.
23. Sun, A.M.; Parisius, W.; Healy, G.M.; et al., Diabetes 1977, 26, 1136-1139.

RECEIVED October 22, 1990

Downloaded by CORNELL UNIV on August 6, 2012 | http://pubs.acs.org
Publication Date: April 3, 1991 | doi: 10.1021/bk-1991-0457.ch008

Chapter 9

Textiles as Bioimplants

Roger W. Snyder

Harbour Biomedical Consultants, Inc., 2716 Bent Tree Trail,
League City, TX 77573

Downloaded by UNIV OF GUELPH LIBRARY on August 6, 2012 | http://pubs.acs.org
Publication Date: April 3, 1991 | doi: 10.1021/bk-1991-0457.ch009

Basic textile structures and yarns have been used in numerous implanted devices. Since variables in structure and yarn are not always independent, trade-offs between ingrowth, strength and handling of medical textiles must be made. Those properties known to affect degradation and biocompatibility include base polymer, fiber shape, processing and contaminants. Primary areas of current research in the medical use of textiles such as biologic composite structures, solvent bonded nonwovens and new yarns are briefly discussed. Although textiles have been used in medical devices for many years, new uses are still being found.

The use of textiles in medicine is an ancient and varied art. Current applications range from external uses such as simple bandages, complicated trusses and stockings; to internal uses ranging from simple sutures to artificial arteries and ligaments. Any application requiring flexibility, uniaxial or biaxial strength and/or porosity can use a textile. A number of materials that can be fabricated into textiles are biostable or at least degrade in a predictable manner. In addition, the fabrication of textiles is an old art and a wide variety of techniques are available which allow the design of an appropriate structure.

Uses

Textiles have long been used externally for wound dressings, pressure bandages or supports, casts, etc. The use of textiles as implants began with the use of threads as sutures. Vorhees (see, for example Callow (1)) noted that a suture inserted into the right ventricle retained fibrin and cells. Soon several investigators were trying various structures as cardiovascular patches and vascular replacements. Certain textiles soon demonstrated the ability to replace or bypass damaged arteries. These textiles functioned by serving as a scaffold for fibrin, collagen or, in some cases, cells.

0097–6156/91/0457–0124$06.00/0

Textile vascular grafts and cardiovascular patches still represent one of the largest uses for textiles as implants. However, other uses have also developed. In the cardiovascular field, vascular grafts have been used for arterial-venous shunts, connectors for the artificial hearts currently under development and felt pledgets to prevent sutures from cutting through fragile tissue. In a related application, many of the early heavy pacemakers were inserted into textile pouches, which prevented migration and encouraged the formation of an intramuscular cavity.

The discovery that textiles could be used to encourage ingrowth led to a number of other applications such as cuffs around various access devices, liners for some artificial heart models, nerve regeneration tubes and tabs to anchor other implants. Many textiles can also be heat set or shrunk into various shapes which turns out to be very useful for improving handling characteristics in some applications such as vascular grafts. The majority of textile vascular grafts are crimped. This is primarily a heat setting process. The crimps allow the length of the graft to be adjusted and keeps the cross section circular, even when the textile is wet and sticky with blood. This makes the surgeon's job easier. These heat setting and shrinking characteristics are also useful in other applications such as fitting sewing rings to various devices.

Finally, textiles also have the property of being very stiff and strong uniaxially or biaxially , at least in tension, and very flexible in bending. This property is very useful in designing unidirectional structures such as artificial ligaments and tendons. Of course, the property of encouraging ingrowth needs to be overcome, especially at the midpoints of these devices, where ingrowth or scar tissue might interfere with movement. Thus these structures are normally designed with minimal porosity, except perhaps at the ends where anchoring is important.

Downloaded by UNIV OF GUELPH LIBRARY on August 6, 2012 | http://pubs.acs.org
Publication Date: April 3, 1991 | doi: 10.1021/bk-1991-0457.ch009

Structures

There are three basic structures for textiles; nonwovens, wovens and knits. Each has properties that directly impact upon the application. Nonwovens are basically piles or mats of short fibers which can be held together in a number of ways. Felts are tangled or intertwined by passing barbed needles back and forth through the thickness. Spun bonded or melt bonded materials have fibers that are bonded together by adhesive, solvent welding, partial melting (by direct heat or ultrasonically) or by another polymer. Typically, nonwovens have been used for sewing rings , pledgets or other applications where thickness or compressibility might be required. Thin nonwoven materials have not demonstrated the strength required for load carrying applications.

Woven materials consist of at least two independent yarns typically crossing each other at right angles (warp and weft), as shown in Figure 1a. These materials tend to be very strong if tightly woven and have minimal porosity. Fine yarns can be woven tightly enough to be nearly waterproof. The patterns can vary from simple over under patterns to complicated tweeds and other patterned textiles. Additional floater yarns can be added to give a napped or plush surface. Yarns can be varied to yield structures that might be partially degradable. One other class of woven structures are braids. Braids are woven structures with the yarns running

Downloaded by UNIV OF GUELPH LIBRARY on August 6, 2012 | http://pubs.acs.org
Publication Date: April 3, 1991 | doi: 10.1021/bk-1991-0457.ch009

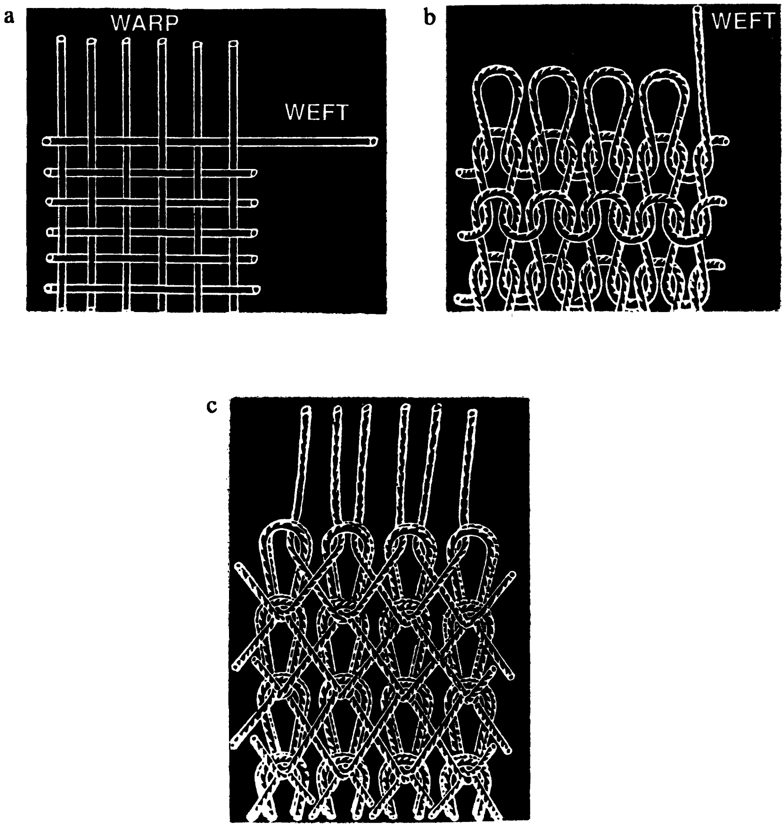

Figure 1. (a) Simple woven structure; (b) Simple weft knit structure; (c) Typical warp knit structure.

at angles to the length of the structure. This structure is very strong in the axial direction, but difficult to stabilize against unraveling. Such structures are commonly used to reinforce tubing, such as cardiovascular catheters, or as braided sutures.

Knits are complicated structures which generally consist of yarns running in one direction or the other. For example, a weft knit might be formed of a single yarn traveling back and forth across the fabric, such as illustrated in Figure 1b. A warp knit consists of yarns all generally traveling along the length of the fabric. Like the woven, additional yarns can be laid in to yield patterns or plush surfaces. An example of one such pattern is illustrated in Figure 1c. In the warp knit, different yarns can be used to form a partially degradable fabric. However, each yarn must be accompanied with a stable yarn to prevent the fabric from unraveling.

Knits are typically more porous and not as strong as wovens. This is because yarns generally must make tighter bends in a knit, decreasing their effective strength and making it difficult to form a tight fabric. On the other hand, because of these bends, knits are in general more pliable, often containing pivot points where the fabric can bend without bending and stretching the actual yarns.

Materials

A number of biostable materials, suitable for implant have been identified over the past 20 years. Probably the material with the most experience in terms of length of implant and number of cases is polyester, specifically polyethylene terephathalate as manufactured by DuPont in fiber form. Dacron vascular grafts have been explanted after 18 years, still functioning (2).

Polytetrafluorethylene, as Teflon fibers by DuPont has shown excellent long term biostability; however with fewer implants to date than polyester. Data out to 17 years for textile vascular grafts demonstrates a lot less decrease in strength than Dacron (2). Polypropylene has also been used successfully in sutures for long implant times.

Materials which have shown mixed results include ivalon, nylon, silk and polyurethane among others. Ivalon and nylon were used in some of the early vascular grafts. Both approached zero strength after approximately two years implant. This is an example which should be remembered by anyone designing implants. Silk sutures are seldom used for any long term application. Some polyurethane fabrications have also shown degradation in long term implant situations.

Some materials have been designed to degrade. Most of these materials to date are based on the polyglycolic acid chemistry. The use of these materials in textiles other than as sutures have been limited.

Several mechanisms have been demonstrated or proposed for polymer degradation. Hydrolysis was the first mechanism proposed and is probably the most prevalent. The ability of some cells and bacteria to actively degrade some polymers, probably through secreted enzymes or change in pH environment has been demonstrated (3).

These degradation mechanisms are affected by a number of factors. The formulation of the polymer will make a difference. For example, textiles formulated from polyester copolymers have shown signs of degradation not seen in the original polyester homopolymer textiles (4). Processing can also make a difference. Cracks and fissures in the polymer can be caused by excessive temperatures in the presence of moisture. Finally the presence of residual surfactants might enhance surface damage.

Downloaded by UNIV OF GUELPH LIBRARY on August 6, 2012 | http://pubs.acs.org
Publication Date: April 3, 1991 | doi: 10.1021/bk-1991-0457.ch009

Filament shapes which increase surface area and cause local stress concentrations accelerate degradation. Fiber bulk will also impact the process. Large filaments or a larger number of filaments increase the bulk to be attacked and decrease the stress levels in individual fibers which will lessen stress mediated degradation.

Finally, sterility and biocompatibility will also impact degradation. The presence of a few bacteria on a "sterile" product may lead to local degradation as well as a long term infection. The presence of certain cells whose function is to remove foreign bodies will also contribute to degradation (3). Sterilization itself is a thermal, chemical or radiation process which can damage polymers.

Downloaded by UNIV OF GUELPH LIBRARY on August 6, 2012 | http://pubs.acs.org
Publication Date: April 3, 1991 | doi: 10.1021/bk-1991-0457.ch009

Biocompatibility

Although the mechanisms of biocompatibility are not fully understood, four factors have been demonstrated to effect how a biological entity reacts to an implanted textile. Probably the most important is porosity. It was demonstrated many years ago by Weslow (5) that an optimum porosity existed which would encourage ingrowth or encapsulation. The lower limit of porosity is normally limited by the type of structure and the upper limit is determined by the stability of the structure and the ability of the implanter. The optimum porosity is normally achieved by a fairly tight knitted structure. A tightly woven structure is too tight for optimum ingrowth. The size and shape of the filaments also effects the host acceptance. Smaller fibers with circular cross-sections are better encapsulated than larger fibers with irregular cross-sections.

Third, toxic substances such as monomers, solvents or polymerization byproducts leaching out of a polymer will have a negative impact on the tissue reaction to the implant. Surface contaminations such as sizing agents, lubricants or surfactants can also negatively impact the results. As shown in a study by Sawyer(6), different methods of processing the same material may result in substances left on the surface or toxic solvents eluting from the polymer, with a negative impact on the host.

Some bacteria, even though killed during sterilization, can leave toxic molecules on the surface of the polymer. These molecules elicit a toxic reaction from the host and are extremely difficult to eliminate. Finally the properties of the polymer itself and certainly the surface configuration of the polymer will effect the outcome. Among the polymers which have been used as implants, nylon seems the most reactive and PTFE the least, with polypropylene and polyester in between.

A fifth area in which the data is not as clear is the compliance of the structure. Evidence suggests that compliance matching at tissue/material interfaces will minimize any stress induced or mediated growth. On the other hand, evidence published by Sauvage (7), among others, suggests that a more rigid textile tube yields better results in certain vascular implant situations. Certainly, textiles made from polymers such as polyester or PTFE have compliances much lower than natural tissue. It may also be that movement of the textile structure causes excessive tissue growth. This is one area in which additional research is needed.

Design of Textiles For Implants

In general implants fall into two categories, synthetic and biological. Biological implants will generally consist of certain organs or tissues treated to increase biocompatibility, host acceptance and decrease antigenicity and perhaps increase fatigue life. These implants may contain synthetic materials as stents, sewing rings, or containment devices. In general, the synthetic components will be less biocompatible but more fatigue resistant and easier to reproduce.

The design of textiles for any implant application is complicated by the number of choices in textile structures and the number of variables present. A number of these variables are not independent and effect the results in opposite directions, as shown in Figure 2.

As an example, those fabrics with superior strength tend to have lower porosity and therefore are less likely to be well encapsulated. Even for a given type of structure, as the structure is tightened, the strength tends to increase, but porosity decreases. Also, in general as porosity increases, the flexibility or handling of the fabric improves. Thus, it is necessary to trade off strength for handling and ingrowth.

As a second example, although PTFE yarn appears to be the most biostable material available, PTFE yarn filaments are relatively large in diameter and textiles fabricated from that yarn generally have higher porosity. Also the yarn feels "different". Thus one might trade off decreased risk of long term failure for lower porosity and better handling achieved with another yarn such as polyester; which, if carefully manufactured, could have sufficient longevity for many applications.

Therefore, like any other good design, it is first of all important to determine what the implant is suppose to accomplish and then decide what priorities exist in terms of some of the other features. The list of parameters to be considered is extensive.

An implant requiring high strength might require a woven or braided structure, particularly if ingrowth must be minimized, such as in an artificial tendon or ligament. However, an implant requiring ingrowth and subjected to relatively low loads might better use a knit, particularly if flexibility and handling are important, such as in a small diameter vascular graft, where the surgeon's skill may be a major contribution to success.

Future Textile Design

The primary area of research in the use of current textiles is composite structures, primarily biological composites. This is an attempt to combine the biocompatibility of biological polymers with the strength and consistency of synthetic polymers. This is currently being accomplished in two ways. The first way is with a coating such as collagen or albumin to seal the pores of the textile. This coating can be adjusted to degrade slowly or to be nearly biostable. Currently, this technology is being used in vascular grafts, but also has applications in other areas such as

Downloaded by UNIV OF GUELPH LIBRARY on August 6, 2012 | http://pubs.acs.org
Publication Date: April 3, 1991 | doi: 10.1021/bk-1991-0457.ch009

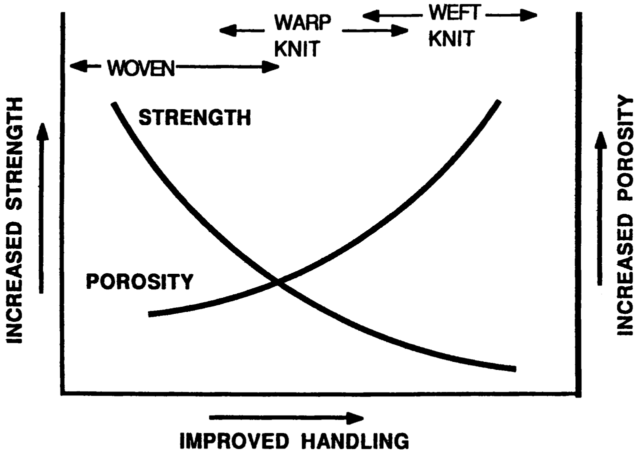

Figure 2. Schematic of variations in porosity, strength and handling characteristics.

artificial ligaments and nerve regeneration tubes. Ligaments have been designed and tested using synthetic materials to coat a carbon filament substrate.

A second type of composite being used, again primarily in vascular grafts, is a seeded material. Autologous cells are removed and cultured until they multiply to a useful level. They are then mixed with a suitable substrate, such as fibrin, and used to coat the textile. Until the implant matures, these cells improve the biocompatibility of the textile. This technology has also been applied to artificial skin.

Another area of research related to textiles is the use of solvent bonded nonwovens as small diameter grafts. These materials are formed by spraying polyurethanes directly onto a rotating mandrel. The overlapping filaments bond while curing on the mandrel, presenting a material such as seen here. Most of the work in this area has been done with polyurethanes or polyurethane/silicone combinations. Degradation remains a problem with these designs. Pore size must be controlled to prevent penetration of macrophage cells, among others.

Finally, new yarns being developed for the commercial sector, such as finer filament polyesters and new polymers will eventually find their way into medical applications. The use of these new materials will be slow to materialize, due to the amount of testing necessary to prove biocompatibility and biostability. However, benefits such as stronger or more flexible textiles will provide the incentive to undertake the expensive testing required.

Conclusions

Although textiles have been used in medical devices for many years, new uses are still being found. Any application requiring a combination of strength and flexibility and perhaps long term ingrowth is a candidate for a textile. Textiles can

Downloaded by UNIV OF GUELPH LIBRARY on August 6, 2012 | http://pubs.acs.org
Publication Date: April 3, 1991 | doi: 10.1021/bk-1991-0457.ch009

serve as scaffolds for natural tissue replacement and, if necessary remain as long term support structures. Certain textiles, used as vascular replacements have demonstrated a longevity approaching twenty years, in an environment that has demonstrated the ability to destroy some polymers.

Literature Cited

1. Callow, A.D. In Biological and Synthetic Vascular Prostheses; Stanley, J.C.; et al, Eds.; Grune and Stratton: New York, 1982; pp 11-26.
2. Botzko, K.; Snyder, R; Larkin, J.; Edwards, W.S. ASTM Spec. Tech. Pub., STP 684 1979; pp76-88.
3. King, M.W.; Guidoin, R.; Blais,P.; Garton, A.; Gunasekera; K.R. ASTM Spec. Tech. Pub., STP 859; 1983; pp294-307.
4. Williams, D.F. ASTM Spec. Tech. Pub., STP 684 1979; pp61-75.
5. Wesolowski, S.A.; Fries, C.C.; Karlson, K.E.; DeBakey, M. E. ; Sawyer, P. N. Surgery (St Louis) 1961, 50, pp91-96 and 105-106.
6. Sawyer, P. N. ;Stanczewski, B. ; Hoskin, G. P. ; Sophie, Z. ; Stillman, R. M. J. Biomed. Mater. Res. 1979, 13, pp 937-956.
7. L. R. Sauvage, L.R. In Vascular Grafting: Clinical Applications and Techniques; Wright,C.B.; et al (Eds.); John Wright - PSG, Inc: Boston, 1983; pp 168-186.

RECEIVED July 5, 1990

Downloaded by UNIV OF GUELPH LIBRARY on August 6, 2012 | http://pubs.acs.org
Publication Date: April 3, 1991 | doi: 10.1021/bk-1991-0457.ch009

Downloaded by UNIV OF ARIZONA on August 6, 2012 | http://pubs.acs.org
Publication Date: April 3, 1991 | doi: 10.1021/bk-1991-0457.ch010

Chapter 10

The Design and Analysis of Laminated Degradable Composite Bone Plates for Fracture Fixation

Mark C. Zimmerman[1], Harold Alexander[2], J. Russell Parsons[1], and P. K. Bajpai[3]

[1]Section of Orthopaedics, University of Medicine and Dentistry of New Jersey, 185 South Orange Avenue, MSB–G574, Newark, NJ 07163
[2]Department of Bioengineering, Hospital for Joint Diseases Orthopaedic Institute, 301 East 17th Street, New York, NY 10003
[3]Department of Biology, University of Dayton, 300 College Park, Dayton, OH 45469

Bone plates for fracture healing were fabricated using a thermoplastic absorbable polymer (polylactic acid polymer) reinforced with high-modulus carbon fiber to produce a semiabsorbable composite and with a calcium phosphate glass fiber to produce a fully absorbable composite. A 0°/±45° laminae layup was used, which composite analysis had indicated would yield an optimum fiber layup. Mechanical testing demonstrated this design to have static and fatigue properties superior to those of laminated or random fiber designs used previously. The production of screwholes during the molding process, rather than machining postmolding, improved the mechanical integrity of the finished plate. Although the 0°/±45° composites possessed adequate mechanical properties and biocompatibility, they were unsuccessful in *in vivo* efficacy testing. Further development to prevent water intrusion and premature loss of mechanical properties is necessary.

Rigid metallic bone plates have two serious disadvantages. The alloys used in the production of the plates leach metallic ions that cause adverse local tissue reactions as well as allogenic responses (1). In a few cases, local tumor formation has been reported (1,2). A second and possibly more serious short-term problem is stress protection atrophy (3-9). As a long bone is loaded, the stress the bone is exposed to causes a compensatory remodeling. The application of a rigid plate alters the loading process and the bone may atrophy. Various studies have demonstrated a loss of bone

0097–6156/91/0457–0132$06.00/0

Downloaded by UNIV OF ARIZONA on August 6, 2012 | http://pubs.acs.org
Publication Date: April 3, 1991 | doi: 10.1021/bk-1991-0457.ch010

mass, decreased cortical thickness, and increased osteoporosis after removing the stress. Thus, it is recommended that metallic fracture fixation hardware be removed once the fracture has healed and there is no danger of refracture.

Researchers have investigated the use of flexible plates as a possible solution to stress protection atrophy. Polymers and composite materials are prime choices because they can be more flexible than metals. Polylactic acid (PLA) is an absorbable polymer that has received considerable attention in fracture fixation; however, the mechanical properties are not adequate for long bone fixation (10). Reinforced composite materials have adequate mechanical properties, and some have been used to successfully fix canine and human fractures. The successful composite systems include glass/epoxy (11), carbon/epoxy (12,13), carbon/methyl methacrylate (3,14), carbon/polypropylene (11), and carbon/polysulfone (11). Because their long-term biocompatibility has not been demonstrated and because of their permanency, they only provide a partial solution to the stress protection dilemma.

The ideal bone plate would be rigid to allow fracture healing, slowly lose its mechanical stiffness to lessen osteoporosis, and completely degrade to biocompatible entities. As a first step toward this goal, PLA polymer reinforced with randomly oriented chopped carbon fiber was used in the authors' laboratories to produce partially degradable bone plates (15). By virtue of the fiber reinforcement, the plates were shown to have mechanical properties superior to those of pure polymer plates. In vivo, the PLA matrix degraded and the plates lost rigidity, gradually transferring load to the healing bone. The degradation products of the polymer matrix as well as the carbon fiber reinforcement are known to be compatible (16-19); hence, it would be unnecessary for the plate to be removed. These partially absorbable composite bone plates were tested in a canine osteotomy model and a canine stress protection osteoporosis model (20). However, the mechanical properties of such chopped-fiber plates were relatively low. Consequently, the plates were only adequate for low-load situations. If a composite plate of these materials was to be successful in a high-load situation, it was felt that an improved design was necessary. Hence, a study was organized to investigate the possibility of using a long-fiber, angle-ply-laminated composite of carbon fiber and PLA (21).

Design criteria were developed with this system; however, a potential totally absorbable material with the necessary criteria is a composite of PLA polymer reinforced with a calcium phosphate (CaP) fiber. An absorbable CaP fiber was developed to reinforce the polymer, and a series of experiments are described evaluating the properties and biocompatibility of this material.

Materials and Methods

Composite Analysis. Theoretical composite analysis was accomplished with the aid of a commercially available computer software package (Comp-Cal, Center for Composite Materials, University of Delaware, Newark, DE). The program combines micro- and macromechanical composite theory to determine in-plane and bending properties. Various parameters are necessary as input data, including the mechanical properties of the fiber and matrix material, the fiber volume fraction, the number of laminae, the laminae orientation, and the external stresses on the system. Elastic moduli (in plane, transverse, and shear), Poisson's ratios, and strength can be theoretically calculated. The analysis is only applicable for a symmetric, balanced, laminated composite. Although limited in scope, the analysis supplies useful theoretical predictions that can be compared to experimental results.

Fabrication Procedure. Fabrication of bone plates included laminae production and composite compression molding. A fiber-winding device was used to produce composite laminae. Fiber (Hercules AF-1: Hercules, Inc., Wilmington, DE) was pulled from a spool, run through a 1.1 wt % polymer solvent solution, and wound onto a drum. The solvent, chloroform, evaporated, leaving a fiber/PLA pre-preg (PLA from Hexcel Medical, Dublin, CA). The pre-pregs were cut into coupons and placed in a mold. The mold was heated to the melt temperature of the polymer, and the composite was compression-molded. The plates were molded at 200°C at a pressure of 1000 psi. The heating rate was 6°C/min, and the cooling rate was 12°C/min. The mean fiber volume fraction of the finished specimens was 56% ± 3%. The plates were fabricated with molded screwholes in the composite.

The fibers used in the fiber compatibility study were 100 μm in diameter and had a ratio of CaO/P_2O_5 of 25.5:74.5. Fiber diameter is directly related to the mechanical properties of the fiber. A thin fiber has less surface flaws that serve as stress concentrations. Any area of stress concentration will allow the fiber to fail at submaterial stresses. Because of these problems with thick fibers, a thin fiber was developed for the composite. The ultimate tensile strength of the 10-μm CaP fiber was 654 MPa. These fibers also contained 3% aluminium oxide.

For biocompatibility experiments, laminae were produced by placing thin CaPAlO fiber (4.8 g) in a bath of PLA (5 g) dissolved in CH_2Cl_2 (300 ml; purity 99.8% $CHCl_3 + C_2H_5OH$). The CH_2Cl_2 evaporated, leaving fiber/polymer laminae. The laminae were cut into coupons (103 × 16 × ~0.2 mm), placed in a mold, and, with the application of pressure and heat, molded into a composite. The maximum temperature was 200°C, and the maximum pressure was 1000 psi. The composite had a volume fraction of 31%, and the fiber was oriented in the 0° direction.

Unmolded porous composite was produced by mixing 1.5 g of PLA, 1.5 g of glass fiber, and 300 ml of CH_2Cl_2. The CH_2Cl_2 evaporated, and a porous composite remained.

Ultrahigh-molecular-weight polyethylene (UHMWPE) was used as a control for the biocompatibility implantations. Both the composite and polyethylene were cut into implants 2.5 × 2.5 × 5.0 mm. All implants were sterilized with ethylene oxide for 12 hr and then ventilated for 24 hr.

In Vitro Testing. The composite plates were mechanically tested in four-point bending in an MTS servohydraulic mechanical testing machine. For static experiments, the machine was used in stroke control (crosshead movement was maintained at a constant rate regardless of load), and the crosshead speed was 0.2 mm/sec. For fatigue testing, the machine was placed in load control (a loading wave form was applied regardless of the deflection) and the test specimens were sinusoidally cycled at 3 Hz. The static tests were carried out in air and the fatigue tests in saline at 37°C.

In a series of experiments, the static and fatigue properties of the composite were investigated.

In vitro degradation studies were performed to determine the decrease in mechanical properties of the fiber/PLA composites as a result of water absorption. Carbon-fiber-reinforced plates with molded holes were soaked in saline maintained at 37°C and mechanically tested after soaking for 1, 2, 4, or 8 weeks. Glass fiber (CaPAlO)

Downloaded by UNIV OF ARIZONA on August 6, 2012 | http://pubs.acs.org
Publication Date: April 3, 1991 | doi: 10.1021/bk-1991-0457.ch010

Downloaded by UNIV OF ARIZONA on August 6, 2012 | http://pubs.acs.org
Publication Date: April 3, 1991 | doi: 10.1021/bk-1991-0457.ch010

samples of 50 mg each, PLA rods (2.6 mm in diameter, 4.8 mm long), and glass-fiber-reinforced composites (1.0 × 1.0 × 0.43 cm) were immersed in tris-buffered saline solution of pH 7.4 maintained at 37°C. To inhibit the growth of microorganisms, 0.002% sodium azide was added to the solutions. Weight loss, PLA, calcium, and phosphorous release, and mechanical properties were determined at time periods from ½ to 8 weeks (22).

In Vivo Studies. NIH guidelines for the use of laboratory animals (23) were followed in all studies. A fracture fixation study was performed to test the carbon-fiber-reinforced plates in the in vivo environment. Eight male coonhounds received transverse middiaphysis femoral osteotomies of their right femurs. Four control animals received metal plates, and four experimental animals received composite plates. All animals received three bone labels: oxytetracycline (24), xylenol orange (25), and 2,4-bis(N,N′-di(carbomethyl)aminomethyl) (26) (DCAF) at 1, 4, and 8 weeks, respectively. When injected, these materials are incorporated in areas of bone that are metabolically active and fluoresce when exposed to ultraviolet light, making it possible to label new bone with a fluorescent marker. All animals were sacrificed at 10 weeks with an overdose of sodium pentobarbitol. In each group three animals had both femurs tested in four-point bending and one animal was utilized for histology. The histological specimens were dehydrated, imbedded in methyl methacrylate, sectioned, and polished. The sections were evaluated with light and UV light microscopy and photographed with an Olympus BH microscope–35mm camera combination.

Calcium phosphate fiber and composites (CaP/PLA) were implanted in two animal models to evaluate their respective biocompatibilities. The criteria for bone compatibility included bone growth around and into the implant and the condition of the new bone (resorption, osteoporosis, or active osteoblastic activity). The criteria for soft tissue compatibility included tissue response and cell type present (macrophage, multinuclear giant cells, or fibrous cells).

A rat model was used for the fiber studies and a rabbit model for the composite studies. Calcium phosphate fiber was implanted in the rat muscle (the dorsum of the back) and bone (transcortically in the femur). The fibers were 100 µm in diameter and 2.0 mm long. The adult male rats weighed 300 g and were sacrificed at 4, 12, 24 weeks.

The composite CaP/PLA specimens were implanted in rabbit muscle (dorsum of the back) and bone (transcortically in the tibia). They received UHMWPE plugs as controls. Two ceramic and two polyethylene plugs were placed in the back muscle, two ceramic implants in the right tibia, and two polyethylene plugs in the left tibia. Six rabbits received implants and two were sacrificed at 6, 12, and 24 weeks.

The unmolded composite of CaP/PLA was also implanted in rabbit muscle and tibia, again in the dorsum of the back, and transcortically in the bone. It was believed that this model would simulate a composite that had experienced biological exposure with subsequent resorption and increased implant surface area. Three animals received implants, as described above, and one animal was sacrificed at 6, 12 and 24 weeks.

The rabbits were adult males and weighed approximately 4 kg. The rabbits received 20 mg/kg/day of Liquimyacin (tetracycline) for 4 days commencing 14 days presacrifice (for bone labeling). They were sacrificed with overdoses of sodium pentobarbitol, and the hard tissue was harvested, dehydrated, and imbedded in Epon.

The blocks were polished and photographed with an Olympus BH microscope–35mm camera combination.

The soft tissue was fixed in formalin, dehydrated, and imbedded in paraffin. The blocks were sectioned, stained with hemotoxalin and eosin, and photographed with the above equipment.

Results

Composite Analysis. Bending is a complex loading situation. The bending moduli are stacking-sequence-dependent, while the in-plane moduli are not (27). A 0/-45/0/+45 stacking sequence was chosen because it produces high transverse and shear moduli (21). This combination of 60% 0° laminae and 40% 45° laminae also provides a laminate with superior fatigue properties (28).

Dimensionally, the composite bone plate was modeled after a popular commercially available plate (AO-ASIF, Davos, Switzerland). The design can be found in Figure 1. Normally, these designs have compression slots—slots that enable the surgeon to compress the bone ends during plate application. As the screws are driven home, the screwheads slide down the slot, putting the plate in tension and forcing the fracture into compression. Tayton et al. (12) found that epoxy composite plates failed when they were produced with multiple compression slots. In order to avoid this problem yet create a small compressive force, a single compression slot was placed at the end of the plate (Slot #6) away from the maximum bending moment. Another important difference from the standard design was the increased curvature of the plate to match the coonhound femur ($r = 13$ mm).

In Vitro Studies. Eight carbon/PLA plates without screwholes were molded in air and tested in bending. The mean bending modulus was 124.4 GPa, and the mean maximum bending stress was 412.0 MPa. The plates with molded holes had a bending modulus of 58.0 GPa and a maximum bending stress of 287.3 MPa. In bending, the maximum interlaminae shear stress is located at the neutral axis. The angle-ply specimens failed in shear at the neutral axis because of the weak interfacial bond between the laminae.

Figure 2 shows the results of the fatigue tests. Six plates were tested without screwholes and five with molded holes. The maximum number of cycles to failure for the plates with molded holes was approximately 1 million at a maximum bending stress of 110 MPa.

The modulus of plates with molded holes declined rapidly with time when soaked in saline (Fig. 3). The residual stiffness (i.e., that remaining after soaking) was 57% after 1 week and declined further to 53%, 48%, and 46% after 2, 4, and 6 weeks in saline, respectively.

The initial mechanical properties of the glass fiber/PLA composite were determined as shown in Table I (29).

From the rule of mixtures, the tensile modulus of the glass fiber is estimated to be approximately 48.3 GPa. This value compares favorably to that of commercial fiberglass (72 GPa).

The tensile properties of the unidirectional CaP/PLA composites degrade in the saline environment. Sixty-three percent of the strength and modulus are retained after 7 days in pH 7.4 tris-buffered saline at 37°C. Following these initial drops, strength

Downloaded by UNIV OF ARIZONA on August 6, 2012 | http://pubs.acs.org
Publication Date: April 3, 1991 | doi: 10.1021/bk-1991-0457.ch010

Downloaded by UNIV OF ARIZONA on August 6, 2012 | http://pubs.acs.org
Publication Date: April 3, 1991 | doi: 10.1021/bk-1991-0457.ch010

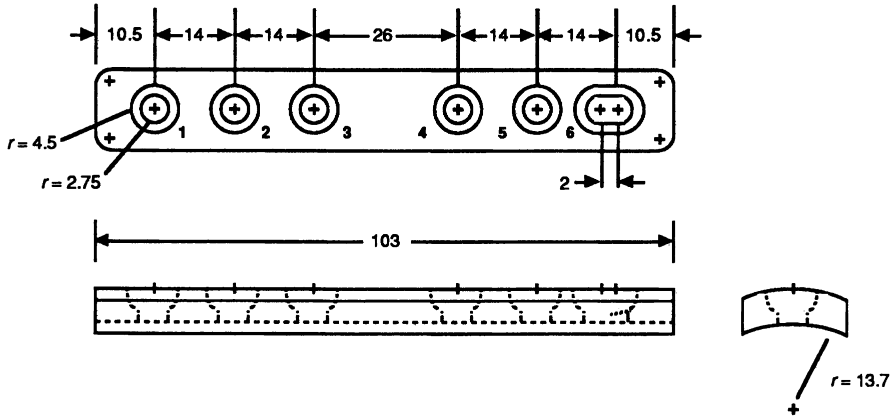

Figure 1. Bone plate design. All measurements are in millimeters.

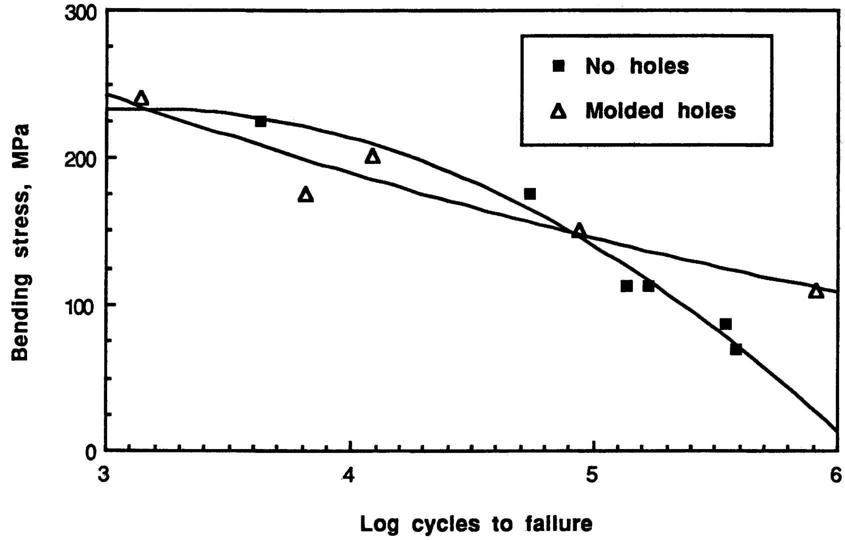

Figure 2. Fatigue results for carbon/PLA composites.

decreases more rapidly than does modulus. Thirty-five percent of the initial strength and 45% of the initial modulus are retained after 23 days of immersion. There is a 3% weight loss by 7 days and a 15% weight loss by 23 days. Similarly, the ±45° composites retain 52% of their flexural strength and 60% of their flexural modulus after 9 days of immersion. The initial loss in properties is attributed to plasticization by adsorbed water. Weight loss of the ±45° composites is much less than that of the unidirectional composites. A weight loss of 0.1% was observed at 2 days, and 0.9% was lost by 9 days.

Table I *GlassFiber/PLA Mechanical Properties*

	Strength (MPa)	Modulus (GPa)
Tension	200.3 ± 7.1	29.9 ± 2.2
Compression	185.5 ± 64.1	—
Flexion	161.3 ± 8.8	27.0 ± 0.3
Short beam shear	19.2 ± 2.0	—

Analysis of the lactic acid, calcium, and phosphorous release from the soaked samples suggested that the PLA–calcium–phosphorous–glass fiber composites degraded at a rate higher than either the PLA or the glass fiber (22). The dissolution profile of the PLA–glass fiber composite showed a burst effect, with the greatest amount of calcium and phosphorous release occurring at week 1. The tris-HCl media obtained from the PLA–glass fiber composites was found to contain a precipitate during the first 1½ weeks of the study. The precipitate was found to contain a significant amount of aluminum, calcium, and phosphorous. These data suggest that the composite degraded at a higher rate than suggested by the data obtained for composite degradation by analyzing the tris-HCl dissolution medium alone.

In Vivo Studies. All dogs with metal plates went on to union. These femurs were mechanically tested ($n = 3$) and histologically evaluated ($n = 1$). The composite plates in the first three dogs failed within 3 weeks. In each case, a bone screw adjacent to the osteotomy backed out of the bone. The resulting increased movement caused an increase in the local stress about the hole resulting in plate failure. The increased flexibility of the composite plate was believed to be the cause of this screw backout. The use of nuts and bolts improved the stability of the system. A second group of four dogs received composite plates with nuts and bolts. They were sacrificed at 10 weeks.

The histological results for the animals with steel plates showed the typical bone remodeling associated with metal plates (30). The femurs were in the process of healing as evidenced by the mechanical results (21). No histology or mechanical testing was performed on the animals with composite plates. Although the second group of plates had not failed catastrophically, they were flexible and extensively delaminated. Hypertrophic nonunions had developed in all four animals.

The biological evaluation of the CaP fibers and the CaP/PLA composites was qualitative. A series of photomicrographs, and a short discussion of each, serve as the results of this study.

Figure 4 is a photomicrograph of a bone sample taken from a rat after 4 weeks of implantation. The CaP fiber was intact, with a surrounding layer of particulate matter

Downloaded by UNIV OF ARIZONA on August 6, 2012 | http://pubs.acs.org
Publication Date: April 3, 1991 | doi: 10.1021/bk-1991-0457.ch010

Downloaded by UNIV OF ARIZONA on August 6, 2012 | http://pubs.acs.org
Publication Date: April 3, 1991 | doi: 10.1021/bk-1991-0457.ch010

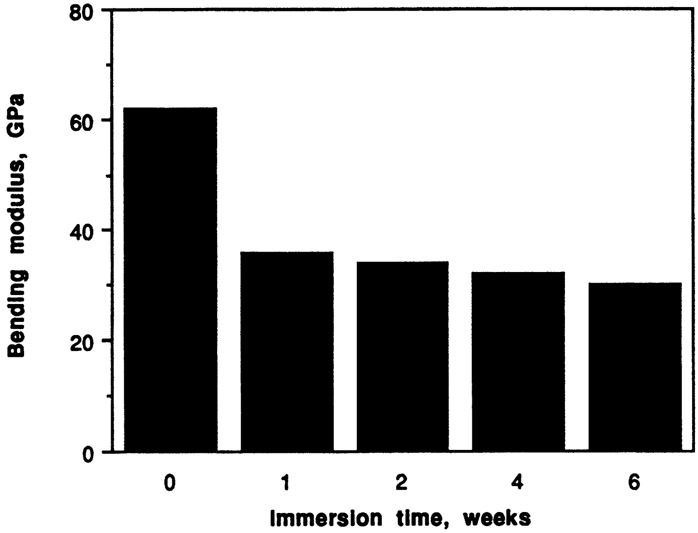

Figure 3. In vitro bending modulus as a function of soak time for carbon/PLA plates.

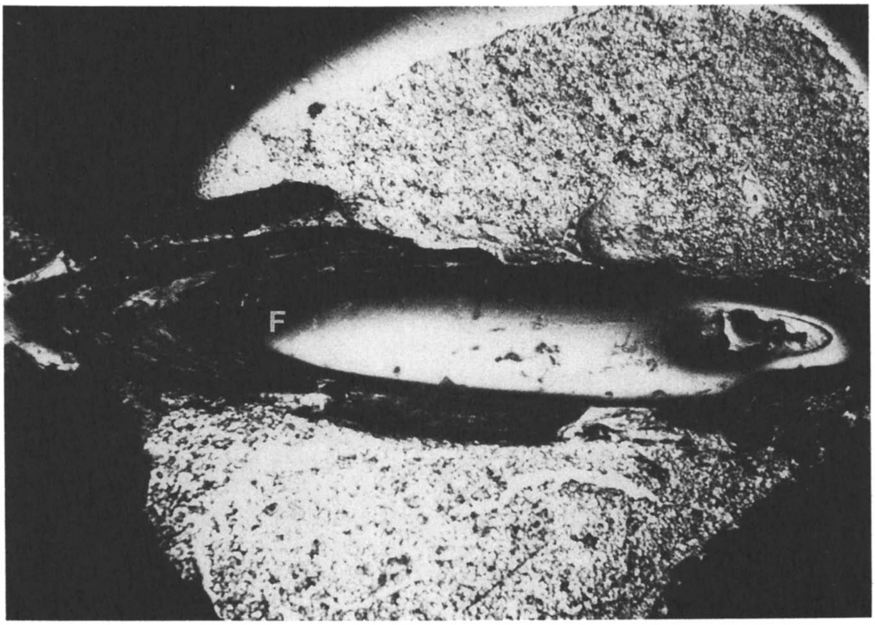

Figure 4. A CaP fiber imbedded in the medullary canal of a rat after 4 weeks of implantation. The fiber (F) was intact with a surrounding layer of particulate matter. 22×

between the fiber and the medullary canal. There was evidence of slight mechanical damage where the fiber had suffered minor cracks in the surface. Figure 5 shows the cross section of the same fiber. The dissolution products are clearly visible at the surface of the fiber.

The mechanical damage became more severe as the length of implantation increased. As shown in Figure 6, a fiber implanted for 12 weeks had cracks throughout its substance and bone growing about a large percentage of its surface area. At 24 weeks the damage was more severe, as the fiber was barely recognizable because of the combined mechanical and chemical degradation (Fig. 7). The fiber was broken apart completely and was in the process of absorbing. Good bone compatibility was evident, with new endosteal bone growing along the substance of the fiber.

Fiber implantation in striated muscle showed the fiber to be a benign intramuscular implant. A thin ring of fibrous cells encapsulated the fiber, and there was no evidence of an excessive inflammatory response. Figure 8 is a representative slide after 12 weeks of implantation.

The remaining figures are of composite materials implanted in bone. Figure 9 is a composite of CaP and PLA. The material was unmolded and was composed of large diameter fibers (100 μm). After 6 weeks of implantation, the PLA degraded minimally, and there was good tissue approximation with the implant. The "woven" bone was disorganized, with oddly shaped haversian systems. Figure 10 is another unmolded CaP/PLA composite; however, it has small-diameter fibers (10 μm). It was implanted for 6 weeks, and the porous nature of this material provided for bone ingrowth. Bone grew into and around the composite material.

Figures 11 and 12 are photomicrographs of molded CaP specimen after 12 weeks of implantation. Figure 11 was implanted for 6 weeks. The specimen was encapsulated with cortical bone. Figure 12 is a higher-power magnification of the same specimen. Bone is in direct contact with the cortical bone. There is no evidence of soft tissue between implant and bone.

Downloaded by UNIV OF ARIZONA on August 6, 2012 | http://pubs.acs.org
Publication Date: April 3, 1991 | doi: 10.1021/bk-1991-0457.ch010

Discussion

Composite Analysis. Theoretical analysis was in reasonable agreement with experimental results. The theoretical bending modulus for a 6.0-mm-thick 37-laminae design was 105 GPa, and the experimental value was 124 GPa. Any parameter that is related to the initial assumptions made for the theoretical determination may be responsible for the small discrepancy (e.g., fibers and matrix are linearly elastic and homogeneous, there are no voids).

In Vitro Studies. The carbon-reinforced PLA with the 0±45 angle-ply design provided a tenfold increase in modulus and a threefold increase in bending strength compared to pure PLA. Also, the angle-ply design used here increased the mean bending modulus 313% and the bending stress 84% above the values for chopped-fiber-reinforced plates (31).

Carbon fiber is a transversely isotropic material, and the mechanical properties of the fiber are greatest in the direction of the long axis of the fiber. Consequently, a composite with long fiber oriented in the direction of maximum stress will have superior properties compared to a short-fiber composite with a random fiber orientation.

Stress concentrations play an important role in structural properties. For an isotropic material, the stress about a circular hole is, in general, three times greater

Downloaded by UNIV OF ARIZONA on August 6, 2012 | http://pubs.acs.org
Publication Date: April 3, 1991 | doi: 10.1021/bk-1991-0457.ch010

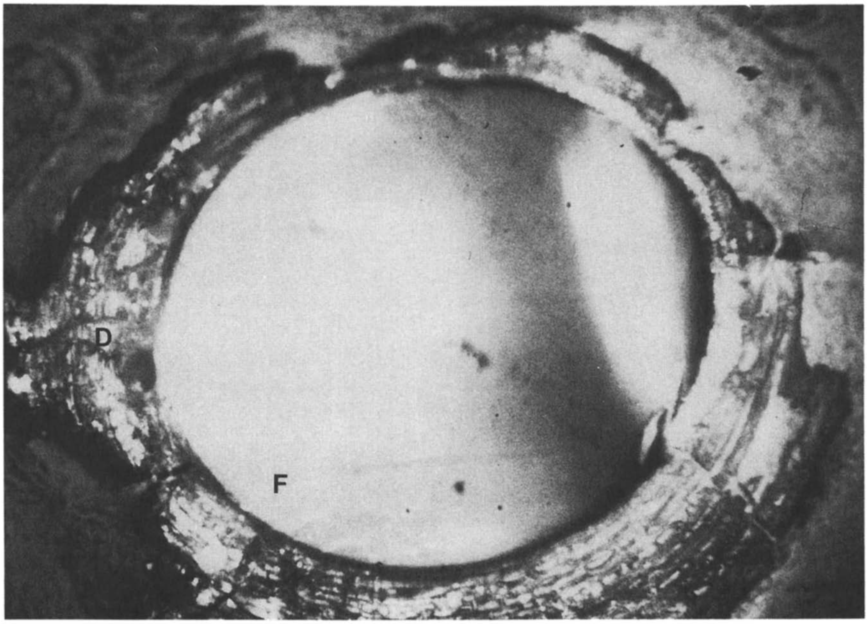

Figure 5. A transverse section of a CaP fiber after 4 weeks implantation. A ring of dissolution products (D) was located about the fiber (F). 90×

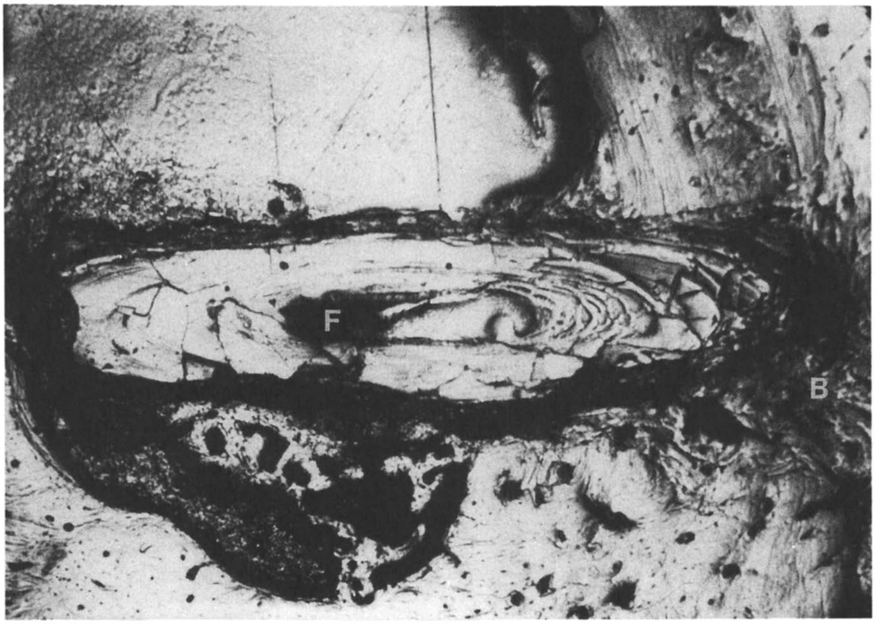

Figure 6. A CaP fiber implanted in a rat for 12 weeks. The fiber (F) had cracks running through its substance, and bone (B) filled in the drillhole entirely. 22×

Downloaded by UNIV OF ARIZONA on August 6, 2012 | http://pubs.acs.org
Publication Date: April 3, 1991 | doi: 10.1021/bk-1991-0457.ch010

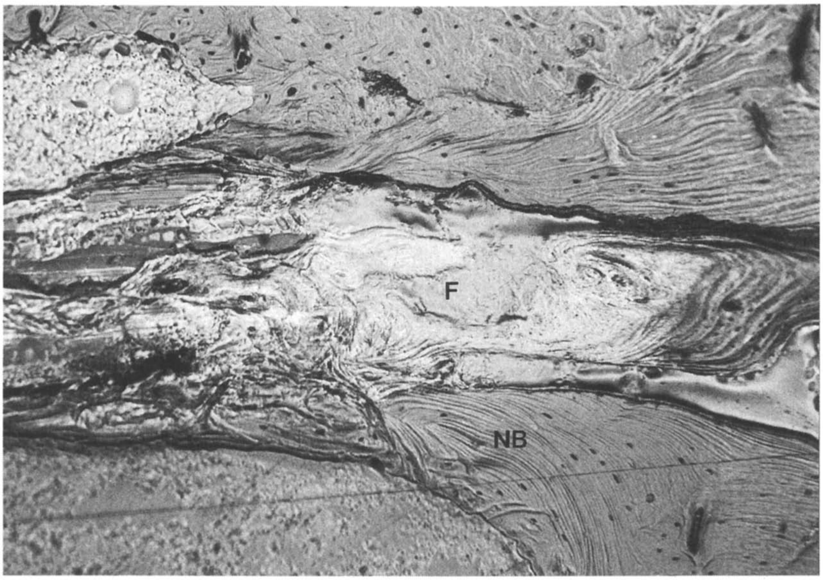

Figure 7. A CaP fiber implanted in a rat for 24 weeks. The fiber was broken apart completely and was in the process of absorbing. There is evidence of good bone compatibility, with new endosteal bone (NB) growing along the substance of the fiber. 42×

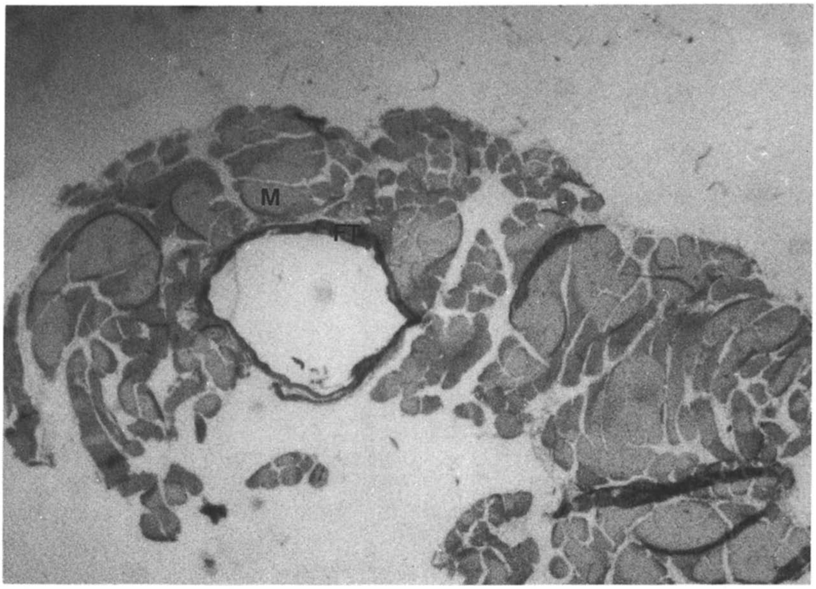

Figure 8. A section of rat muscle (M) after a CaP fiber had been removed. The length of implantation was 12 weeks. A thin ring of a fibrous connective tissue (FT) formed around the fiber (fiber was removed for histology). 8×

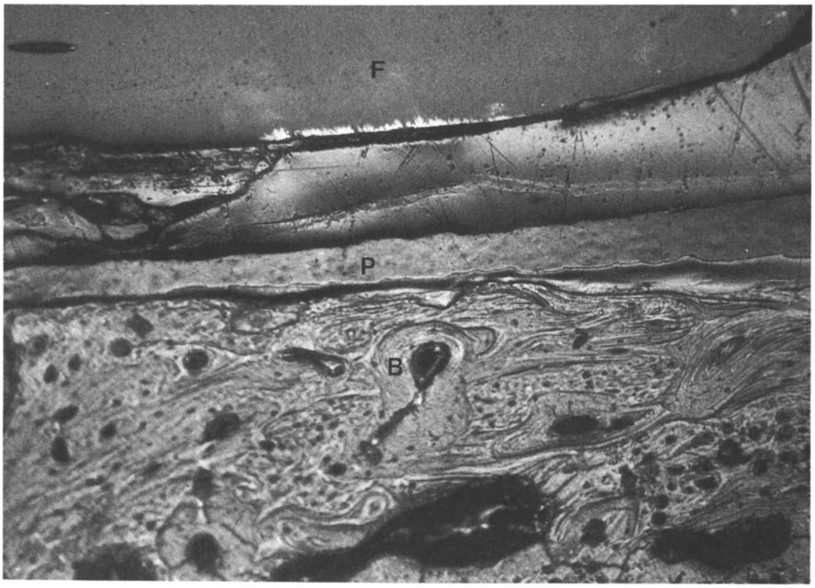

Figure 9. A composite specimen of large diameter fiber coated with PLA imbedded in a rabbit tibia for 6 weeks. The fiber (F) has been polished, and the PLA matrix (P) is between the bone (B) and the fibers. 42×

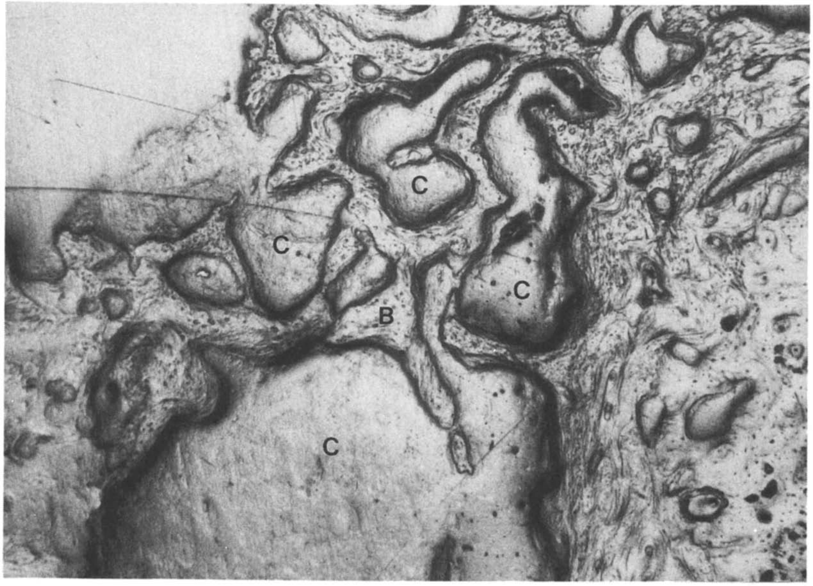

Figure 10. An unmolded composite of CaP and PLA after 6 weeks of implantation. Bone (B) has completely interdigitated the composite (C). 22×

Downloaded by UNIV OF ARIZONA on August 6, 2012 | http://pubs.acs.org
Publication Date: April 3, 1991 | doi: 10.1021/bk-1991-0457.ch010

Downloaded by UNIV OF ARIZONA on August 6, 2012 | http://pubs.acs.org
Publication Date: April 3, 1991 | doi: 10.1021/bk-1991-0457.ch010

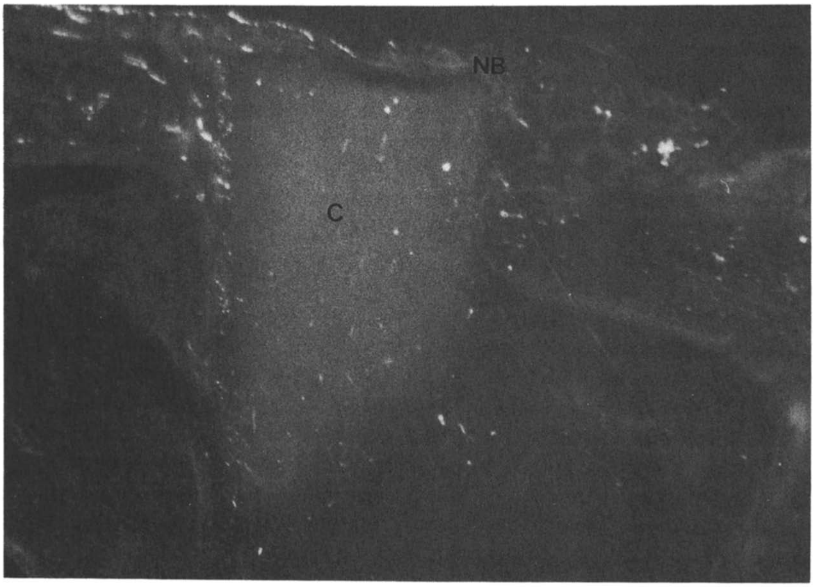

Figure 11. A molded CaP/PLA composite implanted in a rabbit tibia for 6 weeks. The new bone (NB) encapsulated the composite (C) and filled the drillhole. 13×

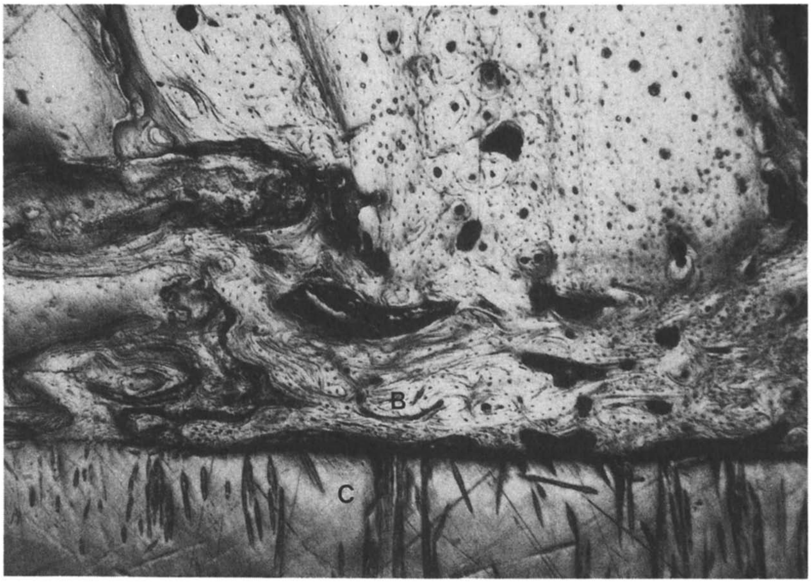

Figure 12. A molded CaP/PLA composite (C) implanted in a rabbit tibia for 12 weeks. There was good bony apposition (B) in the implant. 84×

Downloaded by UNIV OF ARIZONA on August 6, 2012 | http://pubs.acs.org
Publication Date: April 3, 1991 | doi: 10.1021/bk-1991-0457.ch010

than the average stress without the hole (32). This supports the data in (21), where there are large decreases in apparent moduli and stress at failure for the plates with holes. The mode of failure of all the plates with holes was similar. The plates failed on the compressive side at the stress concentration subject to the maximum bending moment, i.e., a hole closest to the middle of the plate.

In the soaking degradation study, the rate of degradation of the CaP/PLA composite material suggests that the manufacturing process and the composition formed allowed for a greater breakdown than did the glass fiber or PLA alone. Since the test materials used in this investigation were sawed from rods into equal lengths, the ends of the samples tended to be rough and jagged. This probably enhanced the seepage of the media between the laminated layers of PLA and glass fiber. The resultant increased surface area in contact with the media caused an increase in dissolution rate, since the PLA and the glass fiber do not bind well. It is also possible that the release of phosphorous resulting in the formation of phosphoric acid could have enhanced the corrosive effect on the fibers of the lactic acid.

In Vivo Studies. Three dogs received carbon-reinforced plates that eventually delaminated and lost mechanical integrity. In all cases, a screw at the area of maximum bending moment backed out of the bone, a rare occurrence with metal plates (33). This lack of fixation in the region of high moment increased stress and led to imminent failure.

Screw loosening was due to the flexibility of the carbon composite system, and subsequently bolts and nuts were added to the system. This modified surgical procedure improved the mechanical stability of the system, although the primary problem of composite hydration eventually led to a poor result. The plates did not fail catastrophically; however, they lost rigidity and delaminated extensively. The fractures did not heal, and hypertrophic nonunions developed.

All polymer matrix composite materials absorb water (34), and in the case of the laminated carbon/PLA composite there was a significant degradation in mechanical performance. The absorption of fluid by a composite with a biodegradable, hydrophilic polymer led to delamination and failure. The high content of continuous fibers that served to wick fluid into the plates accelerated the decay in properties. In a previous experiment, a chopped-fiber composite experienced a decrease in mechanical properties in vivo, although less severely than that observed with the laminated design. The discontinuous arrangement of the fiber in a chopped-fiber composite made it less vulnerable to wicking. Thus, the chopped-fiber plates survived well in the in vivo environment and provided stability for fracture union. Given the in vivo environment, changes in the laminated design to prevent wicking and polymer hydration are indicated.

The purpose of the CaP experiment was to examine the tissue response of an absorbable fiber composed of CaP. The fibers were implanted in the femur of the rat and in the muscles located over the dorsum of the back.

Clearly, the CaP fiber had degraded between 4 and 24 weeks. A completely intact amorphous fiber had a small covering of dissolution products at 4 weeks and was completely fractured and absorbed partially at 24 weeks. The hard tissue response at the three time periods chosen was excellent, with active bone growth present and in intimate contact with the fiber.

The soft tissue response was also excellent. The fibers were held in place by subcutaneous tissue, and there was no evidence of inflammation or rejection. In all cases, a thin ring of a fibrous connective tissue formed around the fiber, and there was a distinct lack of giant cells about the implants. This tissue response was indicative of a benign, nontoxic result.

The dissolution products of the fiber may be the result of several chemical reactions involving water. The fiber was composed of long-chain polymer phosphate anions, connected to each other with modified divalent cations. The cations serve as ionic crosslinks between the nonbridging oxygens of two different chains. Water destroys these ionic crosslinks, thereby allowing the phosphate chains to go into solution. Another possibility concerns the biological milieu. Absorption in vivo is a function of passive dissolution and of cellular and enzymatic attack. All these processes could play a role in the biological degradation of the CaP fiber.

The purpose of the CaP/PLA experiment was to determine tissue response to a CaP/PLA composite. Unmolded composites were implanted in one group of rabbits and molded implants in another. All the animals received polyethylene control implants in their contralateral limb.

Tissue response was identical for the unmolded composite at the three time periods examined. Disorganized "woven" bone infiltrated the drillhole quickly and grew in intimate contact with the composite. Because the composite was unmolded and relatively porous, there was an interdigitation of bone throughout its substance. Again, as in the fiber study, the traumatic stimulation of the endosteum produced intramedullary bone growth. The new endosteal bone used the composite as a trellis to grow into the medullary canal.

The results with the molded composite was similar to the unmolded composite. New bone quickly filled the drillspace and encapsulated the material. Endosteal bone grew into the medullary canal, which was verified with tetracycline labels.

Both the unmolded and molded composites of CaP and PLA were biocompatible. The principal difference, between the composite results and the polyethylene controls, concerned the presence of endosteal bone. Cortical bone surrounded the polyethylene; however, bone was not found advancing into the medullary canal. Medullary canal bone was found with all the composite specimens.

Downloaded by UNIV OF ARIZONA on August 6, 2012 | http://pubs.acs.org
Publication Date: April 3, 1991 | doi: 10.1021/bk-1991-0457.ch010

Conclusions

The studies of pure PLA revealed that the polymer used in this study had mechanical properties equivalent or superior to those reported in the literature. The theoretical composite analysis suggested superiority of a 0°±45° angle-ply design. The experimental mechanical properties proved slightly superior to the theoretical mechanical properties. The plates with molded holes had superior static properties, fatigue properties, and in vitro properties compared to any previous carbon/PLA design. Although the mechanical properties of the plates with molded holes were very good ex vivo, the plates failed in a high-load situation in vivo. Water absorption and delamination ultimately resulted in plate failure. Initial flexibility of the system may have affected screw fixation and played a role in premature mechanical failure.

The best design for a semiabsorbable composite fracture fixation device may be a random chopped-fiber design. It has been successful in the past in low-load situations, and it remains a good model for a semiabsorbable system. Its major limitation is its low mechanical properties, and at the present time it is probably inadequate for fracture fixation in high-load situations.

Calcium phosphate glass is an absorbable and biocompatible material. In soft tissue there was a mild inflammatory response, with a thin ring of fibrous cells formed about the implant. In hard tissue a coating of degradation products formed on the surface of the fiber at the early time period, and bone growth occurred in and around the implant at the two later time periods. The degradation products were nontoxic.

A composite of CaP/PLA was also biocompatible; however, it degraded too rapidly. The composite elicited a minor inflammatory response in soft tissue, and was encapsulated by a thin ring of fibrous cells. Bone also responded well to the material; osteoblastic activity occurred in the medullary canal, and the cortical bone closely approximated it. If a method is found to improve the bonding of the glass fiber to the PLA and no machining is done on the molded specimens, it will probably be possible to develop a slowly degrading composite in which the slowly degrading polymer will protect the fiber from rapid environmental degradation.

Calcium phosphate and CaP composites provide the biomedical engineer with materials that can be used in the design of absorbable implants for high-load situations. A wide variety of applications in orthopaedic and maxillofacial surgery can take advantage of implant absorbability, including fracture fixation plates, intramedullary rods, screws, rivets, and bone graft material. A continuing effort in the authors' laboratories is dedicated to the optimization of the mechanical properties and degradation rates of these materials.

Literature Cited

1. Black, J. *Biological Performance of Materials,* Marcel Dekker: New York, 1981.
2. Sinibaldik, K.; Rosen, H.; Lin, S-K.; De Angelis, M. *Clin. Orthop. Rel. Res.,* 1976, *118,* 257.
3. Hutzchenreuter, P.; Perren, S. M.; Steinmann, S.; Geret, V.; Klebl, M. *Injury,* 1969, *1,* 77.
4. Uhthoff, H. K.; Bardos, D. I.; Liskova-Kiar, M. *Current Concepts of Internal Fixation of Fracture,* Springer-Verlag: New York, 1980.
5. Akeson, W. H.; Woo, S. L-Y. Rutherford, L.; Coutts, R. D.; Gonsalves, M.; Amie, D. *Acta Orthop. Scand.* 1976, *47,* 241.
6. Slatis, P.; Karaharju, E.; Holmstrom, T. Ahonen, J.; Paavolinen, P. *J. Bone Joint Surg.* 1972, *60A,* 516.
7. Tonino, A. J.; Davidson, C. L.; Klopper, P. J.; Linclav, L. A. *J. Bone Joint Surg.* 1972, *58B,* 107.
8. Uhthoff, H. K.; Dubuc, F. L. *Clin. Orthop. Rel. Res.* 1970, *81,* 165.
9. Akeson, W. H.; Woo, S. L-Y.; Coutts, R. D.; Mathews, J. V.; Gonsalves, M.; Amiel, D. *Calcif. Tiss. Res.* 1975, *19,* 27.
10. Vert, M.; Christel, P.; Chabot, F.; Leray, J. In: *Macromolecular Biomaterials;* Hastings, G. W.; Ducheyne, P., Eds.; CRC Press: Boca Raton, FL, 1984.
11. Bradley, G. W.; McKenna, G. B.; Dunn, H. K.; Daniels, A. U.; Statton, W. O. *J. Bone Joint Surg.* 1979, *61A(6),* 866.
12. Tayton, K.; Johnson-Nurse, C.; McKiben, B.; Bradley, J.; Hastings, G. *J. Bone Joint Surg.* 1982, *64B(1),* 105.
13. Tayton, K.; Bradley, J. *J. Bone Joint Surg.* 1980, *65B(3),* 312.
14. Woo, S. L-Y.; Akeson, W. H.; Levenetz, B.; Coutts, R. D.; Mathews, J. V. *J. Biomed. Mater. Res.* 1974, *8,* 321.

American Chemical Society
Library
1155 16th St., N.W.
Washington, D.C. 20036

Downloaded by UNIV OF ARIZONA on August 6, 2012 | http://pubs.acs.org
Publication Date: April 3, 1991 | doi: 10.1021/bk-1991-0457.ch010

15. Corcoran, S.; Koroluk, J.; Parsons, J. R.; Alexander, H.; Weiss, A. B. In: *Current Concepts for Internal Fixation of Fractures;* Uhthoff, H. K., Ed.; Springer-Verlag: New York, 1980, p. 136.
16. Alexander, H.; Parsons, J. R.; Strauchler, I. D.; Corcoran, S. F.; Gona, O.; Mayott, C. W. *Orthop. Rev.,* 1981, *10,* 41.
17. Tayton, K.; Phillips, G.; Ralis, Z. *J. Bone Joint Surg.,* 1982, *64B,* 112.
18. Cutright, D. E.; Beasley, J. D.; Perez, B. *Oral Surg.,* 1971, *32(1),* 165.
19. Brady, J. M.; Cutright, D. E.; Miller, R. A.; Battistone, G. C. *J. Biomed. Mater. Res.* 1973,*7,* 155.
20. Langrana, N.; Parsons, J. R.; Chow, L.; Alexander, H.; Weiss, A. B. *Trans. 29th Orthop. Res. Soc.,* 1983, 381.
21. Zimmerman, M. C.; Parsons, J. R.; Alexander, H. *J. Biomed. Mater. Res.* 1987, *21(A3),* 345.
22. Jenei, S. R.; Bajpai, P. K.; Gustavino, T. D.; Alexander, H. *Proc. 13th Northeast Bioeng. Conf.,* 1987, *1,* 300.
23. NIH publication #85-23, Rev. 1985.
24. Frost, H. M.; *Calc Tiss. Res.* 1969 *3,* 211.
25. Rahn, B. A.; Perren, S. M. *Stain Tech.* 1971, *46(3),* 125.
26. Suzuki, H. K.; Mathews, A. *Stain Tech.* 1966, *41(1),* 57.
27. Pagano, N. J.; Pipes, R. B. *J. Comp. Mater.* 1971, *5,* 50.
28. Hahn, H. T. *Proc. 5th Conf. ASTM STP 674;* Tsai, S. W., Ed.; ASTM: Philadelphia,1979.
29. Lin, T. C.; *Trans. 12th Soc. Biomater.* 1986, 166.
30. Schenk, M. D. *A. O. Bull.* 1978.
31. Parsons, J. R.; Alexander, H., Weiss, A. B. In *Biocompatible Polymers, Metals, and Composites;* Szycher, M., Ed.; Technomics: Westport, CT, 1983.
32. Whitney, J. M.; Daniel, I. M.; Pipes, R. B. *Experimental Mechanics of Fiber Reinforced Composite Materials.* Society for Stress Analysis: Brookfield Center, CT, 1982.
33. Vangness, C. T.; Carter, D. R., Frankel, V. H. *Clin. Orthop.* 1981, *157,* 279.
34. Shen, C-H.; Springer, G. S. *J. Compat. Mater.* 1976, *10,* 2.

RECEIVED October 24, 1990

Downloaded by UNIV OF ARIZONA on August 6, 2012 | http://pubs.acs.org
Publication Date: April 3, 1991 | doi: 10.1021/bk-1991-0457.ch010

Downloaded by UNIV OF GUELPH LIBRARY on August 6, 2012 | http://pubs.acs.org
Publication Date: April 3, 1991 | doi: 10.1021/bk-1991-0457.ch011

Chapter 11

Analysis of Textile-Reinforced Flexible Composites

S. Y. Luo, C. A. Evrensel, and L. Zhou

Mechanical Engineering Department, University of Nevada, Reno, NV 89557

Elastomeric (flexible) composites have had broad applications in synthetic biological materials, various kinds of membrane structures, and pneumatic tires. In this chapter, a constitutive model, for a basic composite element under finite deformation, has been explored. The derivation is based upon the approaches of finite elasticity and a strain-energy function in terms of the Lagrangian strains referring to the initial principal material axes. Both fibre geometric nonlinearity and matrix material nonlinearity have been taken into account. Also, based upon this model, the tensile behavior of flexible composites containing two different types of fiber geometric forms are presented: wavy fibers and straight fiber network (laminates). These theoretical models may be used to analyze the nonlinear finite deformation behavior of textile fabric reinforced flexible composites as well as the biomaterials.

Elastomeric (flexible) composites have had broad applications in synthetic biological materials, various kinds of membrane structures, and pneumatic tires. Their usable deformation can easily reach 10-15% and they can retain their superior strength in a highly controlled manner. Thus, these materials provide engineers with a new degree of freedom in material design through the control of fiber geometric configurations and the proper selection of matrix materials (1).

Some of the best examples of natural flexible composites can be found in biological tissue. Many biological materials are incompressible, viscoelastic, and anisotropic; they often demonstrate nonlinear behavior with a large deformation range (2). For instance, the lung is organized into three basic tissue layers interposed between air and blood: the airway epithelium and vascular endothelium, which are bound together by the fibrous interstitial connective tissue. There is barely any connective tissue in the body where there is only one fibre type. The lung is not an exception and the practically inextensible collagen (less than 2% extensibilty) and the highly extensible elastic fibres (with up to 130% extensibility) occur in tandem anywhere. In a relaxed

0097–6156/91/0457–0149$06.00/0

state, the elastic fibres form a network of straight fibres, whereas the collagen fibres appear wavy (3).

If such a tissue is stretched, the elastic fibres become extended until the collagen fibres are straight. The extension capacity of the connective tissue is accordingly determined by the length of the collagen fibres, whereas the elastic fibres keep the integral fibre network under certain tension at lower levels of expansion. The effect of these two different types of fibres on the mechanical properties of a tissue is presented in Figure 1, which shows mean length-tension curves for canine tracheal smooth muscle in "resting" condition (i.e. non-contracting). The shape of this curve is typical of non-contractile biological tissues and other synthetic textile fabric reinforced composites. The initial, compliant portion (Figure 1) is primarily due to the presence of straight elastic fibres and the final stiffer portion is due to relatively rigid, wavy collagen fibres (4). As shown in Figure 2 the overall airway wall, including smooth muscle, is bimodular, i.e., it has different properties in tension and compression (5). Also, almost all biological fluids and tissues possess viscoelastic behavior which drastically effects the interaction of these tissues with other tissues and fluids (6-8).

Collagen and elastic fibres form networks of interwoven fibres, providing the tissue with what has been called a "nylon-stocking" extensibility (9). Stretching in one direction leads to temporary rearrangement of the fibres. It is the interweaving of such a sheet with elastic fibres that restores the original arrangement upon relaxation and, to some extent, distributes the forces evenly to all fibres of the sheet.

To understand the nonlinear finite strain behavior of natural tissues, many constitutive equations, based upon composite models, have been proposed. It is realized that, under finite deformation, the influences of fiber reorientation usually cannot be neglected, and the geometric and material nonlinearities may be quite significant. Thus, the classical lamination theory, developed for rigid composites, is no longer applicable. Aspden (10) considered the influence of the fibre reorientation in biological materials during finite deformation by using a fibre orientation distribution function and assuming that the fibre carries only axial tension. However, the rigid rotation of fibres and the shear property of the matrix material, which greatly influence the fibre reorientation during deformation, are not seriously considered in the analysis. Humphrey and Yin (11) presented a constitutive model based upon a pseudostrain-energy function, and compared the theoretical analysis with both uniaxial and biaxial experimental results. The parameters used in the energy function are dependent on the experimental data; the fibre spatial arrangements, which are responsible for the geometric nonlinearity, are ignored in their analysis.

In an effort to provide a rigorous treatment of the finite deformation problem, two constitutive models (1, 12), considering both geometric and material nonlinearities, have been developed based on the approaches: (a) Lagrangian description, (b) Eulerian description. In this presentation, the Lagrangian constitutive model is reviewed. Also, based upon this model, the tensile behavior of flexible composites containing two different types of fiber geometric forms are presented: wavy fibers and straight fiber network (laminates) (13).

Constitutive Relation of a Unidirectional Lamina

The description of the relation between the undeformed and deformed configurations of a continuum can be considered as a "mapping" between domains D_0 and D (Figure 3). To find the transformation relation, let X and x be two fixed rectangular Cartesian

Downloaded by UNIV OF GUELPH LIBRARY on August 6, 2012 | http://pubs.acs.org
Publication Date: April 3, 1991 | doi: 10.1021/bk-1991-0457.ch011

Downloaded by UNIV OF GUELPH LIBRARY on August 6, 2012 | http://pubs.acs.org
Publication Date: April 3, 1991 | doi: 10.1021/bk-1991-0457.ch011

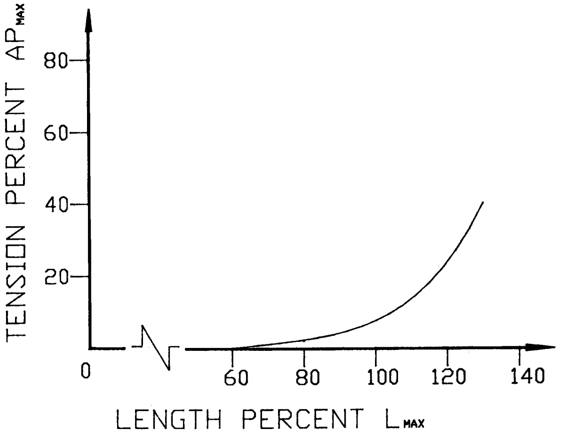

Figure 1. Mean resting tension-length curves of canine tracheal smooth muscle. L max is a unique length where "active" tension is maximum, which is not shown in this figure (Data from Ref. 4).

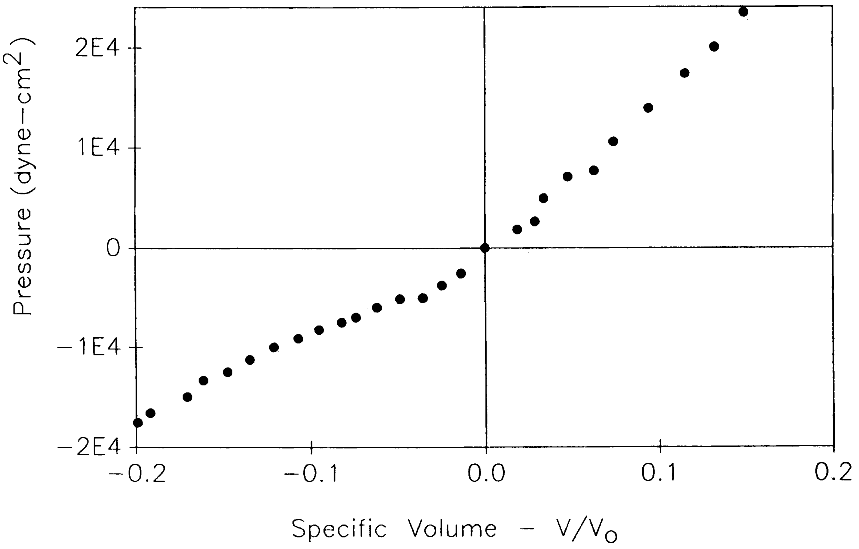

Figure 2. Pressure versus specific volume for canine trachea (Data from Ref. 5).

Downloaded by UNIV OF GUELPH LIBRARY on August 6, 2012 | http://pubs.acs.org
Publication Date: April 3, 1991 | doi: 10.1021/bk-1991-0457.ch011

coordinates associated with the original and deformed configurations, respectively. The position of a generic particle P inside the domain D_0 is defined by the position vector X and coordinates X_j (j=1,2,3). After deformation, this particle assumes the location P' with the new position vector x and coordinates x_i (i=1,2,3). Then, the "mapping" or the deformation of the configuration can be described mathematically by the coordinate transformation between X_j and x_i (14, 15). The definition of deformation, in which the independent variable is the particle position vector X in the original state, is known as the Lagrangian description. The reference system X is known as the Lagrangian coordinate.

The Lagrangian strain, E_{ij}, (also known as Green or St. Venant strain) tensor is defined as

$$E_{ij} = \frac{1}{2}(g_{kj}g_{kj} - \delta_{ij}) \tag{1}$$

where the dummy, or repeating, index denotes a summation with respect to that index over its range, δ_{ij} is the Kronecker Delta, and

$$g_{ij} = \frac{\partial x_i}{\partial X_j} \tag{2}$$

The strain-energy density is assumed to be a function of the Lagrangian strain components referring to the initial principal material coordinate $\bar{X}$ with the axis $\bar{X}_1$ being parallel to the fiber direction (Figure 4). The strain-energy per unit volume of the undeformed lamina is further assumed in the following fourth-order polynomial form

$$W = \frac{1}{2}C_{11}\bar{E}_1^2 + \frac{1}{3}C_{111}\bar{E}_1^3 + \frac{1}{4}C_{1111}\bar{E}_1^4 + C_{12}\bar{E}_1\bar{E}_2 + \frac{1}{2}C_{22}\bar{E}_2^2 + \frac{1}{3}C_{222}\bar{E}_2^3 + \frac{1}{4}C_{2222}\bar{E}_2^4 + \frac{1}{2}C_{66}\bar{E}_6^2 + \frac{1}{4}C_{6666}\bar{E}_6^4 \tag{3}$$

where C_{ij}, C_{ijk}, and C_{ijkl} are elastic constants, and the short-hand notations are used, namely, $\bar{E}_1 = \bar{E}_{11}$, $\bar{E}_2 = \bar{E}_{22}$, and $\bar{E}_6 = 2\bar{E}_{12}$.

The stress matrix referring to the material principal coordinate system $\bar{X}_1$-$\bar{X}_2$, is given in terms of W (15),

$$\bar{\Pi}_{ij} = \frac{\partial W}{\partial \bar{g}_{ji}} \tag{4}$$

With Eqs. (1) and (2), it follows that

Downloaded by UNIV OF GUELPH LIBRARY on August 6, 2012 | http://pubs.acs.org
Publication Date: April 3, 1991 | doi: 10.1021/bk-1991-0457.ch011

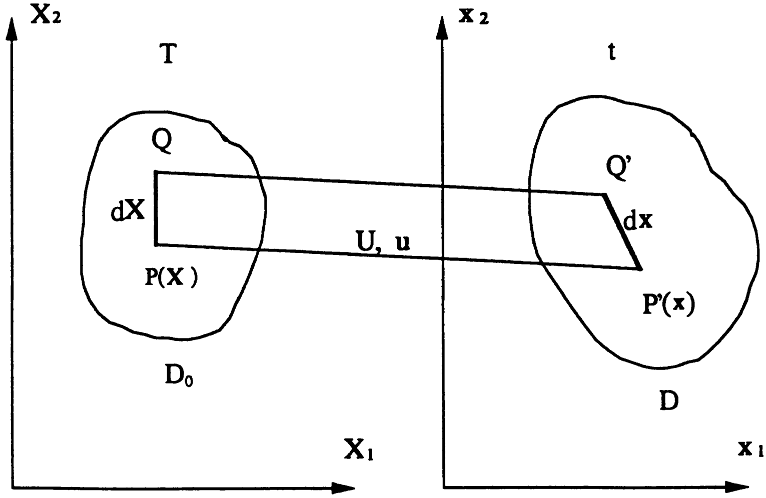
X2
T
Q
dX
P(X)
D0
X1
U, u
x2
t
Q'
dx
P'(x)
D
x1

Figure 3. Deformation of a body from the undeformed configuration D_0 to the deformed configuration D

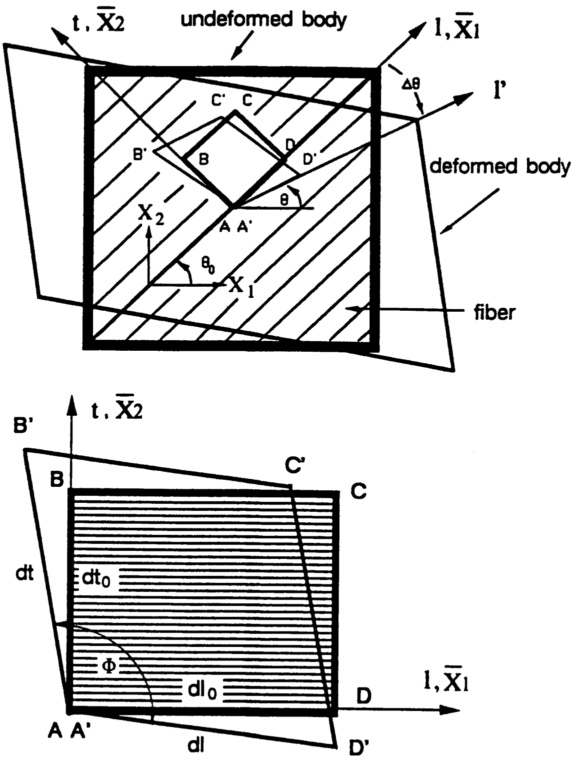
t, X̄2
undeformed body
1, X̄1
Δθ
l'
C' C
B'
B
D
D'
θ
X2
A A'
θ0
X1
deformed body
fiber
B'
t, X̄2
B
C'
C
dt
dt0
Φ
dl0
D
1, X̄1
A A'
dl
D'

Figure 4. A rectangular element of composite lamina before and after loading in the Lagrangian system.

Downloaded by UNIV OF GUELPH LIBRARY on August 6, 2012 | http://pubs.acs.org
Publication Date: April 3, 1991 | doi: 10.1021/bk-1991-0457.ch011

$$\bar{\Pi}_{ji} = \frac{1}{2}\bar{g}_{ip}\left(\frac{\partial W}{\partial \bar{E}_{jp}} + \frac{\partial W}{\partial \bar{E}_{pj}}\right) \qquad (5)$$

To derive the general constitutive equations with reference axes other than the principal material directions, a two-dimensional rectangular Cartesian coordinate system X_1-X_2 is chosen in the plane of the lamina. Let the angle between X_i and $\bar{X}_i$ be θ_0 (Figure 4). The orthogonal transformation matrix,

$$[a] = \begin{bmatrix} \cos\theta_0 & -\sin\theta_0 \\ \sin\theta_0 & \cos\theta_0 \end{bmatrix} \qquad (6)$$

and $[X] = [a][\bar{X}]$. Then, the transformation relations for the deformation gradient and Lagrangian strain between coordinate systems X and $\bar{X}$ are:

$$[\bar{g}] = [a]^T [g] [a] \qquad (7)$$

and

$$[\bar{E}] = [a]^T [E] [a] \qquad (8)$$

With Eq. (6), Eq.(8) yields

$$\begin{aligned} \bar{E}_{11} &= \frac{1}{2}E_{11}(1+\cos2\theta_0) + E_{12}\sin2\theta_0 + \frac{1}{2}E_{22}(1-\cos2\theta_0) \\ \bar{E}_{22} &= \frac{1}{2}E_{11}(1-\cos2\theta_0) - E_{12}\sin2\theta_0 + \frac{1}{2}E_{22}(1+\cos2\theta_0) \qquad (9) \\ \bar{E}_{12} = \bar{E}_{21} &= \frac{1}{2}(E_{22} - E_{11})\sin2\theta_0 + \frac{1}{2}E_{12}\cos2\theta_0 \end{aligned}$$

The stress matrix referring to the coordinate system X is

$$[\Pi] = [a]\,[\bar{\Pi}]\,[a]^T \qquad (10)$$

With Eqs. (6) and (7), Eq. (10) is expressed as

$$\begin{aligned} \Pi_{11} &= [g_{11}c^2 + g_{12}cs]\,W_{11} + [g_{11}s^2 - g_{12}cs]\,W_{22} + [-g_{11}cs + \tfrac{1}{2}g_{12}(c^2-s^2)]\,W_{12} \\ \Pi_{22} &= [g_{22}s^2 + g_{21}cs]\,W_{11} + [\,g_{22}c^2 - g_{21}cs]\,W_{22} + [g_{22}cs + \tfrac{1}{2}g_{21}(c^2-s^2)]\,W_{12} \\ \Pi_{12} &= [g_{22}cs + g_{21}c^2]W_{11} + [\,g_{21}s^2 - g_{22}cs]\,W_{22} + [-g_{21}cs + \tfrac{1}{2}g_{22}(c^2-s^2)]\,W_{12} \\ \Pi_{21} &= [g_{11}cs + g_{12}s^2]\,W_{11} + [\,g_{12}c^2 - g_{11}cs]\,W_{22} + [g_{12}cs + \tfrac{1}{2}g_{11}(c^2-s^2)]\,W_{12} \end{aligned}$$

(11)

Downloaded by UNIV OF GUELPH LIBRARY on August 6, 2012 | http://pubs.acs.org
Publication Date: April 3, 1991 | doi: 10.1021/bk-1991-0457.ch011

where $c = \cos\theta_0$, $s = \sin\theta_0$ and

$$
\begin{aligned}
W_{11} &= \frac{\partial W}{\partial \bar{E}_{11}} = C_{11}\,\bar{E}_{11} + C_{111}\,\bar{E}_{11}^{2} + C_{1111}\,\bar{E}_{11}^{3} + C_{12}\,\bar{E}_{22} \\
W_{22} &= \frac{\partial W}{\partial \bar{E}_{22}} = C_{22}\,\bar{E}_{22} + C_{222}\,\bar{E}_{22}^{2} + C_{2222}\,\bar{E}_{22}^{3} + C_{12}\,\bar{E}_{11} \\
W_{12} &= \frac{\partial W}{\partial \bar{E}_{12}} = 4(C_{66}\,\bar{E}_{12} + 4C_{6666}\,\bar{E}_{12}^{3})
\end{aligned}
\tag{12}
$$

Eq. (11) gives the general constitutive equations for a composite lamina under finite deformation, where the deformation gradients, g_{ij}, represent the geometric nonlinearity induced by the configuration changes of the lamina. The nonlinear expressions of W_{ij} (referring to Eq. (10)) represent the material nonlinearity of the composites. If the deformation of the composite lamina is infinitesimal (i.e. $g_{ij} = \delta_{ij}$) and only the linear terms (i.e. C_{ij}) remain in the expression of W_{ij}, Eq. (11) can be easily reduced to the familiar linear stress-strain equation used for rigid composites.

For a specific deformation, the deformation gradient matrix, [g], is calculated from Eq. (2); the Lagrangian strain referring to the principal material coordinates, $[\bar{E}]$, is obtained from Eqs. (1), (6) and (10); and W_{ij} are obtained by introducing $[\bar{E}]$ into Eq. (12). Then, the corresponding Lagrangian stresses, $[\Pi]$, can be determined from Eq. (11).

Flexible Composites Containing Sinusoidally Shaped Fibers

Introduction. The complex microstructure of some biological material (muscle, skin, and etc.) may be considered as composites with wavy fibres. In this section, a model flexible composite containing sinusoidally shaped fibres is discussed. The spatial position of a fibre with sinusoidal waviness in the X coordinate system is specified as (16)

$$X_2 = a \sin\frac{2\pi X_1}{\lambda} \tag{13}$$

where a and λ are the amplitude and wavelength of the curved fibre, respectively (Figure 5). The angle (θ_0) between the tangent to the fibre and X_1 axis is a function of X_1.

$$\tan\theta_0 = \frac{dX_2}{dX_1} = \frac{2\pi a}{\lambda}\cos\frac{2\pi X_1}{\lambda} \tag{14}$$

Downloaded by UNIV OF GUELPH LIBRARY on August 6, 2012 | http://pubs.acs.org
Publication Date: April 3, 1991 | doi: 10.1021/bk-1991-0457.ch011

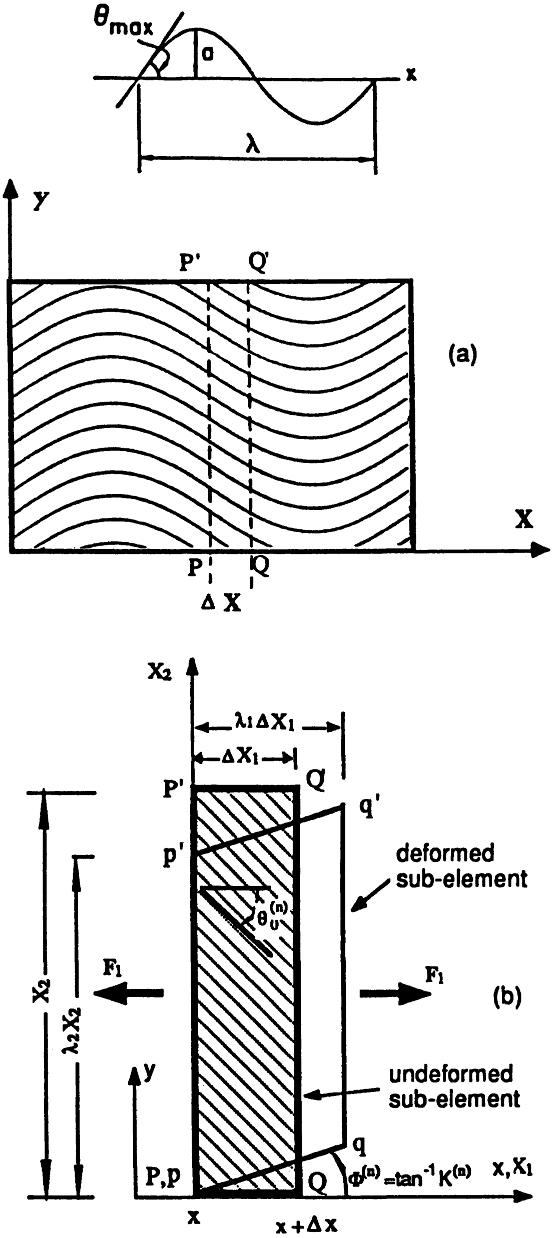
θmax
a
x
λ
Y
P'
Q'
(a)
X
P
Q
ΔX
X2
λ1ΔX1
ΔX1
P'
Q'
q'
p'
deformed sub-element
θu(n)
X2
λ2X2
F1
F1
(b)
y
undeformed sub-element
q
P,p
Q
φ(n)=tan-1K(n)
x,X1
x
x+Δx

Figure 5. (a) Flexible composites containing sinusoidally shaped fibres, (b) the deformation of a sub-element under longitudinal tension.

Downloaded by UNIV OF GUELPH LIBRARY on August 6, 2012 | http://pubs.acs.org
Publication Date: April 3, 1991 | doi: 10.1021/bk-1991-0457.ch011

The deformation of the isophase flexible composite is best understood by examining a representative element which contains a full wave-length of the sinusoidal curve (Figure 5(a)). This element is further divided into sub-elements along the X_1-axis. Each sub-element of the composite between X_1 and X_1+dX_1 is approximated by an off-axis unidirectional fibre composite, in which fibres are inclined at an angle $\theta_0^{(n)}$ to the X_1 axis. Referring to Eq. (14), this initial fibre orientation of sub-element (n), for example, is given as

$$\theta_0^{(n)} = \frac{1}{2}\left[\tan^{-1}\left(\frac{2\pi a}{\lambda}\cos\frac{2\pi X_1}{\lambda}\right) + \tan^{-1}\left(\frac{2\pi a}{\lambda}\cos\frac{2\pi(X_1+dX_1)}{\lambda}\right)\right] \tag{15}$$

It is also assumed that the stress and strain of a sub-element are homogeneous under axial loading. This assumption is supported by the photoelastic analysis (1).

Based upon the above assumptions, the analysis for the isophase model consists of two steps: (1) The constitutive relation of an off-axis sub-element under finite deformation is examined based upon the analysis developed in Sec. 2. (2) The total deformation of the composite is the summation of the deformations of all these sub-elements.

Longitudinal Elastic Behavior. Under the uniaxial tensile force F_1 in the X_1 direction, the following plane stress condition of the flexible composite is assumed:

$$\Pi_{11} = F_1/A_0$$
$$\Pi_{22} = 0$$
$$\Pi_{21} = 0 \tag{16}$$

where A_0 is the initial cross-sectional area perpendicular to the X_1 axis.

Figure 5(b) shows the deformation of a typical sub-element PQQ'P'. pqq'p' represents the configuration in the deformed state. Due to the isophase fibre arrangement, the edge qq' remains perpendicular to the X_1 axis. Let $X_i^{(n)}$ be the coordinates of an arbitrary particle in PQQ'P', and $x_i^{(n)}$ be the corresponding coordinates of this particle in pqq'p'. Here, the superscript refers to the sub-element (n). This deformation is specified as

$$x_1^{(n)} = \lambda_1^{(n)} X_1^{(n)}$$
$$x_2^{(n)} = K\lambda_1^{(n)} X_1^{(n)} + \lambda_2^{(n)} X_2^{(n)} \tag{17}$$

Eq. (17) specifies a deformation, namely, "simple shear superposed on simple extension". From Eqs. (1), (2) and (9), for the sub-element (n), we have

Downloaded by UNIV OF GUELPH LIBRARY on August 6, 2012 | http://pubs.acs.org
Publication Date: April 3, 1991 | doi: 10.1021/bk-1991-0457.ch011

$$[\mathbf{g}] = \begin{bmatrix} \lambda_1 & K\lambda_2 \\ 0 & \lambda_2 \end{bmatrix}, \quad 2[E] = \begin{bmatrix} \lambda_1^2-1 & K\lambda_1\lambda_2 \\ K\lambda_1\lambda_2 & \lambda_2^2(K^2+1)-1 \end{bmatrix} \tag{18}$$

and

$$\bar{E}_{11} = \frac{1}{4}[(\lambda_1^2+\lambda_2^2-2+\lambda_2^2K^2)+(\lambda_1^2-\lambda_2^2-\lambda_2^2K^2)\cos 2\theta_0 + 2K\lambda_1\lambda_2 \sin 2\theta_0]$$

$$\bar{E}_{22} = \frac{1}{4}[(\lambda_1^2+\lambda_2^2-2+\lambda_2^2K^2)+(\lambda_1^2-\lambda_2^2-\lambda_2^2K^2)\cos 2\theta_0 - 2K\lambda_1\lambda_2 \sin 2\theta_0]$$

$$\bar{E}_{12} = \frac{1}{4}[(\lambda_2^2-\lambda_1^2+\lambda_2^2K^2)\sin 2\theta_0 + 2K\lambda_1\lambda_2 \cos 2\theta_0. \tag{19}$$

Then, the components of the Lagrangian stress are obtained from Eq. (11),

$$\begin{aligned} \Pi_{11} &= [\lambda_1 c^2 + K\lambda_2 cs]\, W_{11} + [\lambda_1 s^2 - K\lambda_2 cs]\, W_{22} + [-\lambda_1 cs + \frac{1}{2}K\lambda_2(c^2 - s^2)]\, W_{12} \\ \Pi_{22} &= \lambda_2 [s^2 W_{11} + c^2 W_{22} + cs W_{12}] \\ \Pi_{12} &= \lambda_2 [cs W_{11} - cs W_{22} + \frac{1}{2}(c^2 - s^2) W_{12}] \\ \Pi_{21} &= [\lambda_1 cs + K\lambda_2 s^2]\, W_{11} + [K\lambda_2 c^2 - \lambda_1 cs]\, W_{22} + [K\lambda_2 cs + \frac{1}{2}\lambda_1(c^2 - s^2)]\, W_{12}. \end{aligned} \tag{20}$$

With the stress boundary condition of equation (16), Eq. (20) can be rewritten as

$$\begin{aligned} \Pi_{11} &= \lambda_1 [c^2 W_{11} + s^2 W_{22} - cs W_{12}] \\ 0 = \Pi_{22} &= [s^2 W_{11} + c^2 W_{22} + cs W_{12}] \\ 0 = \Pi_{21} &= [cs W_{11} - cs W_{22} + \frac{1}{2}(c^2 - s^2) W_{12}] \end{aligned} \tag{21}$$

Notice that all superscripts (n) have been omitted in Eqs. (6)-(18). In Eq. (21), W_{ij} is a function of $K^{(n)}$, $\lambda_1^{(n)}$ and $\lambda_2^{(n)}$, and it is obtained from Eqs. (12) and (19). The initial fibre orientation $\theta_0^{(n)}$ is given from Eq. (15). Then, the three unknowns, $K^{(n)}$, $\lambda_1^{(n)}$ and $\lambda_2^{(n)}$ can be solved from Eqs. (21).

The current fibre orientation ($\theta^{(n)}$) of the sub-element (n) (Figure 5) is

$$\theta^{(n)} = \tan^{-1} [K + \frac{\lambda_2^{(n)}}{\lambda_1^{(n)}} \tan\theta_0^{(n)}] \tag{22}$$

The average extension ratio of the wave-length in the X_1 direction can be derived as

$$\lambda_1 = \frac{\Delta x}{\lambda} \sum_{n=1}^{m} \lambda_1^{(n)} \tag{23}$$

Downloaded by UNIV OF GUELPH LIBRARY on August 6, 2012 | http://pubs.acs.org
Publication Date: April 3, 1991 | doi: 10.1021/bk-1991-0457.ch011

Transverse Elastic Behavior. Under the transverse tensile force F_2 (Figure 6), the following conditions for a sub-element (n) of the flexible composite are assumed.

$$\Pi_{11}^{(n)} = 0$$

$$\Delta X \sum_{n=1}^{m} \Pi_{22}^{(n)} = F_2 \tag{24}$$

and the deformation can be written as

$$x_1^{(n)} = \lambda_1^{(n)} X_1^{(n)}$$

$$x_2^{(n)} = \lambda_2^{(n)} X_2^{(n)} = \lambda_2\ X_2 \tag{25}$$

Notice that the extension ratio in the X_2 direction ($\lambda_2^{(n)}$) of each sub-element is identical (i.e. $\lambda_2^{(n)} = \lambda_2$). From Eqs. (1), (2) and (9), for the sub-element (n), we have

$$[g] = \begin{bmatrix} \lambda_1 & 0 \\ K\lambda_1 & \lambda_2 \end{bmatrix}, \quad 2[E] = \begin{bmatrix} \lambda_1^2(K^2+1)-1 & K\lambda_1\lambda_2 \\ K\lambda_1\lambda_2 & \lambda_2^2-1 \end{bmatrix} \tag{26}$$

and

$$\bar{E}_{11} = \frac{1}{4}[(\lambda_1^2+\lambda_2^2-2+\lambda_1^2K^2)+(\lambda_1^2-\lambda_2^2-\lambda_1^2K^2)\cos 2\theta_0+2K\lambda_1\lambda_2\sin 2\theta_0]$$

$$\bar{E}_{22} = \frac{1}{4}[(\lambda_1^2+\lambda_2^2-2+\lambda_1^2K^2)+(\lambda_1^2-\lambda_2^2-\lambda_1^2K^2)\cos 2\theta_0-2K\lambda_1\lambda_2\sin 2\theta_0]$$

$$\bar{E}_{12} = \frac{1}{4}[(\lambda_2^2-\lambda_1^2-\lambda_1^2K^2)\sin 2\theta_0+2K\lambda_1\lambda_2\cos 2\theta_0. \tag{27}$$

The components of the Lagrangian stress obtained from Eq. (11) are:

$$\Pi_{11} = \lambda_1(c^2 W_{11} + s^2W_{22} - csW_{12})$$

$$\Pi_{22} = [\lambda_2 s^2+K\lambda_1 cs]W_{11}+[\lambda_2 c^2-K\lambda_1 cs]W_{22}+\frac{1}{2}[2\lambda_2 cs+K\lambda_1(c^2-s^2)]W_{12}$$

$$\Pi_{12} = [\lambda_2 cs+K\lambda_1 c^2]W_{11}+[-\lambda_2 cs+K\lambda_1 s^2]W_{22}+\frac{1}{2}[-2K\lambda_1 cs+\lambda_2(c^2-s^2)]W_{12}.$$

$$\Pi_{21} = \lambda_1 csW_{11} - \lambda_1 csW_{22} + \frac{1}{2}\lambda_1(c^2 - s^2)W_{12} \tag{28}$$

With Eq. (24), we obtain

$$0 = \Pi_{11} = [c^2 W_{11} + s^2 W_{22} - cs\, W_{12}]$$

$$\Pi_{22}^{(n)} = \lambda_2\, [s^2 W_{11} + c^2 W_{22} + cs\, W_{12}] \tag{29}$$

where W_{ij} is obtained from Eqs. (12) and (27). Also, in Eqs. (26)-(28), all superscripts (n) have been omitted. The initial fiber orientation, $\theta_0^{(n)}$ is given from Eq. (15). Then, for any given λ_2, the two unknowns, $\lambda_1^{(n)}$ and $\Pi_{22}^{(n)}$, in Eq. (27) can be solved from the two equations. The shear stresses of the sub-element (n) can be obtained from Eq. (28). The current fiber orientation ($\theta^{(n)}$) of the sub-element (n) is

$$\theta^{(n)} = \tan^{-1}\left[\frac{\lambda_2}{\lambda_1^{(n)}} \tan\theta_0^{(n)}\right] \tag{30}$$

The average transverse stress acting over the fiber wavelength is

$$\Pi_{22} = \frac{\Delta X}{\lambda} \sum_{n=1}^{m} \Pi_{22}^{(n)} \tag{31}$$

Numerical Examples. The predictions of the longitudinal constitutive relations based upon above analysis are compared to experimental results and other analyses in the finite deformation range. The model composite system consists of silicone elastomer reinforced with sinusoidally shaped Kevlar fibers ($a/\lambda = 0.09$). Due to fiber waviness, the volume fraction may vary among the sub-elements. An average fiber volume fraction $V_f = 9\%$ is used in the calculation. The elastic constants in the strain-energy function (Eq.(3)) are determined experimentally. The second-order constants (C_{ij} etc.) are based on linear theory (i.e., the initial slope of the experimental stress-strain curve). The other constants are obtained by fitting the theoretical curves with experimental data, where 0° and 90° specimens are used to determine the tensile properties. The shear properties are determined by $[\pm 45°]_s$ specimens. The details can be found in the work of Luo & Chou (13). The non-zero elastic constants so obtained are: C_{11}= 8600 MPa, C_{12}= - 1.3 MPa, C_{22}= 2.77 MPa, C_{2222}= -12.5 (MPa)^3, C_{66}= 2.55 MPa, and C_{6666}= 2.45 (MPa)^3.

Figure 7 compares the analytical predictions with experimental results. The heavy solid line indicates theoretical predictions of the present analysis or Lagrangian approach ; the thin solid line indicates theoretical predictions based upon the Eulerian approach (1, 17); and the dotted line is from the incremental analysis (16). Experimental results are also presented.

Figure 8 shows the theoretical predictions of the longitudinal elastic behavior of flexible composites containing sinusoidally shaped fibers with various ratios of a/λ. It indicates that this composite can elongate readily at low stresses, but stiffens when the fibers become fully extended. With different fiber geometric parameter, a/λ, materials with a range of deformation are obtained. Furthermore, the local strains in the sub-element can be predicted directly from Eq. (21). The current fiber orientation angle of the sub-element is given by Eq. (22). These results show that the maximum local tensile strain of the fiber occurs at the region where the initial fiber orientation angle equals to zero (i.e. $X_1 = \pm \lambda/4$). The maximum local shear strain of the composites

Downloaded by UNIV OF GUELPH LIBRARY on August 6, 2012 | http://pubs.acs.org
Publication Date: April 3, 1991 | doi: 10.1021/bk-1991-0457.ch011

Downloaded by UNIV OF GUELPH LIBRARY on August 6, 2012 | http://pubs.acs.org
Publication Date: April 3, 1991 | doi: 10.1021/bk-1991-0457.ch011

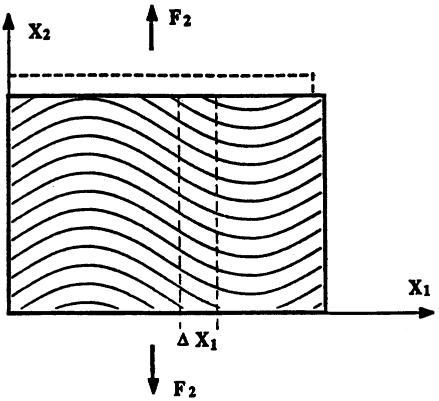

Figure 6. Flexible composites containing sinusoidally shaped fibres under transverse tension.

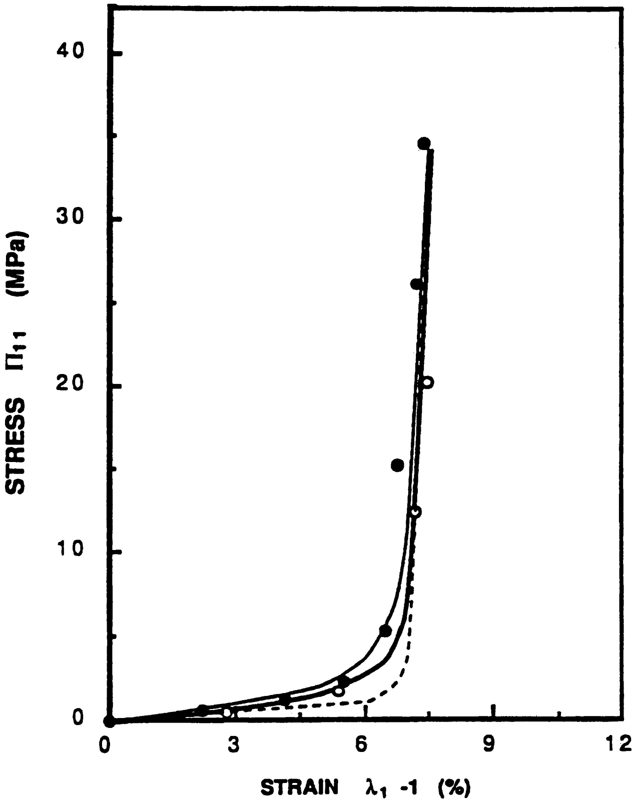

Figure 7. Stress–strain relations of Kevlar/silicone-elastomer composite laminae containing sinusoidally shaped fibres for $a/\lambda = 0.09$. —: Lagrangian description; —: Eulerian description; ---: Incremental analysis; ● and ○ : Experiments of 2 specimens.

occurs in the region where the initial fiber orientation is a maximum (i.e. $X_1 = 0, \lambda/2$). Hence, the strength of the flexible composites may be determined by the maximum tensile strain at $X_1 = \lambda/4$, and the maximum shear strain at $X_1 = 0$.

Flexible Composite Laminate Analysis

Constitutive Relations. Now the constitutive model for composite laminae (Eq. (11) and (12)) is applied to study the constitutive relations of laminated flexible composites (Figure 9) under finite plane deformation. The stress resultant in Lagrangian description (N_{ij}) is defined as

$$N_{ij} = \int_{-h/2}^{h/2} \Pi_{ij} dz \tag{32}$$

where, h is the initial thickness of the laminate. The N_{ij} so defined gives the total force in the i direction per unit length of the undeformed laminate.

Assume that the laminate is composed of n layers of laminae. By neglecting the interlaminar shear deformation, the deformation gradient, g_{ij} (Eq. (2)), has the same value for all the layers, so does E_{ij} (Eq. (1)). For an arbitrary k-th lamina within the laminate, let $\theta_0^{(k)}$ be the fiber orientation angle with respect to the coordinate X_1, and $a_{ij}^{(k)}$ the values given by Eq. (6) for $\theta_0 = \theta_0^{(k)}$. Also, for the k-th lamina, let $\bar{E}_0^{(k)}$ be the values of $\bar{E}_{ij}$ given by Eq. (9), and $W_{ij}^{(k)}$ the values of W_{ij} given by Eq.(12). Then, from Eqs. (11) and (32) the following can be derived (18)

$$N_{ji} = g_{ip} \sum_{k=1}^{n} (h_k - h_{k-1}) \{a_{p1}^{(k)} a_{j1}^{(k)} W_{11}^{(k)} + a_{p2}^{(k)} a_{j2}^{(k)} W_{22}^{(k)} + \tfrac{1}{2}(a_{p1}^{(k)} a_{j2}^{(k)} + a_{p2}^{(k)} a_{j1}^{(k)}) W_{12}^{(k)}\} \tag{33}$$

If the laminae are identical (except the fiber orientation) with thickness t, then equation (33) can be rewritten as

$$N_{ji} = t\ g_{ip} \sum_{k=1}^{n} \{a_{p1}^{(k)} a_{j1}^{(k)} W_{11}^{(k)} + a_{p2}^{(k)} a_{j2}^{(k)} W_{22}^{(k)} + \tfrac{1}{2}(a_{p1}^{(k)} a_{j2}^{(k)} + a_{p2}^{(k)} a_{j1}^{(k)}) W_{12}^{(k)}\} \tag{34}$$

Equations (33) and (34) are the general constitutive equations for flexible composite laminates under finite deformations. The calculation procedure is further exemplified in the following section.

Tensile stress-strain relation. The state of homogeneous deformation is assumed for a symmetric composite laminate with fiber orientation sequences of $+\theta_0/-\theta_0/-\theta_0/+\theta_0$ under unidirectional tension (Figure 10). Because $\bar{E}_{11}$ and $\bar{E}_{22}$ are even functions of θ_0, and $\bar{E}_{12}$ is an odd function of θ_0 (Eq. (9)), we have from Eq. (12)

Downloaded by UNIV OF GUELPH LIBRARY on August 6, 2012 | http://pubs.acs.org
Publication Date: April 3, 1991 | doi: 10.1021/bk-1991-0457.ch011

Downloaded by UNIV OF GUELPH LIBRARY on August 6, 2012 | http://pubs.acs.org
Publication Date: April 3, 1991 | doi: 10.1021/bk-1991-0457.ch011

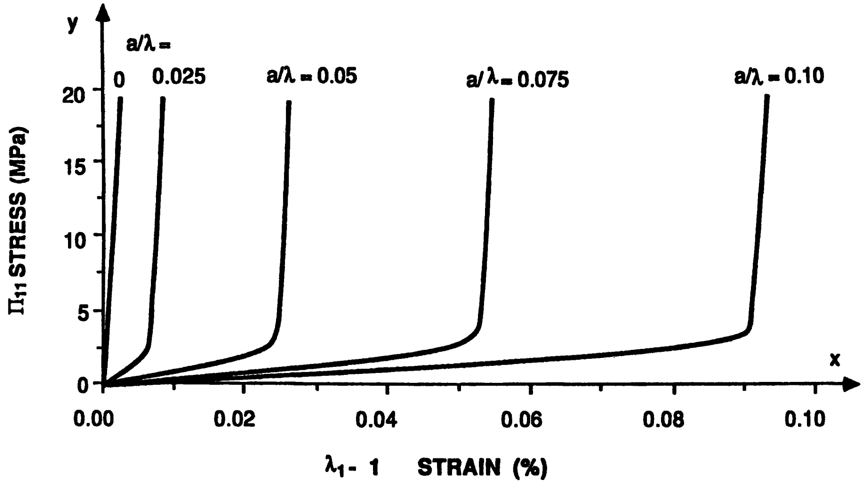

Figure 8. Theoretical stress-strain relation of Kevlar/silicone elastomer composites ($V_f = 9\%$) containing sinusoidally shaped fibers with various ratios of a/λ.

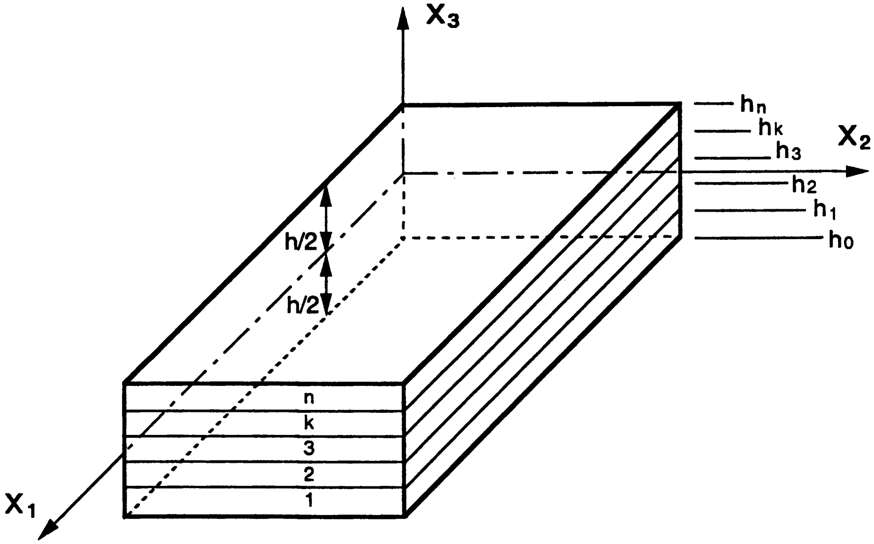

Figure 9. A composite laminate.

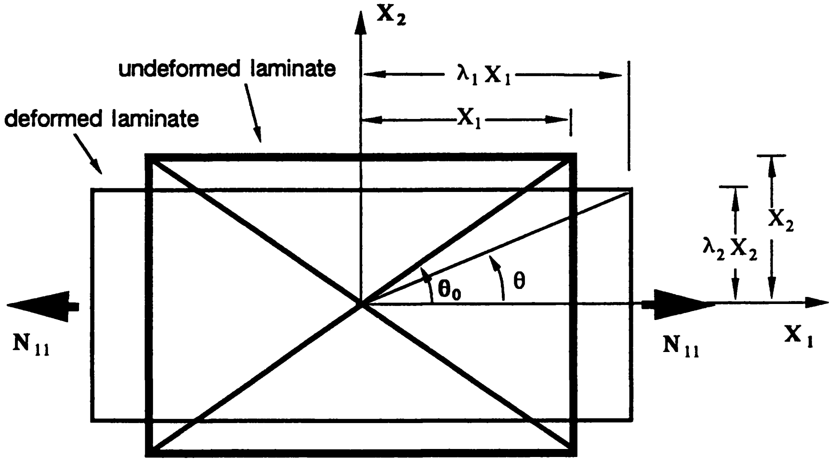

Figure 10. A symmetric flexible composite laminate under a uniaxial load.

$$W_{11}^{(\theta)} = W_{11}^{(-\theta)}$$

$$W_{22}^{(\theta)} = W_{22}^{(-\theta)} \qquad (35)$$

$$W_{12}^{(\theta)} = -W_{12}^{(-\theta)}$$

Eq. (34) is then reduced to

$$N_{11} = \tfrac{h}{2}\lambda_1 \{W_{11}^{(\theta)}(1 + \cos 2\theta_0) + W_{22}^{(\theta)}(1 - \cos 2\theta_0) - W_{12}^{(\theta)}\sin 2\theta_0\}\}$$

$$N_{22} = \tfrac{h}{2}\lambda_2 \{W_{11}^{(\theta)}(1 - \cos 2\theta_0) + W_{22}^{(\theta)}(1 + \cos 2\theta_0) + W_{12}^{(\theta)}\sin 2\theta_0\}\}$$

$$N_{12} = N_{21} = 0 \qquad (36)$$

where h is the thickness of the laminate; $W_{ij}^{(k)}$, obtained from Eqs. (12) and (9) is a function of λ_1 and λ_2. With the stress condition of Eq.(32) and the values of elastic constants, the two unknowns, λ_1 and λ_2, in Eq.(36) can be solved.

For example, let $\theta_0 = 45°$, from Eqs. (10), (2.17) and (36),

$$N_{11}/h = \lambda_1 \{C_{66}(\lambda_1^2 - \lambda_2^2) + \tfrac{1}{4}C_{6666}(\lambda_1^2 - \lambda_2^2)^3\}$$

$$N_{22}/h = 0$$

$$= (D - 4C_{66})\lambda_1^2 - (D + 4C_{66})\lambda_2^2 + \tfrac{1}{4}(C_{111} + C_{222})(\lambda_1^2 + \lambda_2^2 - 2)^2 +$$

$$+ \tfrac{1}{16}(C_{1111} + C_{2222})(\lambda_1^2 + \lambda_2^2 - 2)^3 + C_{6666}(\lambda_2^2 - \lambda_1^2)^3 \qquad (37)$$

Downloaded by UNIV OF GUELPH LIBRARY on August 6, 2012 | http://pubs.acs.org
Publication Date: April 3, 1991 | doi: 10.1021/bk-1991-0457.ch011

Downloaded by UNIV OF GUELPH LIBRARY on August 6, 2012 | http://pubs.acs.org
Publication Date: April 3, 1991 | doi: 10.1021/bk-1991-0457.ch011

where $D = C_{11} + 2C_{12} + C_{22}$. On the other hand, the relation of Eq. $(37)_1$ may be used to experimentally determine the shear constants C_{66} and C_{6666} by a curve fitting method, if the experimental data of N_{11}, λ_1 and λ_2 are given.

Conclusions

1. The constitutive relations for a basic composite element under finite deformation have been exploded. The derivation is based upon the approaches of finite elasticity and a strain-energy function in terms of the Lagrangian strains referring to the initial principal material axes. Both fibre geometric nonlinearity and matrix material nonlinearity have been taken into account.

2. The constitutive equations are applied to study the elastic behavior of flexible composites containing two different types of fiber geometric forms: wavy fibers and straight fiber network (laminates). It has been found that the deformation behavior of such composites is not only influenced by the combination of the material systems, but is also affected by the geometric shape of the fibres and their arrangements. Good agreement also has been found between theoretical predictions and experimental results.

3. The constitutive relations presented in this paper can be used to analyze the nonlinear finite deformation behavior of textile fabric reinforced flexible composites, as well as the biological materials. Both of these studies are under investigation.

Glossary of Terms

a	amplitude of the curved fibre
a_{ij}	component of the orthogonal transformation matrix
C_{ij}, C_{ijk}, C_{ijkl}	elastic stiffness constants related to linear, bi-modular, and nonlinear properties, respectively
c	$= \cos\theta_0$
E_{ij}	Lagrangian strain
g_{ij}	deformation gradient
K	magnitude of shear deformation
s	$= \sin\theta_0$
W	strain-energy density referring to the initial principal material coordinates
W_{ij}	$= \frac{\partial W}{\partial E_{ij}}$
X	Lagrangian coordinate
$\bar{X}$	initial principal material coordinate with $\bar{X}_1$ parallel to the fibre direction
λ	wavelength of the curved fibre
λ_i	extension ratio in X_i direction
θ_0	initial fibre orientation
Π_{ij}	Lagrangian stress (Piola-Kirchoff stress)
‾ (over bar)	for a quantity referring to the initial principal material coordinates $\bar{X}_1$-$\bar{X}_2$

Downloaded by UNIV OF GUELPH LIBRARY on August 6, 2012 | http://pubs.acs.org
Publication Date: April 3, 1991 | doi: 10.1021/bk-1991-0457.ch011

Acknowledgments

This work is partially supported by RAB, University of Nevada, Reno.

Literature Cited

1. Luo, S. Y.; Chou, T. W. Journal of Applied Mechanics 1988, 55, 149-155.
2. Fung, Y. C. Biomechanics: Mechanical Properties of living tissues. New York: Springer-Verlag.
3. Weibel, E.R. in: Handbook of Physiology, 3, Section 3, 1986, 89-111.
4. Stephens, N. L., Kroeger E. and Mehta J. A. J. Appl. Physiol, 1969, 26, 685-692.
5. Winter, D.C., J. Biomechanical Engineering, 1985, 107, 300-303.
6. Evrensel, C.A.; A. Kalnins J. Applied Mechanics, 1988, 55, 660-666.
7. Elli, S. and C.A. Evrensel, Advances in Bioengineering, 1988, BED- 8, 147-150.
8. Evrensel C.A. and S. Elli, Proceedings of the First National Fluid Dynamics Congress, 1988, 2094-2099.
9. Mead, J., Physiol. Rev. 1961, 41 , 281-330.
10. Aspden, R. M. Proc. R. Soc. Lond. 1986, A 406, 287-298.
11. Humphrey, J. D & Yin, F. C. P. Biophysical J., 1987, 52, 563-570.
12. Luo, S. Y., and Chou, T. W., Proceedings of the Royal Society of London, in press.
13. Luo, S. Y. & Chou, T. W. in Micromechanics and Inhomogeneity-The Toshio Mura Anniversary Volume; Weng, G.J., Taya, M. & Abe, H., Ed.; Springer-Verlag, New York, 1989, 243-256.
14. Fung, Y. C. A First Course in Continuum Mechanics, Prentice-Hall, Inc., 1969, Englewood Cliffs, N.J.
15. Rivlin, R. S. in Centro Internazionale Matematico Estivo; Ciclo, II and Rivlin R. S., Ed.; 1970, Edizioni Cremonese, Roma.
16. Chou, T. W. & Takahashi, K. Composites, 18, No.1, 1987, 25-34.
17. Luo, S. Y., and Chou, T. W. In Composites: Chemical and Physicochemical Aspects, T. L. Vigo and B. J. Kinzig, VCH Publishers, 1990, New York.
18. Rivlin, R. S., 1986-88 private communications.

RECEIVED August 13, 1990

Downloaded by STANFORD UNIV GREEN LIBR on August 6, 2012 | http://pubs.acs.org
Publication Date: April 3, 1991 | doi: 10.1021/bk-1991-0457.ch012

Chapter 12

Recent Advancements in Suture Fibers for Wound Closure

C. C. Chu

Department of Textiles and Apparel, Cornell University, Ithaca, NY 14853–4401

This paper reviewed the two most important developments in the field of suture fibers for wound closure. They were antimicrobial sutures for reducing incidence of wound infection and hydrolytic degradation phenomena of synthetic absorbable suture fibers. Experimental findings from other investigators and from the author's lab were given with emphasis on the latter. Many new but unpublished data from the author's lab were also included. Future challenges and directions of research and development for these two areas were briefly discussed. In the area of antimicrobial suture fibers, the chemical, physical and biological properties of a silver metal-coated nylon suture were described, and its antimicrobial performance again seven bacteria in vitro as well as preliminary biocompatibility in vivo were compared with a commercial nylon suture (Nurolon from Ethicon). The data appear promising and may suggest the potential use of this fiber in contaminated wounds or in patients whose immune response have been compromised. In the area of hydrolytic degradation phenomena of synthetic absorbable suture fibers, factors which have been found to influence the hydrolytic phenomena of this class of suture fibers were discussed. This property of hydrolytic degradation of the fibers coupled with the factors affecting it provided a unique opportunity for examining the interior structure and morphology of the fibers. The fibers exhibited a composite morphology with highly oriented microfibrils impregnated within noncrystalline domains. A plasma surface modification of this class of suture fibers for achieving better useful time was also described.

The earliest and most frequent application of textile materials for surgery was believed to be suture materials used to close wounds. As early as 4,000 years ago, linen was used as a suture material. Later, natural fibers from the bark of trees, plaited horsehair, cotton, and silk were also used. Due to the development of synthetic fibers like nylon, polyesters, and polyolefins in 1950's, synthetic fibers have gradually replaced natural fibers for wound closure purposes.

0097–6156/91/0457–0167$12.25/0

Downloaded by STANFORD UNIV GREEN LIBR on August 6, 2012 | http://pubs.acs.org
Publication Date: April 3, 1991 | doi: 10.1021/bk-1991-0457.ch012

Fibers for suture purposes are available in multifilament braid or monofilament form. Most of the braided sutures have 2/2 construction (i.e., each strand of yarn over and under passed two other strands) and they exhibit better handling properties, are more flexible, and are easier to tie knots in than monofilament (1,2). However, the monofilament sutures cause less tissue trauma during application, and induce less tissue reactions. Braided sutures are generally coated with a thin layer of polymer like silicone to facilitate their passage through tissues.

Although suture fibers have been used for several thousand years, the most important technological advancement was the development of synthetic absorbable fibers for wound closure in the early 1970's. Before synthetic absorbable fibers were available, all suture fibers (except catgut and reconstituted collagen) were nonabsorbable. This means they permanently remain inside the human body and cannot be degraded and metabolized. Although the permanence of suture fibers is required for fastening surgical implants like artificial heart valves, they are not needed in most wound closure conditions after the wounds have been healed. When present inside tissues, they do not have any function, but elicit undesirable foreign body tissue reactions which may promote infection, granulomatous reaction, and sinus formation (3). Because of these undesirable tissue reactions associated with nonabsorbable suture fibers, absorbable suture fibers have become increasingly popular. Since absorbable sutures can be degraded and be metabolized by the body after they serve their function, they leave no trace of foreign body to elicit undesirable chronic tissue reactions. Synthetic absorbable suture fibers are considered to be better than natural ones because the latter (catgut and reconstituted collagen) performs inconsistently due to variation in natural source and shows marked tissue reactions due to their foreign protein nature.

Current commercially available synthetic absorbable suture fibers are all derived from linear aliphatic polyesters, particularly polyglycolide and polylactide. These are: polyglycolide (Dexon), poly(glycolide-lactide) random copolymer (Vicryl), poly-P-dioxanone (PDS), and poly(trimethylene carbonate-glycolide) block copolymer (Maxon). Table I lists their chemical repeating units, trade names and manufacturers.

Table I. COMMERCIAL ABSORBABLE SUTURE MATERIALS

Name	Composition	Trade Name	Sources
Poly(glycolic acid) (PGA)	$[-OCH_2CO_2CH_2CO-]$	DEXON	Davis and Geck
Poly(glycolide-co-lactide)	$[-OCH_2CO_2CH_2CO-]_{90}$ $-OCH(CH_3)CO_2CH(CH_3)$ $-CO-]_{10}$	VICRYL	Ethicon
Poly(p-dioxanone)	$[-O(CH_2)_2OCH_2CO-]$	PDS	Ethicon
Poly(glycolide-co-trimethylene carbonate)	$[-OCH_2CO-]_{67}[OCH_2CH_2$ $CH_2OCO-]_{33}$	MAXON	Davis and Geck

All suture materials must have the following basic properties: 1) retaining adequate tensile strength through the critical period of wound healing; 2) adequate handling properties for secured knots; 3) eliciting minimal tissue reactions for minimal interference of healing process; 4) fast degradation and absorption after the suture is no longer needed; 5) no predisposition to wound infection and allergy.

This paper reviews two recent most important developments in the field of wound closure biomaterials. They are: (a) antimicrobial sutures for reducing incidence of wound infection and (b) hydrolytic degradation phenomena of synthetic absorbable suture fibers for a better understanding of fiber morphology. Experimental findings from other investigators and our lab are given with emphasis on the latter. Some new unpublished data from the author's lab are also included when appropriate. Future challenges and directions of research and development for these two areas are also briefly discussed.

The Development of Antiimicrobial Fibers for Wound Closure

The Need To Control Wound Infection. Wound infection is considered to be one of the oldest and most common complications in all injuries and branches of surgery. The incidence of wound infection in this country ranged from 3 to 12% with an average of 8% (4). Despite many recent advances in surgical techniques and medicine, such as new antibiotics and the alteration of the host immune system, the rate of wound infection has not significantly changed in recent years (5). Wound infection often results in additional physiological, psychological and economic burdens to patients as well as their families. Depending on the type of surgery and severity of wound infection, surgical wound infection has been reported to result in an average of 7.4 additional days of prolonged hospitalization with a range of up to 68 additional days (6). Average additional expenses were $839 with a range of $0-$7,900. When other factors, such as the patient's loss of productivity, compensation payments, the cost of implants, and current soaring health care expenses are taken into account, the total cost of wound infection is expected to be even higher (7).

The Role of Sutures in Wound Infection. The development of wound infection depends on several factors, such as the degree of microbial contamination, host resistance, the nature of the wound, the type of surgery, and the presence of foreign materials. Foreign materials like prosthetic devices in wound infection have become increasingly important because of their more frequent use in modern medicine (8). The presence of foreign materials in a wound has been known to significantly enhance propensity of surrounding tissues to infection. Among all foreign materials, suture materials are probably the most important biomaterials for wound infection because they are the most frequently used materials in surgery and because the majority of wound infection begins along and near the suture lines. Thus, suture materials may contribute greatly to the genesis of surgical infections by lowering the clinical dose of a microorganism that is needed to cause wound infection. It has been shown that the number of S. aureus needed to establish infection (e.g., pus formation) can be reduced 10,000-fold by the presence of silk sutures (9,10). Even the most biocompatible suture materials (e.g., monofilament nylon 6,6 and polypropylene) also tend to elicit some degree of surgical infection in contaminated tissues. Edlich, et al., reported that the percentage of gross infection in S. aureus contaminated, nylon-sutured wounds of mice was considerably higher (53.7%) than the needle track (0%) control mice (11). Varma, et al., also reported similar findings in their recent study on dogs (12). They found that the degree of S. aureus infection increased significantly in the presence of suture materials in three bacterial concentrations (7.5 x 10^8, 7.5 x 10^7. 7.5 x 10^6 cells/ml). A recent study of five commercial suture materials (including the newly introduced Gore-tex suture) confirms that the presence of suture

Downloaded by STANFORD UNIV GREEN LIBR on August 6, 2012 | http://pubs.acs.org
Publication Date: April 3, 1991 | doi: 10.1021/bk-1991-0457.ch012

materials in contaminated wounds increases the incidence of infection (13).

All suture materials do not behave similarly in their ability to enhance bacterial infection in surgical wounds. The physical configuration of the suture thread has been suggested to be an important factor in determining its susceptibility toward surgical infection (14-16). The viable bacterial count recovered from the implanted monofilament non-capillary polypropylene sutures, after 41 days in rat muscle, showed a significant decrease from the initial injected amount (from 2.5 x 10^7 to 2.1 to 10^3), while the multifilament twisted nylon sutures with capillarity, maintained roughly the initial count (1.2 x 10^7 to 0.3 x 10^7) (15). The corresponding number of viable bacteria (about 25) recovered from the control (no sutures) was significantly lower than for both sutures. The results were consistent with the study of inflammatory cell reaction near the implanted suture sites (15). It was speculated that bacteria could hide within the interstitial space of the multifilament sutures, where they are difficult to be reached by the body's defense mechanisms, and thus be able to multiply and maintain the infection in the surrounding tissues.

The physical structure of a suture fiber can also serve as a vehicle (or template) for mechanical transportation of bacteria into surgical wounds. This occurs because the outer layer of sutures in the incision traverses the skin barrier and enters the subcutaneous tissues. While the skin is sterilized before surgery, it rapidly becomes contaminated after surgery. The bacteria enter the body via the interstices of a braided suture or along the tract of a monofilament suture. This physical process is aided by capillary action, and the infection that occurs starts in the subcutaneous tissue. If untreated, it can spread to involve the deeper tissues and become clinically significant. Blomstedt et al., reported that the wound infection rates were higher for multifilament sutures with high capillary capability than for non-capillary sutures (17).

Conversely, the chemical structure of the suture has also been considered to be the important factor in the early development of infection in contaminated surgical wounds (11). Extensive tissue reactions arising from the chemical properties of a suture possibly lower the tissue's ability to combat the progress of wound infection. Tissue reactions, however, are not limited to chemical origin of a suture, as different physical configurations of suture materials of the same chemical nature have resulted in different levels of tissue reactions (11).

Several recent studies have suggested that the occurrence of wound infection associated with the presence of suture materials might also be begun by adherence of bacteria onto these materials (18-21). Their results indicate that bacterial adherence to suture materials may occur by a pathogenic mechanism in the etiology of surgical wound infection and play a significant role in the induction of surgical wound infection. It was found that the amount of adhered bacteria depended on (a) the type of suture material, (b) the type of bacteria, and (c) the duration of contact.

However, Chu et al. also reported that a dynamic rather than a static bacterial adherence phenomenon occurred in ten different suture materials (size 2-0 chromic catgut, polyglycolic acid, poly[glycolide-lactide] copolymer, poly-p-dioxanone, poly[ethylene terephthalate], polypropylene and nylon 6,6). Bacteria tested were S. aureus and E. coli. Bacterial adherence was determined quantitatively with radiolabelled cells and qualitatively by scanning electron microscopy. In the group of absorbable sutures, the new PDS sutures exhibited the lowest affinity toward the adherence of both E. coli and S. aureus as shown in Figure 1. Polyglycolic acid sutures had the highest affinity for these two bacteria. With nonabsorbable sutures, the physical configuration of

Downloaded by STANFORD UNIV GREEN LIBR on August 6, 2012 | http://pubs.acs.org
Publication Date: April 3, 1991 | doi: 10.1021/bk-1991-0457.ch012

Downloaded by STANFORD UNIV GREEN LIBR on August 6, 2012 | http://pubs.acs.org
Publication Date: April 3, 1991 | doi: 10.1021/bk-1991-0457.ch012

the sutures contributed more to their ability to attract bacteria than the surface finish. Bacterial adherence to suture materials was also time dependent. Qualitative observations from the scanning electron micrographs (Figure 2) were consistent with the quantitative data. There were very few S. aureus or E. coli adhered to PDS sutures after 60 minutes of contact, whereas other sutures showed a high level of adherence after the same contact period. The scanning electron micrographs confirmed the higher affinity of S. aureus to sutures compared with E. coli (as observed in the radiolabelled study). Not only did the microbes adhere on the rough surface of the interstices among the filaments, but also a major portion of them stayed on the smooth noncrevice parts of the sutures.

Since the majority of wound infections occur along the suture lines, and since suture materials are the most frequently used foreign materials in surgery, it would be ideal to have a suture which not only serves its traditional role as a wound closure, but also able to fight potential wound infection at and around the vicinity of the infected sites. Although it is a standard practice for surgeons not to use sutures to close wounds that are known to be heavily contaminated, most surgical wounds have some degree of microbial contamination which may or may not develop into clinically evident wound infection depending on the degree of host resistance, the dose of microorganisms, and its virulence (22,23). The use of antimicrobial sutures could provide an extra degree of protection in clean or clean-contaminated wounds, particularly those associated with surgical implants. In addition, instead of healing by second-intention, antimicrobial sutures may be used for early secondary closure of incisional abscesses after adequate wound drainage for reducing healing time without complications (24). The potential value of antimicrobial sutures may also be found in traumatic wounds like lacerations in automobile accidents, high risk surgery like cardiovascular and orthopedic operations, frequently-contaminated wound sites like the colon, and in patients whose host resistance has been compromised because of diseases like cancer, AIDS, diabetes, or hemorrhagic shock, or in elderly or new-born patients, organ transplantation, or chemotherapy.

Current Approaches Toward The Development of Antimicrobial Sutures. The most frequent approach to achieve such an ideal suture is to impregnate the sutures with a variety of antimicrobial agents, such as neomycin palmitate, penicillin, sulfonamide, quaternary ammonium complexes, chlorhexidine, and iodine (22,25-29). The main advantage of this approach is the ability to use far lower dosages of antibiotics than the oral or injected route because the drugs are in direct or close contact with the microorganisms in the wound and no loss of drugs occurs due to biotransformation in orally administered cases. It also helps reduce the possibility of bacteria seeding inside the crevices of braided sutures. Although these antibiotic- or antiseptic-impregnated sutures have achieved some degree of success in reducing wound infections in animals, their results are far from perfect for reasons such as the small effective domain, short duration and narrowness of spectrum of the antibacterial effect. For example, the antibacterial activity of neomycin palmitate-impregnated silk and Dacron sutures lasted from 4 to 8 hours (22). The benefits of using antiseptic agents to impregnate sutures have also been questioned because they may be more tissue-toxic than bactericidal.

Downloaded by STANFORD UNIV GREEN LIBR on August 6, 2012 | http://pubs.acs.org
Publication Date: April 3, 1991 | doi: 10.1021/bk-1991-0457.ch012

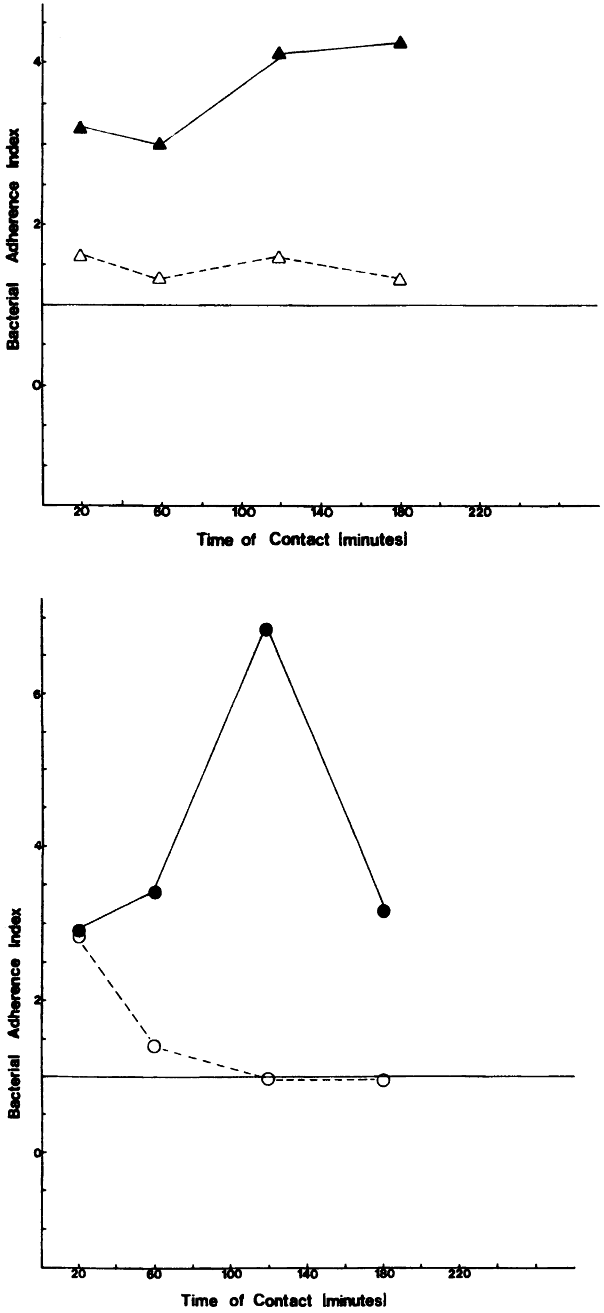

Figure 1. Bacterial adherence index of 2-0 suture materials after various incubation times. Top: Chromic catgut with *S. aureus* and *E. coli.* Bottom: Vicryl with *S. aureus* and *E. coli.* (Reproduced with permission from ref. 18. Copyright 1984 Cahners Publishing Company.)

Downloaded by STANFORD UNIV GREEN LIBR on August 6, 2012 | http://pubs.acs.org
Publication Date: April 3, 1991 | doi: 10.1021/bk-1991-0457.ch012

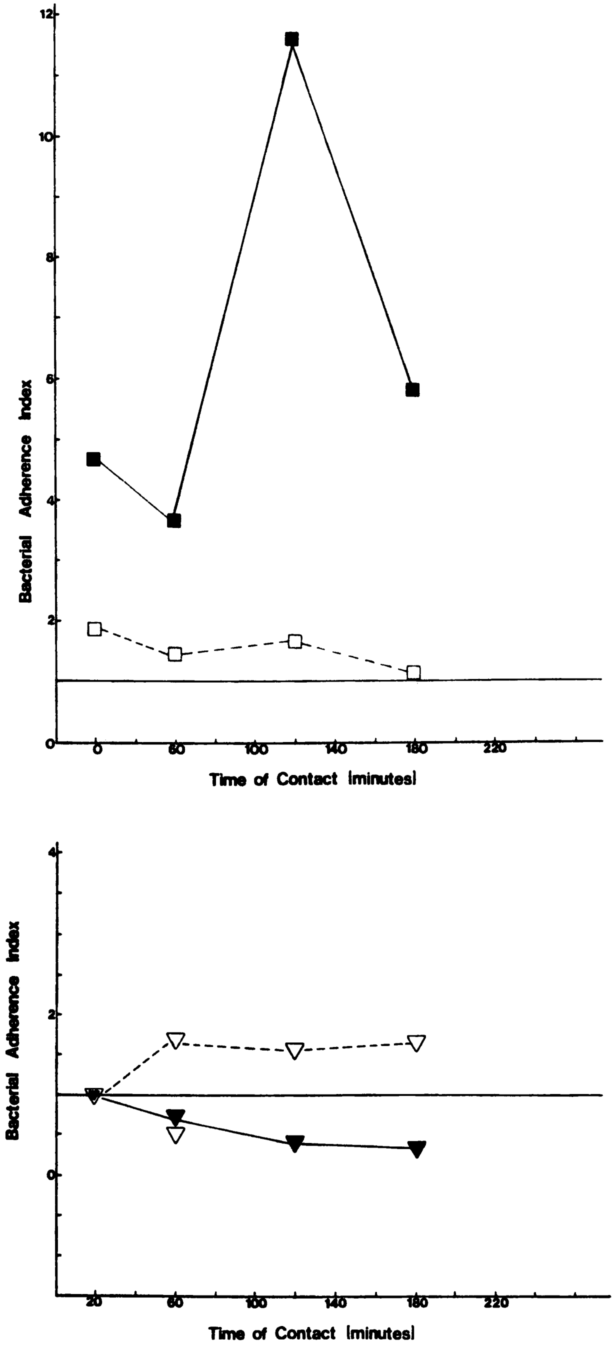

Figure 1. Continued. Bacterial adherence index of 2-0 suture materials after various incubation times. Top: Dexon with *S. aureus* and *E. coli.* Bottom: PDS with *S. aureus* and *E. coli.* (Reproduced with permission from ref. 18. Copyright 1984 Cahners Publishing Company.)

Downloaded by STANFORD UNIV GREEN LIBR on August 6, 2012 | http://pubs.acs.org
Publication Date: April 3, 1991 | doi: 10.1021/bk-1991-0457.ch012

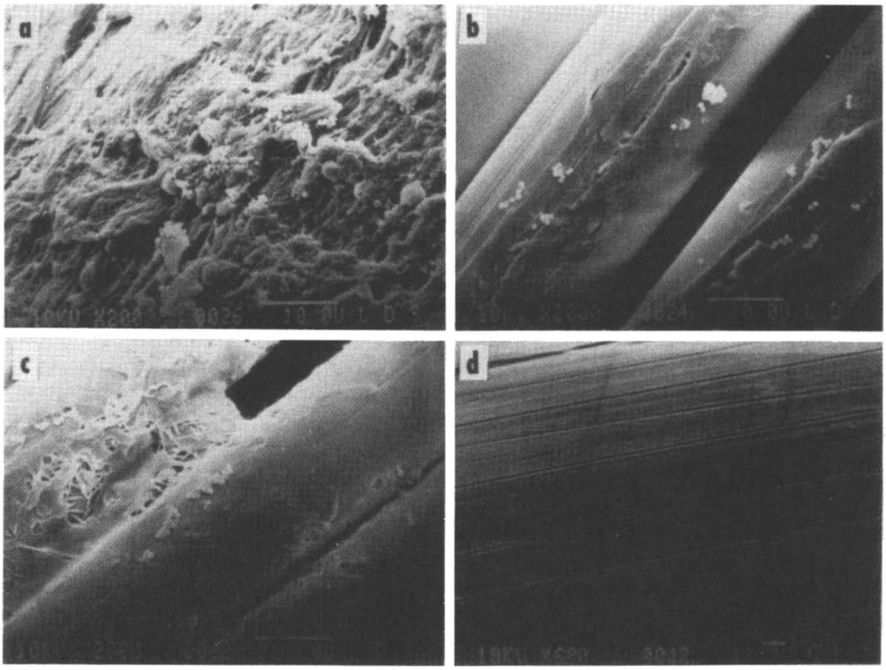

Figure 2. Scanning electron micrograph of S. aureus adherence on 2-0 suture materials after 60 minutes incubation. (a) Chromic catgut; (b) Dexon; (c) Vicryl; and (d) PDS. (Reproduced with permission from Ref. 18. Copyright 1984 C. C. Chu et al.)

Downloaded by STANFORD UNIV GREEN LIBR on August 6, 2012 | http://pubs.acs.org
Publication Date: April 3, 1991 | doi: 10.1021/bk-1991-0457.ch012

Silver Metal-Coated Antimicrobial Suture (SAS). A different approach to control wound infection around the vicinity of suture lines was recently reported (30,31). In those studies, we examined the antimicrobial property of a new direct current-activated, silver, metal-coated nylon 6,6 suture (SAS) in vitro. It was found that a weak direct current (less than 400 μA) could significantly enhance the biocidal property of the new SAS against seven types of bacterial species.

The use of silver in both compound and elemental form for the treatment of wound infection has been known for centuries (32). Recent typical examples are the use of silver sulfadiazine as a topical treatment for burn wounds (33,34) the silver-incorporated Gore-tex vascular graft for the control of prosthetic bacterial infection (35), and the silver anode treatment of chronic osteomyelitis (36). The electrochemical features of direct-current, activated silver and its results in animals and clinical cases were originally reported and recently reviewed by Spadaro (37). Spadaro et al. have shown that silver is bacteriostatic, when used as an anode with an extremely weak electric current (38). Quantitative studies showed that most of this inhibition takes place in a few hours. Silver also exhibited fungicidal properties at concentrations as low as 1.9 μg/ml and its inhibitory and fungicidal concentrations are lower than those reported for other silver compounds (39). Silver has also been incorporated in bone cement composites (40). Even with the wide use of broad-spectrum antibiotics, effective control of osteomyelitis has not been consistent. However, Becker, et al. and Webster et al., used electrically generated silver ions to treat chronic osteomyelitis and controlled the infection in 80% (12 out of 15 patients) (41), and 64% (10 out of 15 patients) (36). Silver ions, because of their small size, have been suspected to be able to penetrate many tissues to some extent, particularly poorly vascularized tissues.

Several bacterial species like E. coli, S. aureus, and P. aeruginosa have been found to have minimum inhibitory and bactericidal concentrations for silver ions 10 to 100 times lower than antibiotics in current use (42); and bacterial resistance to the silver ion is rare (43). Recently, Falcone et al. examined the inhibitory effect of an electrically-activated, silver-coated fabric on six commonly found cutaneous wound bacteria (44). Their results confirm previously reported effective diffusion of the silver ions and their local antibacterial action. Effectiveness of electrically activated silver in reducing bacterial colonization at a percutaneous implant in rats was also recently examined (45). A marked reduction or elimination of S. aureus was observed near the interface by intermittent electrical activation of the percutaneous silver implants.

Silver, metal-coated, multifilament nylon 6,6 yarns were obtained from Saquoit Industries, Inc. The yarns were 129 denier and braided into size 2-0 sutures with an eight-carrier braider. The suture has a structure of 2/2 which indicated that each strand of yarn over and under passed two other strands. This braid structure is identical to commercially available nylon sutures (i.e., Nurolon from Ethicon). It would be more significant to develop an antimicrobial suture with a braid structure because braid sutures are more prone to wound infection than monofilament sutures.

This 2-0 size SAS had a denier of 1278 (denier is defined as the weight in grams per 9000 meters). Its tensile breaking strength (2.8 grams per denier) is comparable to 2-0 size silk sutures, but is slightly lower than 2-0 size Nurolon suture (Figure 3). Characterization of this SAS by energy-dispersive spectrometer (EDS) X-ray elemental analysis indicates that metallic silver of 2-5 μm thickness was chemically bonded into the nylon substrate. An EDS X-ray spectrum of the SAS is given in Figure 4, and the characteristic Ag element peak at 3.0 KeV energy is evident. To identify further where the silver is located in the SAS, area maps of silver element distributions by EDS X-ray analysis along the cross-sectional and longitudinal directions of the SAS were studied (Figure 5). The metallic silver was found to be uniformly distributed on the surface of each nylon fiber within the SAS. The concentration of the metallic silver was about 320 μg Ag per cm length of the SAS. The 2-0 suture was electrically conductive with only 3 ohm resistance per 5 cm SAS length.

The in vitro antibacterial properties of the SAS were evaluated qualitatively by the width and sterility of the clear zone in the bacterial culture plates (30), and quantitatively by standard plate count methods (31). Seven species of bacteria were tested: Staphylococcus aureus, Escherichia coli, Pseudomonas aeruginosa, Klebsiella pneumonia, Shigella dysenteriae, Serratia marcescens and Proteus mirabilis. A weak direct current ranging from 0.4-400 μA was applied to the suture specimens to examine whether the biocidal property of the SAS could be enhanced by anodic micro-current. The commercial size 2-0 Nurolon suture from Ethicon served as the control.

As summarized in Table II, the SAS exhibited very good to moderate bactericidal activity toward these seven bacterial species. P. aeruginosa was the most sensitive species, while P. mirabilis was the least sensitive one. The observed width of the clear zone was further confirmed by the degree of sterility of the clear zone. In general, all stab tests in the clear region showed sterility when the width of a clear zone was greater than 2.0 mm. Application of direct current through the SAS specimens positively enhanced their antimicrobial property and the degree of enhancement depended on the direct current level, bacterial type, mode of current application, and anode versus cathode. pH measurement of the clear zone indicated that the observed clear zone in the bacterial culture plates was due solely to the antibacterial property of the SAS because of the observed constant pH (7.5). Figures 6-8 illustrate the observed clear zone in bacterial culture plates under various conditions.

Increasing current level was found to always increase the width of the clear zone with P. aeruginosa the most sensitive. The ability to adjust the strength of the antimicrobial property would be very useful clinically because the SAS can be tailored to specific clinical conditions (heavily vs. lightly contaminated) simply by either enlarging (i.e., increasing current level) or reducing (decreasing current level) its antimicrobial strength. It is interesting to know that SAS without any current application also exhibited some antimicrobial properties but at a significantly lower level.

The SAS also exhibited an antimicrobial activity toward well-established bacterial colonies, but the effect was less strong than the case when direct current was applied simultaneously with incubation. For example, the width of the clear zone at the anode site for P. aeruginosa was reduced from 7.5mm to 2.5mm when a direct current of 0.4 μA was applied 24 hrs after the established bacterial colonies. These findings are believed to be clinically important because the risk of wound infection is directly proportional to the dose of contaminated bacteria and their virulence, but inversely

Downloaded by STANFORD UNIV GREEN LIBR on August 6, 2012 | http://pubs.acs.org
Publication Date: April 3, 1991 | doi: 10.1021/bk-1991-0457.ch012

Downloaded by STANFORD UNIV GREEN LIBR on August 6, 2012 | http://pubs.acs.org
Publication Date: April 3, 1991 | doi: 10.1021/bk-1991-0457.ch012

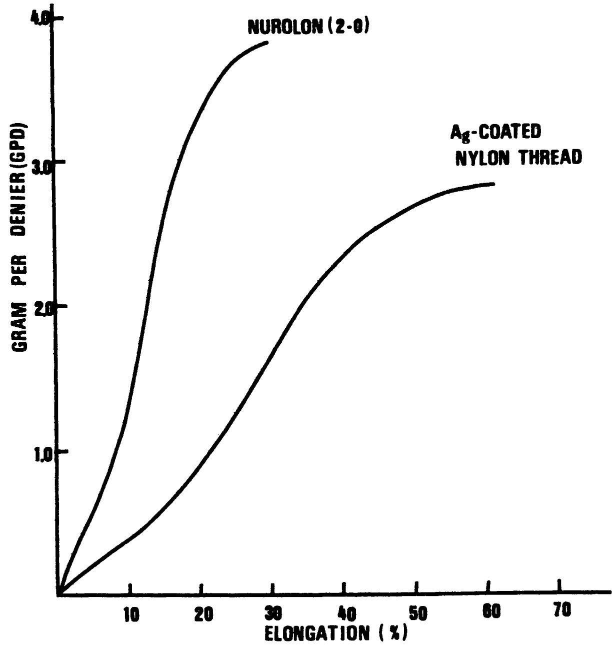

Figure 3. Stress and strain curves of both SAS and commercial 2-0 Nurolon suture. (Reproduced with permission from Ref. 30. Copyright 1987 C. C. Chu et al.)

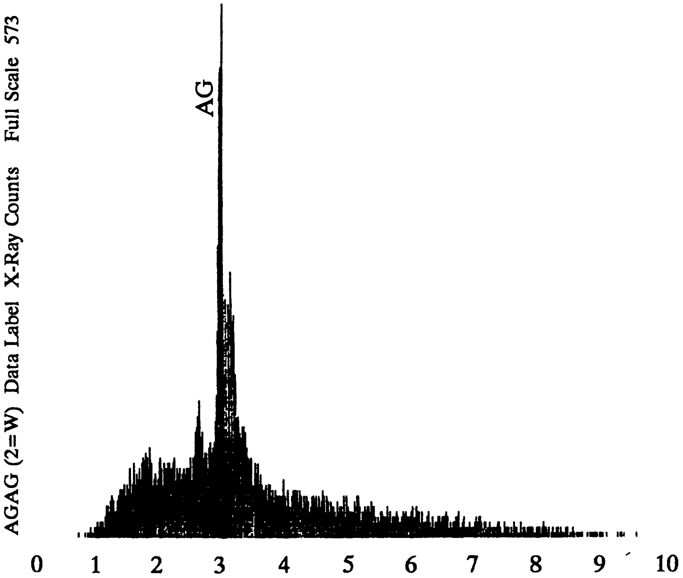

Figure 4. Energy dispersive spectrometer (EDS) spectrum of the new SAS.

Downloaded by STANFORD UNIV GREEN LIBR on August 6, 2012 | http://pubs.acs.org
Publication Date: April 3, 1991 | doi: 10.1021/bk-1991-0457.ch012

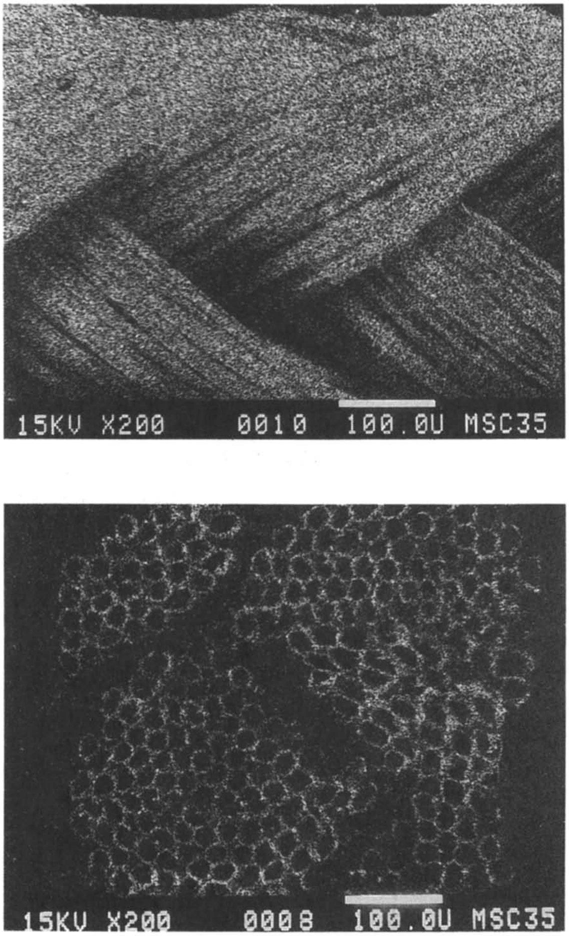
15KV X200 0010 100.0U MSC35
15KV X200 0008 100.0U MSC35

Figure 5. EDS area mapping of silver element for the new silver metal-coated antimicrobial suture (SAS). Top: Longitudinal view. Bottom: Cross-sectional view.

Downloaded by STANFORD UNIV GREEN LIBR on August 6, 2012 | http://pubs.acs.org
Publication Date: April 3, 1991 | doi: 10.1021/bk-1991-0457.ch012

Table II. EFFECTS OF THE MODE OF DIRECT CURRENT APPLIED ON THE *IN VITRO* ANTIBACTERIAL CAPABILITY OF SILVER-COATED NYLON BRAID THREADS

Anti-bacterial Performance	Width of clear zone in culture plate (mm, ± 0.5)								Sterility of clear zone in culture plate[a] (± 0.5)							
—	Anode				Cathode				Anode				Cathode			
Bacterial type and current	24h		48h		24h		48h		24h		48h		24h		48h	
level	X	Y	X	Y	X	Y	X	Y	X	Y	X	Y	X	Y	X	Y
Escherichia coli																
0.4 μA	3.2	2.0	4.0	2.0	0	1.6	0	2.0	IV	IV	IV	III	I	III	I	III
4.0 μA	3.5	2.0	5.0	2.0	0	2.0	0	2.2	IV	III	IV	III	I	III	I	IV
40 μA	4.1	2.4	6.0	2.0	0	1.0	0	1.6	IV	IV	IV	III	I	II	I	III
400 μA	5.0	2.5	6.2	2.8	0	0	0	2.4	IV	IV	IV	IV	I	I	I	IV
Pseudomonas aeruginosa																
0.4 μA	7.5	2.5	8.0	3.0	0	3.1	0	3.0	IV	IV	IV	IV	I	IV	I	IV
4.0 μA	8.1	2.0	9.5	3.0	0	2.8	0	2.5	IV	IV	IV	IV	I	IV	I	IV
40 μA	9.1	3.2	9.5	3.0	0	3.9	0	2.5	IV	IV	IV	IV	I	IV	I	IV
400 μA	10	4.1	9.5	4.7	0	4.1	0	4.1	IV	IV	IV	IV	I	IV	I	IV
Staphylococcus aureus																
0.4 μA	5.6	2.5	6.4	3.0	0	2.8	0	3.5	IV	IV	IV	IV	I	IV	I	IV
4.0 μA	7.0	2.7	7.0	3.0	0	2.3	0	2.8	IV	IV	IV	IV	I	IV	I	IV
40 μA	7.1	3.0	7.1	3.0	0	3.0	0	3.0	IV	IV	IV	IV	I	IV	I	IV
400 μA	8.0	3.1	8.0	3.1	0	3.0	0	3.0	IV	IV	IV	IV	I	IV	I	IV
Shigella dysenteriae																
0.4 μA	6.0	1.8	5.6	1.0	0	1.5	0	1.5	IV	IV	IV	II	I	III	I	III
4.0 μA	6.0	2.0	6.1	1.5	0	1.7	0	1.5	IV	IV	IV	III	I	III	I	III
40 μA	6.9	2.0	6.3	2.0	0	2.0	0	1.2	IV	IV	IV	IV	I	IV	I	II
400 μA	7.0	2.0	6.5	2.0	0	2.0	0	2.0	IV	IV	IV	IV	I	IV	I	IV
Serratia maruslens																
0.4 μA	4.5	1.1	4.0	2.1	0	1.9	0	1.4	IV	II	IV	IV	I	IV	I	III
4.0 μA	4.8	1.5	4.9	2.0	0	1.3	0	1.8	IV	III	IV	IV	I	II	I	IV
40 μA	5.0	1.8	5.3	2.0	0	1.9	0	2.1	IV	IV	IV	IV	I	IV	I	IV
400 μA	5.1	1.8	5.6	2.1	0	1.2	0	2.0	IV	IV	IV	IV	I	II	I	IV

[a] Determined by subculture tests. I - No antibacterial (all 3 stab tests nonsterile); II - Slight antibacterial (1/3 of stab tests sterile; III - Medium antibacterial (2/3 of stab tests sterile); IV - Strong antibacterial (all 3 stab tests sterile). X, Direct Current applied simultaneously during incubation. Y, Direct Current applied after 24 h of incubation without current.

Downloaded by STANFORD UNIV GREEN LIBR on August 6, 2012 | http://pubs.acs.org
Publication Date: April 3, 1991 | doi: 10.1021/bk-1991-0457.ch012

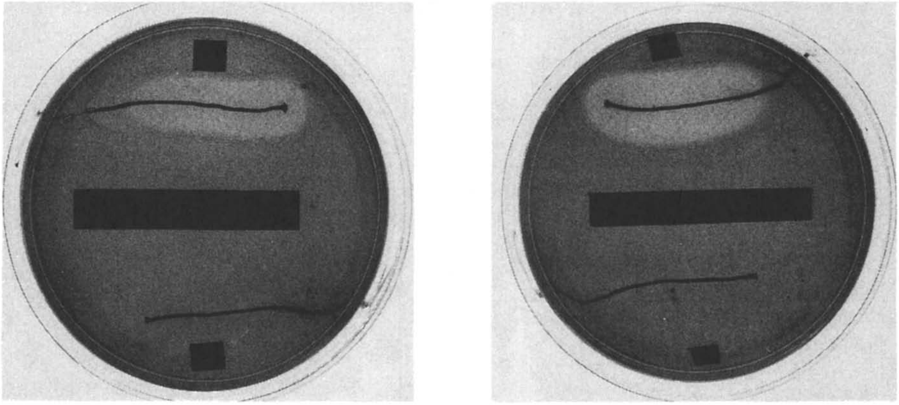

Figure 6. The effect of the magnitude of direct current on the antimicrobial activity of SAS. The SAS was impregnated with *P. aeruginosa*. Left - 0.4μA/24 hrs incubation. Right - 400 μA/24 hrs incubation. (Reproduced with permission from Ref. 30. Copyright 1987 C. C. Chu et al.)

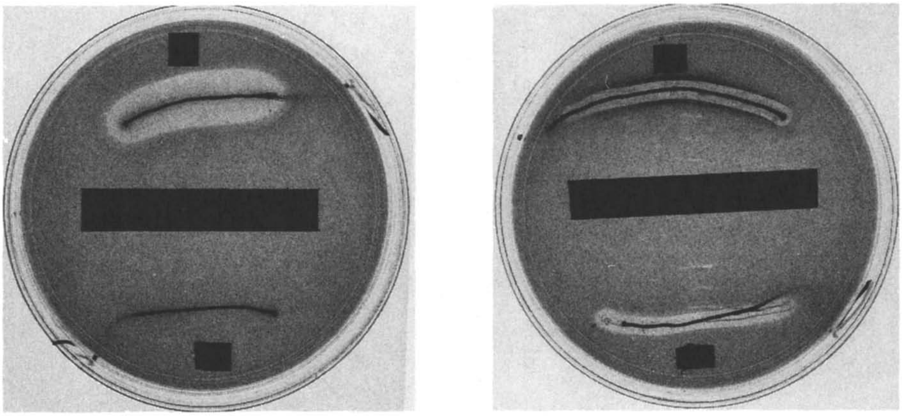

Figure 7. The effect of different mode of direct current application on the antimicrobial activity of SAS. SAS was impregnated with *S. aureus*. Left - 4.0 μA applied simultaneously with incubation for 24 hr; Right - 4.0 μA applied after the bacterial culture plate had been incubated for 24 hr. (Reproduced with permission from Ref. 30. Copyright 1987 C. C. Chu et al.)

Downloaded by STANFORD UNIV GREEN LIBR on August 6, 2012 | http://pubs.acs.org
Publication Date: April 3, 1991 | doi: 10.1021/bk-1991-0457.ch012

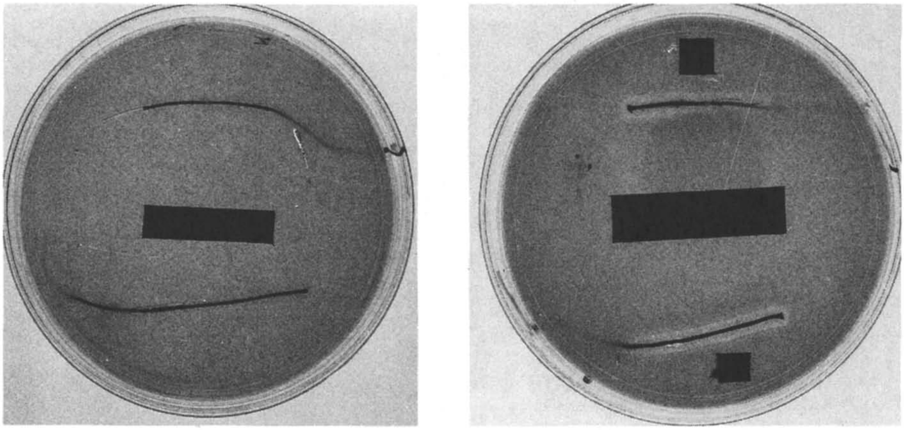

Figure 8. Bacterial culture plates of SAS and control sutures without direct current application. Suture specimens were impregnated with S. aureus for 24 hrs. Left - Nurolon as control; Right - SAS. (Reproduced with permission from Ref. 30. Copyright 1987 C. C. Chu et al.)

Downloaded by STANFORD UNIV GREEN LIBR on August 6, 2012 | http://pubs.acs.org
Publication Date: April 3, 1991 | doi: 10.1021/bk-1991-0457.ch012

proportional to the resistance of the host (23). The observed antimicrobial property of the SAS toward well-established bacterial colonies may make SAS a useful tool to confine contaminated wounds. Another interesting phenomenon associated with this observation was that the antimicrobial activity of the SAS toward 24 hrs well-established colonies was found at both anode and cathode sites instead of at anode site alone as observed when direct current was applied simultaneously with incubation for 24 hrs. A comparison of the strength of antimicrobial property of SAS between the condition where current applied after 24 hrs incubation (Figure 7.b) and the control where no current applied for 24 hrs (Figure 8.a) indicated that these two different modes of current application resulted in an almost identical level of antimicrobial activity. They all had the same size zone of bacterial inhibition and the clear zone appeared at both anode and cathode sites. Since the width of the anode clear zone in the 24 hrs well-established colonies condition remained the same as the cathode clear zone and did not increase with direct current application, the observed clear zone at both anode and cathode sites must be developed during the 24 hrs incubation period where no current was applied as in the no current control. This finding suggests that elemental Ag itself has antimicrobial property too, but its strength is weaker than Ag^+ ions and is limited to the area immediately adjacent to the suture. Thus, only those bacteria adhered onto the SAS would not survive. As mentioned briefly before, the antimicrobial property of the SAS under the condition where direct current was applied simultaneously with incubation, was observed only at the anode site (Figures 6 & 7). This unique finding suggests that the oxidation process of silver metal at the anode site under the influence of electrical force must relate either directly or indirectly to the observed antimicrobial activity of the SAS. It is known that Ag ions would be released into the medium at the anode site (oxidation) and converted into Ag at the cathode site (reduction) as shown below in Equation 1:

$$\begin{array}{lll} Ag \longrightarrow Ag^{+1} + e^{-1} & \text{(anode)} & \\ Ag^{+1} + e^{-1} \longrightarrow Ag & \text{(cathode)} & (1) \end{array}$$

Because antimicrobial activity of the SAS was observed at the anode site when direct current was applied, Ag^+ ions generated at the anode site must be taken up by the surrounding bacteria which subsequently kill them. Thus, the anode-related antimicrobial activity of the SAS indirectly suggests that the uptake of Ag^+ by bacteria must be the first step in the mechanism of the observed antimicrobial property of the SAS. Recent studies on the mechanism of bacterial sensitivity to silver indicated that the amount of silver uptake by bacteria is proportional to their sensitivity level toward silver (46-51). For example, Kaur et al. found that a susceptible K. pneumoniae strain's uptake of silver was three to four times higher than an experimentally derived silver-resistant K. pneumoniae (46). Starodub et al. also reported that by energy dispersive X-ray analysis and transmission electromicroscopy, silver-sensitive E. coli contained dense silver particles inside their cells (47). An Ag^+-resistant strain, however, did not accumulate Ag^+ (47). Similar results have also been reported for other bacteria (48-51).

The next questions to ask are how are Ag^+ ions transported into the interior of cells?, and how do the adsorbed Ag^+ ions inside bacteria inhibit their metabolism? In order for cells to uptake any material from an environment, some type of specific transport system must be required. Brierley et al. reported that accumulation of metals into bacterial cells usually occurs through two stage processes (52). They are: (a) a rapid (in minutes), metabolic-independent surface-binding to cells, followed by (b) a metabolic-dependent and gradual intracellular accumulation of the metal. Because Ag^+ ions are not an essential nutrient, it is doubtful that their transport would go through a specific energy dependent transport system; however, they could be carried into cells via a transport system for an essential metal. This hypothesized mechanism was supported by the study of silver resistance in E. coli (47). It was reported that starved, washed resting cells of strain R1 E. coli were able to uptake Ag^+ ions easily when assayed for Ag^+ ions binding in a buffer lack of essential growth nutrients, but actively growing E. coli of strain R1 (not washed, resting cells) could resist uptake of Ag^+ ions. Ag^+ ions uptaken by bacteria could either interfere in their respiration or/and replication of DNA and hence exhibit antimicrobial activity (53,54). In the former mechanism, $AgNO_3$ was found to inhibit an -SH-containing respiratory enzyme like succinate dehydrogenase. In the latter mechanism, Ag^+ ions were bound to bacterial DNA and interfered with its replication.

The qualitative antimicrobial property of the SAS reported above was further confirmed in our later quantitative examination (31). S. aureus, E. coli and P. aeruginosa were used. In that study, suture specimens of a fixed length were embedded in a custom-built plastic device filled with a fixed concentration of bacteria for predetermined periods of incubation. The bacterial suspension was then removed periodically for a standard plate count. The antibacterial property of the SAS was evident in the anode site of the suture fiber, and at a fixed current, the degree of bacteriostatic effect depended upon the bacterial species as shown in Figures 9 and 10. For example, the P. aeruginosa was reduced to 7.5×10^4/ml, while the three controls (i.e., without suture, with a commercial nylon suture - Nurolon, and the cathode site of the SAS) all reached the same value of 4.5×10^7 over the same period. A reduction of the number of P. aerugionsa by a factor of 10^3 within a period of six hours was observed. The data in Figure 9 also indicated that not only growth of the initial P. aeruginosa was inhibited, but also that the initial bacteria were killed over time. This excellent bactericidal property of the SAS toward P. aeruginosa is consistent with the previous qualitative antimicrobial data, and is clinically significant because this gram negative pathogen is frequently associated with wound infections resulting from severe skin damage, such as burns, and is resistant to many widely used antibiotics. Elimination of S. aureus and E. coli by SAS was not as dramatic as with P. aeruginosa. Bacteriostatic activity toward these two bacteria was not observed until about 3.5 hrs of direct current application (i.e., 40 μA). The silver ion concentration released from the SAS to the medium under various experimental conditions was also quantitatively measured with a Fisher Accumet pH/Ion Meter, Model 815 PM. A silver-ion sensing electrode from Lazar Research Labs, Model IS-146 coupled with a double junction reference electrode was used to measure the change in millivolts of the media. A calibration curve of silver ion concentration vs. millivolts was obtained using a series of deionized water dilution of a silver standard solution ranging from a 10^{-3} to 10^{+3} ppm. The curve could be represented by Equation 2:

$$70 \operatorname{Log} [C]_{Ag+} = -758.20123 + 1.1760913\,[V] \qquad (2)$$

where $[C]_{Ag+}$: concentration of Ag^+ ion,
$[V]$: millivolt reading.

With the assistance of this calibration curve, Ag^+ ion concentrations of the SAS specimens under various current conditions were determined and shown in Figure 11. In general, the silver ion concentration increased with increasing either the current level or

Downloaded by STANFORD UNIV GREEN LIBR on August 6, 2012 | http://pubs.acs.org
Publication Date: April 3, 1991 | doi: 10.1021/bk-1991-0457.ch012

Downloaded by STANFORD UNIV GREEN LIBR on August 6, 2012 | http://pubs.acs.org
Publication Date: April 3, 1991 | doi: 10.1021/bk-1991-0457.ch012

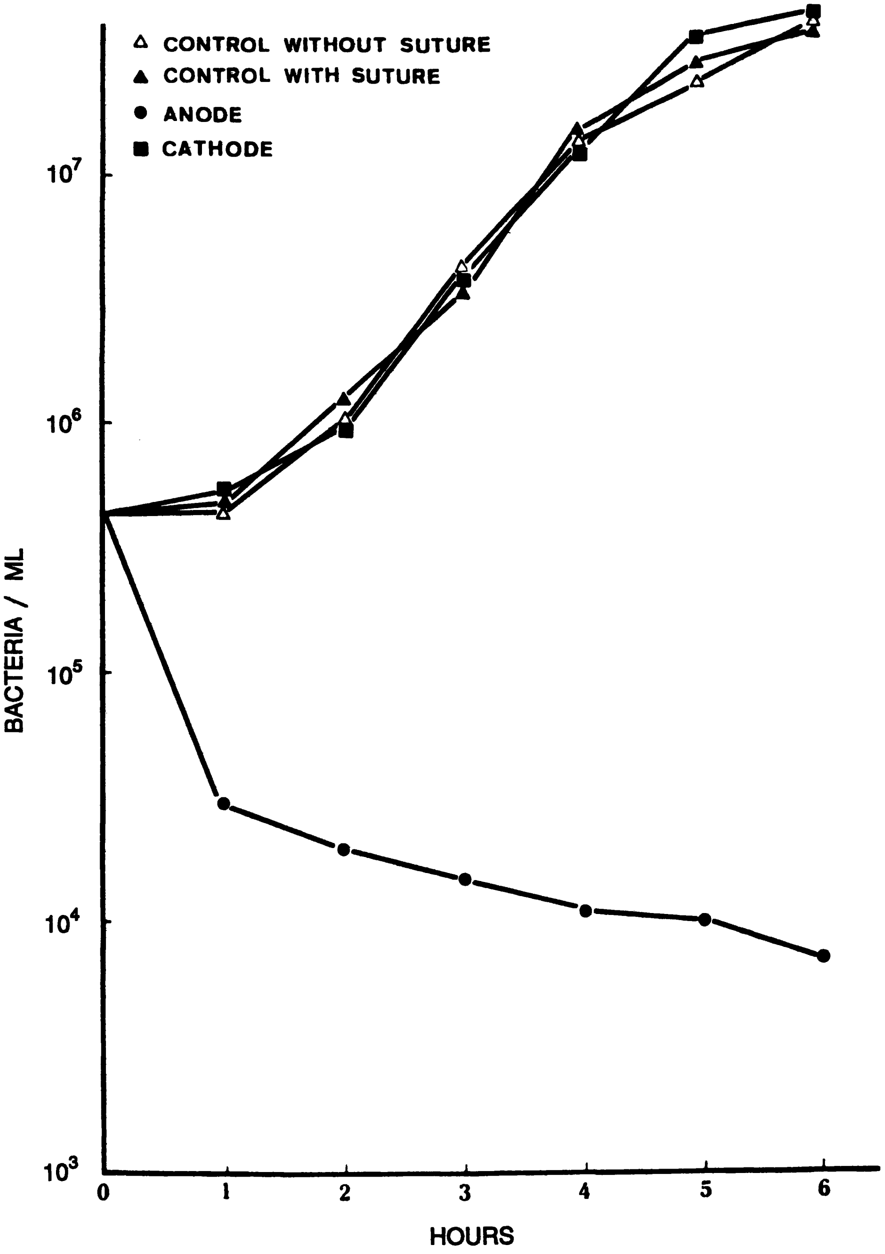

Figure 9. Standard plate counts of P. aeruginosa in the SAS with a direct current of 40 μA. Two controls were without the SAS and with the SAS, but no direct current applied. (Reproduced with permission from Ref. 31. Copyright 1987 W. C. Tsai et al.)

Downloaded by STANFORD UNIV GREEN LIBR on August 6, 2012 | http://pubs.acs.org
Publication Date: April 3, 1991 | doi: 10.1021/bk-1991-0457.ch012

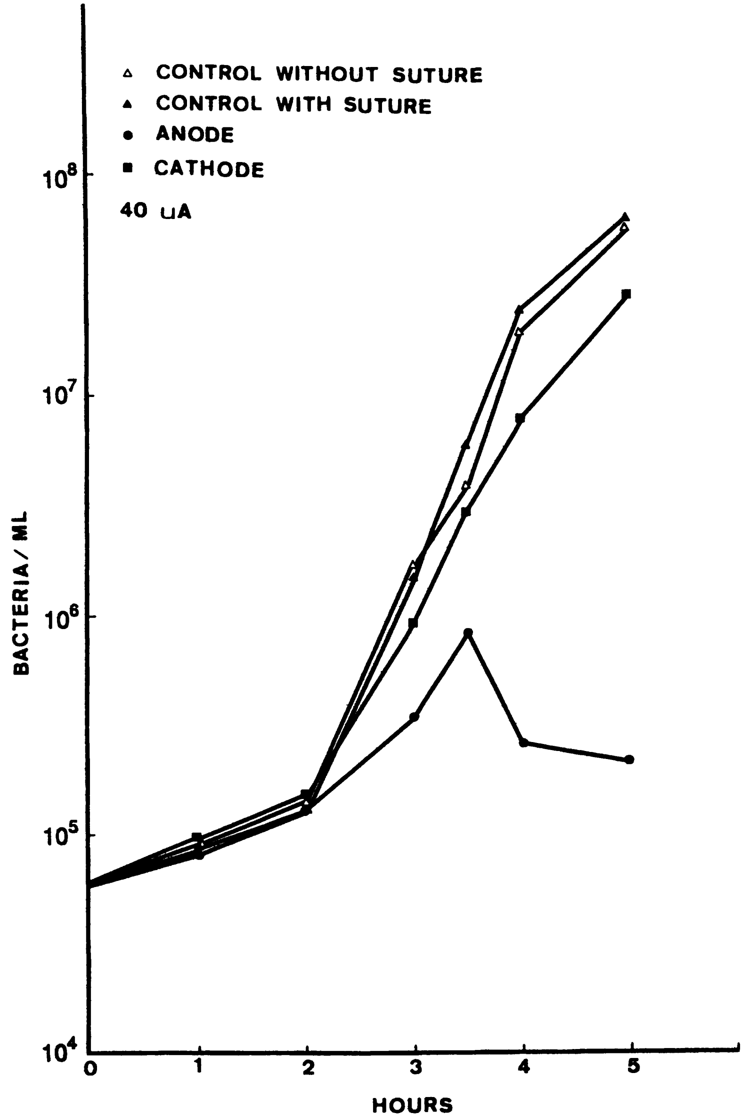

Figure 10. Standard plate counts of S. aureus in the SAS with a direct current of 40 μA. Two controls were identical to those in Figure 9 (Reproduced with permission from Ref. 31. Copyright 1987 W. C. Tsai et al.).

Downloaded by STANFORD UNIV GREEN LIBR on August 6, 2012 | http://pubs.acs.org
Publication Date: April 3, 1991 | doi: 10.1021/bk-1991-0457.ch012

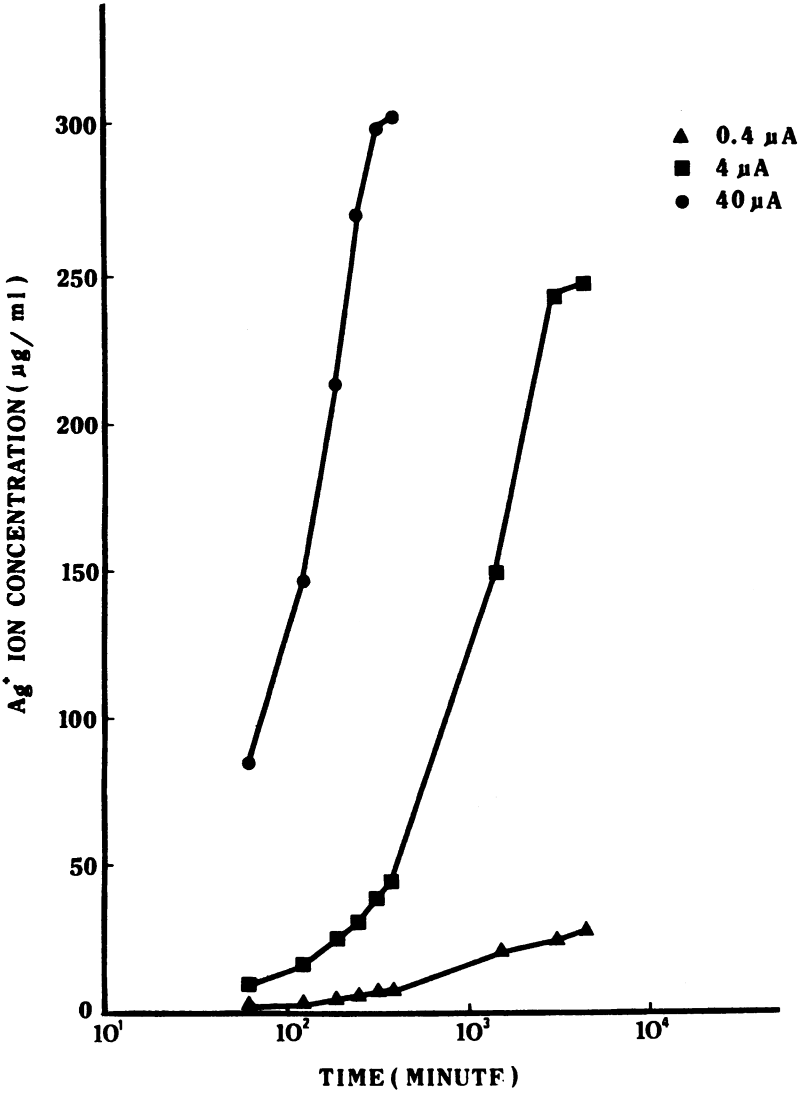

Figure 11. The concentration of silver ions released from the SAS under a wide range of direct current and time. (Reproduced with permission from Ref. 31. Copyright 1987 W. C. Tsai et al.)

In High-Tech Fibrous Materials; Vigo, T., et al.;
ACS Symposium Series; American Chemical Society: Washington, DC, 1991.

Downloaded by STANFORD UNIV GREEN LIBR on August 6, 2012 | http://pubs.acs.org
Publication Date: April 3, 1991 | doi: 10.1021/bk-1991-0457.ch012

time, or both. The increase in Ag^+ ion concentration with time was much faster at a higher current level than the one at a lower current level. At the end of six hours, the silver concentrations were 7.3 μg/ml at 0.4 μA and 305μg/ml at 40.0 μA. It took three days for 0.4 μA to release an Ag^+ ion concentration that was achieved in only 3 hrs for 4.0 μA and less than 1 hr for 40 μA. A comparison between Figure 11 and Figures 9 & 10 indicated the different levels of bacterial sensitivity toward silver ion. As discussed before, Ag^+ ion uptake by bacteria was cell-surface mediated (51). The observed higher sensitivity of S. aureus toward Ag^+ ions than E. coli (as reflected in the need of lower Ag^+ ion concentration for achieving bacteriostatic effects in S. aureus) probably relates to the different cell surface structure and composition between S. aureus (gram-positive) and E. coli (gram-negative). Because gram-positive bacteria do not have LPS-containing outer membranes, they are expected to be inherently more prone to the permeation and transport of Ag^+ ions released by SAS.

A preliminary biocompatibility study of the SAS in rat gluteal muscle was conducted for periods of 7 to 60 days (30). The intensity of the tissue reaction was determined by a modified Sewell et al. method (55) and is given in Table III. It was found that the total scores of histological evaluation of the SAS were always lower (less inflammatory response) than the control suture (Nurolon from Ethicon) up to 60 days of postimplantation. Contrary to the findings in the control suture, the invasion of fibrous connective tissue into the interstitial space of the component yarns was not evident in the new SAS even at the end of the study period (60 days). These results are parallel to the observed mild inflammatory reactions at silver implant sites in rats reported by Spadaro et al. (37,45).

Table III. THE TOTAL SCORES OF HISTOLOGIC EVALUATION

Suture material Implantation period (day)	2/0 Nurolon (Control)	Ag-Coated nylon suture (Testing)
7	84	79.7 ± 1.2
14	a	24.3 ± 3.1
30	36.3 ± 6.5	30.4 ± 2.5
60	32.7 ± 2.5	25.3 ± 0.6

[a] No score could be determined due to the difficulty of differentiating the cells in the slide.

In addition to the demonstrated antimicrobial property, the use of the electrically-activated SAS in treating wound infection may also have one additional advantage - to improve the rate and quality of healing without infection. As recently reported by Becker (56), a rapid and regenerative type of wound healing was found during the treatment of wound infection in humans by electrically activated silver. The production of many dedifferentiated (hence uncommited) fibroblast cells in the wound under the influence of silver ions was suggested to be associated with the observed rapid healing rate. This preliminary finding is consistent with other studies which used endogenous and exogenous electric or magnetic fields to stimulate the healing rate of both soft and hard tissues, particularly the most recent one reported by Dunn et al. (57). In that study, the effects of direct current on the healing of guinea pig dermal wounds were evaluated by using a collagen sponge model. Their preliminary data showed that fibroblast ingrowth and collagen fiber alignment were increased in the collagen sponge when it was stimulated with direct currents ranging from 20 to 100μA through carbon electrodes. Similar results have also been found by Crisp et al. in their study of electrified metallic sutures in pigs (58).

Future Challenges & Opportunities. Further research and development are required before the concept of SAS could be beneficial to surgery in human beings. This may include the examination of other variables, such as (a) the performance of this SAS in deep intracorporeal sites, (b) the possibility of this SAS to directly improve the rate and quality of wound healing without infection, (c) the in vivo performance of this SAS in various types of knotted form, (d) the antimicrobial properties of the SAS in species whose immune response is compromised, and (e) a more thorough understanding of the underlying mechanism for the observed antimicrobial activity of the SAS. Some of our thoughts in this future research work are very briefly described below.

The data reported so far are from in vitro research. Does the SAS perform as well in animals and human beings as we have demonstrated in vitro, and what are the mechanisms involved? To answer these questions and bring the concept of SAS closer to clinical reality, future animal implantation study is essential to demonstrate the efficacy of the SAS in vivo. In addition, it is desirable and beneficial to broaden the use of this SAS in intracorporeal sites, especially in sites having a history of above-average frequency of wound infection (e.g., intestine, wounds around surgical implants, deep-puncture wounds) for taking full advantage of the antimicrobial property of the new SAS for wound infection control. The technical challenge of such a use will be the design of a non-invasive device to activate and enhance the antimicrobial capability of the new SAS in intracorporeal sites. As mentioned before, a rapid and regenerative type of wound healing was also reported by Becker during the treatment of wound infection in humans by electrically activated silver (56). The increase in the rate of wound healing under the influence of silver compounds were also reported by Geronemus et al. (59). However, the role of silver and its compounds in the promotion of healing of cleaned wounds is not conclusive and controversy exists now. For examples, others reported that the presence of silver compounds as topic antimicrobial agents delayed wound healing (60,61). Deitch et al. suggested that the toxicity of the topical antimicrobial agents of silver compound nature (i.e., silver nitrate and silver sulfadiazine) is due to the anionic portion of the agent like NO_3 not the silver ion (62). Therefore, it will be beneficial to study in vivo rate and quality of healing of the wounds treated with the new SAS.

In a quantitative biopsy culture assay of contaminated sutures in Swiss mice, Scher et al. recently reported that the number of S. aureus recovered from six throw-knotted sutures were higher than unknotted ones (63). This finding may suggest that tissues around a knotted suture could be more prone to wound infection than an unknotted suture. Since all sutures are knotted in their clinical use, it is thus important to examine the in vivo antimicrobial performance of the new SAS in knotted form.

While it is known that the oxidation of metallic silver is an important part of the electrical silver activation mechanism, the activated surface under clinically appropriate conditions has not been characterized in detail. For example, serum proteins which tend to decrease the persistence time of bacterial inhibitory effects, may bind to the surface and function to retard oxidation and precipitation of chlorides, or may affect subsequent dissolution rates and so influence effectiveness in vivo. Therefore, to

Downloaded by STANFORD UNIV GREEN LIBR on August 6, 2012 | http://pubs.acs.org
Publication Date: April 3, 1991 | doi: 10.1021/bk-1991-0457.ch012

Downloaded by STANFORD UNIV GREEN LIBR on August 6, 2012 | http://pubs.acs.org
Publication Date: April 3, 1991 | doi: 10.1021/bk-1991-0457.ch012

characterize the sequence of surface morphological and chemical changes of the SAS as a function of current and time in various simulated physiological media, and to relate the microscopic surface characteristics of the SAS to bacterial inhibition observed in vitro and in vivo will provide investigators with a more complete understanding of the underlying antimicrobial mechanism of the SAS. Such an understanding is essential for possible future modification of the SAS, if needed, for specific clinical conditions.

Hydrolytic Degradation of Synthetic Absorbable Sutures

The Importance of Synthetic Absorbable Sutures. One of the most important contributions to wound closure during the past several decades is the development of synthetic absorbable sutures. The most important advantage of synthetic absorbable sutures is their degradability inside a biological environment. This property will enable the sutures not to elicit chronic undesirable tissue reactions after the sutures are not needed because the wound has gained enough strength. Although all the existing sutures are different from each other chemically and configurationally, they are foreign materials to the human body and hence produce an inevitably wide range of biological responses in the living tissues. These responses range from an inflammatory reaction due to the trauma of insertion, to foreign body reaction because of the chemical, physical, and mechanical properties of the suture materials. It is critical for optimal wound healing to minimize these reactions because the healing process, its rate, and complications are greatly influenced by the tissue reactions elicited by sutures.

The degree of tissue reaction depends not only on the chemical and physical nature of the suture and the type of tissues, but also on the mass of the suture and the duration of its presence in the tissue. It is thus ideal to have a suture which would serve its function satisfactorily during the critical wound healing period and then quickly disappear once it is not needed. The longer the suture stays within the body, the more probable it is to serve as the nidus for undesirable tissue reactions which could delay and interfere with normal wound healing, predisposition to wound infection, the formation of suture granuloma, sinus and calculi and thrombogenicity (64-67). A brief summary of these reported undesirable tissue reactions is given below.

Everett reported that sutures which generate a marked tissue response are more liable to cut out and thus weaken wound strength because an excessive inflammatory reaction may lead to edema, and thus weakening of the surrounding tissues with disruption of collagen fibers (68). Barham et al., reported that the wound strength in the rectus muscle of rabbits is greater when closed with polyglycolic acid (Dexon^R) than with chromic catgut (69). By 90 days, the Dexon-sutured wound had begun to plateau near a maximum strength while chromic catgut sutured wounds reached a lower wound strength than Dexon. Thus, the experimental evidence available suggests that the extent of inflammatory reaction that a suture elicits is related to the level of strength that a wound can reach. This, in turn, makes sutures more or less liable to "cut out." The onset of the fibroplasia phase also appears to depend on sutures (68). This fibroplasia phase has an important consequence on the repair of nerve tissues. It has been shown that the presence of sutures in a nerve repair site elicits two distinct tissue responses, the cellular and fibroblastic (70,71). The former reaches maximum activity at an early stage. It is directed to remove the implanted suture and is composed of polymorphonucleocytes, lymphocytes, giant cells, and histocytes. The latter seeks to wall off foreign suture materials, reaches a maximum during the later stage and consists of fibrous tissue cells

Downloaded by STANFORD UNIV GREEN LIBR on August 6, 2012 | http://pubs.acs.org
Publication Date: April 3, 1991 | doi: 10.1021/bk-1991-0457.ch012

in the supporting structure of the nerve itself. The fibroblastic reaction, however, was found to impede the regeneration of nerve tissues more severely than the cellular infiltration reaction; hence Sunderland, et al., recommended that the fibroblast reaction should be as short as possible in nerve repair (71). In nerve anastomosis, DeLee, et al., found histologically that Dexon sutures evoked the next to the most marked (after silk) fibroblastic reaction over a period of 12 weeks (72).

The delay in suture absorption also causes tissue adhesion problems as reported by Vallfors et al., in the closure of dura mater (73). They found Polyglactin 910 (Vicryl^R) sutures were better than Dexon sutures because Vicryl sutures were absorbed more rapidly than Dexon at 60 days; the remaining Vicryl suture mass at 60 days was only 20% of that found for Dexon sutures. Because of the persistence of Dexon sutures in the tissue and the proliferative changes which they elicited in the surrounding tissue, Dexon sutures resulted in strong adhesion to the arachnoid that created holes in the brain surface on dural separation. When dura mater was separated, the effect was to tear off the leptomeninges with their vascular supply to the cerebral cortex.

The persistence of sutures in tissue for protracted periods could also predispose to wound infection. Elek, et al., reported that the number of S. aureus which are needed to establish infection can be reduced 10^5-fold by the presence of silk sutures (9). Edlich et al., reported that the percentage of gross infection in mice with nylon-sutured surgical wounds was considerably higher than that in needle track control mice (11). It was 53.7% and 0%, respectively, for S. aureus and 70.8% and 0%, respectively, for E. coli. Not only the physical presence of a suture, but also the level of tissue reaction it elicits could predispose to wound infection. Edlich et al., found that the strong tissue reactions associated with silk, cotton, and catgut sutures somehow were related to their propensity to wound infection (11). This finding was also supported by Blomstedt (15,16), Alexander (14), Varma's (74), and Peterson-Brown's (13) studies. In an experimental study with absorbable poly-P-dioxanone (PDS^R) and nonabsorbable polypropylene sutures in S. aureus-infected canine arterial anastomoses, Torsello et al. reported there was no difference in the incidence of wound infection between these two sutures (75). Cameron et al. reported that in a randomized comparison between PDS and polypropylene (Prolene) sutures for abdominal wound closure, PDS sutures exhibited 8.6% wound infection which was marginally lower than Prolene sutures (76). The prolonged existence of PDS suture mass in the tissue may be partially responsible for its lack of significant advantage over nonabsorbable Prolene suture toward wound infection in the specified clinical conditions.

Infected wounds can develop sinuses. Bucknell et al., showed a highly significant relationship between sinus formation and postoperative wound infection (77). As high as 86.4% of the patients who developed sinuses had a proved postoperative wound infection prior to the development of the sinus. Suture sinuses are always associated with the prolonged presence of suture materials in the wound. Corman et al., reported that 9% of 102 patients whose wounds were closed with multifilament or monofilament nonabsorbable sutures developed suture sinuses, whereas no sinuses were found in 59 wounds closed with Vicryl sutures (78). Bucknell et al., however, found that the incidence of sinus formation with absorbable sutures (i.e., 11.5% with Dexon) was statistically similar to that with nonabsorbable sutures (i.e., 9.4% with monofilament nylon) in abdominal wound closure (77). Bartone et al. reported that, because of their prolonged mass absorption and subsequent tissue reactions, Dexon and PDS sutures have been associated with wound abscesses and granulomas when used in hypospadias surgery (79).

Downloaded by STANFORD UNIV GREEN LIBR on August 6, 2012 | http://pubs.acs.org
Publication Date: April 3, 1991 | doi: 10.1021/bk-1991-0457.ch012

A prolonged stay of sutures in the blood stream in cardiovascular surgery could also increase the possibility of their thrombogenicity. Although the majority of vascular anastomosis has been closed with nonabsorbable sutures, the use of absorbable sutures in growing patients and animals has certain advantages over nonabsorbable sutures as long as the absorbable sutures retain adequate tensile strength until the anastomosis has reached sufficient strength (80-85). Pae et al., observed the stenosis and/or bowstring formation with subsequent thrombosis development in growing pigs if the diameter of the vessel exceeded the maximum length of the straightened nonabsorbable suture. Considerable inflammatory reaction and intimal roughening occurred in the wounds closed with nonabsorbable sutures. Their results were also supported by other studies (80-82,84,85). Dahlke et al., recently reported that the degradation properties and the chemical nature of the degradation products of Vicryl sutures may modify their thrombogenicity according to the length of implantation (86). Obviously, after the complete absorption of these sutures, they leave no trace of materials as nidus for chronic inflammation which later predisposes to thrombosis formation. This advantage of a relatively faster absorption of suture mass in cardiovascular surgery as observed in Dexon and Vicryl sutures may not be available for PDS and Poly(glycolide-trimethylene carbonate) (Maxon^R) sutures due to their excessive long duration of mass absorption. For example, in venous anastomoses of dogs with PDS sutures, Torsello et al. reported moderate to high incidences of stenoses during the first two months, irrespective of continuous or interrupted suture techniques (82). There are not enough published studies yet to confirm or disprove this observation at the present time.

Due to the high concentration of salts and inorganic compounds in both urinary and biliary tracts, the presence of any foreign body will act as a nidus for stone formation. Because of this concern, absorbable suture materials have almost exclusively been used in these parts of the body. Kaminski et al., reported that no calculi were found after 7 days when the bladder (rabbit) was closed with the absorbable sutures (Dexon and chromic catgut), whereas the incidences of stone formation associated with the nonabsorbable sutures approached 100% at a later period (87). They concluded that surface characteristics and cross-sectional geometry appeared to be less important than the absorbability of a suture material in the formation of persistent urinary calculi. This conclusion was further confirmed by others (88). A faster disappearance of a suture mass after it exhibits no strength could reduce the incidence of stone formation further.

In a randomized trial of interrupted PDS and silk sutures in the gastrointestinal tract (57 patients), Gillatt et al. reported six benign anastomotic stricture, five of which occurred in the PDS group (89). This high rate of stricture formation (19%, 5/27) associated with PDS sutures for large bowel anastomoses forced them to discontinue the trial after 3 1/2 years follow-up study.

The introduction of Dexon and Vicryl sutures in the 1970's has generally reduced the incidences of these undesirable tissue reactions. The recently available PDS and Maxon sutures in the 1980's, however, may not have the advantage (in rate of mass absorption) of Dexon and Vicryl absorbable sutures over nonabsorbable ones. This is because the masses of PDS and Maxon sutures are not completely absorbed until about 6-8 months _in vivo_. This prolonged existence of suture mass in tissue may increase the incidences of the above-mentioned undesirable tissue reactions that Dexon and Vicryl sutures usually do not experience.

Factors Influencing Suture Fiber Degradation. The tensile strength loss and mass absorption of synthetic absorbable sutures depend on several factors as summarized in the recent reviews of Chu (65,67). These factors include the type of tissues (90-93), enzymes (94-99), lipids (100), bacteria (101-104), pH (105), temperature (106-108), inorganic salts (109,110), external force (111,112), and γ-irradiation (94,95,113-115).

On the basis of a microfibrillar model of fiber structure, Chu has recently proposed the degradation mechanism of Dexon in vitro (64-67,113-116). On the basis of this model, hydrolytic degradation proceeds through two main stages, with the first stage in the amorphous region, the second in the crystalline region. Figure 12 is a schematic illustration of this preferential hydrolytic degradation phenomena. Hydrolytic degradation starts in the amorphous regions, as the tie-chain segments, free chain ends, and chain folds in these regions degrade into fragments. As the degradation proceeds, the size of the fragments reaches the stage where they can be dissolved into the buffer medium. This dissolution removes the fragments from the amorphous regions, and loss of material results. As sufficient amounts of chain segments in these regions are removed, the spaces originally occupied by chain segments become vacant and large enough to be visible as cracks (113). The cracks are believed to be initiated on the surface of the fiber and to grow circumferentially around and/or longitudinally into the interior of the fiber. Figure 13 illustrates the appearance of surface cracks of partially in vitro hydrolyzed PDS and Maxon sutures. This is because alkaline hydrolysis of a fiber has been a surface phenomenon. As microcracks form on the surface of fiber, more hydroxyl ions penetrate these areas and microcracks propagate more deeply in the bulk of the fibers until the cracks cut through the whole fiber and scission results.

In a more recent study by Chu et al. on the use of PGA fibers as one of the components for bicomponent woven vascular fabrics, they observed a very unusual but informative morphological change of PGA fibers that resulted from hydrolysis. As shown in Figure 14, similar circumferential surface microcracks as before were observed, but the appearance of the surface microcracks were much more regular along the fiber axis. A detailed examination of the regions where the surface microcracks were formed indicated that not all materials located in the microcrack regions were equally susceptible to hydrolysis. There were many microfibrils remained in the microcrack regions, while the materials surrounding these microfibrils were hydrolyzed and removed. These microfibrils appeared to hold the fiber together by connecting the two adjacent more hydrolytically resistant portions (i.e., the portions without microcracks) of the fiber together before complete fragmentation of the fiber occurred. The dimension of these microfibrils was about 0.5μm. This observed PGA fiber morphology suggests that the fiber itself has a composite structure of microfibrils impregnated within amorphous domains. A recent study of the bulk birefringence of these microfibrils and fibers by Chu indicated that the microfibrils had a birefringence of 0.240 which was significantly higher than the fiber (0.0019). These birefringence data suggest that the observed microfibrils are far more oriented than the PGA fiber where these microfibrils reside. Due to its highly oriented and crystalline nature, microfibrils are more resistant to hydrolysis than the surrounding amorphous domains. As the surrounding amorphous matrix is first hydrolyzed and removed, it reveals the remaining microfibrils as shown in Figure 14. The unique arrangement of surface microcracks on PGA fibers was also observed by Chu et al. in a study of knitted bicomponent vascular fabrics (119). In that study, PGA and Dacron fibers were knitted into jersey tubular fabrics and examined after in vitro hydrolytic degradation. A blue dye was used to differentiate PGA from Dacron fibers in the partially hydrolyzed knitted bicomponent fabrics

Downloaded by STANFORD UNIV GREEN LIBR on August 6, 2012 | http://pubs.acs.org
Publication Date: April 3, 1991 | doi: 10.1021/bk-1991-0457.ch012

Downloaded by STANFORD UNIV GREEN LIBR on August 6, 2012 | http://pubs.acs.org
Publication Date: April 3, 1991 | doi: 10.1021/bk-1991-0457.ch012

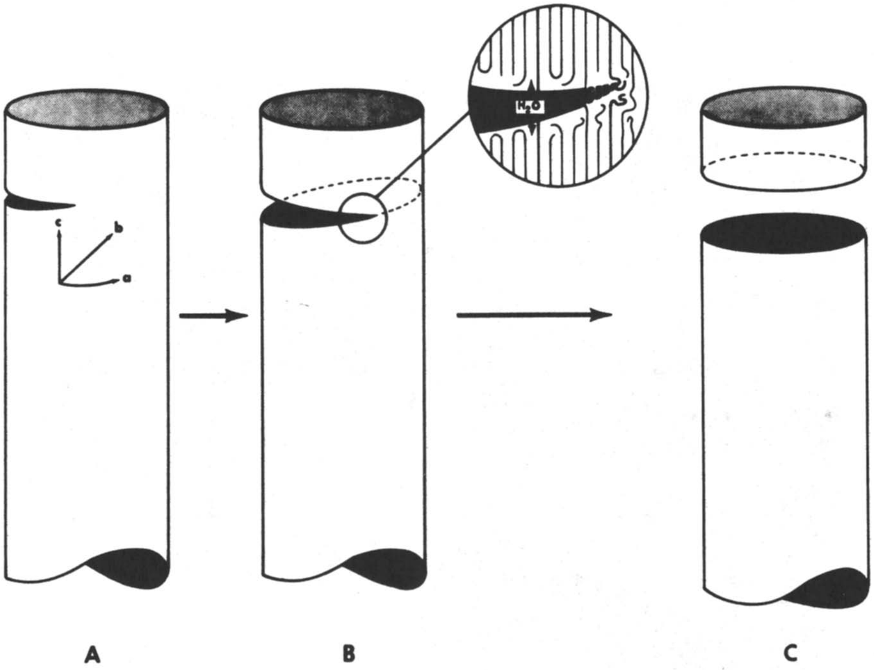

Figure 12. A schematic drawing of the circumferential propagation of a crack on a fiber. (A) initiation of a microcrack. (B) microcrack propagates circumferentially around the fiber and deeply into the fiber along the amorphous regions of each microfibril. Insertion illustrates that water molecules hydrolyze more chain segments located in the amorphous regions than those located in the crystalline regions. (C) as the crack completely propagates through the fiber, fragmentation of fibers results. (Reproduced with permission from Ref. 113. Copyright 1982 C. C. Chu et al.)

Downloaded by STANFORD UNIV GREEN LIBR on August 6, 2012 | http://pubs.acs.org
Publication Date: April 3, 1991 | doi: 10.1021/bk-1991-0457.ch012

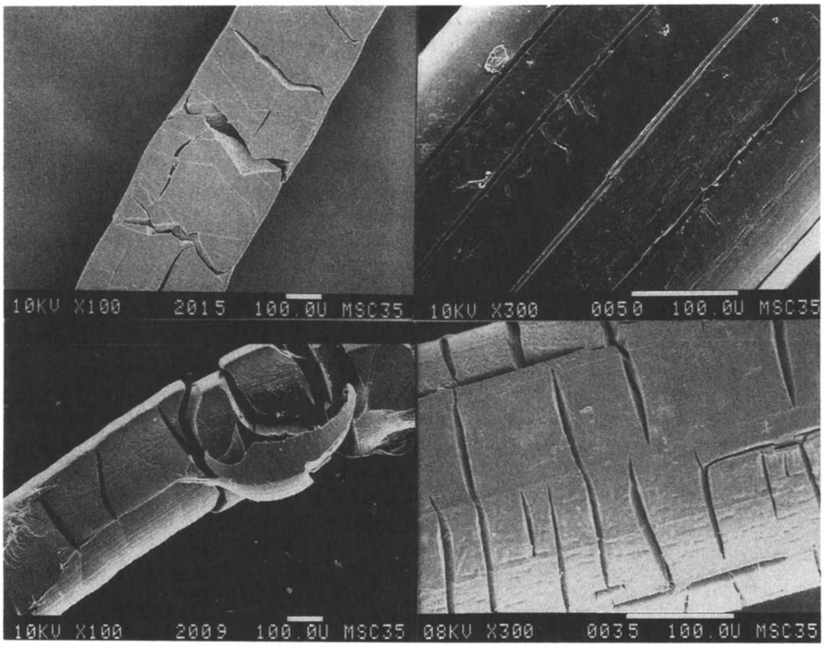
10KV X100 2015 100.0U MSC35
10KV X300 0050 100.0U MSC35
10KV X100 2009 100.0U MSC35
08KV X300 0035 100.0U MSC35

Figure 13. Surface microcracks of PDS and MAXON sutures upon *in vitro* hydrolysis in phosphate buffer solutions at 37°C: Upper left - 90 days hydrolyzed PDS; Lower left - 120 days hydrolyzed PDS; Upper right - 42 days hydrolyzed Maxon; Lower right - 90 days hydrolyzed Maxon.

Downloaded by STANFORD UNIV GREEN LIBR on August 6, 2012 | http://pubs.acs.org
Publication Date: April 3, 1991 | doi: 10.1021/bk-1991-0457.ch012

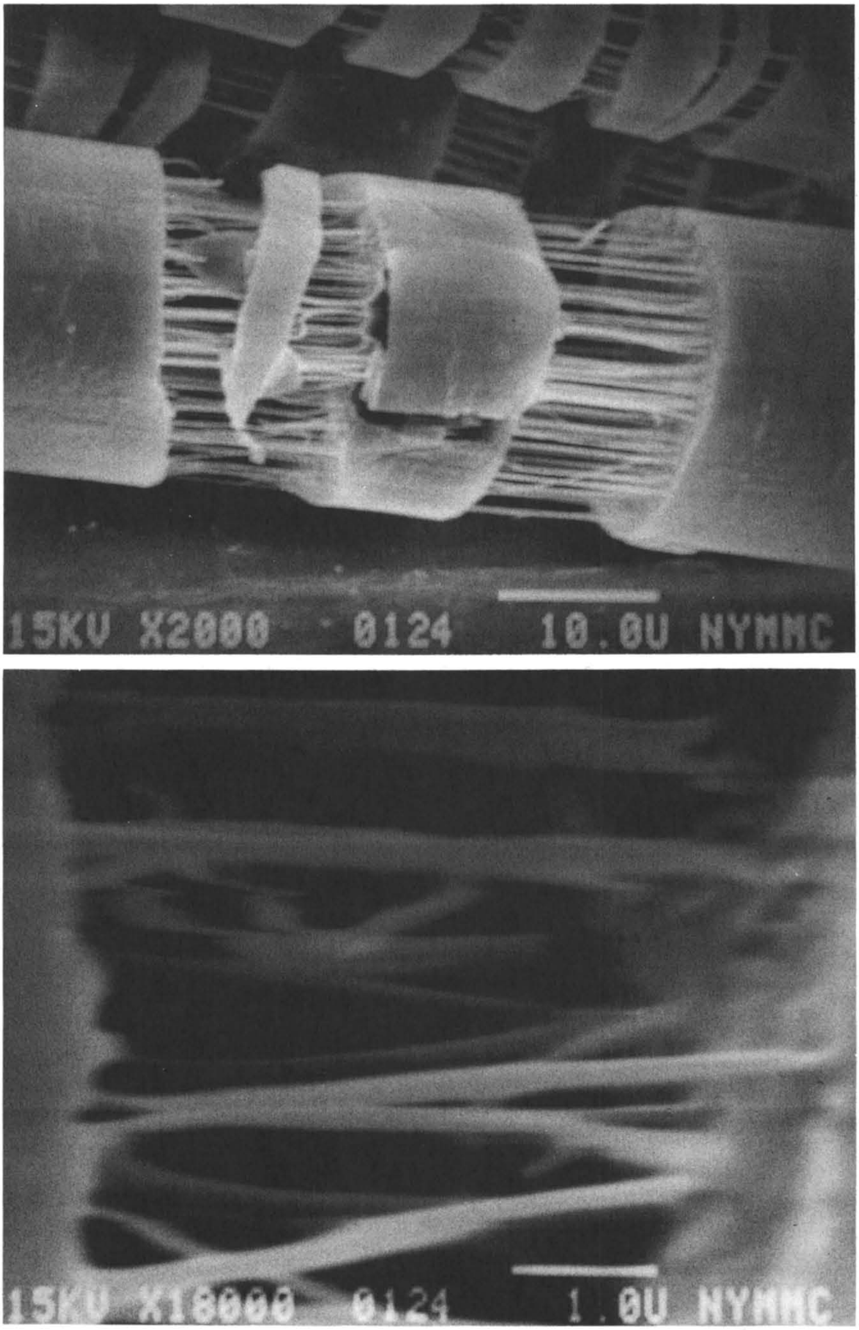

Figure 14. Surface morphology of partially hydrolyzed PGA fiber as one of the yarn components of a bicomponent vascular fabric. Top: Surface microcracks on PGA warp yarns of a bicomponent woven fabric. Bottom: A close-up view (10,000x) of the surface microcrack region. Note the microfibrils connected between two adjacent blocks of PGA fiber.

(i.e., PGA was dyed blue, while Dacron fibers did not dye). During this fiber identification process, the blue dye was only able to selectively dye certain segments of the fiber. As a result, a series of circumferential blue bands alternatively arranged along the length of the fiber were observed. The widths of the dyed and undyed bands, however, were not uniform. This suggests that not every part of the fiber along its axis exhibits the same level of hydrolytic sensitivity; thus, there are some domains which are more susceptible to hydrolysis than the remaining portions of the fiber. These domains are arranged in such a way that they regularly alternate with the more hydrolytic-resistant portion of the fiber. This arrangement of blue bands in the knitted bicomponent fabrics was very similar to the above-mentioned circumferential surface microcracks observed in PGA fibers in bicomponent woven fabrics. The sensitivity of these domains toward degradation was further demonstrated by Chu et. al. in a study of γ-irradiation effects on the hydrolytic degradation of PGA fibers (113). By scanning electron microscopic observations, they found that the regularity and frequency of appearance of surface microcracks (i.e., more hydrolytically sensitive domains) on PGA fibers increased with an increase in the dosage of γ-irradiation and/or the duration of in vitro hydrolysis. This suggests that the hydrolytically sensitive domains distribute irregularly and randomly along the length of the fiber initially. Upon hydrolysis, these domains gradually become visible surface microcracks and appear randomly along the fiber axis. Upon γ-irradiation, chain segments in these initial hydrolytically-sensitive domains are first degraded by a chain scission mechanism. This additional degradation of the chain segments (due to γ-irradiation) would reduce the level of long-chain entanglement in the domains and result in more open structures which later facilitates the access of hydrolytic species and results in a faster hydrolysis as evidenced in the earlier appearance of surface microcracks on γ-irradiated and partially-hydrolyzed PGA fibers. It is still puzzling why the hydrolytically-sensitive domains randomly distribute along the fiber axis. What are the origin and factors which dictate their distribution? Why do the hydrolytically-sensitive and resistant domains alternately arrange along the fiber axis? Answers to these questions will reveal the true fiber morphology of synthetic biodegradable fibers which could lead to a new mode for regulating hydrolytic degradation of this class of fibers for specific clinic applications.

With the hydrolytic degradation in the amorphous regions, chain scission results in a lesser degree of entanglement of long-chain molecules located in the amorphous regions, as well as lower axial elastic moduli and tensile strength. Therefore, the remaining undegraded chain segments in the amorphous regions have better chain mobility; they can move and reorganize themselves from a disordered to an ordered state. Further crystallization is induced and an increase in crystallinity is expected and was indeed observed (106,107,116-118). The degree of crystallinity reaches a maximum at the end of the first stage of degradation, and starts to decrease as hydrolysis proceeds to the second stage and destroys the crystalline lattice. During the first stage, the loss of tensile strength is also the greatest due to the scission of tie-chain segments, while the second-stage degradation is chiefly responsible for the mass loss. This change of the level of crystallinity with hydrolysis could thus be used to monitor the degradation behavior of synthetic absorbable polymers and fibers. For example, Chu et al. recently examined the effect of polymer morphology on the hydrolytic degradation of PGA suture fibers (117). Three types of PGA samples differing in physical form were used: (a) multifilament-braided Dexon suture of 2/0 size from Davis/Geck, (b) PGA polymer chips of M_w about 60,000 from Polyscience, and (c) capillary-rheometer

Downloaded by STANFORD UNIV GREEN LIBR on August 6, 2012 | http://pubs.acs.org
Publication Date: April 3, 1991 | doi: 10.1021/bk-1991-0457.ch012

Downloaded by STANFORD UNIV GREEN LIBR on August 6, 2012 | http://pubs.acs.org
Publication Date: April 3, 1991 | doi: 10.1021/bk-1991-0457.ch012

extruded PGA monofilament fiber from the same PGA chips as in (b). It was found that the levels of crystallinity (obtained from differential scanning calorimetry) of these three types of PGA samples exhibited a different relationship for the duration of hydrolysis (Figure 15). The onset of an accelerated increase in the level of crystallinity was the shortest with the PGA rheometer fiber, followed by PGA chips and Dexon suture fiber. An unoriented PGA rheometer fiber showed a rapid increase in the level of crystallinity during the very early stage of hydrolysis (i.e., 7 days) and its crystallinity remained at a constant level thereafter for a long period of hydrolysis (about 40 days). Dexon sutures, however, showed a characteristic maximum pattern in crystallinity with a very little increase in the level of crystallinity until after 20 days of hydrolysis. The level of crystallinity of Dexon sutures reached a maximum of 57% at or about 30 days hydrolysis and then decreased thereafter. PGA chips showed a similar characteristic in crystallinity vs. hydrolysis time, but the onset of the crystallinity level occurred about 5 days earlier than Dexon sutures and the width of the maximum peak was much more broader than Dexon sutures. This finding suggests that the orientation of molecules is an important factor in influencing the rate of hydrolysis. This difference in crystallinity onset time indicated that unoriented PGA degraded faster than an oriented one. Subsequent weight loss study of these 3 PGA samples also confirmed this observation. Morphologically, the typical circumferential surface cracks observed in oriented PGA sutures, however, were not found in unoriented PGA samples. Instead, micropores were found in unoriented PGA samples and these pores increased in number and size as hydrolysis proceeded as shown in Figure 16.

The role of enzymes in the degradation of synthetic absorbable sutures is controversial. Salthouse, et al., used histochemical procedures to demonstrate that the primary breakdown and absorption of Vicryl sutures are independent of cellular enzyme activity, and the only requirement for their absorption and degradation is an aqueous environment (120). However, Chu and Williams demonstrated that under certain conditions, some enzymes are able to influence the degradation of PGA sutures (94,96,97). The enzymes that did influence the degradation of PGA sutures were mainly (although not exclusively) of the type that might be expected to attack an aliphatic polyester on the basis of its molecular structure, i.e., esterases. Because of the specific action of enzymes with respect to the configuration and chemical structure of the polymer, enzymatic degradation of a polymer is strongly influenced by branching and chain length of the polymer substrate. This influence was recently demonstrated by Chu et al. in their study on the enzymatic degradation of γ-irradiated PGA sutures (94). They found those enzymes like trypsin, which show no effects on unirradiated PGA initially, would influence the degradation of γ-irradiated PGA. The observed γ-irradiation effect on the enzymatic degradation of Dexon, however, was not pronounced in PDS sutures. Williams and Chu recently reported that neither esterases nor trypsin influence the hydrolytic degradation of PDS sutures in a significant manner (95).

The effect of external strain on PGA degradation was recently studied by Chu et al. (111). The purpose was to determine whether strained PGA sutures would degrade differently from unstrained ones because surgeons usually impose stress on sutures by the act of pulling them taut and tying knots. The study indicated that PGA sutures (strained from 0 to 5%) indeed degraded faster than unstrained ones and the level of accelerated degradation depended on the percent of strain applied to the sutures. For example, at 14 days no tensile breaking strength could be detected with 5% strained Dexon sutures, while there was about 84% retention of original tensile strength of unstrained PGA sutures. This accelerated

Downloaded by STANFORD UNIV GREEN LIBR on August 6, 2012 | http://pubs.acs.org
Publication Date: April 3, 1991 | doi: 10.1021/bk-1991-0457.ch012

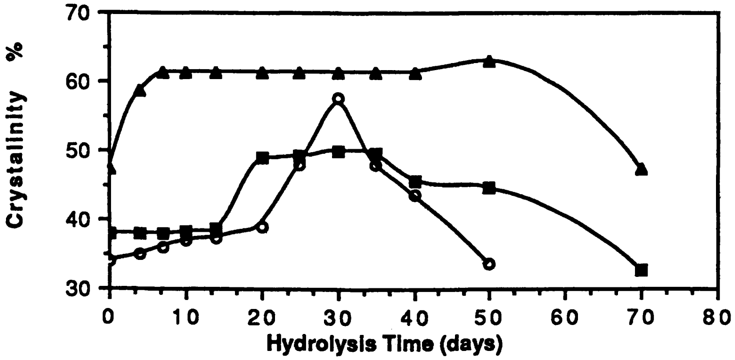

Figure 15. The change of the crystallinity level of three PGA samples differing in morphology as a function of *in vitro* hydrolysis time. (○) Dexon suture fiber, (■) PGA chip, (▲) rheometer fiber from PGA chip.

Downloaded by STANFORD UNIV GREEN LIBR on August 6, 2012 | http://pubs.acs.org
Publication Date: April 3, 1991 | doi: 10.1021/bk-1991-0457.ch012

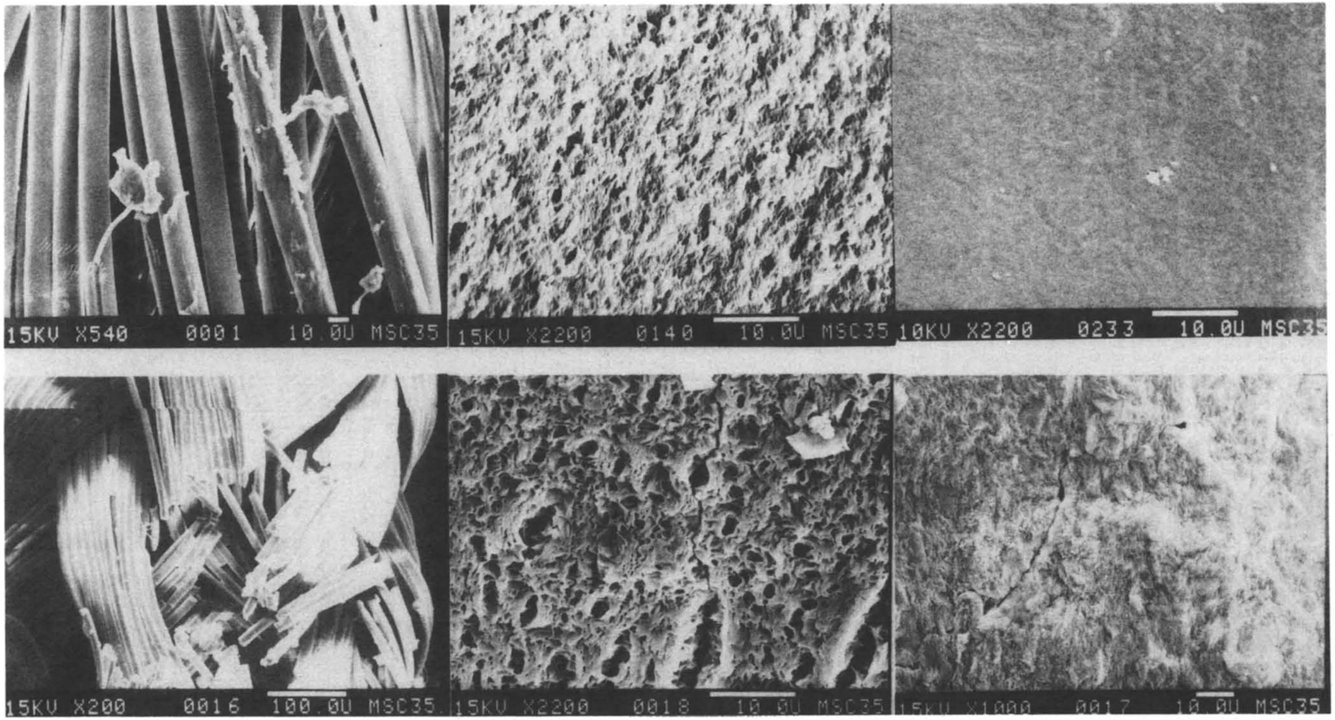
15KV X540 0001 10.0U MSC35
15KV X2200 0140 10.0U MSC35
10KV X2200 0233 10.0U MSC35
15KV X200 0016 100.0U MSC35
15KV X2200 0018 10.0U MSC35
15KV X1000 0017 10.0U MSC35

Figure 16. Surface morphology of partially hydrolyzed three PGA samples differing in morphology: Upper left - unhydrolyzed Dexon suture fiber; Lower left - 42 days hydrolyzed Dexon suture fiber; Upper middle - unhydrolyzed PGA chip; Lower middle - 42 days hydrolyzed PGA chip; Upper right - unhydrolyzed rheometer fiber from PGA chip; Lower right - 42 days hydrolyzed rheometer fiber from PGA chip.

Downloaded by STANFORD UNIV GREEN LIBR on August 6, 2012 | http://pubs.acs.org
Publication Date: April 3, 1991 | doi: 10.1021/bk-1991-0457.ch012

hydrolytic degradation of strained PGA sutures was also evidenced in their changes of the level of crystallinity with hydrolysis time. The onset of an accelerated increase in the level of crystallinity of 5% strained PGA sutures occurred as early as 7 days, while the onset time for the unstrained PGA controls was 20 days. This suggests that the rate of hydrolytic chain scission in the amorphous regions of strained PGA suture fibers is faster than unstrained ones. This observed accelerated hydrolytic degradation of strained PGA sutures was also reported by others (112).

It is known that all fibers whether absorbable or nonabsorbable, synthetic or natural, have one common characteristic - anisotropy. This anisotropic characteristic is expected to affect the hydrolytic degradation of synthetic absorbable suture fibers and was indeed demonstrated in Chu et al's recent study on PDS suture fibers (106). They found that the dye diffusion coefficients perpendicular (lateral) or parallel (longitudinal) to partially hydrolyzed PDS suture fibers were significantly different from each other at all four different dyeing temperatures as shown in Table IV. For example, the longitudinal dye diffusion coefficient of unhydrolyzed PDS was 2.42×10^{-5} mm^2 /sec, while the corresponding lateral dye diffusion coefficient was only 2.38×10^{-8} mm^2/sec at 40°C dyeing temperature. As hydrolysis progressed, both lateral and longitudinal dye diffusion coefficients increased; however, the lateral dye diffusion coefficient showed the most profound increase in percentage with the duration of hydrolysis. For example, a 241% increase in the lateral dye diffusion coefficient was found with 42 days hydrolyzed PDS suture fiber at 50°C dyeing temperature, while the same fiber showed only an 11% increase in the longitudinal dye diffusion coefficient. By measuring the ratio of lateral to longitudinal dye diffusion coefficients (defined as the isotropy index) Chu et al. found that the index increased with the extent of hydrolysis and dyeing temperature. At both low and high dyeing temperatures (30° and 60°C), the increase in the isotropy index with an increasing in hydrolysis time was the least pronounced, while the 40 and 50°C dyeing conditions showed the highest hydrolytic dependent increase in the index. The general trend of increasing isotropy index with the extent of hydrolysis time implies that the anisotropic characteristic of this fiber becomes less pronounced as the fiber degrades through hydrolysis. Thus, the fiber becomes more isotropic (or less oriented) as hydrolysis progresses, and the fiber would eventually lose its most distinguished characteristic - anisotropy. However, bulk birefringence index measurements indicated there was no change of molecular orientation up to 60 days hydrolysis. This lack of change of orientation from the birefringence index study was consistent with the increasing isotropic index from dye diffusion study. It is well known that dye will only diffuse into amorphous regions of the fibers. As the lateral amorphous structure becomes more similar to longitudinal amorphous structure due to hydrolytic scission of chain segments located in amorphous regions, their corresponding dye diffusion coefficient values would become closer to each other and subsequently reflected in the increasing isotropic index. Based on other hydrolytic degradation data, the crystalline regions of PDS fibers were not hydrolyzed until after 60 days hydrolysis. The intact crystalline regions could be attributed to the lack of change in molecular orientation as evidenced in the birefringence index. Therefore, the structure of amorphous regions is more closely related to dye diffusion phenomena, while the structure of crystalline regions is more closely related to the birefringence index.

Most of the reported degradation data are based on mechanical property evaluations. Chu et al. recently developed a chemical means to examine the degradation of Dexon sutures (115). The

Downloaded by STANFORD UNIV GREEN LIBR on August 6, 2012 | http://pubs.acs.org
Publication Date: April 3, 1991 | doi: 10.1021/bk-1991-0457.ch012

Table IV. DYE DIFFUSION COEFFICENT AND ISOTROPY INDEX OF PARTIALLY HYDROLIZED PDS SUTURES AT DIFFERENT DYEING TEMPERATURES

Dyeing Temperature (°)	Hydrolysis Time (days)	Lateral		Longitudinal		Isotropy Index (*E-4)
		√2D*E-4 (mm/√sec)	D*E-8 (mm^2/sec)	√D*E-3 (mm/√sec)	D*E-5 (mm^2/sec)	
30	0	1.87	1.75	6.83	2.33	7.51
	14	2.08	2.17	7.16	2.56	8.48
	28	2.13	2.27	7.37	2.71	8.38
	42	2.15	2.32	7.65	2.92	7.95
40	0	2.18	2.38	6.96	2.42	9.83
	14	2.29	2.62	7.28	2.65	9.89
	28	2.43	2.95	7.61	2.90	10.17
	42	2.76	3.81	7.72	2.98	12.78
50	0	2.24	2.51	7.39	2.73	9.19
	14	3.23	5.51	7.63	2.91	18.93
	28	3.81	7.26	7.73	2.99	24.28
	42	4.14	8.57	7.79	3.03	28.28
60	0	5.37	14.42	7.95	3.16	45.63
	14	5.69	16.19	8.09	3.27	49.51
	28	5.72	16.36	8.27	3.42	47.83
	42	5.77	16.65	8.33	3.47	47.98

advantages of this new method are that it provides quantitative data beyond the unmeasurable strength of Dexon sutures, and is more sensitive than mechanical property evaluations. This method is based on the color change of the reaction of glycolic acid, the principal degradation product, with chromotropic acid. The absorbance of the resulting color change is then determined with a uv-visible spectrophotometer. With the availability of a calibration curve, one can determine how much glycolic acid is released at any specific time due to the degradation of Dexon sutures. As shown in Figure 17, the degradation profiles obtained in this method clearly indicate that a two-stage mechanism is involved in the degradation of this class of polymers and hence further supports the previously hypothesized hydrolytic degradation mechanism of Dexon sutures on the basis of the level of crystallinity data (116). The importance of this method is evident in its ability to identify and quantify both the amorphous and crystalline regions of degradation. As shown by Chu, et al., neither the mechanical property evaluation nor the pH level measurement reveal the characteristic of the two-stage degradation mechanism found in the newly developed chemical method (116). The former (mechanical property) merely reveals a continuous loss of tensile strength as degradation proceeds and does not distinguish the amorphous degradation (first stage) from the crystalline degradation (second stage). The latter (pH level measurement) reveals the second half of the total degradation mechanism, but it is not sensitive enough to identify the first stage degradation.

Surface Modification for Regulating Suture Fiber Degradation. The conventional approach to improve the performance of synthetic absorbable suture fibers has been focused on the research and development of new polymers and fibers. This approach, however, is costly and time consuming. Very recently, Loh and Chu proposed the use of plasma surface modification of existing commercial suture fibers (121).

From the hydrolytic degradation studies of synthetic absorbable sutures, any modification which could retard the diffusion (D) and solubility (S) of H_2O and/or enzyme molecules in the tissues into the suture fibers should be able to slow down their hydrolytic degradation process. The purpose of plasma surface treatment is to generate a unique suture surface layer of a few hundreds of Å thickness for reducing both the rate of water diffusion through the surface and the amount of water solubility in the suture. Such a surface could serve as a temporary (rather than permanent) barrier for water so the adequate tensile strength of the suture could be retained for a longer period during the critical period of wound healing.

It has generally been observed that exposure of polymers to a discharged inert gas plasma results in extensive crosslinking on the polymer surface layer. Both ultraviolet radiation and reactive radicals in the plasma are capable of generating free radicals on the surfaces of many polymers which lead to the formation of crosslinks in the outermost surface. This would slow down the passage of small molecules through the surface layers of the treated suture material, thus resulting in reduction of the rate of hydrolytic degradation during the critical period of wound healing. Because the crosslinked layer will be made to be less than about 100 Å thickness, the surface-modified absorbable sutures would still retain their absorbability. The development of a surface crosslinked layer has been shown to be related to the length of exposure to the plasma, the choice of the plasma conditions, and the nature of the polymer. This crosslinked surface layer can be further modified to reduce its liquid solubility parameter, S, by creating a hydrophobic surface through fluorinated plasma gases.

Downloaded by STANFORD UNIV GREEN LIBR on August 6, 2012 | http://pubs.acs.org
Publication Date: April 3, 1991 | doi: 10.1021/bk-1991-0457.ch012

Downloaded by STANFORD UNIV GREEN LIBR on August 6, 2012 | http://pubs.acs.org
Publication Date: April 3, 1991 | doi: 10.1021/bk-1991-0457.ch012

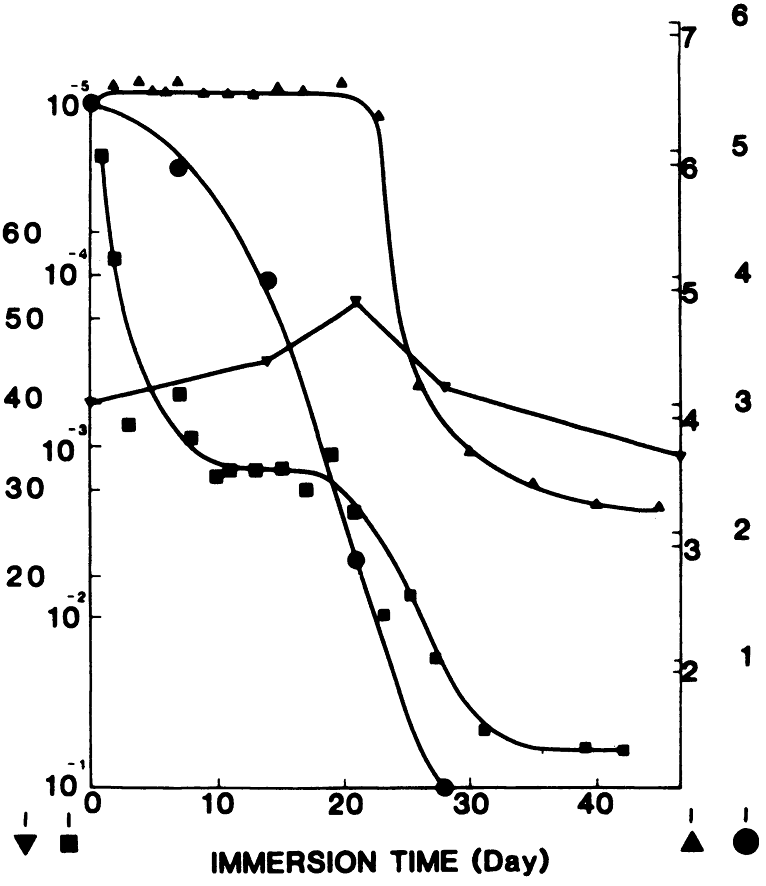

Figure 17. In vitro hydrolytic degradation of PGA suture fibers expressed in terms of the change of glycolic acid concentration (■), tensile strength (●), level of crystallinity (▼), and pH of the medium (▲) as a function of hydrolytic time. (Reproduced with permission from Ref. 115. Copyright 1984 C. C. Chu et al.

This fluorinated layer with a crosslinked and hydrophobic characteristic would be expected to significantly reduce the permeability, P, of solvents.

Table V summarizes the tensile breaking strength of both six plasma-treated and untreated SAS obtained from the initial screening study. The six plasma treatment conditions and their codes were: 400 Å parylene-N (A1), 10^3 Å parylene-N (A3), 400 Å CH_4 (C1), 10^3 Å CH_4 (C3), 400 Å trimethylsilane (D1) and 400 Å tetrafluoroethylene (E1). The data in the parentheses indicate the percentage of the tensile breaking strength remaining using the corresponding plasma surface treated but unimmersed sutures as the controls. The data in the table show, in general, that (i) most of the proposed six plasma surface treatments resulted in better tensile breaking strength retention than the untreated controls, and (ii) the degree of advantage depended on the type of SAS and treatment conditions.

In the Vicryl suture group, the order of the six plasma surface treatments in decreasing effectiveness is: (C3)>(A3)>(C1)=(E1)>(A1)>(D1)>control where (>) means better than and (=) means equal to. (A3) treatment resulted in a tensile breaking strength 418% stronger than the corresponding control after 28 days. Although (D1) treatment resulted in tensile breaking strength very slightly less than the control at 28 days, its tensile breaking strength after 14 days was 123% greater than the corresponding control. As expected, an increase in treatment thickness did improve the tensile strength retention (i.e., C1 vs. C3). None of the six plasma surface treatments adversely affected the initial (0 day) tensile breaking strength of the Vicryl suture.

In the PDS suture group, the data are even more encouraging. The order of the six treatments in decreasing effectiveness is (C1)>(E1)>(C3)=(A1)>(A3)>(D1)>Control. All of the six plasma surface treatments showed consistently far better tensile breaking strength and its retention after hydrolysis than the control. For example, as high as 91% of their original tensile breaking strength was observed with (A3) and (C1) treatments after 28 days, while the control retained only 23.8% of its original tensile breaking strength. Even the worst performance among the six plasma treatments (i.e., D1) retained 63% of its original strength. Contrary to our expectation, increasing depth of plasma treatment did not result in a better retention of tensile breaking strength (e.g., C1 vs C3). Another unexpected observation is that all of the six treatments lowered the initial (0 day) tensile breaking strength of PDS compared to the control. We must, however, recognize that even though plasma-treated PDS sutures had initial lower tensile breaking strength than the controls, their strength retention after 28 days (also 42 days as shown in the in-depth study given below) was significantly higher than the corresponding controls.

In the Dexon suture group, the order of the six treatments in decreasing effectiveness was (E1)>(C3)>(C1)>Control>(A3)>(D1)>(A1). The tensile breaking strength and the percentage strength remaining of the (E1)-treated Dexon was almost double that of the control after 28 days. (C3)- and (C1)- treated Dexon were slightly better than the controls. (A1), (A3), and (D1) treatments, however, were not as good as the other three treatments. None of these six plasma treatments lowered Dexon initial tensile breaking strength compared to the control.

In the Maxon suture group, the order of the six treatments in decreasing effectiveness was (C1)>(D1)>(A1)=(A3)>Control>(E1)>(C3). Although the treated Maxon sutures showed better tensile breaking strength and its retention han the controls after 14 days (e.g., 90% for C1 vs. 73% for control), this advantage disappeared after 28 days. Like PDS sutures, increasing the depth of plasma treatment, however, did not improve the retention of tensile breaking strength of Maxon sutures. None of the six treatments adversely lowered the

Downloaded by STANFORD UNIV GREEN LIBR on August 6, 2012 | http://pubs.acs.org
Publication Date: April 3, 1991 | doi: 10.1021/bk-1991-0457.ch012

Downloaded by STANFORD UNIV GREEN LIBR on August 6, 2012 | http://pubs.acs.org
Publication Date: April 3, 1991 | doi: 10.1021/bk-1991-0457.ch012

Table V. TENSILE STRENGTH OF PLASMA TREATED 2/0 SYNTHETIC ABSORBABLE SUTURES

Treatment		Control		A		B		C1		C3		D1		E1	
Hydrolysis Time		(Kg)	(%)	(Kg)	(%)	(Kg)	(%)	(Kg)	(%)	(Kg)	(%)	(Kg)	(%)	(Kg)	(%)
	0	6.58±0.14	(100)	6.60±1.2	(100.3)	6.57±0.11	(99.9)	6.42±0.11	(99.1)	6.66±0.04	(101.2)	6.73±0.10	(102.3)	6.67±0.16	(101.4)
Dexon	14	5.52±0.08	(69)	5.28±0.20	(80.0)	5.37±0.12	(81.7)	4.97±0.19	(77.4)	5.25±0.17	(78.8)	5.01±0.17	(74.4)	5.12±0.18	(76.8)
	28	0.41±0.03	(6.2)	0.26±0.04	(3.9)	0.32±0.04	(4.9)	0.43±0.04	(6.7)	0.48±0.10	(7.2)	0.37±0.03	(5.5)	0.72±0.11	(10.8)
	0	5.55±0.16	(100)	5.53±0.24	(99.6)	5.52±0.35	(99.4)	5.56±0.13	(100)	5.64±0.27	(101.6)	5.66±0.05	(102)	5.51±0.25	(99.3)
Vicryl	14	3.38±0.25	(60)	3.94±0.20	(71.2)	4.21±0.15	(76.3)	4.31±0.46	(77.5)	4.55±0.09	(80.7)	4.17±0.16	(73.7)	4.29±0.30	(77.9)
	28	0.0598±0.002	(1.1)	0.15±0.02	(2.7)	0.25±0.04	(4.5)	0.18±0.03	(3.2)	0.22±0.01	(3.9)	0.05±0.01	(0.88)	0.19±0.30	(3.6)
	0	5.76±0.3	(100)	3.53±0.15	(61.3)	3.24±0.22	(56.3)	3.53±0.06	(61.3)	4.45±0.03	(77.3)	2.34±0.25	(40.6)	3.67±0.18	(63.7)
PDS	14	5.20±0.2	(90.3)	3.56±0.27	(100.7)	3.17±0.33	(97.9)	3.96±0.20	(112.3)	3.84±0.10	(86.3)	3.06±0.72	(130.8)	3.84±0.11	(104.6)
	28	1.37±0.09	(23.8)	2.99±0.11	(84.7)	2.97±0.37	(91.7)	3.24±0.21	(91.8)	3.21±0.14	(72.1)	1.48±0.24	(63.3)	3.13±0.13	(85.3)
	0	6.60±0.22	(100)	6.09	(92.3)	5.84±0.25	(88.5)	5.93±0.29	(89.8)	6.12±0.25	(92.3)	6.13±0.12	(92.9)	5.95±0.13	(90.2)
Maxon	14	4.85±0.12	(73.5)	5.21±0.00	(85.9)	5.31±0.09	(90.9)	5.20±0.07	(87.7)	5.10±0.11	(83.3)	5.33±0.14	(87.0)	5.11±0.03	(85.9)
	28	4.28±0.34	(64.9)	3.56±0.34	(58.5)	3.29±0.46	(56.3)	3.52±0.38	(59.4)	3.48±0.27	(56.8)	3.10±0.16	(52.1)	3.19±0.01	(52.1)

initial tensile breaking strength of Maxon sutures. Based on these data, Loh and Chu (121) conducted an in-depth evaluation of their approach of using plasma surface treatment to modify the hydrolytic degradation of SAS by examining the wettability, dye diffusion, stiffness, weight loss, and surface morphology of SAS. A complete report of this in-depth study will be published in the near future.

Future Challenge. An examination of the published studies of the four synthetic absorbable sutures indicates that their rate of mass absorption is considerably slower than the rate of tensile strength loss (65). The Absorption Delay (defined as the differential in time between the complete mass absorption and complete loss of tensile strength) of the four synthetic absorbable suture fibers in both in vitro and in vivo conditions is summarized in Table VI. In general, Dexon and Vicryl sutures have been found to exhibit an insignificant amount of tensile strength after 28 days of implantation, while the majority of their mass is still present in tissue for various periods (122-125). For example, Katz, et al., reported that Dexon sutures exhibited insignificant amounts of tensile strength at 28 days of implantation in New Zealand rabbits, while complete absorption of Dexon did not occur until 50 to 75 days in all instances (122). Postlethwait found that Dexon sutures exhibited no tensile strength after 28 days in New Zealand rabbits, while more than 98 to 95% of suture remained at the same period, and close to complete absorption did not occur until about 140 days (124). Reed, et al., reported that most of Dexon suture's strength was lost over the 14-28 day period in vitro (37°C at pH = 7.0), while the mass of the suture remained unchanged during the same period, and the mass loss began in the fourth week and was completed by 70-84 days (125). PDS and Maxon sutures, however, exhibited much more long tensile strength and mass retention than Dexon and Vicryl sutures. PDS sutures retained an average of 58% of their original tensile strength at the end of 4 weeks implantation in the subcutis of rats (126-128). Howevr, there was only 20% of the original mass absorbed at 160 days of post-implantation and complete absorption was not evident until 180 days postimplantation (80,126-128). However, as long as 240 days for complete PDS suture absorption have been reported by others (129,130). Similar results were also found in Maxon sutures (81,127,128,131). They retained 30% of their original tensile strength at 42 days, however, it would take 7 months for complete gross absorption of the suture in rats' subcutaneous tissues. This prolonged suture mass absorption after they have lost all of their function results in a typical chronic inflammation with mononuclear macrophages surrounding the suture.

Table VI. ABSORPTION DELAY OF COMMERCIAL SYNTHETIC ABSORBABLE SUTURES

Suture Materials	Time to Complete Loss of Tensile Strength (Days)	Time to Complete Mass Absorption (Days)	Absorption Delay (Days)	Useful Lifetime* (%)
Dexon®	28	50-140	22-112	20-56
Vicryl®	28	90	62	31
PDS®	63	180-240	117-170	26-35
Maxon®	56	210	155	27

* The ratio of [the time to complete loss of tensile strength] to [the time to complete mass absorption]. The higher percentage is the better absorbable suture.

Downloaded by STANFORD UNIV GREEN LIBR on August 6, 2012 | http://pubs.acs.org
Publication Date: April 3, 1991 | doi: 10.1021/bk-1991-0457.ch012

In High-Tech Fibrous Materials; Vigo, T., et al.;
ACS Symposium Series; American Chemical Society: Washington, DC, 1991.

After the conventional synthetic absorbable sutures become useless (i.e., loss of majority of their original strength), more than 90% of their original mass is still present in the body, providing no tensile strength and resulting in their long term adverse tissue reactions. Prompt removal of the unwanted foreign suture materials without endangering and overloading the metabolic activity of the surrounding tissues is a necessary component of absorbable suture design. Hopefully, such a challenge could be met in the future which will be a major contribution to the field of wound closure biomaterials.

Conclusions

The two most important developments in the field fibrous wound closure biomaterials during the past several decades (i.e., antimicrobial sutures and synthetic absorbable suture fibers) were comprehensively reviewed. The importance for achieving better wound infection control was documented, and an alternative approach of using direct-current activated SAS was described for achieving such a goal. Our preliminary studies indicate that the concept of SAS can be expected to have the following key advantages not available in current commercial or experimental suture materials:

(a) the ability to control and enhance rate of local release of antimicrobial agent from the SAS under a variety of conditions.
(b) the antimicrobial domain of the SAS could be controlled and extended beyond the space immediately occupied by the suture;
(c) the silver material has a wide spectrum of antimicrobial capability and the incidence of bacterial resistance to it has been very rare;
(d) a low dosage of this antimicrobial agent can be used without compromising its effectiveness because of direct and localized release to wound sites;
(e) the SAS appears to elicit less tissue reaction than commercial nylon sutures (i.e., Nurolon) in rats.

A better understanding of the hydrolytic degradation mechanism of synthetic absorbable suture fibers has also been achieved through many studies of the effects of environmental factors like pH, buffer, enzymes, bacteria and material factors like annealing, γ-irradiation, chemical modification on the hydrolysis of this class of fibers and polymers.

The hydrolytic degradation property of this class of fibers coupled with its known dependence on many factors render us a unique opportunity to examine their fiber morphology. Some unusual fiber morphological structures were observed and answers such as the origin of this observation are unknown at the present time. Our preliminary attempts of using plasma surface treatments to regulate the hydrolysis of synthetic absorbable suture fibers were also described. The results obtained so far are encouraging and demonstrate the feasibility of our approach to regulate the hydrolysis of this class of fibers. Further study is underway to confirm this new approach.

Literature Cited

1. Chu, C.C.; Kizil, Z. Surg. Gynecol. Obstet. 1989, 168, 233-238.
2. Tera, H.; Aberg, C. Acta Chir. Scand. 1976, 142(1), 1-7.
3. Chu, C.C. In CRC Critical Reviews in Biocompatibility, Williams, D., Ed.; CRC Press: Boca Raton, Fla, 1986; Vol. 1, p 261-322.
4. Cole, B.; Van Heerfen, J.A.; Kayes, T.F.; and Haldorson, A. Surg. Gynecol. Obstet. 1982, 154:557.

Downloaded by STANFORD UNIV GREEN LIBR on August 6, 2012 | http://pubs.acs.org
Publication Date: April 3, 1991 | doi: 10.1021/bk-1991-0457.ch012

5. Bengamini, T.M.; Polk, H.C. Surg. Gynecol. Obstet. 1989, 168:283.
6. P.S. Brachman, B.B.; Dan R.W. Haley, et al. Surg. Clin. North Amer. 1980, 60(1):15.
7. Cruse, P.J.E.; Ford, R., Surg. Clin. North Amer. 1980, 60:27.
8. Sugarman, B.; Young, E.J. Infections Associated with Prosthetic Devices, CRC Press: Boca Raton, FL, 1984.
9. Elek, S.D.; Conen, P.E., Br. J. Exp. Pathol. 1957, 38:530.
10. Howe, C.W.; Marston, A.T., Surg. Gynecol. Obst. 1962, 115:266.
11. Edlich, R.F.; Panek, P.H., et al., Ann. Surg. 1973, 177(6):679.
12. Varma, S.; Lumb, W.V., et al., Am. J. Vet. Res. 1981, 42(4):571.
13. Paterson-Brown, S.; Cheslyn-Curtis, S.; Biglin, J., et al., Br. J. Surg. 1987, 74:734.
14. Alexander, J.W.; Kaplan, J.Z.; Altemeier, W.A., Ann. Surg. 1967, 165:192.
15. Blomstedt, B.; Osterberg, B., Acta Chir. Scand. 1978, 144:269.
16. Osterberg, B.; Blomstedt, B., Acta Chir. Scand. 1979, 145:431.
17. Blomstedt, B.; Osterberg, B., Acta Chir. Scand. 1977, 43:67.
18. Chu, C.C.; Williams, David., Am. J. Surg. 1984, 147:197.
19. Katz, S.; Izhar, M.; Mirelman, D., Ann. Surg. 1981, 194(1):35.
20. Sugarman, B. & Musher, D., Proc. Soc. for Exp. Biol. and Med. 1981, 167:156.
21. Dankert, J.; Host, A.H.; Feijen, J., CRC Critical Reviews in Biocompatability, D.F. Williams, Ed.; CRC Press: Boca Raton, FL, 1986; 2(3):219-301.
22. Rodeheaver, G.T.; Kurtz, L.D.; Bellamy, W.T., et al., Arch. Surg. 1983, 118:322.
23. Altemeier, W.A.; Culbertson, W.R. "Surgical Infection," In Surgery, Principles and Practice, J. Rhoads and C. Moyer, Eds., 4th Edition; J.B. Lippincott: Philadelphia, 1970.
24. Herman, G.G.; Bagi, P., et al., Surg. Gynecol. Obstet. 1988, 167:16.
25. Glassman, J.A.; Fowler, E.F.; Novak, M.V., Surg. Gynecol. Obstet. 1984, 78:359.
26. Ludewig, R.M.; Rudolf, L.E.; Wangensteen, S.U., Surg. Gynecol. Obstet. 1971, 133:946.
27. LeVeen, H.H.; Falk, G.; Mazzopira, F.A., et al., Surgery 1968, 64:610.
28. Howell, J.J. Br. Med. J. 1965, 5432:449.
29. Echeverria, E.; Olivares, J., Am. J. Surg. 1959, 98:695.
30. Chu, C.C.; Tsai, W.C.; Yao, J.Y.; Chiu, S.S., J. Biomed. Mater. Res. 1987, 21:1281.
31. Tsai, W.C.; Chu, C.C.; Chiu, S.S.; Yao, J.Y., Surg. Gynecol. Obstet. 1987, 165:207.
32. Hill, W.R.; Pillsbury, D.M. The Pharmacology of Silver, Baltimore, Williams and Wilkins, 1939.
33. Fox, C., Surg. Gynecol. Obstet. 1983, 157:82.
34. Carr, H.S.; Wlodkowski, T.J.; Rosenkranz, H.S., Antimicrob. Agents Chemother. 1973, 4:585.
35. Benvenisty, A.I.; Tannenbaum, G.; Ahlborn, T.N., et al., J. Surg. Res. 1988, 44:1.
36. Webster, D.A.; Spadaro, J.A.; Becker, R.O., et al., Clin. Orthop. & Rel. Res. 1981, 161:105.
37. Spadaro, J.A., In Modern Bioelectricity, A.A. Marino, Ed.; M. Dekker: New York, 1988; pp. 629-655.
38. Spadaro, J.S.; Berger, T.J.; Barranco, S.D.; Chapin, S.E.; Becker, R.O. Antimicrob. Agents & Chemother. 1974, 6(5),637.

Downloaded by STANFORD UNIV GREEN LIBR on August 6, 2012 | http://pubs.acs.org
Publication Date: April 3, 1991 | doi: 10.1021/bk-1991-0457.ch012

Downloaded by STANFORD UNIV GREEN LIBR on August 6, 2012 | http://pubs.acs.org
Publication Date: April 3, 1991 | doi: 10.1021/bk-1991-0457.ch012

39. Berger, T.J.; Spadaro, J.A.; Bierman, R.; Chapin, S.E.; Becker, R.O. Antimicrob. Agents & Chemother. 1976, 100,856.
40. Spadaro, J.S.; Webster, D.A.; Becker, R.O. Clin. Orthop. & Rel. Res. 1979, 143, 266.
41. Becker, R.O.; Spadaro, J.A. J. Bone & Joint Surg. 1978, 60A7, 871.
42. Berger, T.J.; Spadaro, J.A.; Chapin, S.E.; Becker, R.O. Antimicrob. Agents & Chemother. 1976, 9:357.
43. Hendry, A.T.; Stewart, I.O. Can. J. Microbiol. 1979, 25:915.
44. Falcone, A.E.; Spadaro, J.A. Plastic and Reconst. Surgeons 1986, 77(3):455.
45. Spadaro, J.A.; Chase, S.E.; Webster, D.A. J. Biomed. Mater. Res. 1986, 20: 565.
46. Kaur, P.; Vadehra, D.V. Antimicro. Agents & Chemother. 1986, 29, 165-167.
47. Starodub, M.E.; Trevors, J.T. J. Med. Microbiol. 1989, 29, 101-110.
48. Trevors, J.T. Enzyme & Microbial Technol. 1987, 9, 331-333.
49. Charley, R.C.; Bull, A.T. Arch. Microbiol. 1979, 123, 239-244.
50. Pooley, F.D. Nature 1982, 296, 642-643.
51. Silver, S., In Molecular Biology, Pathogenicity, and Ecology of Bacterial Plasmids, Levy, S.B. et al., Ed.; Plenum Publ.: New York, 1981; P.179-189.
52. Brierley, C.L.; Kelly, D.P.; Seal, K.J.; Best, D.J., In Biotechnology Principles and Applications, Higgins, J. et al., Ed.; Blackwell Scientific Publ.: Oxford, 1985; P.163-212.
53. Bragg, P.D.; Rainnie, D.J. Can. J. Microbiol. 1974, 20,883-889.
54. Modak, S.M.; Fox, C.L. Biochem. Pharmacol. 1973, 22, 2391.
55. Sewell, W.R.; Wiland, J.; Craver, B.N. Surg. Gynecol. Obstet. 1955, 100, 483.
56. Becker, Robert O., In Proceedings of First International Conference on Gold and Silver in Medicine, Washington, D.C., 1987; pp. 227-243.
57. Dunn, M.G.; Doillon, C.J.; Berg, R.A., et al., J. Biomed. Mater. Res.: Applied Biomater. 1988, 22(A2): 91-206.
58. Crisp, William E., Associated Gynecologist, LTD, Phoenix, AZ, Private Communication, Dec. 15, 1989.
59. Geronemus, R.G.; Merte, P.M., et al. Arch. Dermatol. 1978, 115: 1311.
60. Bellinger, C.G.; Conway, H. Plast. Reconst. Surg. 1970, 15:582.
61. McCauley, R.L.; Linares, H.A.; Pelligrin, V., et al. J. Surg. Res. 1989, 46:267.
62. Deitch, E.A.; Marino, A.A.; Gillespie, T.E., et al. Antimicrob. Agents & Chemother. 1983, 23(3): 356.
63. Scher, K.S.; Bernstein, J.M.; Jones, C.W., Am. Surg. 1985, 51:577.
64. Chu, C.C., In Biocompatible Polymer, Metals, and Composites, M. Szycher, editor, Technomic Press: Lancaster, PA, 1983; Chapter 22.
65. Chu, C.C., In CRC Critical Reviews in Biocompatibility, D.F. Williams, Ed-in-Chief; CRC Press: Boca Raton, FL, 1985; Vol. 1, Issue 3, pp. 261-322.
66. Chu, C.C. "Suture Materials," In Concise Encyclopedia of Medical & Dental Materials, D.F. Williams, Ed.; Pergamon Press: London, In Press.
67. Chu, C.C. "Degradation & Biocompatibility of Synthetic Wound Closure Biomaterials," In Degradation & Biocompatibility of Synthetic Biodegradable Polymers, D.F. Williams, Ed.; CRC Press: Boca Raton, FL, In Press.

68. Everett, W.G. Progr. Surg. 1970, 8, 14.
69. Barham, R.E.; Butz, G.W.; Ansell, J.S. Surg. Gynecol. Obstet. 1978, 146, 901.
70. Guttman, L. Br. J. Surg. 1943, 30, 370.
71. Sunderland, S.; Smith, G.K., Aust. N.Z. J. Surg. 1950, 20, 85.
72. DeLee, J.C.; Smith, M.T.; Green, D.P., J. Hand. Surg. 1977, 2(1), 38.
73. Vallfors, B.; Hansson, Hans-Arne; Svensson, J., Neurosurgery 1981, 9(4), 407.
74. Varma, S.; Johnson, L.W.; Ferguson, H.L., et al. Am. J. Vet. Res. 1981, 42(4), 563.
75. Torsello, G.B.; Sandmann, W., et al., J. Vasc. Surg. 1986, 3:135.
76. Cameron, A.E.; Parker, C.J.; Field, E.S., et al. Ann. R. Coll. Surg. (England) 1987, 69(3):113.
77. Bucknall, T.E.; Ellis, H. Surgery 1981, 89(6), 672.
78. Corman, M.L.; Veidenheimer, M.C.; Coller, J.A., Am. J. Surg. 1981, 141, 510.
79. Bartone, F.; Shore, N.; Newland, J., et al., Urology 1987, 29(5):517.
80. Friberg, L.G.; Mellgren, G.W.; Eriksson, B.D., et al., Scand. J. Thorac. Cardiovasc. Surg. 1987, 21(1):9.
81. Chiu, I.S.; Hung, C.R.; Chao, S.F., et al., J. Throac. Cardiovasc. Surg. 1988, 95(1):112.
82. Torsello, G.; Schwartz, A.; Aulich, A., et al., Eur. J. Vasc. Surg. 1987, 1(5):319.
83. Pae, W.E.; Waldhausen, J.A.; Prophet, G.A.; Pierce, W.S. J. Throac. Cardiovas. Surg. 1981, 81:921.
84. Sauvage, L.R.; Harkins, H.N., Bull. John Hopkins Hosp. 1952, 91:276.
85. Tawes, R.L., Jr.; Aberdeen, E., et al. Surgery 1968, 64:1122.
86. Dahlke, H.; Dociu, N.; Thurau, K., J. Biomed. Mater. Res. 1980, 14, 251.
87. Kaminski, J.M.; Katz, A.R.; Woodward, S.C., Surg. Gynecol. Obstet. 1978, 146, 353.
88. Gorham, S.D.; Anderson, J.D.; Monsour, M.J., et al. Urol. Res. 1988, 16(2):111.
89. Gillatt, D.A.; Corfield, A.P.; May, R.E., et al., Ann. R. Coll. Surg. (England) 1987, 69(2):54.
90. Postlethwait, R.W.; Smith, B.M., Surg. Gynecol. Obstet. 1975, 140, 377.
91. Postlethwait, R.W.,Surg. 1975, 78(4), 531.
92. Salthouse, T.N.; Kaminska, G.Z.; Murphy, M.L., et al., Invest. Opthalm. 1970, 9(11), 844.
93. Salthouse, T.N.; Matlaga, B.F.; Wykoff, M.H., Am. J. Opthalm. 1977, 84(2), 224.
94. Chu, C.C.; Williams, D.F., J. Biomed. Mater. Res. 1983, 17:1029.
95. Williams, D.F.; Chu, C.C., J. Appl. Polym. Sci. 1984, 29:1865.
96. Williams, D.F.; Mort, E., J. Bioeng. 1977, 1:231.
97. Williams, D.F., ASTM Spec. Tech. Publ. 1979, 684, 61.
98. Smith, R.; Oliver, C.; Williams, D.F., J. Biomed. Mater. Res. 1987, 21:991.
99. Persson, M.; Bilgrav, K.; Jensen, L., et al., Eur. Surg. Res. 1986, 18:122.
100. Sharma, C.P.; Williams, D.F., Eng. Med. 1981, 10, 8.
101. Williams, D.F., J. Biomed. Mater. Res. 1980, 14, 329.
102. Sebeseri, O.; Keller, U.; Spreng, P., et al., Invest. Urol. 1975, 12(6), 490.
103. Holbrook, M.C., Br. J. Urology 1982, 54, 313.

Downloaded by STANFORD UNIV GREEN LIBR on August 6, 2012 | http://pubs.acs.org
Publication Date: April 3, 1991 | doi: 10.1021/bk-1991-0457.ch012

104. Elser, C.; Renardy, M.; Planck, H., 3rd international ITV Conference on Biomaterials, Fellbach/Stuttgart, W. Germany, June 14-16, 1989.
105. Chu, C.C.; Moncrief, G., Ann. Surg. 1983, 198, 223.
106. Lin, H.L.; Chu, C.C.; Grubb, D. "Morphological Study of Synthetic Absorbable Sutures," Transactions of the Society for Biomaterials Annual Meeting, 1990, P.134.
107. Chu, C.C.; Browning, A., J. Biomed. Mater. Res. 1988, 22:699.
108. Browning, A.; Chu, C.C., J. Biomed. Mater. Res. 1986, 20:613.
109. Chu, C.C., J. Biomed. Mater. Res. 1981, 15, 19.
110. Zaikov, G.E., J. Macromol. Sci. - Rev. Macromol. Chem. Phys. 1985, C25(4):551.
111. Chu, C.C., In Surgical Research Recent Development, C.W. Hall, Ed.; Pergamon Press: San Antonio, TX, 1985; pp.111-115.
112. Miller, N.D.; Williams, D.F., Biomaterials 1984, 5:365.
113. Chu, C.C.; Campbell, N.D., J. Biomed. Mater. Res. 1982, 16, 417.
114. Campbell, N.D.; Chu, C.C., 27th International Symposium on Macromolecules, Abstracts of Communications, Strasbourg, France, 1981; Vol. II, p. 1348-1352,
115. Chu, C.C.; Louie, May, 2nd World Biomaterials Congress, Washington, DC, 1984; p.209.
116. Chu, C.C., J. Appl. Polym. Sci. 1981, 26(5):1727.
117. Chu, C.C.; Kizil, Z., 3rd International ITV Conference on Biomaterials - Medical Textiles, Stuttgart, W. Germany, 1989; P.24.
118. Fredericks, R.J.; Melveger, A.J.; Dolegiewitz, L.J., J. Polym. Sci. Phys. Ed. 1984, 22:57.
119. Chu, C.C.; Lecaroz, L.E., In Advances in Biomedical Polymers, Gebelein, C. G. Ed.; Plenum Press: New York, 1987; PP.185-214.
120. Salthouse, T.N.; Matlaga, B.F., Surg. Gynecol. Obstet. 1976, 142, 544.
121. Loh, I.H. & Chu, C.C., 1990, NIH-SBIR Phase I Progress Report (1R43AR40454-01).
122. Katz, A.R.; Turner, R.J., Surg. Gynecol. Obstet. 1970, 131, 701.
123. Craig, P.H.; Williams, J.A.; Davis, K.W., et al., Surg. Gynecol. Obstet. 1975, 141, 1.
124. Postlethwait, R.W., Arch. Surg. 1970, 101, 489.
125. Reed, A.M.; Gilding, D.K. Polymer 1981, 22(4), 494.
126. Ray, J.A.; Doddi, N.; Regula, D., et al., Surg. Gynecol. Obstet. 1981, 153(10), 497.
127. Bourne, R.B.; Bitar, H.; Andreae, P.R., et al., Can. J. Surg. 1988, 31(1):43.
128. Sanz, L.E.; Patterson, J.A.; Kamath, R., et al., Obstet. Gynecol. 1988, 71(3 pt 1):418.
129. Knoop, M.; Lunstedt, B.; Thiede, A., Langenbecks Arch. Chir. 1987, 371(1):13.
130. Marti, R.; Burgues, L.; Gabarro, I., et al., J. French Opthalm. 1986, 9(5):373.
131. Katz, A.; Mukherjee, et al., Surg. Gynecol. Obstet. 1985, 161:213.

RECEIVED October 12, 1990

Downloaded by STANFORD UNIV GREEN LIBR on August 6, 2012 | http://pubs.acs.org
Publication Date: April 3, 1991 | doi: 10.1021/bk-1991-0457.ch012

Downloaded by CORNELL UNIV on August 6, 2012 | http://pubs.acs.org
Publication Date: April 3, 1991 | doi: 10.1021/bk-1991-0457.ch013

Chapter 13

New Third-Generation Protective Clothing from High-Performance Polyethylene Fiber

From Knives to Bullets

K. M. Kirkland, T. Y. Tam, and G. C. Weedon

Allied Fibers Technical Center, P.O. Box 31, Petersburg, VA 23804

Ultra high strength polyethylene fibers are finding increased use in a variety of protective clothing applications. The unique combination of properties available with high performance polyethylene fibers such as extraordinary abrasion resistance, high modulus and tensile strength, low specific gravity, excellent chemical resistance, and high cut resistance are extending the use of high performance fibers in applications where existing protective clothing was lacking. Growing awareness of the advantages offered by high strength polyethylene fibers is allowing the fiber to be used to improve existing protective clothing.

Many types of hand and arm protectors making use of the superior cut and abrasion resistance of the high strength polyethylene fibers will be presented. Ballistic armor applications will be highlighted to illustrate the advantages of high performance polyethylene fiber's high tensile strength, high modulus and low specific gravity.

Progress in developing protective clothing has never been more rapid than it is at present. This steady progress has been made possible by advances in both polymer and fiber technology. Improvements in materials have given protective clothing designers more options which lead ultimately to more comfortable, better performing products. Factors such as abrasion and cut resistance are very important for garments designed to protect against mechanical injury. The combination of high modulus, tenacity and energy absorption with low

0097–6156/91/0457–0214$07.00/0

specific gravity and low elongation are desirable for good ballistic performance. It is unusual for a single fiber to possess all of these characteristics. High Performance Polyethylene (HPPE) fibers, however, not only meet all of these requirements but also offer additional benefits.

High Performance Polyethylene Fibers

High performance polyethylene fibers are made from very high molecular weight polyethylene polymer. Polyethylene is a flexible chain macro molecule which normally crystallizes or solidifies by chain folding. The folded portions of the polymer chain do not make a significant contribution to fiber strength. Therefore, polyethylene fibers made by conventional methods which allow the polymer chain to fold back onto itself do not possess outstanding physical properties. In contrast, HPPE fibers are produced by a process which allows the polyethylene molecular chains to crystallize in an extended, highly oriented state. The extension of the polymer chain in combination with their orientation along the fiber axis give rise to the superior physical properties such as high tensile strength and high modulus. Several different versions of HPPE fibers are available commercially. All of the work presented here was done using SPECTRA (a registered trade mark of Allied-Signal) HPPE fibers. The key structural parameters that distinguish high performance polyethylene fibers from conventional melt spun materials are illustrated in Figure 1.(1)

The molecular weight of the polyethylene used to produce the HPPE fibers is generally in the range of 1 to 5 million Daltons. In contrast, the molecular weight of many conventional polymers used in fiber production is typically fifty thousand to several hundred thousand Daltons. HPPE fibers, because of the extension and orientation of the polymer chains, exhibit a very high degree of crystalline orientation (95-99%) and crystalline content (60-85%).(1)

One method of producing HPPE fibers is the solution spinning process. In solution spinning the first step is to dissolve the very high molecular weight polymer using a suitable solvent. The solvent serves to disentangle the polymer chains and is critical in obtaining an extended chain structure. The resulting polymer solution is viscous enough to be processed on conventional melt spinning equipment. The cooled extrudate forms an Extended Chain Polyethylene (ECPE) fiber which can be continuously dried to remove the solvent or the solvent can later be extracted by an another appropriate solvent. The extracted fibers are usually subsequently drawn prior to final packaging.

Downloaded by CORNELL UNIV on August 6, 2012 | http://pubs.acs.org
Publication Date: April 3, 1991 | doi: 10.1021/bk-1991-0457.ch013

Downloaded by CORNELL UNIV on August 6, 2012 | http://pubs.acs.org
Publication Date: April 3, 1991 | doi: 10.1021/bk-1991-0457.ch013

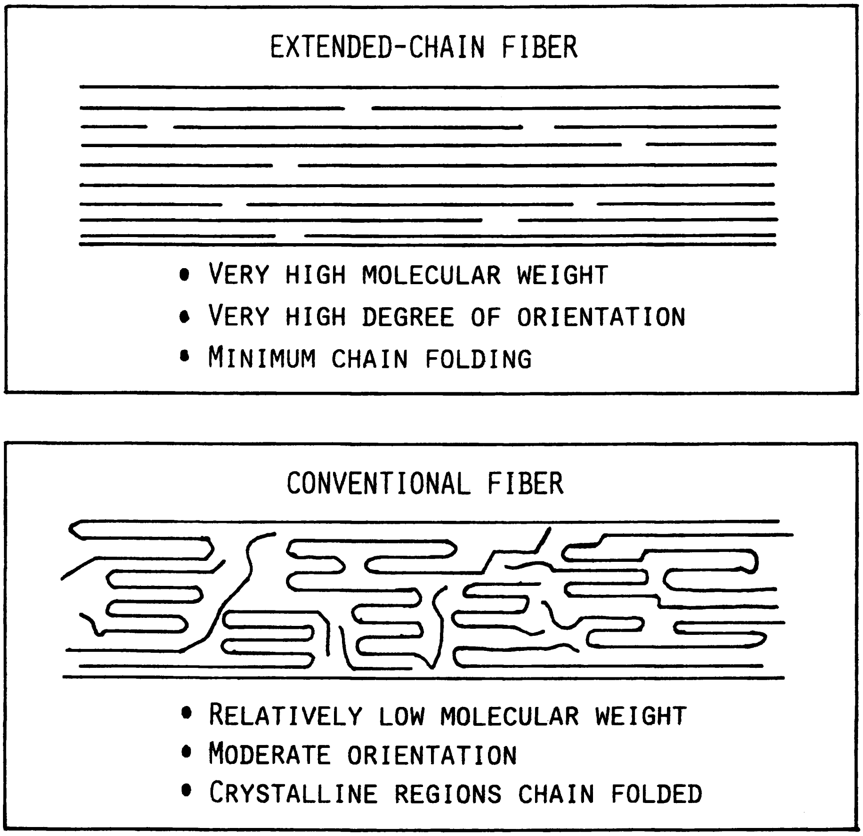
EXTENDED-CHAIN FIBER
• VERY HIGH MOLECULAR WEIGHT
• VERY HIGH DEGREE OF ORIENTATION
• MINIMUM CHAIN FOLDING
CONVENTIONAL FIBER
• RELATIVELY LOW MOLECULAR WEIGHT
• MODERATE ORIENTATION
• CRYSTALLINE REGIONS CHAIN FOLDED

Figure 1. Fiber Morphology. (Reproduced with permission from ref. 1. Copyright 1988. Allied-Signal.)

Downloaded by CORNELL UNIV on August 6, 2012 | http://pubs.acs.org
Publication Date: April 3, 1991 | doi: 10.1021/bk-1991-0457.ch013

Fiber Properties. The tensile strength of HPPE fibers in engineering terms is similar to other high performance fibers such as carbon, aramid, and glass. Because polyethylene has a lower density (0.96 g/cc which is half that of high modulus carbon fiber and two thirds that of aramid) than other high performance fibers, the specific strength of HPPE fibers is extremely high. On a per mass basis the strength of HPPE fibers is at least 35% greater than that of high modulus aramid or S-Glass and approximately two times that of conventional high modulus carbon fiber. Table I gives a comparison of the strengths of several high performance fibers.

Like all materials, HPPE fibers have some limitations: the fiber has a relatively low melting point, and its chemical inertness contributes to difficulties with fiber to matrix adhesion. The melting temperature cannot be significantly improved because it is an inherent property of the polyethylene polymer from which HPPE fiber is made. It is interesting to note that HPPE fiber's 147°C melting temperature is approximately 15°C higher than the melting point of un-oriented polyethylene. The higher melting temperature is a result of the increased crystallinity and extended polymer chain formation in the fiber.

In composite structures using HPPE fibers, the low fiber to matrix adhesion can sometimes present difficulties. Improvements in the fiber's adhesion have been made using corona or gas plasma treatments. However, there are applications where it is desirable to have a low fiber to matrix adhesion.

Cut and Slash Protection

For employers, protecting their workers from injury has become a primary concern since the passage of the Health and Safety at Work act of 1974.(2) This act made employers responsible for providing adequate protective clothing and appliances where necessary. One of the most susceptible parts of the body to injury is the hands. Even after taking measures to protect the hands, such as wearing gloves and installing guards, hand and finger injuries still account for over 25% of all industrial accidents.(2) Clearly, there is still a substantial need for improved types of hand protection. HPPE fibers in this application offer a number of advantages. HPPE fibers can allow the cut protective glove to be made more comfortable because of the fiber's soft hand. Another benefit in using the HPPE fiber in cut protective gloves is the improved abrasion resistance of the HPPE fiber which improves the glove's wear life.

The high cut resistance of HPPE fibers was discovered when the scissors used to cut the fiber during manufacture wore out after a few days of use. While the experience with the scissors indicated that HPPE was cut resistant, a more objective test was needed to quantitatively measure the cut resistance of the fiber. For the cut and slash resistant clothing application a test method to evaluate the fabrics had to be devised before serious product development could begin. A cut and abrasion tester and test method was developed by Allied which is believed to objectively measure the cut resistance of fibers and fabrics.

Cut resistance evaluation. The Beta Tec (a registered trade mark of Allied-Signal) Automatic Abrasion and Cut Tester was designed to measure the cut resistance of protective gloves.(Figure 2.) In addition to gloves, the Beta Tec can be used to evaluate the cut resistance of almost any flexible material. When penetration of the sample occurs, the tester automatically stops. It is possible for the Beta Tec to simulate two types of cutting: slicing and chopping. Cutting motion is determined by cam selection. The cutting arm can accommodate a variety of different types of blades ranging from single edge razor blades to scalpel blades. In order to eliminate the effect of blade dulling from test to test the blade is normally changed after each test.

With the Beta Tec Abrasion and Cut Tester it is possible to realistically test fabrics and obtain unbiased results. To test a fabric sample on the Beta Tec cut tester the specimen is mounted on the mandrel. Either flat fabrics or glove fingers can be tested. The test finger is clamped at the end closest to the cam. Flat fabrics should be clamped at both ends. The proper test cam, rotational speed, and cutting blade load are selected. Once started, the automatic counter records the number of cycles to specimen penetration at which time the tester stops.

Cut Resistant Gloves. Almost all gloves can be considered to provide some degree of cut resistance because the glove is an additional material which must be cut through before the cutting edge reaches the hand. Cotton, leather, and terrycloth all provide some protection from cuts. However, products which have been designed for use in a work environment where there is a high potential for laceration must offer a very high level of cut resistance in order to provide maximum protection. Examples of these work environments are places where the hand can come into contact with very sharp edges; knife blades, broken glass, sheet metal, injection molded plastics, paper and even other fibers. The natural lubricity of high density polyethylene used to make the HPPE fibers facilitates a sliding action of knife blades and other sharp edges across the fiber.

Downloaded by CORNELL UNIV on August 6, 2012 | http://pubs.acs.org
Publication Date: April 3, 1991 | doi: 10.1021/bk-1991-0457.ch013

Downloaded by CORNELL UNIV on August 6, 2012 | http://pubs.acs.org
Publication Date: April 3, 1991 | doi: 10.1021/bk-1991-0457.ch013

Table I.

HIGH PERFORMANCE FIBER PROPERTIES

	HPPE	ARAMID			
	Spectra 1000	HM	UHM*	S-Glass	Graphite HM
PROPERTY					
Density	0.97	1.44	1.47	2.49	1.86
Elongation %	2.7	2.5	1.5	5.4	0.6
Tensile Strength, 10 exp 3 psi	435	400	500	665	375
Specific Strength 10 exp 6 psi	12.4	7.8	9.5	7.4	5.4
Tensile Modulus, 10 exp 6 psi	25	19	25	13	57
Specific Modulus, 10 exp 6 psi	714	365	480	140	850

* Kevlar 149 - Epoxy Impregnated Strand

SOURCE: Reproduced with permission from ref. 1. Copyright 1988 Allied-Signal.

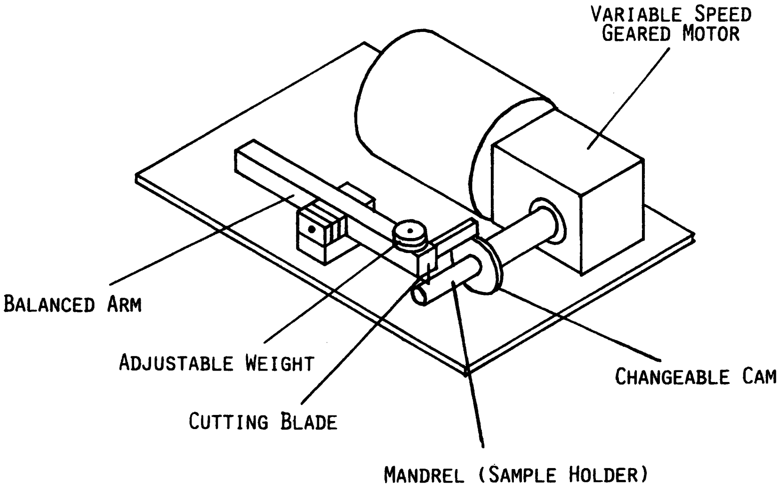
VARIABLE SPEED GEARED MOTOR
BALANCED ARM
ADJUSTABLE WEIGHT
CUTTING BLADE
CHANGEABLE CAM
MANDREL (SAMPLE HOLDER)

Figure 2. The Beta Tec Automatic Abrasion and Cut Tester. (Allied-Signal.)

The natural lubricity of HPPE fibers also makes a significant contribution to the fiber's high abrasion resistance.

HPPE fiber has a white hygienic appearance which, for aesthetic as well as practical reasons, makes it a good choice for food processing or food contact. Because of the fiber's good chemical resistance, gloves made from HPPE fiber do not stain readily and can be easily cleaned, usually with warm water and mild detergent. For food processing the ability to disinfect the gloves is especially important. HPPE fiber's chemical resistance properties allow the use of a variety of disinfectants including bleach in preparing the gloves for reuse. See Table II for HPPE fibers chemical resistance properties. HPPE fibers have a very low moisture absorption (less than 2%) which allows the gloves to be air dried. The fiber's low moisture absorption also reduces the probability of bacterial growth on the fiber surface. Other fibers such as nylon and aramid which are used in cut protective gloves have much higher moisture absorptions on the order of 5% or more.

Because the HPPE fiber glove is more flexible, the user's fingers will not cramp or fatigue as easily as is the case with other less flexible cut protective gloves. The increased flexibility available with gloves made from HPPE fiber can be helpful in reducing worker fatigue and skin irritation. These problems can be the result of using gloves made from abrasive or harsh materials such as metal mesh.

The yarns used to make most cut and slash resistant gloves may be composed of several different fibers or smaller yarns. Highly cut resistant yarns, in many cases, are actually composite yarn structures. In a composite yarn the individual yarns or fibers are combined by twisting, plying, or over wrapping to produce a single highly cut resistant yarn. By combining different fiber types it is possible to increase the performance of the finished yarn. One way of improving the cut resistance of the composite yarns is by constructing the yarn so that it will microscopically alter the cutting edge that contacts the yarn. Past experiments on cutting human skin showed that even microscopic dulling of the cutting edge will significantly reduce the ability of the blade to cut.(3) Several methods can be used to induce the microscopic dulling of the cutting edge. Two of the most common are combining the fibers in the composite yarns with either steel monofilament wire or multi-filament glass fiber. It is important to note that the steel or glass alone would not make very effective cut resistant gloves because the steel wire would not be flexible or strong enough to survive the knitting process and the glass fiber would fracture during knitting. Also, the glass

Downloaded by CORNELL UNIV on August 6, 2012 | http://pubs.acs.org
Publication Date: April 3, 1991 | doi: 10.1021/bk-1991-0457.ch013

Downloaded by CORNELL UNIV on August 6, 2012 | http://pubs.acs.org
Publication Date: April 3, 1991 | doi: 10.1021/bk-1991-0457.ch013

Table II.

CHEMICAL PROPERTIES

	% Strength Retention After 6 Months Immersion	
AGENT	Spectra 900	Aramid
Sea Water	100	100
10% Detergent Solution	100	100
Hydraulic Fluid	100	100
Kerosene	100	100
Gasoline	100	93
Toluene	100	72
Perchlorethylene	100	75
Glacial Acetic Acid	100	82
1M Hydrochloric Acid	100	40
5M Sodium Hydroxide	100	42
Ammonium Hydroxide (29%)	100	70
Hypophosphite Solution (10%)	100	79
Clorox	91	0

Immersed in various chemical substances for a period of 6 months, HPPE fibers retained their original strength.

SOURCE: Reproduced with permission from ref. 1. Copyright 1988 Allied-Signal.

fiber glove would have poor abrasion resistance and a bad hand. Combining different materials in the composite yarn produces a synergistic effect which makes the composite yarn much more cut resistant than its components.

Gloves made from the highly cut resistant yarns are made possible by the invention of computer-controlled knitting machines. This type of knitting machine can knit a seamless glove automatically. In addition to the speed at which the machine can knit, the computer allows tremendous flexibility in the set up and production of many different types of gloves. The knitting machine can be set up to knit tubes with elastic cuffs at the wrist and tube end. These tubes can be worn on the arm or legs to provide these areas of the body with a high level of protection from accidental cuts and slashes.

Downloaded by CORNELL UNIV on August 6, 2012 | http://pubs.acs.org
Publication Date: April 3, 1991 | doi: 10.1021/bk-1991-0457.ch013

Protective Sweater. A further development which exploits the technology used in the cut resistant gloves as well as the abrasion and cut resistant properties of HPPE fibers is a knitted sweater for motorcycle riders. The HPPE yarn used in the cut and slash resistant sweater is essentially the same yarn which is used in the cut resistant gloves. An important difference between the sweater yarn and glove yarn is that the outside of the sweater yarn is over wrapped with nylon or polyester. Using the nylon or polyester yarn in the outer cover allows the yarn to be dyed. Because of the chemical inertness of HPPE fiber it is almost impossible to dye. A leather jacket will scrape, cut and wear out with relative ease. However, the sweater made from HPPE fiber offers a significantly higher level of cut, slash and abrasion protection and is much more durable. (4) Another advantage of the construction of the sweater is that the garment is comfortable because the knitted construction allows better air circulation through the garment than is possible with a leather jacket. This is particularly important in areas where it is hot and humid such as the South and West. A leather jacket would likely not be worn when it is hot or humid because it would be uncomfortable. The sweater made from HPPE fibers could be worn because it would breathe and therefore be more comfortable. A final advantage that the sweater made from HPPE fiber offers is ease of care because it can be washed rather than dry cleaned.

The HPPE fiber sweater may also find application in law enforcement or police work. The sweater would be particularly useful where the need for protection from knife cuts or slashes is greater than the threat from bullets. The knitted fabric is effective at protecting against cuts and slashes, however, the sweater fabric would be ineffective against puncture threats such as knife stabs because of the open nature of the knitted construction.

Downloaded by CORNELL UNIV on August 6, 2012 | http://pubs.acs.org
Publication Date: April 3, 1991 | doi: 10.1021/bk-1991-0457.ch013

Medical Glove Liner. Another glove application where HPPE fiber is uniquely suited is in the medical field. The need has never been more acute for better forms of hand protection for health care professionals. In the past, the main reason for using sterile gloves and clothing was to protect the patient from the doctor. Today, this situation is, in many cases, reversed. Because of Acquired Immune Deficiency Syndrome (AIDS) virus the need to protect the health care workers from the patient has become a major concern. The Center for Disease Control estimates that the number of diagnosed cases of AIDS will increase at the rate of 10,000 per year. By the end of 1992 over 365,000 cases of AIDS will have been diagnosed in the United States. (5) Another less well publicized, but far more prevalent threat to health care workers is the danger posed by other infectious diseases such as the Hepatitis B virus. The Occupational Safety and Health Administration estimates that approximately 300 health care workers die annually from Hepatitis B infections. (6) Many of these workers contract infectious diseases through cuts on their hands and fingers. Another route of infection is through accidental needle sticks. (6)

The first extra precautions taken by health care professionals against accidentally infecting themselves was to wear multiple pairs of latex rubber gloves.(7) Because of the increased use of the latex gloves, both the demand for the gloves and their price have risen dramatically. Ironically, the use of multiple pairs of latex gloves add only a minute amount of additional protection from accidental nicks and cuts. The ideal situation would be to provide a glove which would isolate the hands from the environment and at the same time protect the hands from accidental nicks and cuts. This ideal glove should interfere to the absolute minimum degree with the mobility and sensitivity of the fingers. (8) In addition, the glove should also be comfortable even after being worn for extended periods.

One of the first gloves which attempted to meet this difficult list of requirements was a light metal mesh glove made from very small chain mail. This glove afforded maximum protection from accidental nicks and cuts, but sacrificed tactile sensitivity. Also, the micro chain mail glove was very expensive.

With HPPE fibers it is possible to produce a glove liner which will meet most of the requirements set forth above. The HPPE fiber glove liner provides a high level of cut protection while affording enough tactile sensitivity to touch a quarter and determine by feel if the coin is heads or tails. The HPPE fiber glove liner is worn underneath the standard latex surgeon's glove and is over 30 times more cut resistant than the latex surgeon's glove and 15 times as cut resistant as a leather work glove. By making the glove liner separate from the latex glove, the glove liner can be reused. Tests have shown that the HPPE fiber glove liners can be sterilized for reuse up to twelve times without adversely effecting the glove liner's cut resistance. Unfortunately, the HPPE fiber glove liner, because of its knitted construction, does not provide protection from accidental needle sticks.

The HPPE glove liner has been tested in clinical trials and will soon be commercially available. In addition to the increased protection against accidental nicks and cuts, the surgical glove liner from HPPE fiber provides other benefits. During market evaluation trials, operating room personnel reported that the HPPE glove liners are warm and wick perspiration away from the skin, keeping the hands dry and comfortable. The glove liner can be worn with bleach sterilization or Dakins solution which some doctors and surgeons apply to their hands before putting on the latex glove. HPPE fiber gloves have been sterilized by a variety of methods such as ethylene oxide, radiation, and steam autoclave. When the sterilization process requires high heat it is important not to exceed 121°C (250°F) because of HPPE fiber's low melting temperature. A disinfectant solution made from 5% sodium hypochlorite can be used to disinfect the glove liner without effecting its cut resistant properties. It is recommended that the glove liners be air dried and never machine dried to insure that the fiber is never subjected to temperatures above 121°C (250°F).

Downloaded by CORNELL UNIV on August 6, 2012 | http://pubs.acs.org
Publication Date: April 3, 1991 | doi: 10.1021/bk-1991-0457.ch013

Chain Saw Cut Protection. Another type of protective clothing being developed from HPPE fibers is chain saw cut protective chaps. Early chain saw cut protective chaps were made with over 22 layers of ballistic nylon. Later chaps were produced with multiple layers of aramid material. The HPPE chaps are made from two layers of nonwoven fabric. The nonwoven fabric construction is capable of protecting the user from injury from chain saw cuts at chain speeds in excess of 3200 feet per minute.

Armor Systems

HPPE fibers because of their high strength to weight ratio, good energy absorption, and high modulus are a natural choice for ballistic protective clothing. HPPE fibers can be used in two types of ballistic armor systems. The first type of ballistic clothing, soft body armor, makes use of the high flexibility afforded by HPPE fibers. The second type of armor which exploits HPPE fiber's energy absorbing properties is hard composite armor.

Downloaded by CORNELL UNIV on August 6, 2012 | http://pubs.acs.org
Publication Date: April 3, 1991 | doi: 10.1021/bk-1991-0457.ch013

Soft Armor Systems. The earliest types of armor were generally made from hard rigid materials such as metals. Because of the hard and rigid nature of this type of armor it was assumed that the best method of protecting the human body from missiles was to use hard materials which resisted penetration and spread the impact load.(9) The idea of spreading the impact load was correct, however the use of a hard rigid material as the primary protective layer proved to be undesirable. A hard, rigid material alone does not make efficient use of an effective method of energy dissipation, namely material deformation and breakage.(9)

One of the major factors in armor design after performance is comfort. The three factors which seem to have the greatest influence on the comfort of an armor system are weight, flexibility, and breathability. Metal armor is deficient in all three areas. With the invention of synthetic fibers great improvements in armor design have been possible. The first large scale use of synthetic fibers in armor systems was woven nylon 6,6 used in combination with steel plates to produce "Flak Jackets" during World War II.(9) The next improvement came when glass fiber and resin composite armor called Doron replaced the steel plates.(9) Aramid fibers provided a quantum leap in armor system technology because of their balance of physical properties. Aramid armor systems perform well, however with the invention of HPPE fibers, further improvements in the form of significant weight reductions and increased ballistic performance are possible.

Because of the superior strength to weight ratio of HPPE fibers it is possible to produce armor systems which provide protection equivalent to other armor systems but at a lower weight, or alternatively a significantly higher level of protection at the same weight. The low denier (a measurement of linear density) of the HPPE yarns and the fiber's natural lubricity combine to produce fabrics which can be made into lightweight, flexible ballistic armor. Ballistic protective products made from HPPE fibers are superior in comfort when compared to many other types of ballistic armor. The increased comfort of HPPE armor encourages its continuous use on a routine basis. No matter how good an armor system is it can not provide protection if it is too uncomfortable to be worn.

The chemical resistance of the HPPE fibers again is an advantage for military body armor. Chemical resistance is important if the armor is exposed to chemical agents, especially the type used in decontamination during chemical or biological warfare.

In a typical ballistic vest the ballistic resistance is obtained by using multiple layers of woven fabric. The number of layers necessary is determined by the level of the threat which must be stopped. The higher the threat, the greater the number of fabric panels required to defeat it. Fabric construction and yarn size also influence the ballistic performance of the armor system. Conventional fabric constructions utilizing high performance fibers can be penetrated by ballistic projectiles when the yarn in the projectile path is pushed aside without ever fully engaging the projectile. This phenomena is dependent on several factors such as projectile velocity, yarn to yarn friction, projectile to yarn friction, projectile shape, and fabric construction. To fully utilize the ballistic defeating potential of HPPE fibers it is important that projectiles not penetrate the fabric simply by pushing the fibers out of the way. The tendency of the projectiles to slide between the fibers can be reduced by using lower denier yarns.

Fabric construction is another factor which effects the ability of the projectile to engage the fibers. Plain weaves perform better than satin weaves because the plain weave minimizes the lateral movement of the yarn.(10) Therefore, layers of plain weave fabrics made from lower denier yarns provide better ballistic protection at the same weight than a comparable system of plain weave fabrics made from larger yarns.

To optimize the ideas of decreasing yarn size and reduced yarn mobility a nonwoven 0°, 90° HPPE fiber laminate bonded with an elastomeric resin was developed. The patented construction called Spectra Shield (a trade mark of Allied-Signal) is the strongest, lightest weight ballistic armor in the world.(11) (Figure 3.) By laying two sheets of individual filaments perpendicular to each other and then locking the filaments in place with the elastomeric resin the maximum number of filaments are available to engage the projectile upon its initial contact with the panel. The unidirectional construction does not require the fibers to overcome the built in crimp associated with yarns in a woven structure. Another advantage of the unidirectional construction of Spectra Shield it that it efficiently disperses blunt trauma and minimizes its effects. Damage incurred is localized which results in good multiple hit performance.

The advantages of the unidirectional construction are not in its performance alone. The process for manufacturing The 0°, 90° unidirectional laminates reduces fiber handling such as twisting and weaving which minimizes fiber damage incurred during manufacture. The 0°, 90° laminates of HPPE fiber are available in two forms: with a film covering for soft body armor and without the film for hard composite armor.(11) (Figure 4.)

The ballistic performance of HPPE fiber is not effected by long term exposure to temperatures as high as 71°C (160°F). HPPE fiber test panels have been kept at 71°C (160°F) for over 60 days and ballistically

Downloaded by CORNELL UNIV on August 6, 2012 | http://pubs.acs.org
Publication Date: April 3, 1991 | doi: 10.1021/bk-1991-0457.ch013

Downloaded by CORNELL UNIV on August 6, 2012 | http://pubs.acs.org
Publication Date: April 3, 1991 | doi: 10.1021/bk-1991-0457.ch013

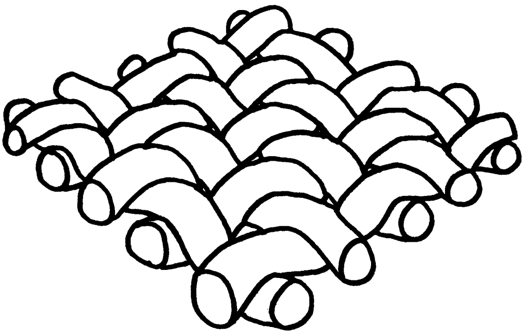

WOVEN FABRIC

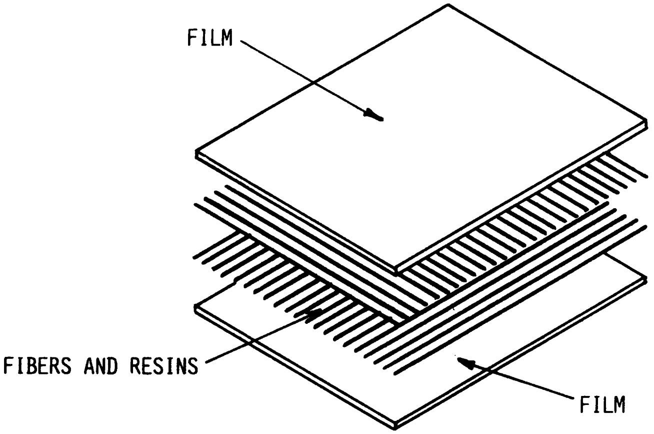

SPECTRA SHIELD

Figure 3. Conventional Fabric compared to Spectra Shield. (Reproduced with permission from ref. 11. Copyright 1989 Allied-Signal.)

Downloaded by CORNELL UNIV on August 6, 2012 | http://pubs.acs.org
Publication Date: April 3, 1991 | doi: 10.1021/bk-1991-0457.ch013

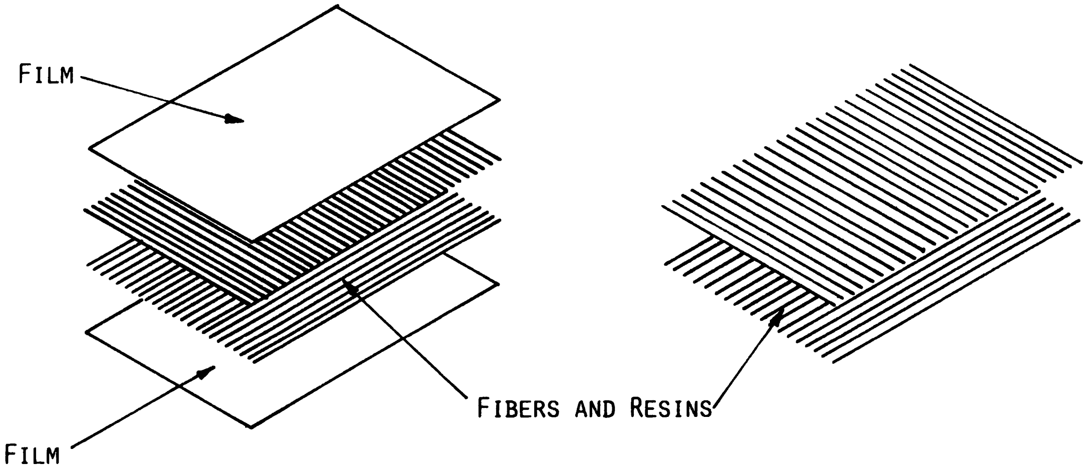

SPECTRA SHIELD SINGLE ELEMENTS
FOR SOFT BODY ARMOR

SPECTRA SHIELD PRECONSOLIDATED
ROLLS OF UNIDIRECTIONAL FIBERS
FOR MOLDING HARD ARMOR

Figure 4. Spectra Shield Products. (Reproduced with permission from ref. 11. Copyright 1989 Allied-Signal.)

Table III. Effect of Temperature on Ballistic Performance of HPPE composite armor

Temperature°C	V50 (m/sec)
23	604.7
80	594.7
100	593.4
120	558.7

Fiber SPECTRA 900, AD = 4.4 ADT = 6.0 matrix Airflex 105 an ethylene-vinylacetate copolymer, a product of Air Products and Chemical Inc.

SOURCE: Reproduced with permission from ref. 11. Copyright 1989 Allied-Signal.

Downloaded by CORNELL UNIV on August 6, 2012 | http://pubs.acs.org
Publication Date: April 3, 1991 | doi: 10.1021/bk-1991-0457.ch013

tested at ambient temperature with no loss in performance. (Figure 5.) When the panels were tested at elevated temperature a slight decrease in performance of approximately 8 % at 120°C (250°F) was measured. (Table III.) From Figure 5 it can be seen that for most practical applications variation in ambient temperature will not adversely effect the performance of the HPPE fiber ballistic armor.(11)

Hard Composite Armor Systems. Hard armor is possibly the oldest type of ballistic protective clothing. When one hears the term armor, a hard protective casing is what usually comes to mind. Modern hard armor is much more sophisticated than earlier metal armors. Most modern hard armor is usually composed of several different materials which are organized in a complex series of layers. For protective clothing the most common type of hard armor is used in helmets. Another less well known application of hard armor technology is in the supplementation of flexible armor systems used to protect against critical threat situations such as high powered ammunition or in bomb disposal.

The high strength to weight ratio, toughness, and ultra high modulus of HPPE fibers allows them to provide a high level of ballistic and impact protection at a lower weight than is possible with many other materials. The lower weight of HPPE armor systems, especially in helmets, can significantly reduce wearer fatigue. Even a small reduction of the weight of the helmet allows the wearer to concentrate more on the surrounding situation and less on how heavy and uncomfortable the helmet is. Composite armor produced from HPPE fibers weighs 30 % to 50 % less than for the same performance level as aramid monolithic composite armor.(12) (Figure 6.)

One application which has benefited immensely from the introduction of HPPE fibers is the police riot helmet. Before availability of HPPE fibers standard riot helmets were made from a fiber glass and epoxy composite. This construction was much heavier than the

Downloaded by CORNELL UNIV on August 6, 2012 | http://pubs.acs.org
Publication Date: April 3, 1991 | doi: 10.1021/bk-1991-0457.ch013

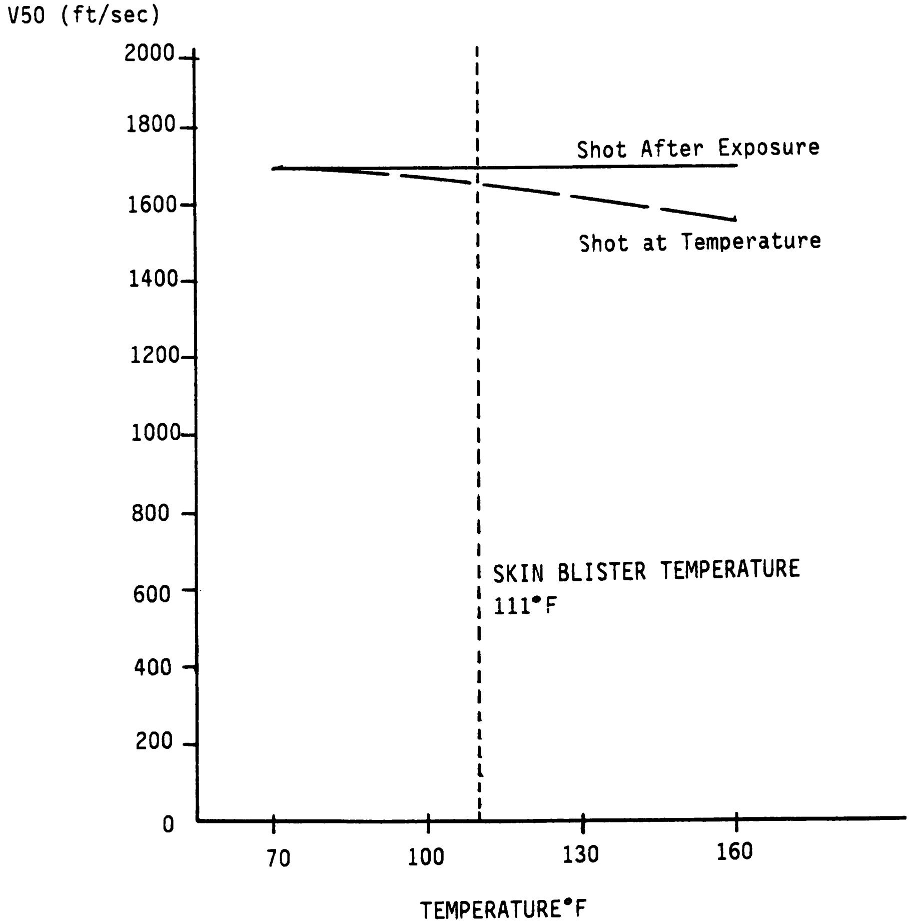

Figure 5. Ballistic Performance V 50 vs. Temperature. (Reproduced with permission from ref. 11. Copyright 1989 Allied-Signal.)

Downloaded by CORNELL UNIV on August 6, 2012 | http://pubs.acs.org
Publication Date: April 3, 1991 | doi: 10.1021/bk-1991-0457.ch013

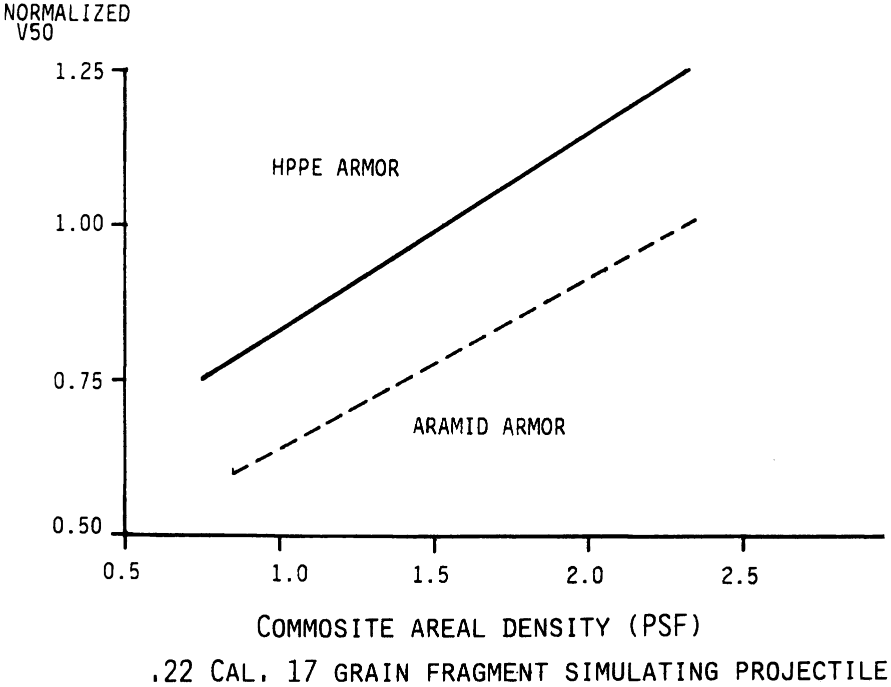

Figure 6. Ballistic Performance of High Performance Polyethylene vs. Aramid composites. HPPE is Spectra 1000 and Aramid is Kevlar 29. (Reproduced with permission from ref. 12. Copyright 1989 Allied-Signal.)

same helmet reinforced with HPPE fibers. A fiber glass riot helmet provides little, if any, ballistic protection. The use of aramid fibers was explored, but they were found to be too heavy. The new riot helmet made with HPPE fibers is lighter weight than the glass fiber or aramid fiber riot helmet. Even at the lighter weight the HPPE fiber helmet provides ballistic protection and superior impact performance.(13)

Combat helmets for military use may also benefit from the use of HPPE fibers. The standard aramid combat helmet currently made from Kevlar 29 weighs three pounds. A combat helmet being developed from HPPE fibers will weigh slightly over two pounds.(13) Decreasing the weight of tactical armor reduces fatigue and increases mobility which translates into a higher probability of survival.

Hard composite armor from HPPE fibers can be produced by a variety of methods. The matrix systems can be epoxy, vinyl ester, polyester, or latex resin. The fiber reinforcement can be provided by either woven fabrics or the 0°,90° unidirectional laminates. The unidirectional laminates without the polyethylene film are used which allows the individual laminate layers to be consolidated using heat and pressure. Another advantage to the HPPE fiber unidirectional prepreg system is that it is moldable which makes manufacture of some types of armor easier. For HPPE fabrics the matrix material can be applied either by wet lay up or the fabric can be preimpregnated with matrix for later use. Again the various layers of material are consolidated using heat and pressure.(14)

Earlier it was stated that the poor fiber to matrix adhesion was a disadvantage for HPPE fibers. For composite armor systems the low level of fiber to matrix adhesion is actually an advantage. This is because the low level of fiber to matrix adhesion allows the dissipation of the impact energy by the breaking of the fiber to matrix interface. The performance of HPPE hard armor against .22 caliber fragment simulating projectiles is shown in Figure 7. The protection afforded by HPPE armor against some common hand gun and rifle ammunition is shown in Table IV. The amount of the HPPE fiber reinforced hard armor required to defeat the threat at the given velocity is shown in pounds per square foot. For comparison purposes 11 pound per square foot dual hardened steel or 9 pound per square foot aramid composite armor is required to defeat the 7.62 M-80 ball round.(14)

Where the ballistic threat possesses high kinetic energy or is a hardened armor penetrating projectile it may be necessary to combine the HPPE armor with a suitable hard "strike face". The type and amount of the high hardness material required is heavily dependent on the type of threat which must be defeated. Use of HPPE

Downloaded by CORNELL UNIV on August 6, 2012 | http://pubs.acs.org
Publication Date: April 3, 1991 | doi: 10.1021/bk-1991-0457.ch013

Downloaded by CORNELL UNIV on August 6, 2012 | http://pubs.acs.org
Publication Date: April 3, 1991 | doi: 10.1021/bk-1991-0457.ch013

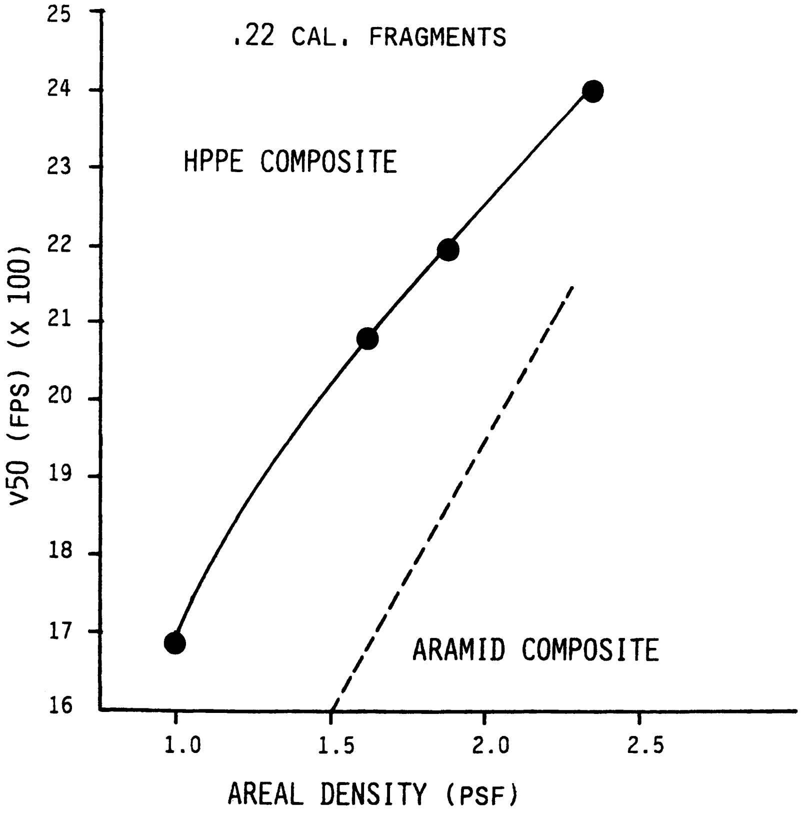

Figure 7. Normalized V 50 ballistic performance of High Performance Polyethylene and Aramid composites. HPPE is Spectra 1000 and Aramid is Kevlar 20. (Reproduced with permission from ref. 15. Copyright 1988 Allied-Signal.)

fiber for the backing of the armor system can reduce the over all weight of the system. To improve the performance of soft body armor, panels of the HPPE fiber composite armor can be added to augment the protection of the vital areas such as the chest. Again, the amount of HPPE composite armor required depends on the type threat to be defeated.

Table IV. HPPE Composite Armor Areal Densities to Defeat Common Ballistic Threats

Threat Description	Velocity (fps)	Nominal Weight (psf)
9 mm Full Metal Jacket	1450	0.8
5.56 mm M-193 ball	3250	4.0
7.62 mm M-80 ball	2750	4.75
7.62 mm AK-47 Steel Core	2400	5.25

SOURCE: Reproduced with permission from ref. 12. Copyright 1989 Allied-Signal.

Because the elevated temperature performance of HPPE fiber rigid composite armor systems may be cause for concern an evaluation of the armor performance was conducted. The HPPE fiber and latex matrix system was used to fabricate five identical panels which were heated to the test temperature and held there for one hour. The panels were tested with the results shown in Table V and plotted in Figure 8. Again armor from HPPE fiber can perform at elevated temperature without a significant loss in ballistic performance.

In addition to the ballistic applications of HPPE fiber in hard armor there are many non ballistic sporting applications of the technology such as protective head gear. Many of the requirements for the sporting applications may not be as critical as the ballistic armor requirements; however, a high level of impact protection at a low weight is desirable. HPPE fibers can easily meet the requirements when used as the reinforcement in these helmets. Helmets for almost every sporting application are being investigated. To date helmets or prototypes have been tested in applications such as: racing crash helmets, polo helmets, rock climbing helmets and white water helmets.

Conclusion

The versatility of HPPE fibers has been demonstrated by the range of applications in which the fiber is finding use. However, for many applications no single fiber by itself can meet all of the requirements. Every high performance fiber has at least one property where its performance is weak. Means must be devised to minimize the fiber's weak areas and still obtain maximum performance.

Downloaded by CORNELL UNIV on August 6, 2012 | http://pubs.acs.org
Publication Date: April 3, 1991 | doi: 10.1021/bk-1991-0457.ch013

Downloaded by CORNELL UNIV on August 6, 2012 | http://pubs.acs.org
Publication Date: April 3, 1991 | doi: 10.1021/bk-1991-0457.ch013

Table V.

HPPE COMPOSITE BALLISTIC RESISTANCE AT ELEVATED TEMPERATURE

Prepreg:	HPPE / Latex
Resin:	Latex
Fabric:	Spectra 1000, 650 d, 34X34 Plain Weave, Treatment B
Fiber Weight Fraction:	92%
Number of Layers:	34
Areal Density:	1.54 lbs/square foot
Fabrication Conditions:	225 F, 20 Minutes, 176 PSI
Threat:	.22 cal. Fragment, 17 Grain

Temperature (F)	V50 (FPS)	% Loss
70 (Room Temp.)	2052	Control
150	2008	2.14
180	1972	3.90
212	1968	4.09
230	1951	4.92

A thermocouple was embedded at the center ply of the laminate. The panels were conditioned one hour in an oven at each test temperature.

SOURCE: Reproduced with permission from ref. 15. Copyright 1988 Allied-Signal.

Downloaded by CORNELL UNIV on August 6, 2012 | http://pubs.acs.org
Publication Date: April 3, 1991 | doi: 10.1021/bk-1991-0457.ch013

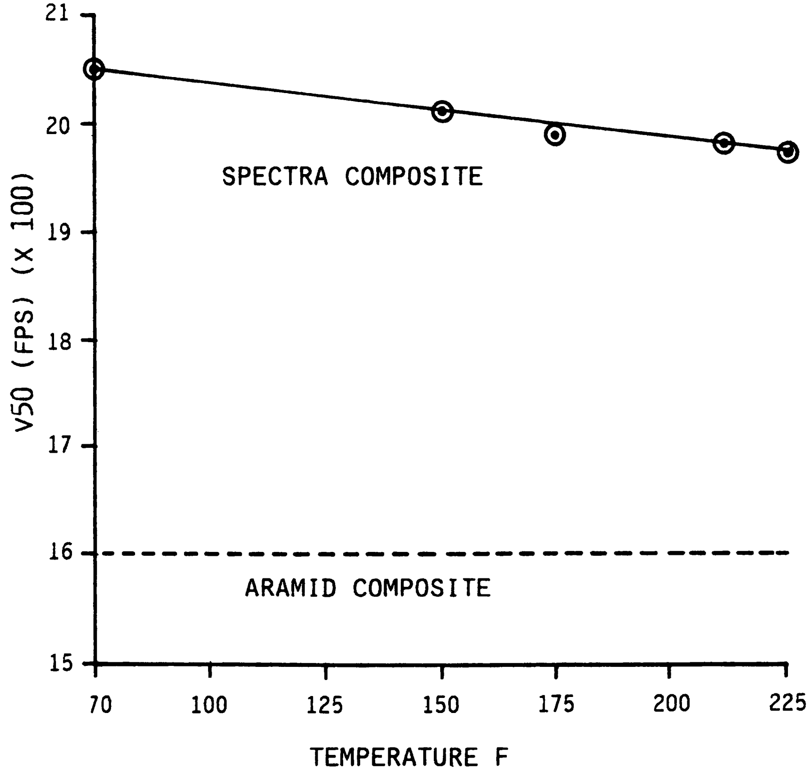

AREAL DENSITY 1.54 POUNDS PER SQUARE FOOT

Figure 8. High Performance Polyethylene composite ballistic resistance at elevated temperature. HPPE is Spectra 1000 and Aramid is Kevlar 29. (Reproduced with permission from ref. 15. Copyright 1988 Allied-Signal.)

Improvements in the performance of products such as protective clothing which are made from high performance fibers can come from two areas. First, the search for the ideal "Super Fiber" which can meet all requirements can continue. Second, a more realistic and immediate solution can be found in hybridization of the various fibers and materials. This is an approach which has been used very successfully in the past. The same methods show great promise for the latest group of high performance fibers. It would probably be accurate to say that fourth generation protective clothing will not be composed of a single type of fiber, but be a highly engineered and complex marriage of several different fibers and materials.

Literature Cited

1. D.S. Cordova, D.S. Donnelly, Spectra Extended Chain Polyethylene Fibers. Allied-Signal. c. 1988 p.1
2. David C. Bennett, Health and Safety at Work, "Hand Protection" May 1981. p.32.
3. John R. Sorrells, et al. Some Cutting Experiments on Human Skin and Synthetic Materials. National Bureau of Standards, Washington, D.C. October 1973. p.17.
4. Kaleidoscope, Winter 1988, Issue 3, Vol. 3, Allied-Signal. c. 1989. p.3.
5. Center for Disease Control Outlook on AIDS. Chemical Week, June 7, 1989 p.44
6. New Products to Prevent Accidental Needle Sticks, Sunday New York Times, March 27, 1988.
7. Peter Truell, "Demand for Rubber Gloves Sky Rockets" The Wall Street Journal. Thursday June 9, 1988. p.6.
8. H.M. Taylor, "Gloves" Textiles. Vol 18. no. 1982. p.20.
9. T.A. Abbott. "Ballistic Protective Clothing" Shirley Publication. S 45 p.41.
10. D.C. Prevorsek, et al. "Ballistic Armor from Extended Chain Polyethylene Fibers" Allied-Signal. c.1989. p.1.
11. Ballistic Applications of Flexible Spectra Products. Allied-Signal. c.1989. p.1.
12. Rigid Composite Armor Performance and Applications. Allied-Signal. c.1989. p.4.
13. Kaleidoscope. Vol.2 no.2 Summer 1987. Allied-Signal. c.1987. p.2.
14. Rigid Composite Armor Performance and Applications. Allied-Signal. c.1989. p.2.
15. L. C. Lin et al., "Ballistic Performance of Lightweight Spectra Composite Hard Armor." c.1988 Allied-Signal. pp.3-5.

RECEIVED July 16, 1990

Downloaded by CORNELL UNIV on August 6, 2012 | http://pubs.acs.org
Publication Date: April 3, 1991 | doi: 10.1021/bk-1991-0457.ch013

Downloaded by NORTH CAROLINA STATE UNIV on August 6, 2012 | http://pubs.acs.org
Publication Date: April 3, 1991 | doi: 10.1021/bk-1991-0457.ch014

Chapter 14

Polybenzimidazole Blends in Protective Apparel

Nona Fahl and Marian Faile

PBI Products Division, Hoechst Celanese Corporation, 2300 Archdale Drive, Charlotte, NC 28210

This paper describes the spectrum of protection available by blending Hoechst Celanese PBI fiber with aramid fibers such as Kevlar and Nomex. Vertical flammability, dynamic flame testing, and gas pit exposures are included to characterize the levels of protective performance of PBI blends for specific end-use requirements. Testimonials confirm the improved comfort and reduced heat stress of PBI blend garments in industrial and fire fighting applications. The importance and development of improved, dynamic, testing techniques are highlighted as key elements in demonstrating unique PBI contributions such as improved comfort and maintenance of fabric integrity after thermal exposure.

The commercial introduction of polybenzimidazole (PBI) fiber in 1983 offered an opportunity for advanced developments in high performance fiber products. PBI or poly[2,2'-(m-phenylene)-5, 5'-bibenzimidazole] is an inherently flame-resistant fiber (1). PBI staple fiber, manufactured by Hoechst Celanese in Rock Hill, South Carolina, offers the following unique properties: 1) Does not burn in air; 2) Remains dimensionally stable at high temperatures; 3) Does not melt or drip; 4) Remains supple even when charred; 5) Has excellent resistance to chemicals and solvents; 6) Provides excellent comfort due to high moisture regain; 7) Processes well on conventional textile equipment.

When blended with other high performance fibers, PBI contributes unique thermal, chemical, and textile properties necessary in critical end-use applications. The blending of PBI with other fibers creates synergies when the flame resistance and comfort of PBI are optimized. PBI's unique contributions are evident in aircraft fire blocking, where PBI blends have captured

0097–6156/91/0457–0238$06.00/0

In High-Tech Fibrous Materials; Vigo, T., et al.;
ACS Symposium Series; American Chemical Society: Washington, DC, 1991.

50% of the market due to flame resistance and durability. The safe egress of passengers from the recent airplanes crashes is an example of the valuable contribution of enhanced flame performance. In fireman's turnout gear, PBI blends are recognized as the state-of-the-art thermal protection.

PBI's fiber properties allow fabric development for comfortable, durable, garments with excellent protection from heat and flame. PBI has unique thermal and textile fiber characteristics, outlined in Table I. Design options include protective fabrics in knitted, woven, needlepunched, and hydroentangled, nonwoven constructions. In each construction, blend ratios are optimized for critical end-use requirements. In blends with other high temperature fibers, PBI's unique properties contribute to significant improvements in protection.

Table I. Physical Properties of Hoechst Celanese PBI Fiber

Property	Value (Metric)
Denier per filament	1.5 denier (1.7 denier tex)
Tenacity	2.7 g/denier (2.4 dN/tex)
Breaking elongation	28%
Density	1.43 g/cm^2
Moisture regain, 25°C, 65% RH	15%
Hot air shrinkage, 204°C	< 1%
Limiting oxygen index	41%

In addition to PBI's thermal stability and flame resistance, PBI fibers exhibit outstanding resistance to solvents, acids, fuels, and steam. Table II illustrates the tensile strength retained following immersion in organic chemicals at 86°F for 168 hours. Furthermore, PBI fiber retains 96% of its original breaking strength after a 72-hour exposure to steam hydrolysis at 300°F and 67 psi. PBI also exhibits excellent resistance to inorganic acids and bases. PBI retains 90% of its original breaking strength following a 24-hour exposure to 50% sulfuric acid vapors at 160°F. The excellent resistance to hydrocarbons is essential in the industrial environment of gas and oil workers. PBI blends are engineered to offer chemical resistance suitable for critical end-use applications.

Table II. PBI Tensile Strength After Immersion in Organic Chemicals

Compound	Tensile Strength Retained
Acetic Acid	100
Methanol	100
Acetone	100
Kerosene	100
Dimethylformamide	100

Downloaded by NORTH CAROLINA STATE UNIV on August 6, 2012 | http://pubs.acs.org
Publication Date: April 3, 1991 | doi: 10.1021/bk-1991-0457.ch014

PBI Blends in Protective Coveralls

The exceptional thermal, chemical, and textile properties make PBI blends an excellent candidate for industrial protective apparel. Blend and fabric design engineering have identified optimum fabrics for comfort, durability, and protection for high risk industrial end-uses. A comparison of thermal and physical properties of industrial coveralls provides a spectrum to identify performance attributes and improvements PBI blends offer for the most critical industrial environments. Table III characterizes fabrics included in the study.

Table III. Protective Industrial Coverall Candidates

Fabric	Construction	Weight(ounces/yd^2)
40/60 PBI/HS Aramid	2X1 Twill	4.5
20/80 PBI/Aramid	Plain weave	4.5
50/50 FR Polyester /Cotton	Plain weave	6.0
100% Aramid	Plain weave	6.0
100% FR Cotton	Sateen	9.0

These fabrics have been selected due to their current availability in industrial protective coveralls. The aramid and PBI blends are inherently flame resistant fibers, while the FR cotton and polyester/cotton have been chemically treated to be flame resistant. PBI blends included have been engineered to optimize performance characteristics for protection above that historically available. A format of standard and engineered test evaluations is designed to evaluate the thermal and flame resistance properties of the coveralls. Flammability test results serve as a means for comparison but, due to the uniqueness of any actual fire scenario, cannot warrant any guarantees. The data presented is therefore an assessment of performance in specific, controlled tests.

Vertical Flammability Testing

Vertical flammability testing measures the amount of flame propagation and char formation characteristics of a fabric (2). Testing consists of a 12-second burn using a specified gas mixture with BTU content of 540 Btu's per cubic foot. After flame, afterglow, and char length are reported. Char length measurements reflect the tear length of the sample when specified weights are suspended on the burned specimen. In this manner, the vertical flammability also reflects the degree of char integrity. As Table IV indicates, the addition of PBI reduces the char length by minimizing the flame spread and increasing the integrity of the char. The fabrics severely weakened by the the flame contact report longer tear lengths than the PBI blends. None of these coverall fabrics exhibited after flame.

Downloaded by NORTH CAROLINA STATE UNIV on August 6, 2012 | http://pubs.acs.org
Publication Date: April 3, 1991 | doi: 10.1021/bk-1991-0457.ch014

Downloaded by NORTH CAROLINA STATE UNIV on August 6, 2012 | http://pubs.acs.org
Publication Date: April 3, 1991 | doi: 10.1021/bk-1991-0457.ch014

Table IV. Vertical Flammability (FTMS-5903)

Fabric	Tear Length(in)
40/60 PBI/HS Aramid	0.8
20/80 PBI/Aramid	2.0
100% Aramid	2.6
50/50 FR Polyester/Cotton	4.6
100% FR Cotton	3.5

Just as vertical flammability testing highlights the PBI advantage of char formation and integrity, the Federal Test Method for High Heat Flux Contact focuses on the PBI fiber properties of dimensional stability during flame exposure and low heat shrinkage (3). The high heat flux contact test consists of two 12-second flame exposures using a Fisher burner and butane fuel. Measurements of after flame and percent consumed indicate the extent of flame propagation. Table V illustrates the performance of the coverall fabrics for high heat flux contact testing. The importance of dimensional stability and low flame shrinkage is critical in high heat flux testing due to the unrestrained position of the samples during flame exposure. The inherent PBI fiber properties of heat stability and low flame shrinkage become obvious benefits in PBI blends with other high temperature fibers. Blends of PBI/H.S. Aramid and PBI/Aramid exhibit little shrinkage and percent consumed values are less than half that of the Aramid, FR cotton, and FR polyester/cotton. The vertical and high heat flux contact burns indicate performance for small flames encountered in industrial applications. PBI, blended with other high temperature fibers, minimizes flame spread. Furthermore, these performance characteristics can be engineered into fabrics by the selection of PBI blend ratios for specific end-use requirements.

Table V. Flame Resistance: High Heat Flux (FTMS-5905)

Fabric	After Flame (sec)	Percent Consumed
40/60 PBI/HS Aramid	0	7
20/80 PBI/Aramid	0	14
100% Aramid	6	35
50/50 FR Polyester/Cotton	7	55
100% FR Cotton	0	31

Thermal Protective Performance

The Thermal Protective Performance tester (TPP) consists of two Meeker burners with a controlled fuel supply of propane and nine quartz tubes calibrated to supply a 50/50 radiant/convective heat source of 2.0 cal/cm^2-sec. A copper calorimeter placed behind the fabric measures the amount of heat passing through the samples and, utilizing the Stoll tissue tolerance model, a time to second degree burn prediction (4). Table VI illustrates the TPP values of the coverall fabrics. Fabric weight, thickness, construction, and insulative properties contribute to the thermal protective performance of a blend. In industrial coveralls, the protection predicted by the TPP test can indicate the amount of time workers have to escape from flame without receiving second degree burns.

Table VI. Thermal Protective Performance

	Weight (oz/yd^2)	TPP (cal/cm^2)	Exposed Fabric
40/60 PBI/HS Aramid	4.5	12.0	Supple
20/80 PBI/Aramid	4.5	13.0	Stiffened
100% Aramid	6.0	14.7	Brittle
50/50 FR Polyester/ Cotton	6.0	8.5	Weak, brittle
100% FR Cotton	9.0	10.2	Weak, brittle

The benefit of PBI is indicated in the amount of protection afforded by blending PBI at the 20% and 40% blend levels. While the FR cotton and FR polyester/cotton are 133% to 200% the weight of the PBI blends, the TPP values are lower. The aramid exhibits a TPP approximately 17% greater than the PBI blends, but also weighs 33% more than the PBI blends. Furthermore, the PBI blends maintain their fabric integrity and allow flexing after a 5-second TPP exposure.

The static nature of the TPP test does not allow for assessment of the char formation and the ability of the fabric to maintain its integrity and protection during periods of movement. To assess char integrity, samples were exposed to the Thermal Protective Performance heat source of 2.0 cal/cm^2-sec for 5 seconds. Using an Instron tensile tester, the burned samples are evaluated for residual grab strength (5). As indicated in Table VII, the characteristic supple char formation of the PBI fiber greatly increases the integrity of the char when blended with other high performance fibers. The 40/60 PBI/H.S. Aramid maintains fabric integrity and flexibility. The 20/80 PBI/Aramid sample is stiffened, but bends easily without cracking. The aramid, FR cotton, and FR polyester/cotton are severely weakened and easily crack open when bent offering no protection from additional flame exposure. Fabric char integrity is critical for emergency escape from flame without exposure of unprotected skin or flammable clothing. Small amounts of PBI fiber, blended with other high temperature fiber will substantially improve char integrity and protection from flame breakthrough in industrial coveralls.

Downloaded by NORTH CAROLINA STATE UNIV on August 6, 2012 | http://pubs.acs.org
Publication Date: April 3, 1991 | doi: 10.1021/bk-1991-0457.ch014

Table VII. Grab Strength Retained Following TPP Exposure

Fabric	Grab Strength Retained (%) 5 sec exposure
40/60 PBI/HS Aramid	28
20/80 PBI/Aramid	18
100% Aramid	8
50/50 FR Polyester/Cotton	0
100% FR Cotton	9

Downloaded by NORTH CAROLINA STATE UNIV on August 6, 2012 | http://pubs.acs.org
Publication Date: April 3, 1991 | doi: 10.1021/bk-1991-0457.ch014

Dynamic Flame Testing

The importance of char integrity and flame dimensional stability is further analyzed using the Hoechst Celanese Dynamic Flame Tester (Figure 1). The test unit consists of two Fisher burners supplied with natural gas. Flames are calibrated at 1600°F. Fabric samples are suspended vertically with a 1000-gram weight hanging on the lower edge of the sample. Burner position is adjusted horizontally and flame contact is initiated. Failure time is depicted as the time the fabric breaks under constant 1000-gram load. The 1000-gram weight is used on all samples regardless of fabric weight and depicts the fabric strain at elbows or knees during escape from flame. Table VIII illustrates failure time for protective coverall fabrics exposed to 1600°F flame under a constant load of 1000 grams. As exhibited in TPP strength retention testing, the PBI fiber properties of supple char formation and dimensional stability with flame exposure offer significant improvements when blended with other high performance fibers. In industrial coveralls, the dynamic flammability test indicates the integrity of the fabric during a flame exposure and therefore the time, under constant load, allowed for escape without encountering flame breakthrough and the subsequent burning of flammable clothing or exposed skin.

Table VIII. Dynamic Flame Test: Time to Failure

Fabric	Weight (oz/yd^2)	Failure Time (sec)
40/60 PBI/HS Aramid	4.5	51
20/80 PBI/Aramid	4.5	20
100% Aramid	6.0	6
50/50 FR Polyester/Cotton	6.0	3
100% FR Cotton	9.0	5

Gas Pit Testing

As a final assessment of coverall performance, a full scale mannequin test was designed using a 9 x 7 x 5 foot pit located at the Charlotte Police and Fire Training Academy. Located in the bottom of the pit is a 4-inch diameter natural gas pipe with a

Downloaded by NORTH CAROLINA STATE UNIV on August 6, 2012 | http://pubs.acs.org
Publication Date: April 3, 1991 | doi: 10.1021/bk-1991-0457.ch014

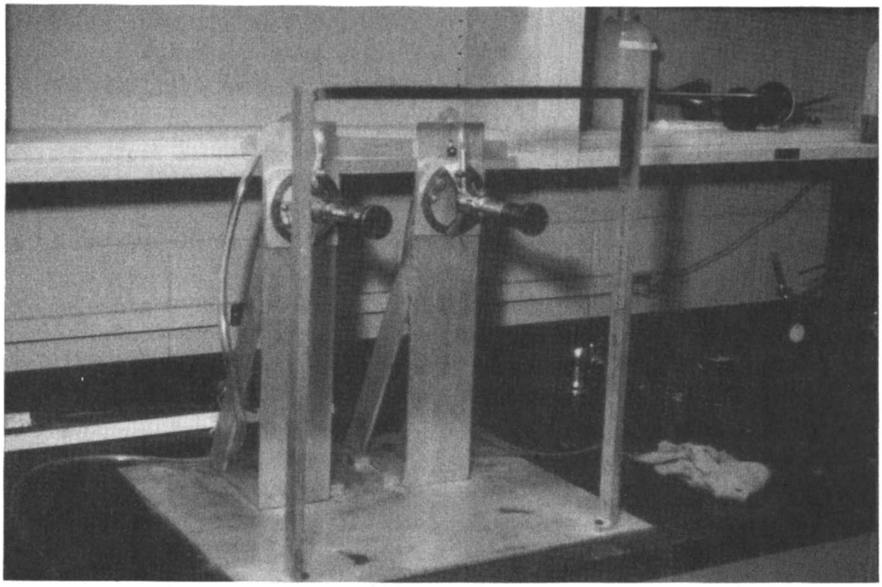

Figure 1. Hoechst Celanese Dynamic Flame Tester.

4-inch triangular gash on the top surface to simulate damage by a backhoe. Mannequins are dressed in cotton underclothes with temperature sensor tapes placed strategically over their bodies. Mannequins are then outfitted in denim jeans and a cotton work shirt, and dressed in protective coveralls. The gas pressure is set at 25 pounds per square inch. Mannequins are placed in the pit approximately two feet from the gas line rupture. Gas flow is initiated and ignites in a voluminous flame approximately 30 feet high. Gas flow ceases after 5 seconds, mannequins are extinguished and temperature sensors and garment damage assessed.

The gas pit test is designed to compare performance of industrial coveralls to actual conditions encountered by gas and oil workers. According to Alberta Occupational Health and Safety, the fireball temperatures exceed 2000°F. Under these conditions, all typical industrial clothing will ignite causing third degree burns. The burns are caused not from the direct flame contact, but from the clothing ignition. In our test sequence, the placement of the mannequin simulates a gas worker caught in a pit as the pipeline ruptures. The performance of protective coveralls in thermal protection and ignition resistance are assessed to predict the extent of the injuries each mannequin would sustain.

Combustion occurred on the FR cotton and FR polyester/cotton coveralls causing ignition of the work shirt and charring the undershirt. The aramid coveralls exhibit severe flame shrinkage and embrittlement. Flame shrinkage in the sleeves exposes the flammable work clothing resulting in ignition and increased body burns according to the temperature sensors. The PBI/aramid blend exhibits slight charring and stiffening of the coverall. Slight scorching is noted on the work shirt. The PBI/H.S. aramid exhibits little visible signs of flame contact. Slight scorching is evident on the work shirt and undershirt. Average temperature sensor readings are noted on Table IX. Little differences were noted in the temperature performance of the PBI blends. The stiffening of the PBI/Aramid creates an insulative air space minimizing temperature rise. The appearance of the PBI/Aramid and PBI/High Strength Aramid after flame exposure offers dramatic visual differences. The PBI/Aramid is stiffened and slightly charred. It is impossible to visually discern if the PBI/High Strength Aramid has been burned. PBI/High Strength Aramid coveralls washed and reburnt, exhibit no reduction in thermal performance.

Table IX. Gas Pit Mannequin Testing

Fabric	Average Temperature in Exposed Area (°F)
40/60 PBI/HS Aramid	135
20/80 PBI/Aramid	139
100% Aramid	174
50/50 FR Polyester/Cotton	178
100% Cotton	153
No coveralls: Flammable work clothing	215

Downloaded by NORTH CAROLINA STATE UNIV on August 6, 2012 | http://pubs.acs.org
Publication Date: April 3, 1991 | doi: 10.1021/bk-1991-0457.ch014

Downloaded by NORTH CAROLINA STATE UNIV on August 6, 2012 | http://pubs.acs.org
Publication Date: April 3, 1991 | doi: 10.1021/bk-1991-0457.ch014

The flammability testing format illustrates the enhanced flame performance at lower fabric weights possible by blending PBI fibers with other high performance fibers. In critical industrial applications, a greater level of protection can be derived by engineered blends to reduce ignition, increase char integrity, and reduce flame shrinkage. PBI fiber characteristics of supple char and low flame shrinkage translate into improved thermal performance when blended with other flame resistant fibers.

Comfort

Garment comfort is of critical importance in designing fabrics for industrial protective coveralls. Measurements of breathability, weight, stiffness, and moisture regain can offer insight into the comfort of a garment. Table X compares comfort determinants for coverall fabrics.

Table X. Comfort Determinants

Fabric	Weight (oz/yd^2)	Air Permeability (ft^3/ft^2-min)	Theoretical Moisture Regain (%)
40/60 PBI/HS Aramid	4.5	99	7.8
20/80 PBI/Aramid	4.5	72	6.3
100% Aramid	6.0	48	3.5
50/50 FR Polyester /Cotton	6.0	85	5.5
100% FR Cotton	9.0	47	8.0

Furthermore, the superior flame resistance offered by PBI allows blends to be engineered lighter in weight than other industrial apparel, without compromising the level of protection. The lighter weight and construction provide improved comfort and breathability. The high moisture regain of PBI fiber translates into improved moisture absorbancy of the fabric blend. Fabric drape, stiffness, and flexibility are illustrated by Handle-O-Meter Stiffness results on Table XI.

Table XI. Handle-O-Meter Stiffness

Fabric	Total Fabric Stiffness (grams/standard width)
40/60 PBI/HS Aramid	93
20/80 PBI/Aramid	71
100% Aramid	167
50/50 FR Polyester/Cotton	111
100% FR Cotton	145

The lighter weight PBI blends provide greater flexibility, breathability, and moisture absorbancy than the aramid, FR cotton, and FR polyester/cotton. These engineered blends have incorporated the unique textile properties of PBI fiber in optimum constructions and blend ratios for maximum comfort and protection.

Conclusions

PBI fiber offers a unique opportunity for enhanced engineering design options to improve the level of protection available in critical industrial end-use applications. The exceptional properties exhibited by PBI fiber such as chemical resistance, dimensional stability, low heat shrinkage, and supple char formation contribute significantly to improved protection when blended with other high performance fibers. PBI blends offer, in addition to enhanced thermal performance, comfortable, flexible garments.

Acknowledgments

Many people where involved in this endeavor: however, J. H. Boykin, J.A. Watts, and S. G. Koknat must be singled out for their contributions. The authors also acknowledge the support of management of PBI Products Division of Hoechst Celanese Corporation.

Literature Cited

1. "Properties of Polybenzimidazole High Performance Fiber," Technical Bulletin, Hoechst Celanese Corporation: Charlotte, NC, 1989.
2. *Federal Standard for Textile Test Methods*, Flame Resistance of Cloth; Vertical, Method 5903, General Services Administration, U.S. Government Printing Office: Washington, DC, 1978.
3. *Federal Standard for Textile Test Methods*, Flame Resistance of Material; High Flux Flame Contact, Method 5905, General Services Administration, U.S. Government Printing Office: Washington, DC 1978.
4. Stoll, A.M.; Chianta, M.A. *Aerospace Medicine*, 1969, *40*, 1232-1238.
5. ASTM, Standard Test Methods for Breaking Load and Elongation of Textile Fabrics, Designation D, 1682-64.

RECEIVED March 20, 1990

Downloaded by NORTH CAROLINA STATE UNIV on August 6, 2012 | http://pubs.acs.org
Publication Date: April 3, 1991 | doi: 10.1021/bk-1991-0457.ch014

American Chemical Society
Library
1155 16th St., N.W.
Washington, D.C. 20036

Downloaded by UNIV OF ARIZONA on August 6, 2012 | http://pubs.acs.org
Publication Date: April 3, 1991 | doi: 10.1021/bk-1991-0457.ch015

Chapter 15

A New Concept in Temperature-Adaptable Fabrics Containing Polyethylene Glycols for Skiing and Skiing-Like Activities

Steven L. Harlan

NeutraTherm, Inc., 1501 Ohio Street, Des Moines, IA 50314

We report the first user test experience with polyethylene glycol (PEG-1000) permanently affixed to fabric as a phase-change material for next-to-skin use. In 50 subjects, NeutraTherm-treated undergarments are evaluated during skiing and skiing-like conditions for comfort and protective function. When compared to untreated cotton thermal undergarments, initial testing indicates that phase-change materials impart superior qualities as protective clothing, particularly in preventing both overheating and chilling. This particular phase-change material was also shown to be superior in preventing moisture and odor at the skin surface and in the outer garments. Independent laboratory testing reported no detectable formaldehyde in NeutraTherm-treated garments. No skin irritancy attributed to the fabric or any other chemical component of the bound polymer was reported in 200 test subjects.

As one of our test subjects succinctly stated, "Few things are as uncomfortable as becoming 'sweaty' in frigid temperatures". During snow sports and physical activities in frigid temperatures, there is an interaction between the insulating qualities of clothing and the physiological factors at play. The heat produced by physical muscular activity adds quickly to the basic metabolic heat production and liquid perspiration ensues. Sudden excess heat build-up continues to be a problem with modern insulation in protective clothing. This is a particularly limiting factor in hi-loft synthetic

0097–6156/91/0457–0248$06.00/0

insulation. Furthermore, with cessation of muscular activity, chilling ensues, particularly if liquid perspiration has appeared.

Ideal protective clothing should do more than simply insulate and transport moisture vapor away from the skin. Part of the function of ideal protective clothing should be its ability to "adapt" to thermal fluctuations at the skin surface to keep the skin temperature at 33 - 35°C, thus preventing perspiration and chilling.

Enthalpic clothing, clothing that absorbs heat and releases heat upon demand, brings us a major technological advancement and a step closer to ideal protective clothing. This technology permits clothing to react to changes in environment and physical activity. This is a new active process of energy absorption and energy return, rather than a passive insulation or moisture transport process. New terms and testing descriptors relating to "active cooling" and "active warming" are now needed.

Thermally adaptable, truly functional fabrics are produced when phase-change materials with enthalpic qualities are bonded to fabric. Enthalpic substances store and release thermal energy, i.e., they contain thermal energy available for release, and they have the ability to absorb excess heat. Several enthalpic materials are known including plastic crystals, inorganic salt hydrates such as calcium chloride hexahydrate, lithium nitrate trihydrate, zinc nitrate hexahydrate, and polyethylene glycols with molecular weights of 600 - 20,000. Historically, it has been very difficult to find suitable (1-3) materials which can be bonded permanently to fabric and retain the ability to absorb and release calories of heat for unlimited cycles of heating and cooling.

A "suitable" enthalpic material must be able to operate at or near the temperature of human skin. It must also be dermatologically safe and pass Draize skin irritancy/sensitization predictive testing (4). When moisture does become present, the ideal enthalpic material should be hydrophilic and draw moisture away from the skin while performing its temperature buffering functions. Finally, fabric that can respond to overheating and chilling should have tactile comfort, softness, and good "hand" (5).

NeutraTherm is the manufacturing name for our adaptation of the crosslinking polyethylene glycol process developed by Vigo and Bruno (6). Polyethylene glycol (PEG) is a material with high enthalpy, since it is a phase-change material. It has effective and prolonged heat storage and release capabilities, because it undergoes a change of state, solid to liquid (melting) or liquid to solid (crystallization). Polyethylene glycols with average molecular weight of 1,000 (PEG-1000) were chosen because of their demonstrated ability to operate or phase change near skin temperatures. The process utilizes the chemical crosslinking agent DMDHEU (dimethylol- dihydroxyethyleneurea) used in the durable press/permanent press fabric finish industry.

Suitable thermal storage and release properties are produced with a minimal add-on of weight to the fabric (20%). Existing finishing

Downloaded by UNIV OF ARIZONA on August 6, 2012 | http://pubs.acs.org
Publication Date: April 3, 1991 | doi: 10.1021/bk-1991-0457.ch015

techniques for fabrics are suitable for application to fabric. Established solvent extraction techniques and drying techniques are suitable for polymerization. Successful impregnation and bonding requires consideration of fabric type, range of solution concentrations, quality of solution, range of curing temperatures and time (1), air drying, and quality of handling.

Reported properties of PEG bound to fibers include thermal storage and release properties (enthalpy), thermal insulation, solar insulation/infrared reflectance, enhanced moisture absorption and wicking, soil resistance, static resistance, abrasion resistance, pilling resistance, and colorfastness to laundering (6-7).

In addition to the above-mentioned properties of PEG bound to fibers, we have observed improved machine washability and machine dryability for delicate fabrics, as well as reduction or prevention of the permanent shrinkage which results from the initial laundering of some fabrics. We have also observed the ability of certain fabrics to be screen-printed and be amenable to sublimation art techniques. Prior to NeutraTherm treatment, these fabrics were unable to tolerate or accept these art forms. Resistance to odor retention is also imparted, as well as the ability to be "pre-warmed" in conventional microwave ovens.

We report our initial experience with next-to-skin, phase-change materials. This is our first attempt to establish the relationship between fiber properties and comfort performance with these materials. This paper presents the application of the phase-change material, polyethylene glycol, in next-to-skin garments through a series of wearer trials under skiing and skiing-like conditions.

Downloaded by UNIV OF ARIZONA on August 6, 2012 | http://pubs.acs.org
Publication Date: April 3, 1991 | doi: 10.1021/bk-1991-0457.ch015

Human Wear Testing

Prior to human testing with next-to-skin use tests, it is important to collect background data on the molecule and related structures. The chemical and physical properties of the PEG and DMDHEU used in the NeutraTherm process are well known. Biological data in animals and man is available because of the widespread use of PEG and DMDHEU over the past thirty years. Polyethylene glycols with average molecular weights of 200 - 4000 are used extensively in topical medicaments, cosmetics, and toothpastes. Many topical medications in dermatology use PEG as a lubricant to make the preparation "smooth and creamy". One of the most common uses of PEG 3350 is a powder-in-water form drank as a colon preparation prior to diagnostic colonoscopy. PEG has been used for years in the durable press finishing industry at concentrations of 1 - 2% as a lubricant and as an agent to scavenge and reduce free formaldehyde. It should be noted that the Cosmetic Product Registry of the FDA shows that formaldehyde in low concentrations is used in about 5% of cosmetic preparations as a preservative (8).

The catalysts used in the process, $MgCl_2 6H_2O$ and citric acid are well known, low toxicity agents used in the food preservation industry. Also, these catalytic agents do not participate in the covalent crosslinking that occurs between the fabric and resin DMDHEU and the PEG. The afterwash of the process eliminates all traces of catalysts.

The crosslinking agent in the NeutraTherm process is the same formaldehyde-containing amide resin (DMDHEU) used in the durable press finishing industry (permanent press). Because of the widespread use in industry, dermatologists have been testing (patch testing) for DMDHEU allergy and formaldehyde allergy since the early 1970s (9). Predictive testing in humans has demonstrated that if repeatedly challenged (Draize testing) with strong concentrations of these chemicals, 3% of humans will become allergic to them. The allergy produced is one of redness, dryness, and itching of the skin. Hives are extremely rare and reported only a handful of times in the medical literature (10-13).

It was determined from the work of Vigo and Bruno that free formaldehyde is consumed more efficiently during PEG finishing and present in amounts 30% less than in durable press/permanent press finishing (Bruno, J. S.; Vigo, T. L.; personal communication of unpublished data.) Use tests with the final formulation in a cotton/polyester T-shirt were then necessary. The sample size of test subjects in user testing must be large enough so that results are valid for the population at large. A test population of 200 random subjects prior to marketing is considered appropriate when previously known and characterized chemicals are involved (4). Use tests are required to determine if in the final product, these substances as part of a multi-component system, are dermatologically reactive. The possibility that the laboratory tests may not predict what is likely to happen in the field stems from a large number of variables that may affect the outcome of the tests. These include the skin site, climatic conditions, the presence of perspiration, ultrastructural presentation of the molecule to the skin, among others.

The work of Vigo and Bruno has demonstrated that the covalent linkages of PEG bonding to fabric remain stable and durable through over 50 launderings (6). NeutraTherm has performed wearer tests in 200 individuals. Those with previously known durable press/formaldehyde allergy were asked not to participate in the initial study. There have been no skin reactions in our 200 subjects.

Bruno and Vigo have found that the PEG application pad bath process releases approximately 30% less formaldehyde than the permanent press process. The process of Vigo and Bruno containing 50% polyethylene glycol, consumes DMDHEU with 99% efficiency versus 85 - 88% efficiency in the permanent press process (Bruno, J. S.; Vigo, T. L.; personal communication of unpublished data.) The permanent press industry uses 1 - 2% PEG (polyethylene glycol) to scavenge excess free formaldehyde. In the NeutraTherm process, 50% PEG is present.

Downloaded by UNIV OF ARIZONA on August 6, 2012 | http://pubs.acs.org
Publication Date: April 3, 1991 | doi: 10.1021/bk-1991-0457.ch015

Traces of formaldehyde are present in clothing finished with DMDHEU. When new durable press clothing is sitting in a warehouse, workers must not be exposed to more than 1 ppm formaldehyde in the air. This OSHA guideline mandates the clothing formaldehyde levels indirectly. Manufacturers of durable press clothing avoid problems with OSHA by maintaining around 50 - 200 ppm free formaldehyde in the durable press products. Our test garment, tested by an independent, CDS Laboratories, contained no detectable formaldehyde by AATCC Method 112, with 50 ppm being the minimum detectable limit. A methylated glycolated form of DMDHEU in the NeutraTherm process allows for essentially "zero formaldehyde" in both the production process and the finished products.

Downloaded by UNIV OF ARIZONA on August 6, 2012 | http://pubs.acs.org
Publication Date: April 3, 1991 | doi: 10.1021/bk-1991-0457.ch015

Garment Preparation

Test garments for next-to-skin use consisted of 50% cotton, 50% polyester, 5 oz. T-shirts. The T-shirts were short sleeved with crew neck. Garments were treated by the pad bath technique of Vigo and Bruno (1-2) consisting of a 50% solution of polyethylene glycol 1000. Garment laundering consisted of a normal warm wash cycle with powdered phosphate detergent. Garments were given a cold rinse and tumbled dry in a permanent press cycle. Garments were laundered once before initial wearing. Garments were tested with an average polymer add-on of 60% or 0.6 grams of PEG polymer per gram of fabric. Thermal storage and release properties, heat of crystallization and heat of fusion, were confirmed by measurements made at USDA Southern Regional Research Center by DSC thermal calorimetry. For a comparative study of thermal calorimetry testing of fabrics, refer to the studies of Vigo and Bruno (3,6,7).

CDS Laboratories, Box 234, Langton, PA, 17747, performed AATCC analytical Method 112 for free formaldehyde in the treated T-shirts. They reported no measurable formaldehyde, stating that 50 ppm is the limit of detection.

Comfort Testing Protocol

Fifty test subjects, thirty-three men and seventeen women (18 - 60 years of age) participated in the study. Thirty-six of the subjects tested the NeutraTherm-treated T-shirts in Alpine and Nordic skiing. Fourteen subjects tested the garments in mountain bicycling and hiking. All testing was performed within a temperature range of 20 - 50°F. The subjects were asked to evaluate the NeutraTherm garments next to skin for a minimum of two full days of activity. They were asked to then compare this to two days of activity wearing untreated cotton thermal underwear, of the cotton "waffle knit" type thermal underwear, next to skin. The subjects were asked to wear their usual accessories over the test garments in the manner of which they ordinarily experience these activities. Subjects were given

Downloaded by UNIV OF ARIZONA on August 6, 2012 | http://pubs.acs.org
Publication Date: April 3, 1991 | doi: 10.1021/bk-1991-0457.ch015

the same garment laundering instructions and instructed to dry the garments in a dryer on medium heat with a permanent press/cool down cycle.

Prior to testing, subjects were asked if they had sensitive skin, asthma, or hay fever allergies. These conditions are known to predispose to irritant and contact dermatitis in general. Fourteen of the fifty subjects answered in the affirmative. None of the fourteen subjects, however, had a history of allergy to formaldehyde or durable press finishes specifically.

In this pilot study, the subjects were given only two sizes (medium and large) of treated cotton shirts. We were unable to control "fit" the treated garments. Fit in the control underwear was controlled by the test subjects themselves. At the time of this pilot study, no control garment existed that could not be easily distinguished from the PEG-bonded garments. The polymer-treated shirts have a unique and variable hand depending upon the ambient temperature, before the garment is put onto the skin. Once at body temperature on the skin, the PEG-bonded fabric cannot be easily distinguished by the wearer until activity begins. Also, there is a distinctly different hand of the treated fabrics during laundering which thwarts blind comparison. The control garments were compared to the treated garments, but not evaluated separately. No attempt was made to apply scientific statistical analysis as blind comparison was not possible in this initial study.

Tables I and II summarize the ranking of NeutraTherm garment performance for the descriptors evaluated.

Table I. Comfort Rating NeutraTherm Treated T-shirt
Results from 33 Men and 17 Women

Comfort Factor	Rating Level		
	Poor	Satisfactory	Excellent
Overall Comfort	0	14	36
Freedom of Movement	0	17	33
Neck Comfort	2	13	33
Sleeve Comfort	1	11	36
Garment Weight*	2	22	26

*5 oz. T-shirt with 60% PEG-Polymer add-on.

Downloaded by UNIV OF ARIZONA on August 6, 2012 | http://pubs.acs.org
Publication Date: April 3, 1991 | doi: 10.1021/bk-1991-0457.ch015

Table II. NeutraTherm Garment Characteristics
Skiing-Like Activity 20 - 50°F

Performance Descriptor	Ranking by Test Subjects			
	Poor	Satisfactory	Excellent	No/NA
Active Cooling	--	06	23	18
Active Warming	--	09	38	03
Thermal Insulation	--	12	38	--
Solar Insulation	--	12	11	21
Wind Insulation	--	09	41	--
Moisture Transport (during exercise)	01	18	28	02
Moisture Transport (after exercise)	02	19	26	06
Outer Garment Dryness	--	14	29	06
Drying Speed (on the body)	--	14	33	--
Shrinkage** (during washing)	36	09	01	03
Drying Speed** (in the dryer)	22	23	01	02
Odor Retention Resitance	01	14	34	01

**Denotes first generation fabrics with poor wet shrinkage behavior. Fabric returns to original dimensions after drying.

Results

This initial comfort evaluation or Phase I evaluation was intended to establish the relationship between fiber properties and comfort performance of NeutraTherm fabric compared to untreated cotton thermal underwear. It was also a part of a larger study of 200 subjects in ordinary use tests. These subjects reported no skin irritancy and also provided preliminary information regarding comfort and laundering experiences. As with all user tests of this type, there is involved a subjective assessment of fabric comfort and correlation of fabric physical properties. This first comfort evaluation was designed to indicate whether NeutraTherm-treated cotton/polyester would have detectable comfort differences and thermal/moisture handling performance differences as compared with untreated cotton thermal underwear. It is readily apparent that, in this initial Phase I study, comparison underwear fabrics are not controlled specifically.

The subjective comfort ratings in Table I demonstrate that the overall comfort with simply treating ordinary T-shirt material with NeutraTherm is quite acceptable. Table I is not a direct comparison to untreated cotton waffle knit underwear. Note that the 60% add-on weight is not a detractor in most circumstances for these types of activities. Add-on was limited to 60%, as our experience with ordinary T-shirt material demonstrated that greater than 60% add-on of polymer contributed to a somewhat "stiff" hand and a noticeable increase in weight of the garment for these activities. It should also be noted that treated ordinary T-shirt material experiences 20% wet shrinkage during laundering. Excessive wrinkling and folding slows drying in machine drying. Interestingly, air drying (hanging) time is more nearly normal. After drying, the garments return to normal size and appearance.

The descriptors "active cooling" and "active warming" are new terms applied to phase-change materials. In this study the fabric was bonded with a mixture of polyethylene glycols with the average molecular weight of 1000. Each individual subunit of the polymer materials absorbs heat (cools) and releases heat at a certain temperature within a range of -17 and 37°C. This creates the potential for what we term the active cooling and active warming of phase-change materials in these functional fabrics. This active cooling and warming is subtle and is not always noted, depending on the subject and the conditions. We realize that statistical analysis of this is premature until test subjects can be dressed with the garments and controls in a manner that provides for blind comparison. Phase-change polymers are being designed with narrower and more specific temperature ranges. It is expected that this will increase the ability of test subjects to observe active cooling or active warming.

Test subjects were asked if they specifically observed active warming or active cooling of the NeutraTherm garment. We asked subjects to note any

Downloaded by UNIV OF ARIZONA on August 6, 2012 | http://pubs.acs.org
Publication Date: April 3, 1991 | doi: 10.1021/bk-1991-0457.ch015

Downloaded by UNIV OF ARIZONA on August 6, 2012 | http://pubs.acs.org
Publication Date: April 3, 1991 | doi: 10.1021/bk-1991-0457.ch015

extraordinary warming or cooling sensations during activity which seemed over and above simply comfort from insulating and wicking. The subjective sensation of active cooling while overheating during activity was a more subtle observation under these circumstances of temperature and activity. As Table II demonstrates, this was noted to a lesser degree than the warming qualities during skiing and skiing-like activities.

Subjective responses regarding thermal insulation were very good. Table II represents a direct comparison but not a blind comparison to untreated cotton waffle knit thermal underwear. Several subjects felt that commenting on solar insulation and effects of overheating contributed by the sun were not applicable or appropriate because of conditions or accessory garments.

A surprise of the study was the very high rating for wind insulation. Prior to the study, this was not thought to be a major feature of the polymer-treated clothing. Even respondents, who were not generally impressed by the garment, gave it excellent ratings for wind insulation. One test subject, an air force pilot, commented that he noted excellent wind insulation wearing the NeutraTherm T-shirt in an open glider in 40°F temperatures.

Test subjects were asked specifically to note the perspiration handling of the garment compared to untreated cotton thermal waffle-knit underwear. They were asked to evaluate the moisture transport and the elimination of perspiration from the skin during exercise. They then evaluated the moisture transport after exercise in the cooling-down period. At the end of the day, test subjects were asked to examine their accessory clothing, sweaters, and ski jackets for perspiration. As expected, almost without exception, accessory clothing was noted to be significantly dryer or completely dry at the end of a day's activity as compared to a day's activity with untreated cotton thermal underwear. This effect is partially due to temperature buffering and overall reduction in perspiration. To a significant degree, however, this is probably due to the very strong hydrophilic properties of the polymer.

The polymer treated T-shirts seem to absorb and dissipate a great deal of moisture before showing any signs of wetness. With first generation ordinary knitted fabrics, wet shrinkage and wrinkling is noted as the NeutraTherm-treated T-shirt becomes thoroughly hydrated, either with perspiration or during washing. The hydrophilic nature of the polymer also increases garment drying time in the dryer, but this was still not a negative factor in 26 of 50 responding subjects.

Some of the test subjects did perspire heavily enough that spots of wrinkling appeared in the shirt over the high perspiration skin sites. Interestingly, when wetness or dampness is noted in the NeutraTherm treated garment, the drying speed on the body and the reversal of this wrinkling is quite good. When activity ceases and the treated shirt remains

Downloaded by UNIV OF ARIZONA on August 6, 2012 | http://pubs.acs.org
Publication Date: April 3, 1991 | doi: 10.1021/bk-1991-0457.ch015

on, it quickly dries so that wrinkling disappears and the shirt returns to its original appearance as noted by drying speed on the body in Table II.

Phase II trials will be conducted with second generation underwear fabrics utilizing specially engineered substrate fabrics. Specially engineered-knitted substrate fabrics when treatd with PEG 1000 can reduce or eliminate the unpleasant wet shrinkage behavior. It should be noted that with skiing and skiing-like activities in temperatures less than 50°F, wet shrinkage behavior even with ordinary fabric substrates is quite acceptable. Substrate fabric engineering for Phase II studies also improves greatly the drying time in the machine dryer. The severe wrinkling and folding which slows machine drying is eliminated.

Also noted was the improved resistance to odor retention that the polymer imparts to underwear fabrics. This was another surprise of the study. Table II demonstrates that 48 of 50 test subjects noted significantly superior to greatly superior odor resistance when compared to untreated cotton underwear. The odor resistance and prolonged freshness of treated garments was quite remarkable and relatively unexpected in this study. Our skiers later reported the ability to ski strenuously for three to five times longer without needing to launder the treated underwear nor the shirt or sweater worn over the treated underwear. The laundering habits of our skiers changed from laundering underwear and accessories after one day's use, to laundering only after three to five days of use. Indeed, NeutraTherm "neutralizes" odor.

For a comparative study of woven, knit, and non-woven materials containing bound PEG, refer to the studies of Vigo and Bruno with regard to thermal, mechanical, and absorbent/moisture-related properties (1,3,6,7,14).

Discussion

Comfortable clothing must maintain the skin temperature at 33 - 35°C with no liquid perspiration present. Extremes of moisture and temperature have been determined to be major cause of discomfort (15-16). Modern cold weather protective clothing in many cases has reached the point where the amount of insulation is limited by the problem of overheating. Liken this problem to the early problems with jet fighter planes. They early on became limited by the pilot's inability to maintain consciousness under high g-forces. It was not until a suit was developed which could inflate and react to those g-forces that the fighter technology could advance further.

Microporous shell fabrics imparting waterproof, windproof, breathable qualities exist in many types of skiwear (Gore-Tex, Thintech, Sympatex, Darlexx, Super-Microft). Synthetic films and polymer coatings are available which impart similar waterproof/breathable qualities (Entrant, Ultrex, Helly-Tech, Dermaflex). Tactel TM is a nylon fiber that is reportedly "warm" to the touch. All insulations basically trap air, "dead air" that blocks transmission and loss of body heat (Thinsulate, Thermolite, Thermore, Thermoloft, Quallofil, Hollofil, Loftguard, Kodofill). The more recent developments in linings (Dryline, Fieldsensor, Qwick) have been designed to absorb or direct moisture away when liquid sweat occurs. There is also a skiwear fabric (Solar Alpha/Descente) which utilizes zirconium carbide particles to transform sunlight into heat.

PEG-bonding and NeutraTherm allows the first opportunity to experience phase-change materials in skiwear and clothing for cold weather activity. The work of Vigo and Bruno have demonstrated that these materials can absorb excess heat for up to thirty minutes, then can release that stored heat for up to thirty minutes in a cyclic fashion. There appears to be no limit to the number of cycles available under conditions of cold weather activity, overheating/chilling.

We report the first experience with this technology under skiing and skiing-like conditions. This study indicates that applying phase-change materials to ordinary T-shirt material creates impressive results in skiing-like conditions. We view NeutraTherm as a breakthrough process which employs hydrophilic phase-change material to "neutralize" overheating, chilling, and moisture problems of physical activity in frigid temperatures. Under many circumstances, it appears to neutralize and prevent odor as well.

Skiers typically experience excess body heat while "bundled-up" indoors and during their descent down the mountain. Riding the chair-lift up produces chilling, particularly when liquid perspiration is present. These heating and cooling cycles typically remain less than thirty minutes and fall within the capability of the PEG to influence and buffer every cycle. Several hundred calories of extra available heat or several hundred calories of heat absorption are subtle and not always immediately or acutely noticed. However, when multiplied by a factor of ten, twenty, thirty, or more cycles of activity throughout the entire day, the difference is considerable. These multiple phase-changes translate into many thousands of calories of heat provided and managed by the thermal adaptability of the NeutraTherm fabric. The user notices that the entire day of activity was more comfortable and that little or no perspiration can be noted at the skin or within the outer garments.

It should be noted that the other desirable qualities imparted by NeutraTherm such as absorbency, wicking, thermal insulation, solar insulation/reflectance, abrasion resistance, are constant and not related to thirty-minute cycles.

Phase-change materials appear to be effective in contributing to comfort, by buffering and reducing overheating, the cause of perspiration. This particular phase-change material also appears to absorb, dissipate, and control moisture that does occur. As a truly adaptable, "functional fabric", it then responds to chilling by providing several hundred calories of stored heat per cycle. With physical activity in frigid temperatures, these warming/cooling cycles repeat continually.

Downloaded by UNIV OF ARIZONA on August 6, 2012 | http://pubs.acs.org
Publication Date: April 3, 1991 | doi: 10.1021/bk-1991-0457.ch015

Downloaded by UNIV OF ARIZONA on August 6, 2012 | http://pubs.acs.org
Publication Date: April 3, 1991 | doi: 10.1021/bk-1991-0457.ch015

Literature Cited

1. Bruno, J. S.; Vigo, T. L. "Temperature-Adaptable Fabrics With Multifunctional Properties", Proceedings AATCC National Technical Conference, 258, Charlotte, N.C., Oct. 15, 1987.
2. Bruno, J. S., and Vigo, T. L. "Thermally Active Fabrics Containing Polyethylene Glycols", J. Coated Fabrics 16, 264, 1987.
3. Vigo, T. L.; Bruno, J. S. "Temperature-Adaptable Textiles Containing Bound Polyethylene Glycols," Textile Research Journal 57:427, 1987.
4. Fisher, A. A. Contact Dermatitis, 3rd ed., Lea & Febiger, Philadelphia, PA., 1986, pp. 30-45, 253-254, 283-298.
5. Fuzac, John F. "Some Factors Affecting the Comfort Assessment of Knit T-Shirts", American Chemical Society, Houston, Texas, March 1980, Vol. 20, pp. 254-259.
6. Vigo, T. L.; Bruno, J. S. "Improvement of Various Properties of Fiber Surfaces Containing Crosslinked Polyethylene Glycols", Journal of Applied Polymer Science, 1989, Vol. 37, pp. 371-379.
7. Vigo, T. L.; Bruno, J. S. "Properties of Knits Containing Cross-linked Polyethylene Glycols," Proceedings AATCC National Technical Conference, 1988.
8. FDA, Division of Cosmetics Technology/Product Experience Branch, April 11, 1972. Subchapter D-Cosmetics, Part 170, 171. Federal Register 37 (70).
9. Epstein, E.; and Maibach, H. I. "Formaldehyde Allergy". Arch. Dermatol. 94:186, 1966.
10. Fisher, A. A. "Contact Urticaria Due To Polyethylene Glycol". Cutis 19:409, 1977.
11. Fisher, A. A. "Immediate and Delayed Allergic Contact Reactions To Polyethylene Glycol. Cont. Derm. 4:135, 1978.
12. Lindskov, R. "Contact Urticaria". Cont. Derm. 8:333, 1982.
13. Maibach. H. I. "Polyethylene Glycol: Allergic Contact Dermatitis Potential". Cont. Derm. 1:247, 1975.
14. Vigo, T. L.; Bruno, J. S. Proceedings of INDA-TECH Conference: Ft. Lauderdale, Fla., May 1988, pp. 427-438.
15. DeMartino, R. N.; et al, Textile Research Journal, 1984, July pp. 445-458.
16. Morris, Mary Ann; et al, "Relationship of Fiber Content and Fabric Properties to Comfort of Socks", Clothing and Textile Research Journal 1984-1985, Vol. 3, pp. 14-19.

RECEIVED July 31, 1990

Chapter 16

Thermal Performance of Wool and Inherently Flame-Retardant Fiber-Blend Fabrics

William H. Marsden

The Wool Bureau, Inc., 225 Crossways Park Drive, Woodbury, NY 11797

Downloaded by COLUMBIA UNIV on August 6, 2012 | http://pubs.acs.org
Publication Date: April 3, 1991 | doi: 10.1021/bk-1991-0457.ch016

The natural chemical and physical properties of the wool fiber are discussed as they relate to the thermal performance of blends of wool with selected inherently flame retardant fibers. Such blends would be utilized to provide flame retardant and thermally insulative protective clothing systems for firefighters and others. These included wool blends with Kevlar, Nomex, Ryton and Inidex. Various blend levels were evaluated in batting form for stability to 500°F oven exposure, vertical flammability performance and thermal protection performance (TPP) ratings in layups with a standard turnout shell and selected lining fabrics and Gore-Tex moisture barriers. The conclusion was that a 60/40 blend of Zirpro flame retardant wool and Kevlar offered a high level of thermal stability, superior vertical flammability performance and good TPP ratings in the batting weight range 5 to 5.5 ozs./yd.^{2}. Previous investigation, plus commercial application in firefighter's turnouts, has also established that high wool content insulative linings are effective in reducing heat stress levels for the wearer (5, 6, 7, 13).

As noted in such publications as the prestigious National Geographic Magazine (1), wool has a history of use that dates back over 12,000 years, and has provided clothing and shelter (protection from the elements) in cold and in warm climates since ancient times. Wool also has a place in the hi-tech textile revolution, where combinations of different types of fibers are used to generate products with new and diverse properties. The scope of this study is to illustrate how the inherent properties of wool may be enhanced to use it for protective clothing for firefighters' uniforms by chemical modification and by judicious blending with inherently flame-retardant and highly heat stable synthetic fibers. The synthetic fibers used for blending were commercially available ones.

0097–6156/91/0457–0260$06.00/0

Downloaded by COLUMBIA UNIV on August 6, 2012 | http://pubs.acs.org
Publication Date: April 3, 1991 | doi: 10.1021/bk-1991-0457.ch016

Structure of Wool and Its Relationship to Comfort.

As one can readily see from the schematic (Figure 1), wool is a complex structure that synthetic fiber producers have been trying to duplicate for many years, but so far without success. This "hi-tech" structure is a protein material composed of more than 20 amino acids containing the elemental building blocks of carbon, hydrogen, oxygen, nitrogen and sulfur. It is comprised of a hydrophobic outer layer of tough overlapping scales called the cuticle and an inner core called the cortex. Although the cuticle is resistant to liquid water penetration, it contains pores of sufficient size to freely permit the entry of water vapor. The inner cortex, which makes up 90% of the weight of the wool fiber, is hydrophilic, so much so that wool is highly water-vapor absorbent, and is greatly superior to the relatively non-absorbent polyamide, aramid, polyester and acrylic synthetic fibers in common use. Wool's moisture regain, or absorbency of water in vapor form from the atmosphere, is 12 to 17% under normal conditions (70°F and 65% relative humidity) and increases to 25 to 30% as the relative humidity approaches 100%, as it can within the garment microclimate existing between the body of a hard-working firefighter and his protective clothing. By contrast, cotton's moisture regain in approximately half that of wool, while the most absorbent common synthetic fiber, polyamide, is about a third as absorbent as wool at a relative humidity of 65% and one-fourth as absorbent at 90 to 95% relative humidity.

Along with absorbency, the cortex, because it is composed of two different cellular structures (a more crystalline ortho-cortex and an amorphous para-cortex) that grow at different rates, imparts a unique helically-coiled and crimped fiber shape that resists deformation because of bonding between the coiled amino acid chains. This singular structure serves to give wool its bulking power and resiliency - both very important in providing bulk without weight (which translates to efficient thermal insulation in a textile material) and the ability to retain that bulk within protective garments.

One result of this chemical and physical structure is that from a comfort standpoint, wool is unsurpassed. Clothing comfort is defined here in the narrow sense as the ability to help the human body maintain an even and healthful microclimate when covered by clothing or other textile materials. Wool's ability to help the human body regulate its internal temperature through the absorption, storage and transport of evaporating perspiration (when clothing constraints make that the only practical means of attainment) is well established. Wool is a "user-friendly" fiber, and its "test of time" has been reinforced by many scientific comfort studies at such places as the Hohenstein Research Institute in West Germany (2) (3), the Polytechnic of Wales in the U.K. (4), the Institute for Perception TNO in the Netherlands (5) and Oakland University in Michigan (6) (7). Wool fiber and fabrics have been compared with polyester, acrylic, nylon, aramid and leather with regards to comfort and the achievement of a more favorable next-to-the body microclimate in products such as blankets, quilts, mattress pads, car seat covers and upholstery, socks and firefighter turnouts.

Downloaded by COLUMBIA UNIV on August 6, 2012 | http://pubs.acs.org
Publication Date: April 3, 1991 | doi: 10.1021/bk-1991-0457.ch016

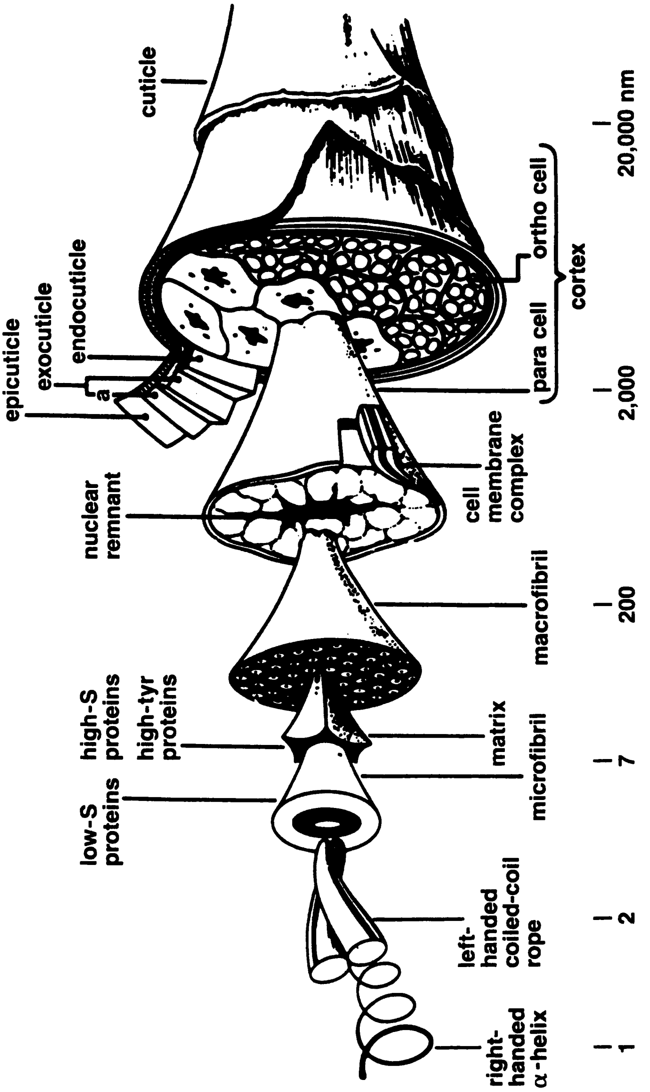
right-handed α-helix
left-handed coiled-coil rope
low-S proteins
microfibril
high-S proteins
high-tyr proteins
matrix
macrofibril
nuclear remnant
cell membrane complex
epicuticle
exocuticle
endocuticle
a
para cell
ortho cell
cortex
cuticle
1
2
7
200
2,000
20,000 nm

Figure 1. Structural Components of Wool

Downloaded by COLUMBIA UNIV on August 6, 2012 | http://pubs.acs.org
Publication Date: April 3, 1991 | doi: 10.1021/bk-1991-0457.ch016

Wool and Breathable Woolen Fabrics for Protective Clothing. Utilizing the comfort factor inherent in wool to enhance modern firefighters protective clothing has been necessitated by an increasing awareness in the fire service that their OSHA/NFPA mandated highly-insulative, but poorly breathable, synthetic turnout gear was creating a high incidence of heat-stress-related injuries and medical problems. The wearing of the synthetic turnouts, coupled with the use of self-contained breathing apparatus that let the firefighters work longer and closer to high radiant heat exposures, meant many U.S. firefighters were approaching or exceeding the heat stress limits a human body could safely endure in the course of their "normal" fire ground activities. In the late 1970's to mid 1980's pioneering work was done by a Swedish turnout manufacturer to establish that all-wool turnouts were significantly more comfortable than competitive synthetic gear. This was done through use and wear trials throughout Europe and the U.S. While some of the wool turnouts incorporated a breathable liquid water barrier like Gore-Tex, most did not. They relied only on the use of a durable fluorochemical oil-and-water repellent fabric treatment to upgrade wool's natural water repellency to the point the wool shell fabric provided excellent protection against liquid water penetration. One notable and well-documented U.S. wear-trial lasted sixteen months and was conducted by the San Francisco Fire Department, November 1984 to February 1986. In a summary report by the participants it was stated that "all members using these turnouts are especially pleased with the ability to prevent body heat build-up" (8).

The primary reasons for this beneficial behavior were the use of wool and the absence of a liquid moisture barrier component such as Gore-Tex or a neoprene-coated layer within the composite. These liquid moisture barriers, by their very nature, have to interfere partially at best (in the case of Gore-Tex) and almost completely at worst (in the case of neoprene-coated barriers) with the cooling evaporation of body moisture and its passage through and out of the clothing system. The preferred all wool turnout consisted solely of a wool lining fabric that was quilted to a needled wool batting and an outer shell fabric of a sturdy wool twill Zirpro treated to impart durable flame retardancy and fluorochemical oil-and-water repellency.

However, the "all-wool/no moisture barrier" turnout was doomed by the ascendency of the Federal OSHA standard (9) for firefighters' protective clothing, which was largely based on the NFPA 1971 standard (10) for protective clothing for structural firefighters. This standard contained one requirement a 100% wool garment couldn't meet. This was that any single fabric used in a turnout had to withstand a 5 minute/500°F. convective hot air oven test with no more than 10% shrinkage in length or width directions. Wool fabrics normally will shrink 12 to 18% under those conditions. The standard also required that a liquid moisture barrier be utilized immediately under the shell or outermost fabric layer. This barrier could be completely impermeable (i.e., a neoprene-coated fabric) or vapor-permeable (such as a Gore-Tex composite), but it had to completely prevent liquid water entry up to a specified hydrostatic pressure.

Downloaded by COLUMBIA UNIV on August 6, 2012 | http://pubs.acs.org
Publication Date: April 3, 1991 | doi: 10.1021/bk-1991-0457.ch016

Wool Blends With Inherently Flame Retardant Fibers for Protective Clothing.

This all led to some development work by an innovative turnout manufacturer located in New Jersey. This company developed a thermal liner system called "Fire Flite" consisting of a 60/40 wool/aramid woven fabric quilted to a 60/40 aramid/wool needled batting, that easily met all requirements of the OSHA and NFPA 1971 standards.

This was utilized with a Gore-Tex liquid moisture barrier, and wear trials around the country, as reported last year in "Chief Fire Executive Magazine" (11), soon indicated that this liner/moisture barrier combination in a turnout generated perceived lower levels of heat stress and increased wearer comfort.

The U.S. Wool Bureau had strongly supported the Swedish turnout manufacturer's efforts in the U.S. It also supplied the innovative U.S. manufacturer with much information on wools behavior in absorbing and transporting body moisture in the early stage of their developmental efforts. Now it is engaged in a program to develop an improved "hi-tech" liner system based on the use of a new engineered wool product from New Zealand. This new product is a durably-crimp enhanced, felt-resist treated and moth-proofed wool. Processed in New Zealand and developed primarily for the under-body bedding area (futons, mattresses, filled mattress pads), it is produced by mechanical crimping of a blend of clean and strong but relatively low-bulk Romcross wools. This wool is then autoclave set to permanently lock in the induced higher crimp level, so that it has the strength and resiliency of carpet wool but the bulk and cohesiveness of the finer and more highly crimped apparel wools. On arrival in U.S., only Zirpro treating to impart durable flame-retardancy is required.

This wool has, in a cooperative program with Tex-Tech Industries, been evaluated in needled batting in blends with the aramid fibers Nomex and Kevlar as well as Ryton and with Inidex. The primary considerations were flammability performance, thermal protective performance (TPP) and stability during the 5 minute/500^{o}F. oven exposure test. Following in Table I are some flammability and 500^{o}F. oven test results of various moderately needle-punched batting compostions (all being in the 6 to 7 oz./yd.^{2} weight range). The flammability test is the Federal Test Method Standard 191, Method 5903, vertical exposure to a 12-second ignition flame specified procedure. Failure to comply with the standard is having an after-flame of more than 2-seconds or a char length of more than 4 inches on average in the flammability test, or a thermal shrinkage greater than 10% in length or width in the oven test.

Based on these results, and giving recognition to the fact that wool/Kevlar blends exhibited a high level of strength and resistance to penetration or tearing both before and after 500^{o}F oven exposure, batting blends of 60% and 70% Zirpro flame retardant artificially crimped wool with 30 or 40% Kevlar were selected for further investigation as to thermal protective performance values they would produce. A range of battings were produced and tested for their thermal protective performance rating. Battings were tested in a composite representative of what would be used in a turnout. Outermost, or closest to the 50/50 convective/radiant heat source, is the shell fabric. In every case, this was a commercial 7.8 oz./yd.^{2} 60/40 Kevlar/PBI product from Amatex. Next comes the moisture

Downloaded by COLUMBIA UNIV on August 6, 2012 | http://pubs.acs.org
Publication Date: April 3, 1991 | doi: 10.1021/bk-1991-0457.ch016

TABLE I. 500°F Oven Shrinkage and 5903 Flammability Results

Batting I.D.			500°F for 5 Mins. - Oven Test (Shrinkage)	5903 Flammability 12 Sec. Ignition			
				A.F. (Secs.)		C.L. (inches)	
Tex-Tech Style No.	Composition	Weight (oz./yd.^{2})	% L X % W	MD	CD	MD	CD
5310	80% FR Wool 20% Kevlar	6.7	13 x 13	.6	-	.6	-
5311	80% FR Wool 20% Ryton	6.6	29 x 33	.3	-	3.0	-
5312	80% FR Wool 20% Nomex	6.0	19 x 20	.3	-	1.7	-
5313	80% FR Wool 20% Inidex	6.7	22 x 24	.8	-	2.1	-
5314	70% FR Wool 30% Kevlar	6.5	10 x 10	0	0	.4	.4
5315	60% FR Wool 40% Kevlar	7.0	5 x 6	0	0	.2	.2
5316	60% Non-FR Wool 40% Kevlar	7.1	6 x 7	0	0	.4	.3
5317	100% FR Wool	7.1	30 x 25	.1	0	3.0	2.5

barrier. This was comprised of Gore-Tex/spun-bonded Nomex composite product known as E-89, at a weight of 4.2 oz./yd.^{2}. Finally, the last component of the composite is the batting/facecloth insulation liner, with the face-cloth innermost or closest to the sensor, representing the body, which measures heat flowing through the composite. A thermal protection performance rating of 35, equivalent to 17.5 seconds of protection from heat build-up sufficient to cause 2nd degree burns, is the minimum called for in the NFPA 1971 standard. For comparative purposes, we included a couple of commercial insulative liners designated as the E-89 thermal liner (a 6.6 oz./yd.^{2} product consisting of 2 layers of spunbonded Nomex quilted to a woven Nomex ripstop fabric) and the Q-9 thermal liner (needled reprocessed Nomex batt quilted to a woven Nomex ripstop fabric at a 10.3 oz./yd.^{2} total weight). As a facecloth for use with all the wool battings we utilized a 5.7 oz./yd.^{2} plain woven flame retardant fabric of 50/50 wool/Conex supplied by Nichimen. Table II gives thermal protection performance test results for the range of composites tested.

In conclusion, based on the overall performance in the protective categories, a 60/40 Zirpro flame retardant durably crimped wool/Kevlar batting in the 5 to 5.5 oz./yd.^{2} weight range is now commercially available from Tex-Tech Industries. It offers excellent flammability performance, good 500°F oven exposure stability, maintains a high degree of strength after the 500°F exposure and provides good thermal protection performance levels. Its added "plus" is its ability to offer enhanced comfort or lowered heat stress, when used in conjunction with a suitable flame retardant wool-blend face-cloth fabric and a vapor-permeable moisture barrier. To quote Dr. Robert Lomas of the British Textile Technology Group, a research chemist and specialist in breathable fabrics for foul-weather clothing, from a 1989 "Textile Technology International" article..."Linings fulfill a second function in breathable garments. They are capable of storing perspiration liberated in periods of high activity and then allowing it to diffuse through the outer breathable fabric when the wearer reduces or ceases activity." (12). This is certainly descriptive of what a high-wool content thermal liner does in a firefighters' turnout.

Currently, while various wool/aramid FR fabrics can be obtained from Japan, Europe and Canada, the Wool Bureau is engaged in a developmental program with a U.S. mill to make available wool/aramid or wool/PBI face-cloth fabrics, so that the entire flame retardant wool-blend turnout thermal liner system can be put together with completely "Made in the USA" materials. In passing, it can be noted that with such wool-blend woven fabrics, not only is it possible to keep shrinkage under 10% during 500°F. hot air exposures, but fabric tear strengths are maintianed at 65 to 80% of original values, whereas 100% wool fabrics would char and retain only 5 to 10% of their original tear strength.

Finally, it is worthwhile to mention that this development can be utilized in the whole protective clothing area. Certainly lowering heat stress and improving comfort would be welcomed by all wearers of insulated flame retardant garments throughout the industrial sector.

Downloaded by COLUMBIA UNIV on August 6, 2012 | http://pubs.acs.org
Publication Date: April 3, 1991 | doi: 10.1021/bk-1991-0457.ch016

Table II. Turnout Composite TPP and Weight Relationships

	Turnout Composite	Total Wgt. (oz./yd.^{2})	TPP	TPP per oz./yd.^{2} Total Composite
I.	Shell + E-89 M.B. + E-89 T.L.	18.6	37	2.0
II.	Shell + E-89 M.B. + Q-9 T.L.	22.3	50	2.2
III.	Shell + E-89 M.B.+ 60/40 FR Wool/Kevlar (5.5 oz./yd.^{2}) + Wool/Conex (5.7 oz./yd.^{2})	23.2	49	2.1
IV.	Shell + E-89 M.B.+ 60/40 FR Wool/Kevlar (6.7 oz./yd.^{2}) + Wool/Conex	24.4	48	2.0
V.	Shell + E-89 M.B.+ 60/40 FR Wool/Kevlar (8.0 oz./yd.^{2}) + Wool/Conex	25.7	51	2.0
VI.	Shell + E-89 M.B.+ 60/40 Non-FR Wool/ Kevlar (7.2 oz./yd.^{2}) + Wool/Conex	24.9	48	1.9
VII.	Shell + E-89 M.B. + 70/30 Non-FR Wool/ Kevlar (5.4 oz./yd.^{2}) + Wool/Conex	23.4	46	2.0
VIII.	Shell + E-89 M.B. + 70/30 FR Wool/Kevlar (6.8 oz./yd.^{2}) + Wool/Conex	24.5	47	1.9
IX.	Shell + E-89 M.B. + 100% FR Wool (7.2 oz./yd.^{2}) + Wool/Conex	24.9	43	1.7
X.	Shell + E-89 M.B. + 60/40 FR Wool/Kevlar (12.9 oz./yd.^{2}) + Wool/Conex	30.6	60	2.0

Downloaded by COLUMBIA UNIV on August 6, 2012 | http://pubs.acs.org
Publication Date: April 3, 1991 | doi: 10.1021/bk-1991-0457.ch016

Downloaded by COLUMBIA UNIV on August 6, 2012 | http://pubs.acs.org
Publication Date: April 3, 1991 | doi: 10.1021/bk-1991-0457.ch016

Glossary of Terms and Trade-Marked Products

1. Conex - Nichimen's trade-marked *meta*-aramid inherently flame-retardant synthetic fiber.
2. Gore-Tex - W. S. Gore's trade-mark process for the lamination/bonding of expanded microporous polytetrafluoroethylene film to textiles to impart breathable water-proofing.
3. Inidex - Courtald's trade-marked acrylic acid/acrylamide cross-linked copolymer inherently flame-retardant synthetic fiber.
4. Kevlar - Dupont's trade-marked *para*-aramid inherently flame-retardant synthetic fiber.
5. National Fire Protection Association (NFPA) - A financially independent non-profit association with voluntary membership that functions to provide methods of implementing fire safety - these include the development and administration of codes and standards for protection of lives and property.
6. NFPA 1971 - A standard for protective clothing for structural fire fighting developed under the auspices of NFPA.
7. Nomex - Dupont's trade-marked *meta*-aramid inherently flame-retardant synthetic fiber.
8. OSHA - The Occupational Safety and Health Administration department of the federal government.
9. PBI - Hoeschst/Celanese's trade-marked polybenzimidazole inherently flame-retardant synthetic fiber.
10. Ryton - Phillips' trade-marked inherently flame-retardant synthetic fiber made from a melt-spinnable aromatic polymer of poly (*p*-phenylene sulfide).
11. Thermal Protective Performance (TPP) - A rating method for the thermal resistance and insulation of textile materials against a specified thermal flux - in this case, test methods and conditions are as given in the NFPA 1971 standard in Chapter 5, Section 5-1.
12. Zirpro - IWS/Wool Bureau's trademark for their licensed process involving the application of zirconium and titanium metal complexes to wool to impart durable flame-retardancy.

Literature Cited

1. Hyde, N.; *National Geographic* 1988, Vol. 173, No. 5, 552-591.
2. *Comparative Thermophysiological Evaluations of Wool and Acrylic Blankets and Wool and Polyester Filled Quilts*, IWS Spec. Products Tech. Info. Letter No. 13, Jan., 1984.
3. *Further Comfort Evaluations of Automobile Seat Covers*, IWS Chem. Processing Tech. Info. Letter No. 5, April, 1989.
4. *An Ergonomic Comparison of Wool and Polyester Filled Quilts*, IWS Spec. Products Tech. Info. Letter No. 26, Feb., 1986.
5. van de Linde, E. J. G.; Lotens, W. A. *Restraint by Clothing Upon Fire-Fighters Performance*, Int. Conf. on Protective Clothing Systems in Stockholm, Sweden, Aug., 1981.

6. Reischl, U.; Stransky, A.; Assessment of Ventilation Characteristics of Standard and Prototype Firefighter Protective Clothing, Textile Research Journal 50, 643-647 1980.
7. Reischl, U.; Stransky, A.; DeLorme, H. R.; Travis, R. Advanced Prototype Firefighter Protective Clothing: Heat Dissipation Characteristics, Textile Research Journal 52, 66-73 1982.
8. O'Connor, Lt. J. J. ; Summation of San Francisco F. D. Field Test: Wool Turnout Equipment, Feb., 1986.
9. OSHA Fire Brigade Standard, 29 CFR 1910.56, Federal Register, Sept. 12, 1980.
10. National Fire Protection Assoc. (NFPA) Standard 1971, Protective Clothing for Structural Firefighting, 1986.
11. Carter, H.; From Factory to Firehouse: Innovations in Protective Clothing, Chief Fire Executive Magazine, Vol. 3, No. 2, March/April, 1988, 21.
12. Lomax, R.; Ways of Waterproofing Breathable Fabrics, Textile Technology Int'l, 1989, 305-310.
13. Mehta, P. N.; Norman, D. L.; Textile Research Journal 53, 153-159, 1983.

RECEIVED July 31, 1990

Downloaded by COLUMBIA UNIV on August 6, 2012 | http://pubs.acs.org
Publication Date: April 3, 1991 | doi: 10.1021/bk-1991-0457.ch016

Chapter 17

Printing Technology for Aramid Fabrics

James D. Hodge and E. Anne Dodgson

Spruance Research Laboratory, E. I. du Pont de Nemours and Company, P.O. Box 27001, Richmond, VA 23261

Downloaded by COLUMBIA UNIV on August 6, 2012 | http://pubs.acs.org
Publication Date: April 3, 1991 | doi: 10.1021/bk-1991-0457.ch017

Fabrics of Du Pont NOMEX aramid fiber can be printed by a conventional rotary screen printing process if the aramid fiber structure is open to allow dyes to migrate in and there is a structural feature to facilitate binding of the dye molecules to the fiber substrate. With Nomex this is achieved by imbibing surfactants into the water swollen fiber structure prior to initial drying. The surfactant provides a much more open structure as well as providing an ionic binding site for the dyes. The special problems of printing military camouflage fabrics where the colors, dye fastness properties, and infrared reflectance properties are critical are discussed.

The primary function of thermal protective clothing is to minimize or even eliminate physical harm as a result of a fire. However, beyond this obvious requirement of flame protection, it is highly desirable and often necessary to provide protective clothing in various colors. This desirability for a variety of colors can be from a need for styling as with uniforms for race car drivers or from a need for high visibility as with the outer shell of the launch and recovery suits used by the space shuttle crews. Quite the opposite is required for flame resistant military camouflage; that is, coloration is necessary to impart invisibility.

Because of the highly crystalline nature and high Tg of aramid fibers, such as Du Pont's NOMEX, it is extremely difficult to dye aramid fabrics in conventional dyeing processes. Colored NOMEX with the best overall properties (fabric strength and colorfastness) is achieved by injecting colorants into the spin dope prior to fiber spinning. These colorants can be dyes of a variety of classes or pigments. No molecular binding of the colorant is necessary in this procedure since the colorant is physically or mechanically locked into the fiber structure.

Dyeing NOMEX in fabric form can only be achieved by using

0097–6156/91/0457–0270$06.00/0

carriers, usually a powerful organic solvent, to swell or disrupt the structure to permit dyes to migrate into the fiber. In this case there must be some sort of molecular bonding of the dye to the aramid structure and only cationic (basic) dyes will bind to the NOMEX polymer structure. Fabrics of NOMEX will dye to deep shades (with a carrier) using cationic dyes but will only lightly stain using acid dyes. This affinity of cationic dyes for the meta aramid structure is not well understood. The most obvious bonding site is the free carboxyl end group. On the other hand, there are very few free amine ends available as sites for bonding to acid dyes. The amide groups may also play a role since amides are hybrid structures of two resonance forms resulting in the carbonyl oxygen being somewhat electronegative. Van der Waals forces between the aromatic rings of the polymer and dye may also be a factor; however this would apply equally to acid or basic dyes (1).

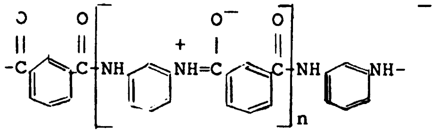

Meta Aramid Structure
(The Two Resonance Forms of the Amide Group Are Shown)

These techniques of adding colorants to the spin dope and carrier dyeing fabrics are fine for protective clothing in solid shades. But for a protective apparel where printed colors are required, such as military camouflage, there are a new set of problems: the requirements of the printing process and limitations on the dyestuffs that may be used.

There are two principal printing procedures used today in textile printing: pigment printing and dye (or wet) printing. The most widely used procedure is pigment printing where the pigment colorant is bound to the fiber substrate with a thermoset resin. This method is not acceptable for thermal protective camouflage because of flammability problems associated with the binder resin. With the pigment colorant only on the surface of the fiber, wash and crockfastness are also problems with pigment prints, especially with military specifications around these parameters. As a consequence, dye printing is the only acceptable method for military camouflage printing at present.

There is a further limitation on the colorants available for military camouflage. The colors, or shades, are chosen to reduce the contrast of battle dress uniforms with the natural background. Nearly all camouflage patterns are composed of various shades of green, brown and black. There is, however, another important criteria: the shades must also minimize the contrast in the near infrared region (600-900 nm) to avoid detection by night surveillance devices. Typical infrared reflectance of some common dye classes are shown in Figure 1. The dye classes that currently meet the IR reflectance requirements of the military, both here and abroad, are limited to acid dyes and vat dyes (2).

This presents a unique problem for NOMEX since aramids are not

Downloaded by COLUMBIA UNIV on August 6, 2012 | http://pubs.acs.org
Publication Date: April 3, 1991 | doi: 10.1021/bk-1991-0457.ch017

Downloaded by COLUMBIA UNIV on August 6, 2012 | http://pubs.acs.org
Publication Date: April 3, 1991 | doi: 10.1021/bk-1991-0457.ch017

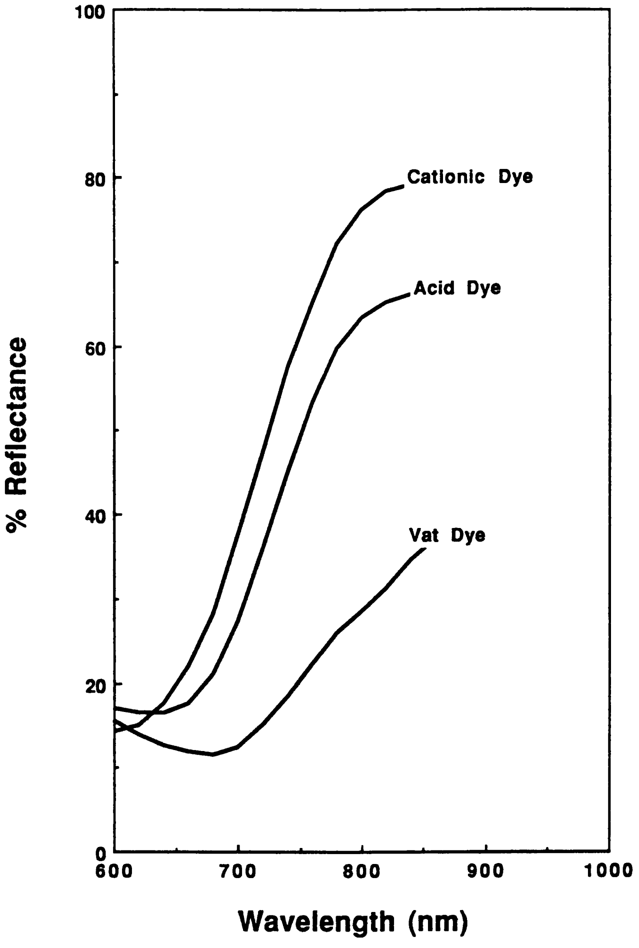

Figure 1. Effect of Dye Class on IR Reflectance.

Downloaded by COLUMBIA UNIV on August 6, 2012 | http://pubs.acs.org
Publication Date: April 3, 1991 | doi: 10.1021/bk-1991-0457.ch017

substantive to either of these classes of dyes. Additional criteria important in the selection of dyes for military camouflage are good colorfastness to light, high temperature washing, and crocking.

U.S. Military camouflage is a four color pattern: light green, dark green, brown and black with infrared reflectance specifications shown in the shaded portion of Figure 2. The printing process can be simplified somewhat if the fiber is produced in the light green base shade. This was easily accomplished by addition of the acid dyes for this color as part of the fiber production process. The real problem was producing a fiber that would accept acid dyes in printing the remaining three colors.

The mechanism for printing with dyes is similar to aqueous dyeing of fabrics--the dyes must migrate from the aqueous phase into the fiber and then bind in some manner to the fiber structure. The textile wet printing process consists of overlaying the dry fabric with a highly viscous print paste containing the dyes in the pattern desired, oven drying the printed fabric, steaming, and washing. Dye "fixation" (molecular binding of the dye to the fiber substrate) is achieved in the steaming step where a miniature aqueous phase is created on the fabric surface allowing the dyes to migrate into the fiber. Without the use of a carrier to swell the meta aramid structure, the NOMEX fiber must be inherently sufficiently open for this dye migration to take place. This was the first problem that had to be solved. Achieving dye migration into the substrate is only half of the battle; the other half is accomplishing the molecular binding to the substrate. The preferred mechanism of binding acid or basic dyes to a substrate is the formation of an ionic bond. For example, a typical acid dye has one or more sulfonate groups, or possibly a carboxylate group, in the structure as shown in these examples of typical acid dyes:

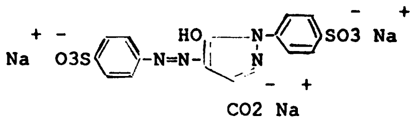

C.I. Acid Yellow 23

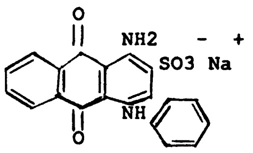

C.I. Acid Blue 25

The sulfonate (or carboxylate) anion will be attracted by a cation that is part of (or contained in) the fiber substrate. The final step in the mechanism is formation of an ionic bond between the anionic dye and the substrate with the associated counter ions forming a salt which will wash out of the structure. Failure to achieve good chemical binding, or fixation, will result in washfastness being poor or nonexistent. In fact, if little or no dye fixation has been accomplished, most of the dye will wash out during the fabric scouring step in the printing process.

Experimental

The two basic properties that had to be incorporated into an aramid fiber substrate to permit printing with acid dyes in a conventional screen printing process were: (a) an open structure to permit dye

Downloaded by COLUMBIA UNIV on August 6, 2012 | http://pubs.acs.org
Publication Date: April 3, 1991 | doi: 10.1021/bk-1991-0457.ch017

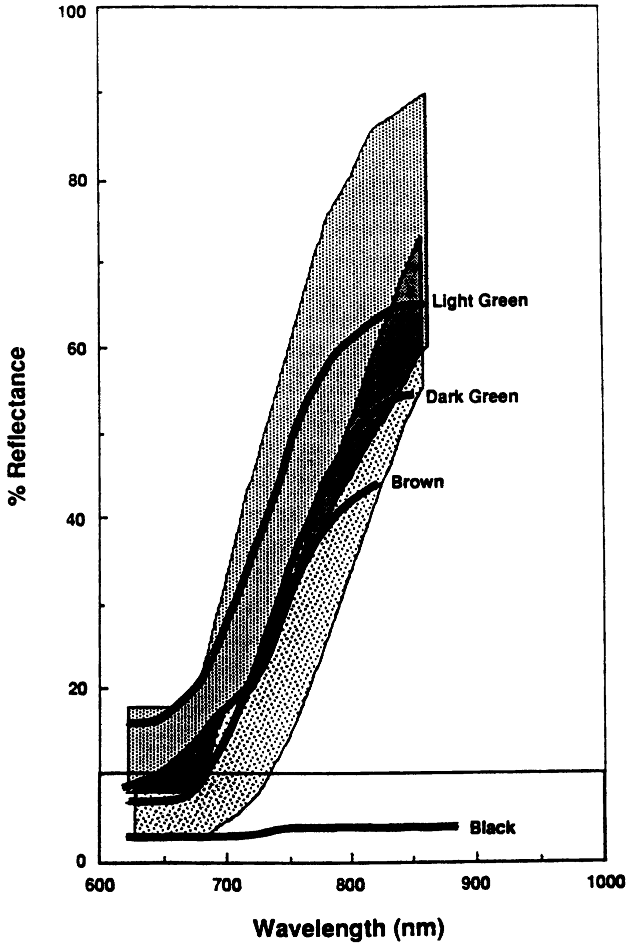

Figure 2. Infrared Reflectance of Camouflage from NOMEX Aramid Fiber.

In High-Tech Fibrous Materials; Vigo, T., et al.;
ACS Symposium Series; American Chemical Society: Washington, DC, 1991.

migration into the fiber without a carrier, and (b) a structural feature that would facilitate binding of an acid dye to the substrate.

Over the past several years Du Pont has developed proprietary technology for imbibing surfactants into water swollen NOMEX before it is dried (3 and 4). It is possible to imbibe as much as 15% of a anionic, cationic or even a neutral surfactant into the aramid fiber. After imbibition, the subsequent drying of the swollen fiber removes the water and the fiber structure collapses to a normal fiber. However, this fiber now has a more open structure due to the surfactant and can be easily dyed without a carrier. The second benefit of this technology is that if an ionic surfactant is used, the surfactant will ionically bond to a dye of the opposite charge. The initial work involved imbibing an anionic surfactant, such as isopropylammonium dodecylbenzene sulfonate, which produced a substrate that was deeply dyeable with cationic dyes. Fabrics prepared from fiber containing the anionic surfactant could also be printed with cationic dyes. Since NOMEX normally has an affinity for cationic dyes, the primary function of the anionic surfactant was to provide the open structure.

To achieve printing with acid dyes, the selection of surfactant is more critical since it must not only provide the open structure, but must bind very well to the acid dye and form a structure that will not wash out. In addition, to improve the lightfastness a UV screener can be imbibed along with the surfactant. Numerous cationic surfactants were tried and although all were quaternary ammonium salts or ammonium hydrochloride salts of one form or another there were significant differences in color yield in printing trials. An imidazoline salt was selected as the best surfactant yielding the best depth of shade in acid dye printing. The amount of surfactant in the fiber (staple through finished fabric) were determined by solvent extraction of the sample followed by HPLC analysis of the extract. Proton magnetic resonance of the sample dissolved in a suitable solvent can also be used if the spectra for the surfactant and the m-phenylenediamine isophthalate structure do not interfere with each other. An approximation of the amount of total imbibed materials can also be done by simple weight loss with solvent extraction.

Acceptable color yield on printing was achieved with acid dyes for the dark green and brown shades, but an acceptable black shade could not be attained with acid dyes. Since the black color is only 16% of the total pattern, it was possible to use a carbon black based pigment print with a flame retardant binder to achieve this color. An added benefit of using the black pigment was that the IR reflectance met the specification of <10% across the near infrared spectral range. This cannot be achieved with acid dyes. These three colors were printed onto the light green base color fabric.

The use of both dyes and pigments in a single printing process required some modification of the process. The drying temperature had to be high enough to cure the pigment binder but low enough to prevent premature crystallization and structure closure which would prevent dye migration. Tests showed that 150 degrees C would work. The total production sequence starting with the light green aramid fabric is as follows: (a) the green and brown acid dye colors and the black pigment/binding resin are rotary screen printed using

Downloaded by COLUMBIA UNIV on August 6, 2012 | http://pubs.acs.org
Publication Date: April 3, 1991 | doi: 10.1021/bk-1991-0457.ch017

appropriate thickeners, (b) the printed fabric is immediately dried, (c) dye fixation is then accomplished with autoclave steaming at 45 45 psig, and (d) washing and frame drying completes the production process.

Results

Several hundred yards of NOMEX fabric were printed in the U.S. Military woodland camouflage pattern using this technology. Analysis of the precursor NOMEX staple used for this fabric showed an average content of 11.6% of cationic surfactant and 2.6% UV screener. The color shades of the finished printed fabric, although not a precise match, were very close to the nylon/cotton standard. Color data in CIELab units, measured using an Applied Color Systems, Inc., SpectroSensor II are given in Table I, below.

Table I. Comparison of Color Data (CIELab) of NOMEX Printed Camouflage with the U.S. Nylon/cotton Standard

	NOMEX Fabric			Nylon/cotton Std		
Color	L*	a*	b*	L*	a*	b*
Light Green	46.6	0.37	14.18	43.0	0.20	14.58
Dark Green	33.5	-9.58	13.88	33.2	-8.56	10.26
Brown	30.6	2.03	10.05	28.3	3.88	10.40
Black	19.8	0.00	- 0.46	16.0	1.49	- 1.19

The infrared reflectance is shown in Figure 2. The spun yarns used to weave the fabric also included producer-colored green KEVLAR aramid (at the 5% level) to provide garment break-open protection in a fire situation and a carbon core fiber (2% level) to provide built-in static protection. The antistatic fiber eliminated the need to apply an antistatic coating to the fabric.

Although the technology presented here deals with producing a military camouflage product and the unique problems associated with such a product, the same technology (in a much simplified version) can be applied to printing NOMEX aramid fabrics in any pattern for any use that a printed protective apparel fabric might be required.

Literature Cited

1. Trotman, E. R. Dyeing and Chemical Technology of Textile Fibres; Wiley-Interscience: New York, 1984; p 276.
2. Ramsley, A. O.; Bushnell, W. B. Development of the U.S. Woodland Battle Dress Uniform; United States Army Natick Research and Development Laboratories Technical Report TR-81/008.
3. Vance, E.; Barton, B. A. U.S. Patent 4 668 234, 1987.
4. Moulds, G. M.; Vance, E. British Patent 1 438 067, 1976.

RECEIVED April 2, 1990

Downloaded by COLUMBIA UNIV on August 6, 2012 | http://pubs.acs.org
Publication Date: April 3, 1991 | doi: 10.1021/bk-1991-0457.ch017

Downloaded by NORTH CAROLINA STATE UNIV on August 6, 2012 | http://pubs.acs.org
Publication Date: April 3, 1991 | doi: 10.1021/bk-1991-0457.ch018

Chapter 18

Measuring the Effects of Intense Heat and Dynamic Mechanical Forces on Thermal Protective Fabrics

A. J. Geshury, R. L. Barker, and W. P. Behnke

Department of Textile Engineering, Chemistry, and Science, College of Textiles, North Carolina State University, Raleigh, NC 27695–8301

The performance of thermal protective fabrics depends on their ability to insulate and to maintain structural integrity when exposed to high heat assault. A novel laboratory test method is described for assessing the thermal transmission of fabrics subjected to the simultaneous application of intense heat and dynamic mechanical forces. This method uses a modification of a Thermal Protective Performance (TPP) tester to subject fabrics to heat and to mechanical stress and bending forces. The intent is to simulate forces created by the movement of an active victim in a real life fire accident. This paper discusses the performance of single-layer flame and heat resistant fabrics including FR cotton, FR wool, and aramid blend fabrics.

Failure of a thermal protective fabric to maintain structural integrity, especially in single layer garments, can be disastrous since stress induced break open in the fabric exposes the wearer directly to the heat hazard and resulting catastrophic heat transfer. Therefore, the ultimate test of a heat resistant protective material is a measure of its ability to provide thermal insulation when exposed simultaneously to intense heat and externally imposed mechanical stress and strain. Laboratory test methods, such as the Thermal Protective Performance (TPP) test, provide valuable information which is directly related to the end-use performance of the heat resistant materials and thermal protective garments. However, these methods assess heat transfer while the fabric is in a static and unstressed state; they do not evaluate thermal performance under conditions simulating body movement generated by an individual escaping from a fire.

The typical reaction of a victim caught in a fire accident is to try to escape the heat hazard by running away from the fire source. Even if the victim already suffers some degree of burn injury, it is unlikely that external burns will affect internal body organs in short exposures. Therefore, we anticipate a scenario where the victim will remain conscious and active at least during the period that immediately follows the fire accident. The active victim's movements impose mechanical strains on clothing fabrics, particularly at the knee, upper leg, arm and back. In these areas the fabrics are subjected to mechanical tensile and bending stresses.

0097–6156/91/0457–0277$06.00/0

The purpose of this paper is to describe a TPP test modified to permit evaluation of the effects of dynamic mechanical forces on the thermal protective insulation of single layer protective fabrics. The research focuses on the performance of fabrics of Nomex® and Kevlar® aramid fibers, and fabrics made of FR cotton and FR wool.

Experimental

Test Fabrics

The fabrics evaluated are described in Table I. They are single layer woven fabrics in the 8.0 oz/yd^2 weight range. The materials used were chosen to represent the range of anticipated reactions to the simultaneous application of thermal and physical stresses. Kevlar and FR cotton fibers were selected for their dimensional stability and represent two levels of high temperature resistance. Similarly, Nomex and FR wool fibers were selected as materials which would shrink with high temperature exposure and represent two levels of resistance to mechanical stresses. Finally, the four fibers represent two mechanisms of achieving flame resistance, either inherent or through a flame retardant treatment. The test materials are commercially available and are currently used in thermal protective apparel. Test fabrics were selected to be as close as possible in weight, since weight is a dominant factor controlling the fabric heating rate.

Downloaded by NORTH CAROLINA STATE UNIV on August 6, 2012 | http://pubs.acs.org
Publication Date: April 3, 1991 | doi: 10.1021/bk-1991-0457.ch018

Table I. Test Fabrics

Fabric	Weight (oz/yd^2)	Flame Resistance	Remarks
Kevlar 100	7.7	Inherent	100%Kevlar aramid
Nomex III	7.9	Inherent	95%Nomex+ 5% Kevlar
FR Cotton	8.2	Treated	Proban® flame retardant
FR Wool	7.8	Treated	Zirpro® flame retardant

Test Methods

Thermal Protective Performance (TPP) Tester. A Thermal Protective Performance tester (Custom Scientific Instruments Co.) was used in this study for evaluating the thermal protective performance of the test materials. This method uses heat flux generated by two Meker burners set at 45° angles and nine electrically heated quartz tubes to expose a 100 cm^2 test specimen to 2.0 cal/cm^2 sec. The balance of radiant to convective heat was set at 50/50 using a commercial radiometer (Hy-Cal Model No. R-8015-C-15-072). The intense heat of 2.0 cal/cm^2 sec. was chosen to simulate industrial or military flash fire conditions. It is similar to the emergency fire hazard condition encountered by fire fighters or the intensity of heat in a large pool fire (1,2) and is equal to the TPP exposure specified in NFPA 1971 (3). The heat sources are isolated from the test specimen with a water-cooled shutter to insure accurately timed exposures. The heat transferred through the test fabric is measured by an instrumented copper calorimeter. The calorimeter consists of a copper disk 40 mm in

Downloaded by NORTH CAROLINA STATE UNIV on August 6, 2012 | http://pubs.acs.org
Publication Date: April 3, 1991 | doi: 10.1021/bk-1991-0457.ch018

diameter and 1.6 mm thick with four type J (iron-constantan) thermocouples positioned on a circle at half the radius of the disc, 120 degrees apart and one in the middle. The copper disc is painted dull black and mounted on an insulating board. The rate of the temperature rise is used in conjunction with the calorimeter constants to compute the heat flux received. The thermal protective performance of the test material is determined by comparing the measured heat transfer to the tolerance time of human tissue to incidental thermal injury as obtained by Stoll (4). The tolerance time required for a 2nd degree burn to occur is read directly from the sensor response curve by comparing the calorimeter trace with the human tissue tolerance to heat obtained by integration of Stoll's curve with respect to time.

The TPP rating is defined as the total exposure energy which causes the test fabric to transfer a sufficient amount of heat to cause a second degree burn injury (blister), and is calculated as:

$$\text{TPP rating (cal/cm}^2\text{)} = \text{Tolerance time (sec.)} \times \text{Heat flux (cal/cm}^2\text{sec.)}$$

Dynamic Thermal Protective Performance (DTPP) Test. A method capable of evaluating the thermal protective performance of fabrics exposed simultaneously to dynamic mechanical forces and flash fire conditions was developed. This method, based on modification of a standard TPP tester, makes use of the TPP test exposure system which is capable of simulating flash-fire conditions.

For the dynamic test, a novel specimen holder was designed and mounted directly to the TPP tester. This butterfly frame subjects the test fabric to dynamic forces during the heat exposure. The dynamic force applied to the test specimen varies depending on the position of the butterfly frame. Maximum tension is developed in the test fabric when the frame is in the lower horizontal position (Fig. 1). This tension results from the mechanical stress in the fabric itself. Therefore, the level of strain which develops is controlled by varying the length of the fabric that is mounted in the holder. The lowest level of tension occurs when the fabric reaches the maximum bending as illustrated in Fig. 2.

To implement these modifications, it was necessary to change the shape of the heat sensor used in the TPP test, and to remove the insulation block to accommodate the new specimen holder. The modified calorimeter consists of a blackened copper strip 12 x 70 mm and 1.6 mm thick. Three type J thermocouples are secured in the strip and positioned at equal intervals along the strip center. This calorimeter uses the same thickness of copper as the TPP calorimeter. This insures an equivalent response to heat transfer in the DTPP test. The location of the heat sensor is adjusted and set to 6.3 mm (1/4 inch) for testing single layer fabrics; the same spacing is used in the TPP test.

The calorimeter sensor is connected to a data acquisition unit which provides a continuous record of the rate of temperature rise of the sensor. Data are processed on a Hewlett Packard computer (Model No. 9122) using software that was specially developed for this research. DTPP test data are processed to predict the time required to cause a burn injury using the Stoll criteria (4). Tolerance time is read directly from the sensor response curve. The DTPP rating is defined as the total exposure energy which causes the test specimen to transfer a sufficient amount of heat to cause a second degree burn (blister). It is calculated as follows:

$$\text{DTPP rating (cal/cm}^2\text{)} = \text{Tolerance time (sec.)} \times \text{Heat flux (2.0 cal/cm}^2\text{sec.)}$$

Downloaded by NORTH CAROLINA STATE UNIV on August 6, 2012 | http://pubs.acs.org
Publication Date: April 3, 1991 | doi: 10.1021/bk-1991-0457.ch018

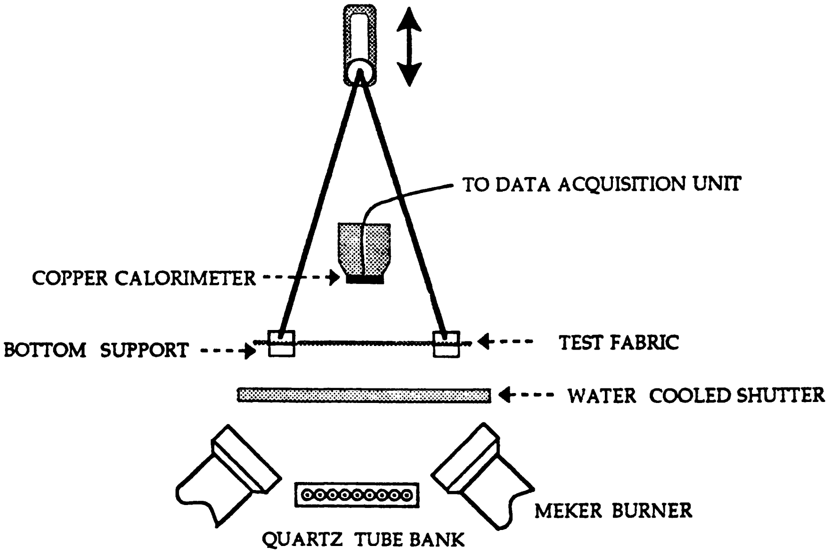
TO DATA ACQUISITION UNIT
COPPER CALORIMETER
BOTTOM SUPPORT
TEST FABRIC
WATER COOLED SHUTTER
MEKER BURNER
QUARTZ TUBE BANK

Figure 1. Schematic diagram of dynamic thermal protective performance (DTPP) tester – horizontal position.

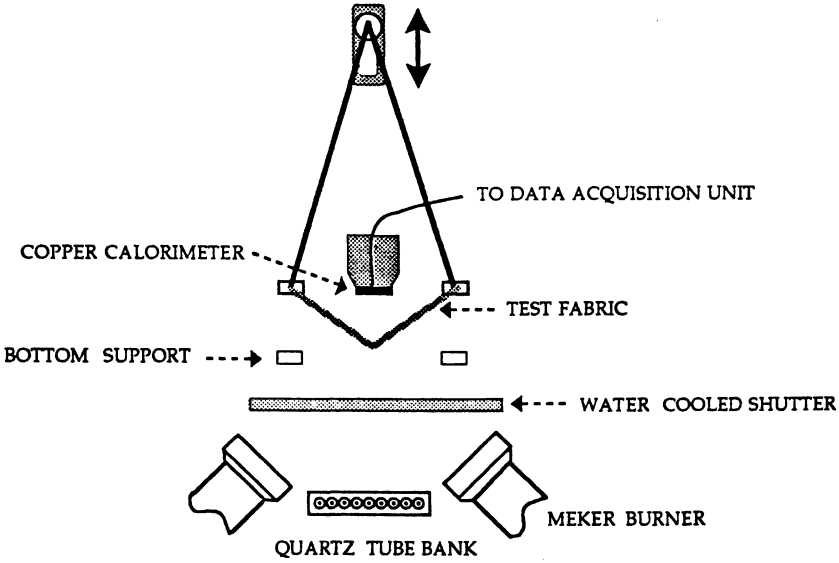
TO DATA ACQUISITION UNIT
COPPER CALORIMETER
TEST FABRIC
BOTTOM SUPPORT
WATER COOLED SHUTTER
MEKER BURNER
QUARTZ TUBE BANK

Figure 2. Schematic diagram of dynamic thermal protective performance (DTPP) tester – flexing (bending) position.

Downloaded by NORTH CAROLINA STATE UNIV on August 6, 2012 | http://pubs.acs.org
Publication Date: April 3, 1991 | doi: 10.1021/bk-1991-0457.ch018

Experimental Approach

Experiments were conducted to evaluate the effect of tension and flexing action on the thermal protective insulation of selected test materials. Testing conditions are summarized in Table II.

Table II. Test Conditions

Test Method	Flexing	Tension
TPP	Static	0%
Modified TPP	Static	-3%, 0%, 2%, 4%
Modified TPP	0.7 sec./cycle	-3%, 0%, 2%, 4%

Assessments were made using the TPP testing arrangement as specified by the standard method (3). Other evaluations were made using a modified TPP apparatus. In this case, the apparatus was used without motion (static test) but with different levels of tension applied to the test fabric. In other tests on the same modified TPP tester, the butterfly specimen holder was activated to flex the test fabric at a cycle duration of 0.7 seconds. This condition was used to represent the time required for a complete cycle in the leg movement of a long distance runner (5,6).

The design of the modified TPP apparatus is such that tension in the test fabric is created by forcing the fabric to stretch as the specimen frame moves in simulation of a running or walking cycle. Variation in the level of tension is achieved by using different mounting conditions. A negative tension of -3% means that the length of fabric between the specimen holder's jaws is longer than the distance between the jaws. This condition represents the case where the garment is loosely mounted. Zero tension in the modified test is comparable to the level of tension experienced by the fabric in the conventional TPP test. Tension of 2% and 4% represent cases where the fabrics are subjected to periodic tension forces during the heat exposure where maximum of 2% or 4% strain is placed on the fabric in the lower horizontal position as illustrated in Fig. 1. The results reported below represent an average of at least three test samples for every fabric at each of the different test conditions.

Results and Discussion

Thermal Protective Performance in the Conventional TPP Test

Table III shows results obtained in the conventional TPP test. These data show that the Nomex III and Kevlar 100 aramid fabrics provide similar levels of thermal insulation when compared on the basis of TPP and TPP normalized by the basis weight of the fabric. The FR wool sample provided a TPP similar to the rating obtained by the aramid fabrics. The FR cotton sample provides the lowest TPP, losing its ability to insulate after 4 seconds of exposure to the intense heat. These TPP ratings are generally in good agreement with results reported by other studies (1,7,8).

Table III. Thermal Protective Performance by Conventional TPP Method

Material	Weight (oz/yd^2)	Tolerance Time to 2nd degree burn (sec.)	TPP Value (cal/cm^2)	TPP/Weight
Nomex III	7.9	7.1	14.2	1.8
Kevlar 100	7.7	6.6	13.2	1.7
FR cotton	8.2	4.4	8.8	1.1
FR wool	7.8	7.2	14.4	1.9

Thermal Protective Performance in Modified TPP Test

Table IV shows data obtained in the modified TPP tests: the TPP values reported were measured using the conventional test method. Results identified as S-DTPP were obtained using the modified TPP tester in a mode of operation that used no motion (static test). DTPP results were obtained using the dynamic test apparatus operating with a 0.7 second per cycle flexing movement. In all the cases, no tension (0%) was applied to the test materials.

Table IV. Comparison of Thermal Protective Performance (TPP value cal/cm^2)

Material	TPP	S-DTPP	DTPP
Nomex III	14.2	13.8	9.8
Kevlar 100	13.2	17.0	14.6
FR Cotton	8.8	11.0	9.8
FR Wool	14.4	8.4	7.2

Instrumental Effects

Our experiments indicate that significant effects are associated with the design of the heat sensing system used in the modified TPP apparatus. Instrumental effects related to the configuration of the fabric sample in the dynamic tests were expected since the arrangement used to hold the sample in the modified test places more restraint on the test fabric. This is an important consideration since the level of sample restraint controls the material shrinkage that can occur during the exposure. Therefore, we notice that the S-DTPP value of the FR wool sample is considerably lower than the TPP value obtained in the conventional TPP test. We attribute this to sample holding conditions which inhibit shrinkage and formation of an insulating char. At the same time, we notice that, operating in a static mode, the thermal insulation provided by the Kevlar 100 and FR cotton samples in the modified tester is higher than the conventional values. We attribute this increase to changes in the shape of the heat sensor (the DTPP test uses a copper strip positioned perpendicular to the flame while the conventional TPP sensor uses a copper disc) and to the removability of the insulating block. In the tests of the Nomex III fabric, the counteracting effects of

Downloaded by NORTH CAROLINA STATE UNIV on August 6, 2012 | http://pubs.acs.org
Publication Date: April 3, 1991 | doi: 10.1021/bk-1991-0457.ch018

higher sample restraint and changes in the heat sensing apparatus appear to be offsetting factors. This would explain the similarity in the S-DTPP and TPP obtained values for this material.

Dynamic Mechanical Effects on TPP. Comparison of S-DTPP and DTPP values (Table IV) shows that the flexing action introduced by the butterfly sample holder contributes to the reduction of the thermal protection insulation of the test samples. However, some materials suffer greater reduction in protective insulation as a result of dynamic mechanical stress. In this regard, it is important to recognize that material stress derives, not only as a result of the external applied dynamic forces, but also from internal physical changes that take place in the heated material itself. These effects can best be explained by considering the behavior of individual test fabrics.

Downloaded by NORTH CAROLINA STATE UNIV on August 6, 2012 | http://pubs.acs.org
Publication Date: April 3, 1991 | doi: 10.1021/bk-1991-0457.ch018

Nomex III. The TPP of Nomex III sample is reduced by 30% as a result of introducing movement during the heat exposure. The explanation for the reduction in thermal insulation is apparent from examination of the calorimetric traces generated in static and dynamic TPP tests (Fig. 3). Therefore, we observe that in the three second interval following the initiation of TPP exposure, the rate of heat transfer, as indicated by the slope of the calorimetric trace, is the same in both static and dynamic tests. However, following the initial period, we observe a stepped increased curve in the rate of heat transfer recorded in the dynamic TPP evaluation. The stepped increase in heat transfer contributes to reduce the protective insulation, as it shortens the time required to exceed Stoll's criterion for heat transmission. We believe that this response is evidence of the effect that fabric shrinkage has on reducing the insulating air layer that exists between the backside of the fabric and the heat sensor surface. In this case, the step-like feature of the heat transfer curve is consistent with those instances that occur during the dynamic flexing cycle when the fabric is close or in actual physical contact with the heat sensing calorimeter. Therefore, intimate contact between the heated backside of the fabric and the heat sensor increases the heat transfer rate by adding a conductive component to the total transmission. However, the rate of heat transfer is ultimately diminished (to produce the moderate slope in the stepped curve) when the test fabric is forced by the frame holder to the lower position (see Fig. 1). This explanation of this phenomenon is confirmed by the observation that a precise correlation exists between the flexing cycle duration (0.7 second) and the steps that occur in the heat sensor response.

We also observed backside flaming in the Nomex III sample. This flaming occurs 4 to 6 seconds into the test and typically lasted for 10 seconds. However, it is important to point out that, in the case of Nomex III, the protection insulation was not much affected by back side burning. This is probably due to the small contribution that the heat released by ignition contributes to the overall heat transfer. In addition, when tension is applied in the dynamic TPP test, the level of tension appears to have little effect on the performance of Nomex III (Fig. 7-A). Since Nomex III is a blend of 95% Nomex with 5% Kevlar, it demonstrates the effect that a small amount of Kevlar has on reducing the shrinkage in heat exposure.

Kevlar 100. Mechanical stress, produced either as a result of dynamic forces or thermal shrinkage had little effect on the thermal protective performance of Kevlar 100 fabric. In fact, calorimetric traces (Fig. 4) show that the rate of heat transfer measured in the modified TPP test (static and dynamic modes) is actually lower than recorded in

Downloaded by NORTH CAROLINA STATE UNIV on August 6, 2012 | http://pubs.acs.org
Publication Date: April 3, 1991 | doi: 10.1021/bk-1991-0457.ch018

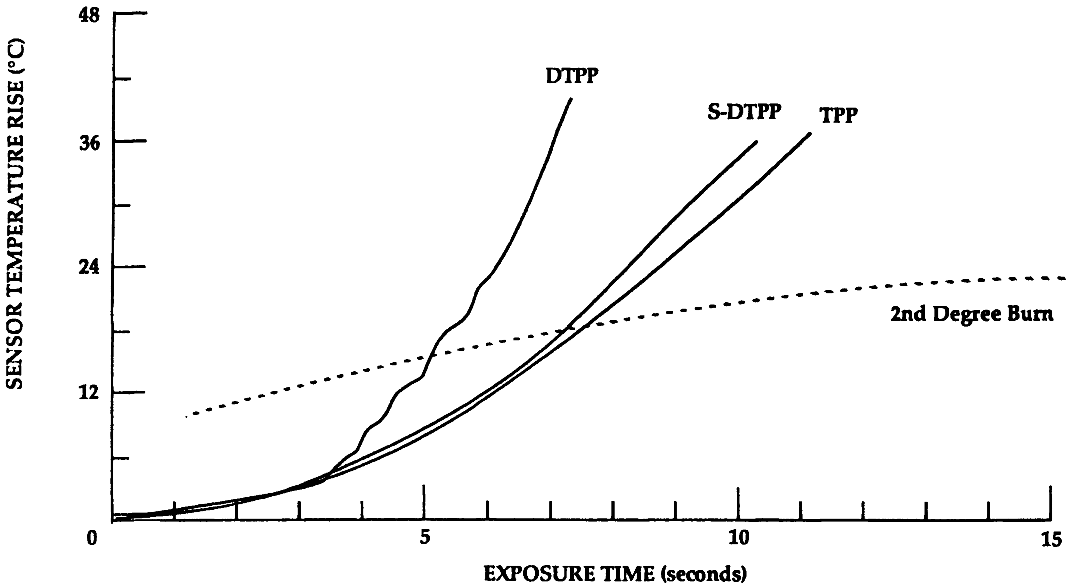

Figure 3. Thermal protective performance graph of Nomex® III fabric.

Downloaded by NORTH CAROLINA STATE UNIV on August 6, 2012 | http://pubs.acs.org
Publication Date: April 3, 1991 | doi: 10.1021/bk-1991-0457.ch018

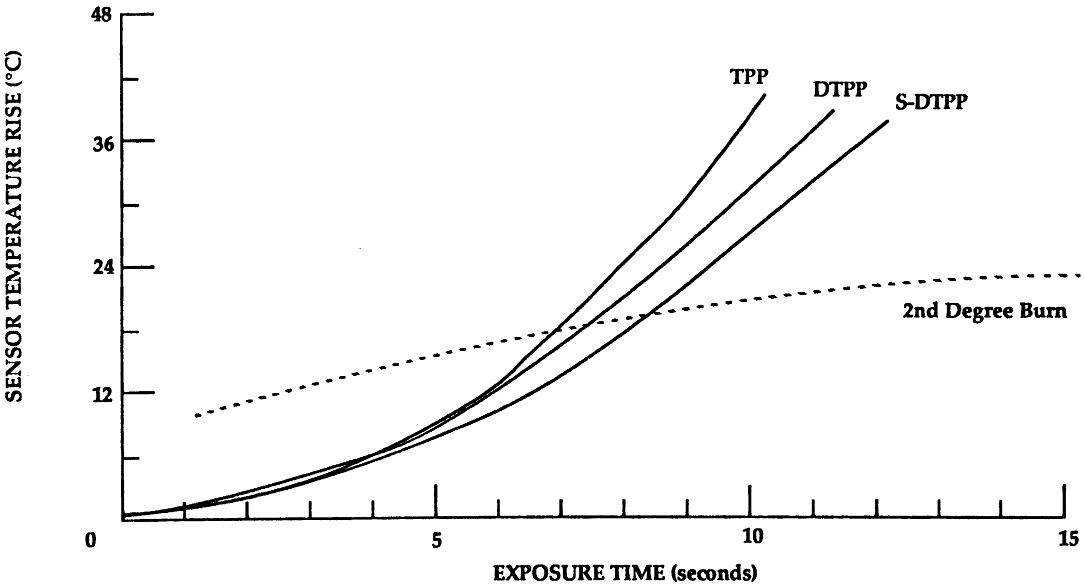

Figure 4. Thermal protective performance graph of Kevlar® 100 fabric.

the convectional TPP method. These results reflect the superior thermal stability of the Kevlar material. The heat stability of Kevlar is further confirmed by experiments showing that applied tension has little effect on the DTPP value (Fig. 7-B). As previously discussed, the higher TPP value recorded in the modified test is directly related to the changes in the configuration of the heat sensor.

FR Wool. The higher level of shrinkage restraint applied in the modified test had the greatest impact on the thermal protective performance of the FR wool sample. We believe that the significant loss in protective insulation suffered by the wool sample in the modified TPP test can be partly attributed to higher sample holding forces which restrain thermal shrinkage and prevent the swelling phenomenon which produces insulating char in the conventional TPP test. Additionally, flexing action in the dynamic test causes the wool fabric to break open producing catastrophic heat transfer to the heat sensor. Fig. 7-C shows that, in the static test condition, the level of applied tension is a significant factor affecting FR wool performance. In Fig. 5, the calorimetric trace labeled S-DTPP(A) is typical of the transfer rate measured in the modified TPP test operated to allow the FR wool sample to shrink with no flexing motion applied to the test sample. By comparison, the curve labeled S-DTPP(B) shows the heat transfer that occurs when the FR wool sample is restrained to prevent shrinkage and swelling. These experiments show that, when the sample holding conditions allow some shrinkage (-3%), the FR wool fabric swells and produces an effective insulating char. In this case, only a small crack is observed in the center of the fabric and the heat transfer rate is comparable to that observed in the conventional test (TPP). By comparison the test conducted with high sample restraint shows a heat transfer rate similar to the dynamic test rate (DTPP).

FR Cotton. The most complex behavior in TPP tests is exhibited by the FR cotton sample (Fig. 6). The process of heat transfer through the cotton fabric can be divided into three distinctive stages: an initial fabric heating period that leasts 3.5 seconds after the onset of the heat exposure. This phase is followed by a period occurring between 3.5 to 5.5 seconds after the test is initiated, in which heat is transferred rapidly through the fabric. This phase is followed by a more moderate heat transfer (> 5.5 seconds). The observed reduction in the rate of heat transmission can be attributed to the formation of insulative char that occurs as a result of carbonization of cellulosic material. Backside flaming of the FR fabric is also observed 4 to 5 seconds into the exposure. Figure 7-D shows that the thermal protective performance of the FR cotton sample is lowered by higher sample mounting tension.

Failure Mechanism in TPP Tests

Significant insight into material performance in TPP tests is gained by considering the mechanism that limits thermal protection. Table V compares the breakthrough time and the tolerance time of the test fabrics in static and dynamic TPP tests. In these cases, the tolerance time is taken as the time required for heat transmission to exceed the level for second degree burn. Breakthrough time is taken as the time at which the fabric was visually observed to break open. Additionally, Table VI identifies the mode of failure that is observed in each of the test samples. Therefore, we notice that, although the FR cotton sample ignites and breaks open in the dynamic TPP test, structural failure is not the limiting factor for this material. This is because the TPP of the FR

Downloaded by NORTH CAROLINA STATE UNIV on August 6, 2012 | http://pubs.acs.org
Publication Date: April 3, 1991 | doi: 10.1021/bk-1991-0457.ch018

Downloaded by NORTH CAROLINA STATE UNIV on August 6, 2012 | http://pubs.acs.org
Publication Date: April 3, 1991 | doi: 10.1021/bk-1991-0457.ch018

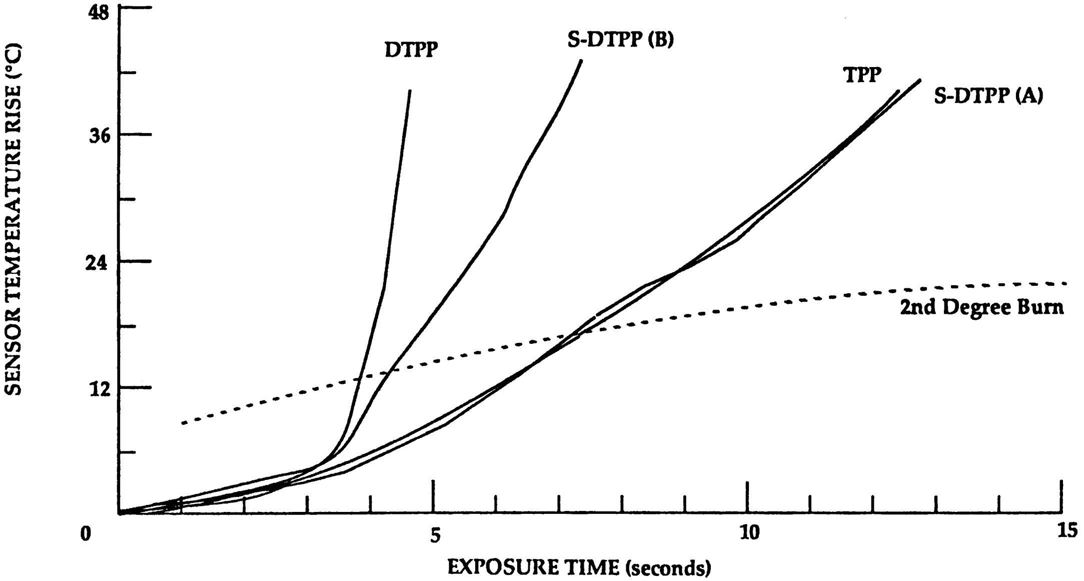

Figure 5. Thermal protective performance graph of FR wool fabric.

Downloaded by NORTH CAROLINA STATE UNIV on August 6, 2012 | http://pubs.acs.org
Publication Date: April 3, 1991 | doi: 10.1021/bk-1991-0457.ch018

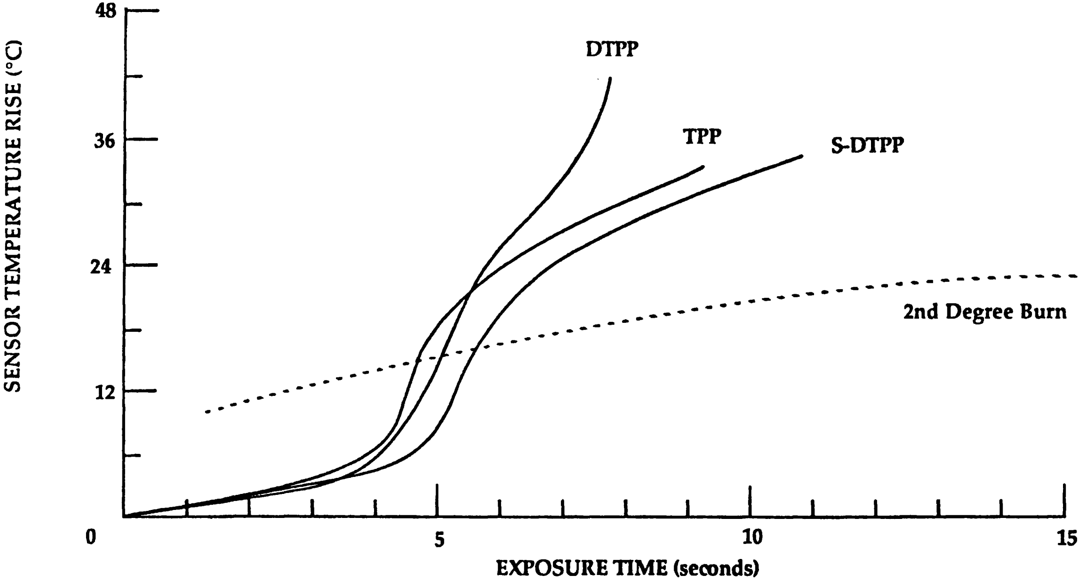

Figure 6. Thermal protective performance graph of FR cotton fabric.

Downloaded by NORTH CAROLINA STATE UNIV on August 6, 2012 | http://pubs.acs.org
Publication Date: April 3, 1991 | doi: 10.1021/bk-1991-0457.ch018

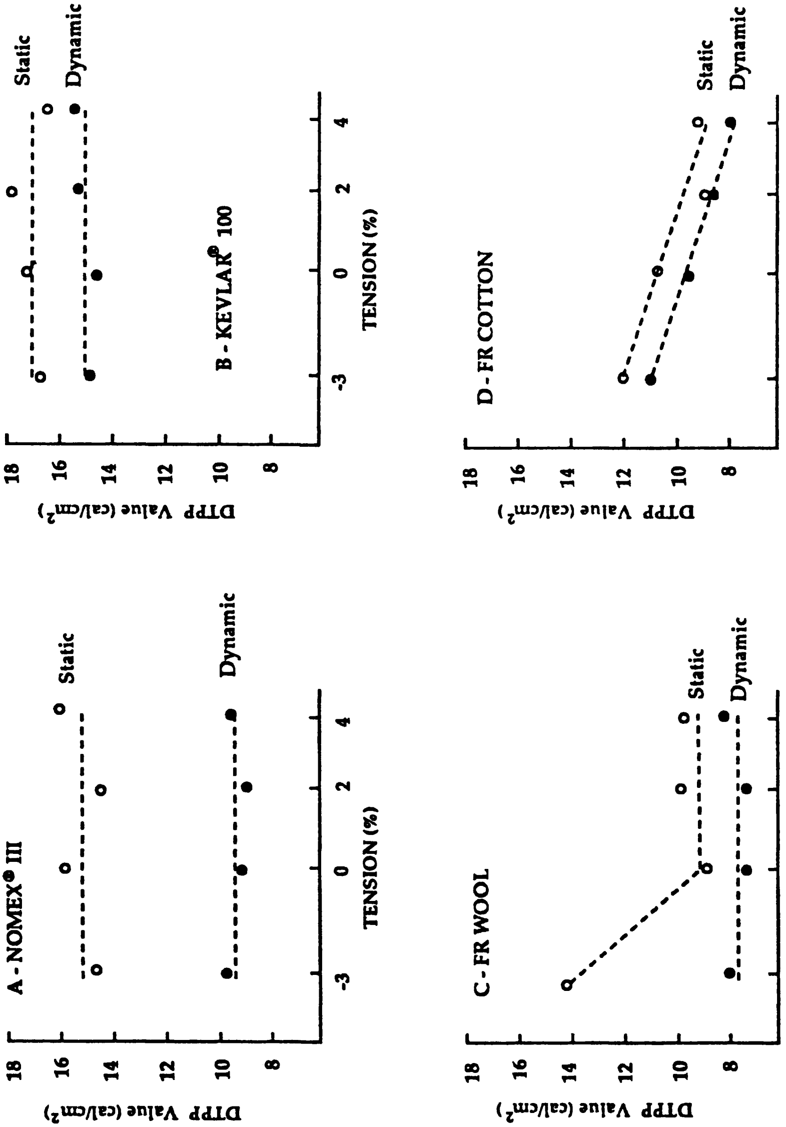

Figure 7. A, B, C, D Effect of tension on the thermal protective performance.

cotton sample is comparably low as measured in the conventional TPP test: thus, failure of the FR cotton sample occurs as a result of its thermal transmission. Break open takes place only after the Stoll criteria is exceeded. In comparison, the FR wool sample clearly fails in the dynamic TPP test as a result of mechanical breakthrough induced shrinkage forces and mechanical flexing. So far as dynamic TPP evaluation of aramid fabrics is concerned, we observed that the protective time afforded by the Nomex III sample is limited by heat transmission and not due to break-open in the fabric structure. This is partly because of the transfer of conductive heat that occurs when the back side of the Nomex III fabric contacts the heat sensor in the dynamic TPP testing configuration. This effect is a result of the shrinkage that occurs in the Nomex III sample during intense heat exposure. The superior thermal dimensional stability of Kevlar 100 is evident in the dynamic TPP test; we notice that heat transmission through the Kevlar 100 is little affected by flexing or by higher levels of sample mounting tension.

Table V. Breakthrough and Thermal Insulation Performance

Material	Test Method	Breakthrough Time (secs)	Tolerance Time (secs)
Nomex III	TPP	-	7.1
	S-DTPP	40.0	6.9
	DTPP	13.0	4.9
Kevlar 100	TPP	-	6.6
	S-DTPP	32.0	8.5
	DTPP	10.2	7.3
FR Cotton	TPP	-	4.4
	S-DTPP	26.0	5.5
	DTPP	6.5	4.9
FR Wool	TPP	-	7.2
	S-DTPP	2.1	4.2
	DTPP	2.0	3.6

Table VI. Mechanism Responsible for Limiting Protective Thermal Insulation under the Dynamic Test Conditions

Material	Failure Mechanism
Nomex III	Conductive heat transfer
Kevlar 100	Pure radiant and convective heat transmission
FR Wool	Mechanical breakthrough
FR Cotton	Pure radiant and convective heat transmission

Downloaded by NORTH CAROLINA STATE UNIV on August 6, 2012 | http://pubs.acs.org
Publication Date: April 3, 1991 | doi: 10.1021/bk-1991-0457.ch018

Conclusions

A dynamic TPP test has been demonstrated that adds an additional component of realism to the laboratory evaluation of the thermal protective performance of fabrics. By incorporating tension and flexing motion, this new procedure simulates forces placed on apparel materials by human movement in response to a fire accident. The modified TPP method permits visual evaluation of the ability of fabrics to resist ignition in fire exposure as it provides a direct measure of the ability of a protective fabric to retain strength and flexibility in flame.

Our research shows that the higher level of sample restraint and mechanical action that are features of a dynamic TPP evaluation, contribute to lower the TPP rating of fabrics that shrink at high temperatures or fabrics that develop a brittle char. Consequently, the upper limit of thermal protective performance is defined either by catastrophic breakthrough that results from mechanical forces, or by limits on heat transmission in fabrics that otherwise retain structural integrity throughout the heat exposure. Whether the TPP limit is defined by accumulated heat transfer or by break open depends on the conditions of sample restraint and movement and on the insulation characteristics of the material itself. Our experiments clearly show that it depends on the ability of the material to maintain strength and flexibility in the face of thermal degradation.

Therefore, thermally stable Kevlar 100 emerges as a superior insulator in dynamic TPP tests. Other materials suffer varying degrees of loss in protective insulation. For example, the TPP of the FR wool sample is severely limited in dynamic evaluations. This is a direct result of high shrinkage restraint and mechanically induced break open of the characteristic char generated when wool is exposed to high heat. The insulation of the Nomex III sample is also reduced as a result of heat shrinkage which causes the fabric to contact the thermal sensor. However, since the Nomex III fabric was the only material that an intimate contact between the backside of the fabric and the heat sensor was observed, care must be taken in evaluating the protective performance. The effect of conductive heat transfer may be overestimated by the heat sensor as a result of the higher thermal conductivity of the copper compared with the thermal conductivity of human skin. FR cotton fabric is observed to form a brittle char which breaks open in dynamic flexing. However, the FR cotton sample does not exhibit poorer thermal protection performance in the dynamic TPP than it does in the conventional static method. This is because the TPP of the FR sample is already comparably low. Therefore, mechanically induced break-open occurs only after the fabric fails by transmitting heat in excess of the Stoll criterion for second degree burn injury.

Although the dynamic TPP test provides a promising means of evaluating the thermal protection of fabrics, more research is needed to qualify and determine the practical significance of these measurements. There is a particular need to determine how dynamic TPP data may be interpolated to predict the field performance of thermal protective garments. Therefore, an effort is ongoing to develop a novel testing arrangement that uses a mechanical leg immersed in flames generated by large gas torches. The mechanical leg, driven to simulate the action of running man, will be used to evaluate materials in garment form as they are subjected to fire and to movement. This approach will establish, under extremely realistic conditions, the correlation between a dynamic TPP test, and the protective performance of clothing systems.

Downloaded by NORTH CAROLINA STATE UNIV on August 6, 2012 | http://pubs.acs.org
Publication Date: April 3, 1991 | doi: 10.1021/bk-1991-0457.ch018

Authors' Note

Care must be taken in deriving conclusions about the safety benefits from these data. The data describe the properties of fabrics in response to specified test conditions and controlled laboratory exposures. The test conditions may not represent actual field conditions which can be physically complicated and unqualified.

Acknowledgments

This research was funded by the Thermal Resistant Systems/Nomex group of E.I. DuPont De Nemours & Company. We also acknowledge the contribution of DuPont in providing the test materials used by this research.

Literature Cited

1. Behnke, W. P. Fire and Materials 1984, 8(2), 57-63.
2. Abbott, N. J.; Schulman, S. Journal of Coated Fabrics, 1976, 6, 48-64.
3. NFPA 1971, Standard on Protective Clothing for Structural Firefighters, National Fire Protection Association: Quincy, Massachusetts, 1986.
4. Stoll, A. M.; Chianta, M. A. Aerospace Medicine, 1968, 39, 1097-1100.
5. Hopper, B. J. The Mechanics of Human Movement; American Elsevier: New York, 1973.
6. Grillner, S.; Halbertsma, J.; Nillson, J.; Thortensson, A. Brain Research, 1979, 165, 177-182.
7. Ghosh, T. K.; Barker, R. L. Journal of Industrial Fabrics, 1986, 4, 20-28.
8. Shalev, I.; Barker, R. L. In Performance of Protective Clothing, ASTM Special Technical Publication 900; Barker, R. L.; Coletta, G. C., Eds.; American Society for Testing and Materials: Philadelphia, 1986; pp 358-375.

RECEIVED August 9, 1990

Downloaded by NORTH CAROLINA STATE UNIV on August 6, 2012 | http://pubs.acs.org
Publication Date: April 3, 1991 | doi: 10.1021/bk-1991-0457.ch018

Downloaded by STANFORD UNIV GREEN LIBR on August 6, 2012 | http://pubs.acs.org
Publication Date: April 3, 1991 | doi: 10.1021/bk-1991-0457.ch019

Chapter 19

Melt–Stick Characteristics of Flame-Retardant-Treated Polyester–Cotton Blend Fabrics

Robert W. Hall

Navy Clothing and Textile Research Facility, 21 Strathmore Road, Natick, MA 01760

The Navy Clothing and Textile Research Facility (NCTRF) conducted a series of heat and flame exposure tests on several blend levels of fire retardant (FR) treated polyester-cotton fabrics. The tests were conducted in an effort to evaluate the relative burn injury potential of the various blend levels as related to melt/stick properties. A combination of four tests procedures were used to rate the fabrics. Test results showed fabrics with 65 percent polyester had high melt/stick characteristics while blends containing up to 50 percent polyester pose little risk of melt/stick induced burn injury. Individual test failures on some fabrics containing 50 percent or less polyester indicate further testing is needed. A new test method for melt/stick testing is described.

Recent development and use of durable fire retardant (FR) treated polyester-cotton blend fabrics in utility and service clothing has raised interest in the melt/stick hazard of polyester. This study used a series of tests to evaluate and rate fire retardant (FR) treated polyester—cotton blend fabrics for risk of melt/stick induced burn injury. It has long been felt that any amount of thermoplastic fiber blended with a non thermoplastic fiber would melt under heat or flame and would cling or stick to the skin contributing to burn injury. The objective of this study was to determine the maximum amount of polyester that could be used in a FR treated polyester-cotton blend fabric without melt/stick occurring. To provide a means of measuring the propensity of molten polymer to stick to the skin, current test methods were surveyed and found to be lacking in definition and reliability. It was therefore decided that existing test methods would require modification or new methods developed. This study summarizes the melt/stick results for the fabrics tested, describes the test

This chapter not subject to U.S. copyright
Published 1991 American Chemical Society

methods used and developed, and makes recommendations for selection of fabric blends to minimize melt/stick characteristics.

Background

There have been several studies comparing the flammability of polyester—cotton blend fabrics with that of 100 percent of either fiber (1,2,3,4). The conclusions drawn from these studies indicate fabrics made from blends of polyester cotton are more flammable and pose a greater risk than fabrics made from 100 percent cotton or polyester. These studies also indicate that the higher the polyester content, the lower the risk of burn injury. Based on the methods employed and the data presented, the conclusions appear to be valid.

Miles (1) showed lower burn injury potential for polyester when A-line dresses were subjected to a remote ignition source simulating a chance flame exposure. Langstaff and Trent (2) reported similar results using the Eastman flat plate (modified MAFT), the TRI convection calorimeter and an instrumented manikin (TIM). Burn tests on TIM showed a decrease in heat release and depth of burn with an increase in polyester content. Fabrics of different weights generated similar amounts of heat release since lighter weight fabrics are consumed faster than heavy fabrics.

Goynes and Trask (3) found that untreated cotton fabrics burn easily and form a fragile char, while polyester shrinks and drips away from the flame. In a polyester-cotton blend, the polyester melts and flows around the cotton, supporting the char and prolonging the flame. An earlier study by Chouinard, Knodel and Arnold (4) found similar results for both nylon—cotton and polyester-cotton blends. The nylon and polyester transmit the flame slowly and often self extinguish when the melting polymer falls away. In these studies, both the nylon and polyester needed cotton to sustain combustion.

These studies suggest that for untreated fabrics, the risk of burn injury is related to the polyester content of the fabric, and that the higher the polyester content the lower the risk. In the case of polyester-cotton blend fabrics that have been finished with a durable FR treatment the polyester again melts and surrounds the cotton, but the FR treatment inhibits flame spread. The result is a somewhat brittle char in the direct flame contact area, with the heat causing the polyester to melt into the adjacent area forming a stiff, durable char.

A number of tests have been used to evaluate the fire and flame resistance of textiles. These tests measure ease of ignition, after flame, self extinguishment, heat release and several other characteristics. None of these tests measure the propensity of the melting polymer contained in a fabric blend to melt and stick to skin. An early attempt to measure the effect of melting polymer on burn injury (4) used heat sensors placed in a board and positioned 1/4 inch below an ignited fabric. Any molten polymer falling from the flaming fabric dropped onto the board containing the sensors and the heat energy was measured. This study found that polyester-rich fabrics transferred less heat than the all-cotton or cotton-rich fabrics tested. The shortfalls of this study were that

Downloaded by STANFORD UNIV GREEN LIBR on August 6, 2012 | http://pubs.acs.org
Publication Date: April 3, 1991 | doi: 10.1021/bk-1991-0457.ch019

none of the fabrics contained a flame retardant finish, and the configuration of the test did not allow the burning, melting fabric to come in contact with the sensors.

The approach taken by the National Fire Protection Association (NFPA) for materials used in the manufacture of firefighter's clothing is the so-called Oven Test (5). Materials are suspended in a convection oven for five minutes at 260° C and must not melt, separate or ignite. The test appears to have poor reproducibility and has little definition of failure criteria. Almost all fabrics containing polyester or nylon gain some stiffness in this test as a result of melting of the polymer. The amount of polyester or nylon in the fabric influences the amount of stiffness. By definition, any resultant stiffness indicates polymer flow and test failure, but there is no indication of melt/stick. This test appears to have been included in the proposed standard for station uniforms for lack of a better test.

Work in the United Kingdom by the Ministry of Defense has centered on what is called a "hot plate" test (6). The fabric sample is placed on a hot plate and heated to 260° C. The amount of melted polymer visible on the surface of the fabric indicates its relative melt/stick propensity. This test is difficult to control since the heated fabrics tend to shrink and/or curl away from the hot plate and provide no means of measuring adhesion.

Methods and Materials

Oven Test

Fabrics were subjected to the 260° C Oven Test for five minutes and evaluated for melt. Problems associated with this test include controlling the oven temperature, the duration of the exposure and interpreting the results. For this test, the fabric ranking was based on the condition of the exposed samples. Fabrics that became stiff, but did not crack when folded, were rated "0", those that cracked, "1"; and those that showed melting on the surface, "2".

Hot Plate Test

A modification of the "hot plate" test using two layers of fabric was used to assess melt/stick in this study. It was decided to use two layers of each fabric evaluated, since it was felt that if the polymer in a fabric, when subjected to these test conditions, flowed in sufficient quantity to stick to another layer of the same fabric, there was a risk of the fabric sticking to skin under the same conditions.

For the hot plate test a 1/4 inch thick copper plate was placed on an electric hot plate and heated above 250° C. The temperature was monitored by a thermocouple set into the copper plate. Samples run with a weight on the fabrics resulted in the fabrics being completely charred with no evidence of sticking. The test procedure was changed to heating a single layer of fabric until the fabric began to melt and char. Shrinking in some of the fabrics required some mechanical manipulation to keep the sample in contact with the heated copper plate. At the time of melting and charring another

Downloaded by STANFORD UNIV GREEN LIBR on August 6, 2012 | http://pubs.acs.org
Publication Date: April 3, 1991 | doi: 10.1021/bk-1991-0457.ch019

sample of fabric was pressed against the heated fabric and the combined sample removed from the hot plate, allowed to cool, and rated.

Two additional melt/stick tests were conducted on double layer fabric samples: (1) exposure to radiant heat and (2) a hot air or convective heat exposure test. Since the objective of these tests was to evaluate melt/stick and not flame resistance, the hot plate, radiant and convective heat tests were run until degradation was observed rather than using a preset exposure time. All fabrics were exposed until melting occurred or the fabric charred. The fabrics were then allowed to cool before melt/stick evaluations were made. This was necessary because the actual time to char or melt varied considerably among fabrics. If preset exposure times had been used, some fabrics may not have melted as they did under a more prolonged exposure.

Radiant Heat Test

The radiant heat exposure tests were conducted using the NCIRF radiant heat tester (Figure 1). This tester uses two sets of quartz lamps set at a 45 degree angle to the face of the test specimen. A concentric ring sample holder was used that provides intimate contact between the fabric samples and prevents the fabric from shrinking during the test. The samples are mounted vertically and were exposed to a combined heat flux of 0.9 gcal/cm sq/sec until charring and melting occurred.

Convective Hot Air Tests

The convective hot air tests were conducted using a Black and Decker Model 9751 heat gun (Figure 2). The temperature measured two inches from the barrel of the gun was 260 to 265^{o} C. A guide was attached to the side of the heat gun to aid in positioning of the sample during the test. Test fabrics were mounted in the ring holder used for the radiant heat testing, exposed until charring and melting occurred, removed from the holder and rated.

Two layers of fabric were used for the hot plate, radiant and convective hot air tests. Melt/stick occurred when the melting polymer flowed between the fabric layers during exposure. Fabrics that did not stick were rated "0" and those experiencing minimal surface sticking were rated "1". In order to be rated "1" the sticking fabrics must separate easily with no transfer of polymer or char between fabrics, otherwise the fabric was rated "2" (melt/stick).

Attempts were made to devise or use other test methods with unsuccessful results. Using a Thermal Protective Performance (TPP) tester (Figure 3), two layers of fabric were evaluated at different heat fluxes and exposure times to allow melting of the fabrics. High heat fluxes or long exposure times resulted in completely charred fabrics with no evidence of sticking. Control of exposure allowed melting without excess char, but no sticking occurred with the samples tested. A 100 percent polyster fabric was tested with the result that the lower fabric melted away with little or no degradation of the upper fabric. Based on these results, it was

Downloaded by STANFORD UNIV GREEN LIBR on August 6, 2012 | http://pubs.acs.org
Publication Date: April 3, 1991 | doi: 10.1021/bk-1991-0457.ch019

Downloaded by STANFORD UNIV GREEN LIBR on August 6, 2012 | http://pubs.acs.org
Publication Date: April 3, 1991 | doi: 10.1021/bk-1991-0457.ch019

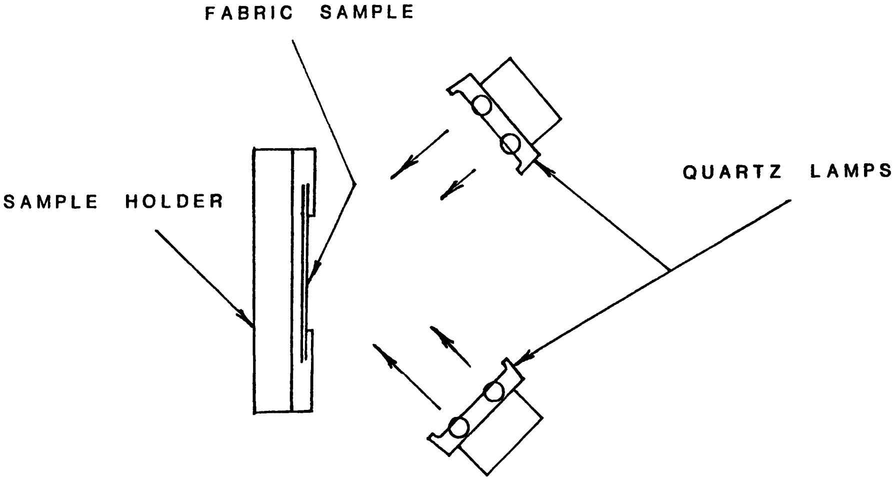
FABRIC SAMPLE
SAMPLE HOLDER
QUARTZ LAMPS

Figure 1. Radiant heat.

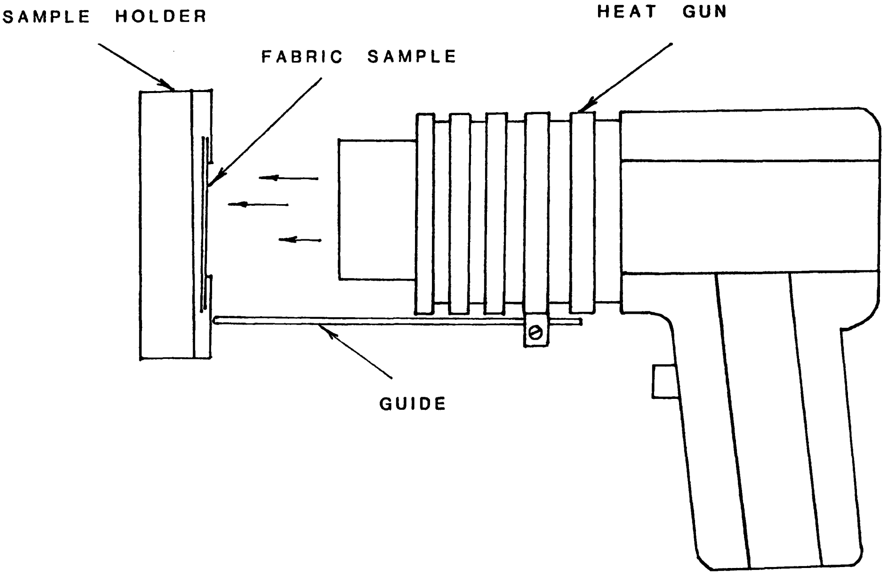
SAMPLE HOLDER
HEAT GUN
FABRIC SAMPLE
GUIDE

Figure 2. Hot air convective heat gun.

Downloaded by STANFORD UNIV GREEN LIBR on August 6, 2012 | http://pubs.acs.org
Publication Date: April 3, 1991 | doi: 10.1021/bk-1991-0457.ch019

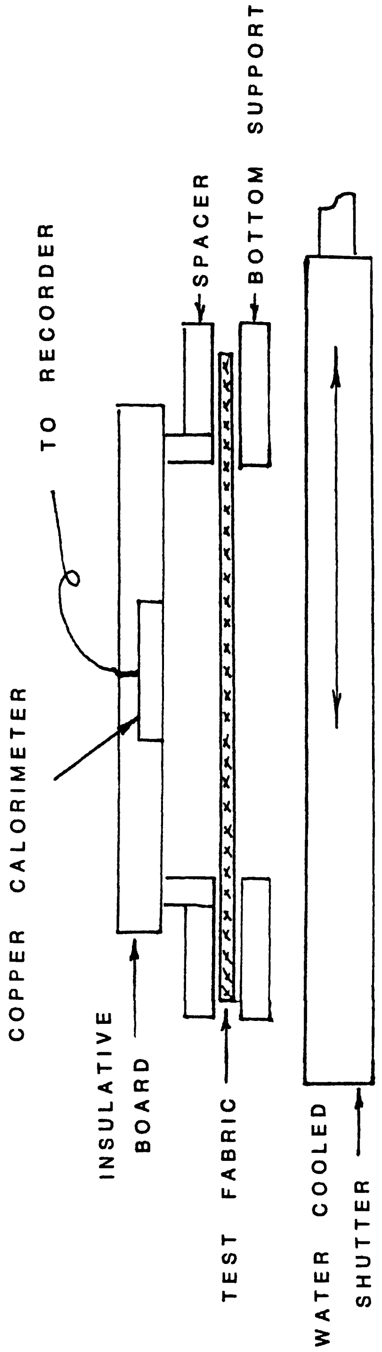
COPPER CALORIMETER
TO RECORDER
INSULATIVE BOARD
SPACER
TEST FABRIC
BOTTOM SUPPORT
WATER COOLED SHUTTER

Figure 3. TPP tester.

Downloaded by STANFORD UNIV GREEN LIBR on August 6, 2012 | http://pubs.acs.org
Publication Date: April 3, 1991 | doi: 10.1021/bk-1991-0457.ch019

decided that this test was not a good indicator of the melt/stick hazard of these fabrics.

Another test used a timed burning tablet placed on the fabric. The tablet was lighted with a match, and the heat passing through the fabric measured by a water cooled heat flux transducer placed against the underside of the fabric. No sticking of polymer to the transducer occurred and the differences in measured heat from sample to sample were more related to fabric weight than fiber content.

All fabrics used in this study were manufacturer's samples or fabrics that were available from previous development programs at NCIRF. No fabrics were manufactured or finished specifically for this study. Table I lists characteristics of the fabrics evaluated. Fabric weights varied from 3.8 to approximately 11.0 ounces per square yard. No specific attempt was made to identify the fire retardant finishes used or to determine the amount of finish applied to the fabrics. Some of the fabrics were identified through previous work.

Table I. Fabric Characteristics

Fabric No.	Blend (%)	Fiber	Weight (oz/sq yd)	Weave	Ends/Picks (in)	Char Length (in)
1	25/75	nylon/cotton	7.6	2/1 TWILL	93/45	4.0
2	25/75	nylon/cotton	8.9	2/1 TWILL	92/56	4.6
3	30/70	nylon/cotton	7.8	2/1 TWILL	81/53	3.6
4	35/65	polyester/cotton	8.9	3/1 TWILL	124/57	5.1
5	40/60	polyester/cotton	11.0	2/2 TWILL	88/39	3.7
6	45/55	polyester/cotton	7.6	3/1 TWILL	124/49	3.0
7	45/55	polyester/cotton	7.8	3/1 TWILL	128/53	4.6
8	45/55	polyester/cotton	7.9	2/1 TWILL	87/48	3.7
9	50/50	polyester/cotton	3.8	PLAIN	86/53	6.0
10	50/50	polyester/cotton	5.9	2x1 BASKET	104/41	5.5
11	50/50	polyester/cotton	6.6	2/1 TWILL	92/48	5.5
12	50/50	polyester/cotton	6.6	2/1 TWILL	104/48	4.6
13	50/50	polyester/cotton	7.3	2/1 TWILL	87/52	4.0
14	50/50	polyester/cotton	8.0	2/1 TWILL	98/46	4.6
15	50/50	polyester/cotton	8.0	2/1 TWILL	102/49	4.5
16	50/50	polyester/cotton	8.1	2/1 TWILL	96/48	5.0
17	50/50	polyester/cotton	8.6	2/1 TWILL	102/49	5.6
18	50/50	polyester/cotton	10.7	2/1 TWILL	81/48	3.7
19	65/35	polyester/cotton	5.5	2/1 TWILL	108/54	5.0
20	65/35	polyester/cotton	6.0	2x1 BASKET	108/72	6.4
21	65/35	polyester/cotton	6.8	2x1 BASKET	108/72	5.0
22	65/35	polyester/cotton	7.7	2/1 TWILL	87/44	3.7
23	65/35	polyester/cotton	7.8	2/1 TWILL	87/44	5.1

In addition to these tests, all fabrics were tested for vertical flammability, in accordance with TM 5903 of FED STD 191, to verify their flame resistance characteristics and were shown to be fire retardant, with char lengths of 3.0 to 6.4 inches.

Downloaded by STANFORD UNIV GREEN LIBR on August 6, 2012 | http://pubs.acs.org
Publication Date: April 3, 1991 | doi: 10.1021/bk-1991-0457.ch019

Results and Discussion

All fabrics were rated in each of the four tests for estimate of melt/stick burn injury potential. A total rating from all four tests was calculated and the fabrics ranked from highest to lowest risk. Table II lists the ratings and order of rank. For fabrics with equal total ratings the fabrics are listed by polyester content and then by weight.

Table II. Fabric Rankings 1/

Fabric No.	Blend	Weight	Hot Plate	Radiant	Heat Gun	Oven	Total
2	25/75 n/c	8.9	0	0	0	0	0
3	30/70 n/c	7.8	0	0	0	0	0
4	35/65 p/c	8.9	0	0	0	0	0
7	45/55 p/c	7.8	0	0	0	0	0
5	40/60 p/c	11.0	0	0	0	0	0
18	50/50 p/c	10.9	0	0	0	0	0
8	45/55 p/c	7.9	0	1	0	0	1
11	50/50 p/c	6.6	1	0	0	0	1
12	50/50 p/c	6.6	1	0	0	0	1
13	50/50 p/c	7.3	0	1	0	0	1
16	50/50 p/c	8.1	1	0	1	0	2
17	50/50 p/c	8.6	0	1	1	0	2
10	50/50 p/c	5.9	0	1	2	0	3
14	50/50 p/c	8.0	1	1	0	1	3
1	25/75 n/c	7.6	0	2	1	1	4
21	65/35 p/c	6.8	0	2	2	0	4
15	50/50 p/c	8.0	1	1	2	1	5
6	45/55 p/c	5.5	0	2	2	2	6
19	65/35 p/c	5.5	2	2	2	2	8
9	50/50 p/c	3.8	2	2	2	2	8
20	65/35 p/c	6.0	2	2	2	2	8
22	65/35 p/c	7.7	2	2	2	2	8
23	65/35 p/c	7.8	2	2	2	2	8

1/ 0 no stick 1 slight stick 2 stick

Oven Tests

Five fabrics were rated "2" in the oven test. In all five cases, considerable molten polymer solidified on the surface of the fabrics which caused them to become very stiff and fragile. Three of the five fabrics contained 65 percent polyester, one was a 50/50 polyester cotton-blend and the other was a 45 percent polyester blend. Four additional fabrics cracked and split when folded and were rated "1". Two of these fabrics contained 50 percent polyester, one 65 percent polyester and the other 25 percent nylon. The balance of the fabrics had varying degrees of stiffness with no cracking.

Hot Plate Tests

Five fabrics rated "2" on this test including four fabrics containing 65 percent polyester and one with 50 percent polyester (#9). Five additional fabrics showed slight sticking and were rated "1". These five fabrics contained 50 percent polyester. One 65 percent polyester fabric (#21) showed no sign of melt/stick on either this or the oven test. This fabric is identical to fabric #20, except that it was treated with a bromine based flame retardant finish in a latex binder, which appeared to help contain the melting polymer under these test conditions.

Radiant Heat Tests

A total of eight fabrics showed a tendency to stick under these test conditions. All five of the 65 percent polyester fabrics failed this test with a rating of "2". Fabric #9 also failed this test, as well as fabric #6 with 45 percent polyester, and #1 with 25 percent nylon. Six fabrics showed slight sticking in this test, five with 50 percent polyester and fabric #8 with 45 percent polyester.

Convective Hot Air Tests

Nine fabrics rated "2" in this test, including the five fabrics containing 65 percent polyester. As in the radiant tests, fabrics #9 and #6 were also rated "2", along with two fabrics containing 50 percent polyester. Fabric #1, with 25 percent nylon, and two 50/50 polyester cotton fabrics showed slight sticking. The balance of the fabrics showed no tendency to stick in either the radiant or heat gun exposure tests.

Conclusions

Of the test methods used in this evaluation, the radiant and heat gun tests appear to be the most reliable. Test equipment can be duplicated at modest cost, the tests are simple to conduct and results are consistent. During these tests the melting polymer is drawn toward the source of heat, which is the face side of the fabric. When sufficient heat is transmitted to the second layer of fabric, the polymer flows toward the front fabric. If there is sufficient flow, the fabrics stick together. Consequently, these tests would be more easily interpreted as a pass/fail test. Any fabric separation during handling should not be considered as "slight stick", as rated in this study. It is felt that any fabric showing slight stick in these tests (samples separating easily with no transfer of polymer), pose little risk of melt/stick induced burn injury.

All test results reported are the worse ratings achieved for each fabric/test condition. Replications (three) on the radiant and heat gun tests showed consistant ratings. The oven and hot

Downloaded by STANFORD UNIV GREEN LIBR on August 6, 2012 | http://pubs.acs.org
Publication Date: April 3, 1991 | doi: 10.1021/bk-1991-0457.ch019

plate tests were more difficult to control, resulting in inconsistent ratings from test to test.

All of the 65/35 polyester-cotton fabrics showed poor results in the radiant and heat gun tests. Fabrics #9 and #6, containing 50 and 45 percent polyester, respectively, also showed poor results in both of these tests. Attempts to explain the poor results achieved with these two fabrics were not successful. It was originally felt that the fabrics may have contained too much finish thus preventing the melting polymer from dispersing into the cotton. As a result, some of the finish was removed and the fabrics were re-tested. This, however, provided no change in results. Two additional 50/50 polyester-cotton fabrics (#15 and #17) failed the heat gun test and fabric #11 failed the radiant test. Discounting the slight stick criteria, thirteen fabrics containing 50 percent or less polyester or nylon demonstrated little risk of melt/stick induced burn injury while five, or 28%, showed a tendency to melt/stick.

Based on the test results of the recommended tests, fabrics containing 65 percent or more polyester are at high risk of causing melt/stick burn injuries, while fabrics containing 50 percent or less thermoplastic fiber appear to be of low risk, although individual failures indicate more testing is needed before definite conclusions can be drawn. Thirteen fabrics showed little or no tendency to melt/stick indicating that with control of fiber blending as well as fabric construction and finishing, polyester or nylon-cotton blend fabrics could be produced that will not add to the risk of burn injury through melt/stick.

This study shows that the radiant and heat gun tests can be used to estimate the relative melt/stick characteristics of FR treated thermoplastic-cotton blend fabrics although additional work is needed to determine the precision of the methods.

Downloaded by STANFORD UNIV GREEN LIBR on August 6, 2012 | http://pubs.acs.org
Publication Date: April 3, 1991 | doi: 10.1021/bk-1991-0457.ch019

Literature Cited

1. Miles, L. B. An investigation of the Flammability Hazard of Apparel Fabrics; Symposium on Textile Flammability; Leblanc Research Corp.: 1978.
2. Langstaff, W. E.; trent, L. C. The Effect of Polyester Fiber Content on the Burn Injury Potential of Polyester/Cotton Blend Fabrics: 1980, 7, 26.
3. Goynes, W. R.; Trask, B. J. Effects of Heat on Cotton, Polyester, and Wool Fibers in Blended Fabrics - A Scanning Electron Microscopy Study; Textile Research Journal: July 1985.
4. Chouinard, M. P.; Knodel, D. C.; Arnold, H. W. Heat Transfer from Flammable Fabrics; Textile Research Journal: March 1973.
5. Anon NFPA 1971 - Protective Clothing for Structural Firefighters, 1986 edition; National Fire Protection Association: Quincy, MA.
6. Randall, A. Correspondence, Stores and Clothing Research and Development, Ministry of Defense, U. K., Dec. 17, 1987.

RECEIVED June 1, 1990

Chapter 20

Polyester Geotextiles

Durability of Polyethylene Terephthalate Fibers and Fabrics

C. J. Sprague[1] and G. W. Davis[2]

[1]Nicolon Corporation, Norcross, GA 30092
[2]Hoechst Celanese Corporation, Charlotte, NC 28209

Downloaded by COLUMBIA UNIV on August 6, 2012 | http://pubs.acs.org
Publication Date: April 3, 1991 | doi: 10.1021/bk-1991-0457.ch020

In the last decade, the use of geotextiles has evolved from specialty "engineering fabrics," considered state-of-the-art in unique geotechnical designs, to commonly used construction materials, considered state-of-the-practice in many civil engineering applications. This relatively quick acceptance of geotextiles can best be explained by their proven track record. Geotextiles have generally performed as expected over their designed service life.

Performance of geotextiles is commonly termed, "durability." Durability can be thought of as relating to changes over time of both the fiber microstructure and the fabric macrostructure. The former involves molecular polymer changes and the latter assesses fabric property changes. This paper takes a look at each of these components of durability as they relate to the use of polyethylene terephthalate (P.E.T.), commonly called polyester, fibers in geotextiles.

For more than two decades, textile materials constructed of synthetic polymer fibers, have been utilized in the construction of roads, drainage systems, and other civil engineering projects. These materials primarily composed of polyester or polypropylene have become known as "geotextiles" because they are textile materials used in conjunction with the ground (hence "geo-"). Geotextiles are designed to perform a function, or combination of functions, within the soil/geotextile system. Such functions as filtration, separation, planar flow, or reinforcement are expected to be performed over the life of the installation, which is often 50 to 100 years, or more.

Geotextiles are accepted construction materials and, like all other materials, they have limitations.

0097–6156/91/0457–0304$06.00/0

While woven geotextiles may be more suitable for reinforcing than are nonwoven geotextiles, they may also be more prone to clogging or piping. Similarly, polyester geotextiles may provide better strength characteristics but poorer chemical resistance than polypropylene geotextiles.

All polymeric materials are susceptible to degradation. For example, polyolefins such as polypropylene and polyethylene undergo oxidative degradation, whereas polyethylene terephthalate (P.E.T.), can be hydrolyzed, and polyamides degrade by both hydrolysis and oxidation. However, it must be emphasized that these reactions can be retarded by the use of suitable additives. Although these processes may be quite slow at ambient temperature, anticipated lifetimes for geotextiles of up to 100 years have been proposed. Furthermore, the degradative processes are readily catalyzed by, for example, transition metals in the case of oxidations and by low pH in the case of polyester hydrolysis [1]. Therefore, an understanding of the geotextile fabric structure and fiber molecular make-up and how these are affected by the in-service environment are necessary to select the appropriate material.

Downloaded by COLUMBIA UNIV on August 6, 2012 | http://pubs.acs.org
Publication Date: April 3, 1991 | doi: 10.1021/bk-1991-0457.ch020

Resistance to Fiber Degradation

Table 1 lists the potential mechanisms of polymer degradation. Table 2 rates the intrinsic resistance of common polymers to degradation. The most predominant degradation concern, especially for polypropylene and polyethylene, involves oxidation. Conversely, solvolysis in the form of hydrolysis is a more pronounced mechanism of degradation for polyesters and polyamides.

Both oxidation and solvolysis are forms of chemical degradation. Generally, significant chemical degradation is observed only at elevated temperatures because the activation energy for these processes is high [2]. The moderate temperatures associated with most installation environments would, therefore, not be expected to promote degradation. Additionally, the majority of synthetic polymers is rather inert towards biological enzymatic attack [2].

Fabric Performance

Fabric performance is most obvious to the geotextile user. Table 3 lists several failure mechanisms which can cause unsatisfactory performance of the geotextile.

In general, long-term piping and clogging resistance, as well as tensile and compression creep resistance, are the most common fabric properties related to durability.

Aging

The exposure environment will generally be characterized by complex air, soil and water chemistry as well as unique radiation, hydraulic and stress conditions. The effect of this combination of exposures, over time, is termed aging. Aging therefore includes both polymer degradation and reduced fabric performance and is dependent on the specific application environment. Durability refers to a geotextile's resistance to aging.

Downloaded by COLUMBIA UNIV on August 6, 2012 | http://pubs.acs.org
Publication Date: April 3, 1991 | doi: 10.1021/bk-1991-0457.ch020

Table 1
Mechanisms of Polymer Degradation†

Chemical Rx	• Oxidation • Ozonization (oxidation initiator) • Solvents • Solvolysis (hydrolysis, ionic reactions) • Trace Metals (oxidation catalyzer)
Thermolysis	(oxidation initiator)
Mechanical Stress	(oxidation initiator)
Photolysis	(oxidation initiator)
Radiolysis	(oxidation initiator)
Biological Attack	• Enzyme (microorganisms) • Mechanical (rodents, insects)

† After Schnabel [2]

Table 2
Intrinsic Material Resistance Against Degradation Mechanisms†

	PA	PE	PET	PP
Photo-oxidation	+	o1)	++	o1)4)
Thermo-oxidation	+	o1)	++	-1)4)
Hydrolysis	o	+	-/o3)	+
Chemical Rx - acid	o	++	+	+
- alkaline	+	++	o	+

Ratings:
-
o improved
+ relative
out.
++ resistance

NOTES:
1) Additives can improve the intrinsic resistance provided they do not leach
2) The resistance of all materials is influenced by material thickness [4].
3) Hydrolysis is primarily a result of exposure to a strongly alkaline, high temperature environment.
4) Exposure to atmosphere or contact with iron can increase the rate of degradation

† After den Hoedt [3]

Downloaded by COLUMBIA UNIV on August 6, 2012 | http://pubs.acs.org
Publication Date: April 3, 1991 | doi: 10.1021/bk-1991-0457.ch020

Table 3
Geotextile Failure Mechanisms*

FUNCTION	FAILURE MODE	POSSIBLE CAUSE
Separation/Filtration	Piping of soils through the geotextile	Openings in the fabric are incompatible with retained soil. Openings may be enlarged as a result of in-situ stress or mechanical damage.
Filtration	Clogging of the geotextile	Permeability of the fabric is reduced as a result of particle build-up on the surface of or within the fabric. Openings may have been compressed as a result of long-term loading.
Reinforcement	Reduced tensile resisting resisting force.	Excessive tensile stress relaxation of the fabric.
Reinforcement	Unacceptable deformation of the soil/geotextile structure	Excessive tensile creep of the fabric.
Planar-Flow	Reduced in-plane flow capability	Excessive compression creep of the fabric.
Cushioning	Reduced resistance to puncture	Excessive compression creep of the fabric.

* These failure mechanisms do not include polymer degradation-related causes.

Do geotextiles commonly encounter problem soil environments? Not according to a 1986 study by the U.S. Army Engineer Waterways Experiment Station which concluded that no cases of fabric failure because of attack from chemicals present in a natural soil environment were found in the literature [5]. However, in cases of fabric burial in soils having a very low or very high pH, consideration should be given to the composition of the geotextile selected. This should be a rare occurrence because most soils have a pH in the range of 3 to 10 [6]. Geotextile composition should also be considered in cases of complex chemical exposure (i.e., leachate), burial in metal-rich soils, and extended exposure to sunlight. In order to evaluate these unique exposure conditions, tests which closely simulate actual exposure conditions on the geotextile selected are recommended. When testing is not possible, most manufacturers can provide data from exposure testing of their specific fibers or fabrics.

Do geotextiles commonly encounter soil conditions which would be expected to cause reductions in fabric performance? Almost always. But, whether its a gap-graded soil which could lead to fabric clogging, or large embankment loads which must be resisted with little fabric creep, fabric properties can be selected to protect against excessive reductions in performance.

PET Fibers and Fabrics

Long-term performance of a geotextile depends on how the specific application environment affects the geotextile's fibers (polymer) and fabric structure. Therefore, it is very important to understand not only the specific environment but also the properties of the specific geotextile selected.

The remainder of this paper provides detailed information on P.E.T. fiber and fabric properties.

When the term polyester fiber is used, it generally refers to poly (ethylene terephthalate) which has been shortened to PET in the trade. PET is the condensation homopolymer of terephthalic acid (or its dimethylester) and ethylene glycol as shown in Figure 1.

PET is a long-chain linear polymer with a typical number-average molecular weight between 15,000 and 30,000. The polymer is thermoplastic and may be converted to a fiber by melt spinning. Chemical functionality is derived from the ester group.

Manufacture

There are two major processes (Fig. 2) used to manufacture polyester geotextiles. These are: (1) the spunbond filament process for producing nonwoven fabrics and (2) the high tenacity filament process for yarns used in producing woven fabrics.

Terephthalic acid and ethylene glycol form a diester monomer which is polymerized to PET. The polymer is melted, extruded, and spun through a spinneret with small holes, forming continuous filaments that are solidified by cooling in air. For spunbond fabrics, polymers with molecular weights of about 20,000 form these filaments which are laid down to form a web, then bonded, in this case by needlepunching, to interlock the filaments to give the spunbond its characteristic tensile strength and dimensional stabi-

Downloaded by COLUMBIA UNIV on August 6, 2012 | http://pubs.acs.org
Publication Date: April 3, 1991 | doi: 10.1021/bk-1991-0457.ch020

Downloaded by COLUMBIA UNIV on August 6, 2012 | http://pubs.acs.org
Publication Date: April 3, 1991 | doi: 10.1021/bk-1991-0457.ch020

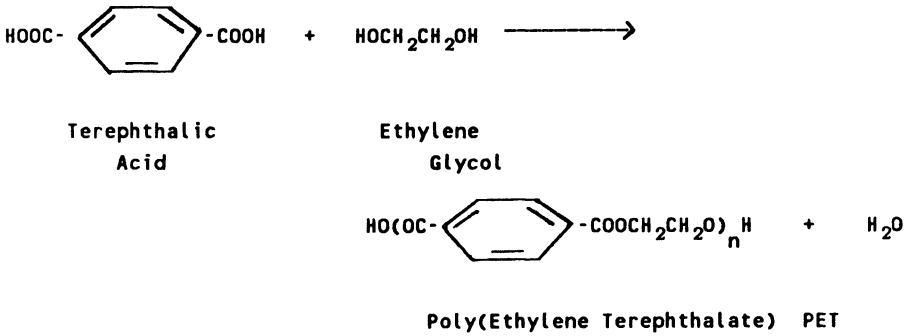
HOOC-
-COOH
+
HOCH$_2$CH$_2$OH
Terephthalic Acid
Ethylene Glycol
HO(OC-
-COOCH$_2$CH$_2$O)$_n$H
+
H$_2$O
Poly(Ethylene Terephthalate) PET

Fig. 1 - Chemical Formulation of PET

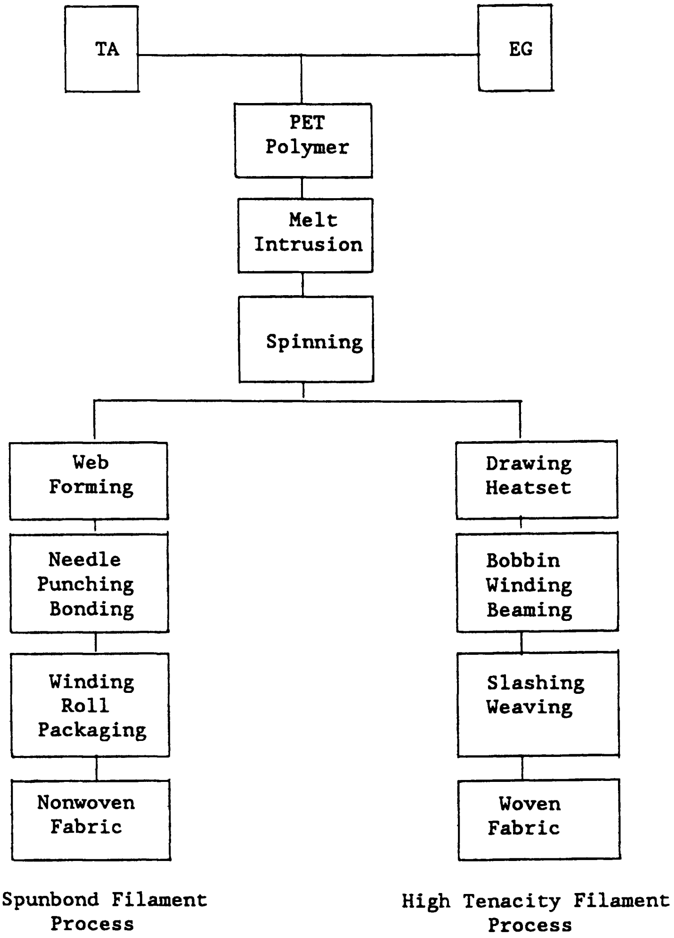
TA
EG
PET Polymer
Melt Intrusion
Spinning
Web Forming
Needle Punching Bonding
Winding Roll Packaging
Nonwoven Fabric
Drawing Heatset
Bobbin Winding Beaming
Slashing Weaving
Woven Fabric
Spunbond Filament Process
High Tenacity Filament Process

Fig. 2 - Polyester Fiber and Fabric Flow Diagrams

Downloaded by COLUMBIA UNIV on August 6, 2012 | http://pubs.acs.org
Publication Date: April 3, 1991 | doi: 10.1021/bk-1991-0457.ch020

lity. Chemical and thermal bonding can also be used. The formed fabric is then wound onto a core package and cut into standard lengths.

For high tenacity filament woven fabrics, the as-spun filaments, which are formed from about 30,000 molecular weight polymer, are drawn by heating and stretching them to several times their original length, followed by heatsetting to form an oriented semicrystalline structure and impart the desired physical properties of high strength, toughness and dimensional stability. The treated filaments in yarn form are wound onto a bobbin, then rewound from many bobbins onto a beam for slashing, followed by weaving on a loom to the specified fabric.

Characteristics

The characteristics that account for the the great versatility of polyester fibers are their high strength, high modulus, toughness, dimensional stability, low shrinkage and heat-settability, low moisture regain and quick drying ability, thermal stability, and resistance to stretching and shrinking, most chemicals, abrasion, wrinkles, cuts, weather, and soil--all this with acceptable economics.

The enormous success of polyester in textile end uses such as apparel and home furnishings, in industrial end uses such as tires and roofing, and in carpet markets is attributed to these outstanding characteristics.

In the following sections, these characteristics will be discussed and related to polyester geotextiles. Most of the data, unless specifically stated otherwise, has been taken from TREVIRA® polyester in-house studies.

PET Resistance to Fiber Degradation

Thermal Resistance

Polyester fibers have outstanding thermal properties. They melt in the range of 478-490°F, crystallize at 250-265°F, have a glass transition temperature of 150-165°F--all well above normal conditions encountered in geotextile applications. In addition, polyester fibers maintain excellent flexibility and strength at temperatures below freezing.

Chemical Resistance - General

Another property critical to geotextile performance in some applications is chemical resistance. Fortunately, many diverse environments have been tested and the results are available. A review of some of that data with the intent of showing general resistance to classes of chemicals as well as the effects of temperature, time, and concentration in select cases follows.

Generally speaking however, polyester geotextiles have excellent stability to many chemical classes such as water, salts, organic acids, organic solvents, dry cleaning solvents, oxidizing agents (bleaches), reducing agents, gases and fuels (petroleum). They are susceptible, under certain conditions, to chemical classes such as inorganic acids, halogenated organic acids, inorganic and organic bases, benzyl alcohol, and halogenated phenols, while the effects of leachates and "buffered solutions" are dependent on their chemical composition.

Downloaded by COLUMBIA UNIV on August 6, 2012 | http://pubs.acs.org
Publication Date: April 3, 1991 | doi: 10.1021/bk-1991-0457.ch020

Chemical Resistance - Water

Polyester is virtually unaffected by rain, seawater or other forms of water.

Polyester's resistance to the effects of water is easily explained. Moisture absorption of polyester is only 0.4% at room temperature and 65% relative humidity. Even at 95% humidity, less than 0.6% moisture is absorbed. Because of its low moisture absorption, polyester geotextiles will not get heavy when wet, will not mildew, and will dry very quickly. Most importantly, polyester's strength is unaffected by water under normal conditions.

The mechanical properties of wet polyester geotextiles are the same as dry. There is no strength loss as mentioned earlier; stretch to break (elongation) is not affected; there is no change in abrasion resistance; and there is no growth or shrinkage (i.e., elasticity is not affected).

Polyester fibers can be plasticized by water, but this plasticization is very slow. The water enters the amorphous regions of the polymer and enhances molecular mobility. The result is a small loss in modulus and strength, but the effect is completely reversible when the water is removed.

PET fibers are only affected by water if conditions are such that hydrolysis of the ester group takes place. The rate of hydrolysis is dependent on temperature and is most sensitive to strong acid or base conditions which can catalyze the hydrolysis reaction. Normally encountered soil temperature and chemistries have not been known to cause hydrolysis.

Chemical Resistance - Acids

Polyester is highly resistant to most mineral and organic acids. Some of them are quite strong, but still have no effect on polyester after a one year exposure as shown in Table 4. Polyester's long-term resistance to sulfuric acid makes it excellent for use in acid rain conditions which become more severe each year.

While polyester is highly resistant to most acids, it is affected by high concentrations of some very strong acids. Generalizations are not appropriate when looking at the effect of pH on acid degradation. In some conditions, polyester can withstand pH's below 0.1. Acid catalyzed hydrolysis is the more important mechanism. Clearly, specific exposure conditions must be known before assessing the effects of acids on polyester geotextile durability.

Chemical Resistance - Alkalis

In contrast to excellent acid resistance, polyester has somewhat limited resistance to alkalis, as shown in Table 5. However, again, generalizations aren't always appropriate. In fact, some alkalies only slightly affect polyester, even after one year of exposure.

As in the case of acids, alkaline degradation increases with higher temperatures, higher concentrations and longer exposure times.

Also, as with acid, the effect of pH on alkaline degradation should not be generalized. pH determines hydroxide ions, but doesn't determine the strength of the hydroxide ions or other nucleophiles (negatively charged ions or fragments), which attack the carboxyl group of an ester. The strength of the nucleophile roughly parallels basicity but is dependent also on the nature of the leaving group displaced and accessability to the ester group. Therefore, strength

Downloaded by COLUMBIA UNIV on August 6, 2012 | http://pubs.acs.org
Publication Date: April 3, 1991 | doi: 10.1021/bk-1991-0457.ch020

Table 4
Acid Resistance of PET Geotextiles

Compound	pH	% Strength Retained After One Year at 70°F
Acetic, concentrate	0.1	100
Benzoic	-	100
Boric	3.5	100
Chlorosulfonic	-	Degraded
Citric, 25%	1.2	100
Formic, conc.	0.1	100
Hydrochloric, 15%	0.1	100
Hydrochloric, 20%	0.1	Degraded
Hydrofloric, 10%	-	Degraded
Lactic, concentrate	0.7	100
Nitric, 15%	0.1	100
Phosphoric, 20%	0.6	Degraded
Sulfuric, 38% (Battery)	0.1	100

Table 5
Alkaline Resistance of PET Geotextiles

Compound	pH	% Strength Retained After One Year at 70°F
Ammonium hydroxide	8-10	88
Ammonium hydroxide, 2%	11.4	SD*
Calcium hydroxide, 15%	12.4	SD
Diethylamine	13.5	SD
Hydrazine, 2%	10.6	76
Hydrazine, 5%	10.8	SD
Potassium hydroxide, 0.1%	12.5	90
Potassium hydroxide, 2%	13.4	SD
Sodium hydroxide, 0.1%	12.1	94
Sodium hydroxide, 2%	12.8	SD
Triethanolamine	13.3	66
Urea	10.4	91

*Severely Degraded.

loss in some cases at pH's above 12 is small. Once again, actual exposure conditions must be known before determining the effect of alkali on polyester geotextiles.

Chemical Resistance - Inorganic Salts

Aside from its susceptibility to acid catalyzed hydrolysis and selective nucleophilysis, polyester is resistant to most other chemicals. These include a wide range of inorganic salts (and organic salts as well) which do not affect polyester after a full year of exposure (Table 6). There are a few exceptions, but again, pH is not necessarily a determining factor.

Chemical Resistance - Organic Solvents

Polyester is insoluble in most organic solvents. The list (Table 7) is very long for organic solvents, including commonly used organic chemicals, fuels and plasticizers, which do not affect polyester strength after a full year of exposure.

Chemical Resistance - Fertilizers

As mentioned, the effect of fertilizer on polyester is dependent on both the chemical composition and the moisture content of the fertilizer (Table 8). Materials which form acids or bases can lead to varying amounts of hydrolytic degradation.

Ultraviolet Resistance. For up to 400 hours of direct sunlight (two-six months aging in calendar time), untreated polyester will retain greater than 90% of its strength (Fig. 3). In the long term, the ultraviolet degradation of polyester slows down and can level out. Half the strength remains after 4000-5000 hours. Actual levels of deterioration vary, depending on the number of sunlight hours and sunlight intensity, which vary each year and depend greatly on geographic location and climatic conditions. For this reason, such conditions should be considered in any prediction of the effects of sunlight on any organic material.

Further, note that polyester is only sensitive to the ultraviolet region between 3000-3300 angstroms. It is very easy to block these rays, allowing a long life, with no effect on strength. In fact, the outer layers of the fabric itself have the ability to filter these rays from inner layers. Therefore, deterioration in thick, heavy fabrics is slight relative to that in yarn. This accounts for the leveling effect over time, as shown in Fig. 3.

PET Fabric Performance Properties

Fabric Properties

When discussing fabric properties, the focus will be on those of polyester fibers and fabrics typically used in geotextiles. Fabrics can be selectively engineered to give very high strength and low elongation with wovens, or moderate strength and high elongation with needlepunched nonwovens, plus quite a range of other properties, to meet a variety of geotextile requirements.

Vivid examples of this flexibility can be seen by looking at the properties of different geotextile fabrics. Polyester spunbond, needlepunched nonwoven fabrics of weights ranging from 3.5 to 16 oz/yd^2 have a range of properties as shown in Table 9.

Downloaded by COLUMBIA UNIV on August 6, 2012 | http://pubs.acs.org
Publication Date: April 3, 1991 | doi: 10.1021/bk-1991-0457.ch020

Downloaded by COLUMBIA UNIV on August 6, 2012 | http://pubs.acs.org
Publication Date: April 3, 1991 | doi: 10.1021/bk-1991-0457.ch020

Table 6
Inorganic Salt Resistance of PET Geotextiles

No strength loss after one year at 70°F

Compound	pH	Compound	pH
Aluminum sulfate	2.9	Potassium nitrate	8.8
Ammonium chloride	5.1	Potassium perchlorate	9.9
Ammonium nitrate	4.8	Potassium permanganate	9.7
Ammonium sulfate	4.6	Potassium sulfate	7.5
Calcium chloride	7.2	Silver nitrate	4.6
Calcium nitrate	3.9	Sodium ammonium hydrogen sulfate	8.2
Copper sulfate	3.5		
Ferric chloride	0.8	Sodium bicarbonate	7.8
Ferrous sulfate	3.0	Sodium carbonate	11.2
Magnesium chloride	4.0	Sodium chlorate	7.4
Magnesium sulfate	6.6	Sodium chloride	7.4
Nickel sulfate	6.6	Sodium nitrate	8.3
Potassium bichromate	3.7	Sodium perchlorate	5.8
Potassium bromide	6.5	Sodium sulfate	5.4
Potassium carbonate	13.1	Sodium tetraborate	9.3
Potassium chlorate	6.9	Sodium thiosulfate	5.4
Potassium chloride	8.0	Zinc chloride	2.4
Potassium chromate	9.4	Zinc sulfate	4.0

Strength Loss

Sodium bisulfite	4.1	(94% after one year)
Ammonium sulfide	9.6	(Destroyed after six months)

Downloaded by COLUMBIA UNIV on August 6, 2012 | http://pubs.acs.org
Publication Date: April 3, 1991 | doi: 10.1021/bk-1991-0457.ch020

Table 7

Organic Solvent Resistance of PET Geotextiles

No strength loss after one year at 70°F		Strength Loss
Acetone	Hydroquinone	Benzyl alcohol
Amyl acetate	Isopropyl alcohol	(Dissolved)
Aniline	Isooctane	Alkyl amines
Asphalt	Jet propellant	(Degraded)
Benzaldehyde	Methyl acetate	Tetrachloroethane
Benzene	Methyl alcohol	(92% after one year)
Butanol	Methylene chloride	
Butyl acetate	Methyl ethyl ketone	
Carbon tetrachloride	Mineral oil	
Chloroform	Nitrobenzene	
m-Cresol	Phenol	
Cyclohexanone	m-Phenylene diamine	
Diesel Fuel	2-Phenylethylalcohol	
Dimethyl formamide	Pyridine	
Dimethyl sulfoxide	Resorcinol	
Epichlorohydrin	Styrene	
Ethanol	Toluene	
Ether	Trichloroethylene	
Ethyl acetate	Trimethylamine	
Formaldehyde, 30%	Turpentine	
Formamide	White spirit	
Gasoline	Xylene	
Glycol		

Table 8
Resistance of Polyester to Fertilizers

	DEGRADATION	
	1 Month	12 Months
Ammonium nitrite	None	None
Ammonium sulphate	None	Slight
Calcium nitrate	None	None
Calcium cyanamide, dry	None	None
Calcium cyanamide, wet	None	Degraded
Lime, slaked	None	Slight
Lime, slaked, moist 50%	None	Destroyed
NPK	None	Slight
Thomas Mead	None	Slight
Thomas Mead, moist 50%	Slight	Appreciable
Urea	None	None

Downloaded by COLUMBIA UNIV on August 6, 2012 | http://pubs.acs.org
Publication Date: April 3, 1991 | doi: 10.1021/bk-1991-0457.ch020

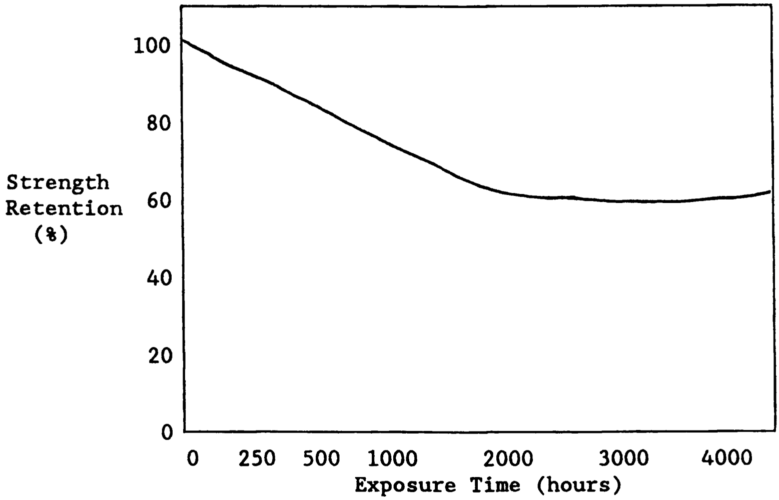

(Simulated outdoor exposure using Xenon Arc or Carbon Arc)

Fig. 3 - Resistance of PET Fibers to Direct Sunlight Exposure

Table 9
Geotextile Properties of PET Spunbond Fabrics

Weight, oz/yd^2	3.5	16
Thickness, mils	60	210
Grab tensile strength, lbs	110/90	625/560
Puncture strength force, lbs	50	240
Mullen burst point, psi	180	840
Trapezoid tear strength, lbs	50/40	205/200
Elongation at break, %	70/85	90/95
Permittivity, sec^{-1}	2.04	0.75
Normal permeability coefficient, cm/sec	0.3	0.4
Vertical water flow, gpm/ft^2	150	55
Apparent opening size, sieve size	70-100	100-170
Thermal shrinkage, % (400°C)	2.9	2.9
Moisture regain, % (65% RH, 72°F)	0.4	0.4
Specific gravity	1.36	1.36

In the case of high tenacity polyester filament yarn, fabrics may be woven in various widths and may vary greatly in weights and thickness. This is accomplished by changing the denier (thickness) of the feeder yarns, the number of yarns in the warp and filling directions on the loom, and the pattern of the weave.

Commercial PET woven geotextiles offer a range of wide width tensile strength from 1000 lbs/inch in both the warp and fill direction up to 3790 and 1180 lbs/inch, respectively, in the warp and fill direction. The extension at failure conversely ranges from 15% to 11% for these fabrics [7]. The important areas are strength and low elongation.

A typical polyester high tenacity filament yarn for this application has the textile properties given in Table 10.

Creep Resistance - Reinforcement

For a fabric to be dimensionally stable, it not only has to be stiff, have low stretch and shrinkage, but it should have good recovery properties. Elongation which occurs due to long-term loading versus instantaneous elongation is referred to as creep. Data in Fig. 4 suggests that polyester can support a load over 50% of its breaking strength with minimal creep for an extended service life. This excellent creep resistance assures that polyester geotextiles maintain acceptable strain levels under load for extended periods.

Creep Resistance - Separation/Filtration, Planar Flow, and Cushioning.

The proper design of a geotextile for drainage and filtration entails selection of a geotextile which inhibits the migration of fines into the core of the drain and induces the formation of a stable filter cake in the soil [8].

Needlepunched nonwovens have been shown to provide an effective balance of thickness, porosity, and pore size distribution to retain fine soils, while inducing a stable filter cake without clogging [10]. PET needlepunched nonwovens exhibit tensile and compression creep resistance that prevents changes in thickness, porosity and pore size distribution over time which can lead to changes in filter behavior.

The ability of PET needlepunched nonwovens to resist compression creep protects their long-term planar flow and cushioning abilities.

Aging of PET

Most of the effects discussed in this presentation have dealt with general properties of polyester fibers and fabrics exposed to a variety of individual conditions. It is not possible to deal with all the factors, nor combinations of factors which could affect the aging and durability of polyester geotextiles. The following sections briefly describe PET's resistance to aging in the most common application environments: atmospheric, soil, and leachate exposure.

Atmospheric Resistance

Polyester's durability in most atmospheric conditions is quite good. This is especially true for normal weather with respect to rain, heat, sunlight and radiation. The excellent water and heat resistance has already been discussed. Sunlight (ultraviolet) resistance is a more controversial area, since untreated polyester can experience slow ultraviolet degradation though much superior to untreated polypropylene. Polyester properties are not affected by moderate doses of high energy radiation.

Downloaded by COLUMBIA UNIV on August 6, 2012 | http://pubs.acs.org
Publication Date: April 3, 1991 | doi: 10.1021/bk-1991-0457.ch020

Downloaded by COLUMBIA UNIV on August 6, 2012 | http://pubs.acs.org
Publication Date: April 3, 1991 | doi: 10.1021/bk-1991-0457.ch020

Table 10
Textile Properties of PET High Tenacity Filament Yarn

Denier/Fils	1000/192
DPF	5.2
Breaking tenacity, gpd	8.9
Breakload, lbs	19.8
Load at 5% elongation, lbs	10
Breaking elongation, %	13
Elastic recovery at 5% elong, %	90
Initial modulus, gpd	110
Toughness, g cm	0.7
Moisture regain, % (65%, RH, 72°F)	0.4
Specific gravity	1.39
Hot air shrinkage, % (350°F)	13.5
Boiling water shrinkage, %	6

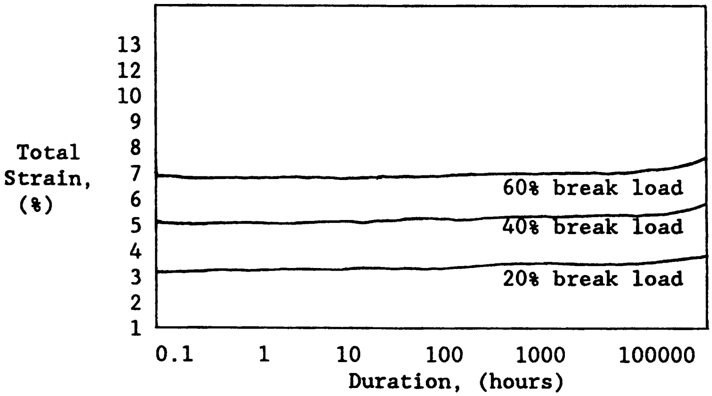

Fig. 4 - Creep Resistance of PET Fibers

Soil Resistance

In the case of soil exposure, polyester durability to moisture, microorganisms, dry fertilizers, dry concrete, asphalt, and bitumen is excellent. However, as discussed earlier, fertilizers can attack polyester under certain moist conditions. Research on concrete in moist conditions is underway.

In an independent study by G. Colin and co-workers [1], polyester nonwoven fabrics buried in soil for seven years showed no significant decrease in bursting strength. Soil burial exposure was carried out in a moist, organically rich soil maintained at 86°F and 85-90% relative humidity.

Leachate Resistance

Leachate is generated as a result of liquid flowing through the soil, forming solutions of both dissolved and suspended materials. The composition of the leachate is highly dependent on the soil and weather conditions and is difficult to predict since there are so many variables which affect this solubilization of organic and inorganic constituents. The characteristics of leachate, however, generally vary greatly in solid waste landfills.

In the case of polyester, it is important to determine if hydrolysis can occur. Equally important in practical terms is to determine if the leachate forms a buffered solution which will inhibit hydrolysis. That is, the acids and bases will react with each other preferentially to form salts instead of attacking the polyester.

Again, because of the variance in composition, caution should be used when describing a typical leachate. Therefore, it is best to characterize the actual leachate before designing the geotextile for a given location.

Downloaded by COLUMBIA UNIV on August 6, 2012 | http://pubs.acs.org
Publication Date: April 3, 1991 | doi: 10.1021/bk-1991-0457.ch020

Summary and Conclusions

Polyethylene terephthalate, more commonly called PET, or just plain polyester, offers great versatility for selective engineering which yields a broad range of geotextile products with excellent strength, toughness and dimensional stability. This is the case in wet or dry conditions. In addition, the weight of the fabric is affected to only a very limited extent by water absorption. Furthermore, resistance to permanent deformation (creep) under long-term loading is excellent. Also, polyester is inert to a wide range of chemical classes encountered in soil. And, superior sunlight resistance allows polyester geotextiles to suit most construction installation requirements. Finally, polyester geotextiles are not affected by microorganisms in soil.

Because of polyester's excellent chemical and physical properties, this material can be used with confidence and is the material of choice for most geotextile applications.

Literature Cited

1. Colin, G., Mitton, M. T., Carlsson, D. J., and Wiles, D. M., Geotextiles and Geomembranes, 1986, Vol. 4, No. 1; p 2.
2. Schnabel, W., Polymer Degradation: Principles and Practical Applications, Hanser Int'l. 1981.
3. den Hoedt, G., Proceedings from Durability and Aging of Geosynthetics, 1988.
4. Plasticization and Hydrolysis: The Effects of Water on Polyethylene Terephthalate in Geotechnical Applications, ITW Enterprises, In-house report, 1988.
5. Geotextiles for Drainage, Gas Venting, and Erosion Control at Hazardous Waste Sites, Environmental Protection Agency, 1986.
6. Encyclopedia of Chemistry, Van Nostrand Reinhold, 1984, p. 706.
7. Paulson, J. N., Proceedings From The Geosynthetic Research Institute Seminar, Very Soft Soil Stabilization Using High Strength Geosynthetics, 1987, p. 239.
8. Williams, N. D., and Abouzakhm, M. A., Geotextiles and Geomembranes, Vol. 8, No. 1; p. 5.

RECEIVED March 14, 1990

Downloaded by NORTH CAROLINA STATE UNIV on August 6, 2012 | http://pubs.acs.org
Publication Date: April 3, 1991 | doi: 10.1021/bk-1991-0457.ch021

Chapter 21

Stabilization of Polypropylene Fiber and Tape for Geotextiles

Robert L. Gray

CIBA-GEIGY Corporation, Ardsley, NY 10502

Recent advances in resin and stabilization technologies have expanded applications of polyolefin fibers in the carpet and geotextile industries. The stabilization requirements of applications such as nonwoven geotextiles, outdoor carpet, or artificial turf demand the use of high performance additives. New, more effective Hindered Amine Light Stabilizers (HALS) have been developed which offer significant advantages over traditional light stabilizers. This paper will discuss process, thermal, and light stability of polypropylene fiber and tape as well as stabilizer extraction resistance.

Geosynthetics have become increasingly important in the construction and environmental industries. Included in the general geosynthetic classification are: geomembranes, geonets, geotextiles, and geogrids. Due to their excellent transmissivity properties, geotextiles are often used as substitutes for natural materials such as gravel or sand (1).

A variety of polymers including polyolefins, polyethylene terephthalate, and polyvinyl chloride are currently being used as geosynthetics. Selection of the polymer is based on the specific physical and chemical requirements for each individual application (2,3).

Polyolefins are often the polymer of choice for use in many of these applications due to their unique physical properties, excellent durability and chemical resistance (4,5). This work discusses stabilization of polypropylene fiber for use in geotextiles.

Degradation.

As with many polymeric materials, the mechanism for polyolefin degradation is generally considered to proceed via a radical chain

0097–6156/91/0457–0320$06.00/0

pathway (6) (Figure 1). Initiation typically occurs through exposure to heat, shear, and/or UV radiation. Additionally, the presence of reactive impurities such as residual catalyst or chromophoric groups can aid in radical initiation. Propagation steps are proposed to involve a reaction with oxygen which can result in the formation of hydroperoxides. Subsequent decomposition of these unstable hydroperoxides lead to the further production of reactive radicals. The effect of this degradation process on the physical characteristics of geosynthetics is of critical importance. Degradation of polyolefins results in two opposing effects on molecular weight distribution. Chain scission (decreased molecular weight) and crosslinking (increased molecular weight) may both occur during aging. Polyethylene typically experiences less chain scission than crosslinking, thus the melt flow rate is usually observed to decrease, reflecting an overall increase in molecular weight. Conversely, polypropylene primarily undergoes chain scission which results in an increased melt flow rate. The practical consequences of these reactions are: discoloration, surface crazing (formation of surface micro-cracks) embrittlement, and loss of mechanical properties (elongation, impact strength, tensile strength).

Downloaded by NORTH CAROLINA STATE UNIV on August 6, 2012 | http://pubs.acs.org
Publication Date: April 3, 1991 | doi: 10.1021/bk-1991-0457.ch021

Mechanisms of Stabilization

Thermal Stabilization. An effective method of thermal stabilization is through the use of a radical terminating antioxidant. The most common class of antioxidant for radical termination is a hindered phenol (7). The mechanism (Figure 2) by which these compounds function is by abstraction of H from the hindered phenol by the reactive peroxy-radical. This produces a less reactive, resonance stabilized phenolic radical. Peroxycyclohexadienones can then be formed after reaction with an second peroxy-radical (8). This type of stabilization is effective at temperatures encountered during both melt processing and long term heat aging.

Phosphites (9-13) and thioethers (14-17) are effective at decomposing hydroperoxides into stable non-radical products. As previously discussed these peroxy moieties are thermally and photolytically unstable and typically decompose producing two radical products. Interrupting this process through the use of phosphites or thioesters can significantly reduce the level of radical initiation. Phosphites are very effective during melt processing (typical temperature range: 220-315°C), providing color and melt flow rate stability. Thioethers (typically used in combination with hindered phenols) are used for elevated temperature (>100°C) applications.

Light Stabilization. UV stabilizers can generally be categorized into three types. The first class of stabilizers function by screening the polymer through absorption of UV radiation. These stabilizers absorb UV radiation and prevent polymer degradation. By undergoing a reversible tautomeric process (18,19), they dissipate the UV energy as heat. As shown in Figure 3, the enol form of the UV absorber (UVA) absorbs the radiation and is

Downloaded by NORTH CAROLINA STATE UNIV on August 6, 2012 | http://pubs.acs.org
Publication Date: April 3, 1991 | doi: 10.1021/bk-1991-0457.ch021

Initiation $PH \xrightarrow[RI^*]{\Delta/UV} P\bullet + H\bullet$

*RI: Reactive Impurities (residual catalyst, chromophoric groups or precursors of chromophoric groups)

Propagation
$P\bullet + O_2 \longrightarrow PO_2\bullet$
$PO_2\bullet + PH \longrightarrow POOH + P\bullet$
$POOH \xrightarrow{\Delta/UV} PO\bullet + \bullet OH$
$2POOH \xrightarrow{\Delta/UV} POO\bullet + PO\bullet + H_2O$
$PO\bullet + PH \longrightarrow POH + P\bullet$
$\bullet OH + PH \longrightarrow H_2O + P\bullet$

Termination
$2PO_2\bullet \longrightarrow POH + P{=}O + O_2$
$PO_2\bullet + P\bullet \longrightarrow POOP$
$P\bullet + P\bullet \longrightarrow P - P$
$2PO_2 \longrightarrow POOP + O_2$

Figure 1. Auto-oxidation Mechanism of Polyolefins

- Trap POO• radicals by donating H•
- Better H• donors than substrate
- Sacrificial (not catalytic) stabilizer

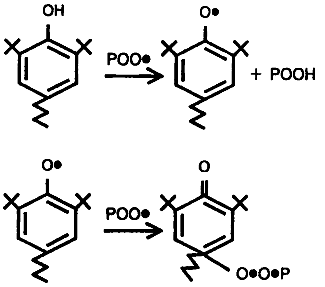

- Produces ⟶ Phenoxyl radicals
  ⟶ Cyclohexadienone derivatives

Figure 2. Hindered Phenol Stabilization Mechanism

Downloaded by NORTH CAROLINA STATE UNIV on August 6, 2012 | http://pubs.acs.org
Publication Date: April 3, 1991 | doi: 10.1021/bk-1991-0457.ch021

converted into its keto-tautomer. This energy is then dissipated as heat in the reverse reaction. The most commonly used UV absorbers are substituted benzotriazoles or benzophenones. A disadvantage of UVA's is that their effectiveness is limited by Beer's Law which requires high concentrations and sufficient polymer thickness. In colored samples, the pigment serves as a screening agent; therefore, the benefit of UVAs are often significantly reduced.

Another class of stabilizers act as UV quenchers or energy transfer agents. These compound function by quenching molecules that have become excited and returning them to the ground state before homolytic bond cleavage can occur (20,21). This class of stabilizers are typically nickel-based coordination complexes.

The most recent class of light stabilizers are the Hindered Amine Light Stabilizers (HALS) which function by interrupting the radical chain degradation mechanism. The proposed stabilization mechanism (Figure 4) involves the formation of a nitroxyl radical from the oxidation of the hindered amine (22), (Klemchuk, P. P.; Gande, M. E.; Cordola, E., Polym. Deg. and Stab., in press.). This nitroxyl radical can in turn react with free radicals in the polymer to eventually yield nonradical products. In contrast to the sacrificial mechanism proposed for hindered phenolic antioxidants, it is believed the nitroxyl radical can be repeatably regenerated and thus function in an efficent manner. This may explain the high level of UV stabilization achieved at relatively low concentrations.

Fiber Stabilization

Stabilization of polypropylene multifilament fiber requires special stabilization approaches. Fiber processing expose the polymer to high shear and often severe extrusion conditions. These conditions require a high performance stabilizer package. The high surface-area-to-volume ratio of the finished polypropylene fiber product requires stabilizers resistant to volatilization and extraction. Additionally, many fiber applications demand color stability through processing, aging, and exposure to NOx type gases (gas fade).

Results and Discussion

Primary Antioxidant.

Polyolefin fiber is often stabilized through the use of a hindered phenol as primary antioxidant in combination with a phosphite. Selection of the hindered phenol (Figure 5) will depend on the particular performance requirements needed for each application. Issues to be considered are color development (aesthetics), thermal stability requirements, and extraction/chemical resistance.

Secondary Antioxidant.

During processing a phosphite can be used to sacrificially stabilize the polymer thus preserving the primary antioxidant for later use as a long term thermal stabilizer. The structure of the phosphite (Figure 6) can have a dramatic effect on both stabilization performance and other physical properties

Downloaded by NORTH CAROLINA STATE UNIV on August 6, 2012 | http://pubs.acs.org
Publication Date: April 3, 1991 | doi: 10.1021/bk-1991-0457.ch021

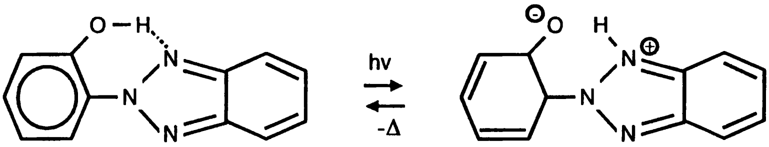

Figure 3. Tautomeric Process by Which Benzotriazoles (and Other UV Absorbers) Dissipate Energy

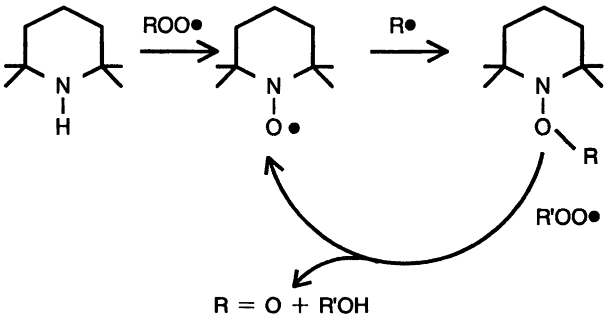

Figure 4. HALS Stabilization Mechanism

Downloaded by NORTH CAROLINA STATE UNIV on August 6, 2012 | http://pubs.acs.org
Publication Date: April 3, 1991 | doi: 10.1021/bk-1991-0457.ch021

Abbrev.	Chemical Name	Trade Name	Structure
AO-1	Tetrakis[methylene(3,5-di-tert-butyl-4 hydroxyhydrocinnamate)]methane	Irganox® 1010	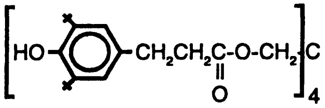
AO-2	Octadecyl 3,5 di-tert-butyl-4-hydroxyhydrocinnamate	Irganox 1076	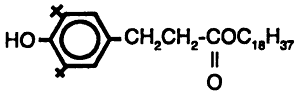
AO-3	1,3,5-tris(3,5-di-tert-butyl-4-hydroxy-benzyl)-s-triazine 2,4,6(1H, 3H, 5H)trione	Irganox® 3114	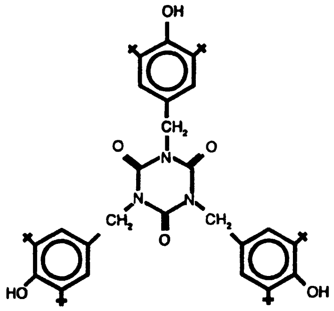
AO-4	Calcium bis[monoethyl(3,5-di-tert-butyl-4-hydroxybenzyl)phosphonate (50% with polyethylene wax)	Irganox 1425wl	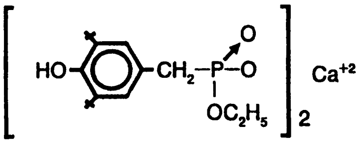

Figure 5. Hindered Phenolic Antioxidant Structures

Downloaded by NORTH CAROLINA STATE UNIV on August 6, 2012 | http://pubs.acs.org
Publication Date: April 3, 1991 | doi: 10.1021/bk-1991-0457.ch021

Abbrev.	Chemical Name	Trade Name	Structure
Phos-1	Tris(2,4-di-tert-butylphenyl) phosphite	Irgafos® 168	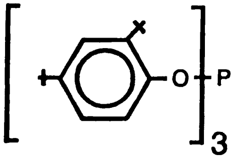
Phos-2	Bis(2,4-di-t-butylphenyl) pentaerythritol diphosphite	Ultranox® 626	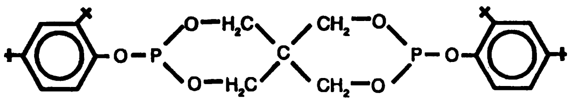

Figure 6. Phosphite Processing Stabilizer Structures

In High-Tech Fibrous Materials; Vigo, T., et al.;
ACS Symposium Series; American Chemical Society: Washington, DC, 1991.

Downloaded by NORTH CAROLINA STATE UNIV on August 6, 2012 | http://pubs.acs.org
Publication Date: April 3, 1991 | doi: 10.1021/bk-1991-0457.ch021

such as hydrolytic stability (PHOS-1 being significantly more resistant to hydrolysis than PHOS-2). Figure 7 shows the stabilizing effect on melt flow of phenol/phosphite additive packages. The large change in melt flow rate found between the compounded resin and final fiber indicates a change in molecular weight and thus the degree of degradation.

Light Stabilizers. Light stability is an important issue for textiles and is particularly critical for geotextiles which may experience extended outdoor exposure. The light stabilizers evaluated in this study are shown in Figure 8. Hindered Amine Light Stabilizers (HALS) outperform traditional UVAs even at one third the concentration as demonstrated in Figure 9 which shows actual outdoor weathering of natural polypropylene tapes. In TiO pigmented fiber, the addition of HALS results in a tenfold increase in light stability (Figure 10). A concentration effect exists where stability can be increased with increasing HALS concentration.

The high performance characteristics of these HALS are due not only to the regenerative mechanism but also to excellent permanence in the polypropylene. HALS-1 and HALS-2 are both oligomeric; consequently, these stabilizers do not readily volatilize during processing and cannot be easily extracted. Table I shows the extraction resistance of the HALS during wash

Table I. Extraction Resistance of HALS-1 & HALS-2 in Polypropylene Multifilament: Washing Test

Base Stabilizer:	0.075% AO-4 0.075% Phos-1 0.10% calcium stearate
Pigmentation	0.25% TiO_2(rutile)
Denier	130/37
Wash Procedure	1. Washed in 7% soap solution for 30 min. @ 60°C 2. Dried for 30 min. @ 60°C 3. 5 Cycles

Light Stabilizer	% Concentration Untreated	% Concentration Treated
HALS-1	0.25%	0.27%
HALS-1	0.49%	0.50%
HALS-2	0.38%	0.40%
HALS-2	0.64%	0.67%

In High-Tech Fibrous Materials; Vigo, T., et al.;
ACS Symposium Series; American Chemical Society: Washington, DC, 1991.

Downloaded by NORTH CAROLINA STATE UNIV on August 6, 2012 | http://pubs.acs.org
Publication Date: April 3, 1991 | doi: 10.1021/bk-1991-0457.ch021

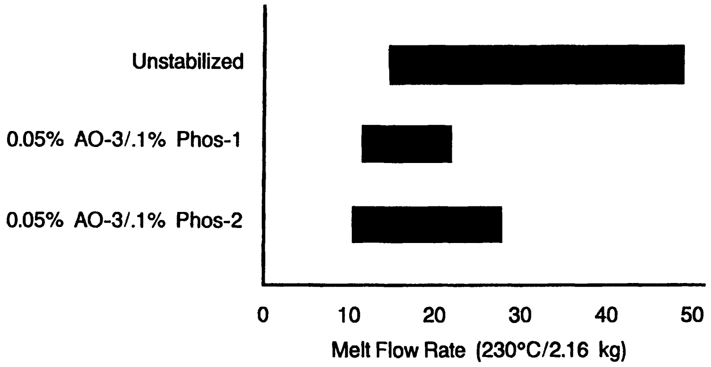

Base: PP homopolymer, 0.1% CaSt & 0.25% TiO_2
Extruder Temp: Compounding 450°F, Fiber 500°F

Figure 7. Processing Stability - Melt Flow Change From Pellets to Fiber

Downloaded by NORTH CAROLINA STATE UNIV on August 6, 2012 | http://pubs.acs.org
Publication Date: April 3, 1991 | doi: 10.1021/bk-1991-0457.ch021

Abbrev.	Chemical Name	Trade Name	Structure
UVA-1	2-Hydroxy-4-n-octyloxy benzophenone	Cyasorb® UV-531	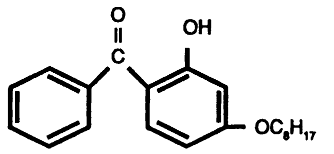 O C OH OC_8H_{17}
HALS-1	Dimethyl succinate polymer with 4-hydroxy-2,2,6,6,-tetramethyl-1-piperidine ethanol	Tinuvin® 622LD	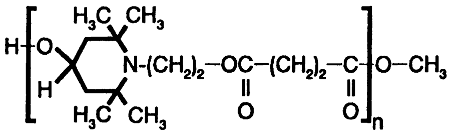 H O H_3C CH_3 H $N\text{-}(CH_2)_2\text{—}OC\text{—}(CH_2)_2\text{—}C$ O O $O\text{—}CH_3$ n
HALS-2	N-N'-bis(2,2,6,6,-tetramethyl-4-piperidinyl)-1,6-hexanediamine, polymer with 2,4,6-trichloro-1,3,5-triazine and 2,4,4-trimethyl-1,2-pentanamine	Chimassorb™ 944FL	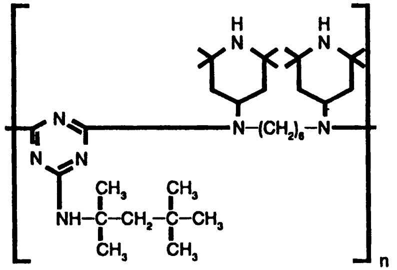 H N H N N N N $N\text{—}(CH_2)_6\text{—}N$ CH_3 CH_3 $NH\text{—}C\text{—}CH_2\text{—}C\text{—}CH_3$ CH_3 CH_3 n

Figure 8. Light Stabilizer Structures

Downloaded by NORTH CAROLINA STATE UNIV on August 6, 2012 | http://pubs.acs.org
Publication Date: April 3, 1991 | doi: 10.1021/bk-1991-0457.ch021

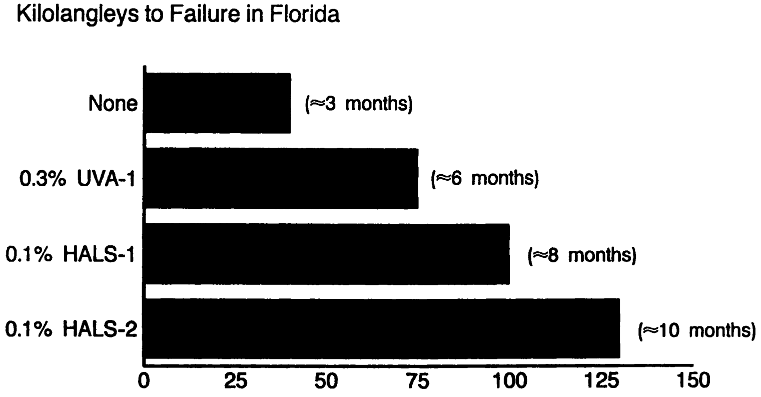

Base: PP homopolymer, 0.1% CaSt, 0.05% AO-1, 0.05% Phos-1

Figure 9. HALS in 2 Mil Polypropylene Tape

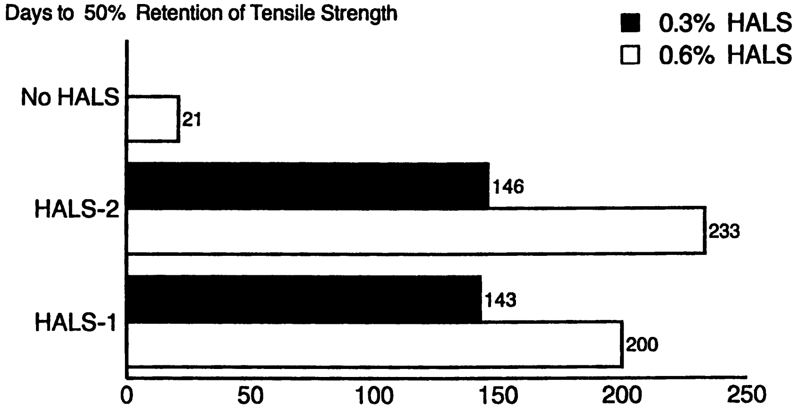

Base: PP homopolymer, 0.1% CaSt2, 0.25% TiO_2 & 0.1% AO-4

Figure 10. HALS in 130/37 Denier Multifilament PP Fiber - Xenon Arc Weatherometer Exposure

cycles at 60°C. After 5 cycles, no loss of HALS was detected by total nitrogen analysis. An analogous study was carried out simulating dry cleaning (Table II). HALS-1 experienced a 31% loss

Table II. Extraction Resistance of HALS-1 & HALS-2 in Polypropylene Multifilament: Dry Cleaning

Base Stabilizer:	0.05% AO-4 0.10% calcium stearate
Pigmentation	0.25% TiO_2(rutile)
Denier	130/37
Wash Procedure	1. 30 min. @ 30°C in perchloroethylene 2. Dried for 30 min. @ 60°C 3. 5 Cycles

	% Concentration	
Light Stabilizer	Untreated	Treated
HALS-1	0.29%	0.20%
HALS-1	0.51%	0.35%
HALS-2	0.26%	0.26%
HALS-2	0.46%	0.49%

while HALS-2 showed no significant loss after exposure. These tests indicate that the HALS evaluated are fairly resistant to extraction. These experiments are, however, somewhat oversimplified and actual extraction resistance may be dependent upon the exposure conditions.

HALS as Thermal Stabilizers. In addition to light stability, thermal stability is an important factor in polypropylene fiber stabilization. Based on the stabilization mechanism proposed for HALS, it might be expected that HALS could function as thermal stabilizers as well as light stabilizers. Indeed, when used in combination with AO-2 and PHOS-1, HALS-2 provides three times the thermal stability of a traditional high performance antioxidant AO-1 in natural polypropylene tape (Figure 11). Figure 12 demonstates that HALS are effective heat stabilizers in TiO-pigmented polypropylene fiber at temperatures below 150°C. The addition of HALS-2 (at 0.30%) to AO-4 increases the thermal stability by over eight-fold. HALS-1 also provides a significant benefit as a thermal stabilizer.

Thiosynergists. The thioether, DSTDP, has been used in combination with primary antioxidants to provide long term thermal stability. As this compound is not particularly effective at low

Downloaded by NORTH CAROLINA STATE UNIV on August 6, 2012 | http://pubs.acs.org
Publication Date: April 3, 1991 | doi: 10.1021/bk-1991-0457.ch021

Downloaded by NORTH CAROLINA STATE UNIV on August 6, 2012 | http://pubs.acs.org
Publication Date: April 3, 1991 | doi: 10.1021/bk-1991-0457.ch021

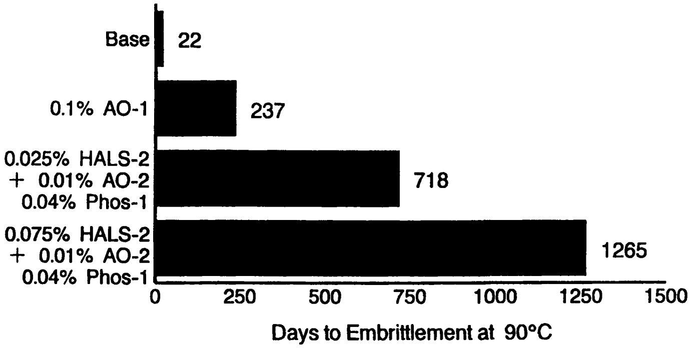

Figure 11. HALS as Heat Stabilizers in PP Tape

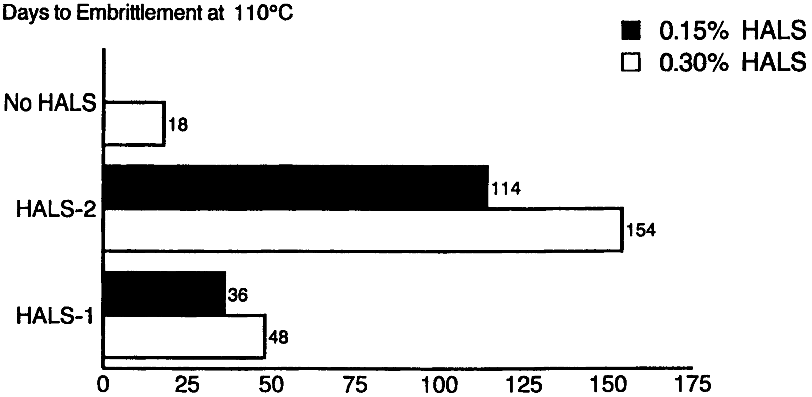

Base: PP homopolymer, 0.1% CaSt2, 0.25% TiO_2 & 0.1% AO-4
130/37 Denier Multifilament

Figure 12. HALS as Heat Stabilizers in Polypropylene Fiber

Downloaded by NORTH CAROLINA STATE UNIV on August 6, 2012 | http://pubs.acs.org
Publication Date: April 3, 1991 | doi: 10.1021/bk-1991-0457.ch021

temperatures (below 50°C), it would not be expected to provide a significant increase in the longvevity of a geosynthetic. At lower test temperatures, HALS provide significantly higher stability than systems containing thiosynergists (Table III). In fact, when HALS are combined with thioesters the thermal stability reduced to less than for systems containing a HALS alone.

Table III. 125°C LTHA of Carbon Black Filled PP Plaques

		Weight %
Control	PP Homopolymer	100.0
	Calcium Stearate	0.1
	UV Grade Carbon Black	2.5
	AO	As indicated

	Analysis (By Nitrogen Content)	
Light Stabilizer	0.1% AO-1 + 0.1% Phos-1	0.1% AO-1 0.3% DSTDP
Control	600	1,900
0.10% HALS-2	2,200	1,100
0.50% HALS-2	5,000	4,700
0.10% HALS-1	2,000	2,000
0.50% HALS-1	5,000	4,000

Carbon Black Filled Systems. Many geotextile applications require grey or black pigmentation. Although carbon black is often included to increase light stability, it typically has a negative effect on thermal stability. As carbon black levels increase, the thermal stability provided by the base antioxidant system decreases (Figure 13). It is believed that the tremendous surface area of the carbon black is capable of adsorbing antioxidants, rendering them ineffective. Apparently, polymeric HALS such as HALS-2 are not as adversely effected by carbon black and can provide a dramatic increase in heat stability.

Traditionally, carbon black alone was believed to provide sufficient light stability. Xenon weatherometer testing on polypropylene tapes has shown that if a HALS is added to carbon black filled polypropylene, carbon black concentrations can be lowered to one quarter their original level and better light stability will still result (Figure 14). As discussed above, reducing the carbon black level has the additional benefit of enhancing other desirable properties. HALS-1 shows better light stability performance than HALS-2. This might be attributed to

Downloaded by NORTH CAROLINA STATE UNIV on August 6, 2012 | http://pubs.acs.org
Publication Date: April 3, 1991 | doi: 10.1021/bk-1991-0457.ch021

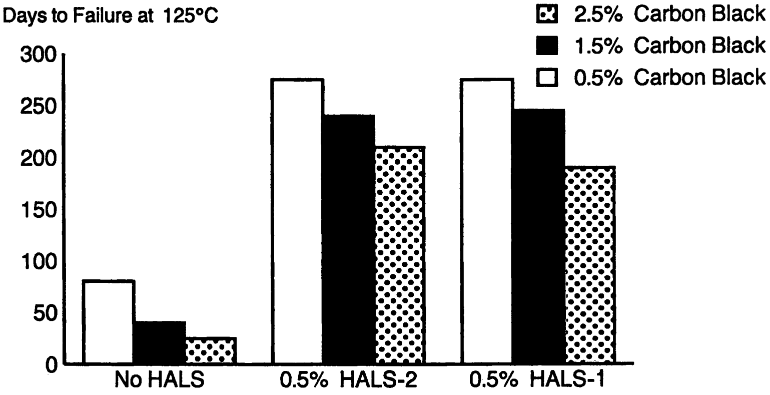

Base: PP homopolymer, 0.1% CaSt2, 0.1% AO-1, 0.1% Phos-1
Vulcan 9 Carbon Black Used

Figure 13. HALS as Heat Stabilizers - Carbon Black Filled PP Tape

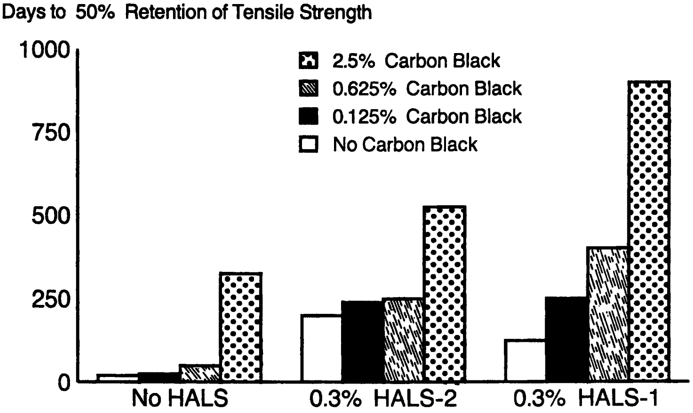

Base: PP homopolymer, 0.1% CaSt2, 0.03% AO-1 and 0.07% Phos-1

Figure 14. HALS in 2 Mil Black Polypropylene Tape - Xenon Arc Weatherometer Exposure

greater steric hinderance of the tertiary amine (HALS-1) which may reduce its interaction with the carbon black surface.

Conclusions

Effective stabilization of polypropylene fiber for geotextile applications requires an additive system capable of preventing polymer degradation during both processing and aging. This is best achieved through a combination of primary antioxidants, phosphites, and HALS. Polymeric HALS provide exceptional extraction resistance and stabilization (both thermal and light) in polypropylene fiber and tape.

In applications requiring the presence of carbon black, high molecular weight HALS show superior performance presumably due to their ability to avoid interaction with the carbon black surface. Long term thermal stability of these products can be dramatically improved with the addition of the proper HALS. The addition of tertiary hindered amines to carbon black containing systems appears to provide excellent UV stability at significantly lower carbon black levels.

Acknowledgments

The contributions and research efforts of the Polyolefin Additives Laboratories in both Ardsley, NY and Basel, Switzerland are gratefully acknowledged. Special appreciation is also extended to Ciba-Geigy Corporation for permission to use the data presented.

Literature Cited

1. Charron, R. M. Geosythetics '89 Conference Proceedings, San Diego, CA, 1989.
2. White, D.F.; Verschoor, K.L. Geotechnical Fabricsreport 1989, 7(3), 16.
3. Ford, J. E., Proc. Fourth International Conference on Polypropylene Fibres and Textiles, Nottingham, UK, September 1987.
4. Tisinger, L.G. Geotechnical Fabricsreport 1989, 7(3), 22.
5. Ramaswamy, S. D.; Rathor, M. N., Proc. Fourth International Conference on Polypropylene Fibres and Textiles, Nottingham, UK, September 1987.
6. Bolland, J. L.; Gee, G., Trans. Faraday Soc., 1946, 42, 236, 244.
7. Das, P. K.; Encinas, M. V.; Scaiano, J. C.; Steenken, S., J. Am. Chem. Soc., 1981, 103, 4162.
8. Pospisil, J., Adv. in Polym. Sci., 1980, 36, 69.
9. Denney, D. B.; Goodyear, W. F.; Goldstein, B., J. Am. Chem. Soc., 1960, 82, 1393.
10. Zuech, E. A., Chem. Comm., 1968, 1182.
11. Chang, B. C.; Denney, D. B.; Denney, D. Z.; Marsi, K. L., J. Am. Chem. Soc., 1969, 91, 5243.
12. Denney, D. B.; Jones, D. H., J. Am. Chem. Soc., 1969, 91, 5821.

Downloaded by NORTH CAROLINA STATE UNIV on August 6, 2012 | http://pubs.acs.org
Publication Date: April 3, 1991 | doi: 10.1021/bk-1991-0457.ch021

13. Walling, C.; Rabinowitz, R., J. Am. Chem. Soc., 1959, 81, 1243.
14. Oae, S. "Organic Chemistry of Sulfur", Plenum: New York, 1977, 529-532.
15. Block, E., J. Am. Chem. Soc., 1972, 94, 642.
16. Shelton, J. R.; Davis, K. E., J. Am. Chem. Soc., 1967, 89, 718.
17. Davis, F. A.; Awad, S. B.; Jenkins, R. H., Jr.; Billmers, R. L.; Jenkins, L. A., J. Org. Chem., 1983, 48, 3671.
18. Calvert, J. G.; Pitts, J. N., Jr.; "Photochemistry", John Wiley & Sons, Inc., New York, 1967, 419.
19. Goeller, G.; Rieker, J.; Maier, A.;Stezowski, J. J.; Daltrozzo, E.; Neureiter, M.; Port, H.; Wiechmann, M.; Kramer, H. E. A., J. Phys. Chem., 1988, 92, 1452.
20. Harper, D. J.; McKellar, J. F.; Turner, P. H., J. Appl. Polym. Sci., 1974, 18, 2805.
21. Allen, N. S.; Homer, J.; McKellar, J. F., Macromol. Chem., 1978, 179, 1575.
22. Klemchuk, P. P.; Gande, M. E., Makromol. Chem., Macromol. Symp., 1989, 28, 117.

RECEIVED August 2, 1990

Downloaded by NORTH CAROLINA STATE UNIV on August 6, 2012 | http://pubs.acs.org
Publication Date: April 3, 1991 | doi: 10.1021/bk-1991-0457.ch021

Downloaded by UNIV MASSACHUSETTS AMHERST on August 6, 2012 | http://pubs.acs.org
Publication Date: April 3, 1991 | doi: 10.1021/bk-1991-0457.ch022

Chapter 22

Impregnated Fiber–Glass Yarn for High-Strength Geosynthetic Reinforcement

Mikhail M. Girgis

**Fiber Glass Research Center, Pittsburgh Plate Glass Industries, Inc.,
P.O. Box 2844, Pittsburgh, PA 15230**

HERCUFLEX Strands are glass fibers which have been impregnated with a polymeric coating. The physical properties of these strands have been determined and compared to fiber glass rovings and organic fibers. These strands can be woven, knitted, or formed into grids. The effects of temperature, humidity, U.V. radiation, and chemical environment on the strength and flexibility of these strands as well as the fabrics were studied. It was found that HERCUFLEX strands satisfy the main performance requirements of high-strength, high-modulus and low creep geosynthetic reinforcement for soft soils and steep embankment. However, other important properties such as survivability, durability, and seamability are now being thoroughly investigated.

The definition of a geotextile according to ASTM is "... any permeable technical material used with foundation, soil, rock, earth or any geotechnical related material as an integral part of a man-made project, structure or system." Jute was the early geotextile fabric made from natural fibers, then synthetic fibers such as polypropylene, polyester and polyethylene which are resistent to degradation by the microorganisms present in the soil were introduced. Use of geotextiles was common in Europe before they were widely accepted in the U.S.A. Until the 1970's, the use of geotextile was limited to a few specific applications such as coastal protection and soil filtration. In recent years, the uses of geotextiles have expanded rapidly from less than one million square yards in 1970 to 290 million square yards in 1988 as shown in Figure 1. The growth is expected to continue at the rate of 10-12% per year well into the next decade.

0097–6156/91/0457–0337$06.00/0

The main reason for this phenomenal growth is that geotextiles offer cost effective solutions to a wide variety of soil problems encountered by civil engineers and contractors. Geotextiles are used now to separate different layers of soil, to protect drainage pipes, to reinforce embankments, to stabilize railroad beds, to consolidate damaged highways, and to protect waterways. The most commonly used fibers are polypropylene, polyester, polyamide, and polyethylene. The fibers may be monofilament, staple or slit film, and are used in the form of woven, knit and nonwoven fabrics. This paper will discuss properties of HERCUFLEX strands and fabrics made from the strands and its potential use as a high-strength, high-modulus, and low creep geosynthetic reinforcement.

Comparison of Fiber Glass to Other Fiber Types

Performance requirements for geosynthetic reinforcement are listed in Table I. The four most widely used fibers in geosynthetics have some significant weaknesses. Polypropylene, the largest volume fiber, has relatively poor resistance to U.V. light. Polyethylene and polypropylene have relatively low melting points and their tensile strength is temperature dependent. Polyester fibers (PET) have relatively poor resistance to hydrolysis in alkaline soils, whereas polyamide fibers (Nylon) have relatively poor resistance in acid soils. Impregnated fiber glass (HERCUFLEX Strands) combines the good properties of fiber glass such as low elongation, very low creep, high tensile strength, high tensile modulus, and temperature insensitivity with improved flex fatigue, abrasion resistance, and resistance to chemical attack. This combination opened the door to new product opportunities in geosynthetic applications. Some of these applications are shown in Figure 2 and comparative properties of fibers used in these applications are listed in Table II.

Fiber glass yarn refers to continuous fibers formed by the rapid attenuation of thousands of streams of molten glass which flow from small orifices in the platinum alloy bushing and are drawn into fibers from 4 to 30 micron in diameter at speeds in excess of 1500 meters/minute (Figure 3a). A protective coating of organic sizing is then applied and the continuous filaments gathered into single multifilament strand before being wrapped onto a winding tube (Figure 3b).

Impregnated fiber glass yarn is produced by impregnating the entire bundle of filaments with a proprietary polymer coating so that each individual filament is separated from each other filament. Significant property improvements have resulted from this process. Tensile strength is nearly doubled, flex fatigue life is increased by several orders of magnitude, and the chemical resistance has improved significantly.

HERCUFLEX Yarns

Yarn properties of HF-1000 (1000 13-micron filaments), HF-2000 (2000 13-micron filaments), HF-4000 (4000 13-micron filaments), and fiber glass roving (not impregnated 1000 13-micron filaments) are listed in Table III. These properties were measured to characterize

Downloaded by UNIV MASSACHUSETTS AMHERST on August 6, 2012 | http://pubs.acs.org
Publication Date: April 3, 1991 | doi: 10.1021/bk-1991-0457.ch022

Downloaded by UNIV MASSACHUSETTS AMHERST on August 6, 2012 | http://pubs.acs.org
Publication Date: April 3, 1991 | doi: 10.1021/bk-1991-0457.ch022

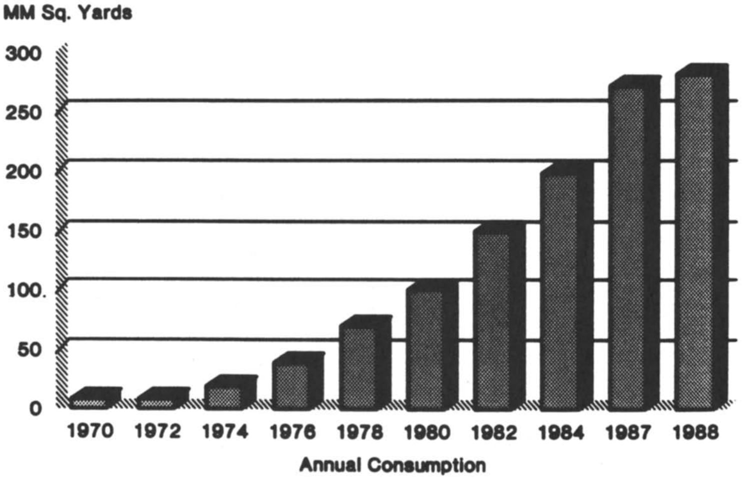

Figure 1. U.S. geotextile consumption.

TABLE I PERFORMANCE REQUIREMENTS FOR GEOTEXTILE REINFORCEMENTS(1)

- High Tensile Strength
- High Elastic Modulus
- Low Elongation
- Creep Resistance
- Resistance to a Wide Range of Chemical Attacks
- Resistance to Hydrolysis
- Insensitive to Temperature and Humidity Variations
- Abrasion Resistance
- Flexible for Easy Installation
- Can Be Sewn or Spliced to Match the Specific Design Dimensions

---

(1)Adapted From Reference 3.

Downloaded by UNIV MASSACHUSETTS AMHERST on August 6, 2012 | http://pubs.acs.org
Publication Date: April 3, 1991 | doi: 10.1021/bk-1991-0457.ch022

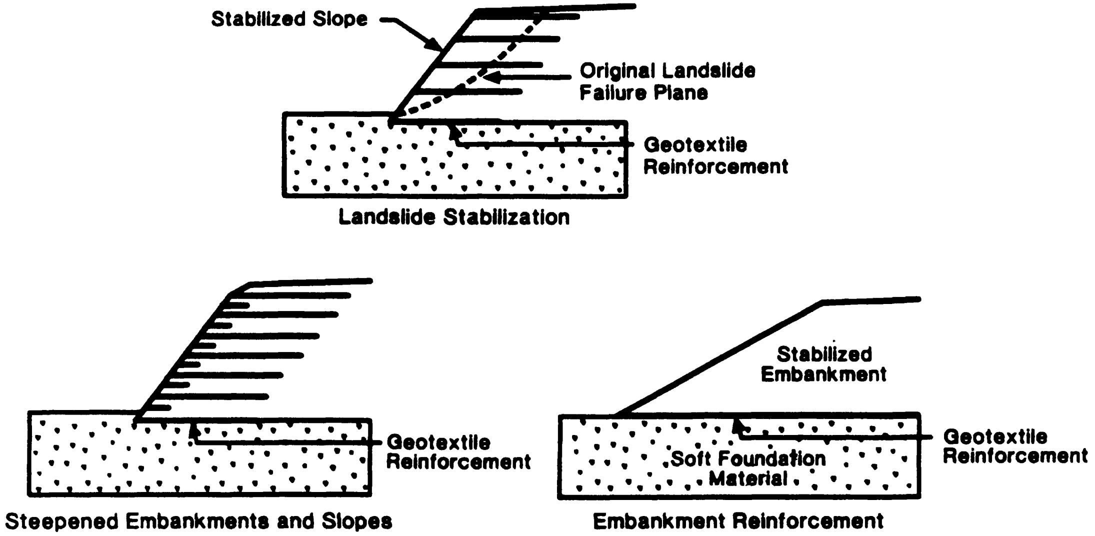
Stabilized Slope
Original Landslide Failure Plane
Geotextile Reinforcement
Landslide Stabilization
Geotextile Reinforcement
Steepened Embankments and Slopes
Stabilized Embankment
Soft Foundation Material
Geotextile Reinforcement
Embankment Reinforcement

Figure 2. HERCUFLEX products - geotextile application soil reinforcement systems (high modulus-high strength materials).

Downloaded by UNIV MASSACHUSETTS AMHERST on August 6, 2012 | http://pubs.acs.org
Publication Date: April 3, 1991 | doi: 10.1021/bk-1991-0457.ch022

TABLE II COMPARATIVE PROPERTIES OF FIBERS USED IN GEOTEXTILE APPLICATIONS

Fiber Type	Density g/cm^3	Tensile Strength psi x 1000	Elongation %	Modulus psi x 1000
Polypropylene	0.91	101	20	942
Polyethylene	0.95	72	30 - 50	580
Polyester	1.38	203	15 - 30	2680
Nylon 6, 66	1.14	145	15 - 35	1810
Aramid	1.45	420	2 - 4	8000
Steel	7.77	312	2	29000
HercuFlex	2.14	447	2 - 4	8000

the yarns and to assess the effects of impregnation on yarn performance under different test conditions.

The impregnating process increases the strength of the glass fibers and protects the surface of the fibers from abrasion damage. The amount of impregnant polymer is at least 12% by weight (30% by volume), and it acts as the stress transfer medium among glass fibers. Therefore, breaking strength of the yarn is increased by 70% and its flexibility improved dramatically. A knotted fiber glass roving (not impregnated) could easily be broken by hand. A knotted impregnated yarn could not be broken by hand. The effect of the knot reduced the strength of the impregnated yarn by 70%. By comparison, the strength of a knotted high tenacity PET yarn was reduced by 52%. Clearly, the impregnation effectively protects the surfaces of glass fibers. It is significant that the strain at break of the knotted HERCUFLEX yarn was reduced by 65%, not much more than the reduction of 40% for the PET yarn. By coating the individual glass fibers, the abrasion effects of mechanical mistreatment have been significantly reduced.

At approximately 5.2 KN/mm, the secant modulus at break of the HERCUFLEX yarn is much higher than the value of 3 KN/mm for the PET yarn. A high value of modulus is a very desirable property in many geosynthetic applications, particularly in geogrids used to reinforce soils. It should be noted that the secant moduli were measured by monitoring machine cross head displacement using PPG rubber drum clamps. Since an extensometer was not used to measure yarn extension, the modulus values could be considered as conservative. However, these values were presented only for the sake of comparison with similar conventional materials.

Downloaded by UNIV MASSACHUSETTS AMHERST on August 6, 2012 | http://pubs.acs.org
Publication Date: April 3, 1991 | doi: 10.1021/bk-1991-0457.ch022

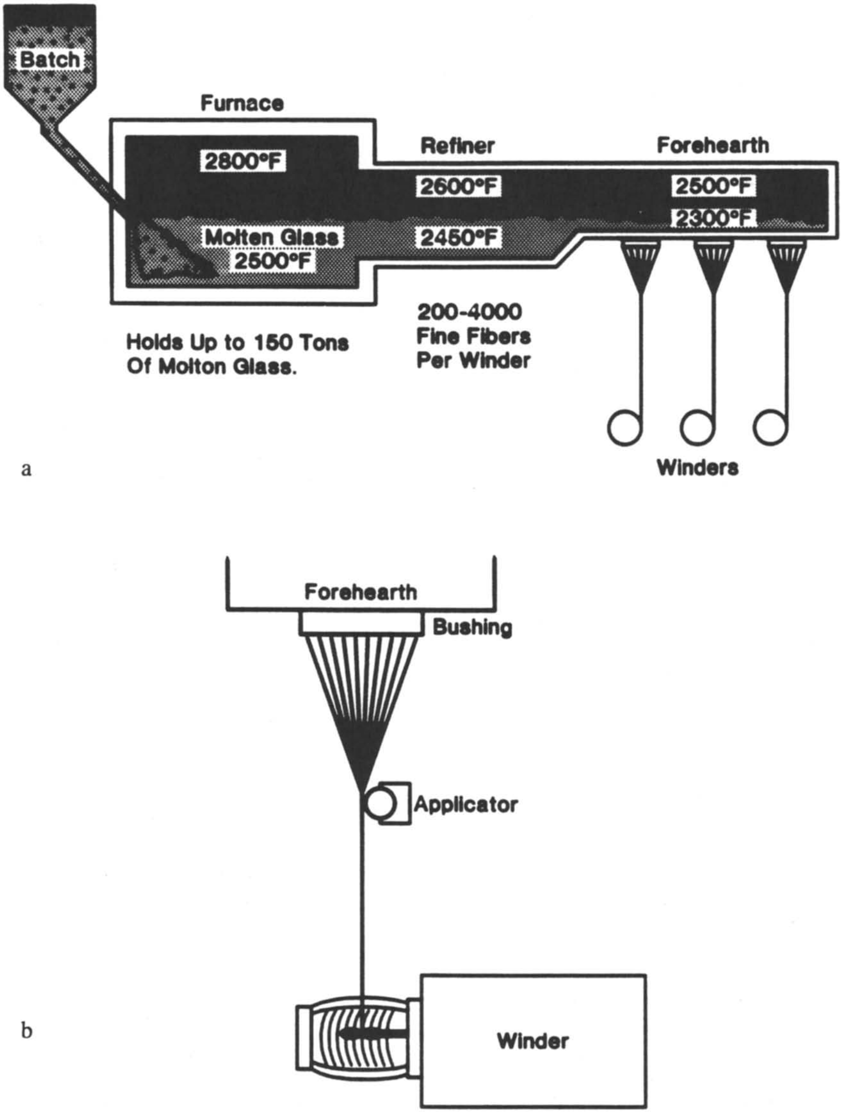
Batch
Furnace
2800°F
Refiner
Forehearth
2600°F
2500°F
2300°F
Molten Glass
2500°F
2450°F
Holds Up to 150 Tons
Of Molton Glass.
200-4000
Fine Fibers
Per Winder
a
Winders
Forehearth
Bushing
Applicator
b
Winder

Figure 3. (a) Glass melting. (b) Fiber glass forming process. (Reproduced with permission from ref. 3. Copyright 1988 Technomic Publishing Company.)

Downloaded by UNIV MASSACHUSETTS AMHERST on August 6, 2012 | http://pubs.acs.org
Publication Date: April 3, 1991 | doi: 10.1021/bk-1991-0457.ch022

TABLE III COMPARATIVE PROPERTIES OF FIBER GLASS IMPREGNATED YARNS(2)

Property	Conventional Fiber Glass	Hercuflex HF-1000	Hercuflex HF-2000	Hercuflex HF-4000
Tensile Strength, Lbs.	32	60	120	240
Typical Modulus of Elasticity, psi	10.5×10^6	8.0×10^6	8.0×10^6	8.0×10^6
Typical Elongation, %	2.5	2.8	2.8	2.8
Thermal Cycling (-40°R, +70°)	Insensitive	Insensitive	Insensitive	Insensitive
Chemical Attack Acid & Alkali Media	Susceptible	Resistant	Resistant	Resistant
PVC Shear Adhesion	Adhesive Failure	Cohesive Failure	Cohesive Failure	Cohesive Failure
Typical Flexibility (MIT Cycles to Failure)	100	3000	5000	7000
Flammability	Self Extinguishing	Self Extinguishing	Self Extinguishing	Self Extinguishing
Flex/Abrasion Test	100	>100,000	>100,000	>100,000
Yield Yards/Lb.	1490	1360	680	340
Denier	2996	3282	6564	13,128
TEX	333	365	730	1460
Area, Cross Section, Sq. In.	$.2 \times 10^{-3}$	$.25 \times 10^{-3}$	$.5 \times 10^{-3}$	1×10^{-3}

(2)Adapted From Reference 3.

Samples of HERCUFLEX yarns were exposed to humidity aging at 95% RH and 49°C temperature for 28 days and to water immersion at 26°C for 28 days. Changes in tensile strength and flex life of the exposed yarns were determined. Testing results are shown in Table IV. Exposure to high temperature and humidity conditions caused a 10% loss in the yarn strength and 50% loss in its flex fatigue life. However, exposure to tap water (immersion) resulted in only a 10% loss in strength and a 28% loss in yarn flexibility.

The exposure of the yarn to U.V. radiation for 1200 hours in an unfiltered carbon arc Atlas Weatherometer indicates that it has a distinct advantage relative to PET yarns. PET yarn retained less than 50% of its strength, while HERCUFLEX yarn retained more than 90% of its strength under these exposure conditions.

Downloaded by UNIV MASSACHUSETTS AMHERST on August 6, 2012 | http://pubs.acs.org
Publication Date: April 3, 1991 | doi: 10.1021/bk-1991-0457.ch022

TABLE IV AGING PROPERTIES OF IMPREGNATED YARN(3)

Impregnated Yarn Property	Aging Conditions	Percent Retention 28 Days
Tensile Strength	1. Water Immersion At 75°F	90
	2. Humidity Chamber, 95% RH & 120°F	90
MIT Flex Life (No. of Cycles to Failure Under Constant Load)	1. Water Immersion At 75°F	72
	2. Humidity Chamber, 95% RH & 120°F	50

(3)Adapted From Reference 3.

TABLE V EFFECTS OF CHEMICAL ENVIRONMENT ON TENSILE STRENGTH OF FIBER GLASS YARN(4)

Yarn Property	Chemical Effect	Percent Retension
Impregnated Yarn	Acidic; 1N, HCl, 80°F, 3 Hrs.	80
Fiber Glass Roving		10
Impregnated Yarn	Alkaline; 1N, NaOH 80°F, 30 Min.	90
Fiber Glass Roving		10

(4)Adapted From Reference 3.

The corrosive effects of acidic and alkaline media on the strength of HERCUFLEX yarns also have been tested. Ten-foot long samples of HF-4000 were soaked in 1 M NaOH at room temperature for 30 minutes, then rinsed with tap water three times, then dried at 250° for 2 hours, and tested at room temperature. Another set of 10-foot long samples of HF-4000 were also soaked for 3 hours at room temperature in 1 M HCl. The samples were then rinsed with tap water three times, then dried at 250°F for 2 hours, and tested at room temperature. The test results showed that the glass yarn retained 80% of its tensile strength after exposure in the acidic medium and 90% in the alkaline medium, as illustrated in Table V.

Downloaded by UNIV MASSACHUSETTS AMHERST on August 6, 2012 | http://pubs.acs.org
Publication Date: April 3, 1991 | doi: 10.1021/bk-1991-0457.ch022

Fabrics of HERCUFLEX Strands

HERCUFLEX yarns HF-1000 and HF-2000 have been woven successfully on the Dornier shuttle loom and the Rapier loom. The yarns have also been knitted on weft-knitting machines such as the Liba or Meyer weft insertion fabric machines. The performance in fabric formation indicates that the yarn is processible with a high efficiency. Woven fabrics of HERCUFLEX strands have been tested along with fabrics made from 2975 denier fiber glass roving, 1000 denier polyester, and 1448 denier aramid fibers. The four fabrics are not equivalent in construction, weight, yarn denier, or volume of yarn. However, these data are presented mainly to show the magnitude of performance parameters expected from HERCUFLEX yarns relative to other industrial yarns.

Geogrids of HERCUFLEX Strands

Geogrids are planar structures with relatively large openings (usually greater than one centimeter in diameter) which have high tensile strength and tensile moduli in one or more of the principal directions. The main function of a geogrid is as reinforcement. Geogrids of HERCUFLEX strand can be made by combining several HF-4000 strands which can be joined together at nodal junctions using PVC plasticized resin.

Properties of HERCUFLEX Woven Fabrics

The properties of woven fabrics made from HERCUFLEX yarns, fiber glass roving, polyester yarns, and aramid fibers were determined and listed in Table VI. Strips of woven fabrics containing 15 ends in the warp direction and 2-feet long were prepared to determine the effects of creasing the fabric on its breaking strengths. Fabric samples were tested without creasing, and they were creased under 10-lb loads for 24 hours. It was found that fiber glass roving lost 70% of its original strength while impregnated yarn samples lost only 20%. However, the breaking strength of aramid and polyester fabric samples did not change significantly after creasing, mainly because of the higher elongation of both fibers at the crease than HERCUFLEX yarn. Higher elongation reduces the compression fatigue of the fibers at the crease. Tongue tear strength of the fabrics were measured using 3 x 8-in. samples. The data indicate that impregnated yarn fabric had the highest strength, more than twice polyester fabric. The mode of failure in all fabrics was the same; i.e., the strands in the fabric samples were roped-up together.

Fabric flexibility was tested using the MIT flex fatigue test (ASTM D-1871) and Stoll abrasion (ASTM D-3885) flex test. Fabric samples containing 5 ends (about 0.5-in. wide) and 6-in. long were tested under load (2.5 lb) using the MIT test. The results indicate that the sensitivity of the fiber glass roving to flex fatigue is dramatically reduced by the impregnation process. Impregnated yarn fabric had more than 10 times the flex life of fiber glass roving. The same trend was observed when the fabric samples were tested on the Stoll Flex test which is mainly used as an abrasion tester.

In general, HERCUFLEX fabric has a distinct advantage in strength over polyester fabric. For the polyester to match the HERCUFLEX yarn in tensile strength, the weight of polyester yarn would have to equal that of HERCUFLEX yarn, and the volume would have to be more than double that of HERCUFLEX yarn. Only a dense polyester fabric could compete with HERCUFLEX yarn in strength; however, such dense fabric structures are not desirable for soil reinforcement.

Samples of woven HERCUFLEX strands and polyester fabrics were exposed to different aging conditions such as tap water, temperature, humidity, or U.V. light. Changes in tensile strength were determined and are summarized in Tables VIIa and VIIb. The data indicate that fabrics of HERCUFLEX strands retained 90% of its strength after immersion in tap water at room temperature and at 72°C for 30 days. A similar trend was observed for aging at 95% relative humidity and 49°C for 28 days. The data also demonstrate that HERCUFLEX fabric is not very sensitive to U.V. degradation. The polyester fabric lost over 50% of its strength after 3000 hours of U.V. exposure in an unfiltered carbon arc Atlas Weatherometer, while HERCUFLEX fabric lost only 20% of its original strength.

Applications

Potential applications for HERCUFLEX products are the following:

Vertical Walls. One of the most rapidly developing geosynthetic applications is the construction of vertical walls which utilizes the concept of soil reinforcement as opposed to the more traditional concept of retaining walls. Geogrids are the preferred reinforcement in this application because the cross-members have a relatively high profile (e.g., a diameter greater than 10 times the soil diameter). This means that the movement of the grid through the soil requires a displacement of the retained soil in addition to overcoming soil-grid friction. The resulting "pull-out" resistance of a geogrid is often 7-10 times the "pull-out" resistance of a simple strip of similar material. As a consequence, the anchoring ability of a high profile geogrid is much higher than that of a strip, and the use of high profile geogrids allows much more flexibility in the selection of fill material and reinforcement spacing. High tensile strengths and moduli geogrids required in design of vertical walls would be easily constructed using HERCUFLEX strand instead of high tenacity PET yarns which have much less creep resistance than HERCUFLEX yarns.

Slope Stabilization. The concept of soil reinforcement can also be used to enable construction of steepened slopes. For example, a slope constructed of soil with an angle of repose of 14 (4:1) could be constructed at a much steeper angle, say 45 (1:1) by internally reinforcing the soil with geosynthetic layers. Geogrids and woven geotextile based on the use of HERCUFLEX yarns may be used to construct such steepened slopes in earth.

Embankment Support. Geosynthetics may also be used to reinforce embankments constructed on weak subgrade soils. At the present

Downloaded by UNIV MASSACHUSETTS AMHERST on August 6, 2012 | http://pubs.acs.org
Publication Date: April 3, 1991 | doi: 10.1021/bk-1991-0457.ch022

Downloaded by UNIV MASSACHUSETTS AMHERST on August 6, 2012 | http://pubs.acs.org
Publication Date: April 3, 1991 | doi: 10.1021/bk-1991-0457.ch022

TABLE VI COMPARATIVE PROPERTIES OF INDUSTRIAL TEXTILE FABRICS(5)

Property (Test Method)	Fiber Glass Roving	Impregnated Fiber Glass Yarn	Kevlar®49	Polyester
Fabric Weight, Oz./Yd ^{2}	7.8	8.5	5.0	2.8
Fabric Construction & Weave Style	10 X 10 Plain Weave	10 X 10 Plain Weave	14 X 12 Plain Weave	10 X 10 Plain Weave
Breaking Strength, Lb./15 Ends	355	716	544	202
Crease Test, (10 Lbs. Load, 24 Hrs.) Tensile Strength Retention (Lb./15 Ends)	106	566	540	200
Toungue Tear Strength Lb. (3" X 8" Sample) Mode of Failure	8	36 Roped Up	30 Roped Up	16 Roped Up
MIT Flex Life (5 Ends, 2.5 Lbs.)	430	4200	>100,000	>100,000
Stoll Flex Life (15 Ends)	316	2000	5952	>100,000

(5)Adapted From Reference 3.

TABLE VIIa PHYSICAL PROPERTIES OF WEAVE SET FABRICS(6)

Fabric Type	Tensile Strength Retention, %					MIT Flex Life
	Water, 75°F 28 Days	Water, 160°F 30 Days	Humidity, 95% RH, 120°F, 28 Days	UV Exposure		Retention, % Water, 75°F, 28 Days
				1600 Hrs.	3000 Hrs.	
Impregnated Fiber Glass	90	90	90	80	80	80
Polyester	-	97	-	53	46	-

(6)Adapted From Reference 3.

TABLE VIIb AGING STUDIES OF STABILIZED KNITTED FABRICS

Fabric Type	Tensile Strength (5 Ends HercuFlex™and 10 Ends Polyester)		
	Original (lb.)	30 Days at 160°F Water, lb.	3000 Hours uv Exposure, lb.
Polyester	250	240	116
HercuFlex™	230	231	188

American Chemical Society
Library
1155 16th St., N.W.
Washington, D.C. 20036

time, the very high tensile strengths and very high moduli required in design are more readily developed by geotextiles than available geogrids. HERCUFLEX products would be particularly amenable to this application since they could be easily constructed into high strength geogrids or geotextiles. In fact, the resulting glass products are likely to be the highest strength and modulus products available in the marketplace.

Railroad Track. In this application, the function of the geosynthetic is to internally reinforce the railroad embankment structure itself, as opposed to walls, slopes, embankments, or other soil structures which might be associated with the track. Within the track structure, three modes of reinforcement are possible: (a) reinforcement in the track-wise direction, which is reinforcing the track or increasing the track modulus, (b) reinforcement in the cross-track direction, which is reinforcing the ballast, and (c) reinforcement in the vertical direction which is reinforcing the subgrade. Very high secant moduli, especially at the 1-3% levels, are required to adequately meet track and subgrade reinforcement requirements. HERCUFLEX products, with their very high moduli, appear to be well-suited to this application. However, the survivability and durability properties of these materials should be thoroughly investigated and determined before recommending their use in such applications.

Comparison of Tensile Properties of Geosynthetic Materials

The primary design parameters for reinforcement applications are the tensile strength and tensile elastic modulus which is the slope of stress-strain curves at a specified strain (typically between 2% to 10%). In civil engineering designs which require very high tensile moduli, the maximum desirable strain should be in the order of 2% to 5%. Table VIII is a comparison of the calculated wide width strip tensile properties of two potential HERCUFLEX geogrids and a prototype HERCUFLEX geotextile with the available high strength/high modulus geosynthetics, extracted from the appropriate manufacturer's technical brochures. The comparative tensile properties were listed at 2% and 5% strains in addition to the ultimate breaking strength. At 2% strain, the tensile strength of potential HERCUFLEX Geogrid #1 and #2 is several times stronger than Tensar (SR3) which is a high strength polypropylene geogrid made by The Tensar Corporaiton, Morrow, GA. At 5% strain, HERCUFLEX products will pass their ultimate tensile strength which are significantly higher than all the other geosynthetics considered.

The ultimate strength of HERCUFLEX Geogrid #1 is comparable to RECO's Matrex 240 high strength geogrid made from high tenacity polyester yarn by The Reinforced Earth Company, Arlington, VA, but significantly higher than the other geogrids. The corresponding elongation at break for the HERCUFLEX products is approximately one-quarter of the elongation at break of the Tensar products. With respect to the geotextiles, fabric of HERCUFLEX strands is significantly stronger than the commercially available high strength geotextiles. Usually, geotextile manufacturers, in their brochures, list breaking strengths of their products because they compare best

Downloaded by UNIV MASSACHUSETTS AMHERST on August 6, 2012 | http://pubs.acs.org
Publication Date: April 3, 1991 | doi: 10.1021/bk-1991-0457.ch022

Downloaded by UNIV MASSACHUSETTS AMHERST on August 6, 2012 | http://pubs.acs.org
Publication Date: April 3, 1991 | doi: 10.1021/bk-1991-0457.ch022

TABLE VIII COMPARATIVE TENSILE PROPERTIES OF GEOSYNTHETIC PRODUCTS

Geosynthetic Products	Tensile Strength, lb/ft at			Strain at Break
	2% Strain	5% Strain	Break	
GEOGRIDS				
HercuFlex 1 (HF-4000, 10 Yarns/ Strand at 1 Inch)	15,000	26,000	26,000	4%
HercuFlex 2 (HF-4000, 10 Yarns/ Strand at 2 Inches)	7,500	13,000	13,000	4%
RECO Matrex, 240	Not Available		23,880	--
TENSAR, SR3	2,600	4,730	8,000	15%
GEOTEXTILES				
HercuFlex HF-4000 (10 x 10 Simple Weave)	16,800	26,400	27,600	5%
Nicolon, 1500NC	Not Available		16,200	12%
Quline, 3600XX	Not Available		18,000	15%
Mirafi, 2120HP	Not Available		12,000	18%

at those levels. This explains why the tensile strengths at both 2% and 5% strains are unavailable for the other geotextiles listed in Table VIII.

Based upon the comparison presented, it can be concluded that HERCUFLEX strand can produce a high strength and high modulus geotextile while all other available geotextiles have high strengths but relatively low moduli and high elongations. Similarly, the tensile properties of HERCUFLEX geogrids, relatively, would appear to surpass those of the other commercial geogrids.

Conclusions

Impregnated fiber glass yarns have been developed and commercialized. Yarns can be woven or knitted into fabrics on industrial looms. These yarns have high modulus, high tensile strength, very low elongation, very low creep, insensitivity to thermal cycling, resistant to acidic and alkaline media, abrasion and flex fatigue resistant, and economical to produce. The coated glass strands are now being used by the wire and cable industry in reinforcing aerial and fiber optic telephone cables. The yarn is also being evaluated by the industrial fabric industry in tension support structures, pond lining, and geosynthetic applications.

Acknowledgment

The author expresses his appreciation to the Fiber Glass Products unit of the Glass Group of PPG Industries, Inc., for their permission to publish this paper.

HERCUFLEX is a registered trademark in the United States Patent and Trademark office.

Literature Cited

1. Girgis, M. M., et.al., "Impregnated Fiber Glass Yarn for Reinforcing Fiber Optic Cables," 35th International Wire and Cable Symposium Proceedings, 1986.
2. HercuFlex. The New Fiber Glass for Cost-Effective, High Performance Cable Reinforcement, PPG Industries, Inc., Product Brochure, 1986.
3. Girgis, M. M., "Impregnated Fiber Glass Yarns for Reinforcing Industrial Coated Fabrics," Journal of Coated Fabrics, Volume 17, (April, 1988) 230-241.
4. Koerner, R. M., Designing with Geosynthetics, Prentice-Hall, Englewood Cliffs, NJ, Second Edition, 1990.

RECEIVED August 13, 1990

Downloaded by UNIV MASSACHUSETTS AMHERST on August 6, 2012 | http://pubs.acs.org
Publication Date: April 3, 1991 | doi: 10.1021/bk-1991-0457.ch022

Chapter 23

The Use of Geotextiles in Waste Containment Facilities

S. D. Menoff, J. W. Stenborg, and M. J. Rodgers

Chambers Development Company, Inc., Pittsburgh, PA 53215

Downloaded by PENNSYLVANIA STATE UNIV on August 6, 2012 | http://pubs.acs.org
Publication Date: April 3, 1991 | doi: 10.1021/bk-1991-0457.ch023

During the past few years, there has been an increased emphasis on technical advancements in the design and construction of waste containment facilities. This has been in response to the demand for environmentally sound landfill sites. This emphasis has resulted in the increased utilization of geosynthetic materials for waste containment applications. While geomembranes have become the basic element for containment in waste disposal facilities, geotextiles are also utilized to satisfy a number of important design and construction considerations.

The principal application for geotextiles in waste disposal facilities are as filters and cushions. They also serve as drainage layers either on their own or in conjunction with geonets. High-strength geotextiles provide soil reinforcement to allow for the construction of steeper side slopes, potentially increasing the available airspace. This paper presents an overview of the design applications and construction considerations for the use of geotextiles in waste containment facilities.

Design Objectives and Applications

In the design of a solid waste disposal facility, the objectives are to provide for the containment of waste and leachate in a manner that ensures long term environmental protection, regulatory compliance, and cost effective utilization of manpower, equipment, and space. To achieve these objectives, landfills are lined with one or more

0097–6156/91/0457–0351$06.00/0

layers of geomembranes. These geomembranes, coupled with natural soil or geosynthetic drainage layers, contain and collect leachate for removal and subsequent treatment and disposition. The objective is to minimize the development of a leachate head build up on the geomembrane liner and thereby reduce the risk to the environment.

Geotextiles are important components of a geosynthetic containment system in a waste disposal facility. Other components include geomembranes, geonets, and geogrids. The major applications of geotextiles in landfill construction are the following:

1. Cushion

   Geotextiles placed directly above or below a geomembrane act as a "cushion" which protects the geomembrane from damage. Puncture can be a particular problem during installation.

2. Filtration

   Geotextiles placed between two different soils or between a soil and a geonet allow liquid to flow perpendicularly to the interface from one material to the other, while preventing the movement of fine grained soil particles (permittivity). Geotextiles used in this application also serve the purpose of separation.

3. Drainage

   Geotextiles allow liquid or gas to move along the plane of the material (transmissivity). Large volumes of liquid are conducted using geotextiles in combination with geonets.

4. Reinforcement

   Geotextiles can be used as the reinforcing elements in a soil mass primarily through stress distribution within the soil mass or direct soil reinforcement. Reinforcement allows side slopes above or below the ground surface to be steepened.

Geotextile Classification

Geotextiles are classified according to the type of polymer, filament, fiber and fabric from which they are manufactured.

The majority of geotextiles are manufactured from polypropylene and polyester. These materials have been shown to be resistant to degradation when exposed to

Downloaded by PENNSYLVANIA STATE UNIV on August 6, 2012 | http://pubs.acs.org
Publication Date: April 3, 1991 | doi: 10.1021/bk-1991-0457.ch023

Downloaded by PENNSYLVANIA STATE UNIV on August 6, 2012 | http://pubs.acs.org
Publication Date: April 3, 1991 | doi: 10.1021/bk-1991-0457.ch023

municipal solid waste leachate. Polyethylene geotextiles have been recently introduced into the market, however, they are not readily available in the United States. The two types of geotextiles used in most geotechnical applications are woven and non-woven. Non-woven geotextiles are used most often in waste containment applications because experience has shown that they perform better as filters and cushions in conjunction with other landfill components. The filaments used in non-woven fabrics are bonded in one of three ways: chemical bonding, thermal bonding, or mechanical bonding by needle punching. The most common bonding procedure is needle punching.

Landfill Application

1. Cushion

A landfill can only be considered environmentally sound when leachate can be collected and removed, thereby preventing contamination of the surrounding hydrogeologic regime. To effectively collect leachate, the integrity of the geomembrane liner system must be preserved. Since high density polyethylene (HDPE) geomembranes are susceptible to damage during and after installation, geotextiles are placed adjacent to the liner to act as a cushion against possible puncture. The properties most important in this application are bulk density and thickness.

In general, non-woven geotextiles in the range of 10 to 16 ounces per square yard have proven adequate for most cushion applications. The evaluation of the effectiveness of cushion materials is best accomplished through a laboratory testing program which includes static load testing to simulate actual landfill conditions.

2. Filtration

When designing a filter system using geotextiles, the same criteria are used as if designing with aggregates. Flow estimates and capacity calculations are essentially the same. The advantage over typical aggregate systems is the saving of valuable landfill airspace and construction time. Three conditions must be met for a geotextile to be considered an effective filter: it must provide adequate drainage capability (permittivity), prevent piping of the soil, and provide the required durability against chemical or biological attack. These conditions are generally met using a non-woven polyester or polypropylene geotextile, especially when fine grained soils are present. Although either woven or non-woven geotextiles can be used in filter applications, industry experience has shown that the performance of non-woven geotextiles is generally superior.

3. Drainage

Geotextiles alone can be used as a drainage medium, although they are most frequently used in conjunction with a geonet to produce a geocomposite. The advantage of a geocomposite is that geotextile prevents soils from clogging the drainage channels of the geonet. When choosing a geonet for a landfill application, one must consider the overburden pressure, strand rollover, or the intrusion of adjacent materials into the geonet channels. Factors that impact the long term performance of a geocomposite include creep, response to elevated temperatures, and the potential for biological or mechanical clogging.

4. Reinforcement

The limited available airspace in existing landfills makes it necessary to look for innovative ways to use the available space. One way is to increase the slopes of the landfill. By incorporating geotextiles such as high tensile strength wovens, steeper slopes can be built. The fabric provides tensile strength to the bottom of the embankment and may also interrupt rotational-type failure. Areas of concern when analyzing soils for reinforcement include soil creep, plastic soil deformation, and stress redistribution. Because these soil analyses are dependent on a number of factors, a relatively high factor of safety of is recommended.

Construction Considerations

The considerations previously discussed relate to the geotextile once it is in place and functioning as designed. During construction and installation, other considerations that become important include installation durability, field seam strength, anchor trench adequacy, and ultra-violet light degradation.

Installation of a geotextile layer begins by unrolling a panel of material down the slope or across the area intended to cover. A series of panels are placed and joined at their edges to form one continuous layer of material. The edges of adjacent panels are overlapped and sewn or heat welded together. Experience has shown that sewing is the preferred method of joining geotextile

Downloaded by PENNSYLVANIA STATE UNIV on August 6, 2012 | http://pubs.acs.org
Publication Date: April 3, 1991 | doi: 10.1021/bk-1991-0457.ch023

Downloaded by PENNSYLVANIA STATE UNIV on August 6, 2012 | http://pubs.acs.org
Publication Date: April 3, 1991 | doi: 10.1021/bk-1991-0457.ch023

panels. The geotextile material and seams must be strong enough to "survive" the installation of subsequent geosynthetics and natural soil layers and remain intact to function as intended by design. The most critical design criteria is for the geotextile to remain intact as a soil layer is being placed over it.

As field seaming progresses, the outer edge of the panels must be anchored to hold it in place and prevent movement into the cell as other layers of material are placed over the geotextile layer. The geotextile is usually placed in an anchor trench with other geosynthetic layers such as geomembranes or geonets. The anchor trench uses horizontal or vertical embedment to hold the material by friction or simple burial in a shallow trench.

Friction considerations or friction angles for geosynthetic materials are a concern when designing access into or placing the final cover system over the waste containment area and in anchor trench designs. Geotextiles have relatively low friction angles when in contact with geomembranes such as HDPE. Geotextiles in contact with soil have relatively high friction angles. The designer must usually consider the stability of a composite layer of soil and geotextile on an HDPE liner. When working below ground surface within the cell, the geotextile in the anchor trench provides a means of holding the layer as waste is placed in the cell. The most critical time for design is immediately after construction. As the area is filled with waste material, the potential for pullout of liner components from the anchor trench is generally reduced. Frictional consideration becomes a concern as waste is placed above the surrounding ground surface and an "above-grade" sideslope is created. The final cover system is constructed over the top and side slopes of the facility. When geosynthetic components are used in the final cover system, the maximum slope permitted because of relatively low friction between geotextiles and HDPE liner is about 6:1 (horizontal : vertical). Final cover systems constructed entirely of soil are usually stable over the long term on slopes as steep as 3:1. Reinforcing geotextiles can be used to steepen sideslopes and provide long-term stability when geosynthetic components are used in final cover systems.

Quality Control and Quality Assurance

The installation of any construction product according to the design plans and specifications is always important. However, it is extremely critical when geosynthetics are used in a waste containment application. Quality control and quality assurance are integral parts of all geosynthetic installations.

It is important that the geotextiles used in the construction of any specific landfill meet the design specifications. A quality control program is needed at the manufacturing plant to assure the manufacturing process is not varied and a consistent product adhering to the specification is produced. Samples should be taken on a regular basis during manufacturing (typically once every 50,000 sq. ft.) and tested to evaluate the appropriate geotextile properties. The manufacturer is generally responsible for providing certifications that each roll of geotextile conforms to the specification. The manufacturer must also maintain detailed records of quality control documentation.

When considering a geotextile manufacturer, only one with a record of consistently producing a quality product and a carefully implemented quality control program should be considered.

A full time quality assurance monitoring team should be assigned to all installations of geotextiles and other geosynthetic components. A qualified professional engineer experienced in geosynthetics should supervise all construction quality assurance programs and certify all quality assurance documents.

A pre-construction meeting should be held prior to the start of construction to review all quality assurance procedures. The agreement of all parties involved should include sampling frequency and quantities, testing procedures, and any site specific problems that may arise.

Careful attention must be paid to any special installation requirements, especially when combinations of geotextiles, geomembranes and geonets are being used. Geotextile must be checked by field inspection personnel to ensure that overlapping and seaming procedures are as specified. Geotextiles must be maintained in a clean condition to prevent clogging of openings.

The past few years have seen an increased emphasis on technical advancements in the design and construction of waste containment facilities. Concurrently, the need for environmentally sound landfill airspace has accelerated. These two factors have resulted in the increased utilization of geosynthetic materials for waste containment applications. While the use of geomembranes as barrier layers is obvious, geotextiles have also been utilized to satisfy a number of significant design and construction concerns. The principal applications of geotextiles in waste disposal facilities are as filters and cushions. They can also serve as drainage layers either on their own or in conjunction with geonets. Finally, high-strength geotextiles can provide soil reinforcement to allow for the construction of steeper slopes, thereby maximizing the available airspace. This

Downloaded by PENNSYLVANIA STATE UNIV on August 6, 2012 | http://pubs.acs.org
Publication Date: April 3, 1991 | doi: 10.1021/bk-1991-0457.ch023

paper provides an overview of the design applications and construction considerations for the use of geotextiles in waste containment facilities.

Summary

The increased use of geotextiles in waste containment applications improves the environmental integrity of the landfill liner, leachate collection and final cover systems; reduces construction costs; and can provide additional airspace for waste disposal.

Downloaded by PENNSYLVANIA STATE UNIV on August 6, 2012 | http://pubs.acs.org
Publication Date: April 3, 1991 | doi: 10.1021/bk-1991-0457.ch023

LITERATURE CITED

1. Bell, J. Richard Ph.D., P.E., M. ASCE, "Design and Construction Using Geosynthetics" ASCE Continuing Education, 1989.

2. O'Leary, Philip, "Solid Waste Landfills", Waste Age, 1986.

3. Lundell, C. M. & Menoff, S. D., "The Design and Construction of Landfill Containment Systems with Geosynthetic Components", presented at Geosynthetic '89, San Diego, 1989.

4. Lundell, C. M. & Menoff, S. D., "The Use of Geosynthetics as Drainage Media at Solid Waste Landfills", presented at National Solid Waste Management Association, Waste Tech, Boston, 1988.

5. Richardson, G. N. and Koerner, R. M., "Geosynthetic Design Guidance for Hazardous Waste Landfill Cells and Surface Impoundments", 1988.

6. Giroud, Jean-Pierre, "Geotextile and Geomembranes Definitions, Properties and Design", Industrial Fabrics Association International, 1984.

RECEIVED July 31, 1990

Downloaded by PENNSYLVANIA STATE UNIV on August 6, 2012 | http://pubs.acs.org
Publication Date: April 3, 1991 | doi: 10.1021/bk-1991-0457.ch024

Chapter 24

The Use of Geotextiles in Transportation Facilities

L. D. Suits

Soil Mechanics Bureau, New York State Department of Transportation, Albany, NY 12232

The ASTM definition for a geotextile is; any permeable textile material used with soil, rock, earth, or any other geotechnical engineering related materials, as an integral part of a man-made project, structure or system. Since their original introduction into the civil engineering community as filter fabrics, the use of geotextiles in transportation facilities has expanded to every aspect related to geotechnical engineering that the civil engineer deals with. This includes the reinforcement of foundation and embankment soils, erosion control including silt fences and turbidity curtains, separation of poor drainage foundation soils from free draining base soils, and pavement rehabilitation. This paper will describe, 1) the use of geotextiles in these various applications, 2) the important critical properties for each use, 3) some of the test methods for determining critical property values, and 4) some of the concerns about their use including construction and long term survivability.

Geotextiles, as they are called today, had their beginnings in the late 1950's to early 1960's as alternatives to granular filters used in erosion control applications related to civil engineering projects. Since then the number of applications has multiplied as has the number of square meters used on an annual basis. The estimated growth in sales of geotextiles in North America during the period from 1976 to 1987 was from five million square meters to 225 million square meters. (1)

Today's uses include the following: 1) highway pavement rehabilitation, 2) separator for two dissimilar soil materials, 3) as a filtration medium, 4) as a reinforcing member, 5) in erosion and pollution control, 6) to assist in the stabilization of unstable foundation soils, 7) as a drainage material, and 8) as part of composite materials used in the above applications. Within each of

0097–6156/91/0457–0358$06.00/0

these applications there are numerous types of installations in which geotextiles are used. Thus there are easily over 100 applications for the use of geotextiles. In many of the installations the geotextile can serve more than one function at the same time.

Each one of these applications require performance properties in the area of geotextile strength, water-carrying capacity, soil retention ability, and resistance to degradation, in order to survive installation procedures, and for long term performance of the installation.

Over the past several years there have been tremendous efforts made to standardize the testing of these materials nationally through ASTM, and internationally through the ISO group. Many of the tests to be described later in the paper now exist as ASTM-approved standards.

When selecting a material for a particular project, it is critical to keep in mind the primary function of the geotextile in the installation as it may be necessary to trade off some performance characteristics in order to obtain a material which will satisfactorily perform the primary function. A more detailed discussion of this can be found later in the paper.

Applications

Pavement Rehabilitation. In the highway pavement rehabilitation application, the geotextile is "tacked" down to the existing pavement with an asphalt emulsion and the new asphaltic pavement placed over it. The geotextile serves two functions in this type of installation: 1) It provides a waterproof barrier preventing water from seeping into the old pavement causing further deterioration of the system, and 2) it retards the reflection of cracks existing in the old pavement into the new pavement. Both of these functions serve to extend the life of the new overlay pavement.

The success of this type of installation has been varied throughout various parts of the country. Installations in the Southeast and Southwest appear to perform very satisfactorily, while in other areas performance has not been as good. Poor performance is particularly noted in the Northeast where the seasonal temperature variations include periods of freezing and thawing of pore water within the pavement system. In this context the pavement system includes the foundation soils, base soils, and the pavement itself. These freeze/thaw cycles cause pavement movement to take place leading to the reappearance of cracks in the pavement regardless of the presence of the geotextile.

In this application, the critical performance properties for the geotextile include strength to withstand installation procedures, and the ability to absorb the asphalt emulsion used to "tack" it to the existing pavement. The "tacking" process consists of applying the asphalt emulsion over the existing pavement, spreading the geotextile on the emulsion, and applying another coat of emulsion on top of the geotextile. During the "tacking" process care must be taken to ensure that no wrinkles or folds appear in the geotextile. If the geotextile does not have intimate contact with the old pavement

Downloaded by PENNSYLVANIA STATE UNIV on August 6, 2012 | http://pubs.acs.org
Publication Date: April 3, 1991 | doi: 10.1021/bk-1991-0457.ch024

Downloaded by PENNSYLVANIA STATE UNIV on August 6, 2012 | http://pubs.acs.org
Publication Date: April 3, 1991 | doi: 10.1021/bk-1991-0457.ch024

surface, water may become trapped between the geotextile and the old pavement, or the remainder of the geotextile may start to peel away from the pavement when the system is subjected to traffic.

During installation care must be exercised from both a safety standpoint, and prevention of installation damage due to traffic driving directly on the emulsion impregnated fabric prior to placement of the overlay pavement. From a safety standpoint, the surface of the fabric may become extremely slippery due to the presence of the emulsion. Also, if traffic is allowed to drive on the geotextile before the pavement is placed, it may become torn or otherwise damaged by the vehicles. If this happens geographic location will have no bearing on the system's poor performance.

Separation. As a separator the geotextile is placed between the foundation soil of a transportation facility and the granular, free-draining base material of the constructed system. This prevents the free-draining base material from becoming contaminated with the finer foundation soil which will decrease the drainage capability of the base material. In New York State this application is routinely the largest use of geotextiles. This is probably also true on a national level.

Reference to the constructed system includes the pavement of a highway or runway, or the track bed of a railroad (tracks and ballast), and the base material which is placed on the foundation soil.

In this application, the critical properties of the geotextile include sufficient strength to withstand the stresses placed on the material during installation, adequate flow capacity to allow passage of water out of the constructed system into the foundation soil, and small enough pore openings to prevent passage of the fine soil portion of the foundation soil into the base material of the constructed system. If the base course of the system becomes contaminated with fine soil from the foundation soil, adequate drainage of the system is unable to take place leading to accelerated system deterioration.

Drainage. Water is one of the chief contributors to the deterioration of a pavement system. Therefore, providing for the drainage of it is one of the chief concerns in the designing of a system. The use of geotextile as part of a drainage system is an instance where it can serve two functions at the same time. When the fabric is used to wrap a pavement edge drain it allows water to drain from the surrounding areas while acting as a filter to keep fine soil from entering into the edge drain and clogging it. Prefabricated drainage composites also fall into this application.

There are several configurations which a pavement edge drainage system can take. Each starts with a trench excavated at the edge of the pavement. The first configuration consists of lining the trench with the geotextile, backfilling the trench with small crushed stone, wrapping the geotextile over the top of the stone, and backfilling with excavated material. The second configuration consists of installing slotted PVC pipe in the geotextile wrapped trench prior to filling the trench with the crushed stone.

A third configuration is to excavate a trench as previously described, wrap the slotted pipe with the geotextile, install the wrapped pipe in the trench, and backfill the trench. The fourth configuration is the use of a prefabricated geocomposite edge drain. The geocomposite edge drain consists of a planar polymeric core wrapped with a geotextile. The core most often has the appearance of an egg carton. In this instance a narrow trench is excavated next to the pavement, the drain installed, and the trench backfilled with excavated material.

When installing a geotextile for this application, attention must be paid to the placement of the geotextile to ensure that it is in intimate contact with the surrounding soil. If void spaces are allowed to remain between the geotextile and surrounding soil, fines from the soil are carried into the voids. The fines then can either build up a cake on the outside of the fabric, become lodged in the pore openings of the geotextile and plug it, or pass through the geotextile into the drain and eventually plug the drain. All of these occurrences lead to failure of the drain.

In this application the most critical property of the geotextile is its water-carrying capacity (permeability), followed by its ability to retain soil, and then having sufficient strength to withstand installation stresses.

There are other instances where the drainage function of the geotextile plays a key role in the installation. These will be described under the specific applications where this occurs.

Reinforcement. An example of the geotextile being used as a reinforcing member is in the construction of a retaining wall as part of the highway. In this application the geotextile acts as the facing as well as a reinforcement member, possibly pretensioned, and buried with the material backfilled against the wall. The purpose of the wall is to stabilize movement of embankments or roadbeds. Other reinforcing applications include placement directly into the highway embankments, or roadbeds.

A dictionary definition of reinforcement is: something designed to provide additional strength. In this application the tensile properties of the geotextile are utilized to provide additional strength to the constructed system, as opposed to preventing failure of the foundation soils, which will be addressed in the next application. In this discussion the constructed system is the wall, highway embankment, or roadbed system.

Varying approaches are taken as to designing for reinforcement using geotextiles. There is the school which use the concept that it is necessary to mobilize the tensile properties of the geotextile through deformation (strain) of the geotextiles, while others design with a safety factor applied to the ultimate strength disregarding the deformation or strain of the geotextile.

In either approach, the strength properties of the geotextile are the critical concern in the design. Permeability is of relatively little concern, and soil retention only a concern to the

Downloaded by PENNSYLVANIA STATE UNIV on August 6, 2012 | http://pubs.acs.org
Publication Date: April 3, 1991 | doi: 10.1021/bk-1991-0457.ch024

Downloaded by PENNSYLVANIA STATE UNIV on August 6, 2012 | http://pubs.acs.org
Publication Date: April 3, 1991 | doi: 10.1021/bk-1991-0457.ch024

point that the backfill or embankment material not wash through the geotextile allowing erosion to take place.

Stabilization. When used to stabilize wet, soft, weak foundation or subgrade soils, the geotextile serves more than one function. It acts as a separator of two dissimilar materials, it acts as a filter and drainage medium for the foundation soil, and it also acts as a reinforcing member for the constructed system.

The difference between this and the previous application is the condition of the foundation or subgrade soil. It is generally accepted that when a geotextile is used with a subgrade soil having a California Bearing Ratio (CBR) of less than three, overall stabilization, of the subgrade soil is the primary function of the geotextile. In a subgrade soil having a CBR greater than three, the primary function is to reinforce the constructed system.

The California Bearing Ratio is a parameter used to measure the strength of the soil. It is determined by a laboratory test performed on the soil.

In this application the geotextile performs each of the functions as described in the separation, drainage, and reinforcement applications.

In this application the geotextile not only has to withstand the stresses encountered during installation, it must also have long term strength to withstand the stresses developed during the soil stabilization process. It must also provide adequate drainage and soil retention properties.

This application is an example of the situation referred to previously, where it may not be possible to have the optimum in all of the geotextile properties in order to perform the primary function.

The primary function is to provide reinforcement, however for the stabilization process to occur, drainage and soil retention must also take place. In order for this to happen, compromises have to be made in each of the properties.

The strongest geotextile may be so tightly constructed that adequate drainage of water may not take place. The same is true for a material that will retain the smallest particle of soil. The material demonstrating the highest permeability may not provide adequate strength, and also allow too much soil to pass through. Therefore, a compromise must be designed which will allow for satisfactory performance of the system.

Erosion and Pollution Control. There are several different types of installations where the geotextile is used as an erosion control agent. It may be installed on a highway cut slope or embankment where it acts as a drainage medium and filter to allow water to exit the slope while preventing the erosion of the underlying soil. It may be used as a silt fence where it is installed similar to a fence and acts as a filter and drainage medium. Water runoff from the site passes through the geotextile, filtering out any fine sediment that may be suspended in the water.

When used on a highway cut slope or embankment, the geotextile is placed on the slope in intimate contact with it and slope protection stone placed over it. Before the advent of geotextiles this function of erosion control was performed by placing a graded aggregate filter on the slope and covering it with the slope protection stone. This filter could range from one to three feet thick. Reduction in material and construction costs with the use of geotextiles are of prime consideration here.

The critical properties in this installation are soil retention, permeability, and sufficient strength to withstand installation stresses.

Care must be taken during construction that the geotextile not be punctured by the slope protection stone dropping on it from too high a height, or that it be torn by construction equipment. Should this happen and go unnoticed, the material cannot perform its prime function of soil retention.

In the silt fence application the geotextile is installed similar to a fence. This may be along an entire construction site or in drainage ditches along the site.

The silt fence serves as both an erosion control and a pollution control agent. As an erosion control agent it acts to prevent soil from being carried away from the site in question. As a pollution control agent, it prevents the fine soil from being carried away from the site and entering surrounding streams or waterways, and creating an unsightly appearance of the water.

In another pollution control application, the geotextile is installed in a stream, lake, river, or other waterway to act as filter for fine soil material stirred up due to construction activities in the water. Bridge construction is an example of an activity where the geotextile may be used in this capacity. This type of an installation is known as a turbidity curtain. (2)

In both the silt fence and turbidity curtain the geotextile must exhibit soil retention, permeability, and strength to withstand loading due to stresses from the water and soil behind it. Besides these properties, the geotextile must exhibit reasonable resistance to ultraviolet deterioration from exposure to the sunlight. Most of the geotextiles today have ultraviolet inhibitors incorporated into them during manufacturing.

Figures 1 through 8 are examples of the major uses of geotextiles described in this section.

Specifications and Testing (3,4)

Specifications for the various geotextile applications take various forms. Some agencies develop project specific specifications, others approach the subject from the approved list concept, and there is a combination of both approaches.

In the project specific approach, a set of generic property values of the geotextile are specified for the specific installation, and could vary from project to project, or there has been the "brand name or equal" approach.

Downloaded by PENNSYLVANIA STATE UNIV on August 6, 2012 | http://pubs.acs.org
Publication Date: April 3, 1991 | doi: 10.1021/bk-1991-0457.ch024

Downloaded by PENNSYLVANIA STATE UNIV on August 6, 2012 | http://pubs.acs.org
Publication Date: April 3, 1991 | doi: 10.1021/bk-1991-0457.ch024

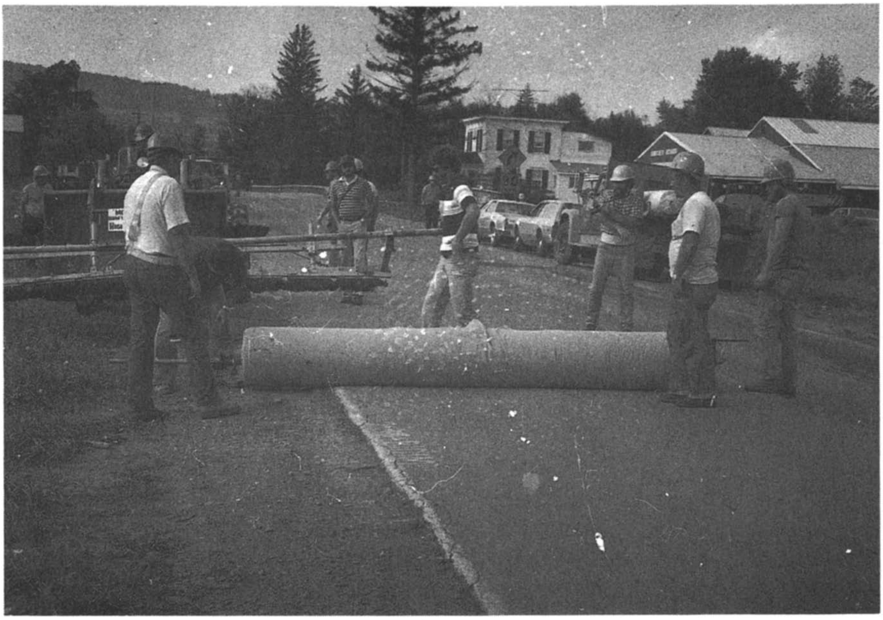

Figure 1. Pavement rehabilitation.

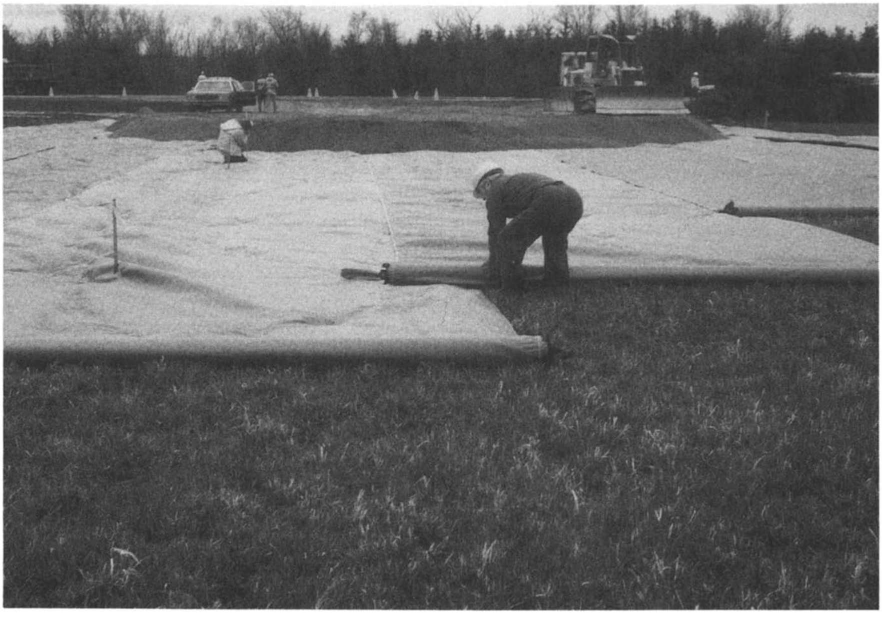

Figure 2. Separation application.

Downloaded by PENNSYLVANIA STATE UNIV on August 6, 2012 | http://pubs.acs.org
Publication Date: April 3, 1991 | doi: 10.1021/bk-1991-0457.ch024

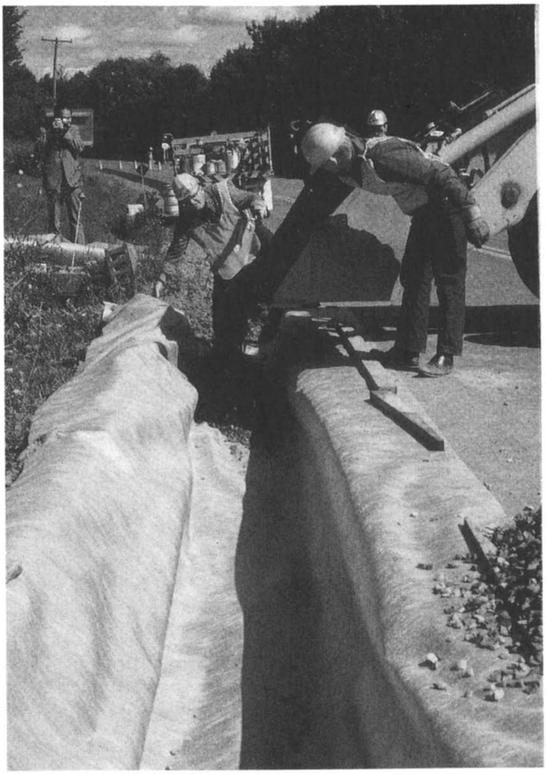

Figure 3. Underdrain (drainage) application.

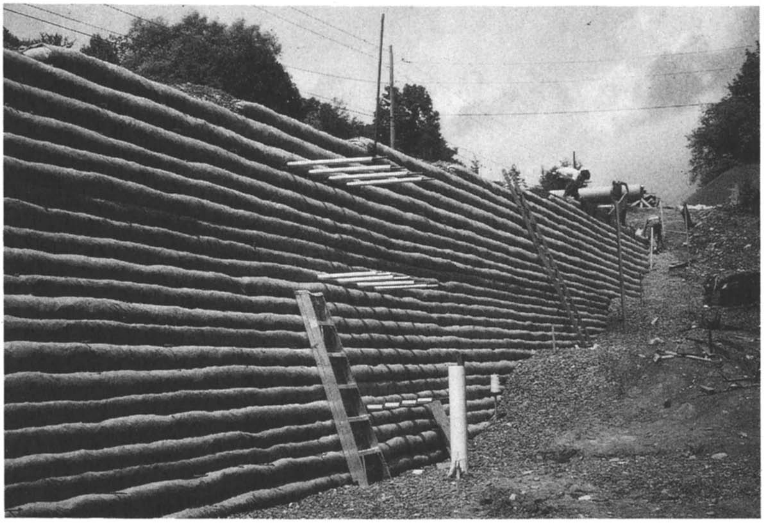

Figure 4. Reinforcement (wall) application.

Downloaded by PENNSYLVANIA STATE UNIV on August 6, 2012 | http://pubs.acs.org
Publication Date: April 3, 1991 | doi: 10.1021/bk-1991-0457.ch024

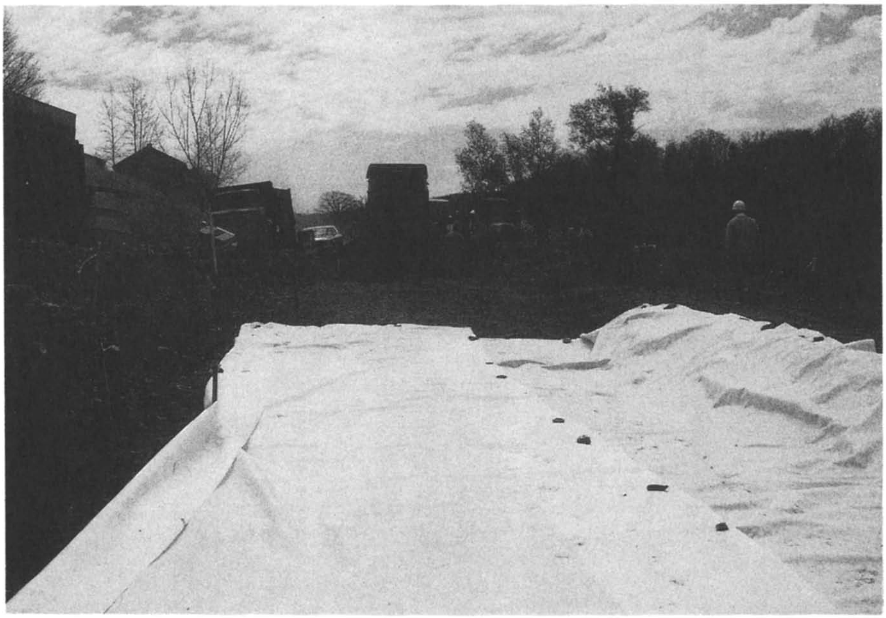

Figure 5. Stabilization application.

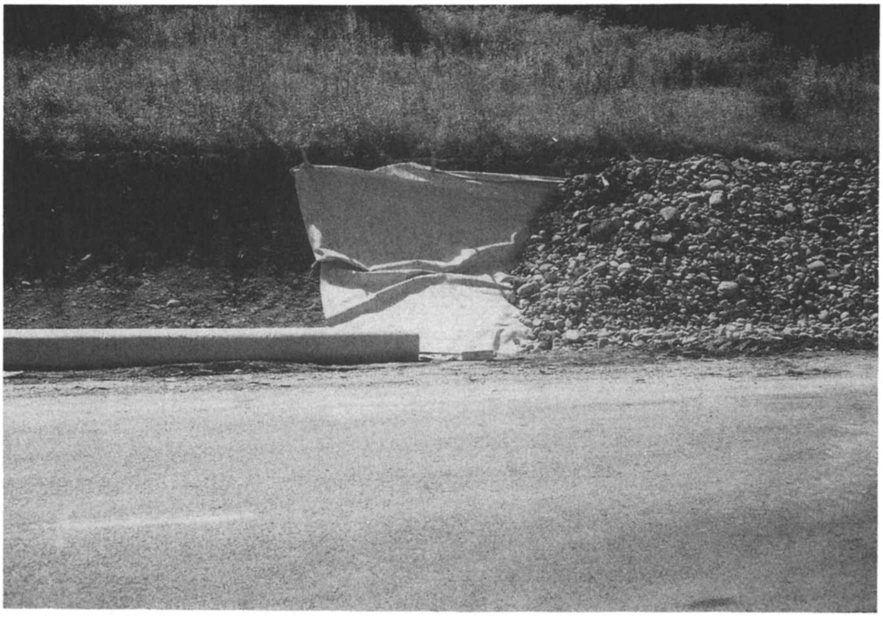

Figure 6. Slope protection application.

Downloaded by PENNSYLVANIA STATE UNIV on August 6, 2012 | http://pubs.acs.org
Publication Date: April 3, 1991 | doi: 10.1021/bk-1991-0457.ch024

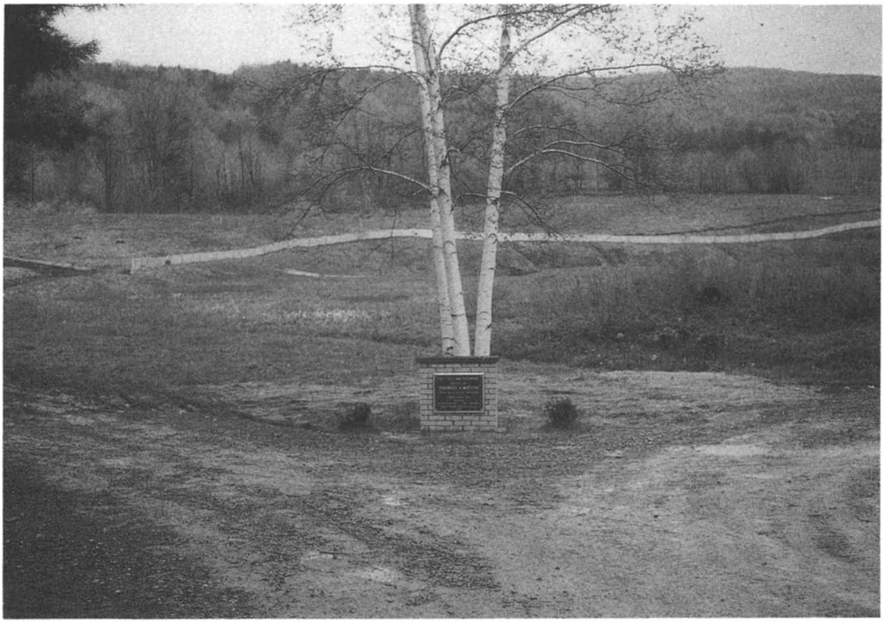

Figure 7. Silt fence application.

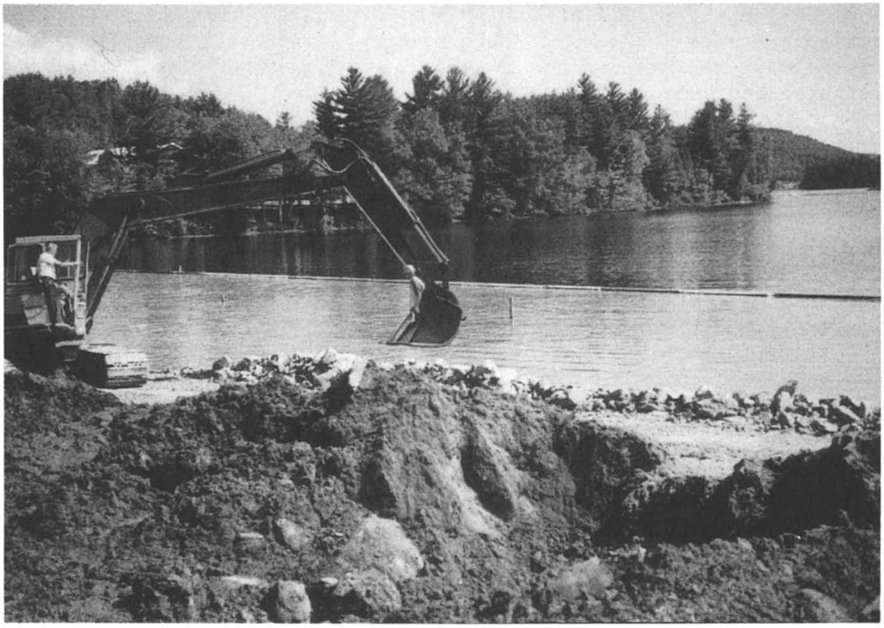

Figure 8. Turbidity curtain.

In the approved list approach, categories of usage such as described in Applications are established, with a set of property values established for each category. The geotextiles are then submitted for approval not related to use on any specific project, but related to the property requirements for the categories of use, and if approved by the specifying agency, placed on an approved materials list for use on any project incorporating geotextiles in one or more of the categories of use.

The combination approach uses the approved list for routine non-critical, non-severe applications, and uses the project specific approach when there is a critical and/or severe installation required. In this instance the required property values are more stringent than in a non-critical, non-severe application. The approved list in this instance is a starting point to locate the proper geotextile for this application.

No matter what approach is taken in regards to the type of specification used, the geotextile must exhibit minimum, or for properties like apparent opening size, maximum property values for the specific application.

These property values are determined by a series of laboratory tests which may or may not simulate the conditions under which the geotextile is going to be used. In the cases where the test does not simulate the field conditions intentionally, the test is referred to as an index property test. Such tests as thickness, mass per unit area, grab tensile, permittivity, and apparent opening size among others are considered as index property tests. In the cases where an attempt is made to simulate the field conditions, the tests are thought of as performance tests.

The properties most generally required in specifications include: grab tensile strength, trapezoid tear strength, wide width strength, seam strength, permittivity, apparent opening size, ultraviolet resistance, and in the case of pavement rehabilitation, asphalt absorption.

Grab Tensile. The grab tensile test is considered to be one of the index property tests. It should be performed according to ASTM Method D4632.

The test is performed using 101.6 by 203.2 mm (4 by 8 in) specimens, with the long direction parallel to the direction of load application. The specimens are clamped into the tensile testing machine with clamps measuring 25.4 by 50.8 mm (1 by 2 in). The longer direction is parallel to the direction of load application. The machine operates at a rate of extension of 300 mm (12 in)/ min. The specimens are loaded until rupture occurs. See Figure 9.

The test is considered an index test because the size of the specimen and rate of straining are not representative of what takes place in a field installation in respect to the area loaded and the rate at which a load is applied. In the field a much larger area is loaded at a much slower rate of strain. However, the test is a good method to compare relative performance of one geotextile to another.

Downloaded by PENNSYLVANIA STATE UNIV on August 6, 2012 | http://pubs.acs.org
Publication Date: April 3, 1991 | doi: 10.1021/bk-1991-0457.ch024

Trapezoid Tear. The trapezoid tear test is another index property test. The purpose of the test is to indicate the tendency for tear propagation to occur should a geotextile become torn during installation.

The test should be performed according to ASTM Method D4533. The dimensions of the specimen are 76.2 mm by 203.2 mm (3 by 8 in). A trapezoid shape is then marked on the specimen with the parallel edges of the trapezoid being 25.4 mm (1 in) and 101.6 mm (4 in). A 15.9 mm long (0.625 in) slit is made in the short parallel edge of the specimen. The specimen is then gripped along the non-parallel edges of the trapezoid with clamps measuring 50.8 mm by 76.2 mm (2 by 3 in), again the longer dimension being in the direction of load application. The specimen is strained at the rate of 300 mm (12 in/min). The specimen is loaded until failure takes place.

Wide Width Strength. The wide width strength test is more of a performance test than the previous tests described, however it still does not represent completely the conditions under which the geotextile is asked to perform in the field. In most applications the geotextile will be confined by the soil in which it is placed. This test is performed in the unconfined state. However, because a larger area is loaded at a much slower strain rate than the grab tensile test the method is considered more of a performance test than an index test.

The test should be performed according to ASTM Method D4595. Specimens 200 mm by 200 mm (8 in by 8 in) are secured in clamps such that the gauge length between the clamps is 100 mm (4 in). The load is applied using a strain rate of 10%/min, much slower than in the grab tensile. The specimen is loaded until failure takes place. See Figure 10.

Seam Strength. In many installations more than a single roll width or length of a geotextile will be required to be placed on the site. In many of these installations adjoining rolls will be required to be joined by sewn seams. This is necessary to insure both strength and coverage continuity.

Where seam strength is of concern, specifications vary in the requirements. There are those specifications which require a certain percentage of the specified wide width strength of the geotextile, or those that require that the seam strength equal the required wide width strength. The argument against the later approach is that while the specification value for geotextile strength does not change, the actual geotextile used will have a higher than required strength in order to meet the equal seam strength specification. This translates into higher costs related to the higher strength geotextile.

Whichever specification approach is taken, there is an ASTM standard method D4884 for evaluating the seam strength of sewn geotextiles. The method is very close to the wide width strength method for geotextiles, except for the fact that two samples of a geotextile joined by the proposed seam configuration are placed in the grips and tested in the same manner as the wide width.

Downloaded by PENNSYLVANIA STATE UNIV on August 6, 2012 | http://pubs.acs.org
Publication Date: April 3, 1991 | doi: 10.1021/bk-1991-0457.ch024

Downloaded by PENNSYLVANIA STATE UNIV on August 6, 2012 | http://pubs.acs.org
Publication Date: April 3, 1991 | doi: 10.1021/bk-1991-0457.ch024

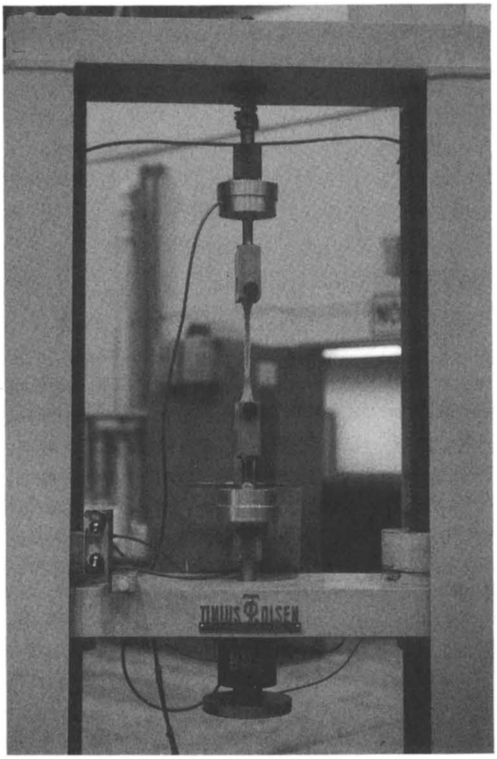

Figure 9. Grab tensile test in progress.

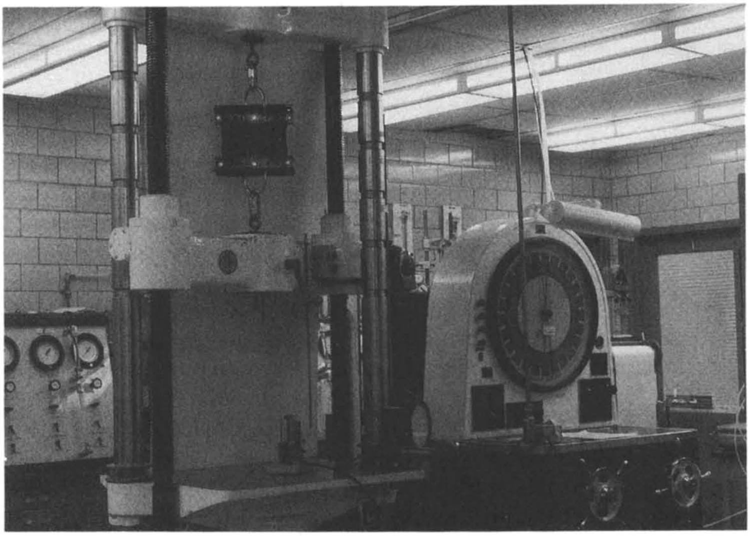

Figure 10. Wide width strength test.

Downloaded by PENNSYLVANIA STATE UNIV on August 6, 2012 | http://pubs.acs.org
Publication Date: April 3, 1991 | doi: 10.1021/bk-1991-0457.ch024

Ultraviolet Degradation. Most of the geotextiles manufactured today have ultraviolet stabilizers incorporated into them to reduce the degradation effects of the sunlight. However, if used in an application where exposure to the sunlight for long periods of time (eg silt fence) is unavoidable, information concerning the tendency of the geotextile to degrade from exposure to ultraviolet rays is important.

The test should be performed according to ASTM Method D4355. The method calls for comparing the effects on strength by exposing test specimens for a total of 150, 300, and 500 hours of alternating ultraviolet light alone and ultraviolet light and water spray to the strength of specimens not exposed. The source of the ultraviolet light is a xenon arc weatherometer. The evaluation of the strength retained or lost is performed using the index grab tensile test.

Specifications regarding this property require that a certain percent of the unexposed strength be retained following the specified length of exposure. To date, no real correlation between the results of this test and actual exposure to sunlight have been made. There are studies in progress attempting to determine if such a correlation exists. That is, it is difficult to say that 300 hours of exposure in the weatherometer is equivalent to a certain length of exposure to actual sunlight. However, a plot of strength for different lengths of exposure in the weatherometer, and a like plot for exposure to sunlight show the same tendencies for degradation. That is the plots take the same form.

Permittivity. ASTM defines permittivity as the volumetric flow rate of water per unit cross sectional area per unit head under laminar flow conditions, in the normal direction through a geotextile.

Permittivity is an expression of the permeability of the geotextile. If a coefficient of permeability is desired, permittivity times the nominal thickness of the geotextile will yield a nominal value for the coefficient of permeability.

Permittivity is used when comparing one geotextile to another. Coefficient of permeability is used when comparing the geotextile to the soil that it will be used with. Because there are varying thicknesses of geotextiles, one geotextile may have the same coefficient of permeability as another, but its volumetric flow rate capacity be entirely different because of having a different thickness.

The test should be performed according to ASTM Method D4491. The method describes procedures for running both a constant head and a falling head test.

The constant head test is performed using a 50 mm (2 in) head of deaired water on the specimen being tested. Quantities of water are collected for five equal time intervals and the permittivity calculated from the results.

The falling head test is performed using an hydraulic gradient loss comparable to the gradient in the constant head test. In this test the time it takes for the head loss to occur is measured. The permittivity is calculated knowing the area of the specimen, the area of the standpipe the head loss occurs in, and the time.

Downloaded by PENNSYLVANIA STATE UNIV on August 6, 2012 | http://pubs.acs.org
Publication Date: April 3, 1991 | doi: 10.1021/bk-1991-0457.ch024

Figure 11 shows a test apparatus which may be used for either test. Round robin test programs have determined that the values of permittivity obtained from either method are in close agreement with one another. Round robin testing has also determined the importance of using deaired water for the test. Water having a dissolved oxygen content above 6 ppm has been shown to produce very erratic and unreproducible results within and between laboratories.

Apparent Opening Size. ASTM defines apparent opening size as a property which indicates the approximate largest particle that would effectively pass through a geotextile. For a woven geotextile, the test provides a reasonable indication of the actual largest opening that occurs in the material. However, for a nonwoven product, the path that the particle has to follow to get through the material may not be a straight line, but a tortuous, winding one. Thus it is possible for a smaller particle to become trapped within the geotextile and indicate a smaller pore size than actually occurs. Thus the name "apparent opening size".

The test should be performed according to ASTM Method D4751. The method calls for shaking various size glass beads on specimens of material and weighing the beads that pass through. A minimum of three different size beads should be used, with at least one size being large enough so that less than five percent by weight passes through the geotextile. The apparent opening size can then be determined by plotting percent by weight passing versus size of glass bead, and determining the size at which five percent would pass. The value is expressed in millimeters, or the nearest Standard US Sieve Size Number. Figure 12 shows the sieve frames and beads used in this test.

When performing the test, care must be taken to not allow buildup of static electricity on the surface of the geotextile. This will cause the glass beads to adhere to the surface of the fabric rather than pass through. There are several methods to prevent this from happening. They range from the simple solution of spraying the surface of the fabric with anti-static laundry spray, to the use of low level radiation staticmasters. The level of radiation is so low that they may be sent through the mail with no restrictions or problems. The laundry spray has not been successful in all climates of the country.

Asphalt Retention. At the present time there is no ASTM Standard for measuring the asphalt retention ability of a geotextile. However, there are tests being performed by laboratories to determine this property. The tests call for submerging a known area of geotextile in an asphalt emulsion for a period of time, allowing the excess asphalt to drain off, weighing the soaked material, and based on the before and after weight of the geotextile, computing the volume of asphalt retained per unit area of geotextile. As previously indicated this information is for the pavement rehabilitation application.

Downloaded by PENNSYLVANIA STATE UNIV on August 6, 2012 | http://pubs.acs.org
Publication Date: April 3, 1991 | doi: 10.1021/bk-1991-0457.ch024

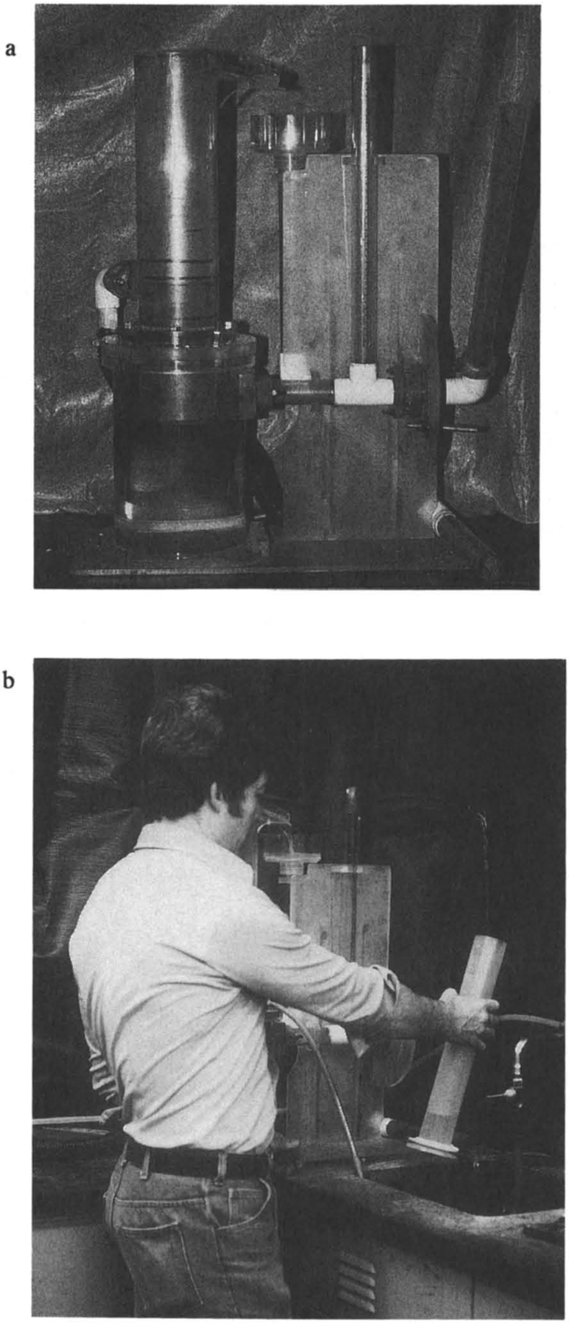

Figure 11. (a) Permittivity test apparatus. (b) Permittivity test in progress.

Downloaded by PENNSYLVANIA STATE UNIV on August 6, 2012 | http://pubs.acs.org
Publication Date: April 3, 1991 | doi: 10.1021/bk-1991-0457.ch024

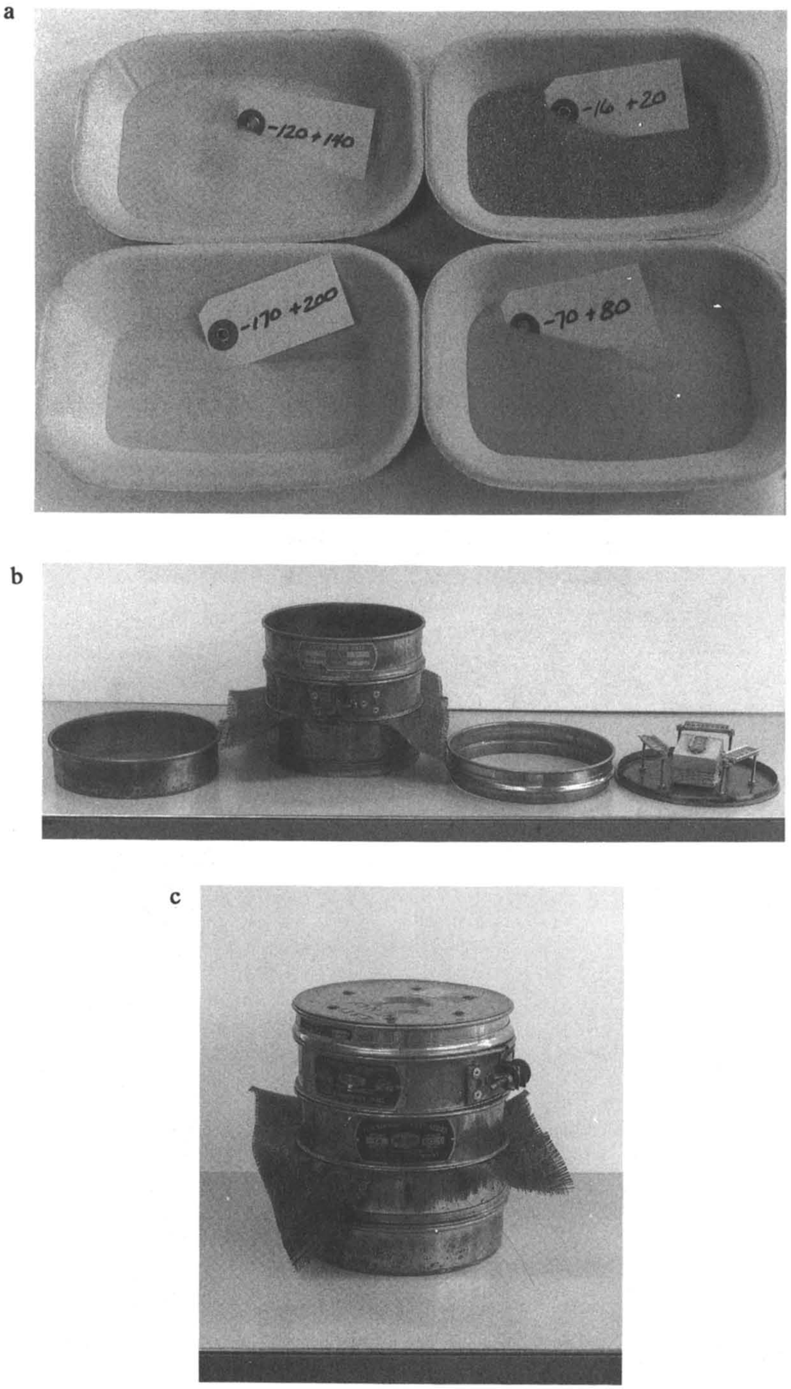

Figure 12. (a) Glass beads for apparent opening size. (b) Unassembled sieve frames and geotextile for apparent opening size. (c) Assembled sieve frame and geotextile for apparent opening size.

Summary

A number of the more routine applications of geotextiles in transportation facilities have been described. There are many other types of applications which incorporate geotextiles as part of the installations. The applications described are the basic ones where geotextiles are used by themselves, and not associated with other synthetic materials. These other applications include prefabricated vertical drains, prefabricated structural drains, and prefabricated edge drains (briefly discussed).

The descriptions of applications were also pretty much limited to highway installations. Other transportation facilities that use geotextiles in similar fashions include airports, waterways, and railroads.

In New York State the estimate of annual savings with the use of geotextile products over previous conventional methods reaches $4 million.

The tests described are the basic tests most often found in geotextile specifications. Other standardized tests include: temperature stability, and puncture resistance. Standardized tests for other materials that are being applied to geotextiles include: burst strength, mass per unit area, stiffness, and thickness.

There are a number of new tests being developed in the standardization process. These include: clogging potential, filtration efficiency, pore size distribution, stiffness, and frictional resistance.

As seen, geotextiles have reached the point where they are considered to be conventional solutions to problems previously solved by more expensive means. As new applications are developed the dollar savings, and the engineering benefits will continue to grow.

Literature Cited

1. Koerner, R. M. Designing with Geosynthetics; Prentice-Hall; Englewood Cliffs, N.J., 1986.
2. Suits, L. D., Minnitti, A., Prototype Turbidity Curtain for the Westway Highway, Transportation Research Board, Washington, D.C., 1989.
3. Minnitti, A.; Suits, L. D.; Dickson, T. H.; New York State Department of Transportation's Experience and Guidelines for the Use of Geotextiles, Transportation Research Board 916, Transportation Board, Washington, D.C., 1983.
4. Suits, L. D.; Guide to New York State Department of Transportation Usage of Geotextiles, New York State Department of Transportation, Albany, N.Y. 1988.

RECEIVED July 13, 1990

Downloaded by PENNSYLVANIA STATE UNIV on August 6, 2012 | http://pubs.acs.org
Publication Date: April 3, 1991 | doi: 10.1021/bk-1991-0457.ch024

Downloaded by UNIV MASSACHUSETTS AMHERST on August 6, 2012 | http://pubs.acs.org
Publication Date: April 3, 1991 | doi: 10.1021/bk-1991-0457.ch025

Chapter 25

Chemical Compatibility Testing of Geotextiles

L. G. Tisinger

**GeoSyntec, Inc., 3050 Southwest Fourteenth Place, Suite 18,
Boynton Beach, FL 33426**

Geotextiles for landfill applications are generally used as an integral part of the leachate collection system. Compatibility with the chemical environment to which the geotextile will be exposed must be demonstrated for long-term exposure to the chemical environment. The geotextile must be capable of retaining its design function throughout the lifetime of the landfill. In order to meet the need of having information regarding the chemical compatibility of a geotextile, test programs are being conducted in which the geotextile is exposed to a chemical environment. During exposure, various properties of the geotextile are monitored. These tests are typically performed over a period of 120 days at temperatures of 23 and 50°C.

Geotextiles are synthetic textile products that are used for civil engineering applications that may include soil reinforcement, soil separation and filtration, and protective cushioning for geomembranes in landfills (1). Geotextiles are clearly important members of the cadre of synthetic materials that are now used for civil engineering.

Since geotextiles are typically permanent components of a reinforcement or drainage system, they must be resistant to the environment in which they will ultimately be exposed. The environments may be highly alkaline soils; contaminated water; or climatological elements such as extreme fluctuations in temperature, rain, and sunlight.

Geotextiles are fabricated in several different configurations such as high-tenacity woven, woven, and nonwoven variations and are typically based on either polypropylene or polyethylene terephthalate (polyester). These polymers have proven to be highly durable through exceptional long-term performance. For instance, in

0097–6156/91/0457–0376$06.00/0

Downloaded by UNIV MASSACHUSETTS AMHERST on August 6, 2012 | http://pubs.acs.org
Publication Date: April 3, 1991 | doi: 10.1021/bk-1991-0457.ch025

Europe, both polypropylene and polyester geotextiles have been used for many years for reinforcement in steep embankments for roads where space was limited. When buried, these materials function for extended periods of time without detectable reduction in strength.

Aggressive environments, such as those observed in landfills or contaminated soils, can be fairly noxious because of their high or low, but not neutral, pH. In landfills, geotextiles must be able to perform as intended for the entire design life of the landfill, which is typically about 30 years. Since a landfill lining system is only as good as its weakest component, failure of any part of the lining system can produce catastrophic consequences. Aggressive environments may include both elevated temperatures and pressures, extreme pH levels, and significant concentrations of organic chemical waste. It is impossible to predict the synergistic effect of all environmental elements; however, the single most deteriorating element by far is the chemical environment. Fortunately, it is possible through laboratory experimentation to observe the effect of the chemical environment through chemical compatibility tests. Physical, mechanical, hydraulic, and microstructural tests are used to monitor the chemical compatibility of geotextiles exposed to leachate (waste liquid produced from rain percolating through waste in landfills).

Leachates for chemical compatibility tests are taken from landfills either close in geographical location or similar in projected waste streams. Leachates are typically very complex matrices containing many organic and inorganic components. Thus, there is great difficulty in preparing a "synthetic" waste solution if such were proposed _in lieu_ of the local or similar leachates. The U.S. Environmental Protection Agency (EPA) has attempted to develop a typical leachate but has not yet been successful.

Chemical compatibility testing for geotextiles was initiated by the EPA and is a requirement for all new hazardous waste and some municipal waste installations. These tests are usually performed for 120 days at 23 and 50°C. Various geotextile properties are monitored after 30, 60, 90, and 120 days. The information obtained from such test programs is valuable; however, caution must be exercised when interpreting test data.

EPA Method 9090, "Compatibility Test for Wastes and Membrane Liners"

EPA Method 9090 is the test method used for the assessment of chemical compatibility of geomembranes (geomembranes are essentially impermeable synthetic barriers used for leachate or waste containment) with landfill leachates (2). In EPA Method 9090, mechanical properties such as yield stress, yield elongation, break stress, break elongation, initial tear resistance, puncture strength, Mullen burst strength, and modulus of elasticity are measured. Physical properties that are measured include dimensions, thickness, mass, specific gravity, volatiles, extractables, and hardness. Every property is monitored after exposure to leachate for 30, 60, 90, and 120 days at temperatures of 23 and 50°C.

Although the majority of the property monitoring tests used in EPA Method 9090 are inappropriate for geotextiles, the fundamental methodology is still applicable. There is currently no standard test method for the assessment of chemical compatibility of geotextiles; however, a standard is currently being drafted by the American Society for Testing and Materials (ASTM). Laboratories, consulting firms, and regulatory agencies are responsible for the development of test protocols for specific landfill projects. After these groups have developed test protocols, the EPA is consulted for final approval of the test program, since the data generated will ultimately be evaluated by the EPA and will be the critical factor for issuance of the landfill permit. Unfortunately, acceptance criteria for geotextile chemical compatibility test results have yet to be developed. Therefore, realistically, approval of test results depends on the ability of the laboratory to provide an accurate interpretation.

Downloaded by UNIV MASSACHUSETTS AMHERST on August 6, 2012 | http://pubs.acs.org
Publication Date: April 3, 1991 | doi: 10.1021/bk-1991-0457.ch025

Experimental Procedures

The geotextiles are carefully inspected upon receipt at the laboratory. Samples are selected from areas free of defects and other obvious anomalies. Mass per unit area is determined for the entire sample. Only specimens with mass per unit area values within one standard deviation of the average mass per unit area of the roll are selected for testing. The individual specimens are then exposed to leachate in order to minimize the quantity of leachate required for the test.

Stainless steel exposure cells are used for leachates containing appreciable concentrations of organic components. Since the interactions are likely to be physical in nature (absorption of the leachate components into the fibers), stainless steel is used in order to preclude absorption of the organic components by the tank, as would occur if a synthetic tank were used. This type of interaction would effectively reduce the leachate components available for testing with the geotextile.

Polyethylene or glass exposure cells are used instead of stainless steel cells for leachates containing largely salts; polyethylene material precludes possible corrosion, which could occur in metallic tanks. The exposure cells are kept airtight for the duration of the test. For leachate containing a high concentration of volatile organic components, the cells are equipped with a reflux condenser to minimize both pressure buildup and possible escape of volatile components. The leachate is continuously agitated to preclude stagnation or stratification of the leachate around the geotextiles.

After each 30-day exposure period, the leachate is pumped from the exposure cell through a vent to a waste drain for proper disposal. The cell is opened and the appropriate number of geotextile specimens is removed. The exposure cell is then closed and fresh leachate is pumped into the cell. After exposure to the leachate, the geotextile specimens are drained and then dipped in deionized water to remove excess leachate. The specimens are kept moist in sealed polyethylene bags prior to testing.

Oxidative induction temperature was measured using a Perkin-Elmer DSC IV equipped with a system IV microprocessor controller and model 3700 data acquisition facility. The tests were conducted in 50 psi air at a scan rate of 20°C/minute. Bulk geotextile samples (about 2 mg) were tested in aluminum pans. The temperature range scanned was 50 to 350°C. The samples were allowed to dry in standard laboratory atmosphere (23°C ± 2°C, 50-65% relative humidity) for 40 hours prior to analysis.

Monitoring Tests. Monitoring tests are performed after each 30-day exposure period. Tests typically include grab tensile strength, grab elongation, puncture strength, Mullen burst strength, dimensions, mass per unit area, and thickness. Other parameters that are measured include hydraulic properties, such as permittivity (flow of water normal to the plane of the geotextile) and transmissivity (flow of water in the plane of the geotextile).

Test Results

Nonwoven geotextiles, which are typically used in landfills, display much inherent variability due to their method of fabrication. Mass per unit area may vary as much as 40 percent across the roll (according to unpublished test results). Many of the properties measured for chemical compatibility are a function of mass per unit area. One such property is grab tensile strength. Percentage changes in grab tensile strength and elongation for a polyester geotextile exposed to leachate are presented in Table I.

TABLE I. Percentage Changes in Mechanical Properties of Nonwoven Polyester Geotextiles

		Exposure Period (days)			
Property	Unit	30	60	90	120
Grab Tensile Strength	%				
23°C		-2.6	1.8	2.0	-8.1
50°C		-5.5	9.0	-9.5	-20.8
Grab Elongation	%				
23°C		7.9	8.4	5.7	13.4
50°C		7.2	10.3	-20.2	3.1

Table I shows percentage changes that may be considered erratic and likely due to material variability, since no discernible trend is observed. All of the leachate for this test was sampled at the same time, thus its character should not have appreciably changed.

The dimensional test results are shown in Table II.

Downloaded by UNIV MASSACHUSETTS AMHERST on August 6, 2012 | http://pubs.acs.org
Publication Date: April 3, 1991 | doi: 10.1021/bk-1991-0457.ch025

TABLE II. Percentage Changes in Dimensions
of Nonwoven Polyester Geotextiles

Property	Unit	Exposure Period (days)			
		30	60	90	120
Dimensions	%				
23°C		0.4	1.4	-0.8	-0.8
50°C		-0.9	-0.8	-0.2	0.2

The dimensional properties are measured nondestructively. Measurements are taken before leachate exposure and measured again on the same specimen at the conclusion of the exposure period. Therefore, material variability is not a significant factor in these measurements.

As shown in Table II, much stability is observed. Such stability indicates that swelling of the fibers did not occur such as that which might be observed with appreciable absorption of volatile organic solvents.

The mechanical property changes are not consistent with those observed in the physical properties. Since mechanical properties are measured destructively, the reference specimens are different than those measured after each exposure period. If localized variances are a material characteristic, their effect may be very influential on the results of destructive, mechanical tests. As presented in Table I, fundamental material relationships may not always apply. For instance, increases in strength should be accompanied by reductions in flexibility. Such a relationship is not always observed for these results. The anomalous behavior of the grab strength and elongation measurements is likely due to material variability.

Hydraulic property values indicate the ability of the geotextile to filter or drain water. In chemical compatibility tests, permittivity and transmissivity are typically measured. Table III presents the results of hydraulic property monitoring testing for a nonwoven polypropylene geotextile.

As shown in Table III, reduction is observed in both transmissivity and permittivity. Both transmissivity and permittivity were measured with water. Transmissivity displays reduction throughout the entire test. Thus, reduction is likely due to either the surface tension of the leachate acting on the fibers, pulling them closer together, or the presence of insoluble leachate components among the fibers. For permittivity, the 23°C specimens show greater reduction than the 50°C specimens. This initially appears anomalous since an elevated temperature accelerates many degradative processes. However, the leachate used in this study contained appreciable quantities of inorganic salts. At higher temperatures, the salts would more likely remain in solution. Conversely, visual examination revealed salt deposits on the 23°C samples. The salt deposits were not observed on the 50°C specimens.

Downloaded by UNIV MASSACHUSETTS AMHERST on August 6, 2012 | http://pubs.acs.org
Publication Date: April 3, 1991 | doi: 10.1021/bk-1991-0457.ch025

TABLE III. Percentage Changes in Hydraulic Properties of Nonwoven Polypropylene Geotextiles

		Exposure Period (days)			
Property	Unit	30	60	90	120
Transmissivity	%				
23°C		-31.0	-50.1	-44.0	-42.0
50°C		-37.5	-48.5	-47.8	-33.5
Permittivity	%				
23°C		2.3	0.2	-23.8	-3.7
50°C		1.0	3.1	-4.6	5.6

Therefore, these results are consistent with the expected behavior under the conditions in which the geotextiles were exposed.

It is clear that an understanding of the microstructural interactions of the geotextile with the leachate is needed, since small changes may not be observed in the short time period (typically 120 days) of chemical compatibility tests. Bulk property measurements are not sensitive enough to detect the onset of degradation of the fibers. Table IV shows the values for oxidative induction temperature as measured using differential scanning calorimetry (DSC) on the polypropylene geotextiles exposed to leachate. Oxidative induction temperature is the temperature at which a material starts to oxidize.

TABLE IV. Percentage Change in Oxidative Induction Temperature of Nonwoven Polypropylene Geotextiles

		Exposure Period (days)			
Property	Unit	30	60	90	120
Oxidative Induction Temperature	%				
23°C		0.5	-2.8	-4.2	-2.4
50°C		-3.2	-4.2	-1.9	-1.9

These results show that the leachate did not appreciably affect the oxidative stability of the polypropylene geotextile under the test conditions. These results were uniform with less variability than that which is typically observed in the bulk properties.

Downloaded by UNIV MASSACHUSETTS AMHERST on August 6, 2012 | http://pubs.acs.org
Publication Date: April 3, 1991 | doi: 10.1021/bk-1991-0457.ch025

Discussion

The geotextiles used for landfill applications are typically nonwoven polyester or polypropylene materials. Nonwoven geotextiles show greater material variability than that of their woven counterparts due to the method of fabrication.

Not surprisingly, results of chemical compatibility test programs show variability, often "hiding" what may be the true behavior of the material to leachate (3). For instance, as shown in Table I, grab tensile strength and elongation displayed variability with no observable trends as a function of duration of exposure to leachate. Conversely, the dimensions showed stability with little indication of swelling of the fibers due to absorption of organic leachate constituents into the fibers.

The hydraulic properties appear less affected by material variability than the mechanical properties. However, the volume flow of water is reduced by retention of insoluble leachate components among the fibers. This reduction, however, is a bulk change and is not due to leachate-induced chemical deterioration of the geotextile.

The leachate for the polypropylene geotextile study contained low levels of organic and inorganic components. Although the concentration of organic components was low, the level of potentially oxidizing species such as nitrates or sulfates was appreciably higher than the level detected in the polyester geotextile test leachate. DSC was used to measure oxidative induction temperature to observe changes in oxidative stability due either to migration of additives out of the fibers or the onset of oxidation. As shown in Table IV, the oxidative induction temperature remained stable throughout the entire 120-day test period, indicating that the deterioration of the geotextile due to leachate exposure was minimal.

The microstructural testing, such as that using DSC, thermal gravimetric analysis, and infrared spectrophotometry provides insight regarding microstructural degradation (4,5). The bulk mechanical tests provide data that are scattered due to material variability. However, the dimensions did not indicate that significant interaction was occurring with the leachate. Furthermore, the fundamental inverse behavior of strength and elongation was not constant in these test results.

The hydraulic properties showed more stability than the mechanical properties and were more greatly affected by bulk interaction with the leachate.

Conclusions

Chemical compatibility testing has typically involved testing of only the bulk mechanical and physical properties. The mechanical properties typically show much variability, precluding accurate assessment of trends in properties as a result of leachate exposure. Conversely, microstructural properties give a clearer indication of the mechanism of degradation. The bulk properties are important parameters because they provide data that can be used by designers. However, for accurate assessment of the chemical resistance of geotextiles to leachate, microstructural properties should also be

Downloaded by UNIV MASSACHUSETTS AMHERST on August 6, 2012 | http://pubs.acs.org
Publication Date: April 3, 1991 | doi: 10.1021/bk-1991-0457.ch025

measured. The onset of degradation, which occurs on the microstructural level, may not be readily detectable in the bulk mechanical properties in the short duration of the immersion tests.

Inclusion of microstructural tests as part of chemical compatibility test programs provides an indication of potential deterioration in the properties of the geotextile after longer term exposure to leachate.

Literature Cited

1. Koerner, R. M. Designing with Geosynthetics; Prentice-Hall, Inc.: Englewood Cliffs, 1988; pp 1-4.
2. EPA Method 9090: Compatibility Test for Waste and Membrane Liners, U.S. Environmental Protection Agency: Washington, DC, 1985.
3. Tisinger, L. G. Geotechnical Fabrics Report May/June 1989, 22-24.
4. Tisinger, L. G. Proc. Geosynthetics '89, 1989, pp 513-524.
5. Tisinger, L. G.; Kimmet, J.; Peggs, I. D. Proc. 10th Annual Madison Waste Conference, 1987, pp 127-145.

RECEIVED July 2, 1990

Downloaded by UNIV MASSACHUSETTS AMHERST on August 6, 2012 | http://pubs.acs.org
Publication Date: April 3, 1991 | doi: 10.1021/bk-1991-0457.ch025

Author Index

Alexander, Harold, 132
Bajpai, P. K., 132
Barker, R. L., 277
Behnke, W. P., 277
Bristow, Daniel, 90
Byun, Joon-Hyung, 22
Casale, Nicholas, 90
Chou, Tsu-Wei, 22
Chu, C. C., 167
Davis, G. W., 304
Dodgson, E. Anne, 270
Du, Guang-Wu, 22
El-Shiekh, Aly, 34
Evrensel, C. A., 149
Fahl, Nona, 238
Faile, Marian, 238
Geshury, A. J., 277
Girgis, Mikhail M., 337
Gray, Robert L., 320
Hall, Robert W., 293
Hammad, Mohamed, 34
Harlan, Steven L., 248
Hodge, James D., 270
Jayaraman, Sundaresan, 53
Kaufmann, James R., 81
Kirkland, K. M., 214
Kokta, B. V., 102
Li, Wei, 34
Luo, S. Y., 149
Lyman, D. J., 116
Marsden, William H., 260
Menoff, S. D., 351
Parsons, J. Russell, 132
Pastore, Christopher M., 90
Raj, R. G., 102
Rodgers, M. J., 351
Snyder, Roger W., 124
Sprague, C. J., 304
Stenborg, J. W., 351
Suits, L. D., 358
Tam, T. Y., 214
Tisinger, L. G., 376
Tung, Peter S., 53
Turbak, Albin F., 1
Vigo, Tyrone L., 1
Weedon, G. C., 214
Zhou, L., 149
Zimmerman, Mark C., 132

Affiliation Index

Allied Fibers Technical Center, 214
CIBA-GEIGY Corporation, 320
Chambers Development Company, Inc., 351
Cornell University, 167
Drexel University, 90
E. I. du Pont de Nemours and Company, 270
GeoSyntec, Inc., 376
Georgia Institute of Technology, 53
Harbour Biomedical Consultants, Inc., 124
Hoechst Celanese Corporation, 81,238,304
Hospital for Joint Diseases Orthopaedic Institute, 132
Navy Clothing and Textile Research Facility, 293
NeutraTherm, Inc., 248
New York State Department of Transportation, 358
Nicolon Corporation, 304
North Carolina State University, 34,90,277
Pittsburgh Plate Glass Industries, Inc., 337
Southern College of Technology, 1
The Wool Bureau, Inc., 260
U.S. Department of Agriculture, 1
Universite du Quebec, Canada, 102
University of Dayton, 132
University of Delaware, 22
University of Medicine and Dentistry of New Jersey, 132
University of Nevada, 149
University of Utah, 116

Downloaded by 89.163.34.136 on August 6, 2012 | http://pubs.acs.org
Publication Date: April 3, 1991 | doi: 10.1021/bk-1991-0457.ix001

In High-Tech Fibrous Materials; Vigo, T., et al.;
ACS Symposium Series; American Chemical Society: Washington, DC, 1991.

Subject Index

A

Absorbable sutures
  advantages, 168
  chemical repeating units, trade names, and manufacturers, 168t
Absorption, suture characteristic, 117
Absorption delay
  definition, 206
  values for commercial synthetic absorbable sutures, 206t,207
Acid dyes, 273
Acid resistance, polyethylene terephthalate fibers, 311,312t
Active cooling, definition, 255
Active warming, definition, 255
Advanced composites
  applications, 53
  description, 82
  fiber reinforcement for property enhancement, 53
  market, 53
  properties, factors affecting, 34
  three-dimensional braiding, use in formation, 34–51
Aerospace industry, use of multiaxial warp knit composites, 85t,86,87
Aggressive environments, effect on waste containment systems, 377
Aging, definition, 305
Aging of polyethylene terephthalate
  atmospheric resistance, 317
  leachate resistance, 318–319
  soil resistance, 318
Aircraft
  high-tech fibers, use, 13
  high-tech textiles, use, 3,5f
Alkali resistance, polyethylene terephthalate fibers, 311,312t,313
Antimicrobial fibers for wound closure
  advantages, 171
  current developmental approaches for sutures, 171
  silver metal coated antimicrobial suture, 171,175–189
  wound infection, 169–174
Antimicrobial sutures, current developmental approaches, 171
Apparent opening size
  definition, 372
  test, 372,374f
Aramid armor systems, advantages, 225
Aramid fabric(s)
  carrier, use for dyeing, 270–271
  dyeing difficulties with conventional dyeing processes, 270
Aramid fabric(s)—*Continued*
  printing technology, 273–276
Aramid fiber(s)
  affinity of cationic dyes, 271
  imbibition of surfactants, 275
  IR reflectance of military camouflage, 273,274f
  structure, 271
m-Aramid structure, affinity of cationic dyes, 271
Architecture, use of high-tech fibers, 4,6–7f
Armor systems, use of high-performance polyethylene fibers, 224–235
Aromatic polyamides, applications, 8
Artificial arteries, use of high-tech textiles, 2,3f
Artificial hearts, use of high-tech textiles, 2,3f
Artificial kidney
  development, 120–121
  high-tech fibers, use, 11
Artificial lung, use of hollow fibers, 122
Artificial pancreas, use of hollow fibers, 121
Asphalt retention test, description, 372
Atmospheric resistance, PET fibers and fabrics, 317
Automobiles, weight savings with carbon fiber composites, 13t
Average extension ratio of wavelength, definition, 158

B

Bacterial adherence, suture materials, 170–171,172–174f
Benzotriazoles, energy dissipation, 321,323,324f
Beta tec abrasion and cut tester, cut resistance evaluation, 218
Bicycle frame, *See* Braided composite monocoque bicycle frame
Biocompatibility, effect on polymer degradation, 128
Biocompatibility of textile implants, 128
Bioimplants, use of textiles, 125–130
Biological composites, 129–130
Biological implants, description, 129
Biomedical uses, high-tech textiles, 2,3f
Blood dialyzer
  development, 120–121
  See also Artificial kidney
Body protection, use of high-tech textiles, 4,5f
Bone plate, requirements, 133

Downloaded by 89.163.34.136 on August 6, 2012 | http://pubs.acs.org
Publication Date: April 3, 1991 | doi: 10.1021/bk-1991-0457.ix002

Braid(s), 125–126
Braided composite monocoque bicycle frame
  braiding over mandrel, 97,99f
  completed bicycle frame, 100f
  curing agent epoxies, properties, 95t
  density of candidate hybrid systems, 92,93t
  fiber selection, 92,93t,94f,95
  frame geometry for finite elemental analysis, 96,98f
  geometry and moments of frame tubes, 97t
  hybrid composites
    tensile moduli, predicted, 93,94f
    tensile strength, predicted, 93,94f
  material selection and verification, 92–96
  matrix system, 95t,96
  prototype fabrication, 97,98–99f
  shaped foam mandrels for preform processing, 97,98f
  Spectra fiber, advantages and disadvantages, 93,95
  structural analysis, 96,97t,98f
Braided sutures, advantages, 168
Breathable woolen fabrics for protective clothing, 263
Burn injury, relationship of risk to polyester content of fabric, 294

C

Canine trachea, pressure vs. specific volume, 150,151f
Carbon black filled systems, thermal stability, 333,334f,335
Carbon fiber(s)
  development, 9,10t,11,12f
  heat shield for NASA space shuttle, use, 10,12f
  precursors, 9,10t,11
  properties, 10t
  prosthetics, use, 122
Carbon fiber reinforced polylactic acid composite
  analysis, 136,140
  analytical procedure, 133–134
  bone plate design, 136,137f
  composite specimen of large-diameter fiber implanted for 6 weeks, 140,143f
  fabrication procedure, 134
  fatigue results, 136,137f
  fiber implanted for 12 weeks, 140,141f
  fiber implanted for 24 weeks, 140,142f
  fiber implanted in medullary canal after 4 weeks, 138,139f,140
  in vitro bending modulus vs. soak time, 136,139f
  in vitro study
    results, 136–140,145
    testing procedure, 134–135
Carbon fiber reinforced polylactic acid composite—*Continued*
  in vivo study
    procedure, 135–136
    results, 138–146
  mechanical properties, 136,138t
  molded composite implanted for 6 weeks, 140,144f
  molded composite implanted for 12 weeks, 140,144f
  section of muscle after fiber removal, 140,142f
  transverse section of imbedded fiber after 4 weeks, 140,141f
  unmolded composite after 6 weeks of implantation, 140,143f
Cardiovascular patches, use of textiles, 124–125
Cationic dyes, affinity for aramid structure, 271
Cellulosic fillers, advantages, 102
Chain saw cut protective chaps, use of high-performance polyethylene fibers, 224
Chemical compatibility testing of geotextiles
  EPA Method 9090, 377–382
  leachate sampling, 377
  material variability, effect on properties, 382
  test conditions, 377
Chemical environment, effect on aging of impregnated fiber glass yarns, 343,344t
Chemical resistance, polyethylene terephthalate fibers, 310
Clothing comfort, definition, 261
Cold-weather activity clothing, use of NeutraTherm, 248–258
Collagen fibers
  extension during stretching, 150
  nylon stocking extensibility, 150
  relaxed conformation, 149–150
Combat helmets, use of high-performance polyethylene fibers, 232
Comfort of protective coveralls
  determinants, 246t
  polybenzimidazole blends, 246t,247
Commodity fibers, changes, 4,8
Compatibility test for wastes and membrane liners, *See* EPA Method 9090
Compliance matrix, calculation, 29
Compliance matrix of spatially oriented yarns, 28–29
Composite(s)
  applications, 22
  curing
    curing cycle, 67,70f
    schematic representation, 67,69f
  description, 82

Downloaded by 89.163.34.136 on August 6, 2012 | http://pubs.acs.org
Publication Date: April 3, 1991 | doi: 10.1021/bk-1991-0457.ix002

Downloaded by 89.163.34.136 on August 6, 2012 | http://pubs.acs.org
Publication Date: April 3, 1991 | doi: 10.1021/bk-1991-0457.ix002

Composite(s)—*Continued*
  testing
    flexure test, 73–74
    procedure, 71,73
    tensile test, 73,75*t*
Composite analysis, carbon fiber reinforced polylactic acid composite, 136,140
Composite characterization, three-dimensional multilayer woven preforms for composites, 71
Composite frame, design and fabrication, 90–100
Composite yarns, cut resistance, 220,222
Conex, description, 268
Construction, use of high-tech fibers, 4,6–7*f*
Construction considerations for waste containment facilities using geotextiles
  friction, 355
  installation of geotextile layer, 354–355
  quality control and quality assurance, 355–357
Convective hot air tests
  description, 296,299
  fabric melt/stick rankings, 300*t*,301
  heat gun, 296,297*f*
Cortex, definition, 261
Cotton, flame retardant, *See* Flame-retardant cotton
Creel, three-dimensional multilayer preforms for composites, 63,64*f*
Creep resistance, polyethylene terephthalate fabrics, 317,318*f*
Cross-linking polyethylene glycol process, *See* NeutraTherm
Curing of composites
  curing cycle, 67,70*f*
  schematic representation, 67,69*f*
Current fiber orientation, definition, 158
Cushion in waste containment facility, use of geotextiles, 352–353
Cut and slash protection, high-performance polyethylene fibers, 217–224
Cuticle, definition, 261
Cut resistance
  evaluation procedure, 218
  testing apparatus, 218,219*f*
Cut-resistant gloves
  advantages of high-performance polyethylene fibers, 218,220,221*t*,222
  work environments, 218
Cystoscope, use of optical fibers, 122

D

Dacron, uses in surgery, 120
Degradation, polymer, *See* Polymer degradation
Degradation mechanism, polyolefins, 320–321,322*f*
Delamination in composites
  importance, 55
  in-service damage, forms, 54
  shearing stresses, effects, 54
Design of textiles for implants
  factors influencing, 129,130*f*
  parameter choice, effect of purpose, 129
  research, future areas, 129–130
Dialysis, extracorporeal, use of high-tech fibers, 11
Dimensional properties, nonwoven polyester geotextiles, 379,380*t*,382
Doron, use in armor systems, 225
Drainage, use of geotextiles, 360–361,365*f*
Drainage in waste containment facility, use of geotextiles, 352,354
Durability, definition, 305
Dye classes, IR reflectance, 271,272*f*
Dye fixation, procedure, 273
Dye printing process, 271,273
Dynamic flame testing
  apparatus, 243,244*f*
  polybenzimidazole blends, 243*t*
Dynamic mechanical force effects on thermal protective fabrics
  dynamic thermal protective performance test, 279,280*f*
  experimental procedure, 281*t*
  instrumental effects, 282–289
  Kevlar 100, 284,285*f*,286,289*f*
  Nomex III, 283,284*f*,289*f*
  test conditions, 281*t*
  test fabrics, 278*t*
  test methods, 278–279,280*f*
  thermal protective performance
    conventional thermal protective performance method, 281,282*t*
    modified thermal protective performance method, 282*t*
    rating, 279
    tester, 278–279
Dynamic thermal protective performance
  rating, 279
  test
    schematic diagram of tester in flexing position, 279,280*f*
    schematic diagram of tester in horizontal position, 279,280*f*
    thermal protective performance, 282*t*

E

Economics, textile industry, 1–2
Elastic fibers
  extension during stretching, 150
  nylon stocking extensibility, 150

Elastic fibers—*Continued*
  relaxed conformation, 149–150
  sutures, 118
Elastic moduli, prediction for three-dimensional braided composites, 23
Elastomeric composites, *See* Flexible composites
Embankment support, use of Herculflex products, 346,348
Enkamat, applications, 14
Enthalpic clothing and materials, 249
Enzymes, role in hydrolytic degradation of synthetic absorbable sutures, 197
EPA Method 9090
  description, 377
  dimensional changes of nonwoven polyester geotextiles, 379,380*t*,382
  experimental materials, 378
  experimental procedure, 378–379
  hydraulic property changes of nonwoven polypropylene geotextiles, 380,381*t*,382
  mechanical property changes of nonwoven polyester geotextiles, 379*t*,382
  monitoring test procedure, 379
  oxidative induction temperature changes of nonwoven polypropylene geotextiles, 381*t*,382
Equipment, three-dimensional multilayer woven preforms for composite, 57,62*f*,63,64*f*,65
Erosion control, use of geotextiles, 362–363,366–367*f*
Evolution of high-tech fiber
  carbon fiber development, 9,10*t*,11,12*f*
  nylon development, 8
  polyethylene development, 9
Expanded polytetrafluoroethylene, use in small-diameter grafts, 119
Extracorporeal dialysis, use of high-tech fibers, 11
Extracorporeal fibers, applications, 117*t*,120–122

F

Fabric flexibility, Herculflex fabric, 345,347*t*
Failure mechanism, thermal protective performance tests, 286,290*t*
Fertilizer resistance, polyethylene terephthalate fibers, 313,315*t*
Fiber(s)
  advantages of high surface area/weight of material, 11
  composites, use, 122
  extracorporeal devices, use, 120–122
  implants, use, 116–122
  medicinal applications, 116–122
Fiber(s)—*Continued*
  three-dimensional multilayer woven preforms for composites, 57,62*f*
Fiber bulk, effect on polymer degradation, 128
Fiber carrier, design, 50,51*f*
Fiber(s) for suture purposes, forms, 168
Fiber glass yarn
  definition, 338
  forming process, 338,342*f*
  impregnated, *See* Impregnated fiber glass yarn
  melting process, 338,342*f*
Fiber-reinforced composites, woven fabric, 53
Fibrous materials, first uses, 116
Filament(s), effect on biocompatibility of textile implants, 128
Filament shapes, effect on polymer degradation, 128
Filtration in waste containment facility, use of geotextiles, 352–354
Filtration of gases and liquids, use of high-tech textiles, 4
Firefighters' protective clothing, use of wool, 263–267
Fire Flite
  composition, 264
  protective clothing fiber, use, 264
Fire victim, typical reaction, 277
Flak jackets, use of synthetic fibers, 225
Flame-retardant cotton
  breakthrough and thermal insulation performance, 286,290*t*
  failure mechanism of thermal protection, 286,290*t*
  thermal protective performance, 286,288*f*,289*f*
Flame-retardant polyester–cotton blend fabrics, melt/stick characteristics, 294–301
Flame-retardant wool
  breakthrough and thermal insulation performance, 286,290*t*
  failure mechanism of thermal protection, 286,290*t*
  thermal protective performance, 286,287*f*,289*f*
Flame-retardant wool blends
  Fire Flite, 264
  Tex-Tech, 264,265*t*,266,267*t*
Flexible composite(s)
  applications, 149
  natural composites, 149
Flexible composite(s) containing sinusoidally shaped fibers
  background, 155,156*f*,157
  longitudinal elastic behavior, 157–158
  numerical examples, 160,161*f*,162,163*f*

Downloaded by 89.163.34.136 on August 6, 2012 | http://pubs.acs.org
Publication Date: April 3, 1991 | doi: 10.1021/bk-1991-0457.ix002

Downloaded by 89.163.34.136 on August 6, 2012 | http://pubs.acs.org
Publication Date: April 3, 1991 | doi: 10.1021/bk-1991-0457.ix002

Flexible composite(s) containing sinusoidally shaped fibers—*Continued*
  schematic representation, 155,156*f*,157
  stress–strain relationship, 160,161*f*,162,163*f*
  transverse elastic behavior, 159–160,161*f*
Flexible composite laminate analysis
  constitutive relations, 162,163*f*
  schematic representation of composite laminate, 162,163*f*
  tensile stress–strain relationship, 162,164*f*,165*f*
  uniaxial load, 162,164*f*
Flexible plates, use as solution to stress protection atrophy, 133
Flexure test, composites, 73–74
Four-step process of three-dimensional braiding
  analytical model, 36
  braiding machine, 36,39*f*,40
  braiding pattern, 36,37*f*
  comparison with two-step process, 45,46*t*
  description, 35
  equipment, 35
  flow chart of control system for braiding machine, 36,39*f*,40
  ratio of machine bed to preform size, 45,47,48*f*,49
  repeat unit, 36,37*f*
  rewinding requirement, 49–50,51*f*
  yarn orientation angle, 36,38*f*
  yarn volume fraction, 36,38*f*
Fracture fixation, laminated degradable composite bone plates, 132–146

G

Gas pit testing
  polybenzimidazole blends, 245*t*
  procedure, 243,245
Gel spinning, description, 9
Geogrids, definition, 345
Geosynthetic(s), 320
Geosynthetic materials, comparison of tensile properties, 348,349*f*,*349t*,350
Geosynthetic reinforcement, performance requirements, 338
Geotextile(s)
  advantages, 338
  applications, 4,304
  chemical compatibility testing, 376–382
  classification, 352–353
  configurations, 376–377
  consumption, 337,339*f*
  definition, 304,337,376
  development, 358
  environmental exposure, 376
  examples, 337
  fiber types, 338
Geotextile(s)—*Continued*
  limitations, 304–305
  performance requirements in waste containment systems, 376
  testing, 368
  uses
    drainage, 360–361,365*f*
    erosion control, 362–363,366–367*f*
    Europe and United States, 337
    pavement rehabilitation, 359–360
    pollution control, 362–363,366–367*f*
    reinforcement, 361–362,365*f*
    separator, 360,364*f*
    stabilization, 362,366*f*
  See also Polyester geotextiles
Geotextile applications, specifications, 363,368
Geotextiles in waste disposal facilities
  applications, 351–352
  classification, 352–353
  construction considerations, 354–355
  design objectives, 351–352
  quality control and quality assurance, 355–357
  uses, 352
Gloves, cut resistance, 218,220,222
Gore-Tex
  applications, 17
  description, 268
Grab tensile test, description, 368,370*f*

H

Hand protection, use of high-performance polyethylene fibers, 217–218
Hard composite armor systems
  composition, 229
  high-performance polyethylene fibers, use, 229,231–235
Health and Safety at Work Act of 1974, description, 217
Herculflex
  products, uses, 346,348
  strands
    comparison of tensile properties with geosynthetic materials, 348,349*t*,350
    fabrics, 345
    geogrids, 345
    properties of woven fabrics, 345–346,347*t*
    See also Impregnated fiber glass
  yarns
    acidic and alkaline media, effect on strength, 344,344*t*
    aging properties, 343,344*t*
    humidity, effect on aging, 343,344*t*
    impregnation, effect on properties, 341
    properties, 338,341,343*t*
    secant modulus, 341

Hercuflex—*Continued*
  yarns—*Continued*
    water, effect on aging, 343,344*t*
    See also Impregnated fiber glass yarn
High-energy sources, modification of fiber and fabric surfaces, 18
High-performance composite materials, 81–88
High-performance polyethylene fibers
  advantages for use in cut-resistant gloves, 218,220,221*t*,222
  ballistic performance vs. that of Aramid composites, 229,231–234
  ballistic resistance at elevated temperatures, 234,235*t*,236*f*
  chemical properties, 220,221*t*
  composite armor, effect of temperature on ballistic performance, 226,229*t*,230*f*,232
  cut and slash protection, 217–224
  fiber morphology, 215,216*f*
  limitations, 217
  mechanical properties, 217,219*t*
  production via solution spinning process, 215
  tensile strength, 217,219*t*
  uses
    chain saw cut protective chaps, 224
    hard composite armor systems, 229,231–235
    medical glove liner, 223–224
    protective sweater, 222
    soft armor systems, 224–230
    sporting helmets, 234
High-tech fiber
  evolution, 8–12
  utilization, 11–18
High-tech textiles
  applications, 2–8
  development, 2
  evolution, 11–18
  evolution or revolution, 1–18
  uses
    airplanes, 2,5*f*
    architecture and construction, 4,6–7*f*
    artificial arteries, 2,3*f*
    artificial heart, 2,3*f*
    civil engineering applications, 4
    gas and liquid filtration systems, 4
    protective clothing, 4,5*f*
    recreational applications, 4
  utilization, 11–18
High-tenacity filament process, manufacture of PET fiber and fabric, 308,309*f*,310
Hi-loft synthetic insulation, limitation, 248–249
Hindered amine light stabilizers
  extraction resistance, 327*t*,331*t*
Hindered amine light stabilizers—*Continued*
  performance
    polypropylene fiber, 327,330*f*
    polypropylene tapes, 327,330*f*
  stabilization mechanism, 323,324*f*
  thermal stabilizers, use, 331,332*f*
Hindered phenolic antioxidants, structures, 323,325*f*
Hollow fibers
  medicinal applications, 120–122
  uses
    artificial kidney, 120–121
    artificial lung, 122
    artificial pancreas, 121
    plasmapheresis, 121
Hot plate test
  description, 295–296
  fabric melt/stick rankings, 300*t*,301
  limitations, 295
Hubert Humphrey dome, use of high-tech textiles, 4,6*f*
Human wear testing of phase-change materials
  comfort testing protocol, 252–253
  garment preparation, 252
  materials, 250–252
  sample size, 251
Humidity, effect on aging of impregnated fiber glass yarns, 343,344*t*
Hydraulic properties, nonwoven polypropylene geotextiles, 380,381*t*,382
Hydrolytic degradation of synthetic absorbable sutures
  anisotropy, effects, 200,201*t*
  chain scission, effects, 196–197
  chemical analytical method, 200,202,203*f*
  crystallinity level vs. hydrolysis time, 197,198–199*f*
  degradation, factors affecting, 191–203
  enzymes, role, 197
  external strain, effects, 197,200
  future challenge, 206*t*,207
  importance of absorbable sutures, 189–191
  mechanism, 192
  regulation via surface modification, 202,204,205*t*,206
  schematic representation, 192,193*f*
  surface microcracks of partially hydrolyzed sutures, 192,194*f*
  surface morphology of partially hydrolyzed fiber, 192,195*f*,196
  tensile breaking strength of surface-modified sutures, 204,205*t*,206
Hyperfiltration, use of high-tech fibers, 11,12*f*

I

Implantable fibers, applications, 116–122

Downloaded by 89.163.34.136 on August 6, 2012 | http://pubs.acs.org
Publication Date: April 3, 1991 | doi: 10.1021/bk-1991-0457.ix002

Impregnated fiber glass
  advantages for use as geotextile, 338
  applications, 346,348,349*t*
  fabrics, 345
  geogrids, 345
  products, 338,340*f*
  properties, 338,341*t*
  woven fabrics, properties, 345–346,347*t*
Impregnated fiber glass yarn
  acidic and alkaline media, effect on strength, 344,344*t*
  aging properties, 343,344*t*
  humidity, effect on aging, 343,344*t*
  impregnation, effect on properties, 341
  production, 338
  properties, 338,341,343*t*
  water, effect on aging, 343,344*t*
Inclined braider yarn, 26,27*f*
Industrial composite, definition, 82
Inidex, description, 268
Inorganic fillers, advantages, 102
Inorganic salt resistance, polyethylene terephthalate fibers, 313,314*t*
Instrumental effects, thermal protective performance tester, 282–289
Integrated design methodology for composites, logical flow, 90,91*f*
In vitro studies, carbon fiber reinforced polylactic acid composite, 136–140,145
In vivo studies, carbon fiber reinforced polylactic acid composite, 138–146
IR reflectance, dye classes, 271,272*f*

K

Kevlar
  advantages and disadvantages for use in braided composite monocoque bicycle frame, 95
  applications, 14
  description, 268
  development, 8
Kevlar 100
  breakthrough and thermal insulation performance, 286,290*t*
  failure mechanism of thermal protection, 286,290*t*
  thermal protective performance, 283,285*f*,286,289*f*
Knits
  advantages and disadvantages, 127
  description, 126
  schematic representation, 126*f*,127
Knot tying and holding, suture characteristic, 117

L

Lagrangian constitutive model of nonlinear finite strain behavior
  deformation from undeformed to deformed configuration, 150,152,153*f*
  rectangular element of composite lamina before and after loading, 152,153*f*
  strain-energy density, 152
  strain tensor, 152
  stress matrix, 152,154–155
Lagrangian strain tensor, definition, 152
Lagrangian stress, components, 158
Laminated composites, 54–55
Landfill, *See* Waste containment facility
Laser(s)
  high-tech fibers, 13
  optical fibers, 122
Latex gloves, cut protection, 223
Leachate(s), sampling for chemical compatibility tests, 377
Leachate resistance, PET fibers and fabrics, 318–319
Light stabilization mechanism, polyolefins, 321,323,324*f*
Light stabilizers, structures, 327,329*f*
Linear low-density polyethylene–silane-coated wood fiber composites
  coupling mechanism at fiber–matrix interface, 105,107*f*
  experimental materials, 103
  mechanical tests, 104
  preparation of composites, 104
  pretreatment of wood fiber, 103–104
  silane pretreatment, effects
    elongation, 105,106*f*
    morphology, 110,111*f*
    tensile modulus, 105,107*f*,110,112*f*
    tensile strength, 104–106,110,112
  silane structure, effect on coupling effectiveness, 110,113
  tensile properties
    peroxide effects, 108,109*t*,110
    silane concentration, effects, 105,108*t*
Linen, use as suture material, 167
Longitudinal elastic behavior, flexible composites sinusoidally shaped fibers, 157–158
Loom, three-dimensional multilayer preforms for composites, 63,64*f*
Low-cost fillers, incentives for use, 102
Lung, components, 149

M

Machine bed, ratio to preform size, 45,47,48*f*,49

Downloaded by 89.163.34.136 on August 6, 2012 | http://pubs.acs.org
Publication Date: April 3, 1991 | doi: 10.1021/bk-1991-0457.ix002

Marine industry, use of multiaxial warp knit composites, 85*t*,86
Materials characterization, three-dimensional multilayer woven preforms for composites, 67
Materials for bioimplants, 127–128
Mechanical properties, nonwoven polyester geotextiles, 379*t*,380,382
Medical glove liner, use of high-performance polyethylene fibers, 223–224
Medicine, use of fibers, 116–122
Melt/stick characteristics of flame-retardant polyester–cotton fabrics
  background, 294–295
  convective hot air tests, 296,297–298*f*,299*t*
  fabric characteristics, 299*t*
  fabric rankings for tests, 300*t*,301
  hot plate test, 295–296
  objective of study, 293–294
  oven test, 295
  radiant heat test, 296,297*f*
Membrane-laminated fabrics, applications, 17
Metal armor, disadvantages, 225
Microchain mail glove, cut protection, 223
Military camouflage
  colorant limitations, 271
  dye criteria, 271,273
  four-color pattern, 273
  IR reflectance, 273,274*f*
  printing technology for aramid fibers, 273,275,276*t*
Monocoque bicycle frame, braided composite, *See* Braided composite monocoque bicycle frame
Monofilament sutures, advantages, 168
Multiaxial warp knit composites, 81,82
Multiaxial warp knit fabrics
  advantages, 84,87
  aerospace applications, 85*t*
  conformability, 84
  end-use applications of industrial composites, 85*t*,86–87
  flooring, use, 87
  future in industrial applications, 87–88
  load-bearing yarn systems, 82
  marine applications, 85*t*,86
  production, 82
  properties, 82–83
  structural geometry, 82,83*f*
  tear propagation resistance, 84
  tensile properties, 83
  web effects, 84
Multifunctional-property fabrics, applications 17–18
Multilayer knitted/stitched fabrics, description, 56
Multilayer woven fabrics, description, 56

N

NASA space shuttle, use of carbon fibers in heat shield, 10,12*f*
Natural tissues, nonlinear finite strain behavior, 150
NeutraTherm
  active cooling and warming, 255–256
  advantages, 258
  comfort
    evaluation, 255
    testing protocol, 252–253
    treated T-shirt, rating, 253*t*
  cross-linking agent, 251
  cross-linking polyethylene glycol process, 249
  garment preparation, 252
  human wear testing, 250–252
  odor retention, 257
  perspiration handling, 256–257
  properties, 258
  thermal insulation, 256
  treated garment characteristics during skiing-like activity, 253,254*t*
  washability and dryability, 255
  wind insulation, 256
Nomex
  applications, 14
  description, 268
  See also Aramid fibers
Nomex III
  breakthrough and thermal insulation performance, 286,290*t*
  failure mechanism of thermal protection, 286,290*t*
  thermal protective performance, 283,284*f*,289*f*
Nonabsorbable sutures, 168
Nonimplantable fibers, applications, 117*t*
Nonlinear finite strain behavior of natural tissues, models, 150
Nonwoven(s), 125
Nonwoven geotextiles
  bonding procedures, 353
  uses, 353–354
Nonwoven orthogonals, 56
Nonwoven polyester geotextiles
  dimensional properties, 379,380*t*,382
  mechanical properties, 379*t*,380,382
Nonwoven polypropylene geotextiles
  hydraulic properties, 380,381*t*,382
  oxidative induction temperatures, 381*t*,382
Nylon, development, 8
Nylon stocking extensibility, description, 150

O

Optical fibers, use in medicine, 122

Downloaded by 89.163.34.136 on August 6, 2012 | http://pubs.acs.org
Publication Date: April 3, 1991 | doi: 10.1021/bk-1991-0457.ix002

Organic solvent resistance, polyethylene terephthalate fibers, 313,315*t*
Oven test
  description, 295
  fabric melt/stick rankings, 300*t*,301
  limitation, 295
Oxidative induction temperatures, nonwoven polypropylene geotextiles, 381*t*,382

P

Pavement rehabilitation, use of geotextiles, 359–360,364*f*
Permittivity
  definition, 371
  test, 371–372,373*f*
Peroxide, effect on tensile properties of wood fiber composites, 108,109*t*,110
PET, *See* Polyethylene terephthalate
Phase-change material, *See* Polyethylene glycol
Phosphite processing stabilizer
  processing stability, 327,328*f*
  structures, 323,326*f*,327
Pigment printing, description, 271
Pitch, use as carbon fiber precursor, 10*t*,11
Plasmapheresis, use of hollow fibers, 121
Pliability, suture characteristic, 117
Police riot helmet, use of high-performance polyethylene fibers, 229
Pollution control, use of geotextiles, 362–363,366–367*f*
Polyacrylonitrile, use as carbon fiber precursor, 10*t*,11
Polyamide fibers, disadvantages for use as geotextile, 338
Polybenzimidazole blends
  applications, 238–239
  comfort, 246*t*,247
  dynamic flame testing, 243*t*,244*f*
  gas pit testing, 243,245*t*
  protective coveralls, 240–247
  thermal protective performance, 241,242–243*t*
  vertical flammability testing, 240,241*t*
Polybenzimidazole fiber
  advantages of blending with other fibers, 238–239
  commercial introduction, 238
  physical properties, 239*t*
  tensile strength after immersion in organic chemicals, 239*t*
  unique properties, 238
Polybenzimidazole yarns, applications, 14,16*f*
Polyester
  waste containment facilities, use, 352–353
  See also Polyethylene terephthalate
Polyester–cotton blend fabrics, flame retardant, *See* Flame-retardant polyester–cotton blend fabrics
Polyester fibers, disadvantages for use as geotextile, 338
Polyester geotextiles
  aging, 305,308
  aging of PET, 317–319
  degradation mechanisms, intrinsic material resistance, 305,306*t*
  fabric failure mechanisms, 305,307*t*
  PET fabric performance properties, 313,316*t*,317,318*f*,318*t*
  PET fibers and fabrics, 308,309*f*,310
  PET resistance to fiber degradation, 310–316
  polymer degradation mechanisms, 305,306*t*
  soil environment, effects, 308
Polyethylene
  development, 9
  disadvantages for use as geotextile, 338
  waste containment facilities, use, 353
  See also Nonwoven geotextiles
Polyethylene geotextiles, long-term performance, 376–377
Polyethylene glycol
  advantages for use in temperature-adaptable fabrics, 249
  applications, 250
  chemical and physical properties, 250
  properties when bound to fiber, 250
Polyethylene terephthalate (PET)
  chemical formulation, 308,309*f*
  fabrics
    aging, 317–319
    creep resistance, 317,318*f*
    properties, 313,316*t*,317,318*t*
  fibers
    acid resistance, 311,312*t*
    aging, 317–319
    alkali resistance, 311,312*t*,313
    characteristics, 310
    chemical resistance, 310
    fertilizer resistance, 313,315*t*
    inorganic salt resistance, 313,314*t*
    manufacture, 308,309*f*,310
    organic solvent resistance, 313,315*t*
    thermal resistance, 310
    UV resistance, 313,316*f*
    water resistance, 311
  manufacture of fibers and fabrics
    high-tenacity filament process, 308,309*f*,310
    spunbond filament process, 308,309*f*,310
Polylactic acid
  composite with carbon fiber, 133–146
  fraction fixation, 133

Downloaded by 89.163.34.136 on August 6, 2012 | http://pubs.acs.org
Publication Date: April 3, 1991 | doi: 10.1021/bk-1991-0457.ix002

Downloaded by 89.163.34.136 on August 6, 2012 | http://pubs.acs.org
Publication Date: April 3, 1991 | doi: 10.1021/bk-1991-0457.ix002

- Polymer degradation
  - factors affecting degradation mechanisms, 127–128
  - potential mechanisms, 305,306*t*
- Polymer properties, effect on biocompatibility of textile implants, 128
- Polyolefin(s)
  - degradation mechanism, 320–321,322*f*
  - light stabilization mechanism, 321,323,324*f*
  - thermal stabilization mechanism, 321,322*f*
- Polyolefin fiber stabilization
  - antioxidants
    - primary, 323,325*f*
    - secondary, 323,326*f*,327,328*f*
  - effect of carbon black on thermal stability, 333,334*f*,335
  - hindered amine light stabilizers as thermal stabilizers, 331,332*f*,333*t*
  - light stabilizers, 327,329–330*f*
- Polyphenylene sulfide fibers, applications, 14
- Polypropylene
  - disadvantages for use as geotextile, 338
  - uses
    - surgery, 120
    - waste containment facilities, 352–353
- Polypropylene geotextiles, long-term performance, 376–377
- Polytetrafluoroethylene, use in small-diameter grafts, 119
- Porosity, effect on biocompatibility of textile implants, 128
- Preform characterization, three-dimensional multilayer woven preforms for composites, 71
- Preform size, ratio to machine bed, 45,47,48*f*,49
- Prepregs, definition, 54
- Printing technology for aramid fabrics
  - comparison of color data with that of nylon–cotton standard, 276*t*
  - dyes and pigments, use, 275–276
  - property requirements of fibers, 273,275
  - surfactant selection, 275
- Printing with dyes, mechanism, 273
- Protective clothing
  - high-tech textiles, use, 4,5*f*
  - progress in development, 214
  - requirements, 214–215
- Protective coveralls using polybenzimidazole blends
  - candidate fibers, 240*t*
  - comfort, 246*t*,247
  - dynamic flame testing, 243*t*,244*f*
  - flame resistance, 241*t*
  - gas pit testing, 243,245*t*
- Protective coveralls using polybenzimidazole blends—*Continued*
  - grab strength retained after thermal protective performance test exposure, 242,243*t*
  - thermal protective performance, 242*t*
  - vertical flammability, 240,241*t*
- Protective sweater, use of high-performance polyethylene fibers, 222
- Prototype fabrication, braided composite monocoque bicycle frame, 97,98–99*f*

Q

- Quality control and quality assurance, geotextiles in waste containment facilities, 355–357

R

- Radiant heat test
  - apparatus, 296,297*f*
  - description, 296
  - fabric melt/stick rankings, 300*t*,301
- Railroad track, use of Hercuflex products, 348
- Rayon as carbon fiber precursor, 9–10
- Recreational uses, high-tech textiles, 4
- Reinforcement, use of geotextiles, 352,354,361–362,365*f*
- Reverse osmosis media, applications, 11,12*f*,13
- Rewinding lengths, determination for three-dimensional braiding processes, 49–50,51*f*
- Rigid metallic bone plates, disadvantages, 132–133
- Riot helmet, use of high-performance polyethylene fibers, 229
- Ryton, description, 268

S

- Saudi Arabian airport, use of high-tech textiles, 4,7*f*
- Seam strength test, description, 369
- Seeded material, 130
- Separation, use of geotextiles, 360,364*f*
- Shearing stresses, source of delamination, 54
- Shear moduli, three-dimensional textile structural composites, 30,32,33*f*
- Silane, effect of concentration on tensile properties of wood fiber composites, 105,108*t*
- Silane-coated wood fibers, composites with linear low-density polyethylene, 102–113

Silicone rubber sutures, advantages and disadvantages, 118
Silver
  bacterial resistance, 175
  wound infection control, 175
Silver metal coated antibacterial suture
  Ag^+ concentrations vs. direct current and time, 183,186*f*,187
  Ag^+ ion bacterial inhibition mechanism, 183
  Ag^+ ion transport into bacterial cells, 182–183
  anode-related antimicrobial activity, 182
  antibacterial activity, effect of knotted vs. unknotted forms, 188
  antimicrobial activity
    anode-related, 182
    direct current application mode, effect, 176,180*f*,182
    direct current magnitude, effect, 176,180*f*,182
  bacterial culture plates without direct current application, 176,181*f*,182
  bacteriostatic effect, effect of bacterial species, 183,184–185*f*
  biocompatibility with tissue, 187
  direct current application mode, effect on antimicrobial activity, 176,180*f*,182
  direct current magnitude, effect on antimicrobial activity, 176,180*f*,182
  future challenges and opportunities, 188–189
  histological evaluation, 187*t*
  improvement in rate and quality of heating, 187–188
  in vitro to in vivo transition, 188
  knotted vs. unknotted forms, effect on antibacterial activity, 188
Silver metal coated antimicrobial suture
  energy-dispersive spectrometric area mapping, 176,178*f*
  energy-dispersive spectrometric spectrum, 176,177*f*
  in vitro antibacterial properties, 176,179*t*
  preparation, 175
  stress–strain curves, 176,177*f*
  structure, 175–176,177–178*f*
  wound infection control, 171,175
Sinus formation, relationship to wound infection, 190
Sinusoidally shaped fibers, flexible composites, 155–163
Ski wear, use of NeutraTherm, 248–258
Slope stabilization, use of Hercuflex products, 348
Small-diameter grafts
  electrostatic spinning of fibers, 120
  expanded polytetrafluoroethylene, 119
Smooth muscle, mean resting tension–length curves, 150,151*f*
Soft armor systems
  conventional fabric vs. Spectra Shield, 226,227*f*
  criteria, 225
  high-performance polyethylene fibers, use, 225–230
Soil resistance, PET fibers and fabrics, 318
Solution spinning process, production of high-performance polyethylene fibers, 215
Solvent-bonded nonwovens, 130
Space shuttle, use of carbon fibers in heat shield, 10,12*f*
Spatially oriented yarns, 28–29
Spectra
  applications, 14
  See also High-performance polyethylene fibers
Spectra fiber, advantages and disadvantages for use in braided composite monocoque bicycle frame, 93,95
Spectra Shield
  comparison to conventional fabrics, 226,227*f*
  products, 226,228*f*
Sporting helmets, use of high-performance polyethylene fibers, 234
Spunbond filament process, manufacture of PET fiber and fabric, 308,309*f*,310
Stabilization, use of geotextiles, 362,366*f*
Stealth bomber, use of high-tech fibers, 13
Sterilization, effect on polymer degradation, 128
Stiffness matrices, calculation, 29
Structural analysis, braided composite monocoque bicycle frame, 96,97*t*,98*f*
Structure compliance, effect on biocompatibility of textile implants, 128
Surface modification, regulation of suture fiber degradation, 202,204,205*t*,206
Surfaces of fiber and fabric, modification via high-energy sources, 18
Surgery, uses of fabrics, 120
Suture(s)
  bacterial adherence, 170–171
  categories according to origin, 117–118
  characteristics, 116–117
  criteria, 116–117
  definition, 116
  infection concerns, 117
  infection susceptibility, 170
  materials, 116
  physical structure, effect on infection susceptibility, 170
  thread configuration, effect on infection susceptibility, 170
  wound infection, role, 169–174

Downloaded by 89.163.34.136 on August 6, 2012 | http://pubs.acs.org
Publication Date: April 3, 1991 | doi: 10.1021/bk-1991-0457.ix002

Suture fibers for wound closure
  development
    antimicrobial fibers, 169–189
    synthetic absorbable fibers, 168
  forms, 168
  hydrolytic degradation of synthetic absorbable sutures, 189–207
Suture materials, basic properties, 168–169
Synthetic absorbable sutures
  absorption delay, 206*t*,207
  advantages, 191
  degradability inside biological environment, 189
  effects
    predisposition to wound infection, 190
    tissue adhesion, 190
    wound strength, 189–190
  importance, 189–191
  stone formation, 189
Synthetic fibers, comparison to wood fiber, 103

T

Temperature-adaptable fabrics, 248–249
Tensile properties, comparison for geosynthetic materials, 348,349*t*,350
Tensile strength, Hercuflex fabric, 346,347*t*
Tensile test, composites, 73,75*t*
Tension, effect on thermal protective performance, 283,286,289*f*
Tension device, three-dimensional multilayer woven preforms for composites, 65,66*f*
Tests for geotextiles
  apparent opening size, 372,373*f*
  asphalt retention, 372,374*f*
  grab tensile, 368,370*f*
  permittivity, 371–372,373*f*
  seam strength, 369
  trapezoid tear, 369
  UV degradation, 371
  wide width strength, 369,370*f*
Tex-Tech wool blend
  flammability, 264,265*t*
  thermal protection performance, 264,266,267*t*
Textile(s)
  bioimplants
    applications, 125
    biocompatibility, 128
    categories, 129
    design, 129,130*f*
    development, 124
    future design, 129–130
    heat setting and shrinking characteristics, 125
    materials, 127–128
Textile(s)—*Continued*
  bioimplants—*Continued*
    stiffness uniaxially or biaxially and flexibility in bending, 125
    structures, 125,126*f*,127
  domestic consumption, 1–2
  external medicinal applications, 124
  high tech, *See* High-tech textiles
  machinery requirements, 1–2
  vascular grafts and cardiovascular patches, uses, 125
Textile industry, 1–2
Textile materials for surgery, 167
Textile printing, procedures, 271
Textile-reinforced flexible composites
  constitutive relation of unidirectional lamina, 150,152–155
  containing sinusoidally shaped fibers, 155–163
  laminate analysis, 162–165
Thermal protective clothing, 270–276
Thermal protective fabrics
  intense heat and dynamic mechanical forces, effects, 278–290
  ultimate test, 277
Thermal protective performance
  dynamic mechanical effects, 283
  polybenzimidazole blends, 242–243*t*
  rating, definition, 279
  test
    apparatus, 241–242,296,298*f*
    breakthrough vs. tolerance times, 286,290*t*
    description, 296,299
    failure mechanism, 286,290*t*
    function, 277
    tester description, 278–279
    thermal protective performance, 281,282*t*
Thermal resistance, polyethylene terephthalate fibers, 310
Thermal stabilization mechanism, polyolefins, 321,322*f*
Thermomechanical properties, prediction for three-dimensional braided composites, 23
Thinsulate, applications, 17
Thiosynergists, thermal stability, 331,333*t*
Three-dimensional braid(s), description, 56
Three-dimensional braided fabrics, 22,24*f*
Three-dimensional braiding
  advantages, 34
  carrier design, 50,51*f*
  development of processes, 35
  equipment, 35
  four-step process, 35–40,46
  process analysis and automation, 35–46
  ratio of machine bed to preform size, 45,47,48*f*,49
  rewinding requirement for fiber carriers, 49–50,51*f*
  two-step process, 35,40–46

Downloaded by 89.163.34.136 on August 6, 2012 | http://pubs.acs.org
Publication Date: April 3, 1991 | doi: 10.1021/bk-1991-0457.ix002

Downloaded by 89.163.34.136 on August 6, 2012 | http://pubs.acs.org
Publication Date: April 3, 1991 | doi: 10.1021/bk-1991-0457.ix002

Three-dimensional multilayer woven preforms for composites
  advantages, 55,74
  composite characterization, 71
  composite curing, 67,69–70*f*
  composite fabrication and testing, 67,69–75
  composite properties, 74,75*t*,76*f*
  composite specifications, 74,75*t*
  composite testing, 71
  creel, 63,64*f*
  C-scan measurements of composites, 77
  design and development, 57–69
  equipment used for fabric formation, 57,62–65
  fabric finish, 67
  fabric specifications, 74,75*t*
  fiber, 57,62*f*
  flexure test, 73–74
  Kevlar 49 yarn, tensile stress–strain curve, 57,62*f*
  literature review, 55–56
  loom, 63,64*f*
  materials characterization, 67
  multilayer knitted fabrics, 56
  multilayer woven fabrics, 56
  nonwoven orthogonals, 56
  photomicrographs, 71,72*f*
  preform characterization, 71
  preparation for weaving, 65
  production of fabric samples, 67,68*f*,69*t*
  properties vs. composite composition, 74,77
  recommendations, 77–78
  sizing the warp, 65
  tensile stress–strain curve for Kevlar 49 yarn, 57,62*f*
  tensile test, 73,75*t*
  tension device, 65,66*f*
  three-dimensional braiding, 56
  weave design, 57,58–61*f*
  weave plan and schematic representation
    weave A, 57,58–59*f*
    weave B, 57,60*f*
    weave C, 57,61*f*
  weaving setup, 57,62*f*
Three-dimensional textile structural composites
  comparison of engineering constants from model prediction with those from experimental results, 30,32*t*
  compliance matrix calculations, 29
  compliance of spatially oriented yarns, 28–29
  elastic moduli prediction, 23
  fiber and matrix properties utilized in prediction of engineering constants, 30*t*
  measured parameters, 30*t*
Three-dimensional textile structural composites—*Continued*
  mechanical property prediction, 22–23
  numerical calculations, 29
  shear moduli vs. process parameters, 30,32,33*f*
  spatially oriented composite cylinder, 28,31*f*
  stiffness matrix calculation, 29
  thermomechanical property prediction, 23
  Young's moduli vs. process parameters, 30,31*f*,32
Tissue reaction, suture characteristic, 117
Tissue reaction to sutures, influencing factors, 189–190
Toxic substances, effect on biocompatibility of textile implants, 128
Transportation
  high-tech fibers, use, 13*t*,14
  high-tech textiles, use, 3,5*f*
Transportation facilities, use of geotextiles, 358–374
Transverse elastic behavior, flexible composites containing sinusoidally shaped fibers, 159–160,161*f*
Transverse normal stress, source of delamination, 54
Trapezoid tear test, description, 369
Two-step braided composites
  axial yarns, volume, 25
  configurations of braider yarns, 26,27*f*
  cross section, 23,24*f*
  geometric relations, 23–27
  inclined braider yarn, length, 26
  schematic representation of inclined braider yarn within unit cell, 26,27*f*
  unit cell, total volume, 25
  yarn dimensions, 23,25
Two-step braiding process, yarn movements, 22,24*f*
Two-step process of three-dimensional braiding
  analytical model, 40
  braiding machine, 43,44*f*,45
  braiding pattern, 40,41*f*
  comparison with four-step process, 45,46*t*
  description, 35
  equipment, 35
  flow chart of control system for braiding machine, 43,44*f*,45
  ratio of machine bed to preform size, 47,48*f*,49
  repeat unit, 40,41*f*
  rewinding requirement, 49–50,51*f*
  yarn orientation angle, 40,42*f*
  yarn volume fraction, 40,42*f*
Tyvek, applications, 14,15*f*

U

Ultrafiltration, use of high-tech fibers, 11
Unidirectional lamina, constitutive relation, 150,152–155
Unit cell, definition, 25
Utilization of high-tech fibers
  aircraft and transportation, structural use, 13*t*,14,15*f*
  artificial kidney, 11
  civil engineering, 14,15*f*
  comparison of strengths and stiffnesses of composites, 14,15*f*
  extracorporeal dialysis, 11
  high-temperature applications, 14,16*f*,17
  hyperfiltration, 11
  laser beams, 13
  multifunctional-property fabrics, 17–18
  protective clothing, 14,17
  ultrafiltration, 11
UV degradation test, description, 371
UV resistance, polyethylene terephthalate fibers, 313,316*f*

V

Vascular grafts
  advantages and disadvantages, 119
  development, 118–119
  textiles, use, 124–125
Vertical flammability testing, 240,241*t*
Vertical walls, use of Herculflex products, 348

W

Warp, sizing, 65
Waste containment facilities, use of geotextiles, 351–357
Waste containment systems, effect of aggressive environments, 377
Water, effect on aging of impregnated fiber glass yarns, 343,344*t*
Water resistance, polyethylene terephthalate fibers, 311
Weave design, three-dimensional multilayer woven preforms for composites, 57,58–61*f*
Wet printing, *See* Dye printing
Wide width strength test, description, 369,370*f*
Wood fiber
  advantages, 102–103
  comparison to synthetic fiber, 103
  coupling agent, effect on filler–polymer matrix adhesion, 103
  disadvantages, 103
  filler–polymer matrix adhesion, effect of coupling agent, 103
  use as filler, 102
Wool
  comfort, 261
  disadvantages of combination with liquid moisture barriers, 263
  flame retardant, *See* Flame-retardant wool
  helically coiled and crimped fiber shape, 261
  high-tech applications, 260
  history of use, 260
  moisture regain, 261
  structure, 261,262*f*
Wool blends with inherently flame retardant fibers for protective clothing
  advantages, 266
  Fire Flite, 264
  Tex-Tech, 264,265*t*,266,267*t*
Wound closure, advancements in suture fibers, 167–207
Wound infection
  influencing factors, 169
  need to control, 169
  sinus formation, relationship, 190
  sutures, role, 169
Woven(s), 125–126*f*
Woven fabrics, advantages, 53

Y

Young's moduli, three-dimensional textile structural composites, 30,31*f*,32

Z

Zirpro, description, 268

Production: Sharon Averell and Donna Lucas
Indexing: Deborah H. Steiner
Acquisition: Cheryl Shanks
Cover design: Amy Meyer Phifer

Printed and bound by Maple Press, York, PA

Paper meets minimum requirements of American National Standard
for Information Sciences—Permanence of Paper for Printed Library
Materials, ANSI Z39.48–1984 ∞

Downloaded by 89.163.34.136 on August 6, 2012 | http://pubs.acs.org
Publication Date: April 3, 1991 | doi: 10.1021/bk-1991-0457.ix002